



HAL
open science

Gold(I) and Silver(I)-Catalyzed Reactions under Visible Light. Bisphosphine Allene based Ligands: from coordination to catalysis

Fen Zhao

► **To cite this version:**

Fen Zhao. Gold(I) and Silver(I)-Catalyzed Reactions under Visible Light. Bisphosphine Allene based Ligands: from coordination to catalysis. Organic chemistry. Sorbonne Université, 2021. English. NNT: 2021SORUS121 . tel-04209082

HAL Id: tel-04209082

<https://theses.hal.science/tel-04209082v1>

Submitted on 16 Sep 2023

HAL is a multi-disciplinary open access archive for the deposit and dissemination of scientific research documents, whether they are published or not. The documents may come from teaching and research institutions in France or abroad, or from public or private research centers.

L'archive ouverte pluridisciplinaire **HAL**, est destinée au dépôt et à la diffusion de documents scientifiques de niveau recherche, publiés ou non, émanant des établissements d'enseignement et de recherche français ou étrangers, des laboratoires publics ou privés.

Sorbonne Université

Ecole Doctorale de Chimie Moléculaire de Paris Centre

Institut Parisien de Chimie Moléculaire / Equipe Méthodes et Applications en Chimie Organique

Gold(I) and Silver(I)-Catalyzed Reactions under Visible Light

Bisphosphine Allene based Ligands: from Coordination to Catalysis

Par Fen ZHAO

Thèse de doctorat de Chimie Organique

Dirigée par le Pr. Louis FENSTERBANK et le Dr. Virginie MOURIES-MANSUY

Présentée et soutenue publiquement le 15 September 2021

Devant un jury composé de :

Mme. Erica BENEDETTI	Chargée de recherche, Université de Paris	Rapportrice
M. Etienne BRACHET	Maître de conférences, Université de Paris	Rapporteur
M. Yongmin ZHANG	Directeur de recherche, Sorbonne Université	Examineur
M. Louis FENSTERBANK	Professeur, Sorbonne Université	Directeur de thèse
Mme Virginie MOURIES-MANSUY	Maître de conférences, Sorbonne Université	Directeur de thèse

Acknowledgments

I would like to thank the members of the jury, BENEDETTI Erica, BRACHET Etienne, and ZHANG Yongmin for agreeing to judge this work and to be present at the defense. Your invaluable comments and suggestions help me improve the quality of this thesis.

This thesis work was conducted from October 2017 to September 2021, under the guidance of Dr. Virginie Mouries-mansuy and Prof. Louis Fensterbank, in the laboratory “Méthodes et Applications en Chimie Organique (MACO)” at Institut Parisien de Chimie Moléculaire (IPCM), Sorbonne Université.

I would like to sincerely thank my supervisor, Professor Louis Fensterbank, who gives me an opportunity to finish my PhD study in MACO group and for his excellent guidance throughout the past four years of my PhD research. He is the excellent boss of MACO group and let everybody live moments of relaxation under the professional context. He also is an excellent chemist with a wide knowledge. During period of exploring chemistry, we always encountered various difficulties; But we can find the solutions under by his candid discussion, pertinent criticism and constant encouragement.

I am truly grateful to my research director, Dr. Virginie Mouries-mansuy, who is always ready for providing help and solving problems very quickly, I have to work very efficiently to follow her step. I would thank her patience teaching for experimental techniques. I really appreciate her humor and cheer me up, especially when my reaction did not work very well, her encouragement motivates me a lot to achieve the goal.

I would like to thank Mehdi Abdellaoul who participate in my second project and helped me to do some mechanism experiments. Thanks for his work on my project and sharing his suggestions in the experiment discussion. Besides, many thanks for Jeremy Forté and Dr. Nicolas Vanthuynne for the X-ray diffraction and chiral HPLC analysis. I am grateful to Omar Khaled and Cédric Przybylski for HPLC and for HRMS analysis.

I also want to thanks Dr. Christophe Desmarets and Dr. Alexandre Pradal, who are my committees in “comité de suivi”, for their suggestions to my research.

I would like to say thanks to the MACO team who accompanied me through my precious four years in Paris and gave me many precious memories. Many thanks for Dr. Corinne Aubert, Dr. Gilles Lemièrre, Dr. Marc Petit, Dr. Marion Barbazanges and Dr. Cyril Ollivier for their kind helps.

Many thanks to my French friend, Valérie-Anne Ramis cladera, a beautiful lady. She is very kindness and friendliness. She helps me a lot in the lab and my life. She shares with me many music and many French story. We can talk about some interesting things about China and France. We can talk about everything in our free time and we share happiness and sadness. I am so glad to meet her in MACO team.

Thanks to my neighbors, Pei Pei, Wei Xian, and Sunbin, we do sports together in our free time, and we share Chinese food in weekend, I didn't feel lonely with them. And many thanks to my friend, Long Yang, Tingting Cheng, and Puqing Xu, we did many sports together and we travelled together during the holidays. We share happiness and sadness; I fell so luckily I have your friends! I also want to thanks my chinese colleagues, Zhonghua Xia, Yufeng Ren, Ye Lyu, Hengrui Zhang, and Xue Xan Zhang. They bring me happiness and company, and let me feel no lonely during my PhD study in France.

Finally, I am very grateful to my parents, baba, and my cats, their love and support always make me happy and successful in my life.

Fen ZHAO
July, 2021, Paris

To my cats



Thank Coco and Honey for staying with me through four years of studying abroad life

Contents

Acknowledgments	1
Contents	5
General Introduction	9
Résumé.....	13
Chapter 1 Background.....	33
1. Gold Catalysis	35
1.1 Homogeneous Gold Catalysis	35
1.2 Vinylgold Intermediates.....	37
1.3 Redox Gold Catalysis Chemistry	40
2. Visible-light-mediated Gold Catalysed Reaction	44
2.1 Dual Photoredox/Gold Catalysis	46
2.2 Photosensitizer Free Gold Catalysis	53
3. Silver Catalysis	57
3.1 Homogeneous Silver Catalysis.....	58
3.2 Silver Catalysis under Visible Light.....	64
4. Reference	69
Chapter 2 Photosensitizer-free Gold Catalysis.....	73
1. External Photosensitizer-free on Photocatalytic Reaction.....	75
2. Project Aim and Introduction	84
3. Results and Discussion.....	87
3.1 Optimization Studies.....	87
3.2 Scope and Limitation	89
3.3 Post-functionalization	93
4. NMR Monitoring Experiment of Vinylgold(I) Intermediate.....	94
5. Conclusion	102

6. Experimental Section	103
7. Reference	149
Chapter 3 Photocatalyzed Silver Catalysis	153
1. Background	155
1.1 Gold-catalysed Sulfonyl Migration	155
1.2 Silver-catalysed Sulfonyl Migration.....	160
1.3 Radical-mediated Sulfonyl Migration	164
2. Project Aim and Introduction	169
3. Results and Discussion.....	172
3.1 Optimization Studies.....	172
3.2 Scope and Limitation	174
3.3 Mechanism Investigation	176
3.4 Conclusion.....	179
4. Experimental Section	180
5. Reference	201
Chapter 4 Bisphosphine Allene based Ligands: from Coordination to Catalysis.....	205
1. Background	207
1.1 Organophosphorus Compounds	207
1.2 Phosphine Ligand and Analogues	208
1.3 Phosphine Ligand in Asymmetric Catalysis	210
1.4 Allene Syntheses.....	215
1.5 Allenes in Catalysis	225
1.6 Luminescence Properties	231
2. Objective of the Project.....	234
3. Synthesis of Allenyl Bisphosphine Boranes	236
4. Resolution of Racemic Allene Bisphosphine Borane.....	238
5. Metal-allenyl Bisphospine Complexes	240

5.1 Platinum-allenyl Bisphosphine Complex	240
5.2 Gold-allenyl Bisphosphine Complex	240
5.3 Rhodium-allenyl Bisphosphine Complex.....	241
6. Rhodium (I)-catalyzed Cyclization Reactions of 1,6-Enynes.....	242
7. Asymmetric Catalysis with Chiral Rh Complexes 4-127	246
8. Gold-allenyl Bisphosphine Complex	247
9. Conclusion and Perspectives	251
10. Experimental Section	252
11. Reference	278
General Conclusion.....	285

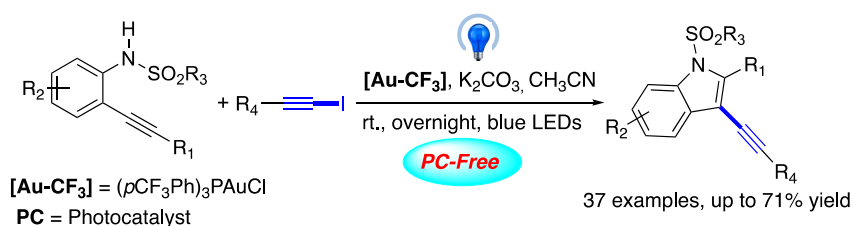
General Introduction

Homogeneous gold catalysis has received great attention over the last decade. The selective electrophilic activation of the carbon-carbon multiple bonds by a gold complex generally constitutes the preliminary triggering event of the catalytic cycle. This step leads to the formation of organogold(I) species, which then typically undergoes fast protodemetalation to afford hydrofunctionalized products. In order to access to higher molecular complexity, the final protodeauration step has to be circumvented and the post-functionalization of organogold intermediates via C-C bond formation appears highly desirable. The research groups of Glorius, Toste and Hashmi have shown the potential of these strategies which involve Au(I)/Au(III) catalytic redox cycles. This approach operates under mild reaction conditions and shows excellent functional group tolerance. In these systems, a photosensitizer, in addition to the gold catalyst, and an aryl radical source, which in this case functions as the oxidant as well as the reagent (aryldiazonium salts or diaryliodonium salts), are used to address the barrier of the Au(I)/Au(III) cycle. In recent years, novel visible-light-mediated gold-catalyzed reactions have been developed. Distinct from the traditional dual photoredox/gold activation mode, no exogenous photosensitizer is required to promote these photocatalytic transformations.

Photoredox catalysis has become a hot topic and emerged as an environmentally friendly and powerful tool in green chemistry, so that the reaction occurs under lower energy consumption and milder conditions. Silver catalysis under visible light has also received great attention in recent years. In order to expand the scope of conventional hydrofunctionalization, various silver catalytic reactions involving visible light have been developed.

In chapter 2, we developed a novel visible-light-mediated photosensitizer- and external oxidant-free photoredox gold-catalyzed Csp^2 - Csp cross coupling of *o*-alkynyl NTs amide and aryl iodoalkynes, which offers various 2,3-disubstituted indole derivatives in moderate to good yields. Very interestingly, iodo-ynamides that have very rarely been used in any organometallic cross coupling reaction could be used as electrophiles in this reaction. The resulting alkynylated indoles lend themselves to various post-functionalization providing valuable scaffolds (Figure GI1).

(I) Gold(I) Catalysis Under Visible Light



(II) Silver (I) Catalysis Under Visible Light

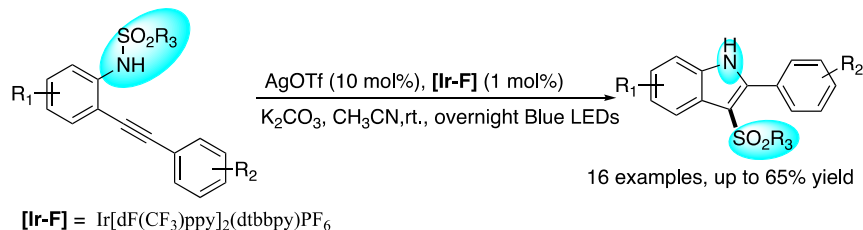


Figure GI1 Gold(I) and silver(I) catalysis under visible light

The indole scaffold is one of a prevalent organic structure, which widely exists in many bioactive natural products and pharmaceuticals. Among them, 3-sulfonylindole derivatives are found in a wide variety of biologically active compounds. Hence, there has been growing interest in developing a general and efficient route to access 3-sulfonylindoles.

In chapter 3, we reported the first facile and efficient protocol for the synthesis of bioactive 3-sulfonylindoles by the visible-light-mediated silver-catalyzed tandem 1,3-migration/cycloaddition of *ortho*-alkynyl-*N*-sulfonylanilines. This reaction occurs smoothly at room temperature in the presence of a silver (I) complex and photocatalyst $\text{Ir}[\text{dF}(\text{CF}_3)\text{ppy}]_2(\text{dtbbpy})\text{PF}_6$ ([Ir-F]) upon irradiation with a sample blue LEDs, provided 3-sulfonylindoles in moderate to good yields (Figure GI1).

Nowadays, there is a growing interest regarding the development of methods to synthesize structurally complexes and biological active products incorporating allenes. Allenes can also be used as organocatalysts or as ligands in organometallic catalysis when it substituted by coordinating groups. Based on our previous works on allenes bearing phosphine moieties. We have known that biphosphine allenes **A** could be prepared following Schmidbaur's procedure. However, it is very sensitive to air which gives a challenge for its purification and limits its application. As show in Figure GI2, we developed a novel facile method for protecting the biphosphine group by using $\text{BH}_3 \cdot \text{Me}_2\text{S}$ (2 eq.). It provided several allenyl biphosphine borane compounds **B** carry different substituents in moderate to excellent yields under the mild conditions. Compared with biphosphine allenes **A**, allenyl biphosphine diborane **B** offers the following advantages: (a) it is very stable in the air since the borane group protects both

phosphine groups on the allene; (b) it is easy to isolate with high yields by chromatography; (c) the borane group can be deprotected easily.

Protecting group BH_3 can be easily removed by using DABCO to form biphosphine allenes **A**, which then directly coordinates with metal such as Rh, Pt and Au to form corresponding metal-allenyl phosphine complexes. Furthermore, dinuclear gold alkynyl phosphine complex **F** can be synthesized start from complex **C1**, which luminescence properties would be investigated. Additionally, the two enantiomers of racemic allenyl biphosphine borane **B1** can be separated in large scale by using preparative chiral HPLC, which opens an access to chiral metal-allenyl bisphosphine complexes. Following previous procedure, we have synthesized enantio-enriched rhodium-allenyl bisphosphine complex (+)-**C1** and digold allene complex (aR)-(+)-**E1** start from chiral allenyl bisphosphine diborane **B1**, there is no oxidation and racemization occur in the process. Moreover, chiral rhodium-allenyl bisphosphine complexes would be tested in asymmetric catalysis for generating various chiral cyclic products.

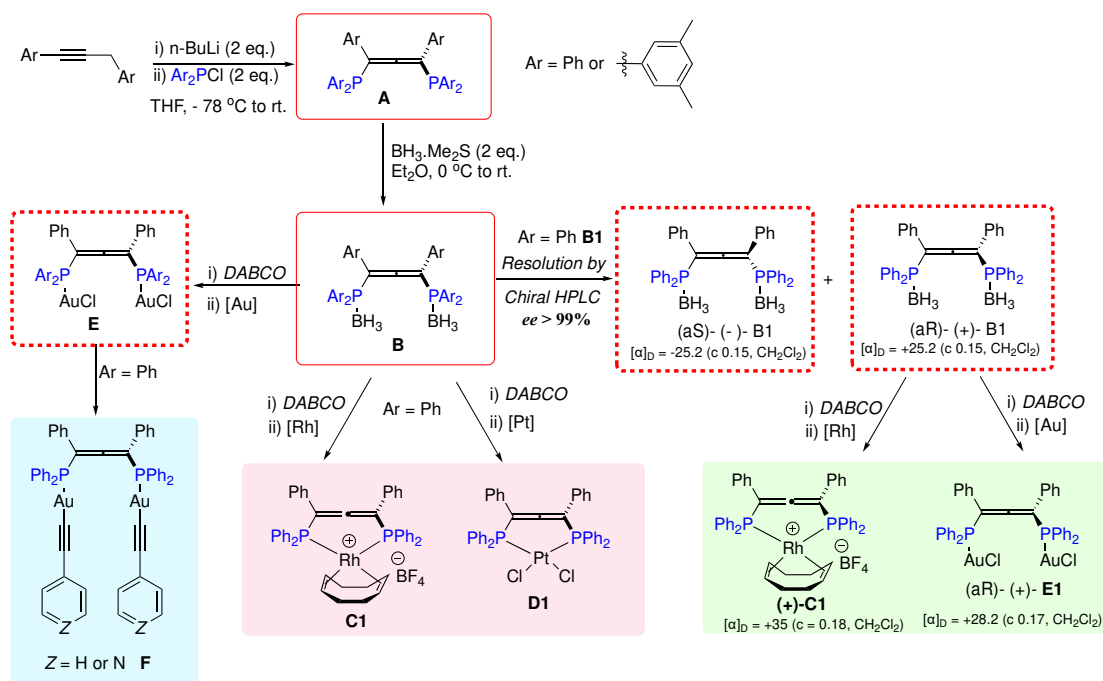


Figure G12 Allenes bisphosphine borane and their applications

Résumé

L'or a longtemps exercé une fascination sur la société en raison de son inertie qui le rend utile pour de nombreuses applications, de la bijouterie aux interconnexions en microélectronique. Le symbole de l'or est Au (du latin : aurum), et son numéro atomique est 79, ce qui en fait l'un des éléments de numéro atomique le plus élevé existant à l'état naturel. L'or est un métal de transition et un élément du groupe 11. C'est l'un des éléments chimiques les moins réactifs et il est solide dans des conditions normales. L'or est souvent présent sous forme d'élément libre (natif), de pépites ou de grains, dans des roches, des veines et des dépôts alluviaux.

La catalyse homogène à l'or a reçu une grande attention au cours de la dernière décennie. L'activation électrophile sélective des liaisons multiples carbone-carbone par un complexe d'or constitue généralement l'événement déclencheur préliminaire du cycle catalytique. Cette étape conduit à la formation d'espèces d'organogold(I), qui subissent ensuite typiquement une protodémétallation rapide pour donner des produits hydrofonctionnalisés. Afin d'accéder à une plus grande complexité moléculaire, l'étape finale de protodésaturation doit être contournée et la post-fonctionnalisation des intermédiaires organogold via la formation de liaisons C-C semble hautement souhaitable. Les groupes de recherche de Glorius, Toste et Hashmi ont montré le potentiel de ces stratégies qui impliquent des cycles redox catalytiques Au(I)/Au(III). Cette approche fonctionne dans des conditions de réaction douces et présente une excellente tolérance aux groupes fonctionnels. Dans ces systèmes, un photosensibilisateur, en plus du catalyseur d'or, et une source de radicaux aryloxy, qui dans ce cas fonctionne comme oxydant ainsi que comme réactif (sels d'aryldiazonium ou sels de diaryliodonium), sont utilisés pour adresser la barrière du cycle Au(I)/Au(III).

La plupart de ces réactions photochimiques se déroulent par un processus de transfert d'électron unique (SET) du photocatalyseur excité au substrat organique ou au réactif, il s'agit donc d'une forme de catalyse photoredox. Comme l'illustre le Schéma R1a, deux cycles de réaction différents (extinction oxydative et extinction réductrice) sont fréquemment invoqués pour expliquer le mécanisme de la catalyse photoredox. Dans ce cas, le photocatalyseur (PC) est initialement excité par irradiation avec de la lumière visible, puis il subit une oxydation ou une réduction à électron unique avec le substrat ou un réactif sacrificiel pour générer diverses espèces radicalaires ou radical-ioniques. Ces espèces hautement réactives peuvent être manipulées pour former de nombreux composés importants et utiles de manière contrôlable.

Les facteurs cruciaux contrôlant le succès de la catalyse photoredox sont les propriétés redox du photocatalyseur excité ainsi que les substrats et réactifs organiques. Cependant, il existe encore de nombreuses molécules organiques dont les potentiels d'oxydation ou de réduction sont incompatibles avec les photocatalyseurs excités, et qui ne peuvent donc pas subir directement un processus de SET dans ces conditions. Compte tenu de l'énergie relativement élevée de l'état triplet du photocatalyseur excité, celui-ci peut également servir de donneur d'énergie, activant un accepteur d'énergie (AE) avec une énergie triplet relativement faible par le biais d'une voie de transfert d'énergie (EnT) (Schéma R1a). Contrairement aux processus SET, les réactions induites par la lumière visible qui se produisent par les processus EnT ne sont pas limitées par les propriétés redox des substrats ; au contraire, elles dépendent principalement des énergies des états triples du substrat organique et du photocatalyseur excité. Le concept général de la photocatalyse EnT est décrit dans le schéma R1 : tout d'abord, le photocatalyseur absorbe la lumière visible et est excité dans l'état bas S_1 à partir de son état singulet de base (S_0). Ensuite, un événement de croisement intersystème (ISC) place le PC dans son état triplet (T_1). Une fois dans son état triplet, le transfert d'énergie intermoléculaire vers l'EA est facile. L'excitation du substrat de son état singulet de base (S_0) à l'état triplet actif (T_1) est possible et le substrat excité participera aux transformations suivantes. Pour que le processus EnT soit efficace, il doit répondre aux trois critères suivants : l'énergie triplet du donneur d'énergie (photocatalyseur) doit être supérieure à celle de l'accepteur d'énergie (substrat/réactif), ii) le donneur d'énergie doit avoir un taux de croisement intersystème élevé, car cela augmentera le rendement quantique de T_1 , et iii) le processus EnT du donneur d'énergie à l'accepteur d'énergie doit libérer de l'énergie.

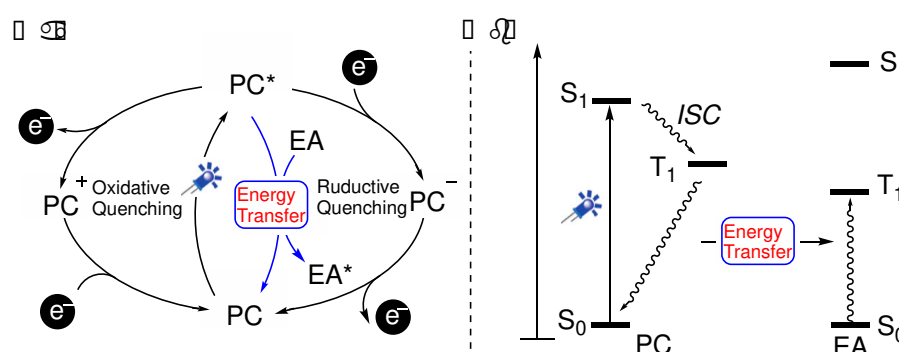


Schéma R1 Voies SET et EnT induites par la lumière visible

Récemment, le groupe de Fensterbank a mis au point une nouvelle méthode de synthèse de précieux dérivés d'alcylnylbenzofurane, qui ont été obtenus à partir des *o*-alcylnylphénols **1-47** et des iodoalcynes **1-48** en présence de complexes catalytiques d'or(I) et d'iridium(III) sous l'irradiation d'une diode électroluminescente bleue. Ils montrent que sous l'irradiation de la

lumière visible, un photocatalyseur d'iridium déclenche via la sensibilisation des triplets l'addition oxydante d'un iodure d'alcynyle sur un intermédiaire de vinylgold(I) pour délivrer des produits de couplage C(sp)²-C(sp) après élimination réductrice. Des études mécanistiques et de modélisation soutiennent qu'un événement de transfert d'énergie a lieu, plutôt qu'une voie redox, comme le montre le Schéma R2. Dans la première étape, la cyclisation des o-alkynylphénols avec le catalyseur or(I) en présence de K₂CO₃ donne le complexe vinylor(I) A. Lors de l'irradiation avec la lumière visible, [Ir-F] est excité dans l'état triplet ³[Ir-F]. Une fois dans son état triplet, le transfert d'énergie intermoléculaire vers la formation de A est facile. Cela conduit à la formation de A dans un état électronique excité B, qui peut ensuite s'additionner par oxydation avec l'alcyne 1-48 pour former les intermédiaires C. Enfin, les produits de couplage C(sp)²-C(sp) ont été obtenus par élimination réductrice. Ces résultats de recherche ouvrent de nouvelles voies dans le domaine de la catalyse à l'or à l'état excité Schéma R2.

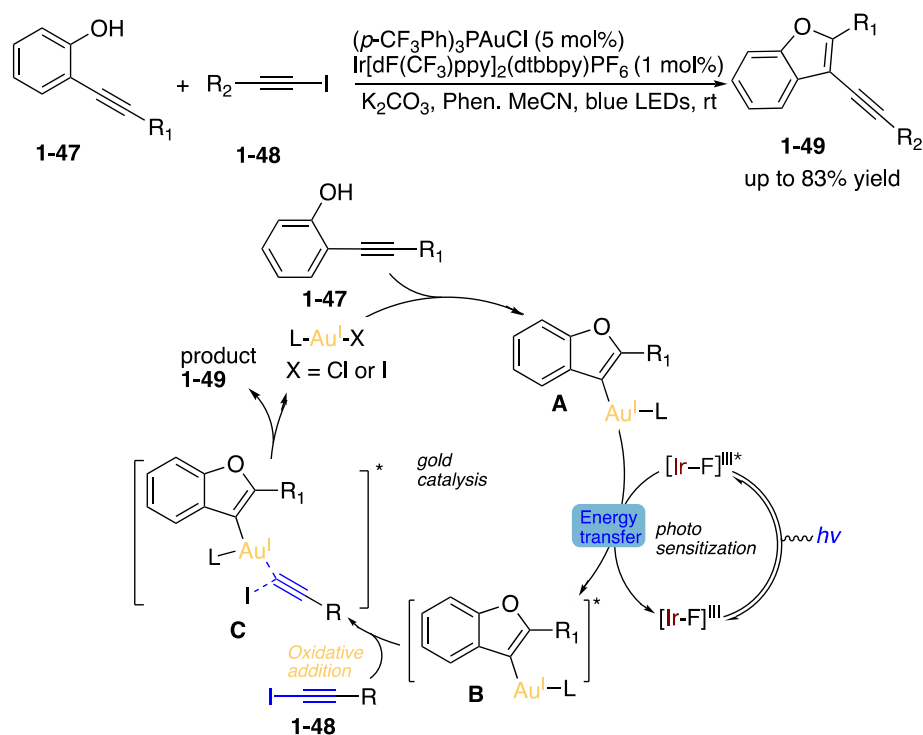


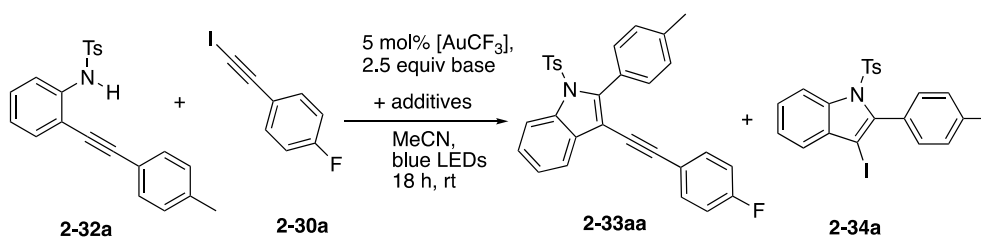
Schéma R2 O-cyclisation alcynylative doublement induite par l'or et photo-induite via l'addition oxydante photosensibilisée et mécanisme proposé

Ces dernières années, de nouvelles réactions catalysées par l'or et médiées par la lumière visible ont été développées. Contrairement au mode traditionnel de double activation photoredox/or, aucun photosensibilisateur exogène n'est nécessaire pour promouvoir ces transformations photocatalytiques. La catalyse photoredox est devenue un sujet brûlant et s'est imposée comme un outil puissant et respectueux de l'environnement dans la chimie verte, de

sorte que la réaction se produit dans des conditions plus douces et avec une consommation d'énergie moindre. La catalyse à l'argent sous lumière visible a également reçu une grande attention ces dernières années. Afin d'élargir le champ d'application de l'hydrofonctionnalisation conventionnelle, diverses réactions catalytiques à l'argent impliquant la lumière visible ont été développées.

Dans le chapitre 2, nous avons mis au point un nouveau couplage croisé Csp^2 - Csp , catalysé par l'or, photosensibilisant et sans oxydant externe, médié par la lumière visible, d'amide de NTs o-alkynyle et d'iodoalkynes aryliques, qui offre divers dérivés d'indole 2,3-disubstitués avec des rendements modérés à bons. Pour ce faire, nous avons d'abord effectué des études d'optimisation. Nous avons commencé notre travail en examinant la réaction modèle entre le 4-méthyl-N-(2-(p-tolyléthynyl)phényl)benzènesulfonamide **2-32a** et le 1-fluoro-4-(iodoéthynyl)benzène **2-30a** dans diverses conditions (tableau R1). Le produit souhaité **2-33aa** a été formé dans les conditions suivantes : un mélange de $[AuCF_3]$ (5 mol%), K_2CO_3 (2,5 éq.) dans MeCN (4,5 mL) a été agité sous irradiation pendant 18h avec des LEDs bleues dans une atmosphère de N_2 . La structure de **2-33aa** a été confirmée par analyse de diffraction des rayons X (XRD). Dans le même temps, le 3-iodo-2-(p-tolyl)-1-tosyl-1*H*-indole **2-34a** a été généré avec un rendement de 16% (Tableau R1, entrée 1). Cependant, l'utilisation de PPh_3AuCl au lieu de $[AuCF_3]$ a été préjudiciable à la réaction puisque seulement 50 % de la conversion a été observée et que seulement 8 % de **2-33aa** a été détecté sur le spectre 1H RMN brut (Tableau R1, entrée 2). Bien que le benzoindole **2-33aa** ait été formé avec un rendement de 38% en utilisant 1 mol% de $[Ir[dF(CF_3)ppy]_2(dtbbpy)PF_6]$ comme photocatalyseur, ce rendement n'est pas aussi élevé que dans des conditions sans photosensibilisateur et la sélectivité **2-33aa** vs **2-34a** était plus faible (Tableau R1, entrées 1 & 3). De plus, l'ajout de 10 % molaire de benzophénone comme photosensibilisateur s'est avéré n'avoir aucun effet en termes de rendement et de sélectivité pour **2-33aa** (Tableau R1, entrée 4). Nous avons diminué la source d'iode dans les conditions de réaction afin de réduire la quantité de **2-34a**. Heureusement, nous avons constaté qu'un rapport 1:1.1 de **2-32a** et **2-30a** (Tableau R1, entrée 5) s'est avéré être aussi productif que les conditions précédentes ((Tableau R1, entrée 1) et plus sélectif envers **2-33aa**. D'autres bases, telles que Na_2CO_3 , Cs_2CO_3 , et $CaCO_3$, sont toutes moins efficaces que K_2CO_3 (Tableau R1, entrées 6-8).

Tableau R1 Optimisation de la formation de l'indole **2-33aa**. [a]



Entrée	2-32a:2-30a (ratio)	Base	additif ^[c]	2-33aa yield (%) ^[b]	2-34a yield (%) ^[b]
1	1 : 1.5	K_2CO_3	-	64	16
2 ^[c]	1 : 1.5	K_2CO_3	-	8	10
3 ^[d]	1 : 1.5	K_2CO_3	1 mol% [Ir]	38	18
4	1 : 1.5	K_2CO_3	10 mol% Ph_2CO	61	16
5	1 : 1.1	K_2CO_3	-	62	10
6	1 : 1.1	Na_2CO_3	-	4	10
7	1 : 1.1	Cs_2CO_3	-	10	6
8	1 : 1.1	CaCO_3	-	0	0

[a] Conditions générales : **2-32a** (0.3 mmol), **2-30a** (1.1 ou 1.5 equiv), $[\text{AuCF}_3]$ (5 mol%, (*p*- CF_3Ph) $_3\text{PAuCl}$), Base (2.5 equiv), additif, et 4.5 mL de MeCN, LEDs bleues, rt pendant 18h.

[b] Rendement NMR en utilisant le 1,3,5-triméthoxybenzène comme étalon interne. [c] 5 mol% PPh_3AuCl a été utilisé au lieu de 5 mol% $[\text{AuCF}_3]$. [d] [Ir] = $[\text{Ir}(\text{dF}(\text{CF}_3)\text{ppy})_2(\text{dtbbpy})\text{PF}_6]$.

De plus, la réaction a pu être conduite en utilisant un sel potassique préformé **2-32a-K**, qui a été préparé à partir d'une déprotonation de **2-32a** avec du KH (0,99 éq.) dans de l'éther à température ambiante, ce qui a donné un rendement de 50 % de **2-33aa** et un rendement de 15 % de **2-34a**. En revanche, quelles que soient les conditions de réaction, toutes les tentatives avec un précurseur amide (acétamide, trifluoroacétamide) ou carbamate (Boc) n'ont donné aucun produit (Figure R1). Dans l'ensemble, cette série de résultats nous a confortés dans l'utilisation d'un nucléophile sulfonamide et d'une base potassique pour les développements ultérieurs.

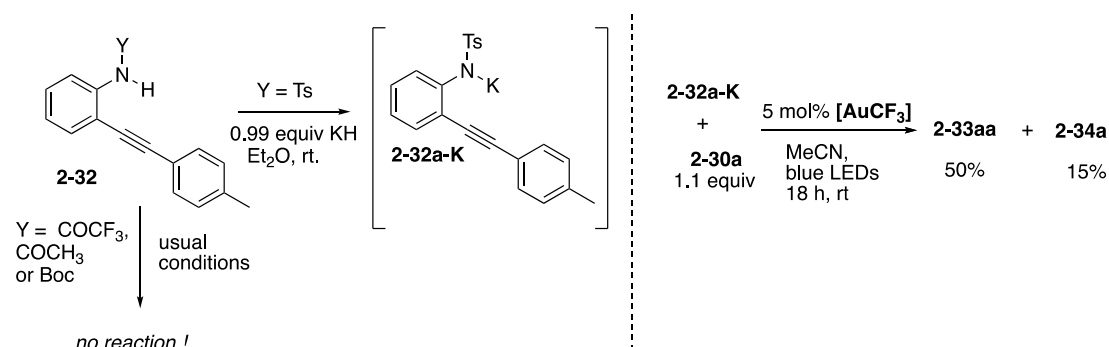
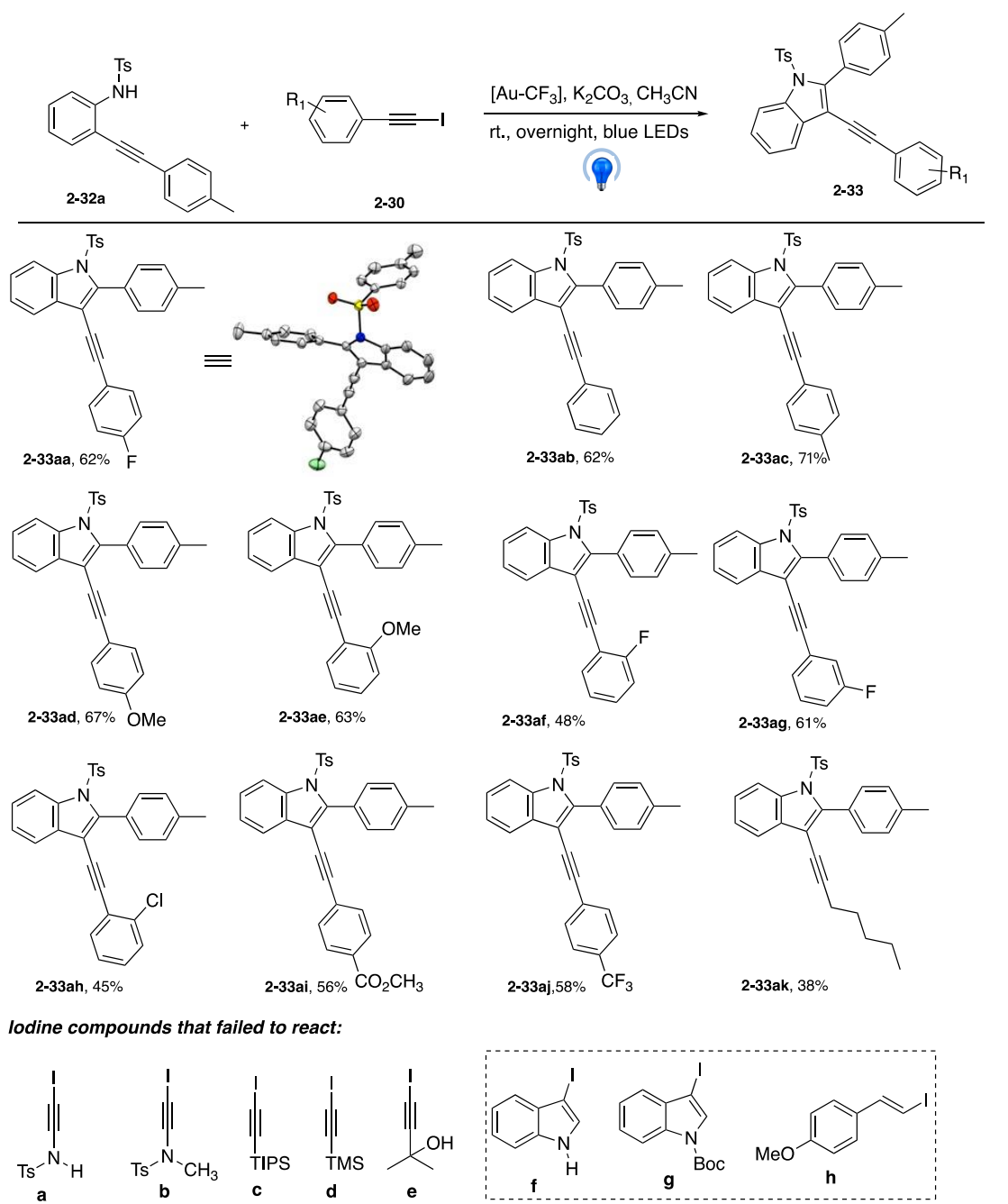


Figure R1 Éléments complémentaires de la réactivité des précurseurs de l'aniline **2-32**

Avec les conditions de réaction optimisées en main (Tableau R1 entrée 5), nous nous sommes ensuite concentrés sur l'expansion de la gamme de substrats en étudiant d'abord une gamme d'iodoalkynes **2-30** (Tableau R2). Une large gamme d'iodoalkynes **2-30** était applicable et des rendements modérés à bons des produits **2-33** ont été obtenus (**2-33aa** - **2-33ak**). Les substrats portant différents groupes électro-attracteurs ou électrodonateurs à différentes positions dans le cycle aromatique des aryl iodoalkynes étaient tous compatibles avec cette réaction.

Tableau R2 Portée des substrats iodoalkyne ^[a]



^[a] **2-32a** (0.3 mmol), **2-30** (0.33 mmol, 1.1 eq.), $[AuCF_3]$ (5 mol%), K_2CO_3 (2.5 equiv), MeCN (4.5 mL), LEDs bleues, rt., overnight.

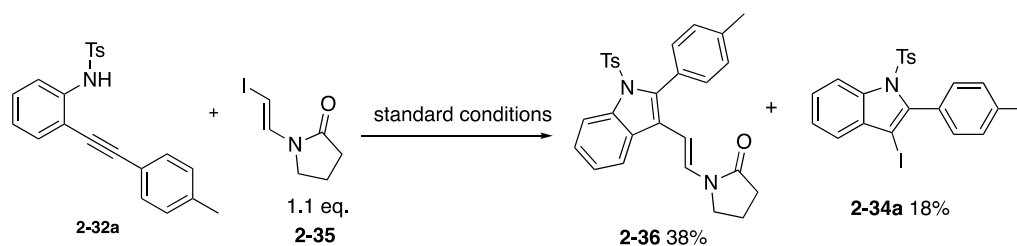
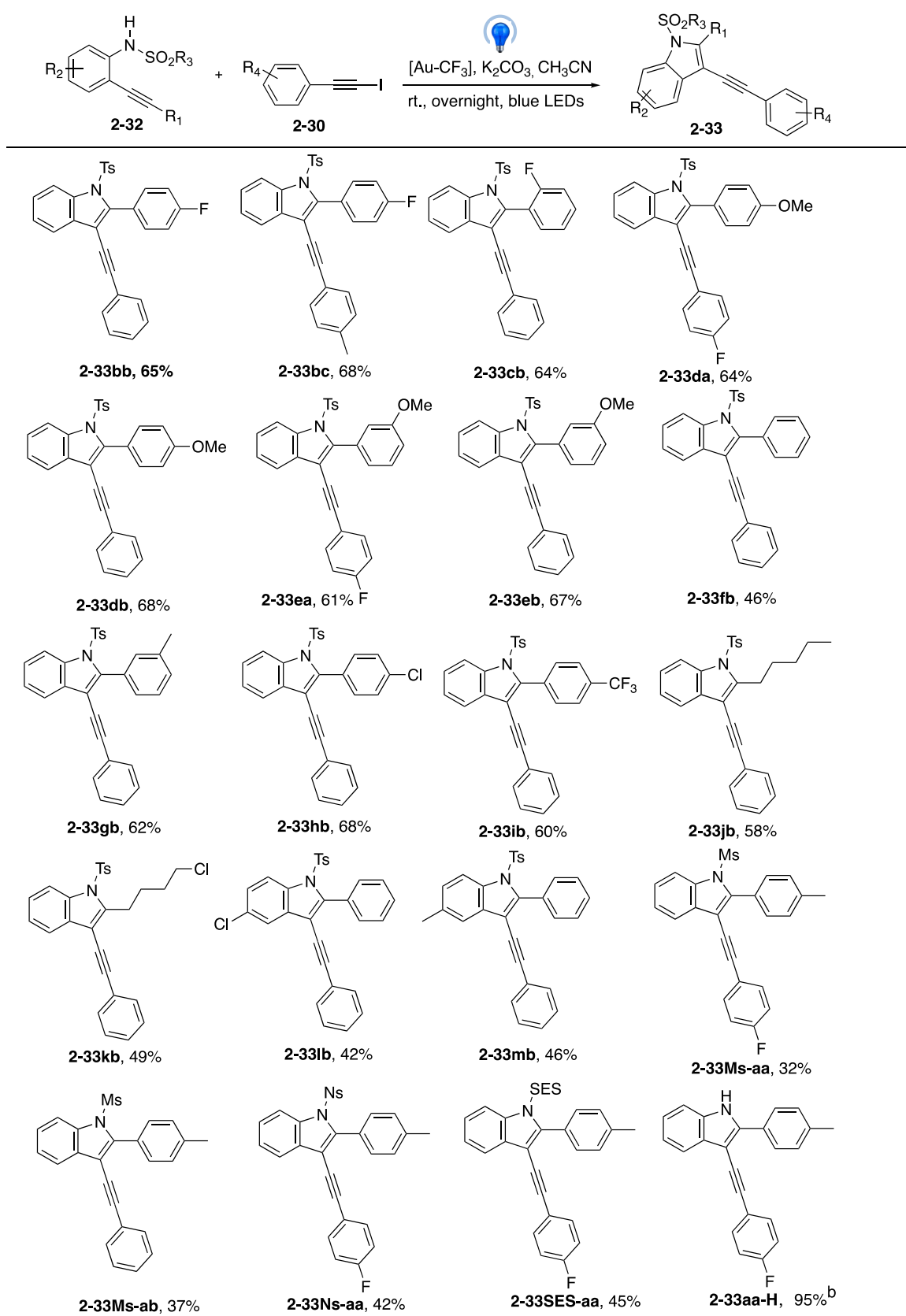


Schéma R3 La réaction de **2-32a** avec l'iodure d'alcényle **2-35**

Nous avons ensuite examiné la portée du substrat par rapport à la plate-forme d'aniline **2-32** (TableauR3). En général, des rendements plus modestes de produits indoliques ont été obtenus avec les précurseurs mésylates, qui ont formé les produits correspondants **2-33Ms-aa** en rendement de 32 % ou **2-33Ms-ab** en rendement de 37 %. Bien que la N-détosylation des indoles soit connue, des groupes sulfonamide encore plus faciles à disposer ont été testés et on a obtenu 42% de nosyl-indole **2-33Ns-aa** et 45% de 2-(triméthylsilyl)éthanesulfonyl (SES) indole **2-33SES-aa**. Ce dernier a pu être facilement converti en l'indole libre NH **2-33aa-H** par traitement avec Bu₄NF.

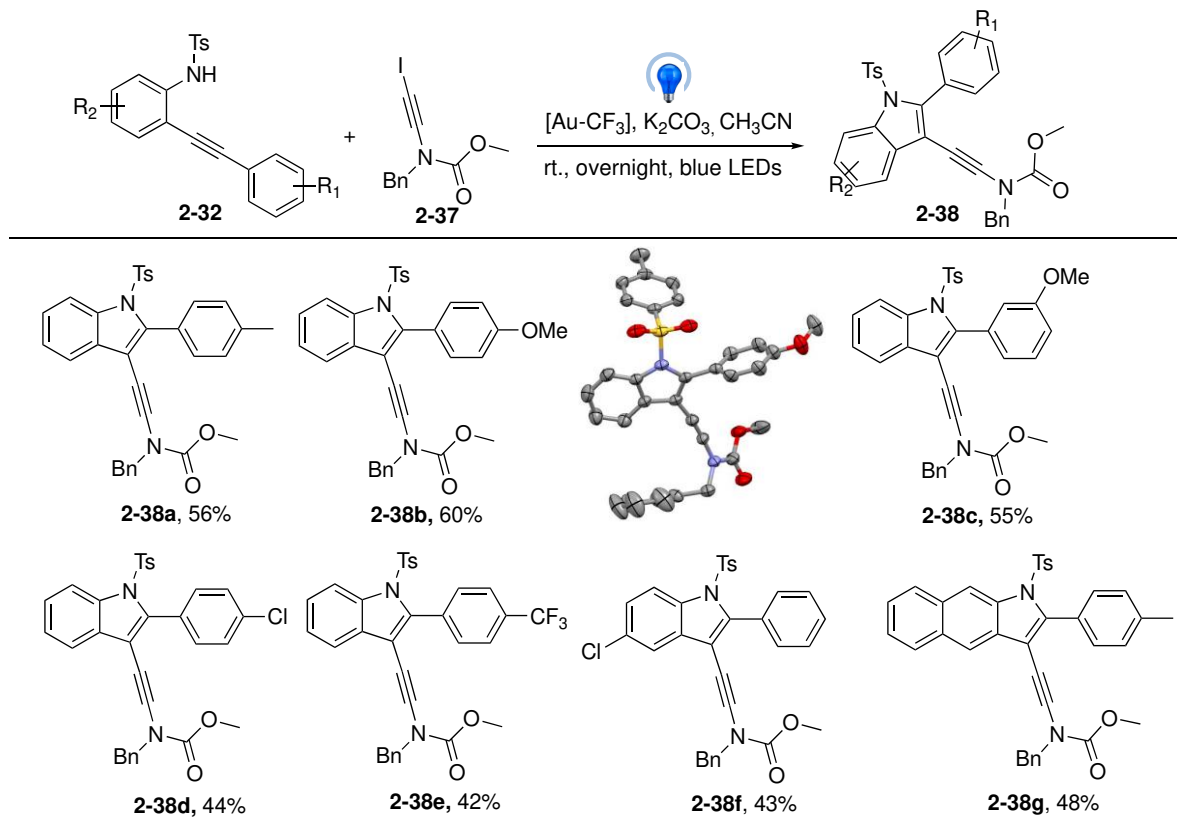
Tableau R3 Champ d'application des anilines^[a]



^[a] **2-32** (0,3 mmol), **2-30** (0,33 mmol, 1,1 éq.), [AuCF₃] (5 mol%), K₂CO₃ (2,5 éq.), MeCN (4,5 mL), blue LEDs, rt., nuit. ^[b] Après traitement avec Bu₄NF.

Afin d'étendre la portée synthétique de ce procédé et également de fournir des substrats pour des post-fonctionnalisations intéressantes, l'iodo-ynamide **2-37** a été testé dans les conditions de réaction optimisées (tableau R4).

Tableau R4 Le champ d'application des iodo-ynamides en tant qu'électrophiles^[a]

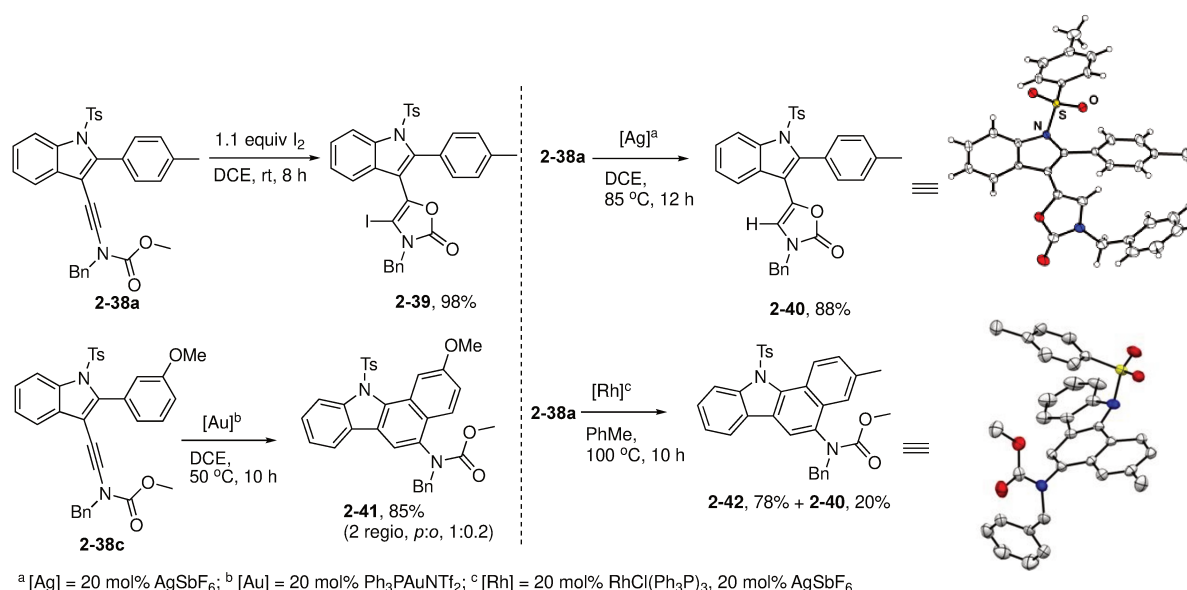


^[a] **2-32** (0.3 mmol), **2-37** (0.33 mmol, 1.1 eq.), $[AuCF_3]$ (5 mol%), K_2CO_3 (2.5 equiv), MeCN (4.5 mL), blue LEDs, rt., overnight.

En profitant de la richesse électronique de la partie ynamide, nous avons conçu plusieurs transformations sur des substrats polyfonctionnalisés **2-38** (Tableau R5). L'iodo-oxazolone **2-39** s'est formée sans problème en présence d'iode (1,1 éq.) dans du DCE frais et sec à température ambiante, ce qui constituait jusqu'à présent un type de dérivés inconnu. De manière très intéressante, la cyclisation catalysée par $Ag(I)$ de **2-38a** dans du DCE (humide) a fourni l'oxazolone **2-40** correspondante avec un rendement de 88 % par protodésilveration. De plus, l'engagement du cycle aromatique pendant dans une réaction d'hydroarylation était possible, que ce soit par catalyse à l'or(I) à partir de **2-38c** ou par catalyse au rhodium cationique à partir du substrat **2-38a** moins activé, pour fournir les carbazoles **2-41** et **2-42** correspondants. La structure de **2-40** et **2-42** a été confirmée par analyse de diffraction des rayons X. Les dérivés de benzo[a]carbazoles sont des unités structurales importantes que l'on retrouve dans de

nombreux produits naturels et molécules biologiquement actives ainsi que dans des matériaux organiques.

Tableau R5 Post-fonctionnalisation des substrats polyfonctionnalisés



Sur la base de l'étendue des substrats, nous avons souhaité avoir un aperçu du mécanisme de cette transformation. Nous avons réalisé des expériences de suivi RMN de l'or vinylique(I) avec des iodoalkynes dans différentes conditions. Tube A : sans PC. Tube B : avec 10 mol% [Ir-F]. Tube C : avec 10 % en moles. Le résultat est montré dans le tableau R6. Nous pouvons savoir que le photocatalyseur, en particulier [Ir-F], ne permet pas de générer le produit **2-33aa** désiré. Enfin, nous constatons que le 3-sulfonylindole a été obtenu en présence de [Ir-F].

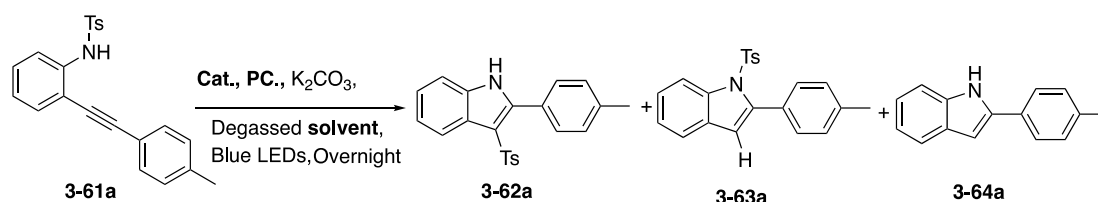
Tableau R6 Rendement de **2-33aa** dans le tube A, le tube B et le tube C sous la lumière des LEDs bleues

Time	Tube A (PC free)	Tube B (with Ir)	Tube C (with Ph ₂ CO)
10 min	50%	40%	18%
20 min	66%	30%	30%
30 min	76%	24%	34%
1h 30min	92%	0%	48%
15 h	95%	0%	60%

L'échafaudage indole est l'une des structures organiques les plus répandues, qui existe largement dans de nombreux produits naturels et pharmaceutiques bioactifs. Parmi eux, les dérivés du 3-sulfonylindole sont présents dans une grande variété de composés biologiquement actifs. Par conséquent, le développement d'une voie générale et efficace pour accéder aux 3-sulfonylindoles suscite un intérêt croissant.

Dans le chapitre 3, nous avons présenté le premier protocole facile et efficace pour la synthèse de 3-sulfonylindoles bioactifs par la 1,3-migration/cycloaddition en tandem, catalysée par la lumière visible, d'ortho-alkynyl-N-sulfonylanilines.

Pour ce faire, nous avons d'abord effectué des études d'optimisation. Nous avons choisi le 4-méthyl-N-(2-(*p*-tolyléthynyl)phényl)benzènesulfonamide **3-61a** comme substrat modèle. La réaction a été conduite dans de l'acétonitrile dégazé à température ambiante en présence de 5 mol% de [Au-CF₃] [(*p*-CF₃Ph)₃PAuCl], 1 mol% de Ir[dF(CF₃)ppy]₂(dtbbpy)PF₆ ([Ir-F]) et 2,5 equiv de K₂CO₃, et sous irradiation de LEDs bleues. La formation du produit **3-62a** a été observée avec un faible rendement (40%) (Tableau R7, entrée 1). La structure de **3-62a** a été confirmée par cristallographie aux rayons X. Les tentatives d'augmentation de la quantité de [Au-CF₃] employée (de 5 % molaire à 10 % molaire) n'ont pas donné de résultats satisfaisants (Tableau R7, entrée 3). Les tentatives d'augmentation de la quantité de [Ir-F] employée (de 1 % en moles à 5 % en moles) ont donné un rendement de 72 % de **3-62a**. Cependant, lorsque nous avons diminué la quantité de [Au-CF₃] à 5 % en moles, le rendement de **3-62a** a diminué à 47 % (Tableau R7, entrée 4). De plus, la réaction n'a pas donné le produit souhaité lorsque nous avons utilisé Ph₂CO comme photocatalyseur (Tableau R7, entrée 5). Comme le catalyseur à l'or est plus cher que celui à l'argent et qu'il nécessite une plus grande quantité de [Ir-F], d'autres catalyseurs, dont AgOTf, AgBF₄ et Ag₂CO₃, ont été examinés (Tableau R7, entrées 6-8). Heureusement, le produit désiré **3-62a** a été obtenu avec un rendement de 65% avec AgOTf comme catalyseur (Tableau R7, entrée 6). Cependant, le rendement du produit **3-62a** a diminué à 35% lorsque la quantité de catalyseur a diminué à 5mol% (Tableau R7, entrée 9). De même, le rendement du produit diminue lorsque la quantité de [Ir-F] augmente (Tableau R7, entrée 10). De plus, seulement 8% du produit souhaité **3-62a** a été généré en utilisant Ru(bpy)₃(PF₆)₂ (5 mol%) au lieu de [Ir-F] (1 mol%) (Tableau R7, entrée 11). La réaction a été examinée en changeant les solvants (Tableau R7, entrée 12-13) dans lesquels CH₃CN s'est avéré être le meilleur solvant pour obtenir le rendement le plus élevé (Tableau R7, entrée 6). On a réalisé que les catalyseurs photoredox (Tableau R7, entrée 14) AgOTf (Tableau R7, entrée 15), K₂CO₃ (Tableau R7, entrée 16), et la lumière visible (Tableau R7, entrée 17) sont nécessaires pour que la réaction se produise. Devant ces résultats, nous avons décidé de poursuivre notre étude en utilisant les conditions de l'entrée 6.

Tableau R7 Optimisation de la condition de réaction.^[a]

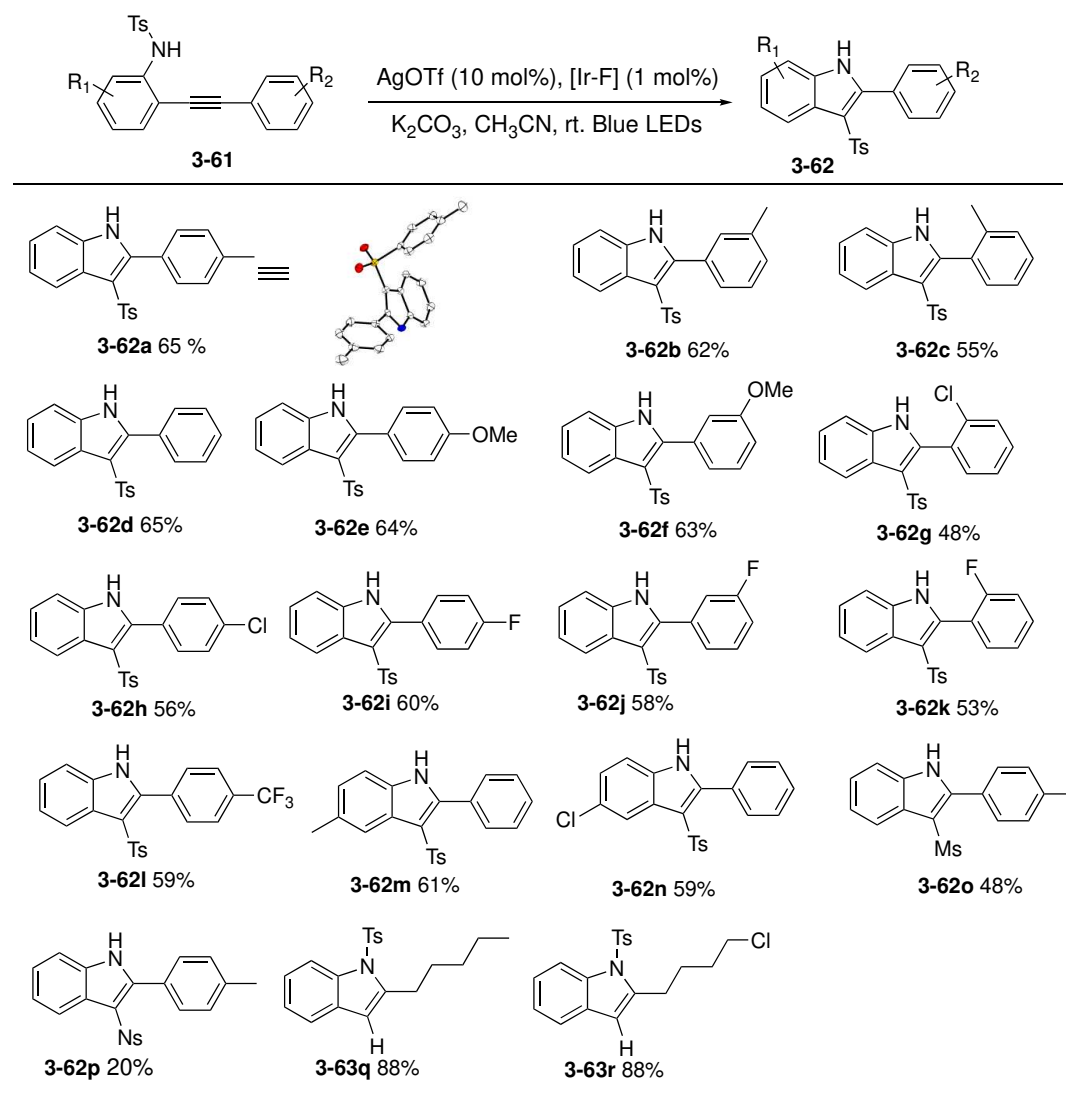
Entry	Cat. (mol%)	Photocat. (mol%)	Solvent	Yield of 3-62a (%) ^b
1	[Au-CF ₃] (5)	[Ir-F] (1)	CH ₃ CN	40
2	[Au-CF ₃] (10)	[Ir-F] (1)	CH ₃ CN	43
3	[Au-CF ₃] (10)	[Ir-F] (5)	CH ₃ CN	72
4	[Au-CF ₃] (5)	[Ir-F] (5)	CH ₃ CN	47
5	[Au-CF ₃] (5)	Ph ₂ CO (5)	CH ₃ CN	0
6	AgOTf (10)	[Ir-F] (1)	CH₃CN	65 (3-64a, 17)
7	AgBF ₄ (10)	[Ir-F] (1)	CH ₃ CN	35 (3-64a , 14)
8	Ag ₂ CO ₃ (10)	[Ir-F] (1)	CH ₃ CN	50 (3-64a , 20)
9	AgOTf (5)	[Ir-F] (1)	CH ₃ CN	35 (3-64a , 15)
10	AgOTf (10)	[Ir-F] (5)	CH ₃ CN	47 (3-64a , 17)
11	AgOTf (10)	Ru(bpy) ₃ (PF ₆) ₂ (5)	CH ₃ CN	8 (3-63a , 58)
12	AgOTf (10)	[Ir-F] (1)	MeOH	18
13	AgOTf (10)	[Ir-F] (1)	THF	15
14	AgOTf (10)	None	CH ₃ CN	0 (3-63a , 82)
15	None	[Ir-F] (1)	CH ₃ CN	NR
16 ^c	AgOTf (10)	[Ir-F] (1)	CH ₃ CN	NR
17 ^d	AgOTf (10)	[Ir-F] (1)	CH ₃ CN	0 (3-63a , 78)

^a **3-61a** (0.2 mmol), catalyst, photocatalyst, K₂CO₃ (2.5 equiv), degassed solvent (3 mL) and stirring for overnight. [Au-CF₃] = (*p*-CF₃Ph)₃PAuCl; [Ir-F] = Ir[dF(CF₃)ppy]₂(dtbbpy)PF₆; ^b Isolated yield. ^c Without K₂CO₃; ^d No light.

Avec les conditions optimisées en main (Tableau R7, entrée 6), la portée des 2-alkynylanilines **3-61** a été étudiée comme indiqué dans le Tableau R8. Tout d'abord, divers substituants (R₂) sur le cycle phényle de la fraction aryléthynyle ont été évalués, ce qui inclut une série de groupes électroniquement différents (Me, OMe, F, Cl, CF₃). La réaction s'est déroulée sans problème pour fournir les 3-sulfonylindoles **3-62a-3-62l** correspondants avec des rendements modérés à bons (de 48% à 65% de rendement). Les 2-alkynylanilines **3-1** portant le groupe Me ou Cl sur le cycle phényle des 2-alkynylanilines ont été bien tolérées et ont donné les 3-sulfonylindoles **3-62m-3-62n** correspondants en bons rendements. L'influence de l'effet stérique a également été soulignée et s'est avérée défavorable aux réactions. Ainsi, les **3-62c**, **3-62g** et **3-62k** ont été obtenus avec des rendements inférieurs à ceux du groupe en autre position.

De plus, le N-(2-(*p*-tolyléthynyl)phényl)méthanesulfonamide **3-61o** contenant des groupes méthylsulfonyle sur l'azote de l'aniline a également été employé dans cette étude. Comme prévu, le 3-(méthylsulfonyle)-2-(*p*-tolyl)-1*H*-indole **3-62o** a été produit avec un rendement de 48 %. Et lorsque le 4-nitro-N-(2-(*p*-tolyléthynyl)phényl)benzènesulfonamide **3-61p** a été utilisé comme composé de départ, **3-62p** a été isolé avec un rendement de 20%. Cependant, lorsque les 2-alkynylanilines **3-61** portant un groupe alkyle, comme **3-61q** et **3-61r**, il n'y a pas de migration tosyle. Cela a seulement généré les produits **3-63q** et **3-63r** avec un rendement de 88%, exactement. (Notes : Les matériaux de départ de **3-61a** à **3-61p**, une petite quantité de produits

Tableau R8 Synthèse des 3-sulfonylindoles **3-62** : portée des 2-alkynylanilines **3-61**^{a,b}



^a Toutes les réactions sont effectuées dans du CH_3CN dégazé (3 mL), en utilisant **3-1** (0,2 mmol), AgOTf (10 % en moles), $[\text{Ir-F}] = \text{Ir}[\text{dF}(\text{CF}_3)\text{ppy}]_2(\text{dtbbpy})\text{PF}_6$ (1 % en moles), et K_2CO_3 (0,5 mmol, 2,5 équiv.) à température ambiante sous des diodes bleues pendant une nuit. ^b Les rendements isolés sont indiqués.

3-63 et **3-64** ont également été générés dans des conditions optimisées. Nous n'avons pas réussi à les séparer car ils ont une polarité similaire ou ne sont présents qu'en petite quantité).

Afin de mieux comprendre le mécanisme de réaction, nous avons réalisé quelques expériences de contrôle (Schéma R4). Lorsque 2 équivalents de TEMPO ont été ajoutés au système réactionnel de **3-61i**, aucun produit souhaité n'a été généré. Le sous-produit **3-63i** a été formé à 89 %. Lorsque 2 équivalents d'un autre piègeur de radicaux (1,1-diphényléthylène) ont été ajoutés au système réactionnel de **3-61i**, il a été constaté que le produit désiré **3-62i** a été obtenu dans un rendement de 20% avec la détection du produit piégé radicalaire **3-62i'** dans 25%. Dans le même temps, les produits secondaires **4-64i** ont été isolés avec un rendement de 35%. Ces résultats ont indiqué que la réaction implique un processus de radical tosyloxy.

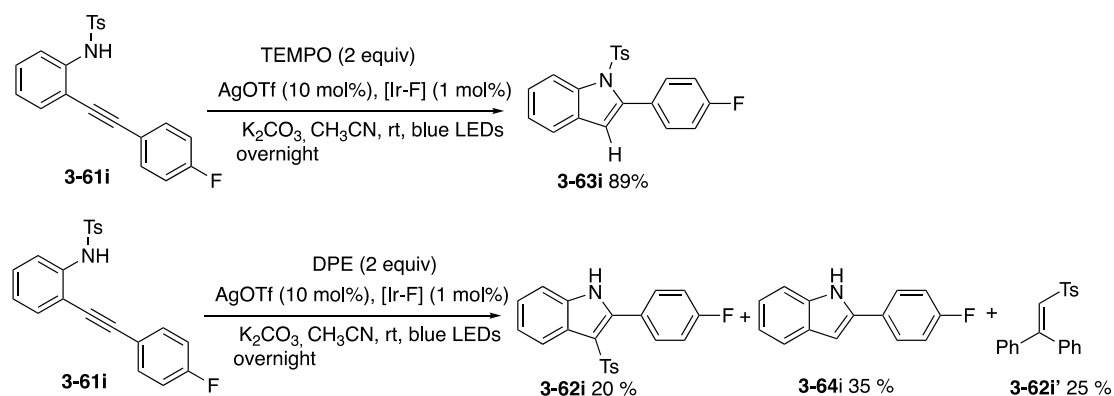


Schéma R4 Expériences de contrôle

Pour savoir si la migration du groupe sulfonyle s'est produite en mode intramoléculaire ou intermoléculaire, une expérience de croisement a été réalisée (Schéma R5). La réaction d'un mélange 1:1 de **3-61i** et **3-61o** dans les conditions optimisées pour former quatre produits 3-sulfonylindoles dans un rapport proche de 0.62 : 1 : 1 : 0.62, ce qui a été confirmé par spectroscopie RMN (Schéma R5, a). De manière intéressante, lorsque nous avons utilisé [Au-CF₃] au lieu de AgOTf, la réaction d'un mélange 1:1 de **3-61i** et **3-61o** a également formé quatre produits 3-sulfonylindoles dans un rapport de près de 0.34 : 1 : 1 : 0.34, ce qui a été confirmé par spectroscopie RMN (Schéma R5, b). Ces résultats indiquent que la migration du groupe sulfonyle peut se faire de manière intra- et intermoléculaire.

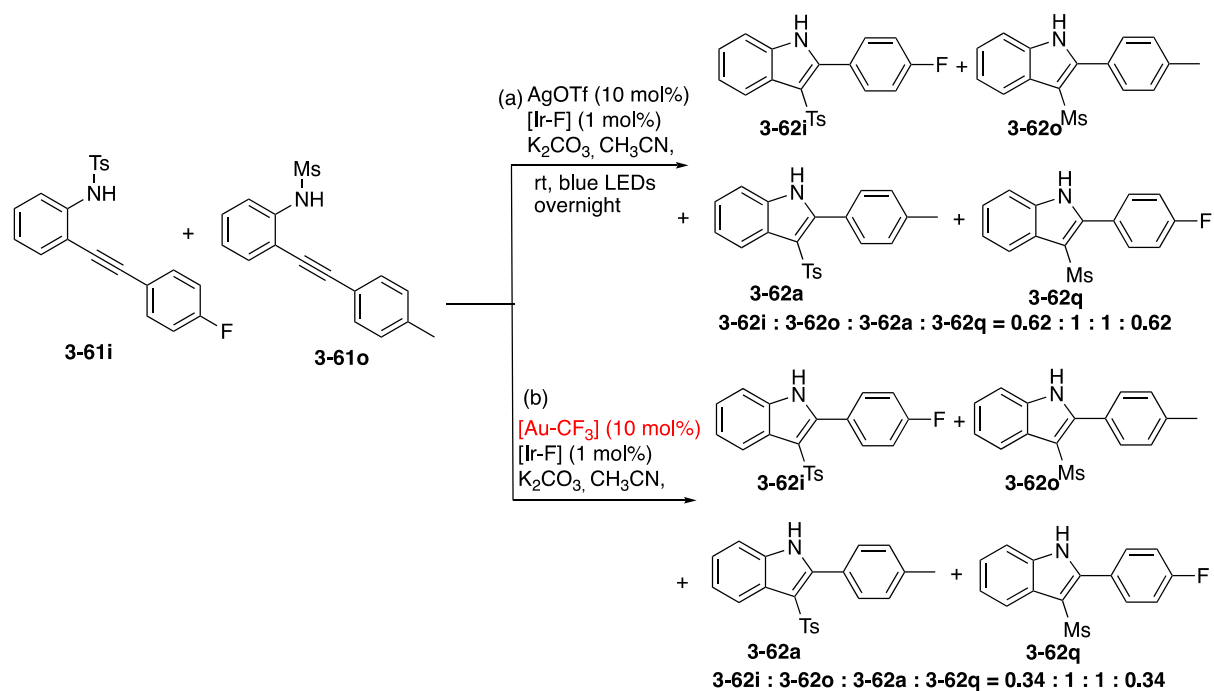


Schéma R5 Expérience de croisement pour sonder la voie possible

Aujourd'hui, il existe un intérêt croissant pour le développement de méthodes de synthèse de complexes structuraux et de produits biologiques actifs incorporant des allènes. Les allènes peuvent également être utilisés comme organocatalyseurs ou comme ligands dans la catalyse organométallique lorsqu'ils sont substitués par des groupes de coordination. Sur la base de nos travaux précédents sur les allènes portant des fragments de phosphine. Nous avons su que les allènes biphosphinés pouvaient être préparés selon la procédure de Schmidbaur. Cependant, il est très sensible à l'air ce qui donne un défi pour sa purification et limite son application.

Dans le chapitre 4, nous avons rapporté la synthèse d'allényl bisphosphine boranes. D'après les travaux précédents, l'allényl bisphosphine **4-90** peut être formée en suivant la procédure de Schmidbaur. Elle est très sensible à l'air ce qui donne un défi pour sa purification et limite son application. La protection du groupe bisphosphine par l'utilisation de BH₃.Me₂S a permis d'obtenir le produit d'addition allényl bisphosphine-borane **4-107** avec un rendement de 85%. L'analyse ³¹P RMNa montrée un pic singulet à 22.1 ppm. L'allényl bisphosphine-borane **4-107** a été caractérisé par cristallographie aux rayons X. À notre grande satisfaction, nous pouvons synthétiser le produit souhaité **4-107** à l'échelle du gramme avec un bon rendement en suivant cette procédure.

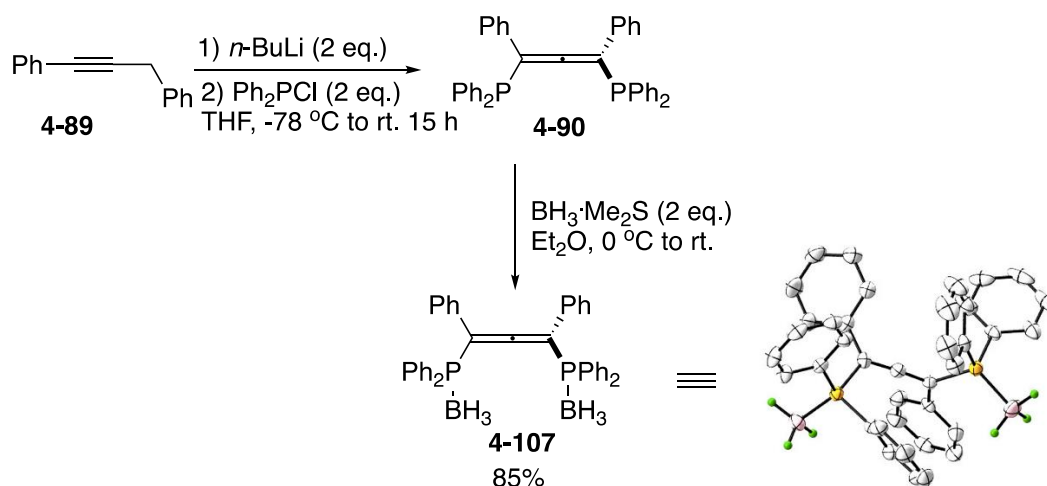


Schéma R6 Synthèse du ligand borane de l'allényl bisphosphine **4-107** par un seul pot.

Par rapport à l'allène bisphosphine **4-90**, l'allényl bisphosphine diborane présente les avantages suivants : (a) il est très stable à l'air car le groupe borane protège les deux groupes phosphine sur l'allène ; (b) il est facile à isoler avec des rendements élevés par chromatographie ; (c) le groupe borane peut être déprotégé facilement ;

Plus tard, nous suivons la même procédure pour synthétiser d'autres boranes allényl bisphosphine **4-109** et **4-121** avec de bons rendements (Schéma R7).

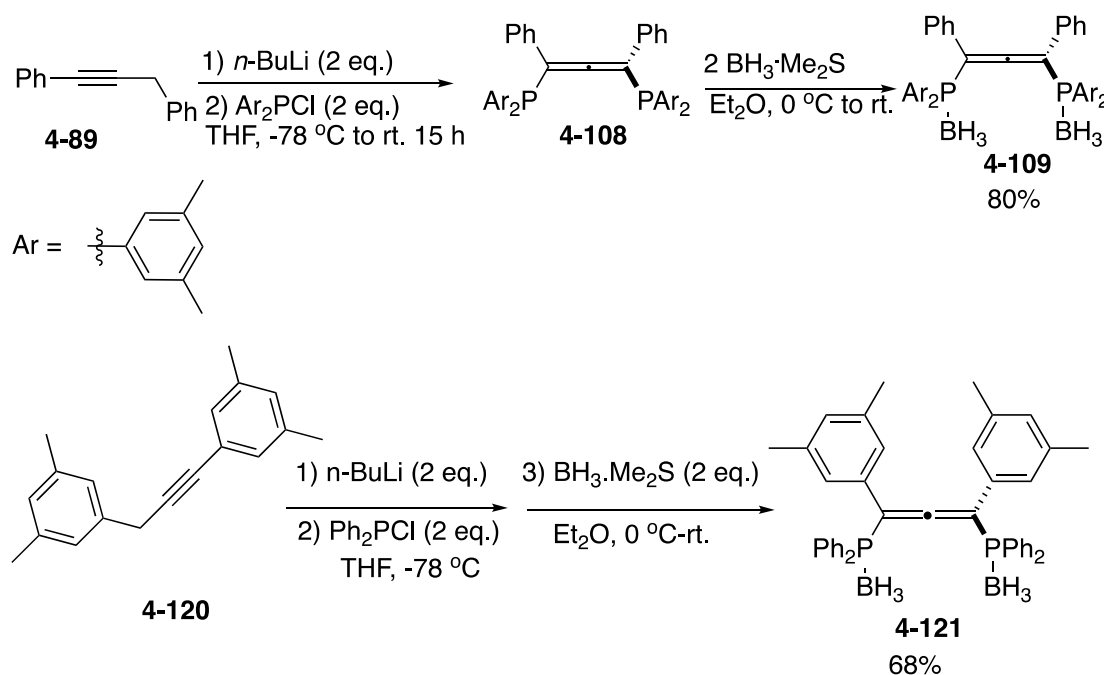


Schéma R7 La synthèse d'autres boranes bisphosphine allényl **4-109** et **4-121**

D'après les travaux antérieurs de notre groupe, nous savons qu'il est impossible de séparer l'allène **4-90** en utilisant la HPLC chirale préparative car une oxydation pour donner un allène contenant de l'oxyde de mono- et bisphosphine s'est produite. Heureusement, le borane allényl bisphosphine racémique **4-107** a été séparé avec succès à grande échelle. La séparation a été

réalisée par la colonne Chiralpak IG et la détection par UV à 254 nm (Figure R2, a) et par dichroïsme circulaire (Figure R2, b). Deux énantiomères de (aR)-(+)-4-107 avec $[\alpha]_D = +25,2$ (c 0,15, CH₂Cl₂) et (aS)-(-)-4-107 avec $[\alpha]_D = -25,2$ (c 0,15, CH₂Cl₂) ont été obtenus en excellent excès énantiomérique (ee > 99 %) (Schéma R8).

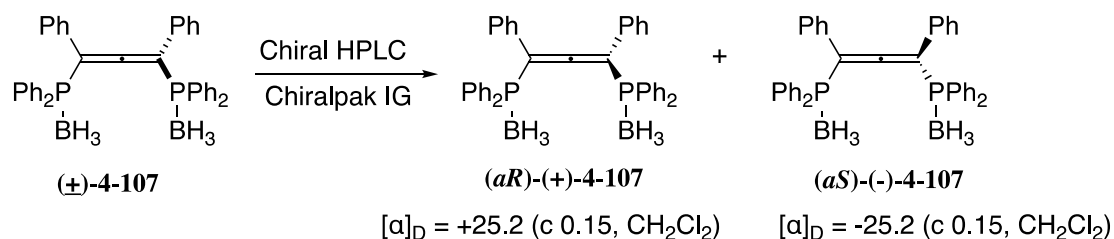


Schéma R8 Résolution de ligands allène bisphosphine borane racémiques par HPLC chirale

Afin d'étendre son application, nous avons synthétisé un complexe d'allène digold (aR)-(+)-4-124 à partir de l'allène chiral (aR)-(+)-4-107, qui a été déprotégé en utilisant le DABCO pour fournir l'allène (aR)-(+)-4-90. Sur la base des travaux précédents, l'or (I) s'est coordonné aux atomes de phosphore de 4-90 de manière sélective pour donner le complexe bisphosphine d'or dinucléaire (aR)-(+)-4-124 avec un rendement de 96 % avec $[\alpha]_D = +28,2$ (c 0,17, CH₂Cl₂) (les mêmes valeurs de rotation spécifiques que précédemment), ce qui signifie qu'il n'y a pas d'oxydation ni de racémisation suivant cette procédure. Et les données spectroscopiques correspondent à celles précédemment rapportées par notre groupe (Schéma R9).

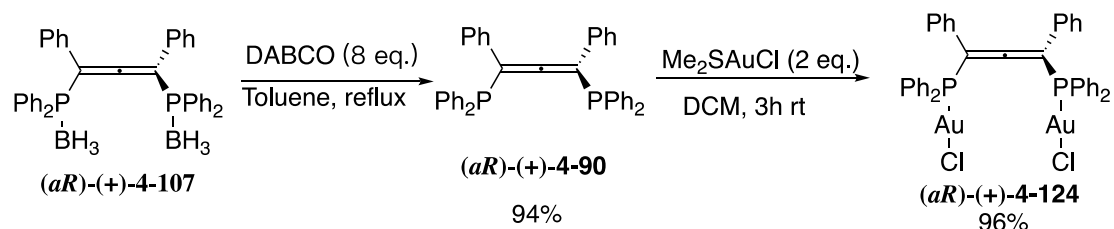


Schéma R9 La synthèse de (aR)-(+)-4-124 à partir de l'allène chiral (aR)-(+)-4-107

Sur la base de ces résultats, nous sommes en mesure de synthétiser le complexe mononucléaire platine-allène bisphosphine 4-125, le complexe or-allène bisphosphine 4-126, le complexe rhodium-allène bisphosphine 4-127, et le complexe rhodium-allène bisphosphine optiquement pur en partant des complexes allène bisphosphine borane correspondants en suivant la même procédure que précédemment (Schéma R10).

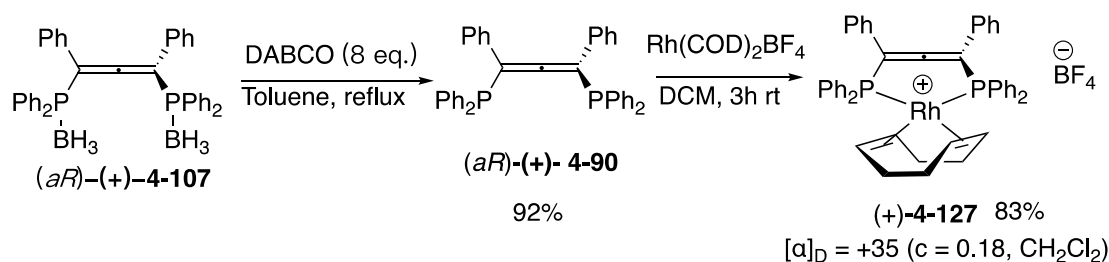


Schéma R10 La synthèse des énantiomères de (+)-4-127

D'autres essais catalytiques pour la cycloisomérisation des 1,6-énynes en utilisant le complexe de rhodium racémique (+)-**4-127** donnent de bons résultats (Schéma R11).

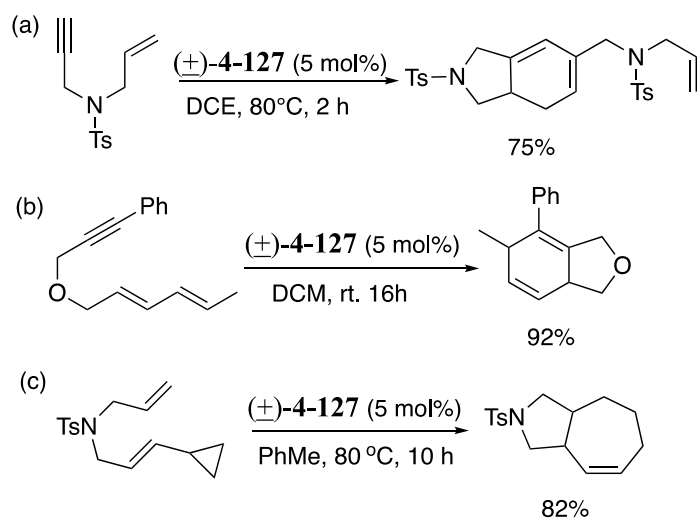


Schéma R11 essais catalytiques avec le complexe de rhodium (\pm)-**4-127**

D'après le succès de la cycloisomérisation des 1,6-énynes en utilisant le complexe de rhodium racémique (\pm)-**4-127**, nous avons ensuite évalué l'activité catalytique de (+)-**4-127** pour la cycloisomérisation asymétrique des 1,6-énynes, ce qui a donné de bons résultats. Nous avons essayé d'obtenir la valeur *ee* par HPLC. Aucun *ee* n'a pu être déterminé précisément mais les produits finaux présentaient une rotation optique (valeur $[\alpha]_D$). Les produits **4-141** et **4-148** ont présenté une valeur de rotation optique, qui était $[\alpha]_D = +32$ ($c = 0,005$, CH_2Cl_2) et $[\alpha]_D = +25$ ($c = 0,005$, CH_2Cl_2), respectivement (Schéma R12, a et b). Nous avons déduit que les valeurs d'*ee* de la **4-148** était de 26% d'après la rotation optique de la littérature ($[\alpha]_D = +85.3$, $c = 2.71$ dans CHCl_3 , 88% *ee*). La réaction de **4-153** a également été examinée avec 5 % molaire de (+)-**4-127** dans le toluène à 80 °C pendant 10 h. Le produit cyclique **4-154** a été obtenu avec un rendement de 81 % avec $[\alpha]_D = +28$ ($c = 0.01$, CH_2Cl_2) (Schéma R12, c). Nous avons également déduit les valeurs d'*ee* du **4-154** était de 89% sur la base de la rotation optique de la littérature ($[\alpha]_D = +30.1$, $c = 0.47\%$, CDCl_3 , 96% *ee*).

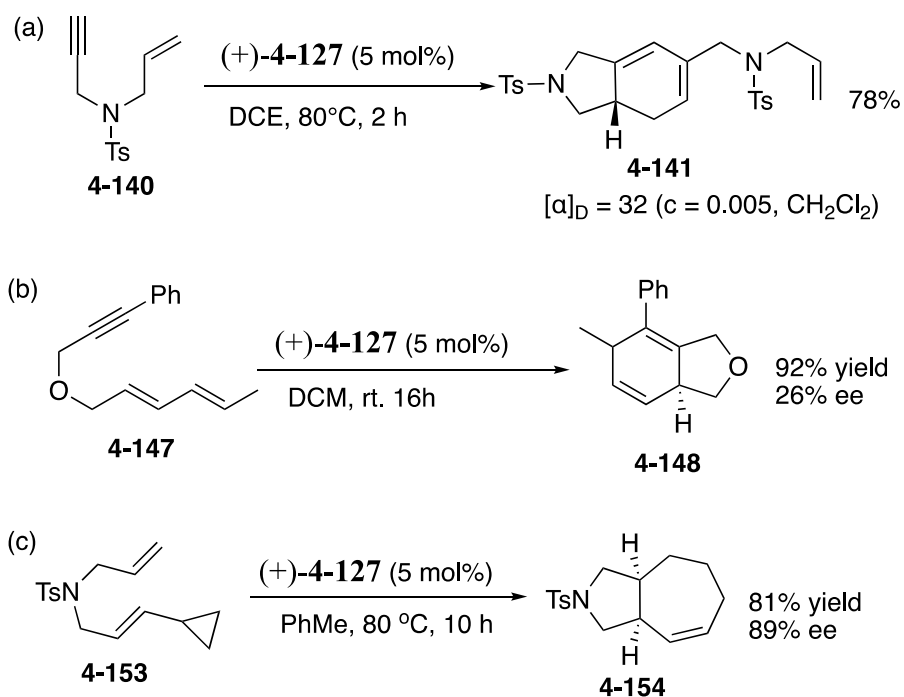


Schéma R12 Catalyse asymétrique des complexes de rhodium optiquement purs (+)-**4-127**

Ces essais préliminaires des complexes de rhodium optiquement purs (+)-**4-127** ont donc donné des résultats prometteurs pour la catalyse asymétrique.

De plus, nous sommes en mesure de synthétiser le complexe dinucléaire d'or alkynyl phosphine **4-155** avec un rendement élevé par la réaction du complexe d'or allényle **4-124** avec le phénylacétylène en présence de *t*-BuLi. Le complexe d'or alkynyl phosphine dinucléaire **4-156** a également pu être formé en suivant la même procédure (Schéma R13).

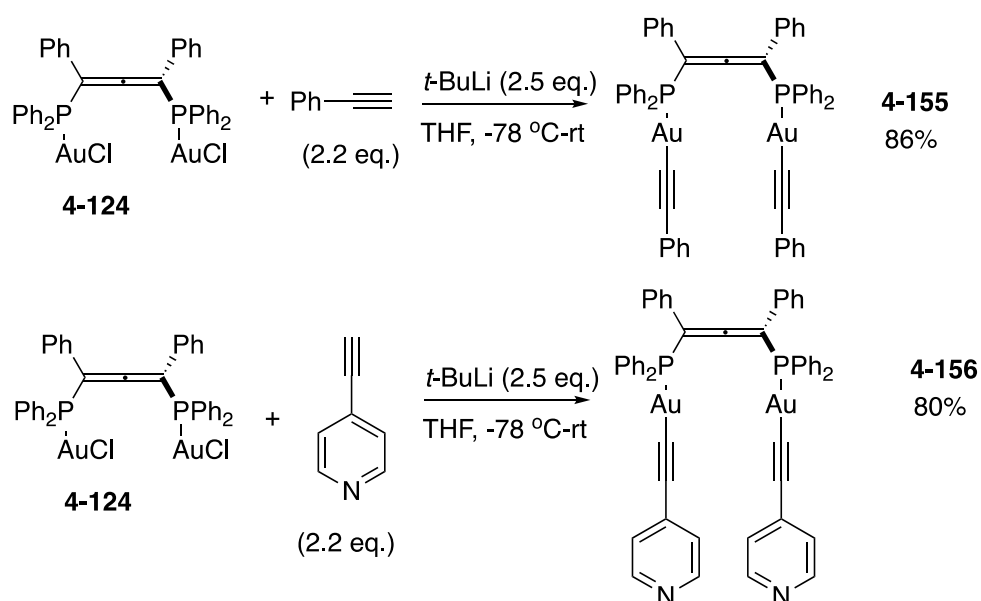


Schéma R13 Synthèse d'un complexe dinucléaire d'or et d'alcynylphosphine

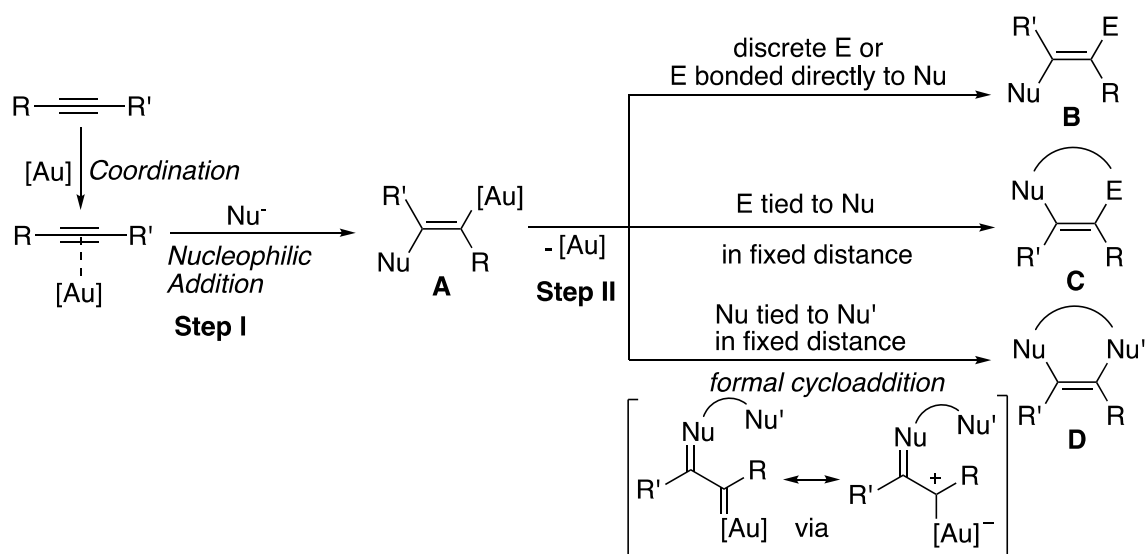
Chapter 1 Background

1. Gold Catalysis

Gold has long held the fascination of society because of its inertness making it useful for many applications from jewellery to interconnects in microelectronics. The symbol of gold is Au (from Latin: *aurum*), and atomic number 79, making it one of the highest atomic number elements that occurs naturally. Gold is a transition metal and a group 11 element. It is one of the least reactive chemical elements and is solid under standard conditions. Gold often occurs in free elemental (native) form, as nuggets or grains, in rocks, in veins, and in alluvial deposits. While the stoichiometric chemistry of gold has intensively and continuously been investigated, this close relationship between gold and chemical applications got lost during the development of catalysis reactions. Probably a low catalytic activity was mistakenly deduced from the inertness of elemental gold that only dissolves in aqua regia or oxidants such as air, the latter only in the presence of strong ligands such as cyanide. For a long time, gold has been considered as a catalytic inert metal element. Until 1973, Bond¹ reported the hydrogenation of olefins over supported gold catalysts, he coined the following statement in one of the milestone publications of gold catalysis, which probably applies to many of the discoveries in this field: “We are at a loss to understand why these catalytic properties of gold have not been reported before, especially since the preparative methods we have used are in no way remarkable.” It completely changed the way people would think about gold. After this, gold-catalysed oxidative hydrochlorination of ethene to vinyl chloride was studied by Hutchings² in 1985. And Haruta et al.³ investigated the low-temperature oxidation of CO, both heterogeneous reactions. For the first time these studies showed gold to be the best catalyst for these reactions, in stark contrast to the previous reports on the poor activity of gold. Up to now, gold catalysis has become a hot spot of research in the field of catalysis. At about the same time a unique milestone in homogeneous asymmetric catalysis was established, as discussed below.

1.1 Homogeneous Gold Catalysis

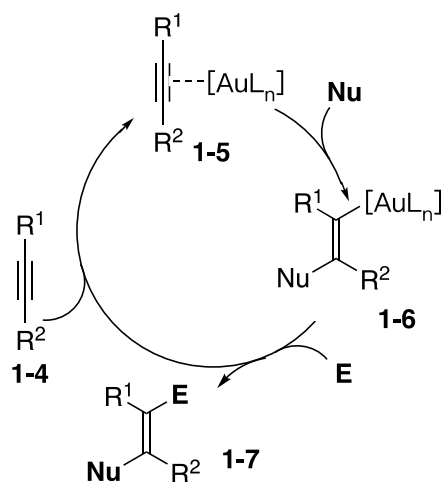
Homogeneous catalysis includes all reactions in which the substrate(s) and the catalyst are in the same state. Homogeneous catalysis by gold is not new: the roots reach back at least 80 years.⁴ In 1986, Ito and Hayashi⁵ reported asymmetric aldol reaction of aldehydes **1-1** with isocyanoacetates **1-2** by using gold(I) complex as a homogeneous catalyst to form enantiomerically pure oxazolines **1-3** (Scheme 1-1). After a few years, Teles and co-workers reported the exceptionally high activity of cationic Au(I)-phosphine complexes for alkyne hydroalkoxylation.⁶ The cationic Au(I) complexes were generated by protonolysis of the



Scheme 1-2 Profile of gold-catalyzed intermolecular transformations with alkynes

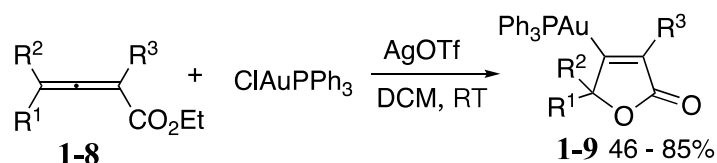
1.2 Vinylgold Intermediates

In homogeneous gold catalysis, which uses well-defined soluble complexes of both gold(I) and gold(III), still the most frequently addressed functional group is the C-C triple bond in alkynes **1-4**.⁸ The alkyne is activated by the interaction with gold (complex **1-5**),⁹ backside-attack of a nucleophile (Nu), either intramolecular or intermolecular, then delivers a vinylgold species **1-6**. From this vinylgold intermediate **1-6** the gold catalyst is liberated by an electrophile (E), typically a proton,⁸ seldom an halogen¹⁰ and palladium.¹¹ During the same step the product **1-7** is also set free (Scheme 1-3). So, the formation of vinylgold compounds as important elementary steps takes place in most gold-catalyzed reactions. For a clear understanding of the mechanism involved in these cationic gold (I) complexes, capture of vinylgold intermediates has become very important.



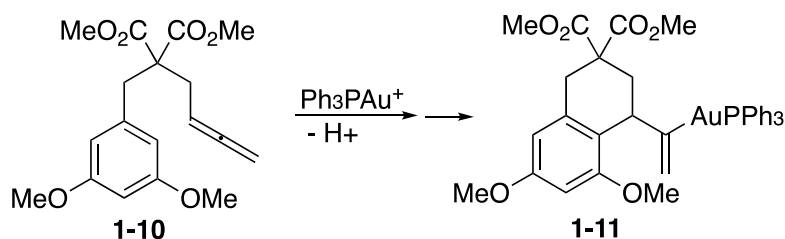
Scheme 1-3 Not detected: Vinylgold intermediates as key intermediates in reactions of alkynes

For a long time, the vinylgold intermediates eluded detection and isolation. In most cases, the gold-catalyzed reactions were interpreted with “suggested” mechanisms of involving vinylgold intermediates.¹² Fortunately, some groups managed to isolate such species and unambiguously characterised them by X-ray crystal structure analyses. The first examples were provided by Hammond et al. in 2008, who observed an only slow cyclisation of allenic esters **1-8** with gold(I) catalysts and finally could show that in stoichiometric rather than catalytic reactions they can conveniently isolate stable vinylgold(I) phosphine complexes **1-9** in good yield (Scheme 1-4).¹³



Scheme 1-4 Vinyl gold complexes obtained from reactions of cationic gold(I) with allenates

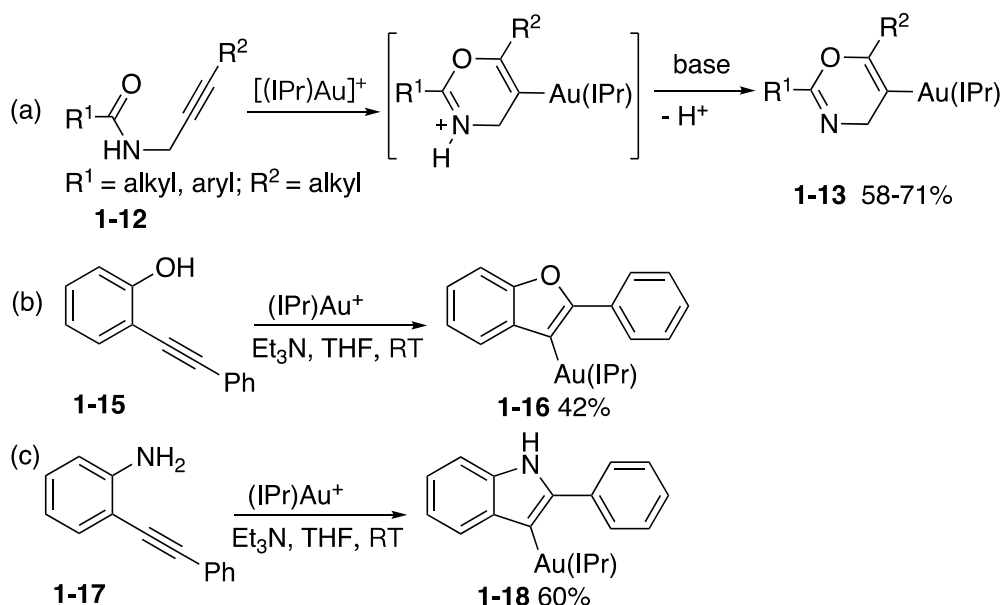
Soon after Hammond’s results had been published, the group of Gagné was able to isolate a related vinylgold(I) species **1-11** with phosphine ligand from intramolecular hydroarylation reactions of allenes **1-10** (Scheme 1-5).¹⁴ Again, a crystal structure analysis unambiguously confirmed the structure of **1-11**.



Scheme 1-5 Gagné’s vinylgold complexes without acceptor substituent

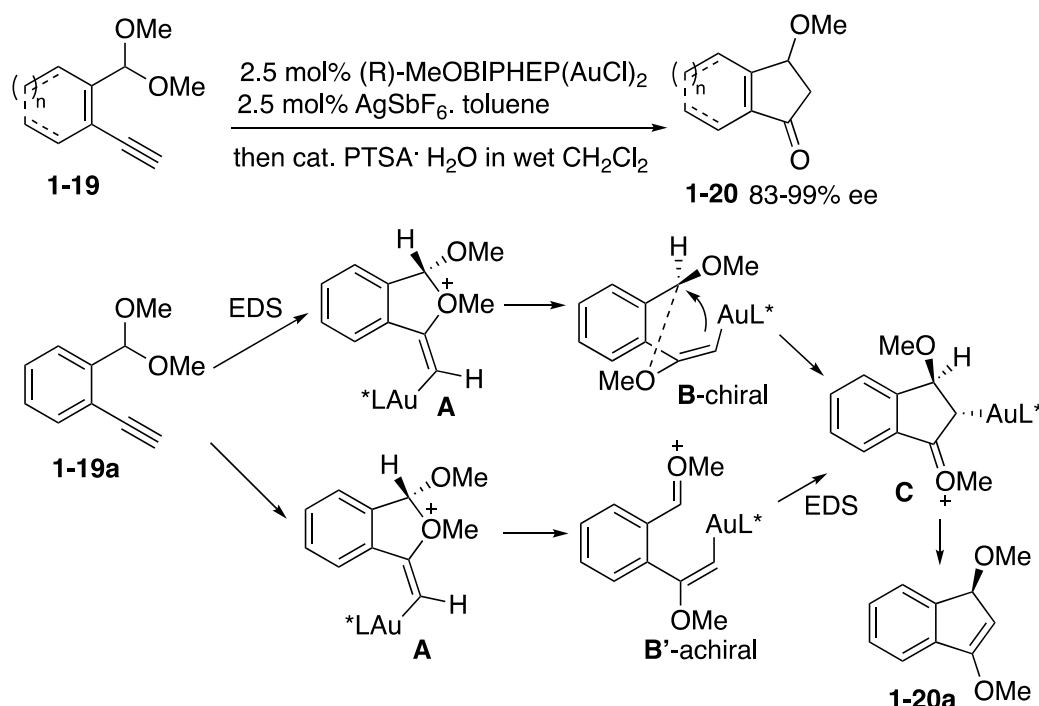
Hashmi et al. reported that vinylgold(I) intermediates can be obtained with alkynes as substrates, a much more frequently used class of substrates than the allenes. Furthermore, it has to be taken into account that allenes (which are thermodynamically less stable than alkynes) are more reactive than alkynes. They isolated stable vinylgold intermediates derived from internal propargylamides in the presence of cationic gold complexes and triethylamine (Scheme 1-6, a).¹⁵ The efficient isolation of the vinylgold complexes **1-13** might originate from the low acidity of the corresponding iminium salt, which allowed a trapping of the proton by the base before this proton could proto-deaurate the vinylgold species and thus close a complete turnover of the catalytic cycle. The results could be transferable to many other reactions proceeding through vinylgold intermediates and allowed an exploration of additional functionalization of

these intermediates in extended catalytic cycles. The simple trick of capturing the proton, which would decompose vinylgold species by protodeauration, by a simple base such as triethylamine, worked beautifully. Based on this result, Hashmi et al. extended the principle to other reaction types as hydroalkoxylation and hydroaminations. In the presence of cationic gold complexes and triethylamine, the vinyl gold complexes could be formed from 2-alkynylphenol **1-15** and 2-alkylaniline **1-17**, respectively (Scheme 1-6, b, c).¹⁶ The synthesis conditions of these two hetaryl gold(I) compounds can broad scope for the isolation of the organometallic intermediates in gold-catalyzed nucleophilic additions to alkynes.



Scheme 1-6 NHC complexes of vinylgold(I) compound

In 2013, Toste reported highly enantioselective carboalkoxylation of alkynes catalyzed by cationic (DTBM-MeO-Biphep)-gold(I) complexes. Various optically active β -alkoxyindanone derivatives were obtained in good yields with high enantioselectivities. Two plausible pathways involving vinylgold(I) intermediates were proposed. In the first possibility, coordination of the chiral cationic gold(I) complex to the alkyne moiety would result in desymmetrizing alkoxylation of the triple bond. The resulting intermediate **A** bearing a chiral acetal-derived cation would undergo rearrangement through chirality-preserving intermediate **B**-chiral to provide **C** and subsequently **1-20a**. In this case, the first step would be the enantiodetermining step (EDS). On the other hand, it is possible that oxocarbenium intermediate **B** is sufficiently long lived to relax to an achiral conformation, **B'**-achiral, that would undergo enantioselective cyclization to afford **C**. In this second possibility, the nucleophilic addition of a vinylgold species to the oxocarbenium intermediate would be the EDS (Scheme 1-7).¹⁷

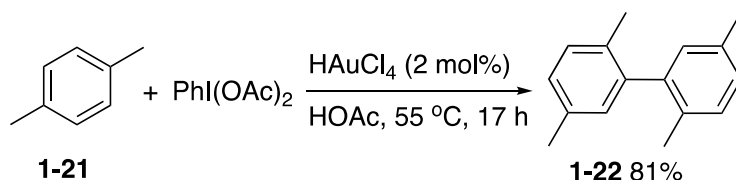


Scheme 1-7 Gold(I)-catalyzed enantioselective carboalkoxylation of alkynes and plausible reaction mechanism

1.3 Redox Gold Catalysis Chemistry

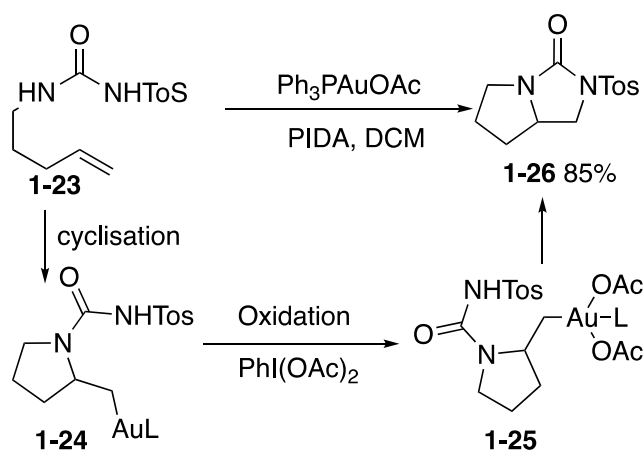
In addition to a superior Lewis acid to catalyze the transformation alkyne and alkene, the fundamental behaviour of gold complexes in the oxidative addition, reductive elimination and transmetalation have also been studied from 1970s. However, contrary to the Pd(0)/Pd(II) cycles which are widely used, gold catalysis involving Au(I)/Au(III) cycles (gold redox catalysis) remains very limited. In that case, the gold catalyst acts not only in its traditional role as a catalyst of nucleophilic addition step but also as a catalyst for the subsequent coupling process. These kinds of redox reactions require the catalyst to undergo two electron oxidation state changes during the catalytic cycle, and while gold(I) and gold(III) are isoelectronic with palladium(0) and palladium(II), respectively, the redox potential of the Au^I/Au^{III} couple is significantly higher ($E_0 = 1.41$ V) than that the Pd⁰/Pd^{II} couple's one ($E_0 = 0.92$ V).¹⁸ Thus, in the gold-catalyzed redox coupling, oxidation of gold(I) to gold(III) is the key step.¹⁹ In the past few years, the oxidations of gold(I) to gold(III) in the gold-catalyzed redox coupling have been developed by using strong external oxidants, strong oxidizing agents (including aryldiazonium salts and hypervalent iodine reagents) and the combination of bidentate ligands with weak oxidizing agent (aryl halides).

The first example of Au-catalyzed oxidative homo-coupling of simple arenes **1-21** involving gold(I)/gold(III) cycle with strong external oxidant reported by Tse et al. in 2007.²⁰



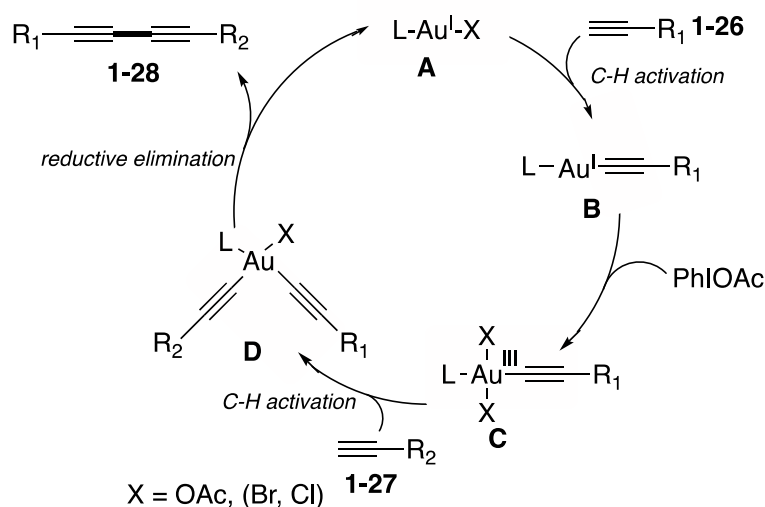
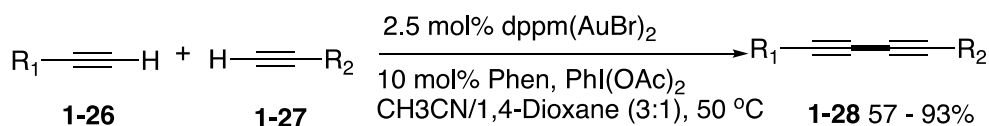
Scheme 1-8 Gold-catalyzed oxidative homo-coupling with PIDA

It can be simply handled in air and no pre-treatment of substrate. A broad range of homo-coupling products **1-22** were obtained by using PhI(OAc)_2 (PIDA) as the oxidant (Scheme 1-8). Mechanistically, these processes are thought to proceed via an organogold intermediate formed upon nucleophilic attack onto multiple bonds activated by gold. Instead of protodeauration of the organogold species in most of gold catalyses, an oxidative pathway has been developed, in which the organogold intermediates were oxidized to gold(III). As an oxidant, PIDA was used in this cascade reaction involving sequential gold-induced nucleophilic addition and oxidative coupling. In 2009, Iglesias and Muñiz²¹ developed a gold-catalyzed diamination of alkenes. The investigation on the individual steps of the catalytic cycle provides strong evidence for the Au(I)/Au(III) cycle. The initial cyclisation of alkene **1-23** proceeds smoothly in the presence of gold(I) to afford the organogold(I) species **1-24**, which was oxidized to gold(III) complex **1-25** with PIDA. The addition of a nitrogen nucleophile to this mixture led cleanly to coupled *N*-methyl urea product **1-26** and regenerate the gold(I) species Ph_3PAuOAc (Scheme 1-9).



Scheme 1-9 Gold-catalyzed bisamination of alkenes

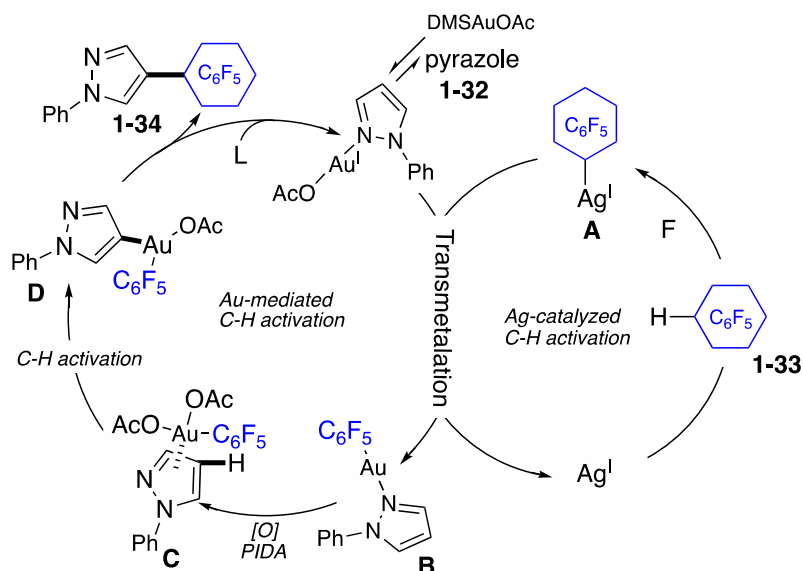
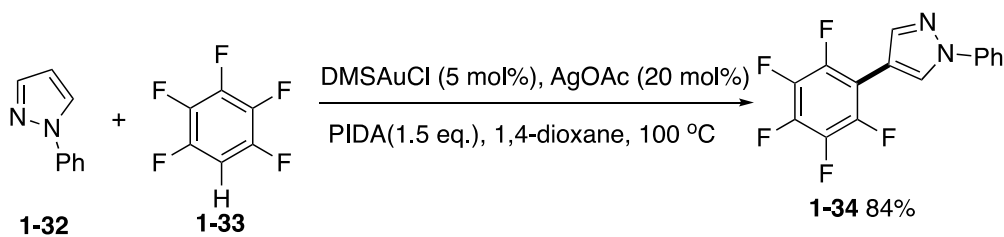
The gold-catalyzed redox coupling involving a sequential gold(I) and gold(III)-induced C-H activation and transmetalation has also been developed. In 2014, Shi et al.²² reported Au-catalyzed alkyne oxidative cross-coupling for the synthesis of unsymmetrical conjugated diynes. A *N,N*-ligand (1,10-Phen) and PhI(OAc)_2 were identified as crucial factors to promote this transformation, giving the desired cross-coupled conjugated diynes in excellent heteroselectivity (>10:1), in good to excellent yields, and with large substrate tolerability. And



Scheme 1-10 Gold-catalyzed oxidative cross-coupling of terminal alkynes

they proposed a mechanism involving Au(I)/Au(III) redox cycle. First, Au(I) **A** induced C-H activation of alkynes **1-26** afford alkyngold(I) complex **B**, followed by oxidation with PIDA to give an alkynylgold(III) complex **C**. A gold(III)-induced C-H activation of another terminal alkyne **1-27** to form Au(III) complex **D**, finally, together with a reductive elimination for giving the desired product **1-28** and Au(I) **A** to finished this catalyzed cycle (Scheme 1-10).

In 2010, Larrosa's group²³ reported that gold(I) could promote selective C-H activation of electron-deficient arenes via σ -bond metathesis. Based on this principle, 5 years later, Larrosa et al.²⁴ developed gold-catalyzed cross-dehydrogenative coupling between protected indoles and polyfluoroarenes, in which a process involving a gold(I)-induced C-H activation of electron-poor arenes and a gold(III)-induced C-H activation of electron-rich arenes was proposed. Although the authors suggested the role of silver salts might be beyond a halogen scavenger, elucidation of its exact role and characterization of key arylsilver(I) intermediate in gold catalysis and evaluation of its possibility for aryl transfer via a transmetalation step to gold as well as the clear mechanistic picture have not been described (Scheme 1-11).



Scheme 1-12 Cooperative Au/Ag dual-catalyzed cross-dehydrogenative biaryl coupling and proposed mechanism

2. Visible-light-mediated Gold Catalysed Reaction

What is visible light? Generally, visible light is defined as the wavelengths that are visible to most human eyes. A typical human eye will respond to wavelengths from about 380 nm to 740 nm. Visible light is only a small part of the electromagnetic spectrum. The colors of the visible spectrum include red, orange, yellow, green, blue, indigo, and violet. As following shows approximate wavelength for the various colors (Figure 1-1). Using visible light as a reagent in combination with catalysts is attractive for developing efficient and selective chemical transformations. Nature impressively demonstrates the power of photosynthesis by converting carbon dioxide and water to carbohydrates and oxygen, a process that is so far unrivaled by any man-made chemical procedure.

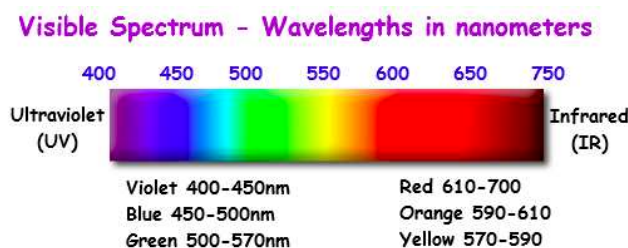


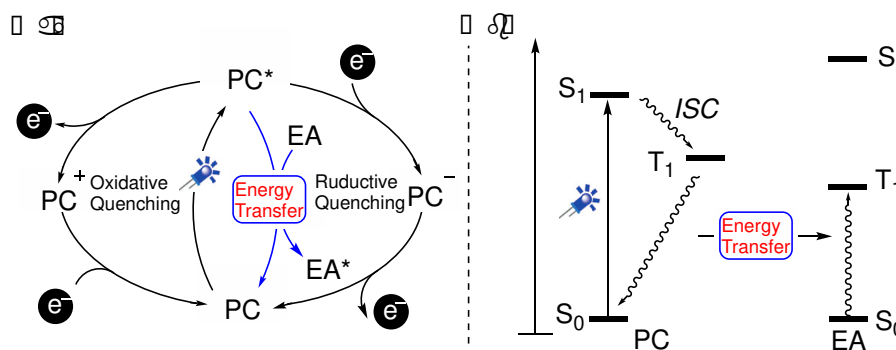
Figure 1-1 Wavelength of visible light

The term photocatalysis may be misleading at the first glance, as light, photons, are used as a reagent, in most cases in large excess and not catalytic. Photocatalysis describes transformations that require light as an energy input to proceed and typically use catalytic amounts of light absorbing photocatalysts, such as metal complexes, organic dyes and semiconductors. Visible-light photocatalysis is a rapidly developing and powerful strategy to initiate organic transformations, as it closely adheres to the tenants of green and sustainable chemistry, documented by a rapidly increasing number of publications in the field since 2008.²⁶

Most of these photochemical reactions proceed through a single-electron transfer (SET) process from the excited photocatalyst to the organic substrate or reagent, thus it is a form of photoredox catalysis. As illustrated in Scheme 1-13a, two different reaction cycles (oxidative quenching and reductive quenching) are frequently invoked to explain the mechanism of photoredox catalysis. In this case, the photocatalyst (PC) is initially excited by irradiation with visible light, and then undergoes a single-electron oxidation or reduction with the substrate or a sacrificial reagent to generate various radical or radical-ion species. These highly reactive species can be manipulated to form many important and useful compounds in a controllable manner.

The crucial factors controlling the success of the photoredox catalysis are the redox properties of the excited photocatalyst as well as the organic substrates and reagents. However, there are still many organic molecules with oxidation potentials or reduction potentials that are incompatible with the excited photocatalysts, and thus they cannot directly undergo a SET process under these conditions. Considering the relatively high energy of the triplet state of the excited photocatalyst, it can also serve as an energy donor, activating an energy acceptor (EA) with a relatively low triplet energy through an energy-transfer (EnT) pathway (Scheme 13a). In contrast to SET processes, visible-light-induced reactions that occur through EnT processes are not constrained by the redox properties of the substrates; instead, they mainly depend on the triplet-state energies of the organic substrate and the excited photocatalyst. The general concept of EnT photocatalysis is described in Scheme 1-13b: first, the photocatalyst absorbs visible light and is excited into the low-lying S_1 state from its ground singlet state (S_0). Subsequently, an intersystem crossing (ISC) event affords the PC in its triplet state (T_1). Once in its triplet state, intermolecular energy transfer to the EA is facile. Exciting the substrate from its ground singlet state (S_0) to the active triplet state (T_1) is possible and the excited substrate will participate in the following transformations. For the EnT process to be efficient, it must meet the following three criteria: the triplet energy of the energy donor (photocatalyst) must be higher than that of the energy acceptor (substrate/reagent), ii) the energy donor should have a high

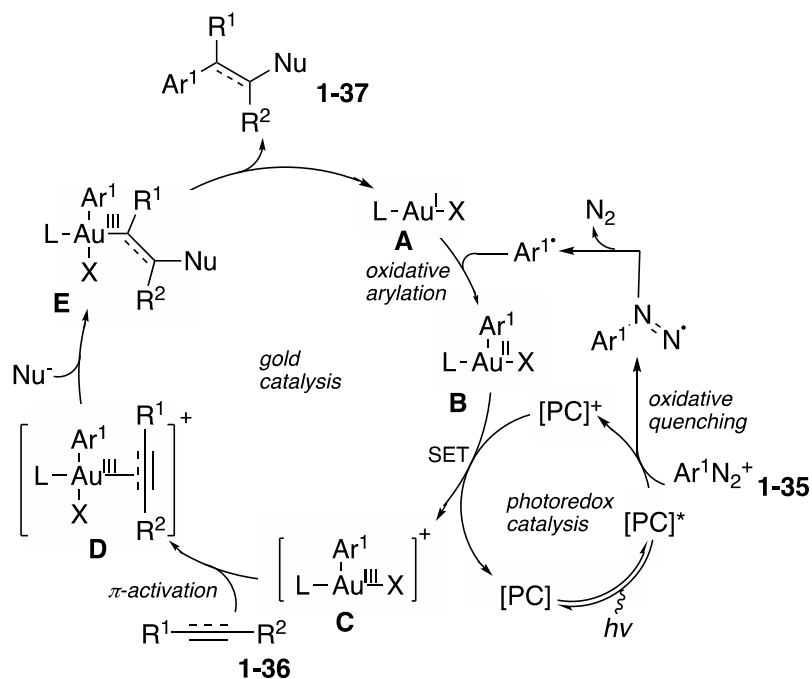
intersystem crossing rate, as this will increase the quantum yield of T_1 , and iii) the process of EnT from the energy donor to the energy acceptor must release energy.²⁷



Scheme 1-13 Visible-light-induced SET and EnT pathways

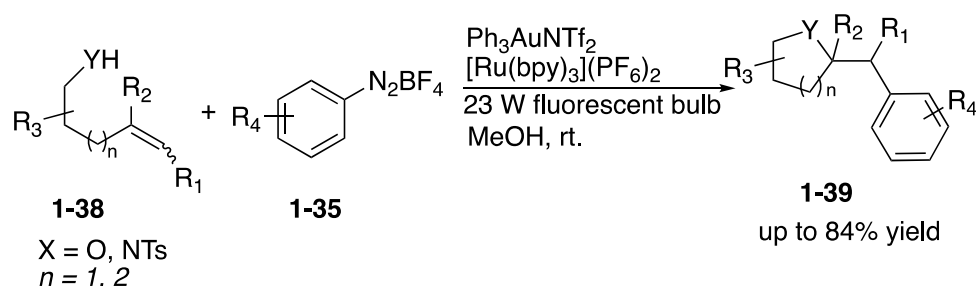
2.1 Dual Photoredox/Gold Catalysis

Au(I) or Au(III) complexes have emerged as efficient carbophilic π -acids in activating unsaturated substrates, especially the alkynes, towards nucleophilic attack.²⁸ In most of these reactions, the resulting organogold species undergo proto-demetalation leading to hydrofunctionalized products. To apply the organogold intermediates in a cross-coupling process mediated by an Au(I)/ Au(III) redox cycle, the reluctance of Au(I) to undergo two-electron oxidation [E_0 (Au(I)/Au(III)) = 1.41 V] has been a hurdle and super-stoichiometric amounts of a strong external oxidant are generally required.²⁹ In this context, in recent years, the combination of gold catalysis with visible-light photoredox catalysis has opened up a new strategy for achieving gold-catalyzed coupling reactions. Visible-light photoredox catalysis can induce the desired redox processes by single electron transfer (SET) in a mild and selective manner,³⁰ shining a light on the redox of Au(I)/Au(III). As shown in the general mechanism in Scheme 14, under visible-light irradiation, arenediazonium salts **1-35** can react with an excited photoredox catalyst [PC]* in an oxidative quenching process to afford aryl radicals. As highly reactive and oxidizing transient species, these radicals are capable of reacting with gold(I) complexes **A** to afford arylgold(II) species **B**,³¹ which can then undergo a single-electron oxidation with the oxidized photocatalyst [PC]⁺, leading to gold(III) complex **C**. Activation of a π -system alkynes **1-36** toward nucleophilic attack either by a gold(I) species or, as shown in Scheme 1-14, by the gold(III) species **C**, followed by reductive elimination then affords the desired arylated product **1-37** and regenerates gold(I) **A**.



Scheme 1-14 General mechanism of dual gold/photoredox-catalyzed difunctionalization reactions of π -systems

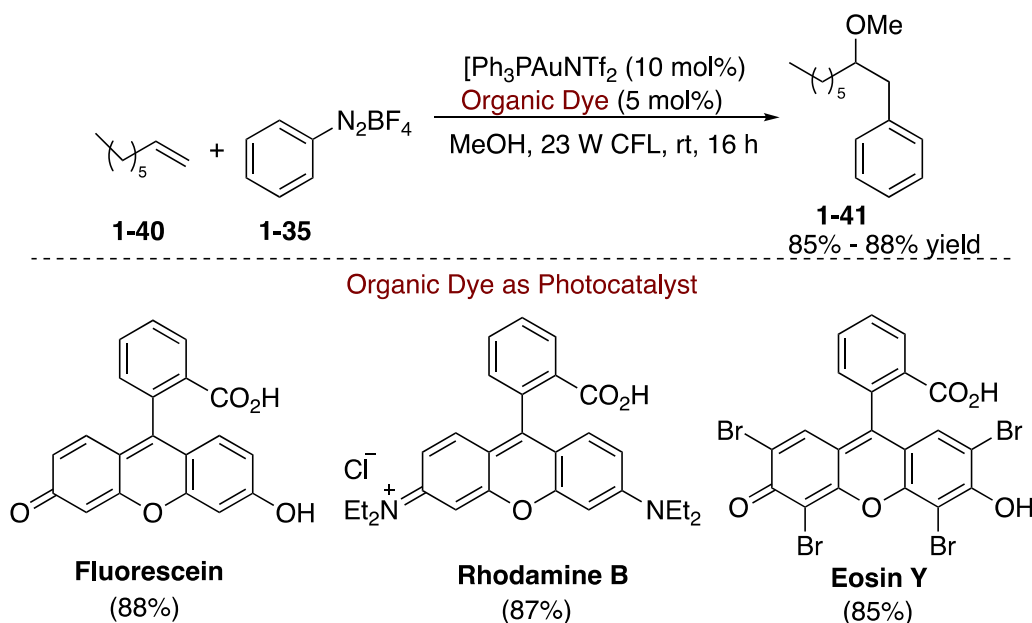
Aryl diazonium salts are a class of reactive electrophiles displaying a large spectrum of reactivities from free-radical chemistry to organometallic synthesis. They have proved to be efficient and more reactive aryl halide and aryl sulfonate surrogates in transition metal-catalyzed coupling reactions. Due to the high nucleofugic properties of the diazonium function, in 2013, Glorius group³² achieved an oxidation of gold(I) complex to gold(III) complex, leading to an intramolecular oxy and aminoarylation of alkenes **1-38** with aryl diazonium salts **1-35** to form the corresponding arylated heterocyclic compounds **1-39**, in which a photosensitizer is essential to activate the diazonium salts **1-35** (Scheme 1-15).



Scheme 1-15 Gold-catalyzed oxy and aminoarylation of alkenes with aryl diazonium salts

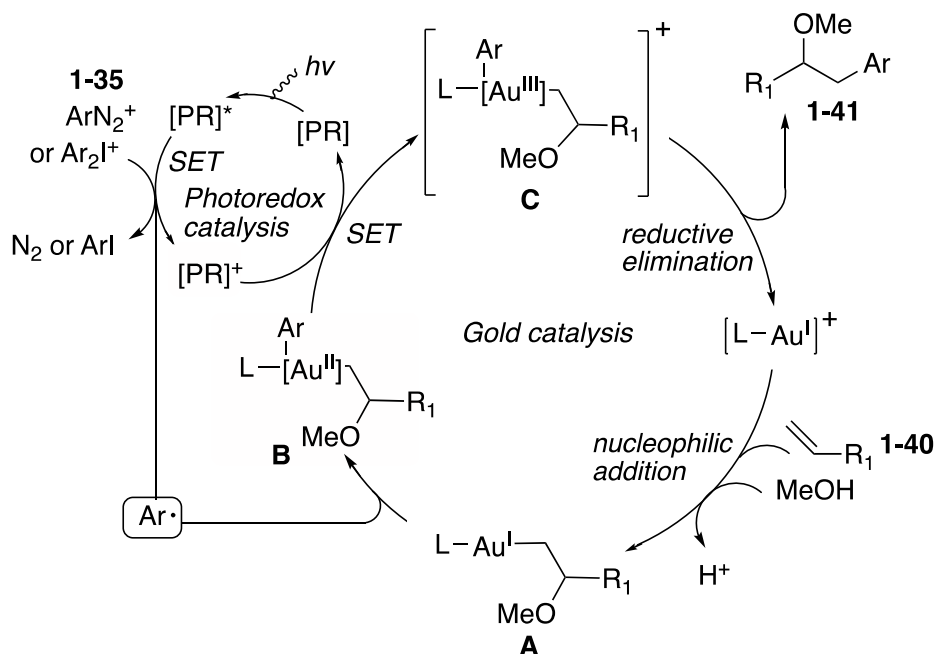
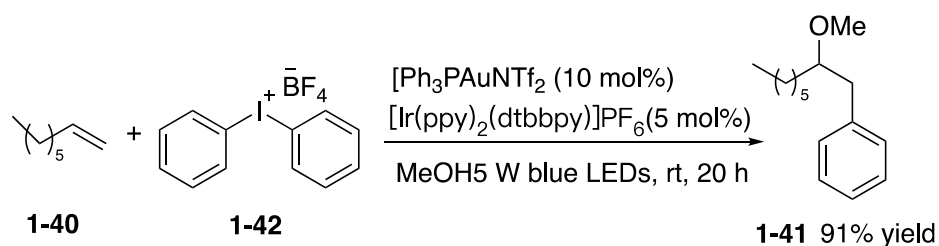
Based on this result, Glorius group turned their attention to expand the scope of the concept and improving the attractiveness of the reaction conditions. In 2014, they developed a novel dual catalysed multicomponent oxyarylation of 1-octene **1-40** combining gold catalysis and

visible light photoredox catalysis. Using aryldiazonium salts **1-35** as sources of the aryl coupling partner, the inexpensive organic dye fluorescein, be used as the photocatalyst. Which is considerably less expensive than $[\text{Ru}(\text{bpy})_3](\text{PF}_6)_2$, led to a single regioisomer of the arylated ether product **1-41** in 88%. Other inexpensive dyes were similarly effective in promoting this transformation (Scheme 1-16).³³



Scheme 1-16 Dual gold/Photoredox-catalyzed intermolecular oxyarylation of 1-octene using organic dyes as photocatalysts

Then they investigate different sources of aryl radicals. Diaryliodonium salts **1-42**, which are generally more stable than aryldiazonium salts and can be purchased commercially could also successfully employed as effective arylating agents. Conducting the three-component coupling reaction of 1-octene **1-40** with diphenyliodonium trifluoromethanesulfonate **1-42** under the standard conditions using the more reducing iridium photocatalyst $[\text{Ir}(\text{ppy})_2(\text{dtbbpy})]\text{PF}_6$ ($E_{1/2}(\text{Ir}^{\text{V}}/\text{Ir}^{\text{III}}) = -0.96 \text{ V}$) and, importantly, 5 W blue LEDs ($\lambda_{\text{max}} = 455 \text{ nm}$) delivered **1-41** in 91% isolated yield. A mechanism involving a photoredox-induced homogeneous $\text{Au}(\text{I})/\text{Au}(\text{III})$ redox cycle was proposed in Scheme 1-17.³³ In accordance with previous reports on the activation of alkenes with sources of cationic gold(I),³⁴ they envisage that initial coordination of the gold to the double bond followed by nucleophilic attack of the methanol solvent would lead to the alkylgold(I) complex **A**.³⁵ Concurrently, in the case of the reaction with aryldiazonium salts **1-35**, excitation of the fluorescein photocatalyst by visible light followed by single electron transfer (SET) to the diazonium compound and subsequent extrusion of nitrogen would generate an aryl radical. With diaryliodonium salts **1-42**, this species would be generated by SET from the excited state of the iridium catalyst

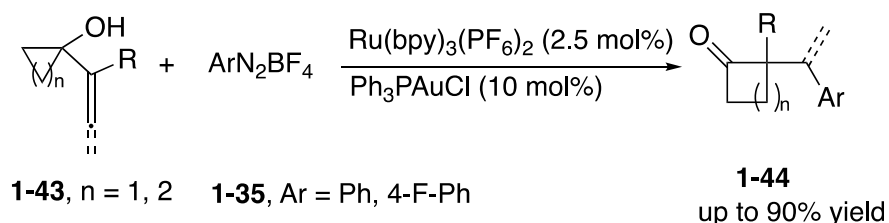


Scheme 1-17 Dual gold/photoredox-catalyzed oxyarylation of alkenes with diaryliodonium salts (isolated yields) and proposed mechanism. PR] = photoredox catalyst {fluorescein for diazonium salts **1-35**, $[\text{Ir}(\text{ppy})_2(\text{dtbbpy})]^+$ for iodonium salts **1-42**}

$[\text{Ir}(\text{ppy})_2(\text{dtbbpy})]^+$ and loss of an aryl iodide molecule. At this stage, oxidation of the gold(I) complex **A** by the aryl radical would afford the gold(II) species **B**, bearing both the alkyl and aryl coupling partners.³⁶ SET between this complex and the oxidized photocatalyst would then deliver the gold(III) species **C** and complete the photoredox catalytic cycle. Subsequent reductive elimination from **C** would then result in product formation and regeneration of the gold(I) catalyst.

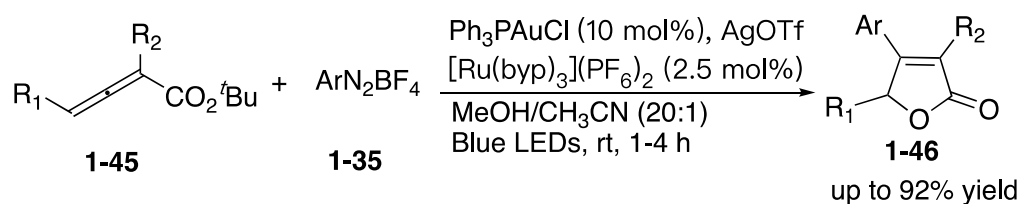
Since Glorius group's initial report on dual gold/photoredox catalysis in 2013, the potential of this methodology has attracted the interest of several research groups and a number of redox-neutral coupling reactions have been developed. In 2014, Toste group reported a ring expansion-oxidative arylation reactions of small sized ring-substituted alkenes and allenes **1-43** with aryldiazonium salts **1-35** affording cyclopentanones **1-44**. The reaction was promoted by dual visible light photoredox catalysis and gold catalysis at ambient conditions. The mechanism of the reaction is consistent with formal oxidative addition of gold(I) to

aryldiazonium salts to form gold(III)-Ar species preceding the reaction with the alkene. These oxidized intermediates react as potent electrophiles toward π -bonds and ultimately provide an entry into formal electrophilic aryl species (Scheme 1-18).³⁷



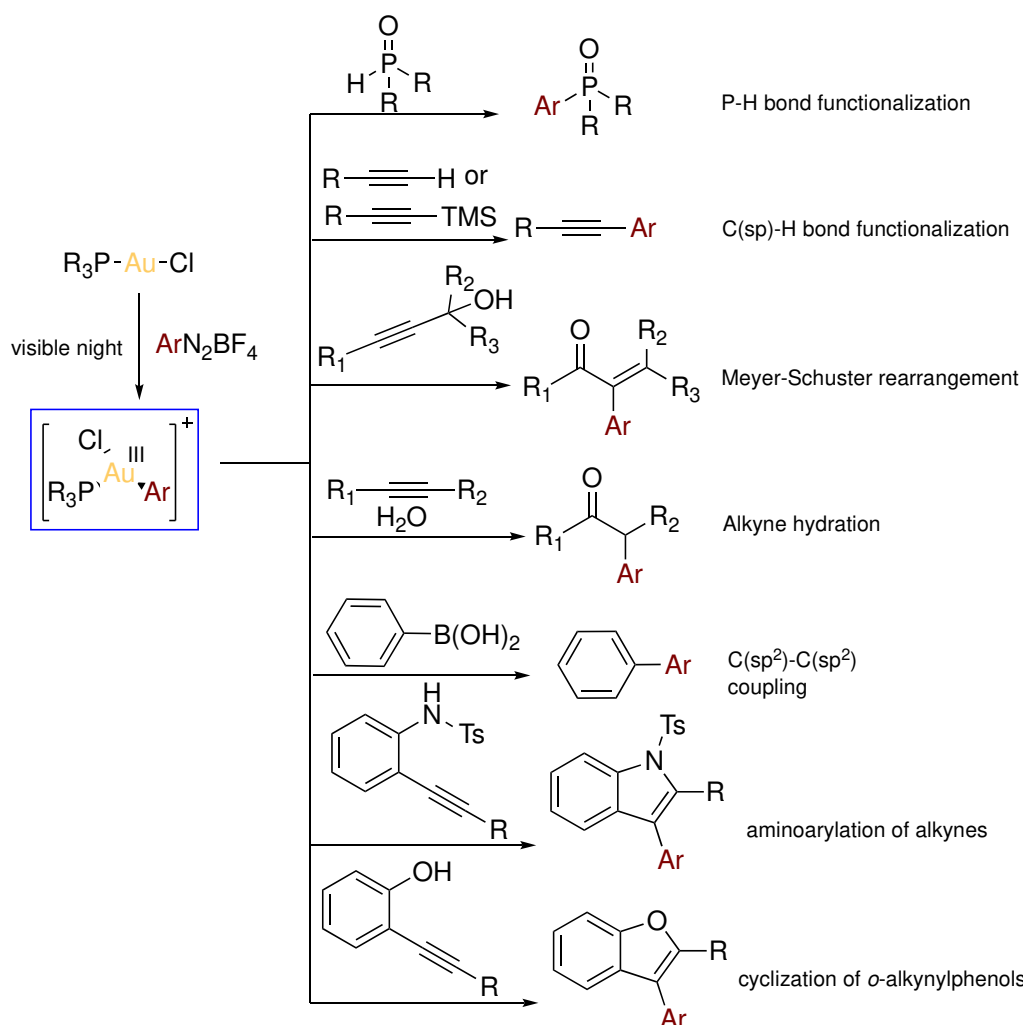
Scheme 1-18 Dual photoredox gold-catalyzed arylative ring expansion

The Shin group, on the other hand, reported an elegant arylative cyclization process involving C(sp²)-C(sp²) coupling with allenates **1-45** delivering butenolides **1-46** (Scheme 1-19).³⁸ The current tandem cyclization/cross-coupling strategy will be particularly valuable since it can combine the structural diversity enabled by gold catalysis with cross-coupling chemistry.



Scheme 1-19 Dual gold/photoredox-catalyzed arylative cyclization of allenates

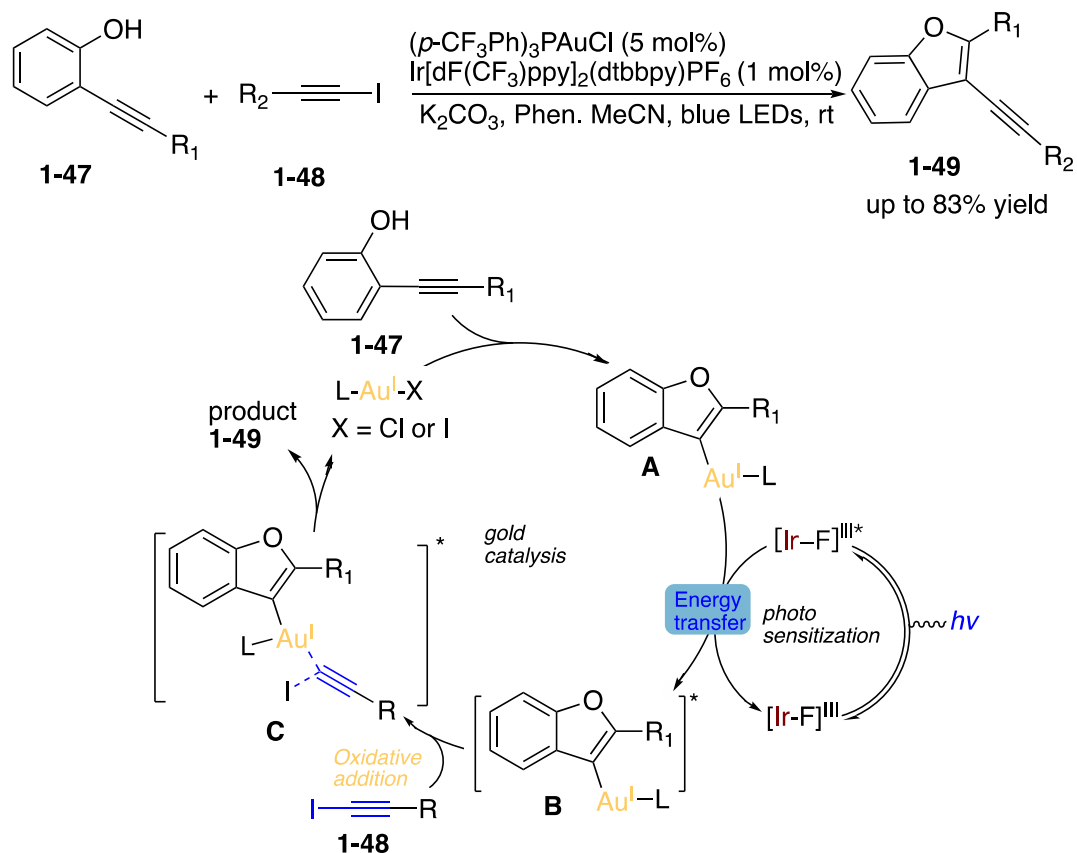
The strategy of this dual gold catalysis was quickly utilized by several research groups in redox-neutral gold-catalyzed coupling reactions, which have been brought about through the merging of homogeneous gold catalysis and visible light photoredox catalysis. The key to success in these systems is the ability of aryl radicals to perform the challenging oxidation of gold(I) first to a transient gold(II) species and then, upon SET oxidation, to arylgold(III) complexes amenable to product-forming reductive elimination. This has led to a number of exciting new difunctionalization reactions of π -systems developed by several groups that combine the traditional reactivity of gold as Lewis acids with coupling chemistry. New transformations continue to be reported at a fast rate, like P-H bond functionalization,³⁹ C(sp)-H bond functionalization,⁴⁰ Meyer-schuster rearrangement,⁴¹ alkyne hydration,⁴² Suzuki-Miyaura reaction,⁴³ amino arylation of alkynes,⁴⁴ and an arylative *o*-alkynylphenol cyclization by Fensterbank (Scheme 1-20).⁴⁵



Scheme 1-20 Further expansion of the concept to various functionalization processes

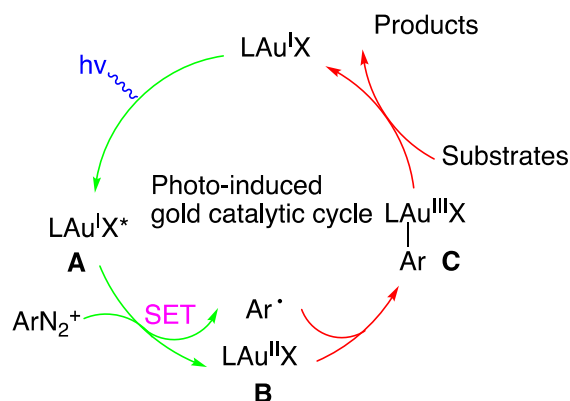
Recently, Fensterbank group developed a new method for the synthesis of valuable alkynyl benzofuran derivatives, which were obtained from *o*-alkynylphenols **1-47** and iodoalkynes **1-48** in the presence of catalytic gold(I) and iridium(III) complexes under blue light-emitting diode irradiation. They show that under visible-light irradiation, an iridium photocatalyst triggers via triplet sensitization the oxidative addition of an alkynyl iodide onto a vinylgold(I) intermediate to deliver C(sp)²-C(sp) coupling products after reductive elimination. Mechanistic and modelling studies support that an energy-transfer event takes place, rather than a redox pathway is shown in Scheme 21. In the first step, the cyclization of *o*-alkynylphenols with the gold(I) catalyst in the presence of K₂CO₃ give vinylgold(I) complex **A**. Upon irradiation with visible light, [Ir-F] is excited into triplet state ³[Ir-F]. Once in its triplet state, intermolecular energy transfer to the formation of **A** is facile. This would lead to the formation of **A** in an excited electronic state **B**, which may further oxidative addition with alkyne **1-48** to form intermediates **C**. Finally, C(sp)₂-C(sp) coupling products was obtained through reductive

elimination. This research results opens new avenues in the field of excited-state gold catalysis (Scheme 1-21).⁴⁶



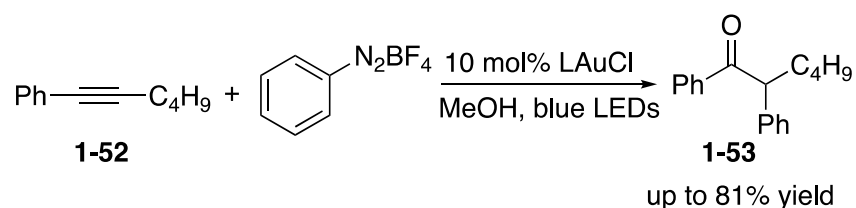
Scheme 1-21 Dual gold and photoinduced alkynylyative O-cyclization *via* photosensitized oxidative addition and proposed mechanism

Very recently, Echavarren group developed a photoredox-initiated gold-catalyzed arylyative alkoxy cyclization of 1,6-enynes with aryldiazonium salts in the presence of alcohols. This three component reaction leads to five-membered ring compounds bearing an exocyclic alkene with the opposite configuration to that obtained by gold(I)-catalyzed cyclization. The reaction occurs under mild conditions and shows high functional group tolerance. A mechanistic proposal for the gold-catalyzed arylyative cyclization of enynes is depicted in Scheme 1-22. The aryl radical generated upon reduction of the diazonium salt in the photoredox cycle adds to Au(I) complex to form Au(II) intermediate **A**, which is further oxidized to Au(III) complex **B** through SET from the photocatalyst or another diazonium salt (radical chain pathway). Next, coordination of the 1,6-enyne **1-50** provides **C**, which undergoes a *5-exo-dig* cyclization to form **D**, followed by addition of the alcohol to generate intermediate **E**. Finally, reductive elimination delivers the desired product **1-51** and regenerates the initial Au(I)



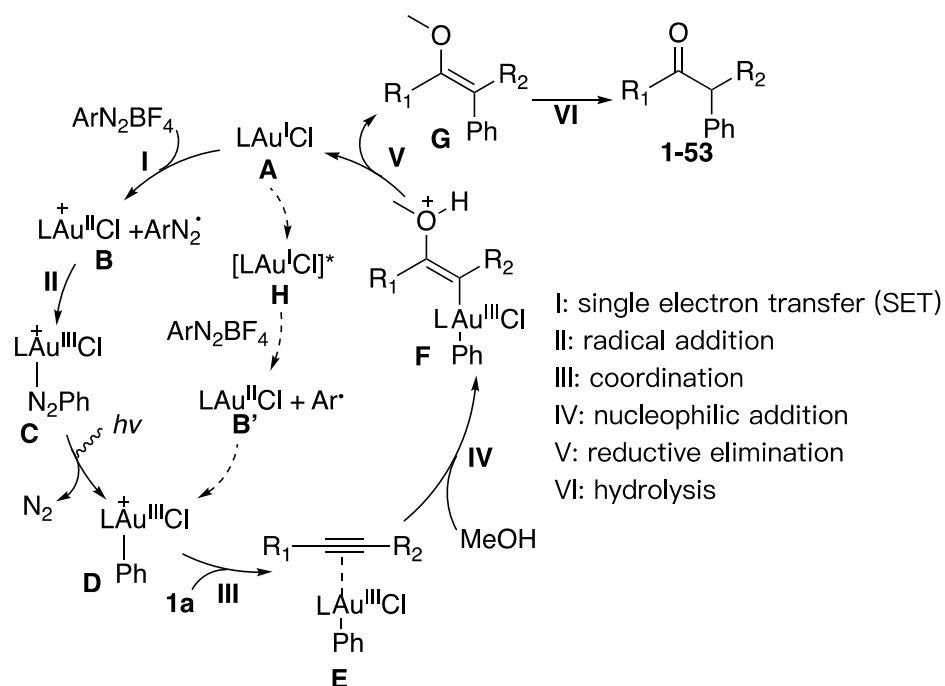
Scheme 1-23 Visible light-induced gold catalysis without exogenous photosensitizer

Recently, Hashmi and co-workers reported exogenous photosensitizer-free visible light-mediated gold-catalyzed 1,2-difunctionalization of 1-phenyl-1-hexyne (**1-52**).⁴⁹ As shown in Scheme 1-24, no exogenous photosensitizer and oxidant, visible light-mediated gold-catalyzed intermolecular 1,2-difunctionalization of **1-52** with aryl diazonium salts affords a variety of α -aryl ketones **1-53** in moderate to good yields.



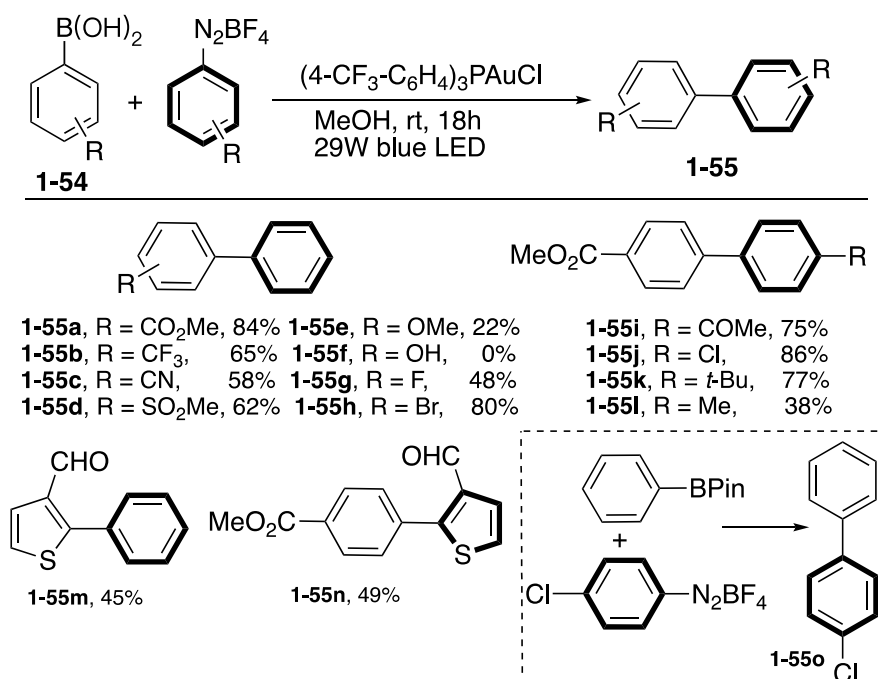
Scheme 1-24 Visible light-mediated gold-catalyzed 1,2-difunctionalization of alkynes

Hashmi⁴⁹ and Gevorgyan⁵⁰ proposed the following mechanism shown in Scheme 1-25. The reaction is initiated by gold-induced SET of gold(I) complex to the aryl diazonium salt, generating an aryl diazo radical and gold(II) species **B**. Diazonium radical addition to gold(II) forms gold(III) intermediate Au^{III}-N₂Ph **C** which evolves to Au^{III}-Ph intermediate **D** by releasing nitrogen. When intercepted by intra- or intermolecularly offered ligands, these arylgold(III) complexes could be intercepted.⁵¹ Then, tandem sequence of coordination, nucleophilic addition, reductive elimination, and hydrolysis occurs to afford the final products. An alternative route toward LCIAu^{III}-Ph intermediate **D** can be envisioned, where the SET of a photoinduced gold(I) complex **H** with the aryl diazonium salt generates an aryl radical and gold(II) complex **B'**. A subsequent recombination would result in intermediate **D**.

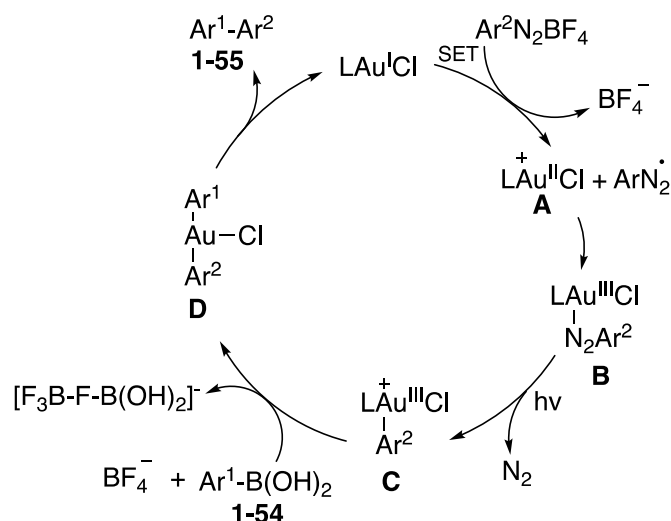


Scheme 1-25 Possible mechanism of the visible light-mediated gold-catalyzed 1,2-difunctionalization of alkyne

Very recently, the same group reported a visible light-induced Au-catalyzed Suzuki-type cross-coupling of boronic acids and aryl diazonium salts.⁵² The scope of the transformation with respect to the boronic acids and aryl diazonium salts substrates was broad. However, substrates possessing an electron-releasing group did not work well (**1-55e-f-l**). Notably, both boronic acid-based and aryl diazonium salt-based heterocycles can be utilized, resulting in acceptable yields of their respective cross-coupling adducts (**1-55m-n**). Employment of aryl boronic pinacol esters also worked well (**1-55o**) (Scheme 1-26). The authors proposed the following mechanism (Scheme 1-27). The Au(I) catalyst undergoes a SET process with the aryl diazonium salt to form the electrophilic Au(II) complex **A** and the aryl diazo radical. The latter recombines with **A** to generate Au(III) complex **B**. A subsequent photoinduced extrusion of N₂ from **B** yields Au(III) intermediate **C**. Next, transmetalation of the in situ activated boronic acid complex with **C** produces diarylated Au complex **D**. Finally, reductive elimination of the latter delivers the desired cross-coupling products **1-55** and closes the catalytic cycle.



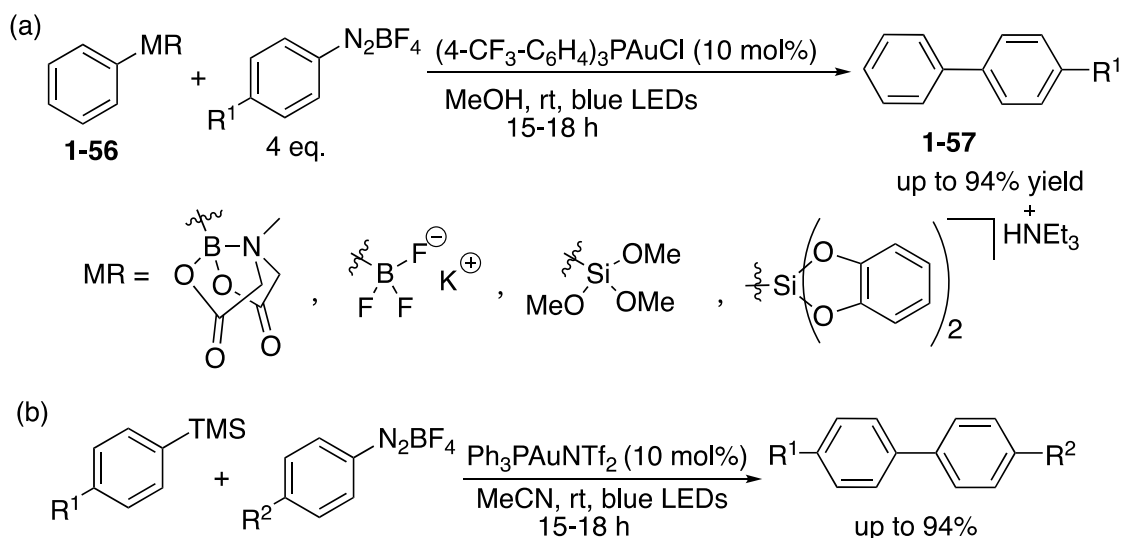
Scheme 1-26 Hashmi's visible light-induced Au-catalyzed cross-coupling reaction



Scheme 1-27 Proposed mechanism of visible light-induced Au catalyzed cross-coupling reaction

Based on these results, Hashmi groups extended their method from using arylboronic acids to pinacol esters, MIDA boronates and potassium trifluoroboronates and showed that they function as an efficient coupling partner with four equivalents of aryldiazonium salts in the photosensitizer-free gold-catalyzed photoredox reactions. Also, organosilicon species, such as trimethoxysilanes and bis(catecholato)silicates, could be transformed by using this method to obtain functionalized biaryls in moderate to excellent yields. The reactions can be conducted under very mild reaction conditions, with a reduced amount of aryldiazonium salt (1.2 equiv.)

by using a catalytic amount of $\text{Ph}_3\text{PAuNTf}_2$ in MeCN under irradiation with blue LEDs at room temperature (Scheme 1-28).⁵³



Scheme 1-28 Photosensitizer-free gold-catalyzed photoredox reactions with aryldiazonium salts

3. Silver Catalysis

Silver is a malleable, ductile, and precious metal that has been known since ancient times (its first debut around 5000 BCE). It is located in group 11 (Ib) and period 5 of the periodic table, between the coinage metal copper (period 4) and gold (period 6), which is inexpensive compared to gold. Silver has the atomic number 47 and atomic weight of 107.880, and its ground state electronic configuration is $[\text{Kr}] 4d^{10}5s^1$, just the same as copper and gold. The oxidation states of silver are 0, +1, +2, +3, and the most common oxidation state are 0 and +1.

The outer orbital electronic configuration of silver is $5s^1$, it allowed to form numerous silver(I) salts/complexes with a wide variety of counterions (halide, sulfide, nitrate, oxide, acetylide compounds, cyano-derivatives, and olefin complexes). Generally, silver salts are mostly utilized as either σ -Lewis acid or π -Lewis acid, with preference to σ -coordination over π -coordination due to the ready availability of empty f orbitals and relativistic contraction of the electron cloud. In addition, the typical d^{10} electronic configuration of silver salts could easily coordinate with most of the unsaturated bonds (π -donors) like $\text{C}=\text{C}$, $\text{C}\equiv\text{C}$, $\text{C}=\text{X}$, and $\text{C}\equiv\text{X}$ bonds (X = heteroatom) and n -donors such as (thio)ethers, amines, and phosphine than other metals.⁵⁴ Because of these aforementioned advantages, silver catalysis has provided an unique opportunity in organic synthesis (Figure 1-2).

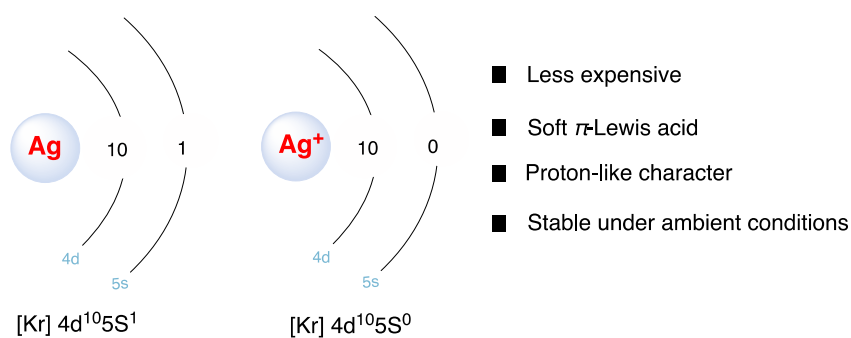


Figure 1-2 Properties of silver (I) catalysts

3.1 Homogeneous Silver Catalysis

The first silver-catalyzed reaction appeared in 1933, in which silver oxidizes the ethylene into ethylene oxide, and has been used on preparative and industrial scales for decades.⁵⁵ Catalysis by silver more economical than other expensive transition metals (TM), excellent selectivity and stability, and environmentally benign nature. But, in comparison with other TM, silver catalysts have long been believed to have low catalytic efficiency, and the rapid development of silver chemistry was achieved only in the past few decades.⁵⁶ The use of silver in organic chemistry today can be classified into two well-defined areas: heterogeneous oxidation processes and homogeneous silver-mediated and catalyzed reactions. Silver (I) cation favouring to interact with carbon-carbon π -bond of alkynes **1-58**, referred to as alkynophilicity in homogeneous catalysis. As shown in Figure 1-3, upon coordination to the carbon-carbon triple bond of alkynes, silver salts lead to the formation of a silver- π -complex **1-59**, facilitating the formation of C-X bonds (X = C, N, O, Halo, P, etc.) by nucleophilic attack on this activated multiple bond. For a terminal or silylated alkyne **1-60**, silver acetylide **1-61** can be formed in the presence of a suitable base and then react with carbon nucleophile.⁵⁷

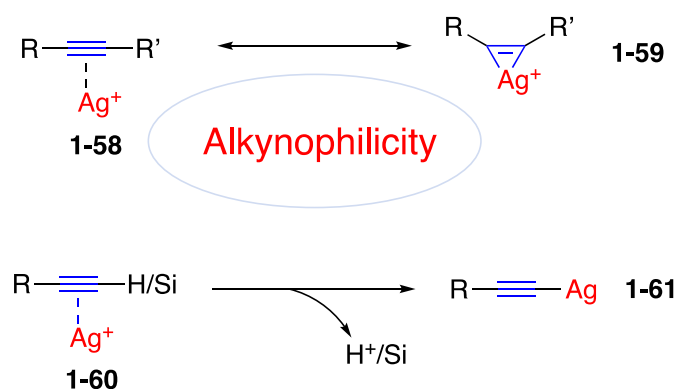
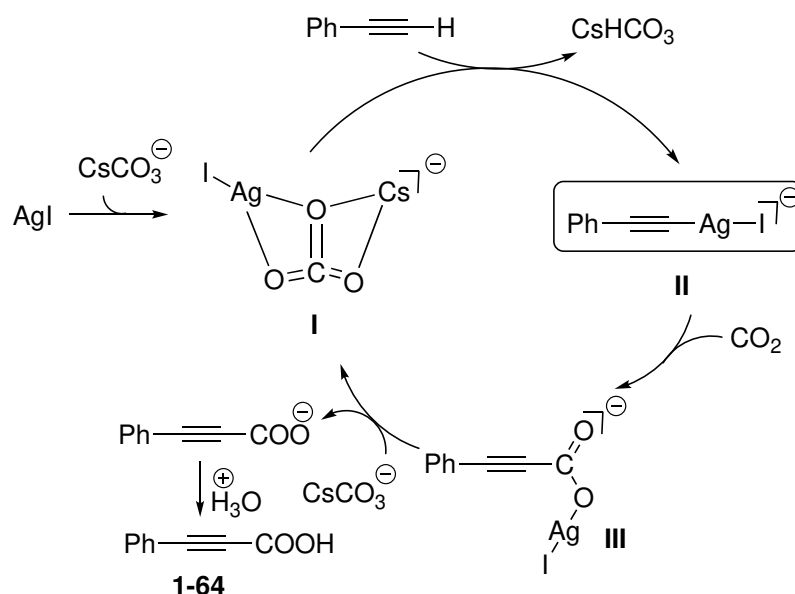


Figure 1-3 Activation of alkyne by silver catalyst

The transition metal-catalyzed Sonogashira coupling of terminal alkynes with aryl and alkenyl halides has become one of the most efficient and straightforward methods to form Csp^2 -

The above carboxylation of terminal alkynes with CO₂ recognized that silver(I) acetylide (R–C≡C–Ag) is generally proposed as the active catalytic species or the key intermediate in silver-catalyzed alkyne reactions. However, in 2014, the DFT studies performed by Luo and Zhang et al. disclosed an unexpected and new catalytically active species, the [IAgCsCO₃][−] anion species **I**, rather than the conventionally considered Ph–C≡C–Ag or AgCO₃[−] anion. Aided by theoretical calculations, the authors found that the iodine anion functions as an inorganic anion ligand to promote the insertion of CO₂ into the alkyne-silver bond (from **II** to **III**). Finally, the acidification after affords propiolic acid product **1-64**. Cs₂CO₃ play dual roles: as a base abstracting hydrogen from the terminal alkyne and a crucial player in generating the catalytically active species **I** (Scheme 1-31).⁶⁰

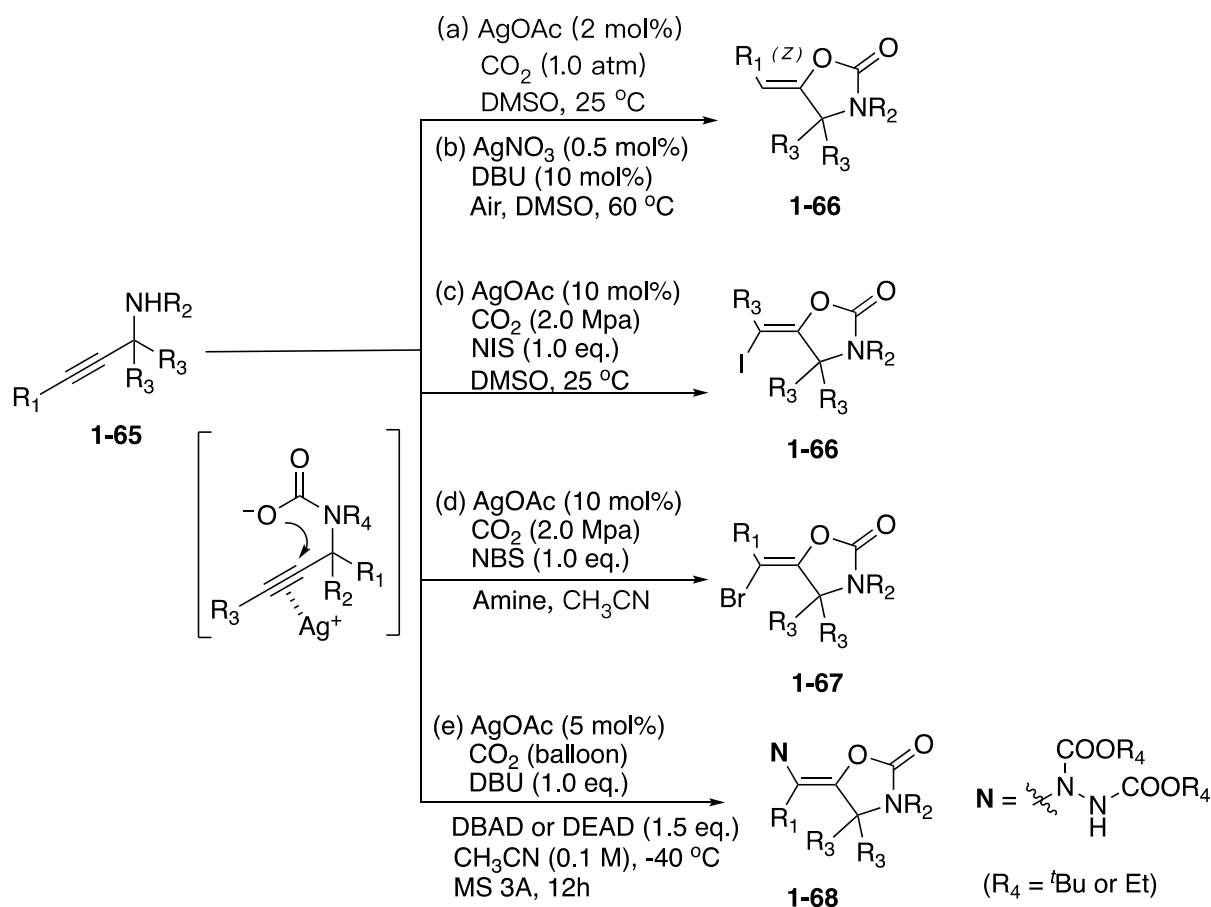


Scheme 1-31 Possible Reaction Mechanism

The oxazolidinone preparation from silver-catalyzed CO₂ incorporation is one of the most attractive synthetic methods. Yamada group reported CO₂ incorporation into various propargylic amines **1-63** proceeded to give the corresponding oxazolidinone derivatives **1-64** in high yields under mild reaction conditions, i.e., 2 mol% of AgOAc and 1.0 atm of carbon dioxide (Scheme 1-32a).⁶¹ Later, Yoshida and co-workers reported that the silver/DBU catalytic system promoted the fixation of carbon dioxide into propargyl amines even under atmospheric carbon dioxide (Scheme 1-32 b).⁶² DBU was found to be necessary for the reaction. They proposed that the DBU-CO₂ adduct generated in situ from DBU and the atmospheric carbon dioxide promoted the reaction with the propargyl amine and carbon dioxide. This assumption was supported by the attempted reaction of propargyl amine and the DBU-CO₂ adduct. In these reactions, the corresponding cyclic carbonates and carbamates bearing *Z* *exo*-olefin were

obtained through the anti-addition of a hemicarboxylate or -carbamate to the internal alkyne activated by a silver catalyst, followed by the protonation of the vinyl-silver intermediate. It was elucidated that the vinyl-silver intermediate generated from the carbon dioxide fixation on the propargyl amine through the anti-addition could also be applied for further transformation, such as iodination **1-66**,⁶³ and bromination **1-67** (Scheme 1-32c, d),⁶⁴ to give functionalized vinyloxazolidinones without the loss of the geometry.

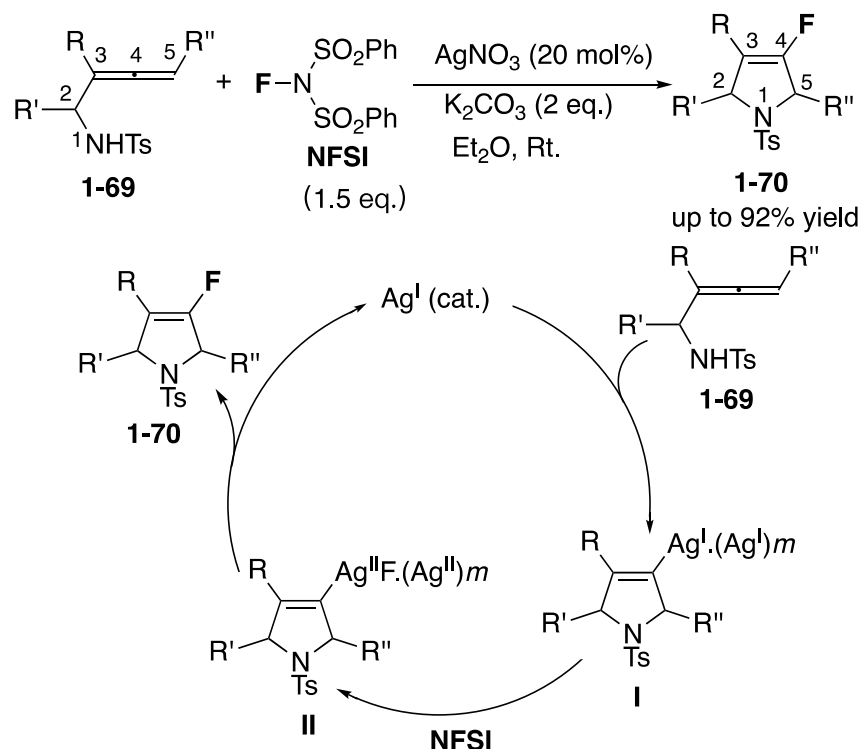
Very recently, Yamada group reported the amination of the vinyl-silver intermediate generated from the silver-catalyzed carbon dioxide incorporation reaction on the propargyl amine (Scheme 1-32e). And the azodicarboxylate reacted with this intermediate to afford the corresponding aminated product **1-68** in high yield. This reaction is the first example of the amination of a vinyl-silver bond, and it was suggested that this amination would proceed by a radical mechanism.⁶⁵



Scheme 1-32 Carboxylation and cyclization of propargyl amines

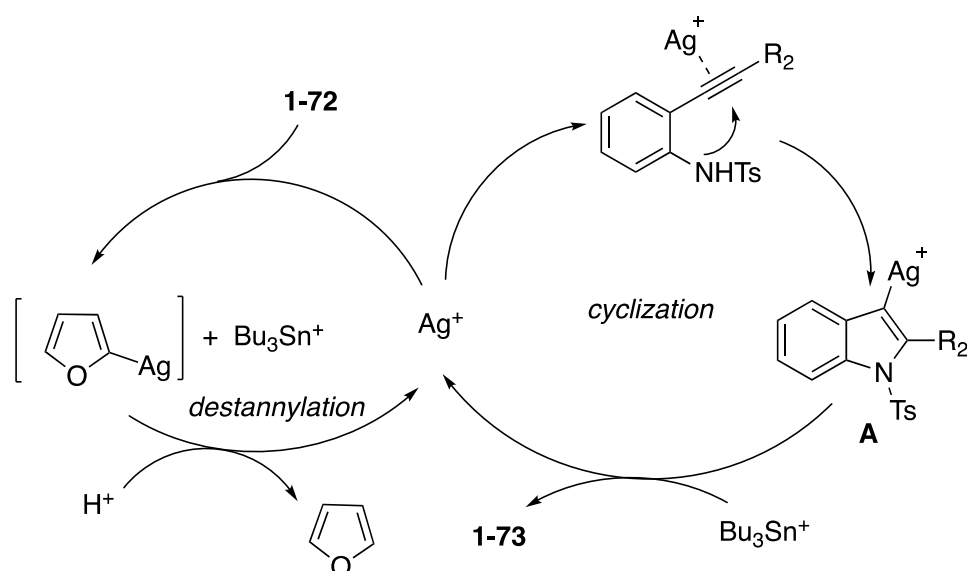
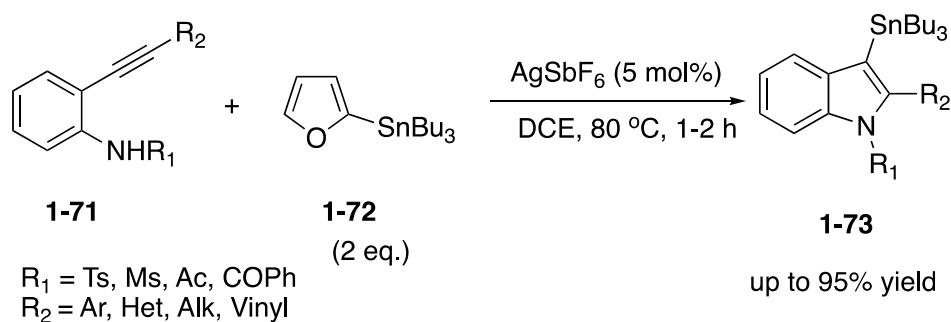
The formation of a vinyl-silver complex has been often proposed as an intermediate in the silver-catalyzed reactions,⁶⁶ due to their instability, the reactivity of a vinyl-silver complex is not completely understood. However, the catalytic reaction based on the vinyl-silver intermediates is still being developed. In 2011, Liu group developed silver-catalyzed

intramolecular aminofluorination of allenes **1-69** for the synthesis of 4-fluoro-2,5-dihydropyrroles **1-70**, in which the vinyl C-Ag bond is cleaved using NFSI to afford vinyl C-F bonds. In addition, further convenient aromatization of fluorinated dihydropyrroles readily afforded the corresponding 4-fluoropyrrole derivatives. For the proposed mechanism, first, silver-catalyzed amination of allene to generate vinyl-silver intermediate **I**. Then, an oxidation of the vinyl-Ag^I intermediate **I** by NFSI to afford a vinyl-Ag^{II} fluoride **II**. Finally, corresponding product **1-70** was formed by reductive elimination (Scheme 1-33).⁶⁷



Scheme 1-33 Silver (I)-catalyzed aminofluorination of allenes and the proposed mechanism

In 2013, Liu and co-workers reported a silver-catalyzed tandem cyclization-stannylation of *N*-protected *ortho*-alkynylanilines **1-71** with 2-tributylstannylfuran **1-72**, which afforded 3-tributyltin substituted indoles **1-73** in fair to excellent yields (42–95%). This work represented the first example of a silver-catalyzed metalative benzannulation reaction. And the resulting stannanes can be transformed into various functionalized indoles. A possible reaction mechanism is shown in Scheme 1-34. It is likely that the reaction is initiated through the formation of 3-indolyl silver(I) intermediate **A** via attack of the amino group onto the silver coordinated alkyne. Meanwhile, silver could catalyze the destannylation of 2-tributylstannylfuran through the transmetalation and protodemetalation. The resulting electrophilic Bu₃Sn⁺ would then react with **A** to give the stannylated product **1-73**.⁶⁸

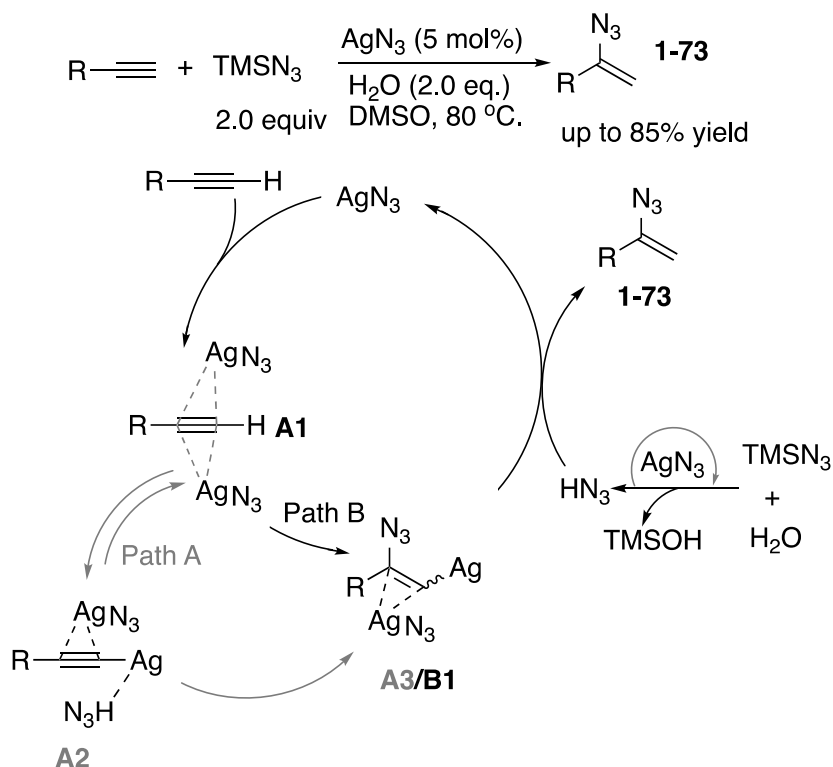


Scheme 1-34 Silver-catalysed tandem cyclization-stannylation of *N*-protected *ortho*-alkynylanilines

One year later, Bi group reported Ag_2CO_3 -catalyzed hydroazidation reaction of terminal alkynes. The reaction has a broad substrate scope of terminal alkynes, affording the corresponding vinyl azides in good-to-excellent yields. However, the high catalyst loading seriously limits its practicality, and moreover, the exact reaction mechanism remains unclear.⁶⁹

Very recently, they developed AgN_3 -catalyzed hydroazidation of terminal alkynes and reported the identification of AgN_3 as the real catalytic species in this reaction.⁷⁰ AgN_3 proved to be a highly robust catalyst, as the loading of AgN_3 could be as low as 5 mol %, and such a small proportion of AgN_3 is still highly efficient even at a 50 mmol reaction scale. Further, on the basis of the experimental and calculation results, they proposed two plausible reaction pathways A and B. A silver- π complex **A1** with two molecules of AgN_3 is first formed from alkyne in the presence of the AgN_3 catalyst. **A1** AgN_3 -silver acetylide- HN_3 complex **A2**, and this process was proven to be in a fast equilibrium during the reaction. Then, the nucleophilic addition step produces alkenylsilver intermediate **A3** (path A). Alternatively, from **A1**, the slightly more favorable concerted addition of cationic silver and azido anion to the triple bond

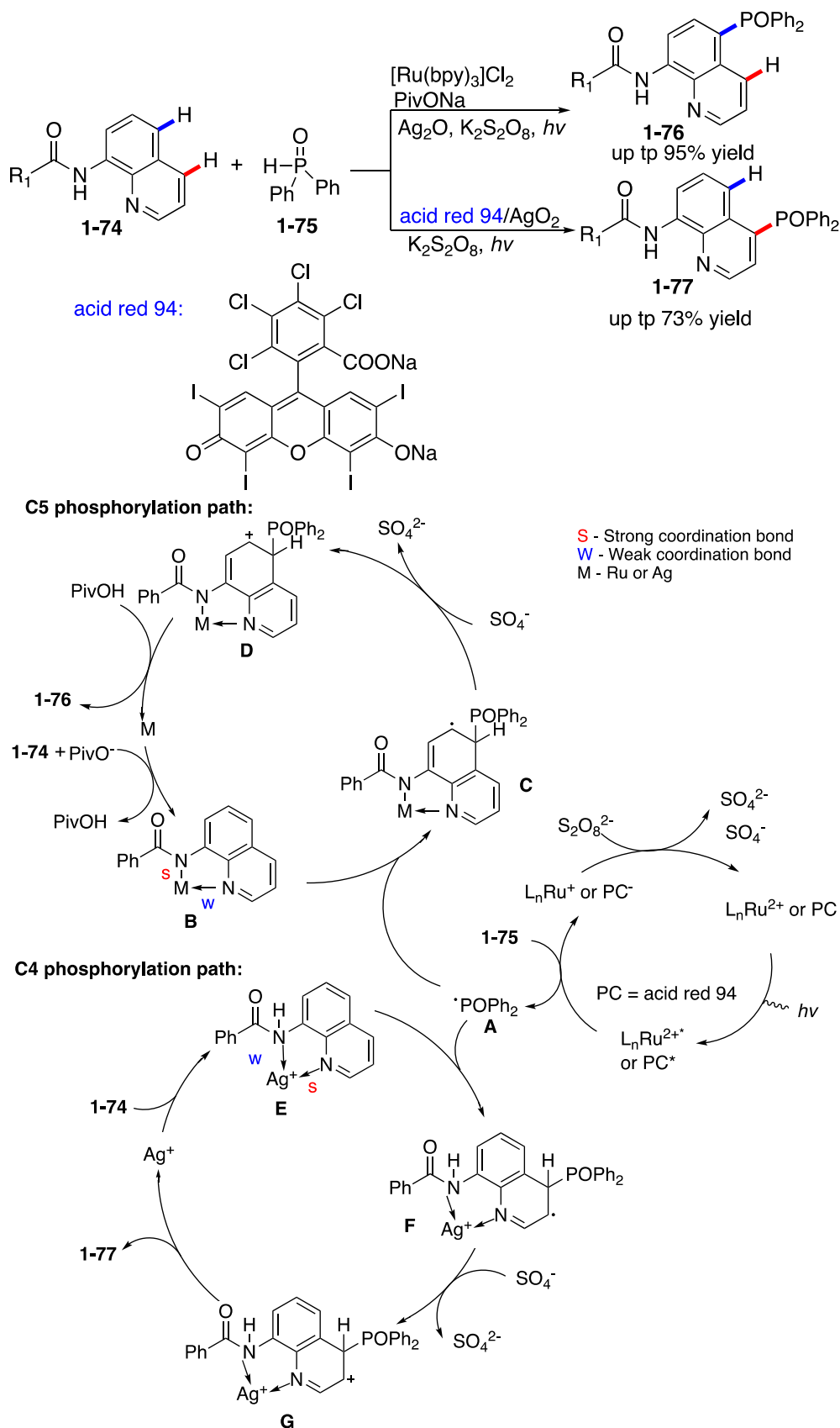
of alkyne could also produce an alkenylsilver intermediate **B1** (**A3** and **B1** are isomers, path B). Subsequently, protonation of **A3** or **B1** by HN_3 formed in situ occurs and delivers the vinyl azide product **1-73**, in which the generation of HN_3 proceeds through the reaction of water with TMSN_3 catalyzed by AgN_3 . Moreover, AgN_3 was for the first time exploited in organic synthesis, thus opening an avenue to the exploration of its synthetic potency as a promising azido reagent (Scheme 1-35).



Scheme 1-35 AgN_3 catalyzed hydroazidation of terminal alkynes and proposed mechanism

3.2 Silver Catalysis under Visible Light

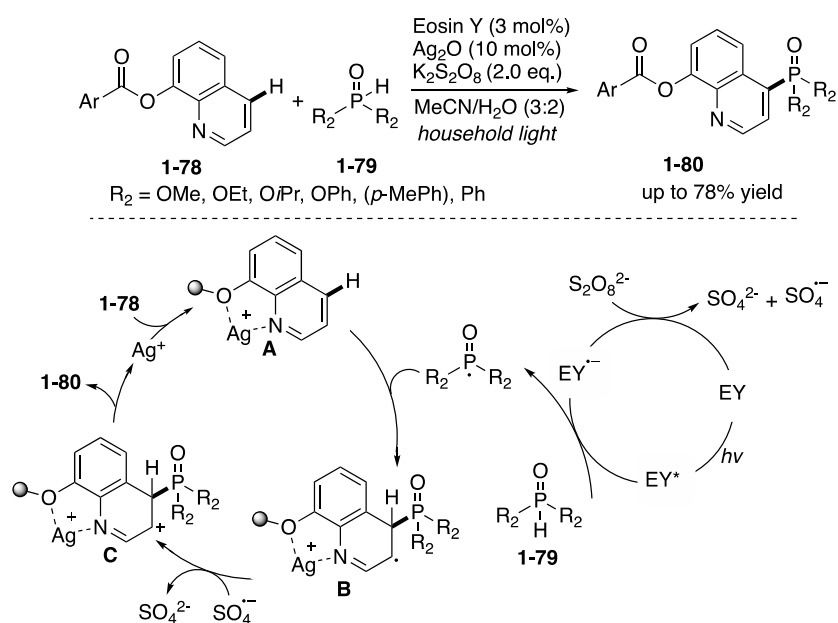
Photoredox catalysis has become a hot topic and emerged as an environmentally friendly and powerful tool in green chemistry, making the reaction occur under lower energy consumption and milder conditions. In recent years, silver catalysis under visible light has received great attention. In order to expand the scope of conventional hydrofunctionalization, various silver catalytic reactions involving visible light have been developed. In 2017, the group of Wu reported the regioselective C4 and C5-selective C-H phosphonation of 8-aminoquinoline amides **1-74** with diarylphosphine oxide **1-75** under the merging photoredox-catalyzed with silver catalysis to form the C5-H quinolinyolphosphonate derivatives **1-76** or unusual C4-H **1-77** quinolinyolphosphonate derivatives (Scheme 1-36).⁷¹ The protocol is characterized by simple, mild and environmentally friendly conditions that avoid stoichiometric loading of a silver salt and high temperature.



Scheme 1-36 Transition metal-catalyzed site-selective C-H phosphonation of 8-aminoquinolines with diarylphosphine oxide via a photoredox process and proposed mechanism

The mechanism was proposed in Scheme 1-36. First, photocatalyst (LnRu^{2+} or PC = acid red 94) is excited by the household light, generating the excited state of LnRu^{2+*} or PC^* . Then, LnRu^{2+*} or PC^* undergoes a reductive quenching process with diarylphosphine oxide **1-75**, generating a LnRu^+ or PC radical anion and an intermediate radical **A**. The LnRu^+ or PC radical anion could be oxidized by $\text{K}_2\text{S}_2\text{O}_8$, regenerating the ground state LnRu^{2+} or PC to complete a photocatalytic cycle. Meanwhile, the C5 phosphonation path starts from coordination of **1-74** and transition metal with the assistant of PivONa, affording an intermediate **B**. Then, the addition of **A** to the intermediate **B** at the C5 position would result in the formation of a radical intermediate **C**. After that, oxidation of **C** by sulfate radical anion and subsequent deprotonation could occur to afford the product **1-76**, along with the regeneration of metal ion species to fulfill the catalytic cycle of C5 phosphonation. On the other hand, the C4 phosphonation path starts from the coordination of **1-74** with Ag(I), affording a chelated intermediate **E**. Then, an intermediate radical **F** is formed by the addition of **A** to the intermediate **E** at the C4 position. Subsequently, an intermediate radical **G** is generated through oxidation of the intermediate **F**. Finally, the decomposition process of the intermediate **G** occurs after the proton transfer process, providing the desired product **1-77**.

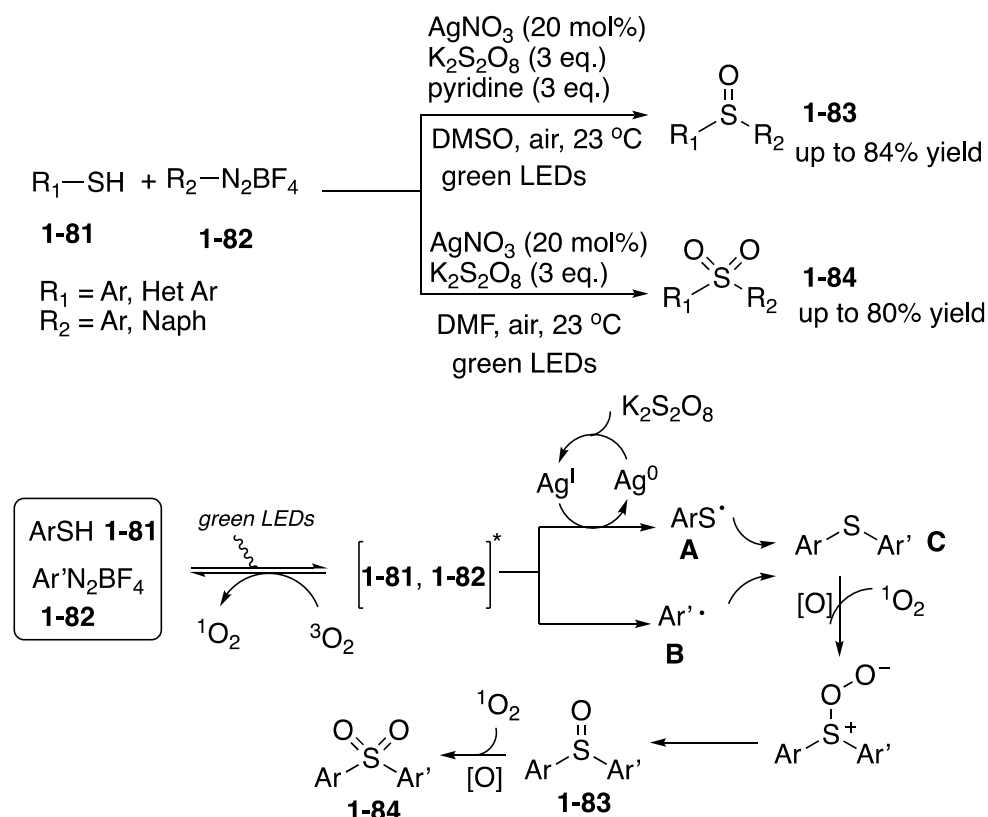
One year later, the same group reported the C4-phosphonation of 8-hydroxyquinolines **1-78** by merging photoredox catalysis with silver catalysis in the presence of a persulfate salt as an oxidant.⁷² The authors propose that the excited state **Eosin Y** (EY^*) is able to generate the P-centered radical out of diphenylphosphine oxide **1-79**. Next, the addition of this radical to



Scheme 1-37 C-H bond phosphonylation by merging photoredox catalysis with silver catalysis

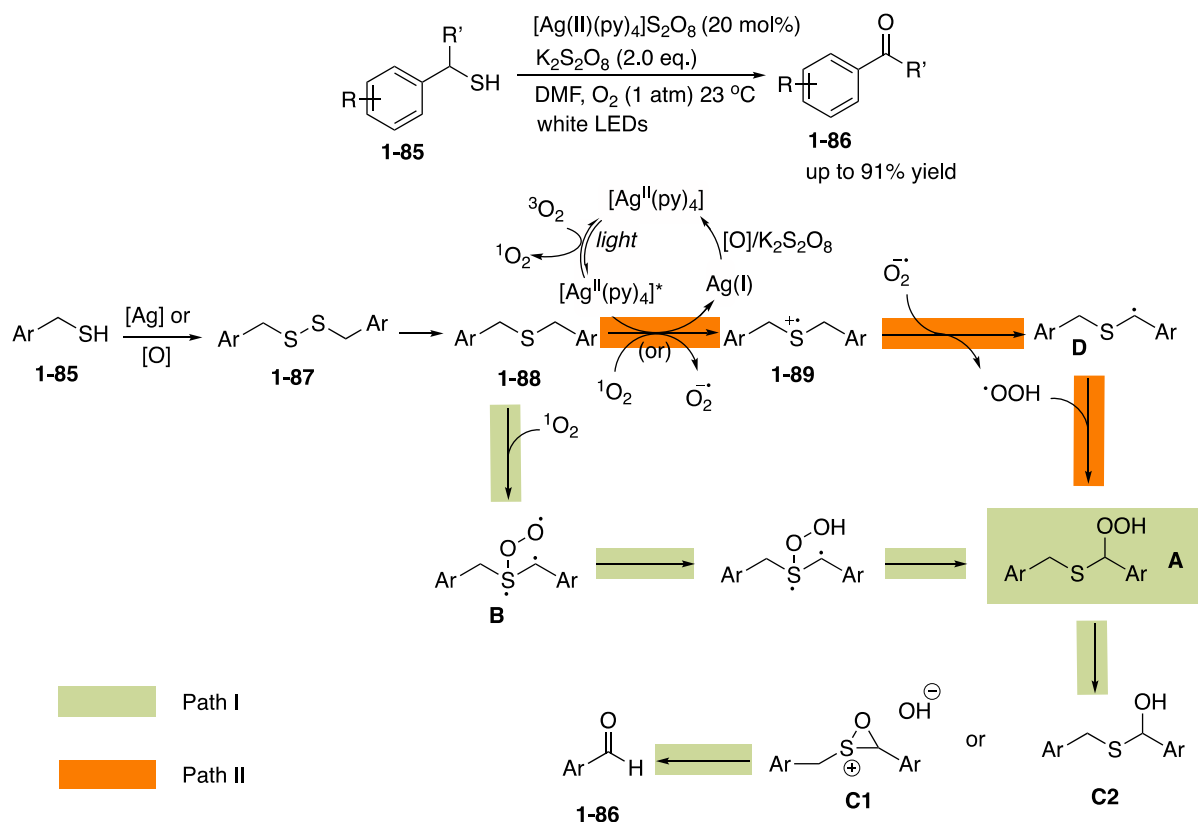
the quinoline **A**, which is activated by the coordination of Ag^+ to the lone-pairs of the oxygen and nitrogen atoms of the chelating substrate **1-78**, takes place. The quinoline phosphine adduct **B** is oxidized by SO_4^{2-} to generate the intermediate **C**. Finally, decomposition of the intermediate **C** occurs, releasing a proton and successfully affording the desired product **1-80**, along with the regeneration of the active Ag(I) species to fulfil the catalytic cycle (Scheme 1-37).

At the same years, Lee group reported visible-light driven silver-catalyzed the selective synthesis of diaryl sulfoxides **1-83** and diaryl sulfones **1-84** by using aryl thiols **1-81** and aryl diazonium salts **1-82**.⁷³ The reactions were carried out under mild reaction conditions, and the desired products were obtained under air atmosphere at room temperature. The method facilitates the rapid access to various aryl sulfoxides and aryl sulfones, providing more opportunities for the synthesis of important bioactive compounds and other key synthetic intermediates. A proposed reaction pathway was shown in Scheme 1-38. Diazonium salt **1-82** are excited through visible light irradiation. Then, thiyl radical **A**, generated by the silver catalyst from thiol **1-81** reacts with aryl radical **B**, generated from diazonium salt **1-82**, to afford sulfide **C** as an intermediate. Subsequent oxidation by $^1\text{O}_2$ would provide the desired sulfoxide **1-83** or sulfone **1-84**.



Scheme 1-38 Visible-light-driven silver-catalyzed the synthesis of diaryl sulfoxides and diaryl sulfones

Very recently, Lee group developed the visible-light-mediated silver(II)-catalyzed C-S bond cleavage of benzyl thiols **1-85** and focuses on controlling the oxidation process to afford the resulting carbonyl compounds **1-86**. Various benzyl thiols can be converted into the corresponding aldehydes or ketones in good to excellent yields under mild reaction conditions (Scheme 1-39).⁷⁴ A proposed reaction pathway is shown in Scheme 1-39. Two different reaction pathways are hypothesized for the formation of oxidative C-S bond cleavage products from sulphide **1-88**, which can be isolated when the reaction was carried out at low temperature (15 °C). In path I, a thiyl radical is generated from thiol **1-85** by the silver catalyst. The subsequent formation of disulfide **1-87** and sulfide **1-88** also occur. After the reaction with $^1\text{O}_2$, which would be generated by the silver(II)-pyridine complex, α -hydroperoxy sulfide **A** is formed. Then, the desired carbonyl product **1-86** would be formed by either an inter- (**C2**) or intramolecular (**C1**) oxygen transfer process. In path II, they suggest that the Ag(II) species was converted to a Ag(I) species by a SET process, generating sulfur radical cation **1-89**. After the reaction with a superoxide radical anion, which would be generated from $^1\text{O}_2$, **D** is formed. A subsequent reaction with **D** and hydroperoxyl radical would provide a key intermediate, α -hydroperoxy sulfide **A**. Then, carbonyl compound **1-86** would be obtained through intermediate **C1** or **C2**.



Scheme 1-39 Visible-light-mediated silver(II)-catalyzed C-S bond cleavage of benzyl thiols and proposed reaction pathway

4. Reference

- [1] G. C. Bond, P. A. Sermon, G. Webb, D. A. Buchanan, P. B. Wells, *J. Chem. Soc. Chem. Commun.* **1973**, 444.
- [2] G. J. Hutchings, *J. Catal.* **1985**, *96*, 292.
- [3] M. Haruta, T. Kobayashi, H. Sano, N. Yamada, *Chem. Lett.* **1987**, *16*, 405.
- [4] A. S. K. Hashmi, *Gold Bull.* **2004**, *37*, 51.
- [5] Y. Ito, M. Sawamura, T. Hayashi, *J. Am. Chem. Soc.* **1986**, *108*, 6405.
- [6] J. H. Teles, S. Brode, M. Chabanas, *Angew. Chem. Int. Ed.* **1998**, *37*, 1415.
- [7] (a) D. Pflasterer, A. S. K. Hashmi, *Chem. Soc. Rev.* **2016**, *45*, 1331; (b) A. M. Asiri and A. S. K. Hashmi, *Chem. Soc. Rev.* **2016**, *45*, 4471.
- [8] (a) A. S. K. Hashmi, *Gold Bull.* **2003**, *36*, 3; (b) A. S. K. Hashmi, *Gold Bull.* **2004**, *37*, 51; (c) A. S. K. Hashmi, G.J. Hutchings, *Angew. Chem. Int. Ed.* **2006**, *45*, 7896; (d) D. J. Gorin, F. D. Toste, *Nature* **2007**, *446*, 395; (e) A. S. K. Hashmi, *Chem. Rev.* **2007**, *107*, 3180; (f) A. Arcadi, *Chem. Rev.* **2008**, *108*, 3266; (g) E. Jiménez-Núñez, A. M. Echavarren, *Chem. Rev.* **2008**, *108*, 3326; (h) Z. G. Li, C. Brouwer, C. He, *Chem. Rev.* **2008**, *108*, 3239.
- [9] M. Pernpointner, A.S.K. Hashmi, *J. Chem. Theory Comput.* **2009**, *5*, 2717.
- [10] (a) A. Buzas, F. Gagosz, *Org. Lett.* **2006**, *8*, 515. (b) S.F. Kirsch, *Angew. Chem. Int. Ed.* **2007**, *46*, 2310. (c) A. S. K. Hashmi, T.D. Ramamurthi, F. Rominger, *J. Organomet. Chem.* **2009**, *694*, 592.
- [11] A. S. K. Hashmi, C. Lothschütz, R. D. M. Rudolph, T.D. Ramamurthi, F. Rominger, *Angew. Chem. Int. Ed.* **2009**, *48*, 8243.
- [12] (a) A. S. K. Hashmi, J. P. Weyrauch, W. Frey, J. W. Bats, *Org. Lett.* **2004**, *6*, 4391; (b) J. W. Weyrauch, A. S. K. Hashmi, A. Schuster, T. Hengst, S. Schetter, A. Littmann, M. Rudolph, M. Hamzic, J. Visus, F. Rominger, W. Frey, J.W. Bats, *Chem. Eur. J.* **2010**, *16*, 956.
- [13] (a) L. -P. Liu, B. Xu, M. S. Mashuta, G. B. Hammond, *J. Am. Chem. Soc.* **2008**, *130*, 17642; (b) L. -P. Liu, G. B. Hammond, *Chem. Asian J.* **2009**, *4*, 1230.
- [14] D. Weber, M. A. Tarselli, M. R. Gagné, *Angew. Chem. Int. Ed.* **2009**, *48*, 5733.
- [15] A. S. K. Hashmi, A. M. Schuster, F. Rominger, *Angew. Chem. Int. Ed.* **2009**, *48*, 8247.
- [16] A. S. K. Hashmi, T. D. Ramamurthi, F. Rominger, *Adv. Synth. Catal.* **2010**, *352*, 971.
- [17] W. Zi, F. D. Toste, *J. Am. Chem. Soc.* **2013**, *135*, 12600.
- [18] S. G. Bratsch, *J. Phys. Chem. Ref. Data* **1989**, *18*, 1.
- [19] M. Joost, A. Amgoune, D. Bourissou, *Angew. Chem. Int. Ed.* **2015**, *54*, 15022.
- [20] A. Kar, N. Mangu, H. M. Kaiser, M. Beller, M. K. Tse, *Chem. Commun.* **2008**, 386.

- [21] A. Iglesias, K. MuÇiz, *Chem. Eur. J.* **2009**, *15*, 10563.
- [22] H. Peng, Y. Xi, N. Ronaghi, B. Dong, N. G. Akhmedov, X. Shi, *J. Am. Chem. Soc.* **2014**, *136*, 13174.
- [23] P. Lu, T. C. Boorman, A.M. Z. Slawin, I. Larrosa, *J. Am. Chem. Soc.* **2010**, *132*, 5580.
- [24] X. C. Cambeiro, N. Ahlsten, I. Larrosa, *J. Am. Chem. Soc.* **2015**, *137*, 15636.
- [25] W. Li, D. Yuan, G. Wang, Y. Zhao, J. Xie, S. Li, C. Zhu, *J. Am. Chem. Soc.* **2019**, *141*, 3187.
- [26] (a) T. P. Yoon, M. A. Ischay, J. Du, *Nat. Chem.* **2010**, *2*, 527; (b) C. K. Prier, D. A. Rankic, D. W. C. MacMillan, *Chem. Rev.* **2013**, *113*, 5322; (c) J. D. Nguyen, E. M. D'Amato, J. M. Narayanam, C. R. J. Stephenson, *Nat. Chem.* **2012**, *4*, 854; d) M. D. Kärkäs, J. A. Porco, Jr., C. R. J. Stephenson, *Chem. Rev.* **2016**, *116*, 9683; (e) R. Brimiouille, D. Lenhart, M. M. Maturi, T. Bach, *Angew. Chem. Int. Ed.* **2015**, *54*, 3872.
- [27] Q. Zhou, Y. Zou, L. Lu, W. Xiao, *Angew. Chem. Int. Ed.* **2019**, *58*, 1586.
- [28] A. M. Asiri, A. S. K. Hashmi, *Chem. Soc. Rev.* **2016**, *45*, 4471; (b) Z. Zheng, Z. Wang, Y. Wang, L. Zhang, *Chem. Soc. Rev.* **2016**, *45*, 4448; (c) L. Liu and J. Zhang, *Chem. Soc. Rev.* **2016**, *45*, 506; (d) D. B. Huple, S. Ghorpade, R. Liu, *Adv. Synth. Catal.* **2016**, *358*, 1348; (e) D. Qian and J. Zhang, *Chem. Soc. Rev.* **2015**, *44*, 677.
- [29] (a) M. N. Hopkinson, A. D. Gee, V. Gouverneur, *Chem. Eur. J.* **2011**, *17*, 8248; (b) H. A. Wegner, M. Auzias, *Angew. Chem. Int. Ed.* **2011**, *50*, 8236.
- [30] (a) X. Z. Shu, M. Zhang, Y. He, H. Frei, F. D. Toste, *J. Am. Chem. Soc.* **2014**, *136*, 5844; (b) Y. He, H. Wu, F. D. Toste, *Chem. Sci.* **2015**, *6*, 1194; (c) S. Kim, J. Rojas-Martin, F. D. Toste, *Chem. Sci.* **2016**, *7*, 85.
- [31] C. Aprile, M. Boronat, B. Ferrer, A. Corma, H. García, *J. Am. Chem. Soc.* **2006**, *128*, 8388.
- [32] B. Sahoo, M.N. Hopkinson, F. Glorius, *J. Am. Chem. Soc.* **2013**, *135*, 5505.
- [33] M. N. Hopkinson, B. Sahoo, F. Glorius, *Adv. Synth. Catal.* **2014**, *356*, 2794.
- [34] R. L. LaLonde, W. E. Brenzovich Jr, D. Benitez, E. Tkatchouk, K. Kelley, W. A. Goddard III, F. D. Toste, *Chem. Sci.* **2010**, *1*, 226.
- [35] X. Z. Shu, M. Zhang, Y. He, H. Frei, F. D. Toste, *J. Am. Chem. Soc.* **2014**, *136*, 5844.
- [36] M. S. Winston, W. J. Wolf, F. D. Toste, *J. Am. Chem. Soc.* **2014**, *136*, 7777.
- [37] X. Shu, M. Zhang, Y. He, H. Frei, F. D. Toste, *J. Am. Chem. Soc.* **2014**, *136*, 5844.
- [38] D. V. Patil, H. Yun, S. Shin, *Adv. Synth. Catal.* **2015**, *357*, 2622.
- [39] Y. He, H. Wu, F. D. Toste, *Chem. Sci.* **2015**, *6*, 1194.
- [40] (a) A. Tlahuext-Aca, M.N. Hopkinson, B. Sahooab, F. Glorius, *Chem. Sci.* **2016**, *7*, 89; (b) S. Kim, J. Rojas-Martinab, F. D. Toste, *Chem. Sci.* **2016**, *7*, 85.

- [41] (a) J. Um, H. Yun, S. Shin, *Org. Lett.* **2016**, *18*, 484; (b) B. Alcaide, P. Almendros, E. Busto, A. Luna, *Adv. Synth. Catal.* **2016**, *358*, 1526.
- [42] A. Tlahuext-Aca, M. N. Hopkinson, A. Garza-Sanchez, F. Glorius, *Chem. Eur. J.* **2016**, *22*, 5909;
- [43] (a) T. Cornilleau, P. Hermange, E. Fouquet, *Chem. Commun.* **2016**, *52*, 10040; (b) V. Gauchot, A. Lee, *Chem. Commun.* **2016**, *52*, 10163.
- [44] C. Qu, S. Zhang, H. Du, C. Zhu, *Chem. Commun.* **2016**, *52*, 14400.
- [45] Z. Xia, O. Khaled, V. Mouriès-Mansuy, C. Ollivier, L. Fensterbank, *J. Org. Chem.* **2016**, *81*, 7182.
- [46] Z. Xia, V. Corcé, F. Zhao, C. Przybylski, A. Espagne, L. Jullien, T. L. Saux, Y. Gimbert, H. Dossmann, V. Mouriès-Mansuy, C. Ollivier, L. Fensterbank, *Nature Chem.* **2019**, *11*, 797.
- [47] J. G. Mayans, J. Suppo, A. M. Echavarren, *Org. Lett.* **2020**, *22*, 3045.
- [48] (a) M. S. Winston, W. J. Wolf, F. D. Toste, *J. Am. Chem. Soc.* **2014**, *136*, 7777; (b) J. R. Deng, W. C. Chan, N. C. H. Lai, B. Yang, C. S. Tsang, B. C. B. Ko, S. L. F. Chan, M. K. Wong, *Chem. Sci.* **2017**, *8*, 7537; (c) J. Xie, J. Li, V. Weingand, M. Rudolph, A. S. K. Hashmi, *Chem. Eur. J.* **2016**, *22*, 12646.
- [49] L. Huang, M. Rudolph, F. Rominger, A. S. K. Hashmi, *Angew. Chem. Int. Ed.* **2016**, *55*, 4808.
- [50] M. Parasram, V. Gevorgyan, *Chem. Soc. Rev.* **2017**, *46*, 6227.
- [51] L. Huang, F. Rominger, M. Rudolph, A. S. K. Hashmi, *Chem. Commun.* **2016**, *52*, 6435.
- [52] S. Witzel, J. Xie, M. Rudolph and A. S. K. Hashmi, *Adv. Synth. Catal.* **2017**, *359*, 1522.
- [53] S. Witzel, K. Sekine, M. Rudolph, A. S. K. Hashmi, *Chem. Commun.* **2018**, *54*, 13802.
- [54] (a) M. Naodovic, H. Yamamoto, *Chem. Rev.* **2008**, *108*, 3395; (b) M. P. Munoz, *Chem. Soc. Rev.* **2014**, *43*, 3164. (c) G. Fang, X. Bi, *Chem. Soc. Rev.* **2015**, *44*, 8124; (d) P. Sivaguru, S. Cao, K. R. Babu, X. Bi, *Acc. Chem. Res.* **2020**, *53*, 662.
- [55] (a) G. E. Hamilton, A. B. Metzner, *Ind. Eng. Chem.* **1957**, *49*, 838; (b) D. F. Othmer, M. S. Thakar, *Ind. Eng. Chem.* **1958**, *50*, 1235.
- [56] (a) H. V. R. Dias, C. J. Lovely, *Chem. Rev.* **2008**, *108*, 3223; (b) Q. Zhenga, N. Jiao, *Chem. Soc. Rev.* **2016**, *45*, 4590; (c)
- [57] U. Létinois-Halbes, P. Pale, S. Berger, *J. Org. Chem.* **2005**, *70*, 9185.
- [58] P. Li, L. Wang, *Synlett*, **2006**, 2261.
- [59] (a) X. Zhang, W.-Z. Zhang, X. Ren, L.-L. Zhang, X.-B. Lu, *Org. Lett.* **2011**, *13*, 2402; (b) M. Arndt, E. Risto, T. Krause, L. J. Gooen, *Chem. Cat. Chem.* **2012**, *4*, 484.
- [60] C. Liu, Y. Luo, W.-Z. Zhang, J.-P. Qu and X.-B. Lu, *Organometallics*, **2014**, *33*, 2984.

- [61] S. Yoshida, K. Fukui, S. Kikuchi and T. Yamada, *Chem. Lett.* **2009**, *38*, 786.
- [62] M. Yoshida, T. Mizuguchi and K. Shishido, *Chem. Eur. J.* **2012**, *18*, 15578.
- [63] K. Sekine, R. Kobayashi and T. Yamada, *Chem. Lett.* **2015**, *44*, 1407.
- [64] N. Sugiyama, M. Ohseki, R. Kobayashi, K. Sekine, K. Saito and T. Yamada, *Chem. Lett.* **2017**, *46*, 1323.
- [65] Y. Sadamitsu, K. Saito, T. Yamada, *Chem. Commun.* **2020**, *56*, 9517.
- [66] (a) M. P. Munoz, *Chem. Soc. Rev.*, 2014, *43*, 3164; (b) G. Fang and X. Bi, *Chem. Soc. Rev.* **2015**, *44*, 8124.
- [67] T. Xu, X. Mu, H. Peng, G. Liu, *Angew. Chem. Int. Ed.* **2011**, *123*, 8326.
- [68] J. Liu, X. Xie, Y. Liu, *Chem. Commun.* **2013**, *49*, 11794.
- [69] Z. Liu, P. Liao, X. Bi, *Org. Lett.* **2014**, *16*, 3668.
- [70] S. Cao, Q. Ji, H. Li, M. Pang, H. Yuan, J. Zhang, X. Bi, *J. Am. Chem. Soc.* **2020**, *142*, 7083.
- [71] H. Qiao, S. Sun, Y. Zhang, H. Zhu, X. Yu, F. Yang, Y. Wu, Z. Li, Y. Wu, *Org. Chem. Front.* **2017**, *4*, 1981.
- [72] X. Su, F. Yang, Y. Wu, Y. Wu, *Org. Biomol. Chem.* **2018**, *16*, 2753.
- [73] D. H. Kim, J. Lee, A. Lee, *Org. Lett.* **2018**, *20*, 764.
- [74] B. Hong, K. C. C. Aganda, A. Lee, *Org. Lett.* **2020**, *22*, 4395

Chapter 2 Photosensitizer-free Gold Catalysis

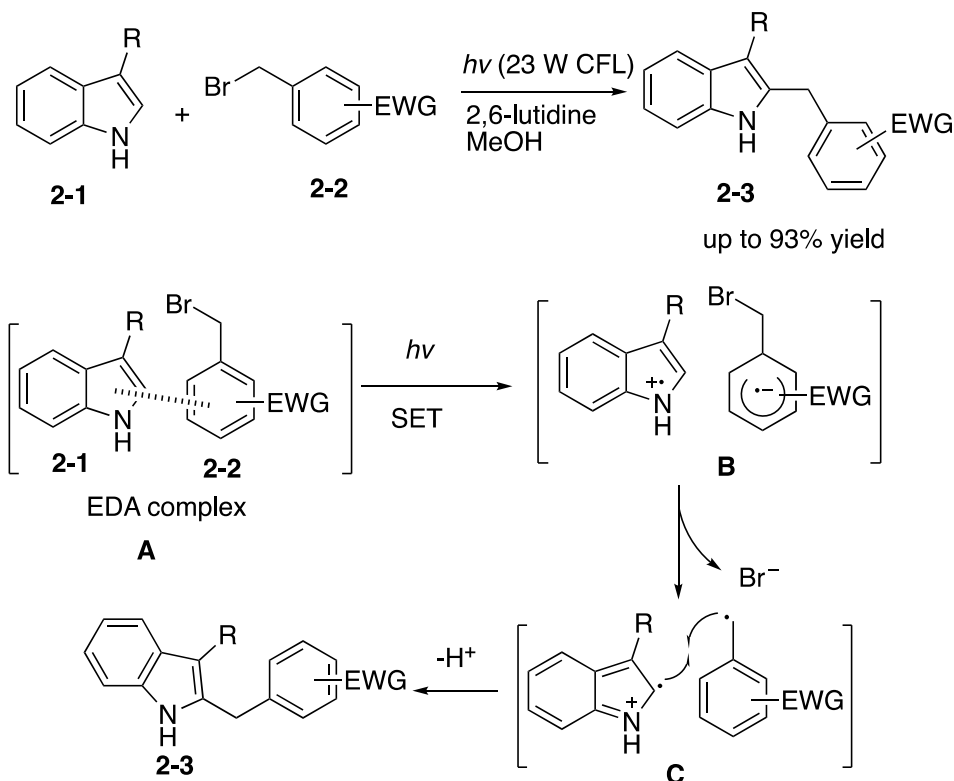
1. External Photosensitizer-free on Photocatalytic Reaction

In order to effectively utilize natural resources and reduce the environmental impact of chemical production, it is imperative to develop new greener chemical production tools to replace the traditional high energy consuming and resource wasteful processes.¹ Photoreactions offer opportunities towards such development.² Photoreactions could achieve the desired reactivity without using harsh conditions, which can avoid the safety issues caused by high temperature and high pressure, often required by thermal reactions. In addition, many light-driven reactions could proceed but are unattainable under thermal activation.

Presently, a lot of elegant photoreactions have been developed for the synthesis of valuable compounds under mild conditions.³ In such reactions, typically, catalytic quantities of photosensitizers, such as transition metal complexes, organic dyes, or inorganic semiconductors, are necessary to absorb visible light and trigger subsequent organic transformations. These photosensitizers could serve as strong single-electron transfer (SET) reagents or energy transfer reagents in many novel and efficient synthetic methods.^{3a,c} However, photosensitizers based on transition-metals and organic dyes raise concerns of resource sustainability and complicate product purification in various applications such as pharmaceuticals and materials. Furthermore, photosensitizers are often too expensive to be used in large-scale industrial productions. In order to solve this problem, the development of photosensitizer-free photoreactions provides promising alternatives. The recent surge in this field shows that synthetic chemists have taken serious notice and started to realize the great potential of this strategy. For example, in 2013, the Melchiorre group found that an electron donor-acceptor (EDA) complex between key chiral enamine intermediates and substrates allowed visible-light-promoted organocatalytic asymmetric alkylations of aldehydes without requiring an external photosensitizer.⁴ Later, the photo cross-coupling of thiols with aryl halides was reported without a photosensitizer using DMSO as the solvent. The mechanistic studies revealed that aryl halides and thiols could form an EDA complex in DMSO, and the transformation was realized *via* a light-driven SET process between the EDA complexes.⁵ These examples demonstrated that the utilization of expensive photosensitizers could be avoided *via* the development of new photoreactions.

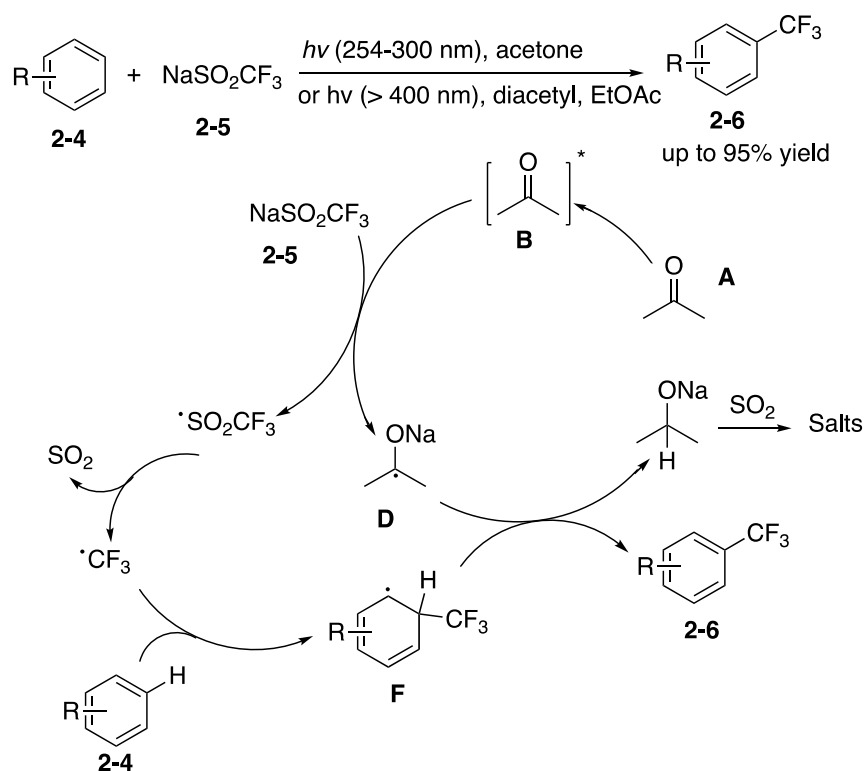
In 2015, Melchiorre and co-workers reported a photoinduced alkylation of indoles **2-1** with electron deficient benzyl and phenacyl bromides **2-2** to form coupling product **2-3** (Scheme 2-1). Additionally, the formation of EDA complex **A** was identified by X-ray single-crystal analysis, which provided firm evidence of the proposed mechanism. EDA complex **A** between indoles **2-1** and electron deficient benzyl bromides **2-2** underwent a photoinduced SET

process to generate radical pair **B**, upon leaving of the bromide anion, and the radical-radical coupling process with radical pair **C** generated the desired coupling product **2-3**.⁶



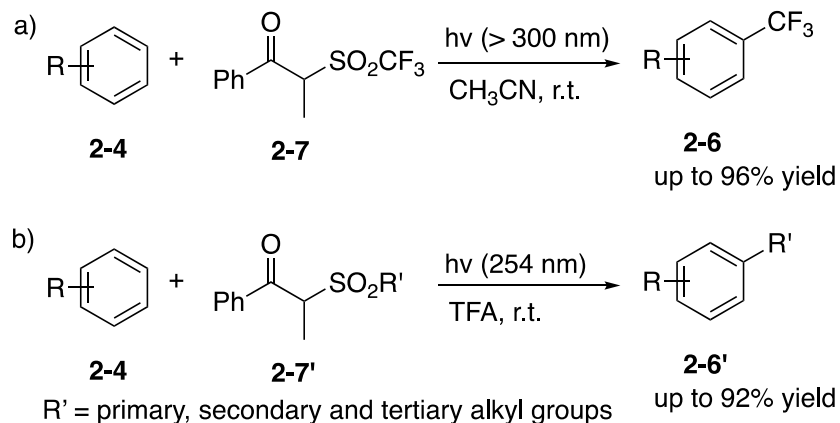
Scheme 2-1 Photoinduced alkylation of indoles *via* the EDA complex

One year later, Li group developed an efficient and practical approach to the photoinduced trifluoromethylation of arenes and heteroarenes **2-4** with easily handled sodium triflate **2-5** (Scheme 2-2).⁷ This reaction provided a simple and clean method to modify biologically active and pharmaceutical molecules with the trifluoromethyl group under mild conditions. Significantly, this photochemical strategy employed acetone, one of the most widely used and cheapest organic solvents, instead of expensive metal catalyst or dangerous peroxides to generate CF_3 radical, which provides a greener route to cost-effective large-scale synthesis of trifluoromethylated chemicals. The proposed mechanism was shown in Scheme 2-2. The SET process between excited acetone **B** and sodium trifluoromethanesulfinate **2-5** generates alkyl radical **D** and SO_2CF_3 radical **C**, which can further fragment to form CF_3 radical **E**. Then, CF_3 radical **E** attacks arenes **2-4** to form aryl radical **F**, which subsequently generates the desired product **2-6** *via* the hydrogen-atom-transfer (HAT) process with alkyl radical **D**.



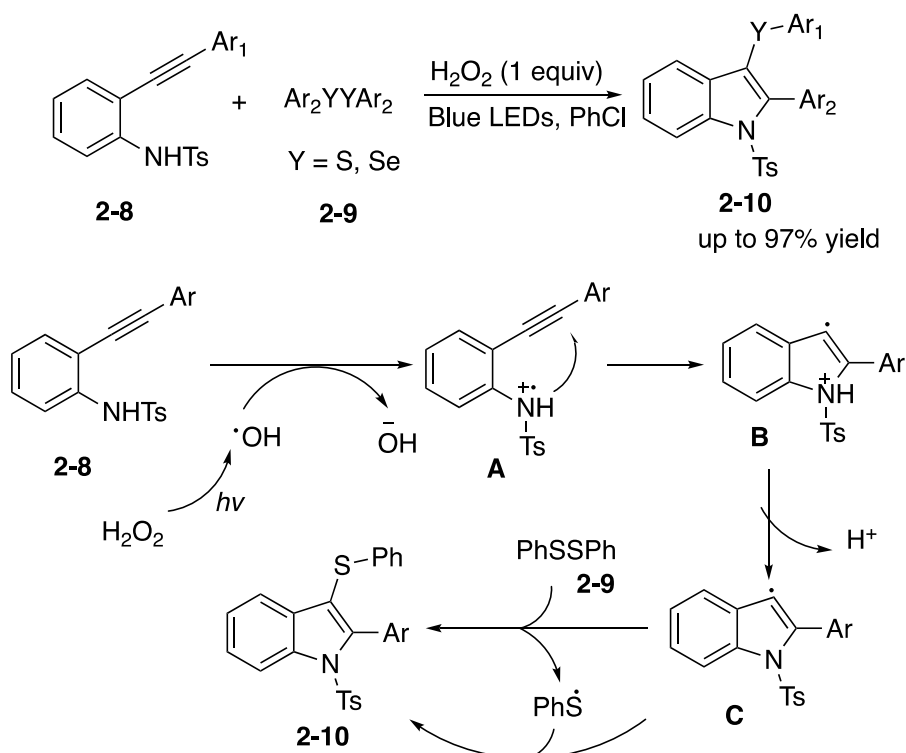
Scheme 2-2 Photoinduced trifluoromethylation of arenes and heteroarenes and proposed mechanism

Based on this reaction, they used trifluoro reagent **2-7** instead of sodium triflate **2-5**. The trifluoromethylation of arenes and heteroarenes can be conducted at room temperature *via* a household CFL as the light source. This transformation tolerates various functional groups and produces the corresponding products **2-6** in moderate to excellent yields (Scheme 2-3, a). The success of this approach hinges upon the identification of a series of sulfone compounds **2-7'**, which can be homolytically cleaved under light irradiation (Scheme 2-3, b). These trifluoromethylation and alkylation reagents are stable to air and water, are soluble in all common organic solvents, and can be readily synthesized from cheap starting materials.⁸



Scheme 2-3 Photoinduced trifluoromethylation and alkylation of aromatics

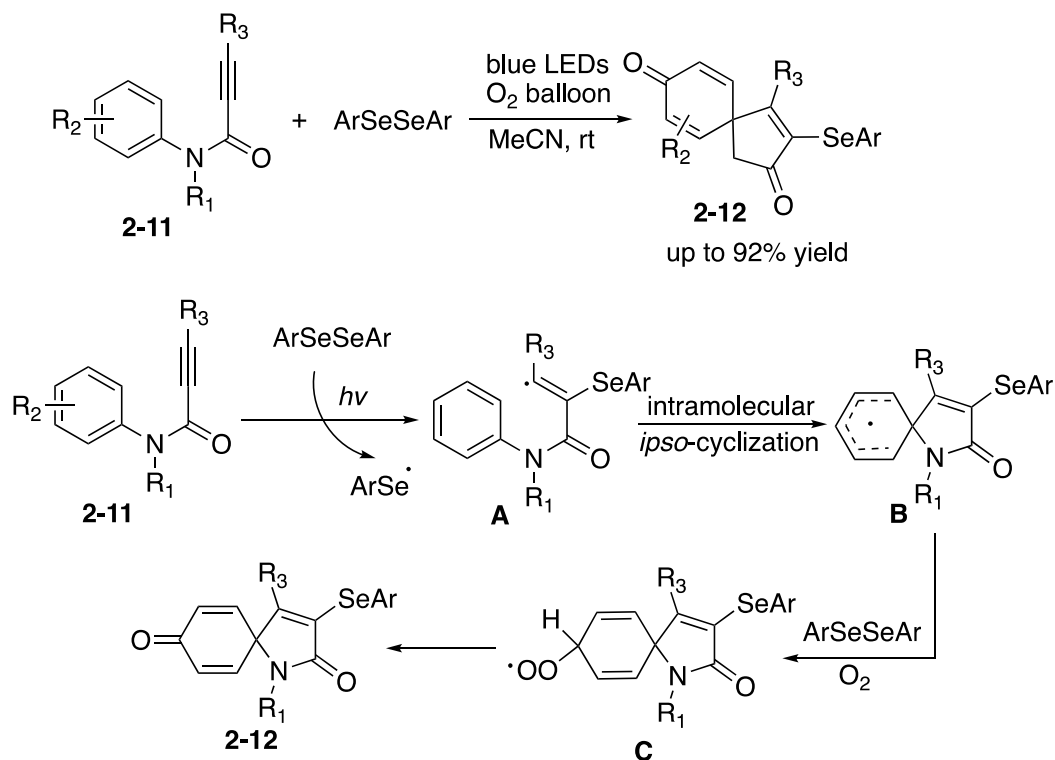
From their continuous study of visible-light-photoredox catalysis, also in 2017 Wang group found that the strategy also provided simple and efficient access to 3-sulfanyl- and 3-selanylindoles **2-10** via tandem cyclization between 2-alkynylanilines **2-8** and diaryl disulfides or diaryl diselenides **2-9** under mild reaction conditions in one-pot without a photocatalyst (Scheme 2-4).⁹ Under the best reaction conditions, the desired products 3-sulfanyl- and 3-selanylindoles **2-10** was generated in good to excellent yields with good functional group compatibility. Based on the preceding literature and radical capture experiments, a plausible reaction mechanism was proposed in Scheme 2-4. Firstly, the irradiation of H₂O₂ to undergo homolytic cleavage to produce hydroxyl radicals, which reacted with 2-alkynylaniline **2-8** through a single electron transfer (SET) pathway to form intermediate **A**. Then, the obtained **A** underwent an intermolecular cyclization to afford intermediate **B**, followed by a deprotonation to generate intermediate **C**, which further interacts with diphenyl disulfide **2-9** to give the desired product **2-10**.



Scheme 2-4 Visible-light-induced tandem oxidative cyclization and proposed catalytic cycle

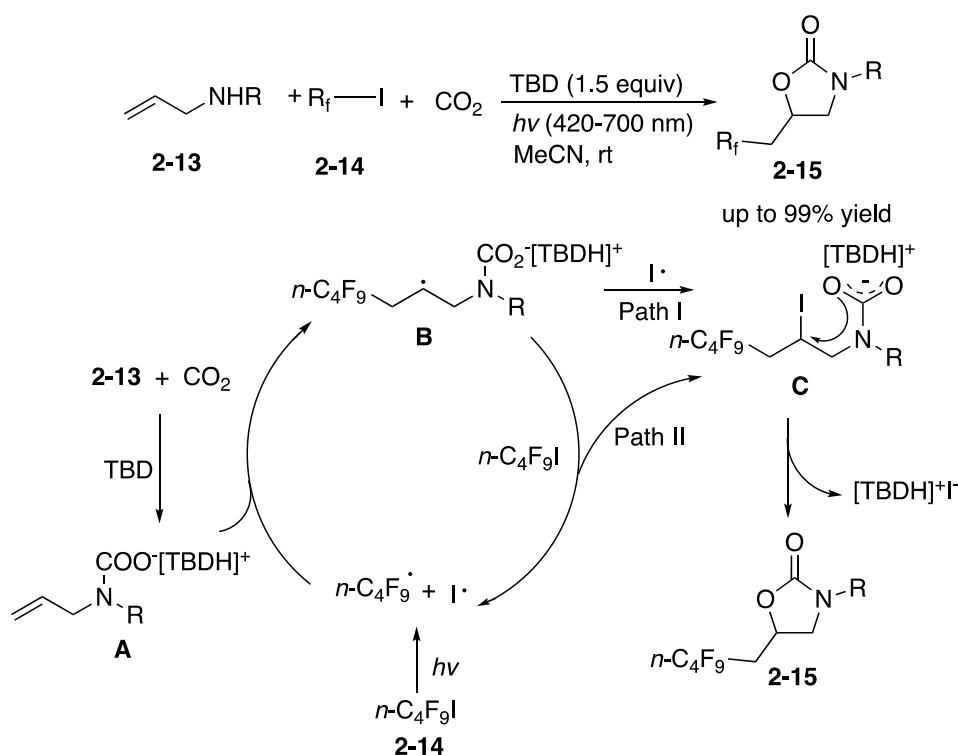
The arylselenium radical could also be used in the construction of spiro compounds. In 2018, the Baidya group explored a visible-light-induced tandem radical cyclization/dearomatization reaction in the absence of photocatalyst, providing an efficient approach to selenium substituted 1-azaspiro[4.5]decatrionediones **2-12** (Scheme 2-5). The protocol features operational simplicity, scalability, broad substrates scope, and uses molecular oxygen as an oxidant. Based on the results of control experiments, a tentative mechanism was

proposed, as shown in Scheme 2-5. The arylselenium radical was generated upon illumination with blue LEDs, adds to *N*-alkynoylanilines **2-11** to deliver radical **A**, which subsequently undergoes an intermolecular radical *ipso*-cyclization to afford **B**. In the oxygen atmosphere with diaryl diselenide, radical **B** is converted into intermediate **C**, which finally leads to spirocyclized product **2-12** after O-O bond cleavage.¹⁰



Scheme 2-5 Visible-light-induced selenylative spirocyclization and proposed mechanism

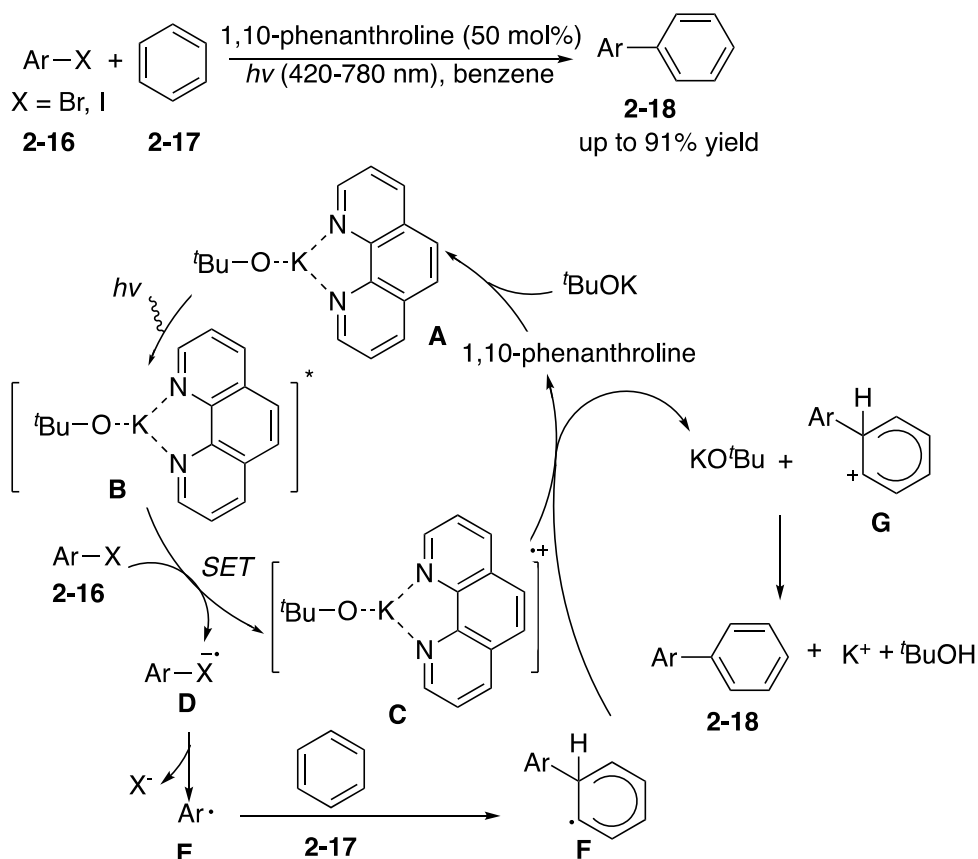
The group developed an unprecedented radical protocol for carboxylative cyclization of allyl amines **2-13** with CO₂ promoted by visible light irradiation with high efficiency under ambient conditions. By using perfluoroalkyl iodides **2-14** as radical and fluorine sources, this strategy achieves concurrent and direct incorporation of both CO₂ and perfluoroalkyl moiety into oxazolidinones **2-15** in excellent yields (Scheme 2-6).¹¹



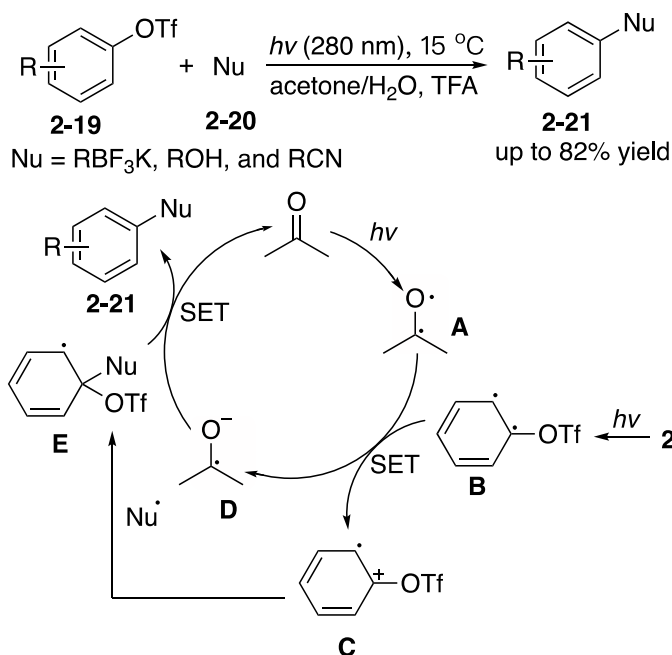
Scheme 2-6 Visible-light-induced carboxylative cyclization and proposed mechanism

A possible mechanism for the reaction is described in Scheme 2-6. Firstly, the $n\text{-C}_4\text{F}_9\cdot$ and $\text{I}\cdot$ radical species were generated *via* a homolytic cleavage process of $n\text{C}_4\text{F}_9\text{I}$ under the irradiation of visible light. Then, addition of the $n\text{-C}_4\text{F}_9\cdot$ radical to carbamate intermediate **A**, which is formed from allylamines **2-13** and CO_2 in the presence of TBD (1,5,7-triazabicyclo[4.4.0]dec-5-ene), gives the carbon radical **B**, which is trapped by $\text{I}\cdot$ radical to produce the iodo-perfluoroalkylated carbamate intermediate **C** (path I). Alternatively, the intermediate **C** might be formed *via* a radical propagation of **B** with $n\text{C}_4\text{F}_9\text{I}$ (Path II). Finally, intramolecular nucleophilic cyclization of **C** gives the desired product **2-15** with release of $[\text{TBDH}]^+\text{I}^-$.

Yuan and co-workers developed a visible light photoredox catalysed coupling reaction of aryl halides **2-16** with benzene **2-17** through using 1,10-phenanthroline as ligand. Under the standard conditions, a variety of aryl halides **2-16** with different functional groups were compatible in this reaction, affording the desired products **2-18** in high efficiency (Scheme 2-7).¹² A possible mechanism was shown in Scheme 2-7. Under visible light irradiation, the SET from electron-donor $\text{KO}t\text{-Bu}$ to electrondeficient phenanthroline *via* complex **A** provides the phenanthroline radical anion. Then, the electron of the excited intermediate **B** is transferred to aryl halides **2-16** to give the aryl radical **E** and intermediate **C**. Radical addition of **E** and oxidation of **F** afford cation intermediate **G**, which will be transformed to the final products **2-18** with the assistance of $\text{KO}t\text{Bu}$.



Recently, Li group reported a general protocol to a photoinduced C-C, C-O and C-N cross-coupling of aryl triflates **2-19** using trifluoroborates, aliphatic alcohols and nitriles as nucleophiles **2-20**, respectively. Desired biaryls products, aryl alkyl ethers and anilides **2-21** were synthesized in the absence of any transition-metal catalyst promoted by light at mild temperature (15 °C) (Scheme 2-8). Based on DFT calculations as well as CV and fluorescence investigations. The proposed mechanism was depicted in Scheme 2-8. Under light irradiation, both acetone and aryl triflate can be excited to their triplet states (**A** and **B**). The SET process would occur to produce radical cation **C** and radical anion **D** since high reactivity of **A** and **B**. The aryl radical cation **C** would be converted to radical intermediate **E** following reaction with the nucleophile. Another SET from intermediate **D** to **E** with the triflate ion as the leaving group would deliver the desired aromatic substitution product **2-21**.¹³

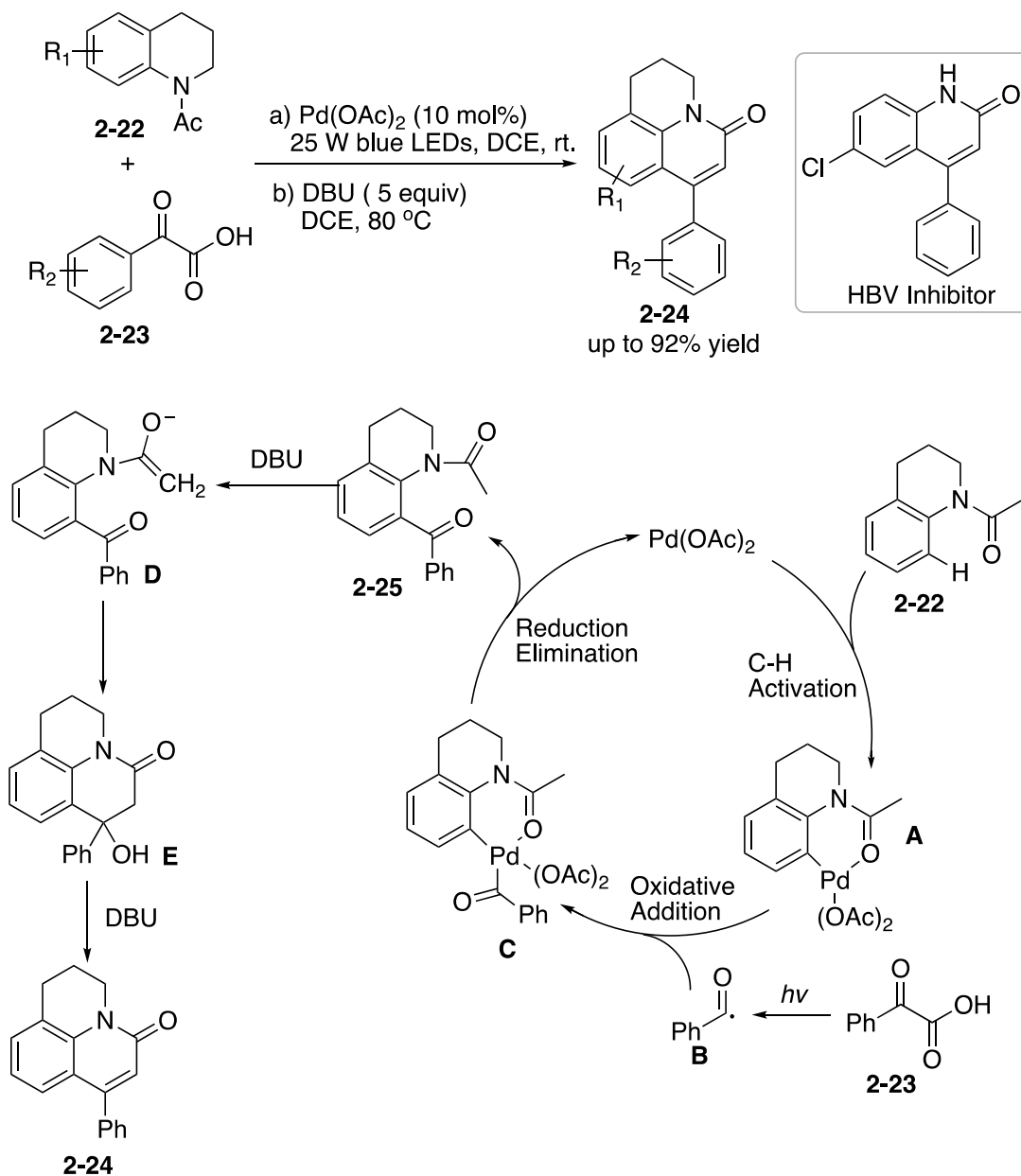


Scheme 2-8 Photoinduced C-C, C-O and C-N cross-coupling with aryl triflates and proposed mechanism.

Photoreactions have become powerful synthetic tools with a broad scope of application. Above reactions focus on photoreactions in the absence of transition-metals and photosensitizers. Photoinduced transition-metal-catalyzed reactions without photosensitizers also have been reported. We have made a short summary about photosensitizer-free gold catalysed reaction in Chapter 1. Visible-light-driven another metals such as Pd- and Cu-catalyzed reactions without photosensitizer also have been reported.

Chu and co-workers reported decarboxylative coupling/intramolecular cyclization cascade between tetrahydroquinolines **2-22** and 2-aryl-2-oxoacetic acids **2-23** induced by visible light leading to a mild, efficient, and atom economical one-pot access for the construction of 4-aryl-2-quinolinones **2-24** (Scheme 2-9).¹⁴ The reaction tolerates various functional groups with excellent yields. In addition, the protocol could be used for the synthesis of HBV inhibitor in excellent yield. Although the reaction mechanism is unclear at this stage, a tentative mechanism to rationalize this transformation is illustrated on the basis of previous reports in Scheme 2-9.¹⁵ First, intermediate **A** was generated from the active palladium catalyst reacts with **2-22** via chelation-directed C-H activation. Meanwhile, 2-oxo-2-phenylacetic acid **2-23** absorbs visible light to generate the benzoyl radical **B** through a decarboxylation process. Subsequently, **A** undergoes oxidative addition with **B** to give intermediate **C**. Subsequently, the intermediate **2-25** was obtained by the reductive elimination of **C** and Pd(II) catalyst continuing to participate

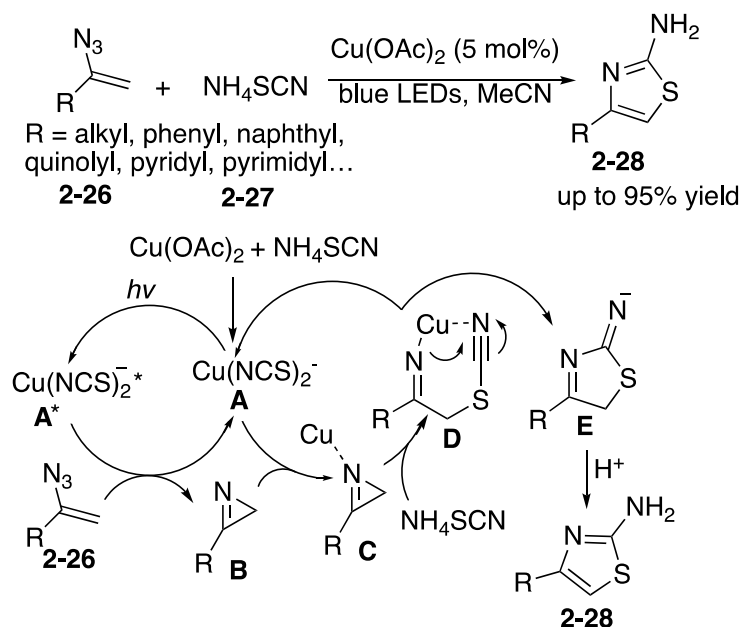
in the next catalytic cycle. Then the compound **2-25** is converted to the target compound **2-24** by the aldol condensation in the presence of DBU.



Scheme 2-9 Visible-light-driven decarboxylative coupling-intramolecular cyclization cascade and postulated mechanism

In 2017, Liu group disclosed a new methodology about synthesizing a broad range of 4-alkyl/aryl-2-aminothiazoles **2-28** *via* copper-promoted intermolecular cyclization under visible light irradiation without photocatalyst.¹⁶ In this process, the generated Cu(NCS)₂⁻ plays a dual role as both photosensitizer and Lewis acid. Under the optimized conditions, various vinyl azides with different functional groups were all well tolerated in high yields. According to the results of mechanistic investigation. A proposed mechanism involving energy transfer was described in Scheme 2-10. Following in situ formation of Cu(NCS)₂⁻ by the reaction of

Cu(OAc)₂ with NH₄SCN. Photoactivation of Cu(NCS)₂⁻ **A** produces its excited state A*, Then energy transfer from the excited Cu(NCS)₂⁻ to vinyl azides **2-26** takes place and produces 2*H*-azirines. Lewis acid activated intermediate 2*H*-azirines **C** then undergo nucleophilic ring opening with thiocyanide **2-27** providing intermediate **D**. Finally, intramolecular nucleophilic attack of the cyanide with imino anion forms the desired 2-aminothiazoles **2-28**.



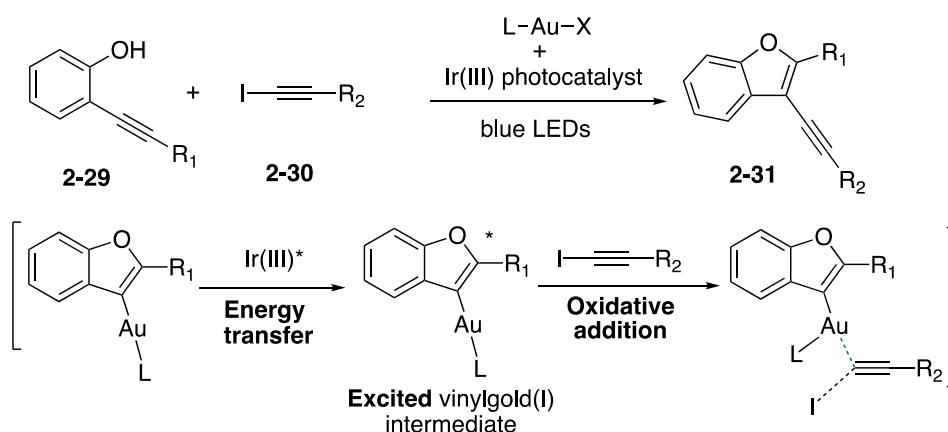
Scheme 2-10 Visible-light-driven construction of thiazoles and proposed catalytic cycle

2. Project Aim and Introduction

Over the last two decades, homogeneous gold catalysis has become a powerful tool and versatile tool for C-C and C-heteroatom bond formation.¹⁷ In the majority of cases, the gold catalyst acts as a soft π -Lewis acid and selectively activates a carbon-carbon multiple bond in the starting material toward intra- or intermolecular nucleophilic addition. This step leads to the formation of organogold(I) species, which then typically undergoes fast protodemetalation to afford hydrofunctionalized products. Based on this reactivity, numerous organogold intermediates have been proposed to support the advanced mechanisms. The reactivity of organogold(I) intermediates has recently elicited strong interest.¹⁸ In order to access to higher molecular complexity,¹⁹ the final protodeauration step has to be circumvented and the post-functionalization of organogold intermediates *via* C-C bond formation appears highly desirable. Nevertheless, the oxidative addition at gold(I) is difficult compared with the commonly used metals in catalysis since the high redox potential of the Au(I)/Au(III) couple,²⁰ which requires strong external oxidants such as hypervalent iodine reagents or F⁺ donors in stoichiometric amount.²¹ These conditions diminish one of the attractive features of gold catalysis, mild reaction conditions and excellent functional group tolerance. There has been a need to devise

pathways in order to circumvent these harsh conditions.²² The research groups of Glorius²³ and Toste²⁴ have shown the potential of these strategies which involve Au(I)/Au(III) catalytic redox cycles, this approach operates under mild reaction conditions and shows excellent functional group tolerance. In these systems, a photosensitizer, in addition to the gold catalyst, and an aryl radical source, which in this case functions as the oxidant as well as the reagent (aryldiazonium salts or diaryliodonium salts), are used to address the barrier of the Au(I)/Au(III) cycle. Hashmi,²⁵ Toste²⁶ and Patil²⁷ groups have showed that these strategies can also be conducted without the need for an additional photosensitizer. While ligand design for gold(I) has emerged to trigger oxidative addition, versatile catalytic cross coupling reactions, notably thanks to the use of hemilabile (P,N) ligands, have been recently worked out.²⁸

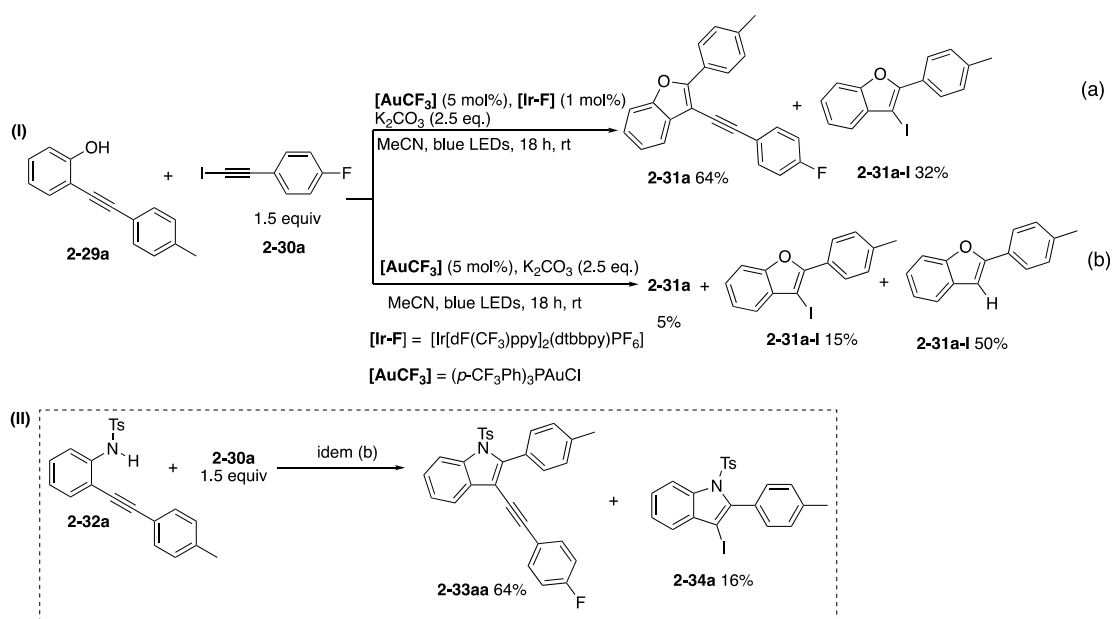
Recently, we have reported the first example of a new reactivity paradigm by providing an energy transfer promoted oxidative addition at gold(I). Upon visible light irradiation, an iridium photocatalyst triggers *via* triplet sensitization the oxidative addition of an alkynyl iodide onto a vinylgold(I) intermediate to deliver *Csp*²-*Csp* coupling products after reductive elimination. Mechanistic and modelling studies suggest that an energy transfer²⁹ event takes place to generate a triplet state of vinylgold intermediate, rather than a redox pathway. The latter can engage in oxidative addition with an alkynyl or a vinyl iodide. This novel mode of activation in gold homogenous catalysis was applied in several dual catalytic processes. Especially, alkynylbenzofuran derivatives like **2-31** could be obtained from *o*-alkynylphenols **2-29** and iodoalkynes **2-30** in the presence of catalytic gold(I) and an iridium(III) complexes under blue LEDs irradiation (Scheme 2-11).³⁰



Scheme 2-11 Previous work: alkynylative cyclization of *o*-alkynylphenols *via* photosensitized oxidative addition

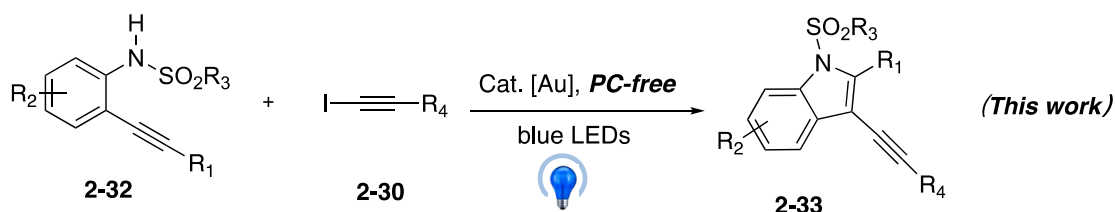
While we were studying possible synthetic extensions of this chemistry, we made some puzzling observations when comparing the reactivity of *o*-alkynylphenol precursor **2-29a** and

o-alkynyl NTs amide **2-32a** in the presence of 5 mol% $[\text{AuCF}_3]$ ($(p\text{-CF}_3\text{Ph})_3\text{PAuCl}$) and K_2CO_3 under blue LEDs irradiation. In the first case, desired product benzofuran **2-31a** was obtained with 64% yield in the presence of 1 mol% $[\text{Ir}[\text{dF}(\text{CF}_3)\text{ppy}]_2(\text{dtbbpy})\text{PF}_6]$ photocatalyst (Scheme 2-12, I(a)). However, It's very little amount of **2-31a** (5%) was observed in the absence of the photocatalyst (Scheme 2-12, I(b)). In sharp contrast, 3-((4-fluorophenyl)ethynyl)-2-(*p*-tolyl)-1-tosyl-1*H*-indole **2-33aa** was generated in 64% yield from the reaction NTs amide **2-32a** with 1-fluoro-4-(iodoethynyl)benzene **2-30a** under the photocatalyst-free reaction conditions (Scheme 2-12,II). (Notes: in part from a manuscript in preparation.)



Scheme 2-12 Contrasting reactivity between a phenol **2-29a** and the sulfonamide precursors **2-32a**

Based on this result, we are very interesting to examine the generality of this reaction since indoles are key motifs in many relevant natural products and indole systems exhibit pharmacological activities, and are also present in commercially important products such as agrochemicals, essential oils, cosmetics, flavoring fragrance, dyes, and photosensitizer compounds.³¹ Herein, we successfully developed a new type of visible light-mediated gold-catalyzed $\text{Csp}^2\text{-Csp}$ cross coupling reaction to formed 2,3-disubstituted indole derivatives **2-33** without photosensitizers or an external oxidant (Scheme 2-13).

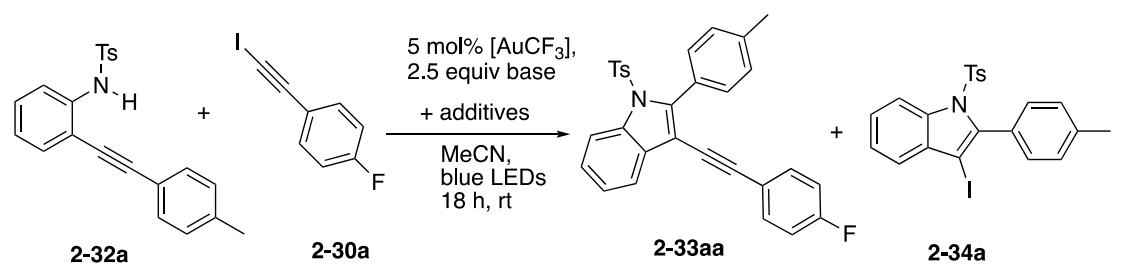


Scheme 2-13 This work: Reactant induced photoactivation of a gold-catalyzed Csp^2 - Csp cross coupling leading to benzoindoles **2-33**

3. Results and Discussion

3.1 Optimization Studies

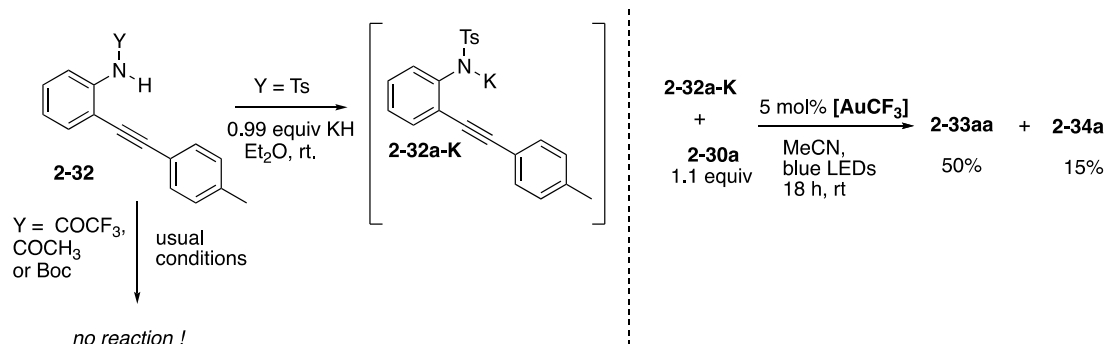
We initiated our work by examining the model reaction between 4-methyl-*N*-(2-(*p*-tolylethynyl)phenyl)benzenesulfonamide **2-32a** and 1-fluoro-4-(iodoethynyl)benzene **2-30a** under various conditions (Table 2-1). Desired product **2-33aa** was formed under the conditions: a mixture of [AuCF₃] (5 mol%), K₂CO₃ (2.5 eq.) in MeCN (4.5 mL) was stirred under irradiation for 18h with Blue LEDs in a N₂ atmosphere. Structure of **2-33aa** was confirmed by X-ray diffraction (XRD) analysis. On the same time, 3-iodo-2-(*p*-tolyl)-1-tosyl-1*H*-indole **2-34a** was generated in 16% yield (Table 2-1, entry 1). However, it was detrimental for the reaction when we used PPh₃AuCl instead of [AuCF₃] since only 50% of conversion was observed and only 8 % of **2-33aa** was detected on the crude ¹H NMR spectrum (Table 2-1, entry 2). Although benzoindole **2-33aa** was formed in 38% yield by using 1 mol% [Ir[dF(CF₃)ppy]₂(dtbbpy)PF₆] as photocatalyst, it is not as much as in photosensitizer free conditions and the selectivity **2-33aa** vs **2-34a** was lower (Table 2-1, entries 1 & 3). Additionally, the addition of 10 mol% benzophenone as photosensitizer proved to have no effect in terms of yield and selectivity for **2-33aa** (Table 2-1, entry 4). We diminished the source of iodine in the reaction conditions in order to reduce the quantity of **2-34a**. Fortunately, we found that a 1:1.1 ratio of **2-32a** and **2-30a** (Table 2-1, entry 5) proved to be as yielding as previous conditions ((Table 2-1, entry 1) and more selective toward **2-33aa**. Other base, such as Na₂CO₃, Cs₂CO₃, and CaCO₃, are all less effective than K₂CO₃ (Table 2-1, entries 6-8).

Table 2-1 Optimization of the formation of indole **2-33aa**.^[a]

Entry	2-32a:2-30a (ratio)	Base	Additives ^[c]	2-33aa yield (%) ^[b]	2-34a yield (%) ^[b]
1	1 : 1.5	K ₂ CO ₃	-	64	16
2 ^[e]	1 : 1.5	K ₂ CO ₃	-	8	10
3 ^[d]	1 : 1.5	K ₂ CO ₃	1 mol% [Ir]	38	18
4	1 : 1.5	K ₂ CO ₃	10 mol% Ph ₂ CO	61	16
5	1 : 1.1	K ₂ CO ₃	-	62	10
6	1 : 1.1	Na ₂ CO ₃	-	4	10
7	1 : 1.1	Cs ₂ CO ₃	-	10	6
8	1 : 1.1	CaCO ₃	-	0	0

^[a] General conditions: **2-32a** (0.3 mmol), **2-30a** (1.1 or 1.5 equiv), [AuCF₃] (5 mol%, (*p*-CF₃Ph)₃PAuCl), Base (2.5 equiv), additive, and 4.5 mL MeCN, blue LEDs, rt for 18h. ^[b] NMR yield using 1,3,5-trimethoxybenzene as internal standard. ^[c] 5 mol% PPh₃AuCl was used instead of 5 mol% [AuCF₃]. ^[d] [Ir] = [Ir[dF(CF₃)ppy]₂(dtbbpy)PF₆]

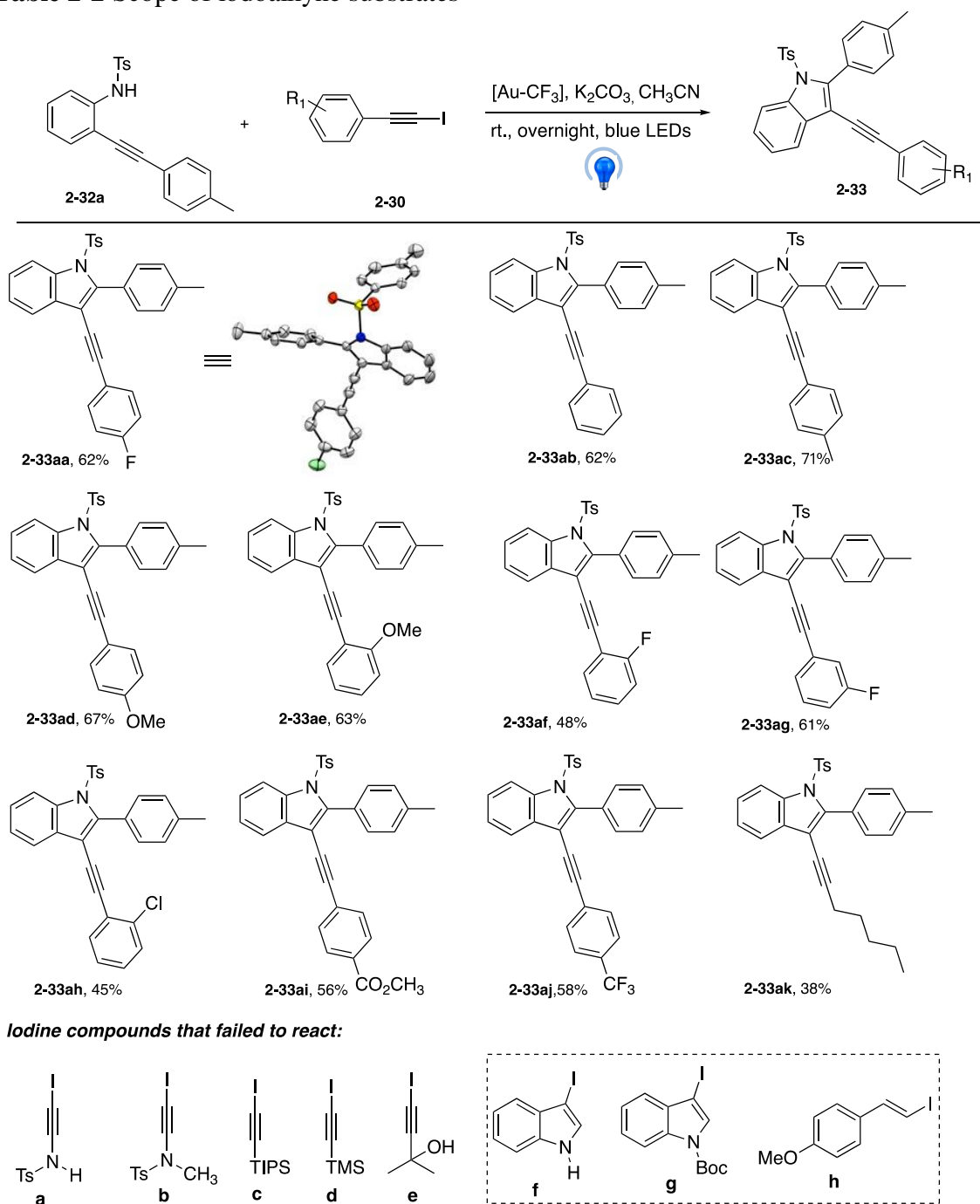
Furthermore, the reaction could be run by using a preformed potassic salt **2-32a-K**, which was prepared from a deprotonation of **2-32a** with KH (0.99 eq.) in ether at room temperature, resulting 50% yield of **2-33aa** and 15% yield of **2-34a**. In contrast, whatever the reaction conditions, all attempts with an amide (acetamide, trifluoroacetamide) or a carbamate (Boc) precursor failed to give any products (Figure 2-1). Overall, this series of findings confirmed us in using a sulfonamide nucleophile and a potassium base for further developments.

**Figure 2-1** Complementary elements of reactivity of aniline precursors **2-32**

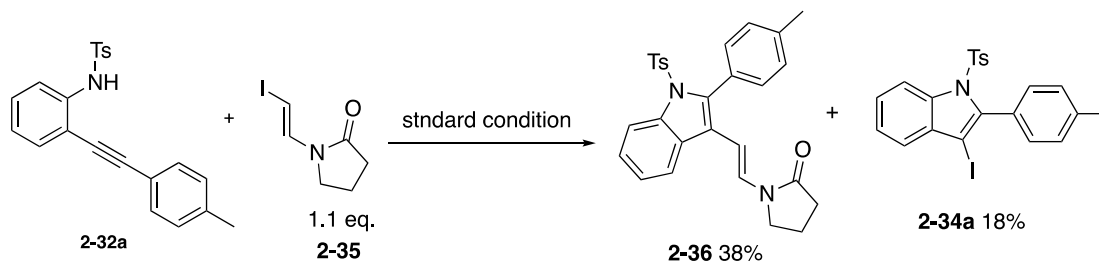
3.2 Scope and Limitation

With the optimized reaction conditions in hand (Table 2-1 entry 5), we next turned our focus on the expansion of the substrate scope by first investigating a range of iodoalkynes **2-30** (Table 2-2). A wide range of iodoalkynes **2-30** were applicable and moderate to good yields of the products **2-33** were achieved (**2-33aa** – **2-33ak**). Substrates bearing different electron-withdrawing or electron-donating groups at different positions in the aromatic ring of aryl iodoalkynes were all compatible with this reaction. When the aryl iodoalkynes **2-30** bearing electron-donating groups such as -Me and OMe, resulting provided **3-33ac**, **3-33ad** and **3-33ae** in slightly better yields (62% - 71%). Additionally, aryl iodoalkynes **2-30** bearing electron-withdrawing groups such as -F, -Cl, -CF₃ and -CO₂Me provided corresponding products **3-33** slightly lower yields. It was noted that *ortho*-substitution in the aromatic ring of aryl iodoalkynes **2-30** gave comparably lower yields, probably due to steric reasons. For example, aryl iodoalkynes **2-30** containing groups such as -OMe and -F provided the corresponding products **2-33ae** and **2-33af** in 63% and 48% yields (**2-33ad** vs **2-33ae**, **2-33af** vs **2-33aa** and **2-33ag**), respectively. Notably, the reaction was well tolerated with iodoalkyne **2-30** bearing an alkyl chain and provided product **2-33ak** in 38% yield. It is worth mentioning that among the tested starting materials, iodine compounds (from **a** to **h**) failed to afford the desired cross-coupled products. Except previous examples, other alkenyl iodide **2-35** was performed in standard reaction conditions, provided product **2-36** in 38% yield and **2-34a** in 18% yield.

Table 2-2 Scope of iodoalkyne substrates^[a]



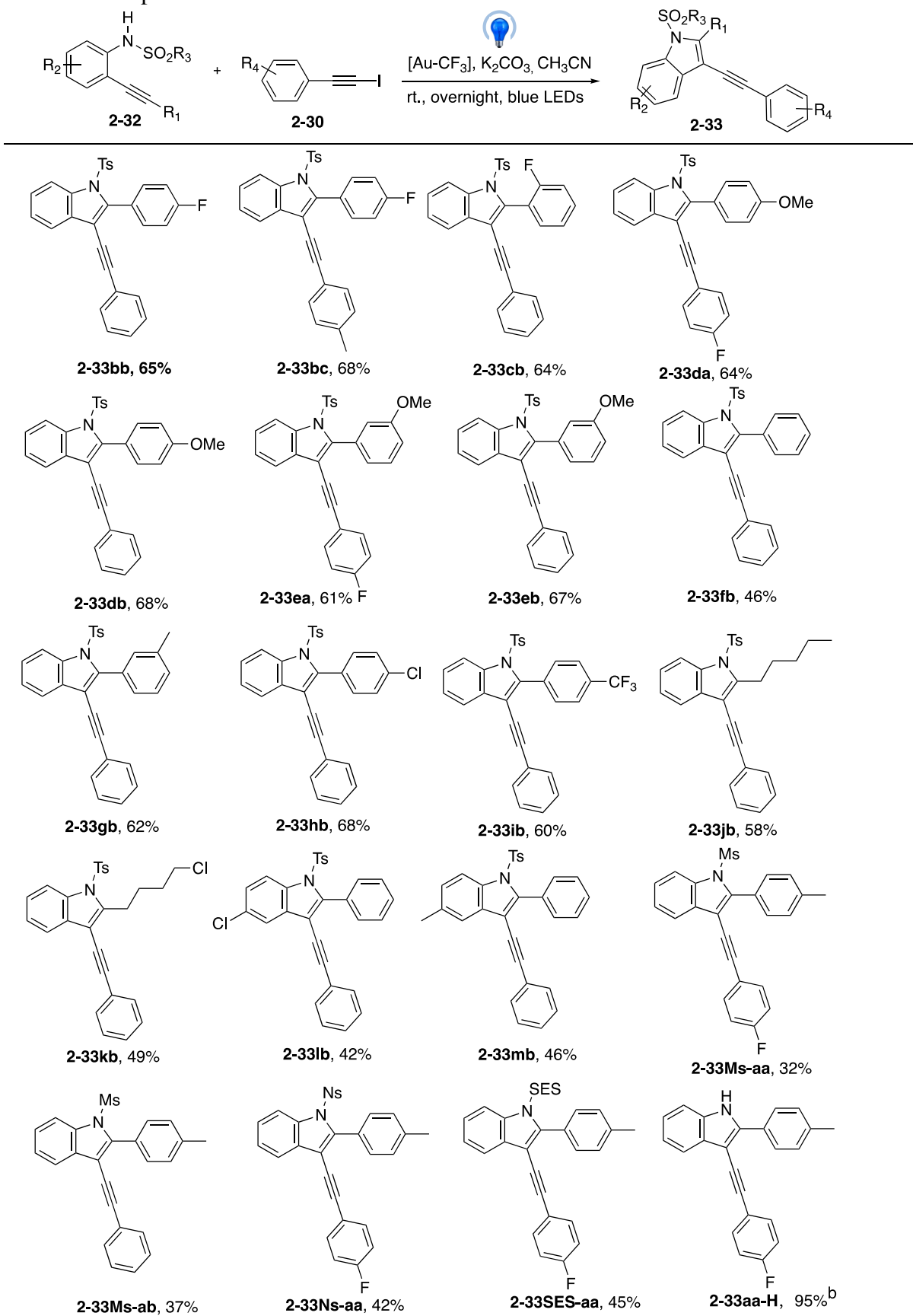
^[a] **2-32a** (0.3 mmol), **2-30** (0.33 mmol, 1.1 eq.), $[\text{AuCF}_3]$ (5 mol%), K_2CO_3 (2.5 equiv), MeCN (4.5 mL), blue LEDs, rt., overnight.



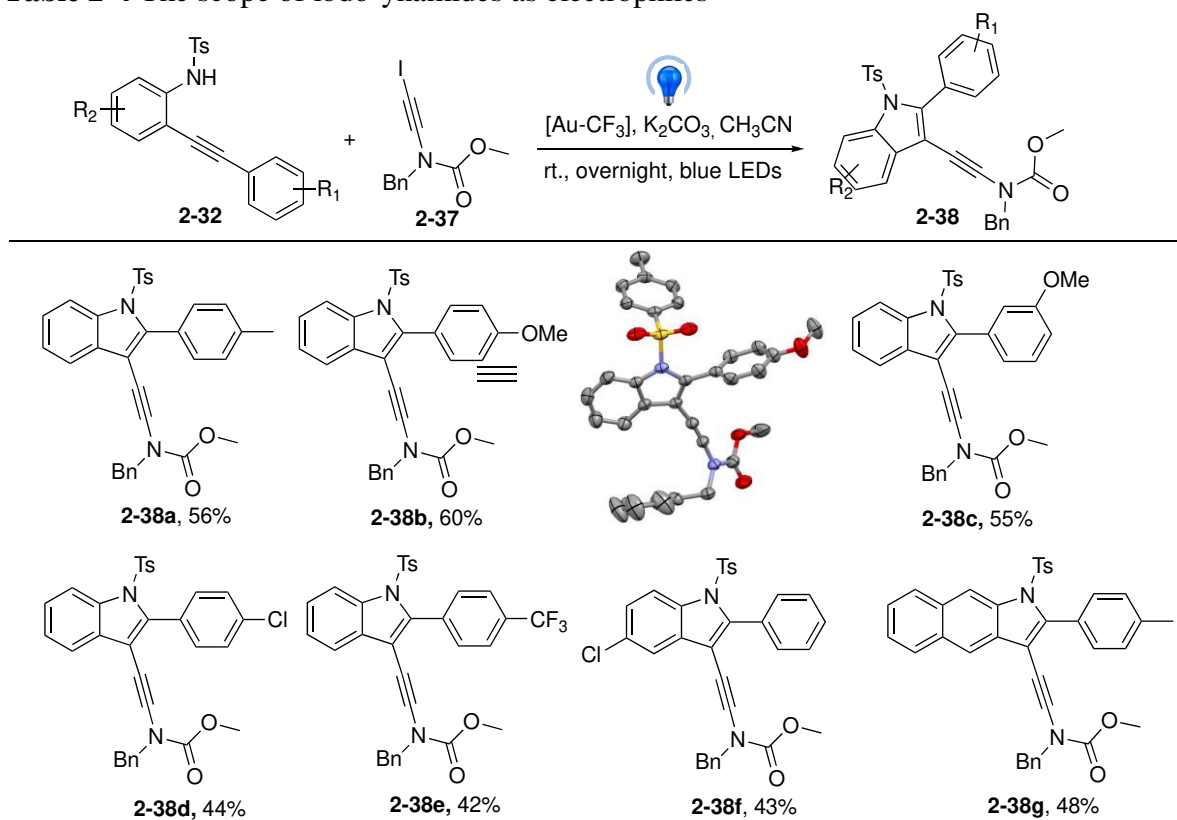
Scheme 2-14 The reaction of **2-32a** with alkenyl iodide **2-35**

We next examined the substrate scope with respect to the aniline platform **2-32** (Table 2-3). First, we examined the reaction *via* variation of the alkynyl substituent R₁. The reaction was found to be general irrespective of the substituents (electron-withdrawing/donating group) present in the aromatic rings of aromatic alkyne (**2-33bb** - **2-33ib**). The reaction was well tolerated with aromatic alkyne containing halogen group such as -F and -Cl substituents at the *para* position, giving **2-33bb**, **2-33bc**, and **2-33hb** in 65%, 68% and 68% yields, respectively. Besides, the aromatic alkyne bearing electron-withdrawing groups such as -F and -CF₃ provided **2-33cb** and **2-33ib** in good yields. Additionally, electron-donating substituents such as -Me and -OMe in any position of aromatic alkyne provided **2-33** in good yields. However, both of starting materials with no substitution gave **2-33fb** in low yield (46%). It was noted that donor alkyl groups on the alkyne were also competent providing 2-alkyl indoles **2-33jb** and **2-33kb** respectively in 58% and 49% yields. Introduction of a chlorine or a methyl groups in 4 position on the aniline precursor gave average yields (< 50%) of products **2-33lb** and **2-33mb**. Further, replacing the R₃ group to survey the importance of a sulfonyl group attached on the nitrogen atom of the aniline precursor. In general, more modest yields of indole products were obtained with mesylate precursors, which formed corresponding products **2-33Ms-aa** in 32% yield or **2-33Ms-ab** in 37% yield. Although the *N*-detosylation of indoles is known,³² even more easily disposed sulphonamide groups were tested and 42% of nosyl-indole **2-33Ns-aa** and 45% of 2-(trimethylsilyl)ethanesulfonyl (SES) indole **2-33SES-aa** were obtained. The latter could be easily converted into the free NH indole **2-33aa-H** *via* treatment with Bu₄NF.

Table 2-3 Scope of anilines^[a]



^[a] **2-32** (0.3 mmol), **2-30** (0.33 mmol, 1.1 eq.), [AuCF₃] (5 mol%), K₂CO₃ (2.5 equiv), MeCN (4.5 mL), blue LEDs, rt., overnight. ^[b] After treatment with Bu₄NF.

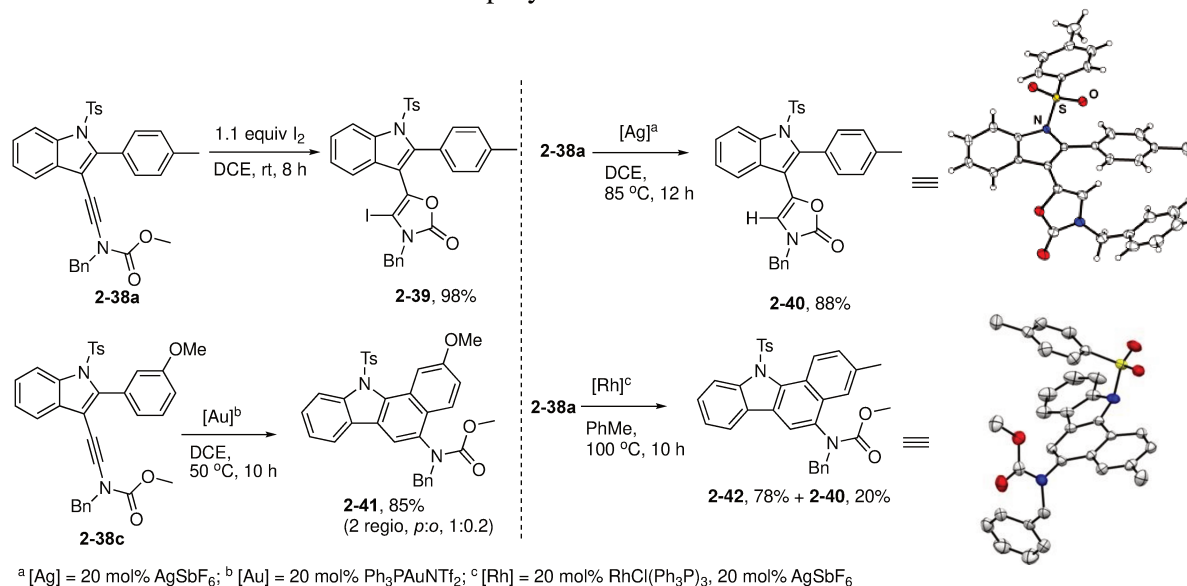
Table 2-4 The scope of iodo-ynamides as electrophiles^[a]

^[a] **2-32** (0.3 mmol), **2-37** (0.33 mmol, 1.1 eq.), [AuCF₃] (5 mol%), K₂CO₃ (2.5 equiv), MeCN (4.5 mL), blue LEDs, rt., overnight.

In order to extend the synthetic scope of this process and also to provide substrates for valuable post-functionalizations, iodo-ynamide **2-37** was tested under the optimized reaction conditions (Table 2-4). Interestingly, this substrate has been only described once by Danheiser who used it as a [2+2] cycloaddition partner.³³ Gratifyingly, iodo-ynamide **2-37** reacted a little bit less efficiently than iodoalkynes **2-30** with a series of anilines **2-32**, but it provided valuable functionalized scaffolds **2-38**. The aromatic ring substrates bearing electron-donating group (Me, OMe) appear to react more efficiently than those with electron-withdrawing group (Cl, CF₃). Furthermore, *para*-substitution in the aromatic ring of aniline platform **2-32** gave comparably higher yields (60% yield **2-38b** vs 55% yield of **2-38c**). The structure of **2-38b** has been confirmed by X-ray diffraction analysis. Notably, a naphthyl aniline precursor could also be engaged to give adduct **2-38g** in 48% yield.

3.3 Post-functionalization

Taking advantage of the electron-richness of the ynamide moiety, we devised several transformations on polyfunctionalized substrates **2-38** (Table 2-5). Iodo-oxazolone **2-39** was

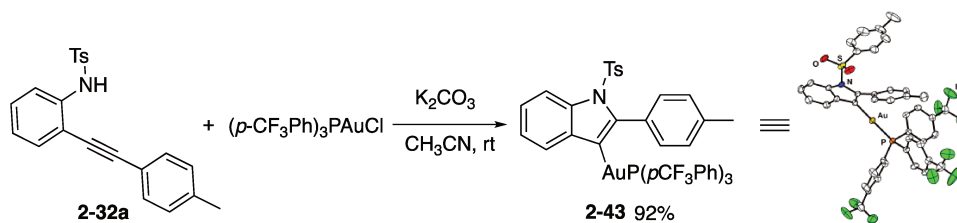
Table 2-5 Post-functionalization of polyfunctionalized substrates

smoothly formed in the presence of iodine (1.1 eq.) in fresh dry DCE at room temperature, so far, which was an unknown type of derivatives. Very interestingly, the Ag(I)-catalyzed cyclization of **2-38a** in (wet) DCE provided the corresponding oxazolone **2-40** in 88% yield *via* protodesilveration.³² Additionally, engaging the pendant aromatic ring in hydroarylation reaction was possible whether by gold(I) catalysis from **2-38c** or by cationic rhodium catalysis from less activated substrate **2-38a** to provide the corresponding carbazoles **2-41** and **2-42**. The structure of **2-40** and **2-42** have been confirmed by X-ray diffraction analysis. Benzo[a]carbazoles derivatives are important structural units found in many natural products³⁴ and biologically active molecules³⁵ as well as organic materials.³⁶

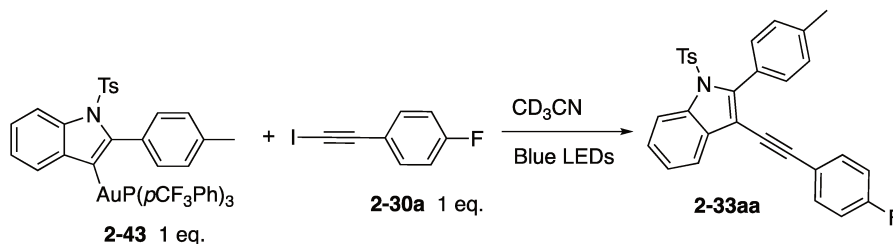
4. NMR Monitoring Experiment of Vinylgold(I) Intermediate

Based on the scope of substrates, we wished to get some insight into the mechanism of this transformation. The fact that a photo-triggered event occurs without any photocatalyst logically led us to consider the optical properties of the different partners present during the reaction. The detail NMR monitoring experiment will be discussed below.

Firstly, we prepared vinylgold intermediate **2-43** in 92% yield by reacting an equimolar mixture of **2-32a** and [Au-CF₃] in the presence of K₂CO₃ (2.5 eq.) in MeCN (Scheme 2-15). X-ray diffraction analysis of suitable crystals of **2-43** confirmed its structure and provided useful structural data for further studies.



With vinylgold(I) **2-43** in hand, we did the NMR monitoring experiment of the reaction between vinylgold(I) **2-43** and iodoalkynes **2-30a**.



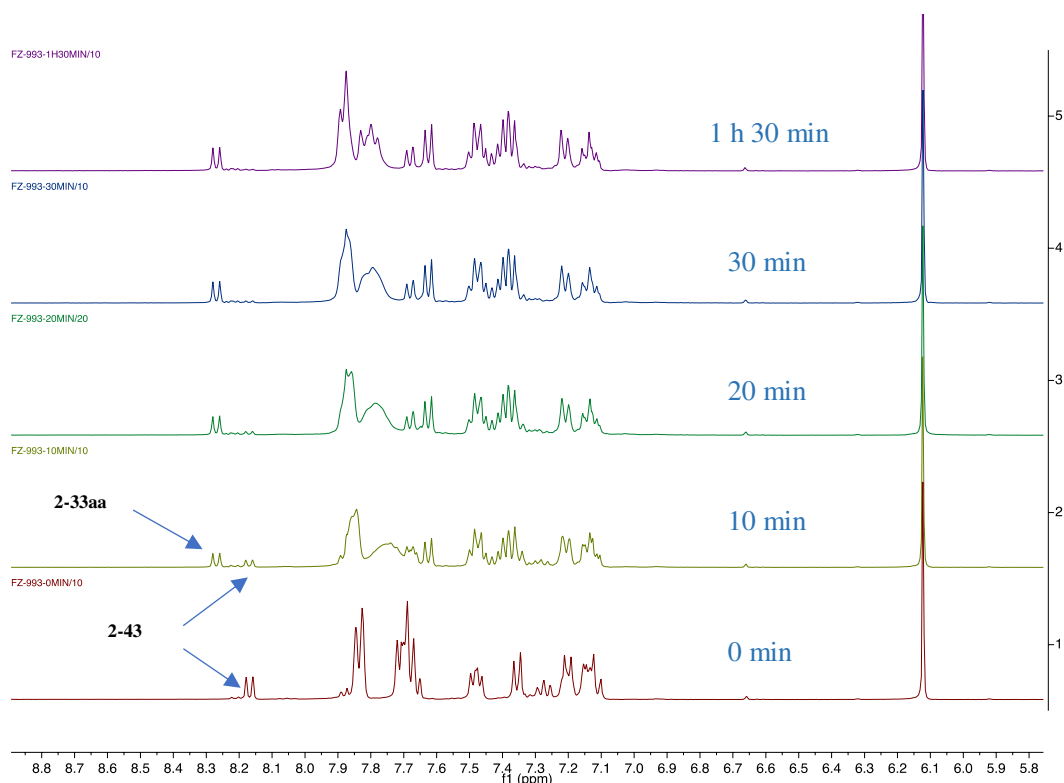
Tube A: Vinylgold(I) **2-43** (12.2 mg, 0.012 mmol) was treated with a stoichiometric amount of of iodoalkynes **2-30a** (2.9 mg, 0.012 mmol, 1.0 equiv.) in 0.6 mL of CD₃CN in a NMR tube. Added 1,3,5-trimethoxybenzene (2.0 mg, 0.012 mmol) as internal standard. Protected by aluminum paper in advance. Stirring in blue LEDs light for 10 min, 20 min, and 30 min until overnight, do ¹H NMR and ¹⁹F NMR analysis.

Tube B: Vinylgold(I) **2-43** (12.2 mg, 0.012 mmol) and [Ir[dF(CF₃)ppy]₂(dtbbpy)PF₆] (0.0012 mmol, 10 mol%) was treated with a stoichiometric amount of of iodoalkynes **2-30a** (2.9 mg, 0.012 mmol, 1.0 equiv.) in 0.6 mL of CD₃CN in a NMR tube. Added 1,3,5-trimethoxybenzene (2.0 mg, 0.012 mmol) as internal standard. Protected by aluminum paper in advance. Stirring in blue LEDs light for 10 min, 20 min, and 30 min until overnight, do ¹H NMR and ¹⁹F NMR.

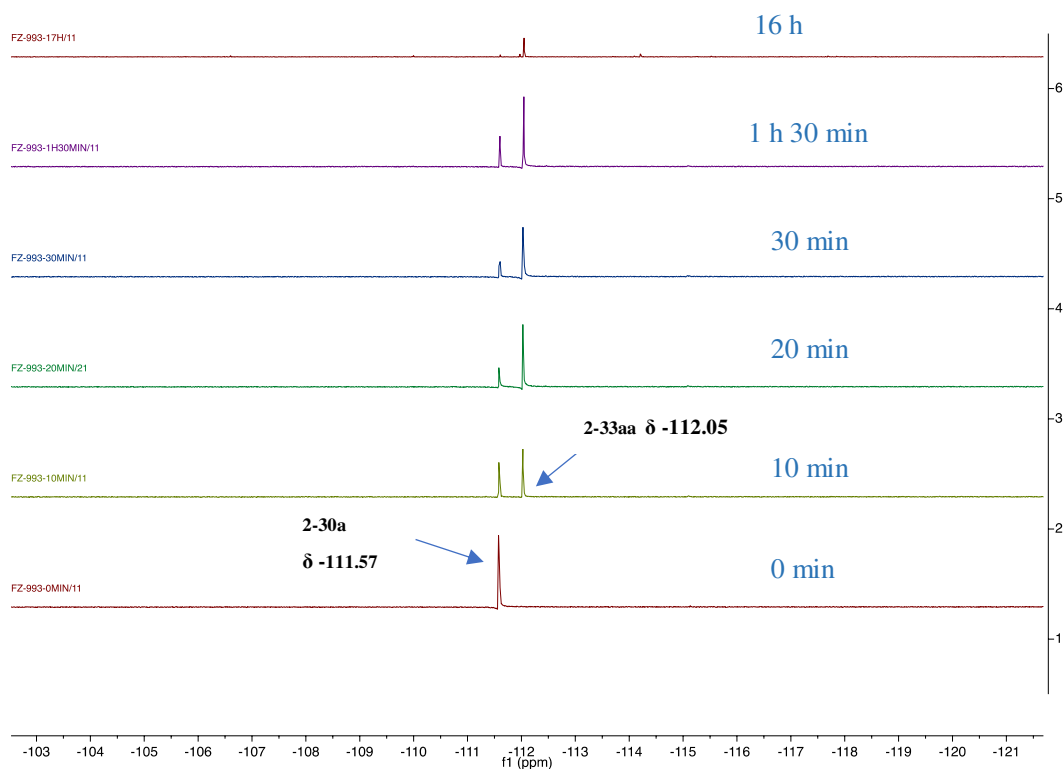
Tube C: Vinylgold(I) **2-43** (12.2 mg, 0.012 mmol) and Ph₂CO (0.0012 mmol, 10 mol%) was treated with a stoichiometric amount of of iodoalkynes **2-30a** (2.9 mg, 0.012 mmol, 1.0 equiv.) in 0.6 mL of CD₃CN in a NMR tube. Added 1,3,5-trimethoxybenzene (2.0 mg, 0.012 mmol) as internal standard. Protected by aluminum paper in advance. Stirring in blue LEDs light for 10 min, 20 min, and 30 min until overnight, do ¹H NMR and ¹⁹F NMR analysis.

Table 2-6 Yield of **2-33aa** in Tube A, Tube B and Tube C under blue LEDs light

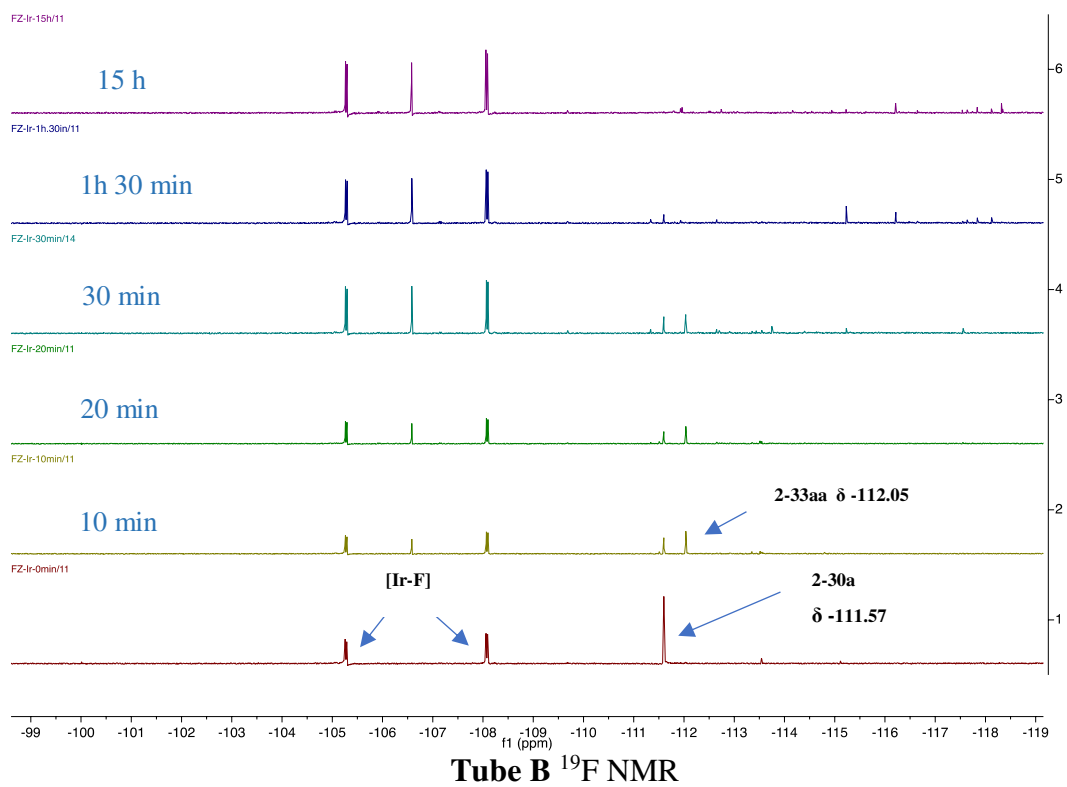
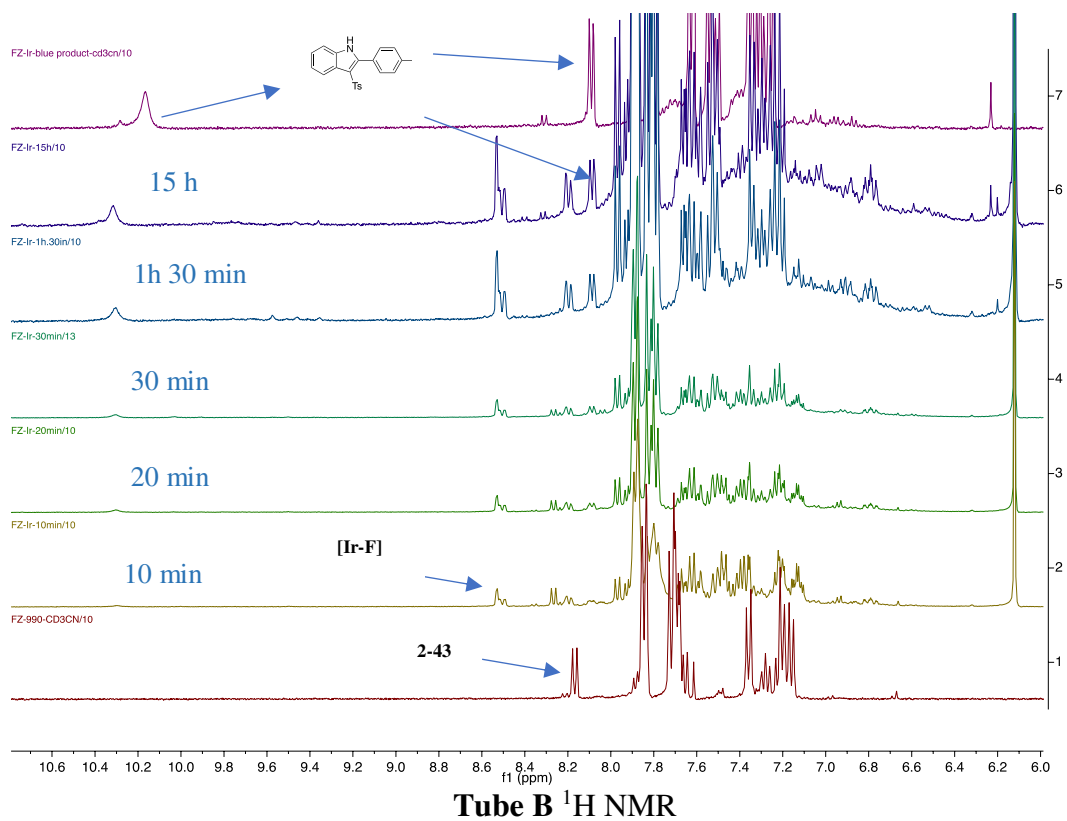
Time	Tube A (PC free)	Tube B (with Ir)	Tube C (with Ph ₂ CO)
10 min	50%	40%	18%
20 min	66%	30%	30%
30 min	76%	24%	34%
1h 30min	92%	0%	48%
15 h	95%	0%	60%

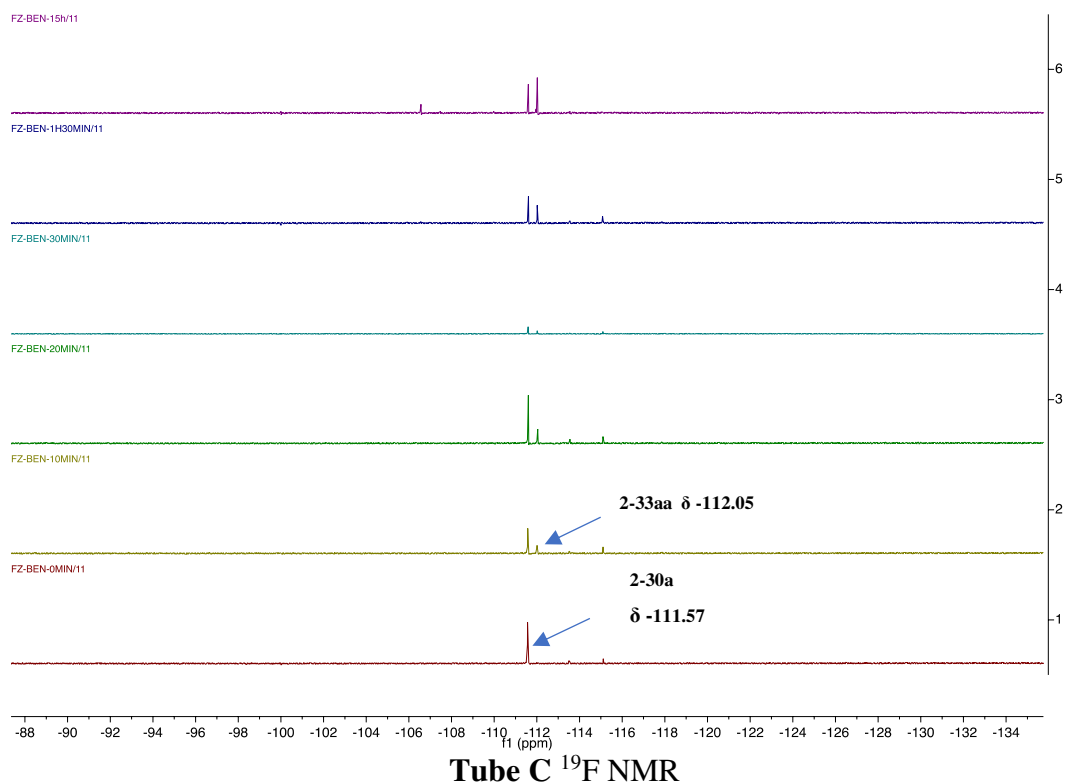
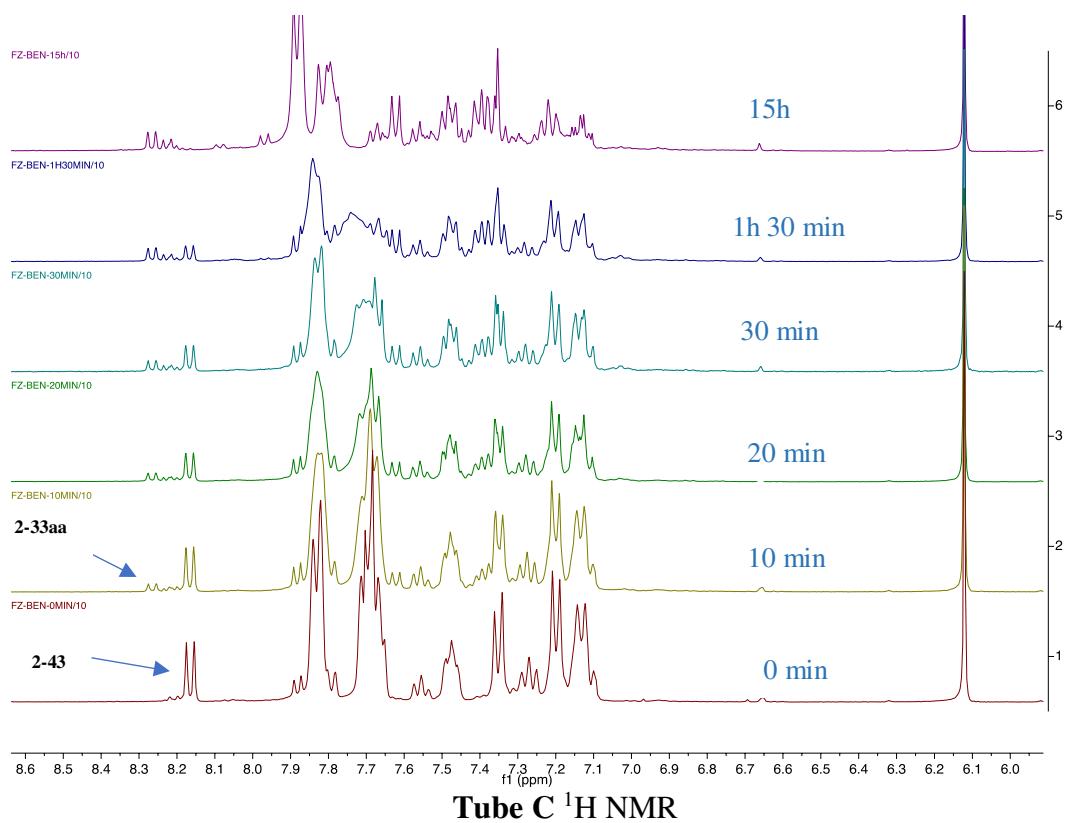


Tube A ¹H NMR

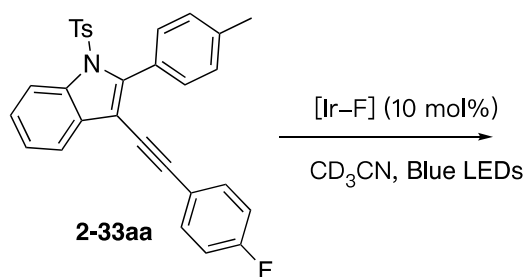


Tube A ¹⁹F NMR

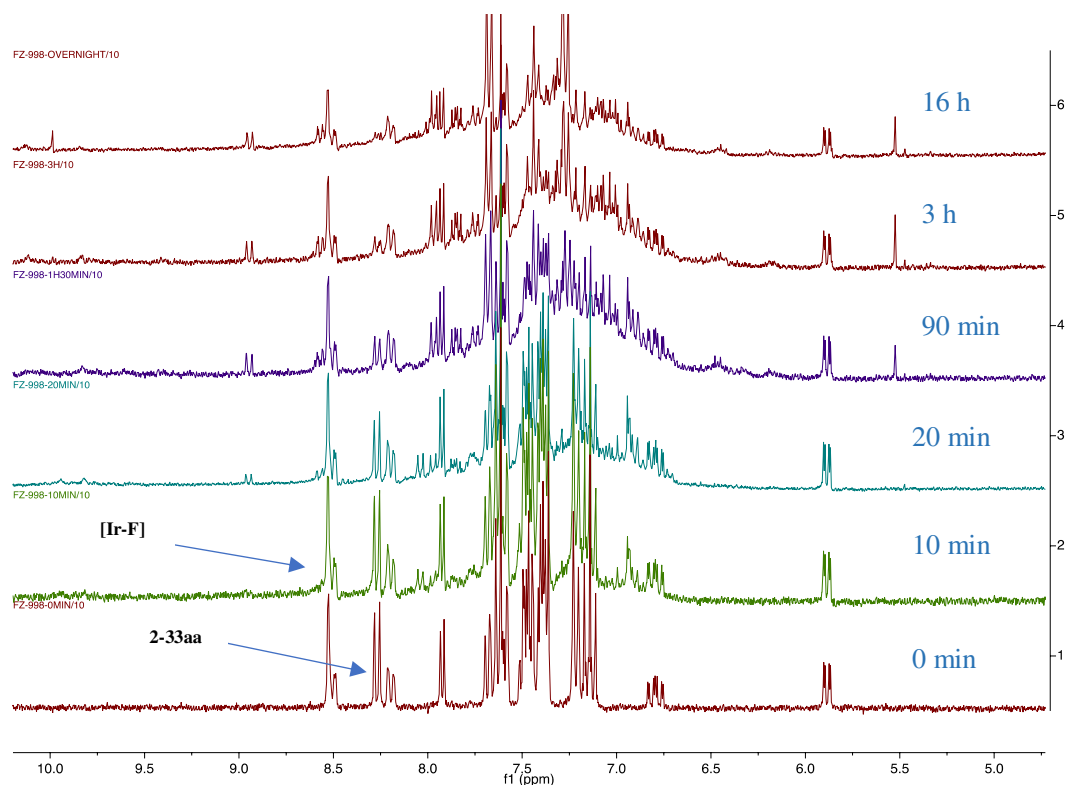




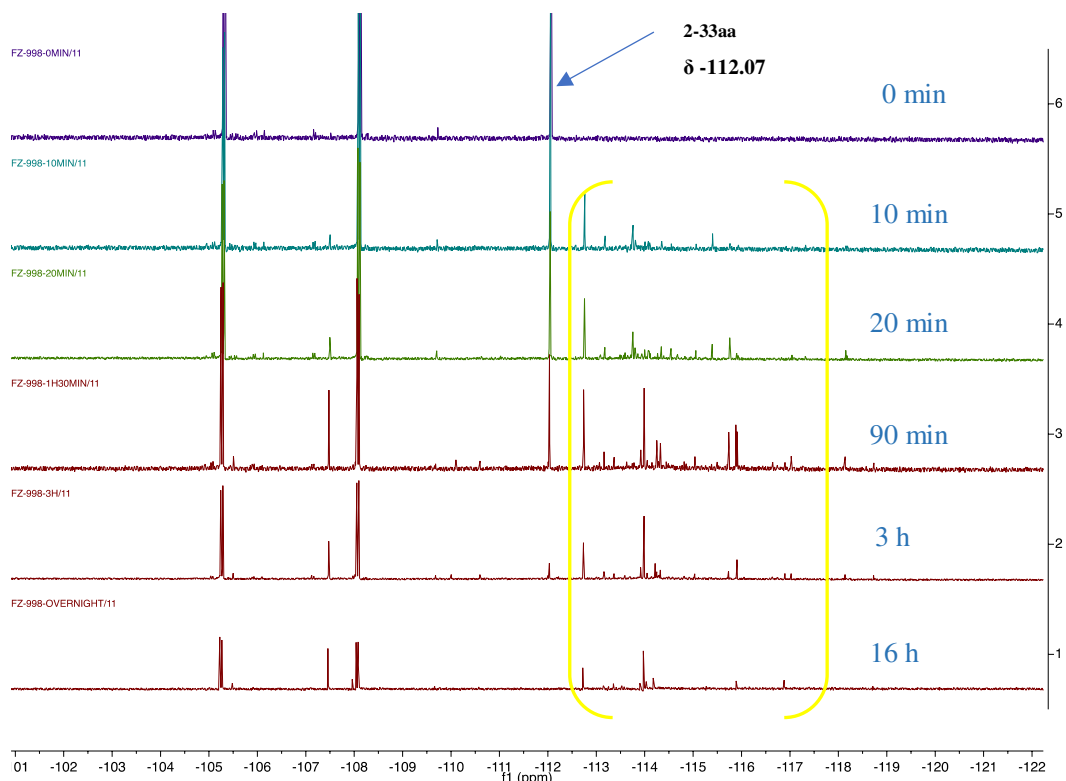
Based on above results, photocatalyst, especially [Ir-F], is not conducive to generate desired product **2-33aa**. Surprisingly, the yield of **2-33aa** from 40% decrease to 0% after 1 h 30 min. In order to understand what happened in this process, we did the NMR monitoring experiment of the reaction of **2-33aa** under 10 mol% [Ir-F] (See below for details).



Tube D: **2-33aa** (5.7 mg, 0.012 mmol) and $[\text{Ir}[\text{dF}(\text{CF}_3)\text{ppy}]_2(\text{dtbbpy})\text{PF}_6]$ (0.0012 mmol, 10 mol%) in 0.6 mL of CD_3CN in a NMR tube. Protected by aluminum paper in advance. Stirring in blue LEDs light for 10 min, 20 min, 90 min, 3h, 16h, do ^1H NMR and ^{19}F NMR analysis.



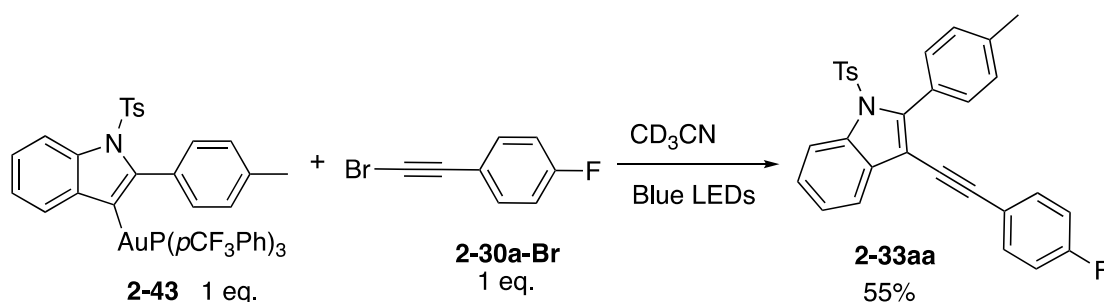
Tube D ^1H NMR



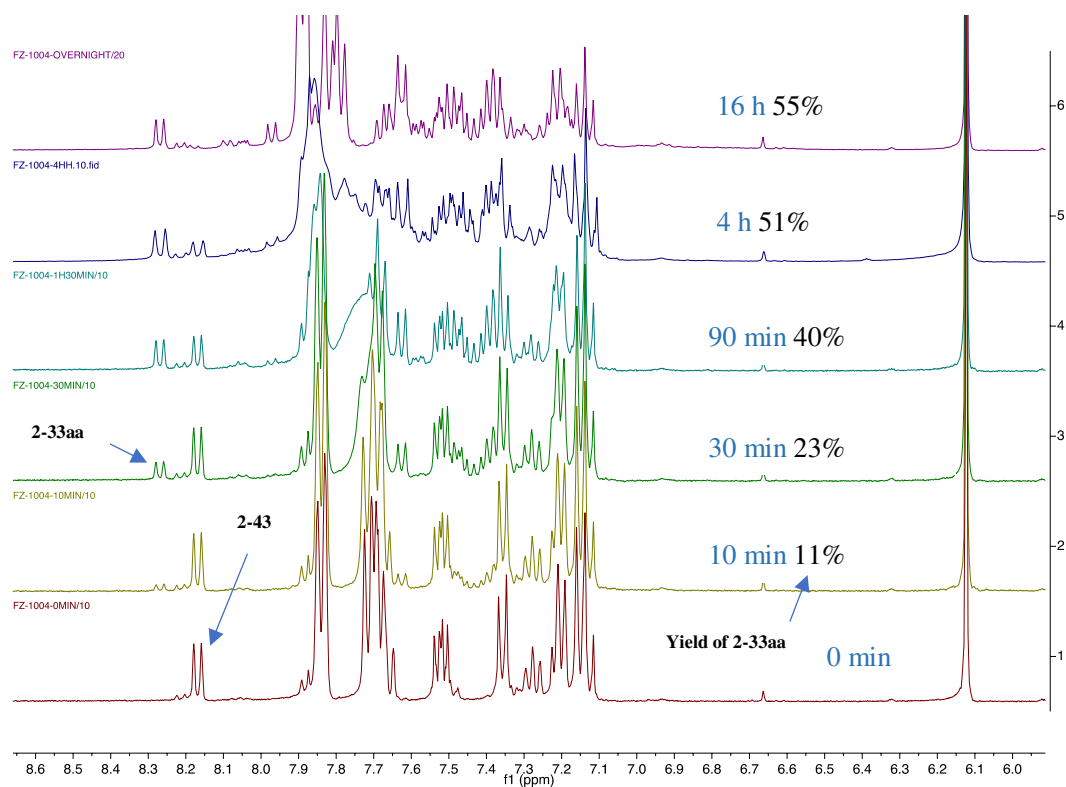
Tube D: ^{19}F NMR

It shows that **2-33aa** was totally decomposed in the presence of $[\text{Ir-F}]$. Unfortunately, we did not obtain any pure compound in this reaction.

Additionally, we also did the NMR monitoring experiment of the reaction between vinylgold(I) **2-43** and 1-(bromoethynyl)-4-fluorobenzene, as detail below:

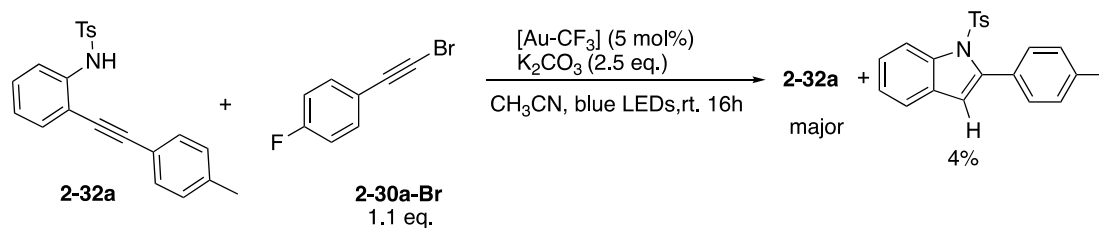


Tube E: Vinylgold(I) **2-43** (12.2 mg, 0.012 mmol) was treated with a stoichiometric amount of 1-(bromoethynyl)-4-fluorobenzene **2-30a-Br** (2.4 mg, 0.012 mmol, 1.0 equiv.) in 0.6 mL of CD_3CN in a NMR tube. Added 1,3,5-trimethoxybenzene (2.0 mg, 0.012 mmol) as internal standard. Protected by aluminum paper in advance. Stirring in blue LEDs light for 10 min, 20 min, and 30 min until overnight, do ^1H NMR analysis. The formation of **2-33aa** was observed by NMR in 55% yield after irradiation by blue LEDs 16 h.



Tube E: ^1H NMR

Based on this result, furthermore, we did the reaction between **2-32a** and **2-30a-Br** in standard reaction conditions. Unfortunately, the desired product **2-33aa** could not be obtained in the one-pot process.



5. Conclusion

In conclusion, we have developed the first application of photosensitizer- and external oxidant-free photoredox gold-catalyzed Csp^2 - Csp of *o*-alkynyl NTs amide and aryl iodoalkynes. It provides various 2,3-disubstituted indole derivatives in moderate to good yields under very mild reaction conditions. Additionally, the reaction was well tolerated with iodoalkynes bearing an alkyl chain. Donor alkyl groups on the alkyne of *o*-alkynyl NTs amide were also competent providing 2-alkyl indoles. It can give corresponding 2,3-disubstituted indole derivatives in quite good yields when Ts group was instead by Ms, Ns, and SES. In contrast, whatever the reaction conditions, all attempts with an amide (acetamide, trifluoroacetamide) or a carbamate (Boc) precursor failed to give any products. Of note, iodo-ynamides that have very rarely been used in any organometallic cross coupling reaction could be used as electrophiles. The resulting alkynylated indoles lend themselves to various post-functionalization providing valuable scaffolds. NMR monitoring experiments on the vinylgold(I) intermediate showed that photocatalyst, especially [Ir-F], is not conducive to generate desired product. Further investigations of the reaction mechanism are ongoing.

6. Experimental Section

6.1 General Informations

All reactions involving air sensitive reagents or intermediates were carried out in pre-heated glassware under an argon atmosphere using standard Schlenk techniques. All solvents and chemicals were used as received from suppliers (Alfa Aesar, Sigma Aldrich, TCI). Acetonitrile and methanol were purified by distillation over calcium hydride under dry Argon atmosphere.

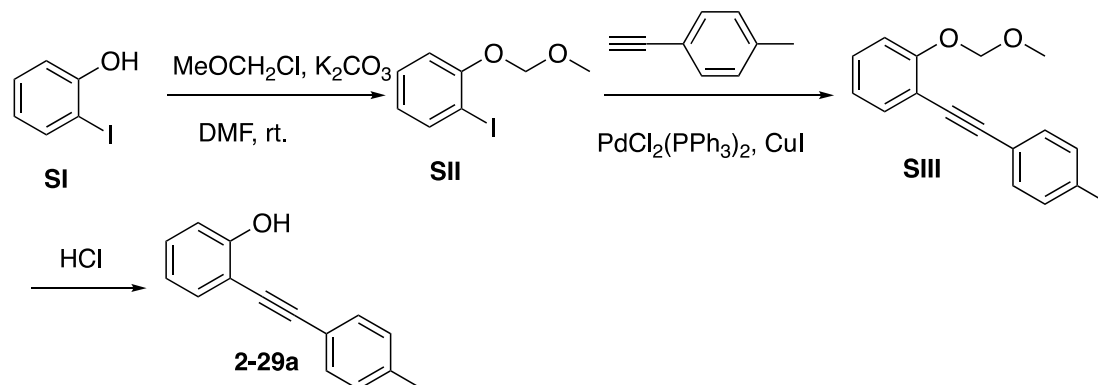
Chromatographic purifications of products were accomplished using force-flow chromatography (FC) on Davisil (LC60A) SI 60 Å (40 – 63 µm) silica gel according to the method of Still. Thin layer chromatography (TLC) was performed on Merck 60 F254 silica gel plates. Filtrations through Celite® were performed using Hyflo Super Cel from Fluka.

¹H NMR spectra were recorded on a Bruker 400 AVANCE or 300 AVANCE (400 and 300 MHz respectively) and are calibrated with residual CDCl₃ protons signals at δ 7.26 ppm. ¹³C NMR spectra were recorded on a Bruker 400 AVANCE or 300 AVANCE (100 and 75 MHz respectively) and are calibrated with CDCl₃ signal at δ 77.16 ppm. ¹⁹F spectra were recorded at 376.5 or 282.4 MHz and were calibrated with trifluorotoluene in CDCl₃ as external standard at δ -63.0 ppm. Data are reported as follows: chemical shift (δ ppm), multiplicity (s = singlet, d = doublet, t = triplet, q = quartet, qt = quintuplet, m = multiplet, bs = broad signal), coupling constant (Hz) and integration. High resolution mass spectrometries were performed on a microTOF (bruker) or a LTQ-Orbitrap (Thermo Fisher Scientific) by electrospray (ESI) or Atmospheric Pressure Chemical Ionization (APCI).

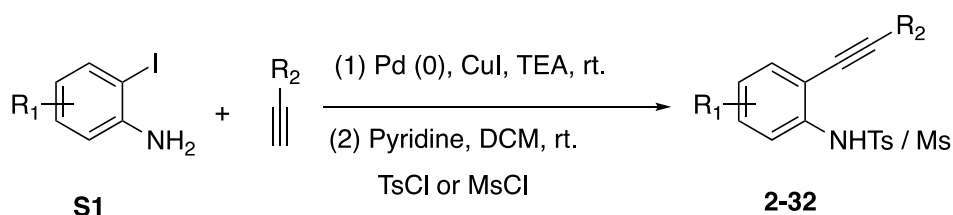
6.2 Substrate Synthesis

6.2.1 Synthesis of Starting Materials 2-(Phenylethynyl)phenol 2-29a and Anilines 2-32

2-(Phenylethynyl)phenol 2-29a³⁷:

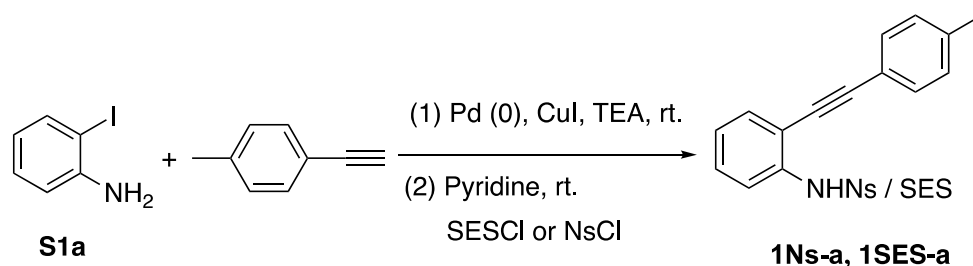


MOMCl (1.1 g, 13.6 mmol, 1.5 equiv.) was added to a mixture of 2-iodo phenol **SI** (2 g, 9.1 mmol, 1 equiv.) and K₂CO₃ (5.0 g, 36.36 mmol, 4 equiv.) in DMF (8 mL). The mixture was stirred at room temperature for 2 hours. The completion of the reaction was monitored by TLC (Pent/Et₂O: 9/1). The solution was diluted with diethyl ether (100 mL) and 60 mL of water were added. The layers were separated and the aqueous phase was extracted with diethyl ether (3 × 30 mL). The combined organic layers were washed with brine, dried over MgSO₄, filtered and concentrated under reduced pressure to afford the iodide **SII** (2.4 g, quant). The latter was engaged without further purification in the next step. To a stirred solution of 1-ethynyl-4-methylbenzene (1.2 g, 10.0 mmol, 1.1 equiv.) and **SII** (2.4 g, 9.1 mmol, 1.0 equiv.) in triethylamine (90 mL) were added PdCl₂(PPh₃)₂ (126.3 mg, 0.18 mmol, 2 mol%) and CuI (34.3 mg, 0.18 mmol, 2 mol%). The mixture was stirred at 65°C until complete consumption of **SII** was observed by TLC (Pent/Et₂O: 9/1). The reaction mixture was cooled to room temperature, diethyl ether was added (50 mL) and the mixture was filtered through a plug of cotton wool. After removal of the solvent, the residue was purified by silica gel chromatography (Pent/Et₂O: 9/1) to afford **SIII** (2.07 g, 90%). The deprotection of MOM was conducted by addition of aqueous HCl (0.85 mL, 9.0 mmol, 6N) to a solution of **SIII** (2.07 g, 8.2 mmol) in MeOH (15 mL). The reaction mixture was stirred until the deprotection was completed. The mixture was diluted with water (50 mL) and diethyl ether (30 mL). The layers were separated and the aqueous phase was extracted with diethyl ether (3 × 30 mL). The combined organic layers were washed with brine, dried over MgSO₄, filtered and concentrated under reduced pressure. The residue was purified by flash chromatography (Pent/Et₂O: 9/1) to afford **2-29a** (1.25 g, 65%) as a yellow solid.

General Procedure 1 (GP1): Synthesis of 2-32a - 2-32n.

To a solution of corresponding 2-iodo anilines **S1** (4.0 mmol, 1.0 eq.) in dry Et₃N (5 mL), respective terminal alkynes (6.0 mmol, 1.5 eq.) and PdCl₂(PPh₃)₂ (0.04 mmol, 10 mol%) was added. After 5 min stirring at rt, CuI (0.08 mmol, 20 mol%) was added and the reaction mixture stirred at same temperature for completion (4 to 12 h). After reaction completed, reaction mixture was poured into ice-cold water and extracted into EtOAc. The combined organic layer was washed with brine solution, dried and evaporated under reduced pressure. The crude residue was purified by flash chromatography on silica gel to give the products in good to excellent yields.

Then the obtained compound (1 mmol) taken in dichloromethane (20 ml) was added with pyridine (3 equiv) followed by tosyl chloride or methanesulfonyl chloride (1.3 eq) at 0 °C over a period of 15 min. After addition completes, reaction stirred at rt for ~12 hours. After reaction completed (monitored by TLC), reaction mass quenched with ice-cold water and extracted into dichloromethane. The combined organic layer was washed with 2N HCl and brine solution, and dried and evaporated to give crude residue. The obtained crude material passed through flash column chromatography to give pure product in good yield (**2-32**).

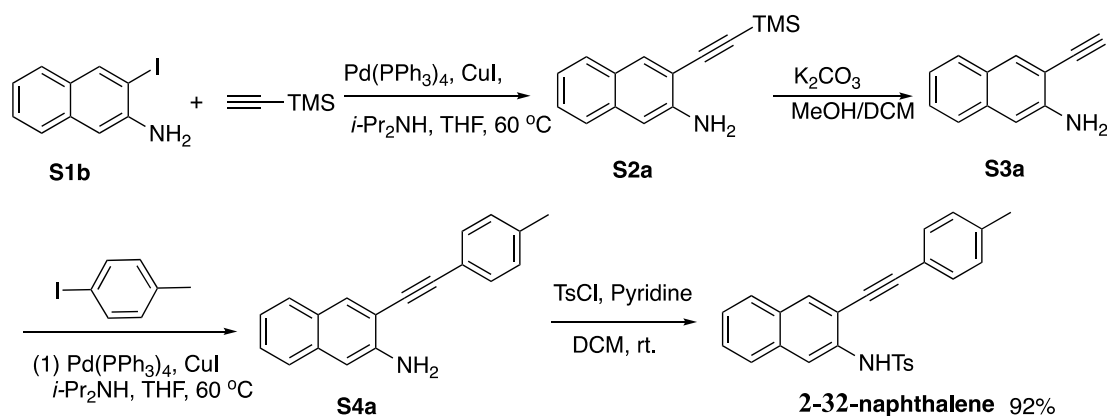
General Procedure 2 (GP2): Synthesis of 2-32Ns-a and 2-32SES-a.

To a solution of 2-iodoaniline **S1a** (0.876 g, 4.0 mmol, 1.0 eq.) in dry Et₃N (5 mL), respective 1-ethynyl-4-methylbenzene (0.696 g, 6.0 mmol, 1.5 eq.) and PdCl₂(PPh₃)₂ (28 mg, 0.04 mmol, 10 mol%) was added. After 5 min stirring at room temperature, CuI (15 mg, 0.08 mmol, 20 mol%) was added and the reaction mixture stirred at same temperature for completion (4 to 12 h). After reaction completed, reaction mixture was poured into ice-cold water and extracted into EtOAc. The combined organic layer was washed with brine solution, dried and

evaporated under reduced pressure. The crude residue was purified by flash chromatography (Pent/Et₂O: 9/1) to give the product in 92% yields as a yellow solid.

Then the obtained compound (1 mmol) taken in pyridine (10 ml) was added 4-nitrobenzenesulfonyl chloride (NsCl, 0.288 g, 1.3 eq.) or 2-trimethylsilylethylsulfonyl chloride (SES-Cl, 0.261g, 1.3 mmol, 1.3 eq.) at 0 °C over a period of 15 min. After addition completes, reaction stirred at rt for 12 hours. After reaction completed (monitored by TLC), reaction mass quenched with ice-cold water and extracted into dichloromethane. The combined organic layer was washed with 2N HCl and brine solution, and dried and evaporated to give crude residue. The obtained crude material passed through flash column chromatography to give pure product (**2-32Ns-a**, **2-32SES-a**) in good yield.

General Procedure 3 (GP3): Synthesis of starting materials **2-32-naphthalene**³⁸



A solution of 3-iodo-2-naphthalenamine **S1b** (1.05 g, 3.93 mmol) in a 1:1 mixture of THF:DIPA (21 mL) was sparged for 12 min with N₂. Five minutes into the sparge, ethynyltrimethylsilane (2.25 mL, 15.69 mmol) was added *via* syringe. After an additional 5 min sparging, CuI (27 mg, 0.15 mmol) and $\text{Pd}(\text{PPh}_3)_4$ (49.5 mg, 0.03 mmol) were added to the reaction mixture. The flask was then sparged for an additional 2 min, then sealed and stirred at 60 °C for 12 h. After cooling, the mixture was concentrated and the residue chromatographed on silica (5:1 hexanes:EtOAc) to give **S2a** (779mg, 83% yield) as a peach-colored solid.

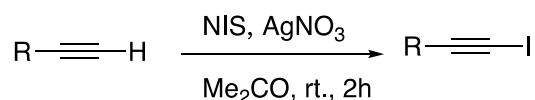
To a solution of alkyne **S2a** (1.0 equiv) in MeOH/ CHCl_3 (1:1, 0.01 M) was added an excess amount of K_2CO_3 (3 equiv). The suspension was stirred at room temperature for 3 h, and then filtered through a bed of celite. After evaporation of the solvent, the crude material was used directly in the next reaction. To an solution of 1-iodo-4-methylbenzene and terminal acetylene **S3a** (1.0 equiv) in 1:1 THF:DIPA was added 1 mol% $\text{Pd}(\text{PPh}_3)_4$ and 2 mol% CuI . The solution was heated to 60 °C for 12 h under an N₂ atmosphere. The reaction mixture was

cooled, concentrated in vacuo and purified *via* flash chromatography to give the desired product **S4a** as a yellow-orange solid in 85%.

Then the obtained compound **S4a** (1 mmol) taken in dichloromethane (20 ml) was added with pyridine (3 equiv) followed by tosyl chloride or methanesulfonyl chloride (1.3 eq) at 0 °C over a period of 15 min. After addition completes, reaction stirred at RT for ~12 hours. After reaction completed (monitored by TLC), reaction mass quenched with ice-cold water and extracted into Dichloromethane. The combined organic layer was washed with 2N HCl and brine solution, and dried and evaporated to give crude residue. The obtained crude material passed through flash column chromatography to give pure product **2-32-naphthalene** in 92% yield.

6.2.2 Synthesis of Iodoalkynes Derivatives

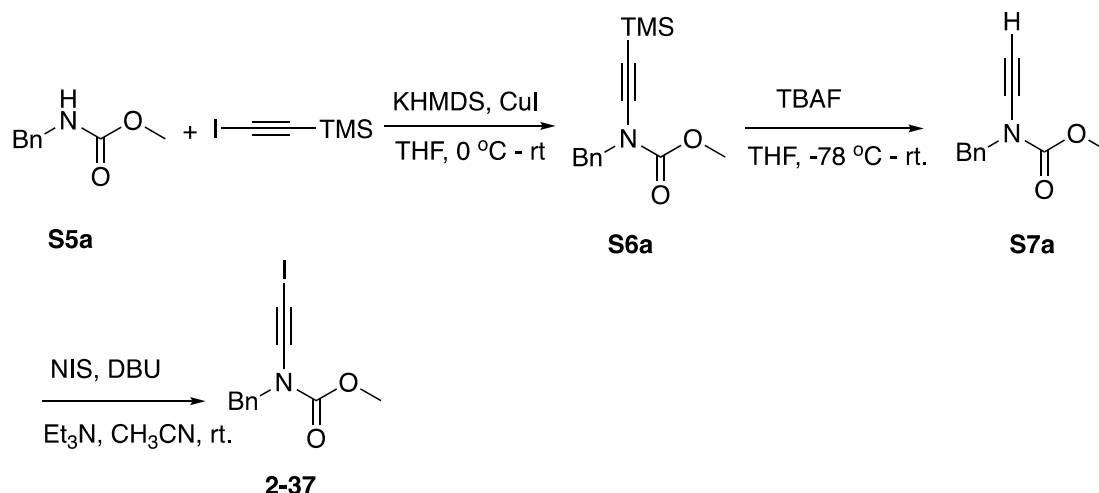
General Procedure 4 (GP4): Synthesis of (iodoethynyl)benzene derivatives **2-30a-2-30k**³⁹



To a stirred solution of the terminal alkyne (2 mmol, 1eq.) in acetone (5 mL) was added NIS (2.2 mmol, 1.1 eq.) and AgNO₃ (0.2 mmol, 10 mol%). The reaction mixture was stirred at room temperature for 3 h. On completion, the solvent was removed under reduced pressure and the residue was filtered through a pad of celite with petroleum ether. Removal of the solvent reduced pressure followed by purification by flash column chromatography on silica gel (petroleum ether as eluent) afforded the title compound **2-30** in 78-98% yield.

General Procedure 5 (GP5):

Methyl benzyl(iodoethynyl)carbamate **7**⁴⁰



A 250-mL, three-necked, round-bottomed flask equipped with a rubber septum, glass stopper, and argon inlet adapter was charged with carbamate **S5a** (1.50 g, 9.10 mmol, 1.0 equiv), 70 mL of THF, and 18.3 mL of pyridine. The colorless solution was cooled at 0 °C and a solution of KHMDS (1.0 M in THF, 10.0 mL, 10 mmol, 1.0 equiv) was added dropwise *via* syringe over 30 min. The resulting suspension was stirred for 15 min and CuI (1.73 g, 9.10 mmol, 1.0 equiv) was added in one portion. The resulting grass-green suspension was allowed to warm to rt and stirred for a total of 3 h. A solution of iodo(trimethylsilyl)acetylene (2.24 g, 10 mmol, 1.1 equiv) in 8 mL of THF was added to the dark green reaction mixture dropwise over 1 h *via* syringe, and the reaction mixture was stirred at rt for 16 h. The resulting brown solution was diluted with 100 mL of Et₂O and washed with three 75-mL portions of a 2:1 mixture of brine and concentrated NH₄OH solution. The combined aqueous phases were extracted with two 80-mL portions of Et₂O, and the combined organic phases were washed with two 80-mL portions of 3 M aqueous HCl solution and 80 mL of brine, dried over MgSO₄, filtered, and concentrated to afford 4.23 g of dark brown oil. Column chromatography on silica gel (gradient elution with 0-5% EtOAc-Petroleum ether) afforded 1.31 g (58%) of ynamide **S6a** as a yellow oil.

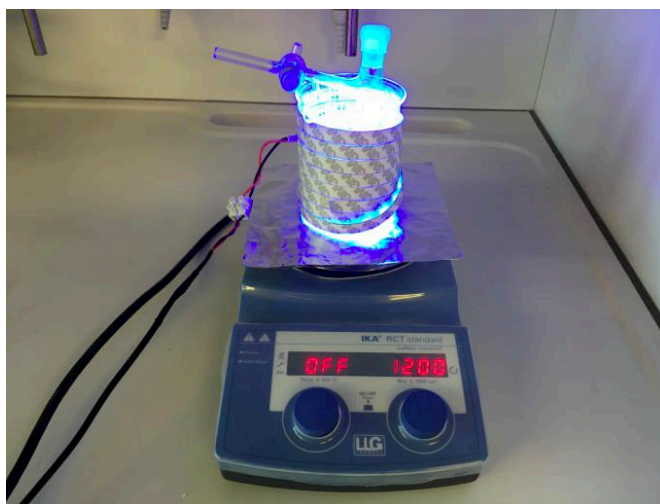
A 100-mL, round-bottomed flask equipped with a rubber septum and argon inlet needle was charged with ynamide **S6a** (0.500 g, 1.91 mmol, 1.0 equiv) and 25 mL of THF. The yellow solution was cooled at -78 °C and TBAF (2.1 mL, 1.0 M in THF, 2.1 mmol, 1.1 equiv) was added dropwise *via* syringe over 5 min. The resulting brown suspension was stirred for 10 min and then diluted with 25 mL of Et₂O, 25 mL of water, and 5 mL of brine. The aqueous phase was extracted with two 20-mL portions of Et₂O, and the combined organic phases were washed with 30 mL of brine, dried over MgSO₄, filtered, and concentrated to afford 0.441 g of orange oil. Column chromatography on 12 g of acetone-deactivated silica gel (elution with 4% EtOAc and 1% Et₃N in petroleum ether) afforded 0.294 g (81%) of ynamide **S7a** as a viscous pale yellow oil.

To a stirred solution of ynamide **S7a** (290 mg, 1.5 mmol) in MeCN (5.0 mL) was added NIS (383 mg, 1.7 mmol) and DBU (258 mg, 1.7 mmol). The mixture was stirred at room temperature for 5 min. The reaction mixture was poured into water and then extracted with EtOAc (3 × 20 mL). The combined organic phase was washed with saturated brine (10 mL), dried over MgSO₄ and filtered. The solvent was removed under reduced pressure and the crude product was purified by flash chromatography (silica gel, petroleum ether or n-pentane as eluent) to give **2-37** (425 mg, 90%) as a yellow solid.

6.3 General Procedure for the Ethynylative Cyclization

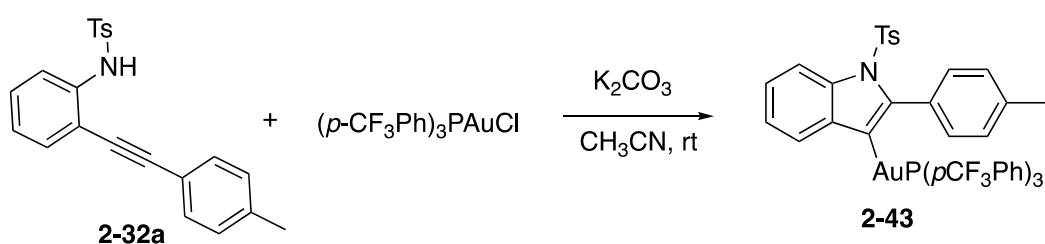
General Procedure 6 (GP6): Ethynylative Cyclization of *o*-alkynyl tosylanilines derivatives with Iodoalkynes

The gold(I) complex $(p\text{CF}_3\text{Ph})_3\text{PAuCl}$ (5 mol %), K_2CO_3 (2.5 equiv), the appropriate iodoalkynes **2-30** (0.33 mmol, 1.1 eq.) and *o*-alkynyl tosylanilines derivatives **2-32** (0.3 mmol, 1.0 eq.) were introduced in a *Schlenk* tube equipped with a magnetic stirring bar in which MeCN (4.5 mL) was added. The mixture was degassed using three freeze pump-thaw cycles and purged with Ar, then irradiated with blue LEDs light for 15 h (unless mentioned). The stirring speed is equal or more than 1200 rpm. The reaction was quenched with EtOAc (5 mL) and a 2 M HCl solution (6 mL) and the solution was extracted by EtOAc (3×5 mL). The combined organic layer was dried over MgSO_4 , filtered and concentrated under reduced pressure to give the crude product. The residue was purified by FC on silica gel to afford the desired product or determined by ^1H NMR using 1,3,5-trimethoxybenzene as internal standard.



The simple photoreactor which is equipped with LED stripes ($\lambda_{\text{max}} = 470$ nm) on a beaker (the diameter is 7.5 cm, the height is 9.5 cm). An aluminum paper is put between the stirring plate and the beaker to reflect the light.

6.3 Synthesis of Vinylgold(I) Complex **2-43**

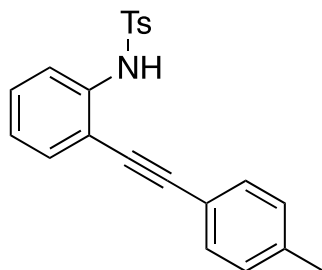


In a 25-mL Schlenk tube 4-methyl-*N*-(2-(*p*-tolylethynyl)phenyl)benzenesulfonamide **2-32a** (0.1 mmol, 36 mg, 1.0 eq.), (*p*-CF₃Ph)₃PAuCl (0.1 mmol, 69.5mg, 1.0 eq.), and K₂CO₃ (0.25 mmol, 34 mg, 2.5 eq.) was dissolved in 10 mL of dry CH₃CN. The reaction mixture was stirred for 16 h at room temperature, filtered over a small column of basic aluminum oxide and wash with 20 mL of dry CH₃CN. The solvent was removed on the rotary evaporator without heating.

Light yellow solid, 94 mg, 92%; M.P. = 270 °C, ¹H NMR (400 MHz, CDCl₃) δ 8.27 (d, *J* = 8.2 Hz, 1H), 7.71 (dd, *J* = 8.3, 1.9 Hz, 6H), 7.66 - 7.60 (m, 3H), 7.56 (dd, *J* = 11.8, 8.0 Hz, 6H), 7.35 (d, *J* = 8.1 Hz, 2H), 7.24 (d, *J* = 1.2 Hz, 1H), 7.14 (d, *J* = 7.7 Hz, 3H), 7.02 (d, *J* = 8.1 Hz, 2H), 2.44 (s, 3H), 2.26 (s, 3H); ¹³C NMR (101 MHz, CDCl₃) δ 155.54, 154.36, 147.35, 143.73, 139.67, 138.71, 136.84, 135.27, 134.75, 134.61, 134.02, 133.86, 133.69, 133.37, 131.14, 129.02, 127.65, 126.78, 126.26, 126.11, 124.61, 123.72, 123.32, 121.89, 116.16, 21.43, 21.34; ¹⁹F NMR (376 MHz, CDCl₃) δ -63.28; ³¹P NMR (162 MHz, CDCl₃) δ 44.96; HRMS (ESI) calc. for C₄₃H₃₀AuF₉NaO₂P⁺ [M+Na]⁺: 1046.1257, found 1046.1259.

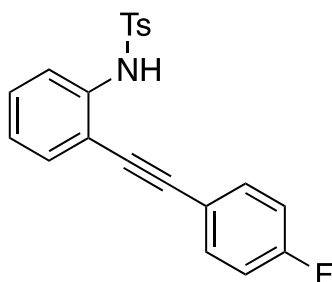
6.4 Compound Characterizations

4-Methyl-*N*-(2-(*p*-tolylethynyl)phenyl)benzenesulfonamide (**2-32a**)



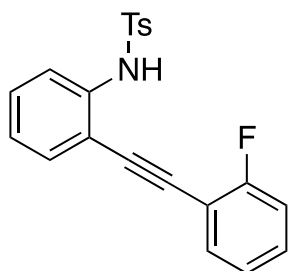
Prepared according to the general procedure **GP1** on 1.0 mmol scale as a yellow solid (347 mg, 96% yield). The spectroscopic data match those previously reported in the literature.⁴¹ ¹H NMR (400 MHz, CDCl₃) δ 7.65 (d, *J* = 8.3 Hz, 2H), 7.62 (s, 1H), 7.37 - 7.32 (m, 3H), 7.28 - 7.24 (m, 1H), 7.22 - 7.19 (m, 1H), 7.16 (dd, *J* = 12.3, 7.9 Hz, 4H), 7.03 (td, *J* = 7.6, 1.2 Hz, 1H), 2.38 (s, 3H), 2.31 (s, 3H).

N-(2-((4-Fluorophenyl)ethynyl)phenyl)-4-Methylbenzenesulfonamide (**2-32b**)



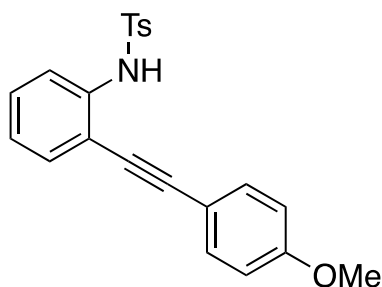
Prepared according to the general procedure **GP1** on 1.0 mmol scale as a yellow solid (328 mg, 90% yield). The spectroscopic data match those previously reported in the literature.⁴⁰ ¹H NMR (300 MHz, CDCl₃) δ 7.67 (d, *J* = 8.3 Hz, 2H), 7.61 (d, *J* = 8.2 Hz, 1H), 7.50 - 7.41 (m, 2H), 7.40 - 7.27 (m, 2H), 7.18 (d, *J* = 8.0 Hz, 3H), 7.13 - 7.03 (m, 3H), 2.35 (s, 3H). ¹⁹F NMR (376 MHz, CDCl₃) δ -109.38.

N-(2-((2-Fluorophenyl)ethynyl)phenyl)-4-methylbenzenesulfonamide (**2-32c**)



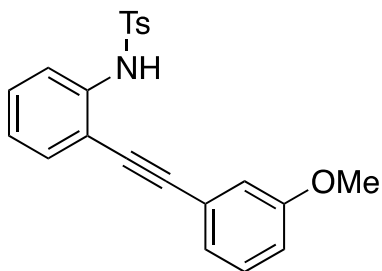
Prepared according to the general procedure **GP1** on 1.0 mmol scale as a yellow solid (328 mg, 90% yield). The spectroscopic data match those previously reported in the literature.⁴⁰ ¹H NMR (400 MHz, CDCl₃) δ 7.71 (t, *J* = 9.0 Hz, 3H), 7.50 - 7.41 (m, 2H), 7.40 - 7.34 (m, 2H), 7.34 - 7.27 (m, 1H), 7.16 (dd, *J* = 11.6, 7.8 Hz, 4H), 7.05 (t, *J* = 7.6 Hz, 1H), 2.29 (s, 3H).

N-(2-((4-Methoxyphenyl)ethynyl)phenyl)-4-methylbenzenesulfonamide (**2-32d**)



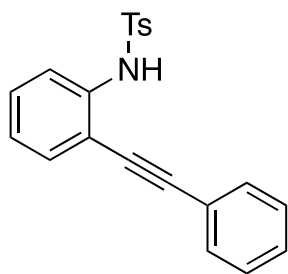
Prepared according to the general procedure **GP1** on 1.0 mmol scale as a grey solid (358 mg, 95% yield). The spectroscopic data match those previously reported in the literature.⁴¹ ¹H NMR (400 MHz, CDCl₃) δ 7.67 (d, *J* = 8.3 Hz, 2H), 7.61 (d, *J* = 8.1 Hz, 1H), 7.41 (d, *J* = 8.8 Hz, 2H), 7.35 (d, *J* = 9.0 Hz, 1H), 7.28 (d, *J* = 8.9 Hz, 1H), 7.23 - 7.15 (m, 3H), 7.05 (t, *J* = 7.6 Hz, 1H), 6.91 (d, *J* = 8.8 Hz, 2H), 3.86 (s, 3H), 2.34 (s, 3H).

N-(2-((3-Methoxyphenyl)ethynyl)phenyl)-4-methylbenzenesulfonamide (**2-32e**)



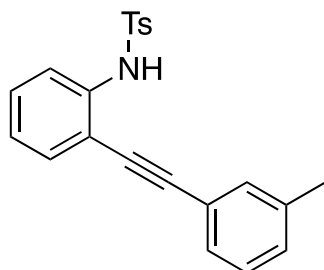
Prepared according to the general procedure **GP1** on 1.0 mmol scale as a grey solid (359 mg, 96% yield). The spectroscopic data match those previously reported in the literature.⁴² ¹H NMR (400 MHz, CDCl₃) δ 7.68 (d, *J* = 8.2 Hz, 2H), 7.63 (d, *J* = 8.2 Hz, 1H), 7.37 (d, *J* = 7.1 Hz, 1H), 7.28 (t, *J* = 7.9 Hz, 3H), 7.14 (s, 2H), 7.06 (dd, *J* = 10.1, 7.7 Hz, 2H), 7.00 (s, 1H), 6.94 (d, *J* = 8.3 Hz, 1H), 3.82 (s, 3H), 2.31 (s, 3H).

4-Methyl-N-(2-(phenylethynyl)phenyl)benzenesulfonamide (2-32f)



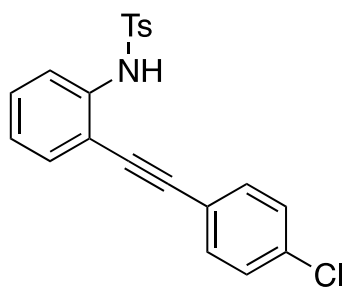
Prepared according to the general procedure **GP1** on 1.0 mmol scale as a yellow solid (312 mg, 90% yield). The spectroscopic data match those previously reported in the literature.⁴⁰ ¹H NMR (300 MHz, CDCl₃) δ 7.70 (d, *J* = 8.2 Hz, 2H), 7.65 (d, *J* = 8.2 Hz, 1H), 7.50 (dd, *J* = 6.7, 3.0 Hz, 2H), 7.45 - 7.37 (m, 4H), 7.32 (s, 1H), 7.26 - 7.15 (m, 3H), 7.09 (t, *J* = 7.6 Hz, 1H), 2.37 (s, 3H).

*4-Methyl-N-(2-(*m*-tolylethynyl)phenyl)benzenesulfonamide (2-32g)*



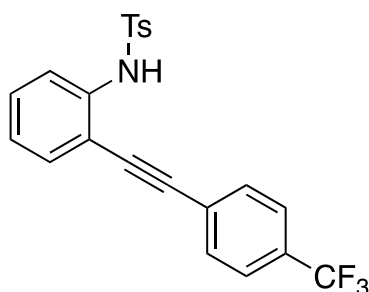
Prepared according to the general procedure **GP1** on 1.0 mmol scale as a yellow solid (343 mg, 95% yield). The spectroscopic data match those previously reported in the literature.⁴⁰ ¹H NMR (300 MHz, CDCl₃) δ 7.72 (d, *J* = 8.3 Hz, 2H), 7.66 (d, *J* = 8.0 Hz, 1H), 7.39 (d, *J* = 7.7 Hz, 1H), 7.29 (d, *J* = 3.3 Hz, 5H), 7.21 (dd, *J* = 13.7, 5.9 Hz, 3H), 7.12 - 7.04 (m, 1H), 2.41 (s, 3H), 2.35 (s, 3H).

N-(2-((4-Chlorophenyl)ethynyl)phenyl)-4-methylbenzenesulfonamide (2-32h)



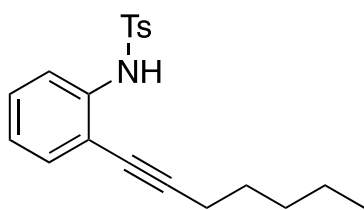
Prepared according to the general procedure **GP1** on 1.0 mmol scale as a yellow solid (335 mg, 88% yield). The spectroscopic data match those previously reported in the literature.⁴⁰ ¹H NMR (300 MHz, CDCl₃) δ 7.66 (d, *J* = 8.2 Hz, 2H), 7.61 (d, *J* = 8.3 Hz, 1H), 7.37 (d, *J* = 7.6 Hz, 5H), 7.29 (d, *J* = 8.3 Hz, 1H), 7.21 - 7.13 (m, 3H), 7.07 (t, *J* = 7.6 Hz, 1H), 2.35 (s, 3H).

4-Methyl-N-(2-((4-(trifluoromethyl)phenyl)ethynyl)phenyl)benzenesulfonamide (2-32i)



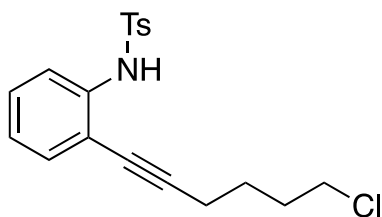
Prepared according to the general procedure **GP1** on 1.0 mmol scale as a gray solid (369 mg, 89% yield). The spectroscopic data match those previously reported in the literature.⁴⁰ ¹H NMR (300 MHz, CDCl₃) δ 7.71 (d, *J* = 8.3 Hz, 2H), 7.65 (d, *J* = 7.5 Hz, 3H), 7.59 (d, *J* = 8.4 Hz, 2H), 7.45 - 7.39 (m, 1H), 7.39 - 7.31 (m, 1H), 7.29 (s, 1H), 7.19 (d, *J* = 8.2 Hz, 2H), 7.11 (t, *J* = 7.6 Hz, 1H), 2.36 (s, 3H). ¹⁹F NMR (376 MHz, CDCl₃) δ -62.89.

N-(2-(Hept-1-yn-1-yl)phenyl)-4-methylbenzenesulfonamide (2-32j)



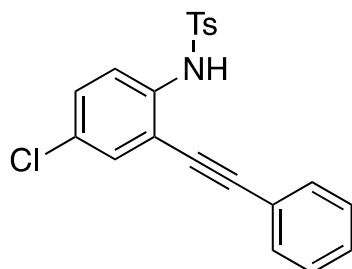
Prepared according to the general procedure **GP1** on 1.0 mmol scale as a yellow solid (279 mg, 82% yield). The spectroscopic data match those previously reported in the literature.⁴³ ¹H NMR (400 MHz, CDCl₃) δ 7.66 (d, *J* = 8.3 Hz, 2H), 7.56 (d, *J* = 8.2 Hz, 1H), 7.26 - 7.17 (m, 5H), 6.97 (t, *J* = 7.6 Hz, 1H), 2.41 (t, *J* = 7.1 Hz, 2H), 2.36 (s, 3H), 1.60 (p, *J* = 7.1 Hz, 2H), 1.46 - 1.35 (m, 4H), 0.95 (t, *J* = 7.0 Hz, 3H).

N-(2-(6-Chlorohex-1-yn-1-yl)phenyl)-4-methylbenzenesulfonamide (**2-32k**)



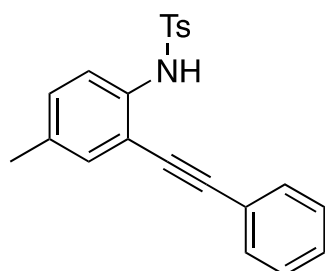
Prepared according to the general procedure **GP1** on 1.0 mmol scale as a yellow solid (282 mg, 78% yield). The spectroscopic data match those previously reported in the literature.⁴³ ¹H NMR (400 MHz, CDCl₃) δ 7.70 - 7.64 (m, 2H), 7.55 (dd, *J* = 8.3, 1.1 Hz, 1H), 7.26 - 7.16 (m, 5H), 6.97 (td, *J* = 7.6, 1.2 Hz, 1H), 3.59 (t, *J* = 6.4 Hz, 2H), 2.46 (t, *J* = 7.0 Hz, 2H), 2.35 (s, 3H), 1.96 - 1.85 (m, 2H), 1.74 (p, *J* = 7.1 Hz, 2H).

N-(4-Chloro-2-(phenylethynyl)phenyl)-4-methylbenzenesulfonamide (**2-32l**)



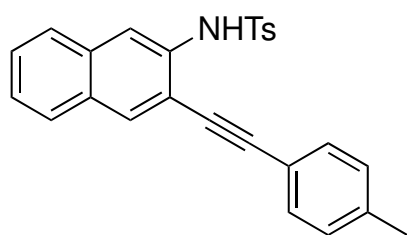
Prepared according to the general procedure **GP1** on 1.0 mmol scale as a gray solid (324 mg, 85% yield). The spectroscopic data match those previously reported in the literature.⁴⁰ ¹H NMR (400 MHz, CDCl₃) δ 7.66 (s, 2H), 7.58 (s, 2H), 7.40 (t, *J* = 20.9 Hz, 6H), 7.17 (s, 3H), 2.34 (s, 3H).

4-Methyl-*N*-(4-methyl-2-(phenylethynyl)phenyl)benzenesulfonamide (**2-32m**)



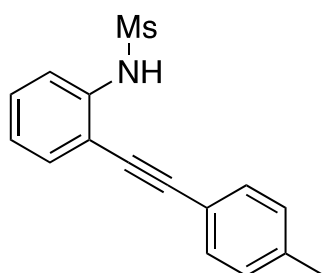
Prepared according to the general procedure **GP1** on 1.0 mmol scale as a gray solid (322 mg, 89% yield). The spectroscopic data match those previously reported in the literature.⁴⁰ ¹H NMR (400 MHz, CDCl₃) δ 7.66 (d, *J* = 8.2 Hz, 2H), 7.53 (d, *J* = 8.3 Hz, 1H), 7.45 (dd, *J* = 6.6, 3.0 Hz, 2H), 7.41 - 7.34 (m, 3H), 7.20 - 7.08 (m, 5H), 2.32 (s, 3H), 2.26 (s, 3H).

4-Methyl-N-(3-(p-tolylethynyl)naphthalen-2-yl)benzenesulfonamide (2-32n)



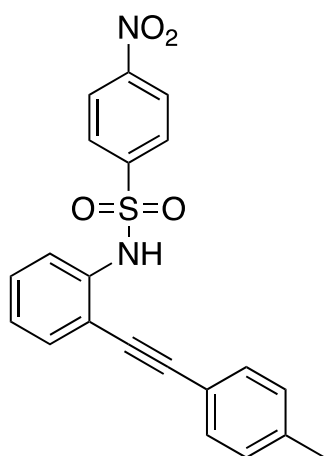
Prepared according to the general procedure **GP3** on 1.0 mmol scale as a yellow solid (378 mg, 92% yield). ^1H NMR (400 MHz, CDCl_3) δ 8.03 (s, 1H), 7.90 (s, 1H), 7.79 (d, $J = 8.2$ Hz, 1H), 7.70 (dd, $J = 7.8, 5.7$ Hz, 3H), 7.51 - 7.45 (m, 1H), 7.41 (t, $J = 7.8$ Hz, 3H), 7.35 (s, 1H), 7.22 (d, $J = 7.9$ Hz, 2H), 7.13 (d, $J = 8.1$ Hz, 2H), 2.42 (s, 3H), 2.30 (s, 3H). ^{13}C NMR (101 MHz, CDCl_3) δ 143.92, 139.48, 136.04, 133.42, 133.33, 132.21, 131.51, 130.21, 129.56, 129.35, 127.71, 127.45, 127.36, 127.28, 125.91, 118.84, 117.48, 114.53, 96.36, 83.42, 21.58, 21.46; HRMS (APCI) calc. for $\text{C}_{26}\text{H}_{22}\text{NO}_2\text{S}^+$ $[\text{M}+\text{H}]^+$: 412.1293, found 412.1289.

N-(2-(p-Tolylethynyl)phenyl)methanesulfonamide (2-32Ms-a)



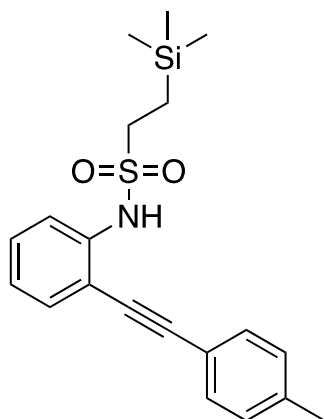
Prepared according to the general procedure **GP1** on 1.0 mmol scale as a yellow solid (257 mg, 90% yield). The spectroscopic data match those previously reported in the literature.⁴² ^1H NMR (400 MHz, CDCl_3) δ 7.62 (d, $J = 8.2$ Hz, 1H), 7.54 (d, $J = 7.3$ Hz, 1H), 7.43 (d, $J = 7.9$ Hz, 2H), 7.37 (t, $J = 7.5$ Hz, 1H), 7.18 (dd, $J = 15.0, 7.7$ Hz, 3H), 7.04 (s, 1H), 3.04 (s, 3H), 2.39 (s, 3H).

4-Nitro-N-(2-(p-tolylethynyl)phenyl)benzenesulfonamide (2-32Ns-a)



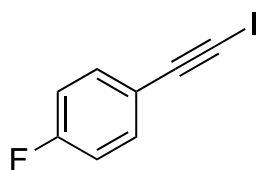
Prepared according to the general procedure **GP2** on 1.0 mmol scale as a yellow solid (267 mg, 68% yield). ^1H NMR (400 MHz, CDCl_3) δ 8.16 (d, $J = 8.9$ Hz, 2H), 7.89 (d, $J = 8.8$ Hz, 2H), 7.66 (dd, $J = 8.2, 1.1$ Hz, 1H), 7.41 - 7.34 (m, 2H), 7.29 (d, $J = 8.2$ Hz, 2H), 7.23 - 7.13 (m, 4H), 2.41 (s, 3H). ^{13}C NMR (101 MHz, CDCl_3) δ 150.26, 144.58, 139.81, 136.08, 132.16, 131.34, 129.66, 129.47, 128.49, 125.98, 124.08, 122.14, 118.44, 116.24, 96.69, 82.78, 21.59. HRMS (APCI) calc. for $\text{C}_{21}\text{H}_{17}\text{N}_2\text{O}_4\text{S}^+$ $[\text{M}+\text{H}]^+$: 372.1448, found 372.1449.

N-(2-(*p*-Tolylethynyl)phenyl)-2-(trimethylsilyl)ethane-1-sulfonamide (**2-32SES-a**)



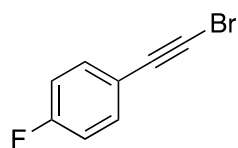
Prepared according to the general procedure **GP2** on 1.0 mmol scale as a yellow solid (156 mg, 42% yield). ^1H NMR (400 MHz, CDCl_3) δ 7.66 (d, $J = 8.2$ Hz, 1H), 7.52 (dd, $J = 7.8, 1.5$ Hz, 1H), 7.42 (d, $J = 7.9$ Hz, 2H), 7.34 (ddd, $J = 8.6, 7.6, 1.5$ Hz, 1H), 7.19 (d, $J = 7.8$ Hz, 2H), 7.13 (dd, $J = 8.2, 7.1$ Hz, 1H), 7.05 (s, 1H), 3.06 - 2.97 (m, 2H), 2.39 (s, 3H), 1.14 - 1.07 (m, 2H), -0.08 (s, 9H). ^{13}C NMR (101 MHz, CDCl_3) δ 139.50, 137.87, 132.20, 131.44, 129.74, 129.33, 124.42, 119.38, 118.73, 114.14, 97.13, 83.25, 47.86, 21.53, 10.52, -2.24. HRMS (APCI) calc. for $\text{C}_{20}\text{H}_{26}\text{NO}_2\text{SSi}^+$ $[\text{M}+\text{H}]^+$: 372.1448, found 372.1449.

1-Fluoro-4-(iodoethynyl)benzene (**2-30a**)



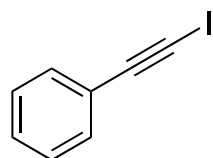
Following general procedure **GP4** with 1-ethynyl-4-fluorobenzene (480 mg, 4 mmol) to afford **2-30a** (0.88 g, 3.6 mmol, 90%) as colorless oil. The spectroscopic data match those previously reported in the literature.³⁰ ^1H NMR (400 MHz, CDCl_3) δ 7.45 - 7.39 (m, 1H), 7.04 - 6.98 (m, 1H). ^{19}F NMR (376 MHz, CDCl_3) δ -109.72.

1-(Bromoethynyl)-4-fluorobenzene (2-30a-Br)



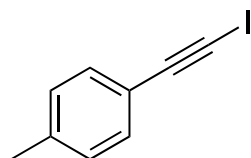
To the mixture of 1-ethynyl-4-fluorobenzene (1 mmol), NBS (1.2 mmol) and 10 mL acetone, AgNO₃ (5 mol %) was added and the mixture was stirred at room temperature for three hours. After completion the reaction, the solvent was evaporated and extracted with 10 mL petroleum ether (30-60 °C), then evaporated the solvent to provide **2-30a-Br** in 92% yield. The spectroscopic data match those previously reported in the literature.⁴⁴ ¹H NMR (300 MHz, CDCl₃) δ 7.50 - 7.41 (m, 2H), 7.08 - 6.99 (m, 2H). ¹⁹F NMR (282 MHz, CDCl₃) δ -109.91.

1-(Iodoethynyl)benzene (2-30b)



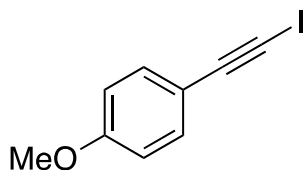
Following general procedure **GP4** with phenylacetylene (408 mg, 4 mmol) to afford **2-30b** (0.866 g, 3.8 mmol, 95%) as colorless oil. The spectroscopic data match those previously reported in the literature.³⁰ ¹H NMR (400 MHz, CDCl₃) δ 7.44 (m, *J* = 7.4, 2.3 Hz, 2H), 7.32 (m, *J* = 5.2, 2.0 Hz, 3H).

1-(Iodoethynyl)-4-methylbenzene (2-30c)



Following general procedure **GP4** 1-ethynyl-4-methylbenzene (464 mg, 4 mmol) to afford **2-30c** (0.94 g, 3.9 mmol, 98%) as colorless oil. The spectroscopic data match those previously reported in the literature.³⁰ ¹H NMR (400 MHz, CDCl₃) δ 7.33 (m, *J* = 7.9 Hz, 2H), 7.11 (m, *J* = 7.8 Hz, 2H), 2.35 (s, 3H).

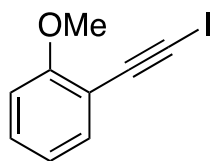
1-(Iodoethynyl)-4-methoxybenzene (2-30d)



Following general procedure **GP4** with 1-ethynyl-4-methoxybenzene (528 mg, 4 mmol) to afford **2-30d** (0.94 g, 3.8 mmol, 98%) as white solid. The spectroscopic data match those

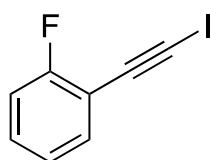
previously reported in the literature.³⁰ ¹H NMR (400 MHz, CDCl₃) δ 7.47 - 7.34 (m, 2H), 6.82 - 6.85(m, *J* = 8.4 Hz, 2H), 3.81 (s, 3H).

1-(Iodoethynyl)-2-methoxybenzene (2-30e)



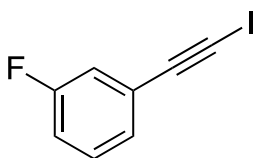
Following general procedure **GP4** with 1-ethynyl-2-methoxybenzene (528, 4 mmol) to afford **2-30e** (0.95 g, 3.7 mmol, 93%) as white solid. The spectroscopic data match those previously reported in the literature.³⁰ ¹H NMR (400 MHz, CDCl₃) δ 7.40 (d, *J* = 7.6 Hz, 1H), 7.30 (d, *J* = 7.8 Hz, 1H), 6.92 - 6.85 (m, 2H), 3.88 (s, 3H).

1-Fluoro-2-(iodoethynyl)benzene (2-30f)



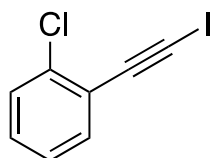
Following general procedure **GP4** with 1-ethynyl-2-fluorobenzene (480 mg, 4 mmol) to afford **2-30f** (0.86 g, 3.5 mmol, 88%) as colorless oil. The spectroscopic data match those previously reported in the literature.³⁰ ¹H NMR (400 MHz, CDCl₃) δ 7.47 - 7.40 (m, 1H), 7.34 - 7.27 (m, 1H), 7.08 (q, *J* = 9.5, 8.7 Hz, 2H). ¹⁹F NMR (376 MHz, CDCl₃) δ -110.07.

1-Fluoro-3-(iodoethynyl)benzene (2-30g)



Following general procedure **GP4** with 1-ethynyl-2-fluorobenzene (480 mg, 4 mmol) to afford **2-30g** (0.85 g, 3.48 mmol, 87%) as colorless oil. The spectroscopic data match those previously reported in the literature.³⁰ ¹H NMR (400 MHz, CDCl₃) δ 7.28 (d, *J* = 8.5 Hz, 1H), 7.23 (d, *J* = 7.6 Hz, 1H), 7.14 (d, *J* = 9.2 Hz, 1H), 7.08 - 7.01 (m, 1H). ¹⁹F NMR (376 MHz, CDCl₃) δ -112.5.

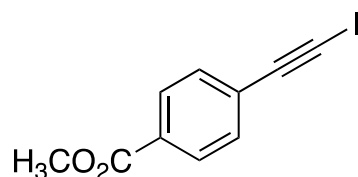
1-Chloro-2-(iodoethynyl)benzene (2-30h)



Following general procedure **GP4** with 1-chloro-2-ethynylbenzene (544 mg, 4 mmol) to afford **2-30h** (0.84 g, 3.2 mmol, 80%) as brown oil. The spectroscopic data match those previously

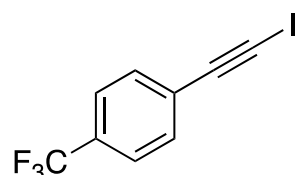
reported in the literature.³⁰ ¹H NMR (400 MHz, CDCl₃) δ 7.50 - 7.44 (m, 1H), 7.42 - 7.36 (m, 1H), 7.27 - 7.18 (m, 2H).

Methyl 4-(iodoethynyl)benzoate (2-30i)



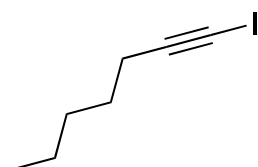
Following general procedure **GP4** with 1-ethynyl-4-(trifluoromethyl)benzene (640 mg, 4 mmol) to afford **2-30i** (0.89 g, 3.1 mmol, 78%) as yellow solid. The spectroscopic data match those previously reported in the literature.⁴⁵ ¹H NMR (400 MHz, CDCl₃) δ 7.98 (d, *J* = 8.0 Hz, 2H), 7.49 (d, *J* = 8.0 Hz, 2H), 3.91 (s, 3H).

1-(Iodoethynyl)-4-(trifluoromethyl)benzene (2-30j)



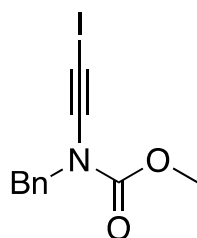
Following general procedure **GP4** with 1-ethynyl-4-(trifluoromethyl)benzene (680 mg, 4 mmol) to afford **2-30j** (1.0 g, 3.4 mmol, 85%) as yellow oil. The spectroscopic data match those previously reported in the literature.³⁰ ¹H NMR (300 MHz, CDCl₃) δ 7.64–7.52 (m, 4H). ¹⁹F NMR (376 MHz, CDCl₃) δ -62.95.

1-Iodohept-1-yne (2-30k)



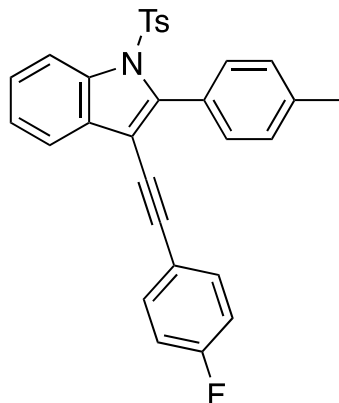
Following general procedure **GP4** with hept-1-yne (384 mg, 4 mmol) to afford **2-30k** (0.78 g, 3.5 mmol, 88%) as yellow oil. The spectroscopic data match those previously reported in the literature.³⁰ ¹H NMR (400 MHz, CDCl₃) δ 2.35 (t, *J* = 6.8 Hz, 2H), 1.55-1.48 (m, 2H), 1.40-1.27 (m, 4H), 0.90 (t, *J* = 7.2 Hz, 3H).

Methyl benzyl(iodoethynyl)carbamate (2-37)



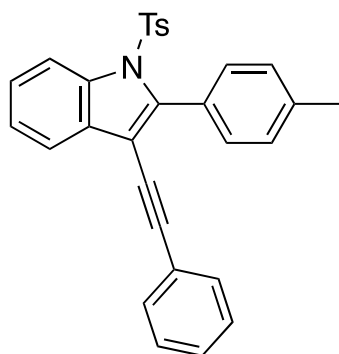
Following general procedure **GP5** to afford **7** (425 mg, 90%) as a yellow solid. The spectroscopic data match those previously reported in the literature.⁴⁰ ¹H NMR (300 MHz, CDCl₃) δ 7.41 - 7.29 (m, 5H), 4.63 (s, 2H), 3.81 (s, 3H).

3-((4-Fluorophenyl)ethynyl)-2-(p-tolyl)-1-tosyl-1H-indole (2-33aa)



Following general procedure **GP6** with 4-methyl-*N*-(2-(*p*-tolylethynyl)phenyl)benzenesulfonamide **2-32a** (108 mg, 0.3 mmol) and 1-fluoro-3-(iodoethynyl)benzene **2-30a** (81 mg, 0.33 mmol). The crude product was purified by flash column chromatography (Petroleum ether : EtOAc = 20 : 1) to afford **2-33aa** as a Yellow solid (89 mg, 62%). Mp 108 °C; ¹H NMR (400 MHz, CDCl₃) δ 8.32 (d, *J* = 8.3 Hz, 1H), 7.63 (d, *J* = 6.4 Hz, 1H), 7.54 (d, *J* = 8.1 Hz, 2H), 7.44 - 7.39 (m, 1H), 7.38 - 7.36 (m, 1H), 7.36 - 7.32 (m, 2H), 7.32 - 7.29 (m, 2H), 7.28 (d, *J* = 3.1 Hz, 2H), 7.05 (d, *J* = 7.7 Hz, 2H), 6.99 (t, *J* = 8.7 Hz, 2H), 2.48 (s, 3H), 2.29 (s, 3H); ¹³C NMR (101 MHz, CDCl₃) δ 163.68, 161.19, 144.81, 143.80, 139.16, 137.12, 134.51, 133.34, 133.26, 131.07, 130.81, 129.30, 128.07, 127.77, 126.86, 125.64, 124.69, 119.94, 119.32, 119.28, 116.72, 115.71, 115.49, 107.68, 93.50, 81.36, 21.60, 21.54; ¹⁹F NMR (376 MHz, CDCl₃) δ -112.07. HRMS (APCI) calc. for C₃₀H₂₃FNO₂S⁺ [M+H]⁺: 480.1428, found 480.1426.

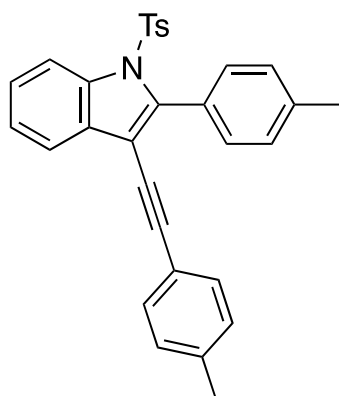
3-(Phenylethynyl)-2-(p-tolyl)-1-tosyl-1H-indole (2-33ab)



Following general procedure **GP6** with 4-methyl-*N*-(2-(*p*-tolylethynyl)phenyl)benzenesulfonamide **2-32a** (108 mg, 0.3 mmol) and (iodoethynyl)benzene

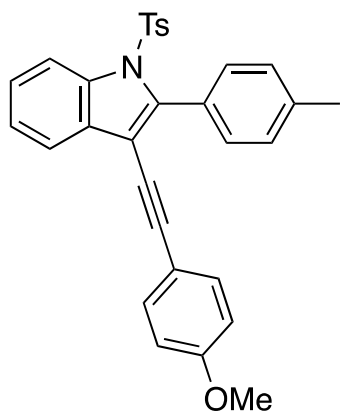
2-30b (75 mg, 0.33 mmol). The crude product was purified by flash column chromatography (Petroleum ether : EtOAc = 15 : 1) to afford **2-33ab** as a white solid (86 mg, 62%). Mp 118 °C. ¹H NMR (400 MHz, CDCl₃) δ 8.32 (d, *J* = 8.2 Hz, 1H), 7.65 (d, *J* = 7.4 Hz, 1H), 7.56 (d, *J* = 8.1 Hz, 2H), 7.44 - 7.35 (m, 4H), 7.34 - 7.27 (m, 7H), 7.05 (d, *J* = 8.2 Hz, 2H), 2.48 (s, 3H), 2.29 (s, 3H); ¹³C NMR (101 MHz, CDCl₃) δ 144.79, 143.77, 139.11, 137.15, 134.48, 131.44, 131.09, 130.94, 129.29, 128.28, 128.22, 128.16, 128.07, 127.81, 126.86, 125.61, 124.69, 123.21, 120.01, 116.73, 94.66, 81.64, 21.62, 21.55; HRMS (APCI) calc. for C₃₀H₂₄NO₂S⁺ [M+H]⁺: 462.1522, found 462.1521.

2-(p-Tolyl)-3-(p-tolylethynyl)-1-tosyl-1H-indole (2-33ac)



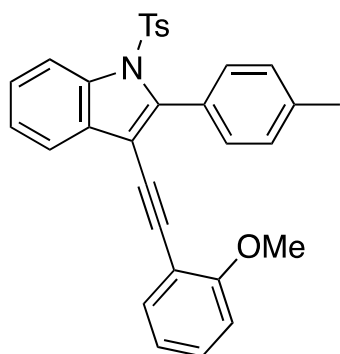
Following general procedure **GP6** with 4-methyl-*N*-(2-(*p*-tolylethynyl)phenyl)benzenesulfonamide **2-32a** (108 mg, 0.3 mmol) and 1-(iodoethynyl)-4-methylbenzene **2-30c** (80 mg, 0.33 mmol). The crude product was purified by flash column chromatography (Petroleum ether : EtOAc = 15 : 1) to afford **2-33ac** as a white solid (101 mg, 71%). Mp 118 °C. ¹H NMR (400 MHz, CDCl₃) δ 8.32 (d, *J* = 8.3 Hz, 1H), 7.65 (d, *J* = 7.6 Hz, 1H), 7.57 (d, *J* = 7.7 Hz, 2H), 7.44 - 7.33 (m, 2H), 7.29 (d, *J* = 8.1 Hz, 6H), 7.11 (d, *J* = 7.8 Hz, 2H), 7.05 (d, *J* = 8.0 Hz, 2H), 2.47 (s, 3H), 2.34 (s, 3H), 2.29 (s, 3H); ¹³C NMR (101 MHz, CDCl₃) δ 144.74, 143.49, 139.01, 138.40, 137.17, 134.45, 131.34, 131.07, 131.02, 129.27, 129.04, 128.04, 127.87, 126.84, 125.56, 124.66, 120.11, 120.03, 116.73, 108.15, 94.87, 80.91, 21.59, 21.52, 21.49; HRMS (APCI) calc. for C₃₁H₂₆NO₂S⁺ [M+H]⁺: 476.1679, found 476.1671.

3-((4-Methoxyphenyl)ethynyl)-2-(p-tolyl)-1-tosyl-1H-indole (2-33ad)



Following general procedure **GP6** with 4-methyl-*N*-(2-(*p*-tolylethynyl)phenyl)benzenesulfonamide **2-32a** (108 mg, 0.3 mmol) and 1-(iodoethynyl)-4-methoxybenzene **2-30d** (85 mg, 0.33 mmol). The crude product was purified by flash column chromatography (Petroleum ether : EtOAc = 20 : 1) to afford **2-33ad** as a Yellow solid (99 mg, 67%). Mp 110 °C; ¹H NMR (400 MHz, CDCl₃) δ 8.32 (d, *J* = 8.2 Hz, 1H), 7.64 (d, *J* = 8.4 Hz, 1H), 7.57 (d, *J* = 8.1 Hz, 2H), 7.43 - 7.38 (m, 1H), 7.33 (d, *J* = 8.8 Hz, 3H), 7.28 (s, 4H), 3.80 (s, 3H), 2.47 (s, 3H), 2.29 (s, 3H); ¹³C NMR (101 MHz, CDCl₃) δ 159.61, 144.72, 143.22, 138.95, 137.18, 134.42, 132.90, 131.05, 129.25, 128.02, 127.94, 126.84, 125.54, 124.65, 120.03, 116.74, 115.30, 113.95, 108.29, 94.68, 80.21, 55.28, 21.59, 21.51; HRMS (APCI) calc. for C₃₁H₂₆NO₃S⁺ [M+H]⁺: 492.1550, found 492.1545.

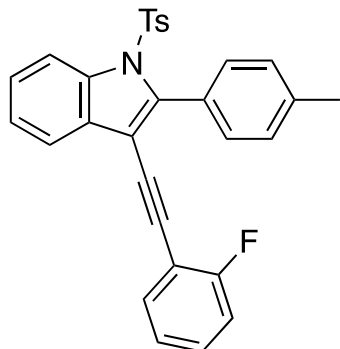
3-((2-Methoxyphenyl)ethynyl)-2-(p-tolyl)-1-tosyl-1H-indole (2-33ae)



Following general procedure **GP6** with 4-methyl-*N*-(2-(*p*-tolylethynyl)phenyl)benzenesulfonamide **2-32a** (108 mg, 0.3 mmol) and 1-(iodoethynyl)-2-methoxybenzene **2-30e** (85 mg, 0.33 mmol). The crude product was purified by flash column chromatography (Petroleum ether : EtOAc = 20 : 1) to afford **2-33ae** as a Yellow solid (93 mg, 63%). Mp 107 °C; ¹H NMR (400 MHz, CDCl₃) δ 8.33 (d, *J* = 8.2 Hz, 1H), 7.71 (d, *J* = 7.6 Hz, 1H), 7.64 (d, *J* = 7.8 Hz, 2H), 7.46 - 7.34 (m, 3H), 7.30 (dq, *J* = 10.1, 4.1 Hz, 5H), 7.05 (d, *J* = 8.0 Hz, 2H), 6.93 - 6.84 (m, 2H), 3.88 (s, 3H), 2.49 (s, 3H), 2.30 (s, 3H); ¹³C NMR (101 MHz, CDCl₃) δ 159.97, 144.71, 143.31, 138.85, 137.23, 134.38, 133.15, 131.22, 131.15, 129.68,

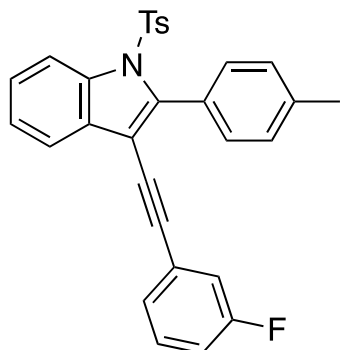
129.24, 127.97, 127.89, 126.84, 125.52, 124.69, 120.40, 120.19, 116.74, 112.52, 110.67, 108.52, 91.27, 85.64, 55.76, 21.60, 21.50; HRMS (APCI) calc. for $C_{31}H_{26}NO_3S^+$ $[M+H]^+$: 492.1628, found 492.1625.

3-((2-Fluorophenyl)ethynyl)-2-(p-tolyl)-1-tosyl-1H-indole (2-33af)



Following general procedure **GP6** with 4-methyl-*N*-(2-(*p*-tolylethynyl)phenyl)benzenesulfonamide **2-32a** (108 mg, 0.3 mmol) and 1-fluoro-2-(iodoethynyl)benzene **2-30f** (81 mg, 0.33 mmol). The crude product was purified by flash column chromatography (Petroleum ether : EtOAc = 20 : 1) to afford **2-33af** as a Yellow solid (69 mg, 48%) Mp 102 °C; 1H NMR (400 MHz, $CDCl_3$) δ 8.33 (d, J = 8.2 Hz, 1H), 7.68 (d, J = 7.6 Hz, 1H), 7.59 (d, J = 7.7 Hz, 2H), 7.42 (t, J = 7.7 Hz, 1H), 7.39 - 7.34 (m, 2H), 7.30 (dd, J = 8.1, 4.0 Hz, 5H), 7.06 (t, J = 8.0 Hz, 4H), 2.48 (s, 3H), 2.29 (s, 3H); ^{13}C NMR (101 MHz, $CDCl_3$) δ 163.83, 161.32, 144.84, 144.08, 139.17, 137.12, 134.43, 133.14, 131.07, 130.84, 129.92, 129.85, 129.30, 128.09, 127.60, 126.84, 125.66, 124.79, 123.88, 123.84, 120.05, 116.70, 115.53, 115.32, 111.95, 111.79, 107.64, 88.05, 86.81, 86.78, 21.59, 21.52; ^{19}F NMR (376 MHz, $CDCl_3$) δ -109.56. HRMS (APCI) calc. for $C_{30}H_{23}FNO_2S^+$ $[M+H]^+$: 480.1355, found 480.1356.

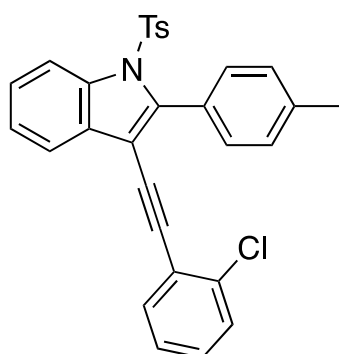
3-((3-Fluorophenyl)ethynyl)-2-(p-tolyl)-1-tosyl-1H-indole (2-33ag)



Following general procedure **GP6** with 4-methyl-*N*-(2-(*p*-tolylethynyl)phenyl)benzenesulfonamide **2-32a** (108 mg, 0.3 mmol) and 1-fluoro-3-(iodoethynyl)benzene **2-30g** (81 mg, 0.33 mmol). The crude product was purified by flash

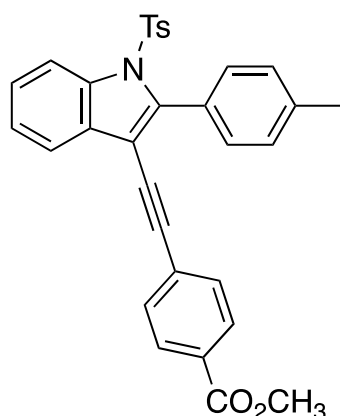
column chromatography (Petroleum ether : EtOAc = 20 : 1) to afford **2-33ag** as a Yellow solid (87 mg, 61%); Mp 104 °C; ¹H NMR (400 MHz, CDCl₃) δ 8.33 (d, *J* = 8.2 Hz, 1H), 7.64 (d, *J* = 7.6 Hz, 1H), 7.54 (d, *J* = 7.8 Hz, 2H), 7.41 (d, *J* = 7.6 Hz, 1H), 7.37 (d, *J* = 7.5 Hz, 1H), 7.30 (dd, *J* = 8.1, 4.6 Hz, 4H), 7.25 (d, *J* = 5.4 Hz, 1H), 7.15 (d, *J* = 7.7 Hz, 1H), 7.06 (d, *J* = 8.3 Hz, 3H), 7.00 (d, *J* = 2.5 Hz, 1H), 2.48 (s, 3H), 2.30 (s, 3H); ¹³C NMR (101 MHz, CDCl₃) δ 163.53, 161.08, 144.87, 144.26, 139.29, 137.08, 134.53, 131.07, 130.67, 129.89, 129.81, 129.33, 128.10, 127.65, 127.30, 127.27, 126.85, 125.69, 125.08, 124.99, 124.73, 119.93, 118.24, 118.01, 116.69, 115.62, 115.41, 107.36, 93.33, 93.30, 82.71, 21.60, 21.54; ¹⁹F NMR (376 MHz, CDCl₃) δ -112.96. HRMS (APCI) calc. for C₃₀H₂₃FNO₂S⁺ [M+H]⁺: 480.1428, found 480.1427.

3-((2-Chlorophenyl)ethynyl)-2-(p-tolyl)-1-tosyl-1H-indole (2-33ah)



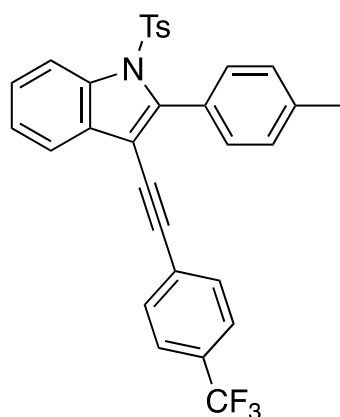
Following general procedure **GP6** with 4-methyl-*N*-(2-(*p*-tolylethynyl)phenyl)benzenesulfonamide **2-32a** (108 mg, 0.3 mmol) and 1-chloro-2-(iodoethynyl)benzene **2-30h** (86 mg, 0.33 mmol). The crude product was purified by flash column chromatography (Petroleum ether : EtOAc = 15 : 1) to afford **2-33ah** as a yellow solid (67 mg, 45%); Mp 109 °C; ¹H NMR (400 MHz, CDCl₃) δ 8.33 (d, *J* = 8.2 Hz, 1H), 7.72 (d, *J* = 7.6 Hz, 1H), 7.59 (s, 2H), 7.45 - 7.35 (m, 4H), 7.30 (dd, *J* = 8.3, 2.1 Hz, 4H), 7.20 (ddd, *J* = 9.3, 6.8, 1.9 Hz, 2H), 7.06 (d, *J* = 8.0 Hz, 2H), 2.48 (s, 3H), 2.30 (s, 3H); ¹³C NMR (101 MHz, CDCl₃) δ 144.86, 144.17, 139.19, 137.08, 135.59, 134.51, 133.10, 131.16, 130.87, 129.33, 129.21, 129.13, 128.10, 127.62, 126.86, 126.37, 125.67, 124.79, 123.18, 120.14, 116.63, 107.60, 91.41, 86.93, 77.32, 77.00, 76.68, 21.60, 21.53; HRMS (APCI) calc. for C₃₀H₂₃ClNO₂S⁺ [M+H]⁺: 496.1133, found 496.1136.

Methyl 4-((2-(p-tolyl)-1-tosyl-1H-indol-3-yl)ethynyl)benzoate (2-33ai)



Following general procedure **GP6** with 4-methyl-*N*-(2-(*p*-tolylethynyl)phenyl)benzenesulfonamide **2-32a** (108 mg, 0.3 mmol) and methyl 4-(iodoethynyl)benzoate **2-30i** (94 mg, 0.33 mmol). The crude product was purified by flash column chromatography (Petroleum ether : EtOAc = 15 : 1) to afford **2-33ah** as a yellow solid (87 mg, 56%); Mp 125 °C; ¹H NMR (400 MHz, CDCl₃) δ 8.33 (d, *J* = 8.2 Hz, 1H), 7.96 (d, *J* = 8.4 Hz, 2H), 7.68 - 7.63 (m, 1H), 7.58 - 7.52 (m, 2H), 7.45 - 7.40 (m, 3H), 7.37 (dd, *J* = 7.5, 1.1 Hz, 1H), 7.33 - 7.27 (m, 4H), 7.08 - 7.01 (m, 2H), 3.91 (s, 3H), 2.49 (s, 3H), 2.29 (s, 3H); ¹³C NMR (101 MHz, CDCl₃) δ 166.46, 144.90, 144.50, 139.35, 137.08, 134.51, 131.23, 131.10, 130.58, 129.44, 129.33, 128.10, 127.88, 127.59, 126.84, 125.73, 124.75, 119.93, 116.69, 107.28, 93.92, 84.92, 52.19, 21.61, 21.53; HRMS (APCI) calc. for C₃₂H₂₆NO₄S⁺ [M+H]⁺: 520.1577, found]⁺: 520.1577.

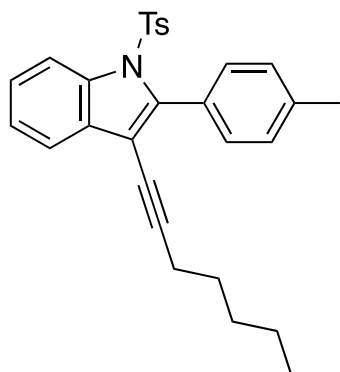
2-(p-Tolyl)-1-tosyl-3-((4-(trifluoromethyl)phenyl)ethynyl)-1H-indole (2-33aj)



Following general procedure **GP6** with 4-methyl-*N*-(2-(*p*-tolylethynyl)phenyl)benzenesulfonamide **2-32a** (108 mg, 0.3 mmol) and 1-(iodoethynyl)-4-(trifluoromethyl)benzene **2-30j** (98 mg, 0.33 mmol). The crude product was purified by flash column chromatography (Petroleum ether : EtOAc = 15 : 1) to afford **2-33aj** as a yellow solid (92 mg, 58%); Mp 119 °C; ¹H NMR (400 MHz, CDCl₃) δ 8.34 (d, *J* = 8.3 Hz, 1H), 7.65 (d, *J*

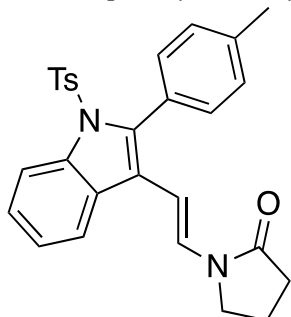
= 7.6 Hz, 1H), 7.55 (dd, $J = 8.3, 2.5$ Hz, 4H), 7.44 (dd, $J = 14.3, 7.6$ Hz, 3H), 7.41 - 7.26 (m, 6H), 7.07 (d, $J = 8.2$ Hz, 2H), 2.49 (s, 3H), 2.30 (s, 3H); ^{13}C NMR (101 MHz, CDCl_3) δ 144.95, 144.61, 139.40, 137.07, 134.57, 131.57, 131.12, 130.53, 129.37, 128.12, 127.59, 126.88, 125.77, 125.27, 125.24, 125.20, 125.16, 124.77, 119.91, 116.69, 107.11, 93.17, 84.35, 21.62, 21.55; ^{19}F NMR (376 MHz, CDCl_3) δ -62.82; HRMS (APCI) calc. for $\text{C}_{31}\text{H}_{23}\text{F}_3\text{NO}_2\text{S}^+$ $[\text{M}+\text{H}]^+$: 530.1396, found 530.1399.

3-(Hept-1-yn-1-yl)-2-(p-tolyl)-1-tosyl-1H-indole (2-33ak)



Following general procedure **GP6** with 4-methyl-*N*-(2-(*p*-tolylethynyl)phenyl)benzenesulfonamide **2-32a** (108 mg, 0.3 mmol) and 1-iodohept-1-yne **2-30k** (73 mg, 0.33 mmol). The crude product was purified by flash column chromatography (Petroleum ether : EtOAc = 20 : 1) to afford **2-33ak** as a yellow solid (52 mg, 38%); Mp 125 °C; ^1H NMR (400 MHz, CDCl_3) δ 8.33 (d, $J = 8.2$ Hz, 1H), 7.96 (d, $J = 8.4$ Hz, 2H), 7.68 - 7.63 (m, 1H), 7.58 - 7.52 (m, 2H), 7.45 - 7.40 (m, 3H), 7.37 (dd, $J = 7.5, 1.1$ Hz, 1H), 7.33 - 7.27 (m, 4H), 7.08 - 7.01 (m, 2H), 3.91 (s, 3H), 2.49 (s, 3H), 2.29 (s, 3H); ^{13}C NMR (101 MHz, CDCl_3) δ 166.46, 144.90, 144.50, 139.35, 137.08, 134.51, 131.23, 131.10, 130.58, 129.44, 129.33, 128.10, 127.88, 127.59, 126.84, 125.73, 124.75, 119.93, 116.69, 107.28, 93.92, 84.92, 52.19, 21.61, 21.53; HRMS (APCI) calc. for $\text{C}_{29}\text{H}_{30}\text{NO}_2\text{S}^+$ $[\text{M}+\text{H}]^+$: 456.1992, found 456.1992.

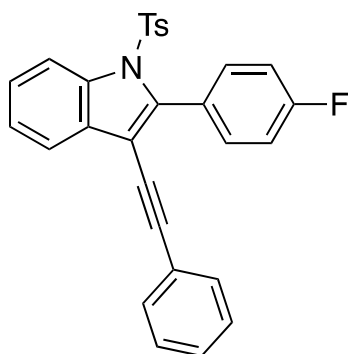
(E)-1-(2-(2-(p-Tolyl)-1-tosyl-1H-indol-3-yl)vinyl)pyrrolidin-2-one (2-36)



Following general procedure **GP6** with 4-methyl-*N*-(2-(*p*-tolylethynyl)phenyl)benzenesulfonamide **2-32a** (108 mg, 0.3 mmol) and (*E*)-1-(2-

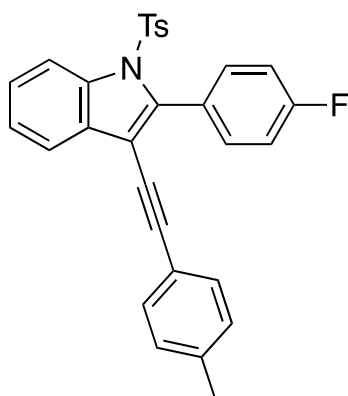
iodovinyl)pyrrolidin-2-one **2-35** (78 mg, 0.33 mmol). The crude product was purified by flash column chromatography (Petroleum ether : EtOAc = 5 : 1) to afford **2-36** as a yellow solid (54 mg, 38%). Mp 148 °C. ¹H NMR (400 MHz, CDCl₃) δ 8.35 (d, *J* = 8.2 Hz, 1H), 7.77 (d, *J* = 7.8 Hz, 1H), 7.61 (d, *J* = 15.1 Hz, 1H), 7.39 (t, *J* = 7.7 Hz, 1H), 7.36 - 7.26 (m, 7H), 7.05 (d, *J* = 8.0 Hz, 2H), 5.59 (d, *J* = 15.2 Hz, 1H), 3.45 (t, *J* = 7.2 Hz, 2H), 2.50 (t, *J* = 8.2 Hz, 2H), 2.46 (s, 3H), 2.30 (s, 3H), 2.14 - 2.01 (m, 2H). ¹³C NMR (101 MHz, CDCl₃) δ 173.07, 144.54, 138.62, 137.74, 137.54, 134.76, 131.48, 129.22, 128.70, 128.34, 128.22, 126.78, 125.12, 124.55, 120.47, 119.82, 116.53, 103.79, 44.82, 31.20, 21.53, 17.35. HRMS (APCI) calc. for C₂₈H₂₇N₂O₃S⁺ [M+H]⁺: 471.1737, found 471.1737.

2-(4-Fluorophenyl)-3-(phenylethynyl)-1-tosyl-1H-indole (2-33bb)



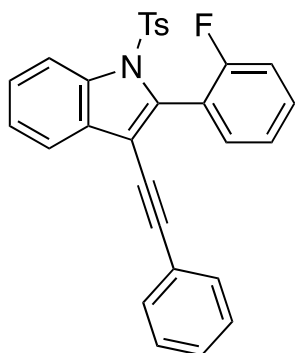
Following general procedure **GP6** with *N*-(2-((4-fluorophenyl)ethynyl)phenyl)-4-methylbenzenesulfonamide **2-32b** (109 mg, 0.3 mmol) and 1-iodohept-1-yne **2-30b** (75 mg, 0.33 mmol). The crude product was purified by flash column chromatography (Petroleum ether : EtOAc = 20 : 1) to afford **2-33bb** as a yellow solid (90 mg, 65%); Mp 104 °C; ¹H NMR (400 MHz, CDCl₃) δ 8.35 (d, *J* = 8.3 Hz, 1H), 7.65 (ddd, *J* = 14.1, 8.4, 6.1 Hz, 3H), 7.47 - 7.41 (m, 1H), 7.40 - 7.35 (m, 3H), 7.30 (dd, *J* = 6.6, 3.2 Hz, 4H), 7.27 (s, 1H), 7.19 (t, *J* = 8.6 Hz, 2H), 7.07 (d, *J* = 8.1 Hz, 2H), 2.30 (s, 3H); ¹³C NMR (101 MHz, CDCl₃) δ 164.48, 162.00, 145.02, 142.26, 137.11, 134.52, 133.19, 133.10, 131.40, 130.58, 129.39, 128.38, 128.34, 126.76, 126.72, 126.69, 125.89, 124.79, 122.92, 120.13, 116.62, 114.60, 114.38, 108.31, 94.89, 81.18, 21.53; ¹⁹F NMR (376 MHz, CDCl₃) δ -111.53. HRMS (APCI) calc. for C₂₉H₂₁FNO₂S⁺ [M+H]⁺: 466.1272, found 466.1265

2-(4-fluorophenyl)-3-(p-tolylethynyl)-1-tosyl-1H-indole (**2-33bc**)



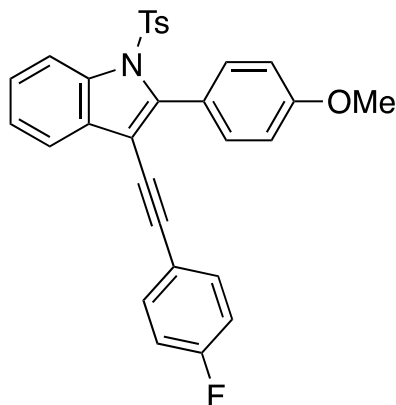
Following general procedure **GP6** with *N*-(2-((4-fluorophenyl)ethynyl)phenyl)-4-methylbenzenesulfonamide **2-32b** (109 mg, 0.3 mmol) and 1-(iodoethynyl)-4-methylbenzene **2-30c** (80 mg, 0.33 mmol). The crude product was purified by flash column chromatography (Petroleum ether : EtOAc = 20 : 1) to afford **2-33bc** as a yellow solid (98 mg, 68%); Mp 110 °C; ¹H NMR (400 MHz, CDCl₃) δ 8.36 (d, *J* = 8.2 Hz, 1H), 7.71 - 7.62 (m, 3H), 7.48 - 7.42 (m, 1H), 7.39 (d, *J* = 7.5 Hz, 1H), 7.29 (d, *J* = 8.0 Hz, 4H), 7.20 (t, *J* = 8.7 Hz, 2H), 7.12 (d, *J* = 7.8 Hz, 2H), 7.07 (d, *J* = 8.0 Hz, 2H), 2.35 (s, 3H), 2.30 (s, 3H); ¹³C NMR (101 MHz, CDCl₃) δ 164.41, 161.93, 144.96, 141.97, 138.59, 137.11, 134.44, 133.15, 133.06, 131.28, 130.66, 129.35, 129.08, 126.78, 126.75, 126.72, 125.83, 124.76, 120.14, 119.80, 116.61, 114.55, 114.33, 108.54, 95.12, 80.46, 21.49, 21.46; ¹⁹F NMR (376 MHz, CDCl₃) δ -111.58; HRMS (APCI) calc. for C₃₀H₂₃FNO₂S⁺ [M+H]⁺: 480.1428, found 480.1422.

2-(2-Fluorophenyl)-3-(phenylethynyl)-1-tosyl-1H-indole (**2-33cb**)



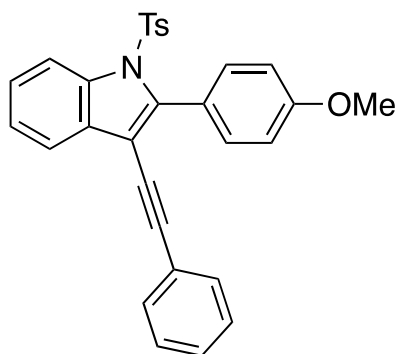
Following general procedure **GP6** with *N*-(2-((2-fluorophenyl)ethynyl)phenyl)-4-methylbenzenesulfonamide **2-32c** (109 mg, 0.3 mmol) and (iodoethynyl)benzene **2-30b** (75 mg, 0.33 mmol). The crude product was purified by flash column chromatography (Petroleum ether : EtOAc = 20 : 1) to afford **2-33cb** as a yellow solid (94 mg, 64%); Mp 115 °C; ¹H NMR (400 MHz, CDCl₃) δ 8.29 (d, *J* = 8.3 Hz, 1H), 7.70 (d, *J* = 7.7 Hz, 1H), 7.57 - 7.49 (m, 2H), 7.41 (t, *J* = 8.3 Hz, 3H), 7.38 - 7.33 (m, 3H), 7.31 - 7.26 (m, 4H), 7.23 (t, *J* = 9.1 Hz, 1H), 7.10 (d, *J* =

8.1 Hz, 2H), 2.31 (s, 3H); ^{13}C NMR (101 MHz, CDCl_3) 162.01, 159.52, 144.99, 136.89, 136.76, 134.79, 132.91, 132.89, 131.46, 130.25, 129.51, 128.27, 126.82, 125.91, 124.45, 123.17, 123.00, 120.28, 115.93, 115.60, 115.39, 109.13, 95.43, 80.68, 21.55; ^{19}F NMR (376 MHz, CDCl_3) δ -109.70; HRMS (APCI) calc. for $\text{C}_{29}\text{H}_{21}\text{FNO}_2\text{S}^+$ $[\text{M}+\text{H}]^+$: 466.1272, found 466.1271.
3-((4-Fluorophenyl)ethynyl)-2-(4-methoxyphenyl)-1-tosyl-1H-indole (2-33da)



Following general procedure **GP6** with *N*-(2-((4-methoxyphenyl)ethynyl)phenyl)-4-methylbenzenesulfonamide **2-32d** (113 mg, 0.3 mmol) and 1-fluoro-4-(iodoethynyl)benzene **2-30a** (81 mg, 0.33 mmol). The crude product was purified by flash column chromatography (Petroleum ether : EtOAc = 15 : 1) to afford **2-33da** as a yellow solid (95 mg, 64%); Mp 113 °C; ^1H NMR (400 MHz, CDCl_3) δ 8.37 (d, J = 8.3 Hz, 1H), 7.68 (d, J = 7.6 Hz, 1H), 7.45 (d, J = 8.3 Hz, 1H), 7.43 - 7.35 (m, 5H), 7.34 (s, 1H), 7.27 (s, 1H), 7.22 (d, J = 2.1 Hz, 1H), 7.09 (d, J = 8.1 Hz, 3H), 7.03 (d, J = 9.1 Hz, 2H), 3.90 (s, 3H), 2.32 (s, 3H); ^{13}C NMR (101 MHz, CDCl_3) δ 163.69, 161.20, 158.56, 144.88, 143.29, 137.16, 134.51, 133.34, 133.26, 131.80, 130.58, 129.31, 128.25, 126.88, 125.82, 124.70, 123.75, 120.05, 116.66, 116.53, 115.72, 115.50, 115.24, 108.00, 93.81, 81.16, 55.35, 21.52; ^{19}F NMR (376 MHz, CDCl_3) δ -110.59. HRMS (APCI) calc. for $\text{C}_{30}\text{H}_{23}\text{FNO}_3\text{S}^+$ $[\text{M}+\text{H}]^+$: 496.1377, found 496.1375.

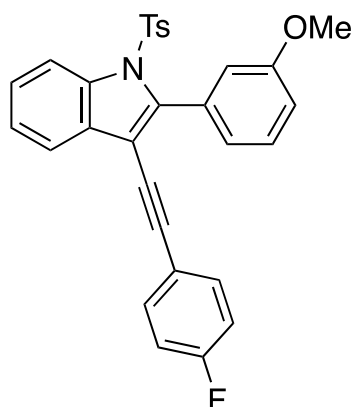
2-(4-Methoxyphenyl)-3-(phenylethynyl)-1-tosyl-1H-indole (2-33db)



Following general procedure **GP6** with *N*-(2-((4-methoxyphenyl)ethynyl)phenyl)-4-methylbenzenesulfonamide **2-32d** (113 mg, 0.3 mmol) and (iodoethynyl)benzene **2-30b** (75

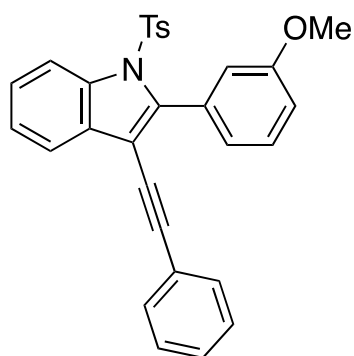
mg, 0.33 mmol). The crude product was purified by flash column chromatography (Petroleum ether : EtOAc = 20 : 1) to afford **2-33db** as a yellow solid (97 mg, 68%); Mp 108 °C; ¹H NMR (300 MHz, CDCl₃) δ 8.33 (d, *J* = 7.6 Hz, 1H), 7.65 (d, *J* = 7.2 Hz, 1H), 7.60 (d, *J* = 8.8 Hz, 2H), 7.44 - 7.35 (m, 4H), 7.32 - 7.27 (m, 4H), 7.25 (s, 1H), 7.03 (t, *J* = 8.8 Hz, 4H), 3.92 (s, 3H), 2.29 (s, 3H); ¹³C NMR (75 MHz, CDCl₃) δ 160.29, 144.79, 143.58, 137.10, 134.54, 132.68, 131.41, 130.89, 129.29, 128.28, 128.19, 126.84, 125.52, 124.69, 123.20, 122.96, 119.92, 116.75, 112.79, 107.53, 94.57, 81.71, 55.31, 21.54; HRMS (APCI) calc. for C₃₀H₂₄NO₃S⁺ [M+H]⁺: 478.1399, found 478.1397;

3-((4-Fluorophenyl)ethynyl)-2-(3-methoxyphenyl)-1-tosyl-1H-indole (3ea)



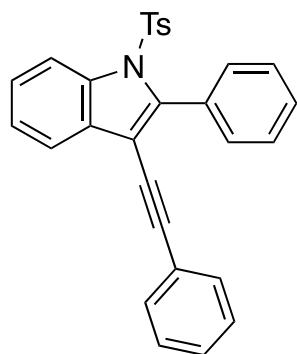
Following general procedure **GP6** with N-(2-((3-methoxyphenyl)ethynyl)phenyl)-4-methylbenzenesulfonamide **2-32e** (113 mg, 0.3 mmol) and 1-fluoro-4-(iodoethynyl)benzene **2-30a** (81 mg, 0.33 mmol). The crude product was purified by flash column chromatography (Petroleum ether : EtOAc = 16 : 1) to afford **2-33ea** as a yellow solid (90 mg, 61%); Mp 115 °C; ¹H NMR (400 MHz, CDCl₃) δ 8.36 (d, *J* = 8.3 Hz, 1H), 7.67 - 7.64 (m, 1H), 7.63 - 7.57 (m, 2H), 7.46 - 7.41 (m, 1H), 7.41 - 7.36 (m, 3H), 7.31 - 7.28 (m, 2H), 7.11 - 6.97 (m, 6H), 3.94 (s, 3H), 2.32 (s, 3H); ¹³C NMR (101 MHz, CDCl₃) δ 163.66, 161.17, 160.31, 144.82, 143.61, 137.07, 134.56, 133.31, 133.23, 132.66, 130.77, 129.30, 126.83, 125.56, 124.69, 122.92, 119.85, 119.31, 119.28, 116.73, 115.71, 115.49, 112.79, 107.31, 93.42, 81.41, 55.31, 21.53; ¹⁹F NMR (376 MHz, CDCl₃) δ -110.78. HRMS (APCI) calc. for C₃₀H₂₃FNO₃S⁺ [M+H]⁺: 496.1377, found 496.1375.

2-(3-Methoxyphenyl)-3-(phenylethynyl)-1-tosyl-1H-indole (2-33eb)



Following general procedure **GP6** with *N*-(2-((3-methoxyphenyl)ethynyl)phenyl)-4-methylbenzenesulfonamide **2-32e** (113 mg, 0.3 mmol) and (iodoethynyl)benzene **2-30b** (75 mg, 0.33 mmol). The crude product was purified by flash column chromatography (Petroleum ether : EtOAc = 15 : 1) to afford **2-33eb** as a yellow solid (105 mg, 67%); Mp 112 °C; ¹H NMR (400 MHz, CDCl₃) δ 8.35 (d, *J* = 8.3 Hz, 1H), 7.68 (d, *J* = 7.4 Hz, 1H), 7.45 (d, *J* = 7.4 Hz, 1H), 7.43 – 7.34 (m, 5H), 7.33 (s, 1H), 7.30 (dd, *J* = 6.4, 3.1 Hz, 4H), 7.22 - 7.19 (m, 1H), 7.05 (t, *J* = 7.2 Hz, 3H), 3.87 (s, 3H), 2.30 (s, 3H); ¹³C NMR (101 MHz, CDCl₃) δ 158.55, 144.86, 143.26, 137.20, 134.50, 131.82, 131.42, 130.70, 129.30, 128.28, 128.27, 128.24, 126.89, 125.78, 124.70, 123.80, 123.08, 120.12, 116.66, 116.45, 115.32, 108.23, 94.97, 81.44, 55.35, 21.52; HRMS (APCI) calc. for C₃₀H₂₄NO₃S⁺ [M+H]⁺: 478.1471, found 478.1472.

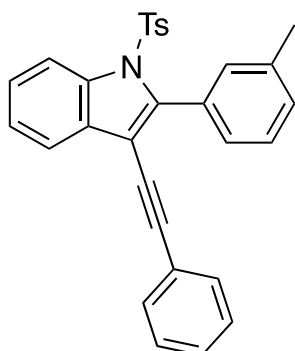
2-Phenyl-3-(phenylethynyl)-1-tosyl-1H-indole (2-33fb)



Following general procedure **GP6** with *N*-(2-((3-methoxyphenyl)ethynyl)phenyl)-4-methylbenzenesulfonamide **2-32f** (113 mg, 0.3 mmol) and (iodoethynyl)benzene **2-30b** (75 mg, 0.33 mmol). The crude product was purified by flash column chromatography (Petroleum ether : EtOAc = 15 : 1) to afford **2-33fb** as a yellow solid (62 mg, 46%); Mp 105 °C; ¹H NMR (400 MHz, CDCl₃) δ 8.36 (d, *J* = 8.2 Hz, 1H), 7.72 - 7.65 (m, 3H), 7.53 - 7.48 (m, 3H), 7.44 (t, *J* = 7.2 Hz, 1H), 7.40 - 7.35 (m, 3H), 7.30 (d, *J* = 6.6 Hz, 5H), 7.06 (d, *J* = 8.2 Hz, 2H), 2.30 (s, 3H); ¹³C NMR (101 MHz, CDCl₃) δ 144.85, 143.49, 137.14, 134.50, 131.39, 131.23, 130.72, 130.69, 129.31, 129.07, 128.26, 128.24, 127.26, 126.82, 125.74, 124.69, 123.07, 120.10,

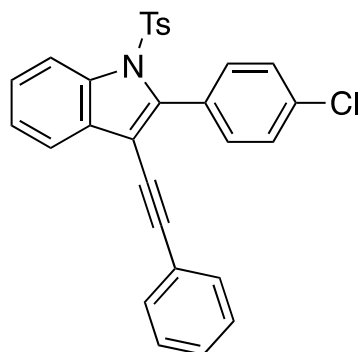
116.63, 108.20, 94.70, 81.46, 21.52; HRMS (APCI) calc. for $C_{29}H_{22}NO_2S^+$ $[M+H]^+$: 448.1366, found 448.1365.

3-(Phenylethynyl)-2-(m-tolyl)-1-tosyl-1H-indole (2-33gb)



Following general procedure **GP6** with 4-methyl-*N*-(2-(m-tolylolethynyl)phenyl)benzenesulfonamide **2-32g** (108 mg, 0.3 mmol) and (iodoethynyl)benzene **2-30b** (75 mg, 0.33 mmol). The crude product was purified by flash column chromatography (Petroleum ether : EtOAc = 15 : 1) to afford **2-33gb** as a yellow solid (62 mg, 46%); Mp 110 °C; 1H NMR (400 MHz, $CDCl_3$) δ 8.34 (d, J = 8.2 Hz, 1H), 7.67 (d, J = 7.3 Hz, 1H), 7.50 - 7.41 (m, 3H), 7.40 - 7.34 (m, 4H), 7.30 (ddd, J = 6.5, 4.0, 2.3 Hz, 6H), 7.06 (d, J = 8.2 Hz, 2H), 2.46 (s, 3H), 2.30 (s, 3H); ^{13}C NMR (101 MHz, $CDCl_3$) δ 144.80, 143.75, 137.15, 136.72, 134.58, 131.86, 131.41, 130.75, 130.58, 129.86, 129.28, 128.28, 128.21, 127.17, 126.89, 125.66, 124.65, 123.17, 120.07, 116.63, 108.01, 94.73, 81.61, 21.52, 21.47; HRMS (APCI) calc. for $C_{30}H_{24}NO_2S^+$ $[M+H]^+$: 462.1522, found 462.1520.

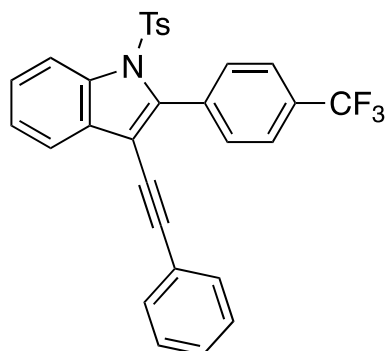
2-(4-Chlorophenyl)-3-(phenylethynyl)-1-tosyl-1H-indole (2-33hb)



Following general procedure **GP6** with *N*-(2-((4-chlorophenyl)ethynyl)phenyl)-4-methylbenzenesulfonamide **2-32h** (114 mg, 0.3 mmol) and (iodoethynyl)benzene **2-30b** (75 mg, 0.33 mmol). The crude product was purified by flash column chromatography (Petroleum ether : EtOAc = 15 : 1) to afford **2-33hb** as a yellow solid (98 mg, 68%); Mp 115 °C; 1H NMR (400 MHz, $CDCl_3$) δ 8.35 (d, J = 8.3 Hz, 1H), 7.68 (d, J = 7.4 Hz, 1H), 7.63 (s, 2H), 7.49 (d, J = 8.5 Hz, 2H), 7.45 (d, J = 8.5 Hz, 1H), 7.43 - 7.37 (m, 3H), 7.32 (s, 3H), 7.29 (d, J = 8.4 Hz,

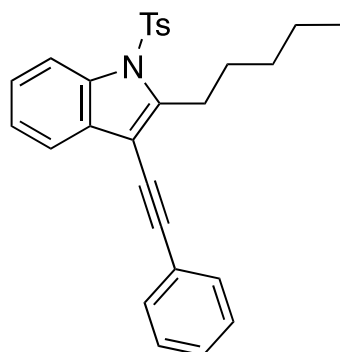
2H), 2.32 (s, 3H); ^{13}C NMR (101 MHz, CDCl_3) δ 145.06, 142.02, 137.25, 135.19, 134.36, 132.46, 131.45, 130.69, 129.42, 129.20, 128.46, 128.37, 127.65, 126.78, 126.03, 124.87, 122.85, 120.21, 116.71, 108.67, 95.18, 81.06, 21.55; HRMS (APCI) calc. for $\text{C}_{29}\text{H}_{21}\text{ClNO}_2\text{S}^+$ $[\text{M}+\text{H}]^+$: 482.0976, found 482.0979.

3-(Phenylethynyl)-1-tosyl-2-(4-(trifluoromethyl)phenyl)-1H-indole (2-33ib)



Following general procedure **GP6** with 4-methyl-*N*-(2-((4-(trifluoromethyl)phenyl)ethynyl)phenyl)benzenesulfonamide **2-32i** (124 mg, 0.3 mmol) and (iodoethynyl)benzene **2-30b** (75 mg, 0.33 mmol). The crude product was purified by flash column chromatography (Petroleum ether : EtOAc = 12 : 1) to afford **2-33ib** as a yellow solid (92 mg, 60%); Mp 120 °C; ^1H NMR (400 MHz, CDCl_3) δ 8.33 (d, J = 8.3 Hz, 1H), 7.80 (d, J = 8.2 Hz, 2H), 7.75 (d, J = 8.3 Hz, 2H), 7.68 (d, J = 7.3 Hz, 1H), 7.46 (t, J = 8.5 Hz, 1H), 7.41 - 7.35 (m, 3H), 7.34 - 7.30 (m, 3H), 7.29 (s, 1H), 7.26 (s, 1H), 7.07 (d, J = 8.1 Hz, 2H), 2.30 (s, 3H); ^{13}C NMR (101 MHz, CDCl_3) δ 145.19, 141.42, 137.37, 134.41, 134.20, 131.46, 131.42, 130.65, 129.47, 128.60, 128.40, 126.76, 126.33, 124.98, 124.30, 124.26, 122.68, 120.39, 116.71, 109.51, 95.50, 80.77, 21.55; ^{19}F NMR (376 MHz, CDCl_3) δ -62.82. HRMS (APCI) calc. for $\text{C}_{30}\text{H}_{21}\text{FINO}_2\text{S}^+$ $[\text{M}+\text{H}]^+$: 516.1240, found 516.1239.

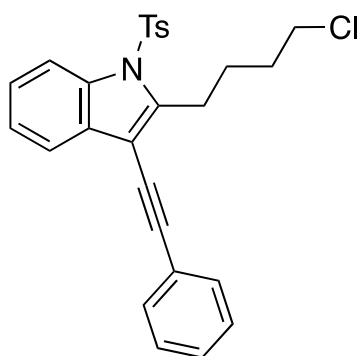
2-Pentyl-3-(phenylethynyl)-1-tosyl-1H-indole (2-33jb)



Following general procedure **GP6** with *N*-(2-(hept-1-yn-1-yl)phenyl)-4-methylbenzenesulfonamide **2-32j** (102 mg, 0.3 mmol) and (iodoethynyl)benzene **2-30b** (75 mg, 0.33 mmol). The crude product was purified by flash column chromatography (Petroleum ether :

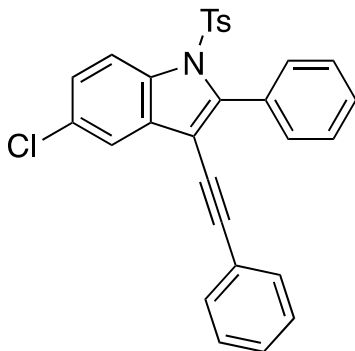
EtOAc = 18 : 1) to afford **2-33jb** as a yellow solid (77 mg, 58%); Mp 128 °C; ¹H NMR (400 MHz, CDCl₃) δ 8.23 - 8.13 (m, 1H), 7.68 - 7.60 (m, 3H), 7.54 (dd, *J* = 7.2, 2.3 Hz, 2H), 7.39 - 7.29 (m, 5H), 7.19 (d, *J* = 8.0 Hz, 2H), 3.24 (t, *J* = 7.6 Hz, 2H), 2.33 (s, 3H), 1.85 (s, 2H), 1.43 (dt, *J* = 6.6, 3.6 Hz, 4H), 0.92 (t, *J* = 6.9 Hz, 3H); ¹³C NMR (101 MHz, CDCl₃) δ 145.86, 144.92, 136.12, 135.88, 131.37, 129.89, 129.85, 128.38, 128.20, 126.32, 124.81, 123.99, 123.40, 119.56, 115.02, 105.57, 95.66, 81.04, 31.53, 30.13, 28.14, 22.35, 21.52, 14.01; HRMS (APCI) calc. for C₂₈H₂₈NO₂S⁺ [M+H]⁺: 442.1835, found 442.1834.

2-(4-Chlorobutyl)-3-(phenylethynyl)-1-tosyl-1H-indole (2-33kb)



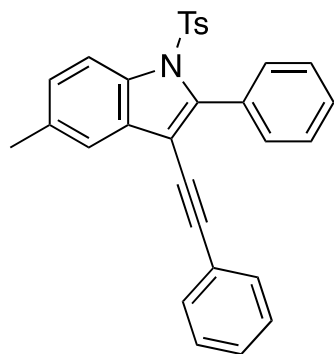
Following general procedure **GP6** with *N*-(2-(6-chlorohex-1-yn-1-yl)phenyl)-4-methylbenzenesulfonamide **2-32k** (138mg, 0.3 mmol) and (iodoethynyl)benzene **2-30b** (75 mg, 0.33 mmol). The crude product was purified by flash column chromatography (Petroleum ether : EtOAc = 18 : 1) to afford **2-33kb** as a yellow solid (68 mg, 49%); Mp 125 °C; ¹H NMR (400 MHz, CDCl₃) δ 8.18 (d, *J* = 7.2 Hz, 1H), 7.63 (d, *J* = 8.6 Hz, 3H), 7.55 (dd, *J* = 7.3, 2.4 Hz, 2H), 7.41 - 7.28 (m, 5H), 7.19 (d, *J* = 8.1 Hz, 2H), 3.61 (t, *J* = 6.6 Hz, 2H), 3.28 (t, *J* = 7.2 Hz, 2H), 2.34 (s, 3H), 2.02 (dt, *J* = 14.3, 6.4 Hz, 2H), 1.92 (dt, *J* = 13.5, 6.5 Hz, 2H); ¹³C NMR (101 MHz, CDCl₃) δ 145.09, 144.50, 136.16, 135.70, 131.44, 129.77, 128.43, 128.37, 126.31, 126.20, 125.06, 124.11, 123.15, 119.69, 115.05, 106.15, 96.00, 80.72, 44.65, 32.02, 27.63, 27.33, 21.54; HRMS (APCI) calc. for C₂₇H₂₅ClNO₂S⁺ [M+H]⁺: 462.1289, found 462.1287.

5-Chloro-2-phenyl-3-(phenylethynyl)-1-tosyl-1H-indole (2-33lb)



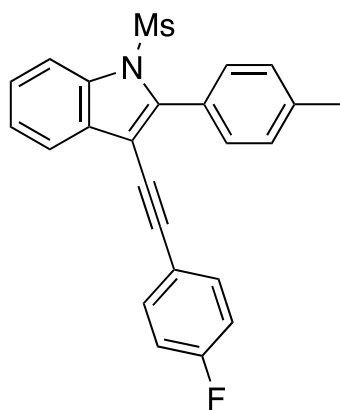
Following general procedure **GP6** with *N*-(4-chloro-2-(phenylethynyl)phenyl)-4-methylbenzenesulfonamide **2-32l** (114 mg, 0.3 mmol) and (iodoethynyl)benzene **2-30b** (75 mg, 0.33 mmol). The crude product was purified by flash column chromatography (Petroleum ether : EtOAc = 12 : 1) to afford **2-33lb** as a brown solid (60 mg, 42%); Mp 102 °C; ¹H NMR (400 MHz, CDCl₃) δ 8.28 (d, *J* = 8.8 Hz, 1H), 7.65 (dd, *J* = 4.2, 1.8 Hz, 3H), 7.50 (dd, *J* = 5.1, 1.9 Hz, 3H), 7.41 - 7.35 (m, 3H), 7.32 - 7.25 (m, 5H), 7.08 (d, *J* = 8.1 Hz, 2H), 2.32 (s, 3H); ¹³C NMR (101 MHz, CDCl₃) δ 145.18, 144.65, 135.46, 134.30, 131.98, 131.43, 131.25, 130.62, 130.21, 129.45, 129.38, 128.43, 128.30, 127.33, 126.83, 125.91, 122.79, 119.78, 117.74, 107.45, 95.05, 80.68, 21.55; HRMS (APCI) calc. for C₂₉H₂₁ClNO₂S⁺ [M+H]⁺: 482.0976, found 482.0955.

5-Methyl-2-phenyl-3-(phenylethynyl)-1-tosyl-1H-indole (2-33mb)



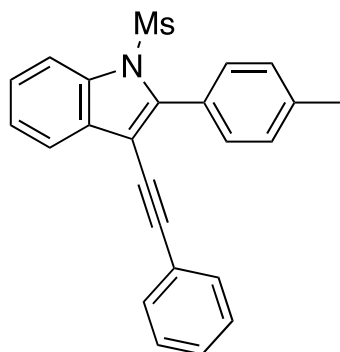
Following general procedure **GP6** with 4-methyl-*N*-(4-methyl-2-(phenylethynyl)phenyl)benzenesulfonamide **2-32m** (108 mg, 0.3 mmol) and (iodoethynyl)benzene **2-30b** (75 mg, 0.33 mmol). The crude product was purified by flash column chromatography (Petroleum ether : EtOAc = 12 : 1) to afford **2-33mb** as a brown solid (64 mg, 46%); Mp 106 °C; ¹H NMR (400 MHz, CDCl₃) δ 8.21 (d, *J* = 8.5 Hz, 1H), 7.66 (dd, *J* = 6.6, 2.9 Hz, 2H), 7.49 (t, *J* = 2.7 Hz, 3H), 7.45 (s, 1H), 7.41 - 7.36 (m, 2H), 7.29 (dd, *J* = 7.5, 3.2 Hz, 5H), 7.26 - 7.22 (m, 1H), 7.05 (d, *J* = 8.2 Hz, 2H), 2.48 (s, 3H), 2.29 (s, 3H); ¹³C NMR (101 MHz, CDCl₃) δ 144.73, 143.61, 135.36, 134.54, 134.49, 131.41, 131.21, 130.94, 130.80, 129.28, 129.01, 128.26, 128.21, 127.23, 127.13, 126.83, 123.14, 119.97, 116.36, 108.06, 94.59, 81.64, 21.52, 21.29; HRMS (APCI) calc. for C₃₀H₂₄NO₂S⁺ [M+H]⁺: 462.1449, found 462.1446.

3-((4-Luorophenyl)ethynyl)-1-(methylsulfonyl)-2-(p-tolyl)-1H-indole (2-33Ms-aa)



Following general procedure **GP6** with *N*-(2-(*p*-tolylethynyl)phenyl)methanesulfonamide **2-32Ms-a** (86mg, 0.3 mmol) and 1-fluoro-4-(iodoethynyl)benzene **2-30a** (81 mg, 0.33 mmol). The crude product was purified by flash column chromatography (Petroleum ether : EtOAc = 18 : 1) to afford **2-33Ms-aa** as a yellow solid (43 mg, 37%); Mp 128 °C; ¹H NMR (400 MHz, CDCl₃) δ 8.17 - 8.12 (m, 1H), 7.81 - 7.76 (m, 1H), 7.61 (d, *J* = 7.9 Hz, 2H), 7.48 - 7.38 (m, 4H), 7.30 (d, *J* = 7.8 Hz, 2H), 7.02 (t, *J* = 8.7 Hz, 2H), 2.77 (s, 3H), 2.45 (s, 3H); ¹³C NMR (101 MHz, CDCl₃) δ 163.76, 161.28, 143.48, 139.43, 136.89, 133.45, 133.36, 130.81, 130.57, 128.35, 127.31, 126.00, 124.95, 120.32, 115.94, 115.76, 115.54, 107.46, 93.77, 80.98, 39.77, 21.57; ¹⁹F NMR (376 MHz, CDCl₃) δ -110.59; HRMS (APCI) calc. for C₂₄H₁₉FNO₂S⁺ [M+H]⁺: 404.1115, found 404.1116.

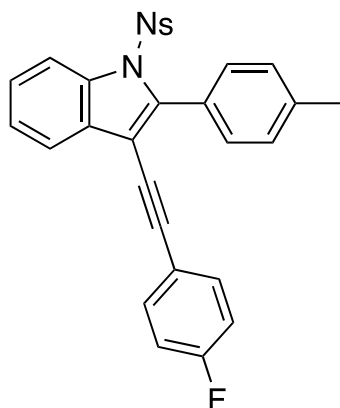
1-(Methylsulfonyl)-3-(phenylethynyl)-2-(*p*-tolyl)-1*H*-indole (**2-33Ms-ab**)



Following general procedure **GP6** with *N*-(2-(*p*-tolylethynyl)phenyl)methanesulfonamide **2-32Ms-a** (86mg, 0.3 mmol) and (iodoethynyl)benzene **2-30b** (75 mg, 0.33 mmol). The crude product was purified by flash column chromatography (Petroleum ether : EtOAc = 18 : 1) to afford **2-33Ms-ab** as a yellow solid (43 mg, 37%); Mp 123 °C; ¹H NMR (400 MHz, CDCl₃) δ 8.19 - 8.14 (m, 1H), 7.83 (dd, *J* = 6.3, 2.8 Hz, 1H), 7.65 (d, *J* = 8.0 Hz, 2H), 7.49 - 7.44 (m, 4H), 7.37 - 7.30 (m, 5H), 2.79 (s, 3H), 2.47 (s, 3H); ¹³C NMR (101 MHz, CDCl₃) δ 143.45, 139.37, 136.92, 131.52, 130.83, 130.68, 128.68, 128.33, 128.32, 127.33, 125.96, 124.94,

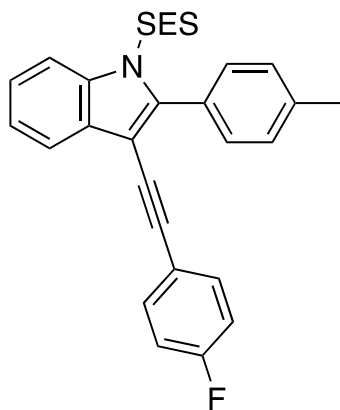
123.13, 120.38, 115.94, 107.68, 94.92, 81.25, 39.69, 21.56; HRMS (APCI) calc. for $C_{24}H_{20}NO_2S^+$ $[M+H]^+$: 386.1209, found 386.1210.

3-((4-Fluorophenyl)ethynyl)-1-((4-nitrophenyl)sulfonyl)-2-(p-tolyl)-1H-indole (2-33Ns-aa)



Following general procedure **GP6** with 4-nitro-*N*-(2-(*p*-tolylethynyl)phenyl)benzenesulfonamide **2-32Ns-a** (117mg, 0.3 mmol) and 1-fluoro-4-(iodoethynyl)benzene **2-30a** (81 mg, 0.33 mmol). The crude product was purified by flash column chromatography (Petroleum ether : DCM = 1 : 1) to afford **2-33Ns-aa** as a yellow solid (64 mg, 42%); Mp 145 °C; 1H NMR (400 MHz, $CDCl_3$) δ 8.30 (d, J = 8.3 Hz, 1H), 8.10 (d, J = 8.7 Hz, 2H), 7.66 - 7.61 (m, 1H), 7.60 - 7.52 (m, 4H), 7.46 (t, J = 7.7 Hz, 1H), 7.42 - 7.30 (m, 5H), 7.00 (t, J = 8.6 Hz, 2H), 2.49 (s, 3H); ^{13}C NMR (101 MHz, $CDCl_3$) δ 163.85, 161.36, 150.56, 143.19, 142.11, 139.76, 136.91, 133.46, 133.38, 131.07, 130.96, 128.36, 128.15, 127.21, 126.27, 125.55, 123.88, 120.44, 118.94, 118.90, 116.77, 115.80, 115.58, 108.98, 94.39, 80.64, 21.62; ^{19}F NMR (376 MHz, $CDCl_3$) δ -110.20; HRMS (APCI) calc. for $C_{29}H_{20}FNO_4S^+$ $[M+H]^+$: 511.1122.

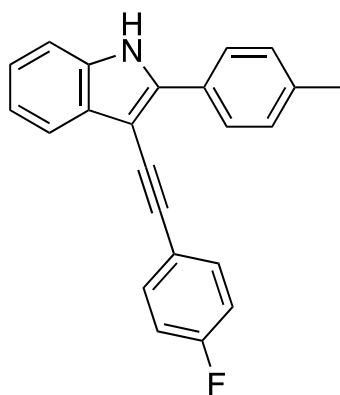
3-((4-Fluorophenyl)ethynyl)-2-(p-tolyl)-1-((2-(trimethylsilyl)ethyl)sulfonyl)-1H-indole (2-33SES-aa)



Following general procedure **GP6** with *N*-(2-(*p*-tolylethynyl)phenyl)-2-(trimethylsilyl)ethane-1-sulfonamide **2-32SES-a** (111mg, 0.3 mmol) and 1-fluoro-4-(iodoethynyl)benzene **2-30a** (81

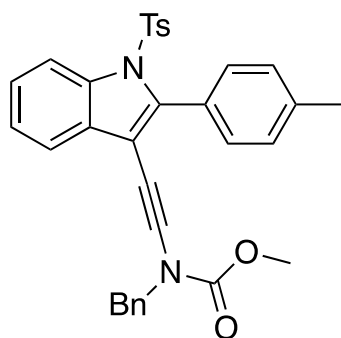
mg, 0.33 mmol). The crude product was purified by flash column chromatography (Petroleum ether : DCM = 1 : 1) to afford **2-33SES-aa** as a yellow solid (64 mg, 42%); Mp 155 °C; ¹H NMR (400 MHz, CDCl₃) δ 8.18 - 8.13 (m, 1H), 7.81 - 7.75 (m, 1H), 7.58 (d, *J* = 7.9 Hz, 2H), 7.45 - 7.38 (m, 4H), 7.29 (d, *J* = 7.9 Hz, 2H), 7.01 (t, *J* = 8.6 Hz, 2H), 2.96 - 2.88 (m, 2H), 2.45 (s, 3H), 0.69 - 0.61 (m, 2H), -0.12 (s, 9H); ¹³C NMR (101 MHz, CDCl₃) δ 163.72, 161.23, 143.88, 139.35, 137.20, 133.38, 133.30, 131.07, 129.87, 128.27, 127.42, 125.71, 124.41, 120.18, 119.44, 119.40, 115.71, 115.58, 115.50, 106.27, 93.37, 81.26, 50.83, 21.54, 9.56, -2.24; ¹⁹F NMR (376 MHz, CDCl₃) δ -110.85. HRMS (APCI) calc. for C₂₈H₂₉FNO₂SSi⁺ [M+H]⁺: 490.1667, found 490.1655.

3-((4-Fluorophenyl)ethynyl)-2-(p-tolyl)-1H-indole (**2-33aa-H**)



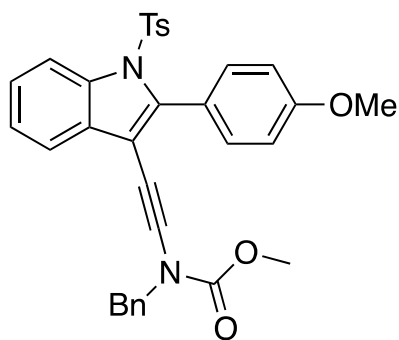
To a stirred solution of 3-((4-fluorophenyl)ethynyl)-2-(p-tolyl)-1-((2-(trimethylsilyl)ethyl)sulfonyl)-1H-indole **2-33SES-aa** (48.9 mg, 0.1 mmol, 1 eq.) in THF (4.0 mL) was added TBAF (0.4 mmol, 4 eq.). The mixture was stirred at room temperature for 3 h. The reaction mixture was poured into water and then extracted with EtOAc (3 × 10 mL). The combined organic phase was washed with saturated brine (10 mL), dried over MgSO₄ and filtered. The solvent was removed under reduced pressure and the crude product was purified by flash chromatography to give **2-33aa-H** (31 mg, 95%) as a yellow solid; Mp 119 °C; ¹H NMR (400 MHz, CDCl₃) δ 8.32 (s, 1H), 7.92 (d, *J* = 6.1 Hz, 2H), 7.82 (d, *J* = 6.6 Hz, 1H), 7.55 (s, 2H), 7.39 (d, *J* = 6.8 Hz, 1H), 7.32 (d, *J* = 6.6 Hz, 2H), 7.27 - 7.21 (m, 2H), 7.07 (t, *J* = 7.4 Hz, 2H), 2.43 (s, 3H); ¹³C NMR (101 MHz, CDCl₃) δ 163.32, 160.85, 139.84, 138.55, 135.21, 133.02, 132.94, 130.28, 129.62, 128.72, 126.44, 123.36, 120.93, 120.53, 120.49, 119.95, 115.66, 115.44, 110.95, 95.29, 92.29, 83.87, 21.35; HRMS (APCI) calc. for C₂₃H₁₇FN⁺ [M+H]⁺: 326.1340, found 326.1340.

Methyl benzyl((2-(p-tolyl)-1-tosyl-1H-indol-3-yl)ethynyl)carbamate (2-38a)



Following general procedure **GP6** with 4-methyl-*N*-(2-(*p*-tolylethynyl)phenyl)benzenesulfonamide **2-32a** (108mg, 0.3 mmol) and methyl benzyl(iodoethynyl)carbamate **2-37** (104 mg, 0.33 mmol). The crude product was purified by flash column chromatography (Petroleum ether : EtOAc = 10 : 1) to afford **2-38a** as a yellow solid (92 mg, 56%); Mp 129 °C; ¹H NMR (400 MHz, CDCl₃) δ 8.28 (d, *J* = 8.3 Hz, 1H), 7.45 (d, *J* = 7.8 Hz, 2H), 7.36 (t, *J* = 8.4 Hz, 1H), 7.32 - 7.22 (m, 11H), 7.03 (d, *J* = 8.2 Hz, 2H), 4.60 (s, 2H), 3.83 (s, 3H), 2.46 (s, 3H), 2.29 (s, 3H); ¹³C NMR (101 MHz, CDCl₃) δ 155.50, 144.66, 142.15, 138.73, 137.02, 135.70, 134.44, 131.04, 130.96, 130.94, 129.24, 129.15, 128.51, 128.02, 127.98, 127.96, 126.82, 126.42, 125.44, 124.49, 119.87, 116.56, 107.72, 54.15, 53.88, 21.58, 21.50; HRMS (APCI) calc. for C₃₃H₂₉N₂O₄S⁺ [M+H]⁺: 549.1844, found 549.1843.

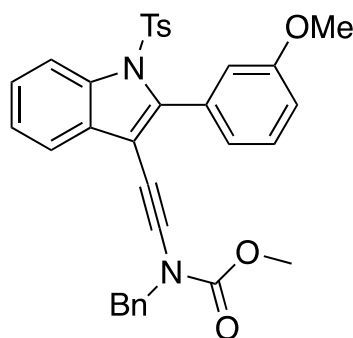
Methyl benzyl((2-(4-methoxyphenyl)-1-tosyl-1H-indol-3-yl)ethynyl)carbamate (2-38b)



Following general procedure **GP6** with *N*-(2-((4-methoxyphenyl)ethynyl)phenyl)-4-methylbenzenesulfonamide **2-32d** (108mg, 0.3 mmol) and methyl benzyl(iodoethynyl)carbamate **2-37** (104 mg, 0.33 mmol). The crude product was purified by flash column chromatography (Petroleum ether : EtOAc = 10 : 1) to afford **2-38b** as a yellow solid (101 mg, 60%). Mp 135 °C; ¹H NMR (300 MHz, CDCl₃) δ 8.28 (d, *J* = 8.3 Hz, 1H), 7.47 (d, *J* = 8.7 Hz, 2H), 7.40 - 7.28 (m, 6H), 7.26 - 7.20 (m, 4H), 7.03 (d, *J* = 7.7 Hz, 2H), 6.94 (d, *J* = 8.8 Hz, 2H), 4.60 (s, 2H), 3.90 (s, 3H), 3.83 (s, 3H), 2.28 (s, 3H). ¹³C NMR (75 MHz, CDCl₃) δ 160.06, 155.50, 144.66, 142.06, 136.97, 135.71, 134.52, 132.51, 129.38, 129.23, 128.67, 128.51, 128.15, 128.03, 127.92, 126.80, 125.34, 124.49, 123.09, 119.78, 116.58,

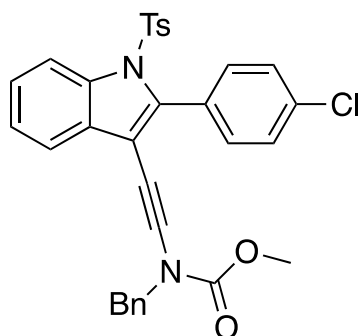
112.70, 107.30, 55.24, 54.16, 53.91, 21.50; HRMS (APCI) calc. for $C_{33}H_{29}N_2O_5S^+$ $[M+H]^+$: 565.1792, found 565.1791.

Methyl benzyl((2-(3-methoxyphenyl)-1-tosyl-1H-indol-3-yl)ethynyl)carbamate (2-38c)



Following general procedure **GP6** with *N*-(2-((3-methoxyphenyl)ethynyl)phenyl)-4-methylbenzenesulfonamide **2-32e** (113 mg, 0.3 mmol) and methyl benzyl(iodoethynyl)carbamate **2-37** (104 mg, 0.33 mmol). The crude product was purified by flash column chromatography (Petroleum ether : EtOAc = 8 : 1) to afford **2-38c** as a yellow solid (93 mg, 55%). Mp 126 °C; 1H NMR (300 MHz, $CDCl_3$) δ 8.31 (d, J = 8.3 Hz, 1H), 7.44 - 7.35 (m, 2H), 7.35 - 7.27 (m, 9H), 7.19 - 7.10 (m, 2H), 7.10 - 7.00 (m, 3H), 4.62 (s, 2H), 3.86 (s, 3H), 3.85 (s, 3H), 2.31 (s, 3H); ^{13}C NMR (75 MHz, $CDCl_3$) δ 158.50, 155.46, 144.73, 141.47, 137.09, 135.65, 134.44, 132.05, 130.84, 129.43, 129.25, 128.53, 128.37, 128.15, 128.05, 127.94, 126.87, 125.62, 124.51, 123.67, 119.98, 116.59, 116.53, 114.74, 108.10, 55.23, 54.16, 53.91, 21.50; HRMS (APCI) calc. for $C_{33}H_{29}N_2O_5S^+$ $[M+H]^+$: 565.1792, found 565.1790.

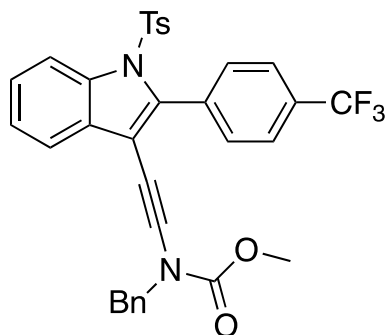
Methyl benzyl((2-(4-chlorophenyl)-1-tosyl-1H-indol-3-yl)ethynyl)carbamate (2-38d)



Following general procedure **GP6** with *N*-(2-((4-chlorophenyl)ethynyl)phenyl)-4-methylbenzenesulfonamide **2-32h** (114 mg, 0.3 mmol) and methyl benzyl(iodoethynyl)carbamate **2-37** (104 mg, 0.33 mmol). The crude product was purified by flash column chromatography (Petroleum ether : EtOAc = 8 : 1) to afford **2-38d** as a yellow solid (75 mg, 44%). Mp 125 °C; 1H NMR (400 MHz, $CDCl_3$) δ 8.27 (d, J = 8.4 Hz, 1H), 7.45 (d, J = 8.3 Hz, 2H), 7.41 - 7.35 (m, 3H), 7.34 - 7.27 (m, 5H), 7.25 - 7.18 (m, 4H), 7.03 (d, J = 8.1 Hz, 2H), 4.60 (s, 2H), 3.83 (s, 3H), 2.28 (s, 3H); ^{13}C NMR (101 MHz, $CDCl_3$) δ 155.43,

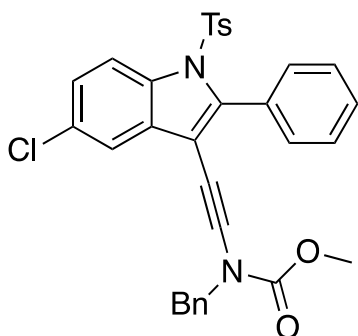
144.93, 140.50, 137.12, 135.54, 134.82, 134.30, 132.28, 130.83, 129.35, 129.29, 128.58, 128.41, 128.38, 128.27, 128.14, 127.55, 126.75, 125.85, 124.67, 120.06, 116.56, 108.50, 54.26, 53.84, 21.52; HRMS (APCI) calc. for $C_{32}H_{26}ClN_2O_4S^+$ $[M+H]^+$: 569.1296, found 569.1298.

Methyl benzyl((1-tosyl-2-(4-(trifluoromethyl)phenyl)-1*H*-indol-3-yl)ethynyl)carbamate (**2-38e**)



Following general procedure **GP6** with 4-methyl-*N*-(2-((4-(trifluoromethyl)phenyl)ethynyl)phenyl)benzenesulfonamide **2-32i** (114 mg, 0.3 mmol) and methyl benzyl(iodoethynyl)carbamate **2-37** (104 mg, 0.33 mmol). The crude product was purified by flash column chromatography (Petroleum ether : EtOAc = 18 : 1) to afford **2-38e** as a yellow solid (52 mg, 42%); Mp 130 °C; 1H NMR (400 MHz, $CDCl_3$) δ 8.28 (d, J = 8.4 Hz, 1H), 7.65 (s, 4H), 7.32 (dt, J = 5.5, 2.8 Hz, 4H), 7.30 - 7.21 (m, 6H), 7.05 (d, J = 8.1 Hz, 2H), 4.62 (s, 2H), 3.83 (s, 3H), 2.30 (s, 3H); ^{13}C NMR (75 MHz, $CDCl_3$) δ 155.38, 145.05, 137.31, 135.46, 134.50, 134.08, 131.21, 130.82, 130.56, 130.13, 129.52, 129.40, 128.59, 128.34, 128.18, 126.74, 126.17, 125.94, 124.81, 124.18, 122.33, 120.24, 116.63, 109.45, 54.26, 53.81, 21.53. ^{19}F NMR (376 MHz, $CDCl_3$) δ -62.47; HRMS (APCI) calc. for $C_{33}H_{26}F_3N_2O_4S^+$ $[M+H]^+$: 603.1560, found 603.1551.

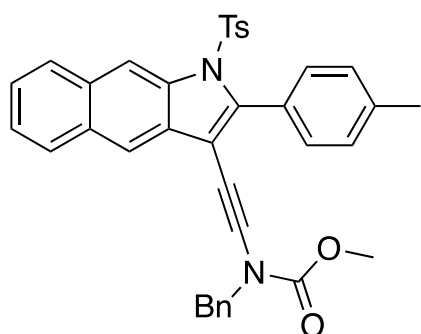
Methyl benzyl((5-chloro-2-phenyl-1-tosyl-1*H*-indol-3-yl)ethynyl)carbamate (**2-38f**)



Following general procedure **GP6** with *N*-(4-chloro-2-(phenylethynyl)phenyl)-4-methylbenzenesulfonamide **2-32i** (114 mg, 0.3 mmol) and methyl benzyl(iodoethynyl)carbamate **2-37** (104 mg, 0.33 mmol). The crude product was purified by flash column chromatography (Petroleum ether : EtOAc = 18 : 1) to afford **2-38f** as a yellow

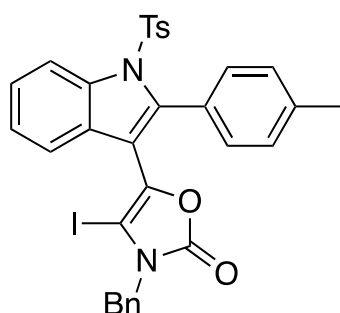
solid (73 mg, 43%). Mp 124 °C; ¹H NMR (400 MHz, CDCl₃) δ 8.20 (d, J = 8.9 Hz, 1H), 7.52 (d, J = 6.4 Hz, 2H), 7.45 (dd, J = 11.5, 7.1 Hz, 3H), 7.36 - 7.30 (m, 4H), 7.26 - 7.19 (m, 5H), 7.05 (d, J = 8.1 Hz, 2H), 4.59 (s, 2H), 3.83 (s, 3H), 2.31 (s, 3H); ¹³C NMR (101 MHz, CDCl₃) δ 155.38, 145.04, 135.42, 135.37, 134.22, 132.21, 131.11, 130.44, 130.44, 130.36, 130.36, 129.39, 129.39, 129.09, 128.63, 128.59, 128.31, 127.25, 126.81, 125.75, 119.65, 117.63, 107.34, 54.22, 53.69, 21.54; HRMS (APCI) calc. for C₃₂H₂₆ClN₂O₄S⁺ [M+H]⁺: 569.1296, found 569.1300;

Methyl benzyl((2-(p-tolyl)-1-tosyl-1H-benzo[f]indol-3-yl)ethynyl)carbamate (2-38g)



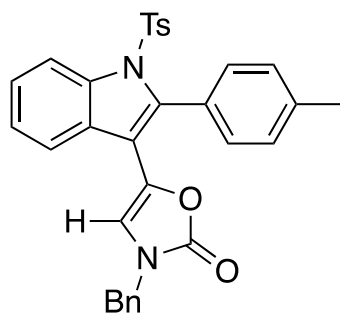
Following general procedure **GP6** with 4-Methyl-*N*-(3-(*p*-tolylethynyl)naphthalen-2-yl)benzenesulfonamide **2-32-naphthalene** (123 mg, 0.3 mmol) and methyl benzyl(iodoethynyl)carbamate **2-37** (104 mg, 0.33 mmol). The crude product was purified by flash column chromatography (Petroleum ether : EtOAc = 18 : 1) to afford **2-38g** as a yellow solid (86 mg, 48%). Mp 135 °C; ¹H NMR (400 MHz, CDCl₃) δ 8.72 (s, 1H), 8.07 - 8.02 (m, 1H), 7.88 - 7.83 (m, 1H), 7.63 (s, 1H), 7.56 (d, J = 7.8 Hz, 2H), 7.52 - 7.46 (m, 2H), 7.39 - 7.30 (m, 5H), 7.29 - 7.22 (m, 5H), 6.97 (d, J = 8.1 Hz, 2H), 4.66 (s, 2H), 3.88 (s, 3H), 2.48 (s, 3H), 2.23 (s, 3H); ¹³C NMR (101 MHz, CDCl₃) δ 155.53, 144.62, 139.08, 136.44, 135.66, 133.85, 131.94, 131.21, 131.18, 130.79, 129.24, 128.80, 128.71, 128.65, 128.60, 128.30, 128.18, 128.18, 128.08, 128.05, 127.76, 126.93, 125.22, 125.19, 117.80, 114.49, 108.01, 54.25, 53.82, 21.63, 21.47; HRMS (APCI) calc. for C₃₇H₃₁N₂O₄S⁺ [M+H]⁺: 599.1999, found 599.2008.

3-Benzyl-4-iodo-5-(2-(p-tolyl)-1-tosyl-1H-indol-3-yl)oxazol-2(3H)-one (2-39)



A mixture of **2-38a** (55 mg, 0.1 mmol), I₂ (28 mg, 0.11 mmol) and DCE (2 mL) was stirred at room temperature for 8 h. The mixture was concentrated in vacuo, added to water, and extracted with EtOAc (3×10 mL). Organic layers were combined, dried over MgSO₄, filtered, concentrated, and purified by flash column chromatography to afford product **2-39** (65 mg, 98%) as a yellow oil. ¹H NMR (400 MHz, CDCl₃) δ 8.39 (d, *J* = 8.4 Hz, 1H), 7.44 (dd, *J* = 8.3, 5.8 Hz, 3H), 7.38 - 7.30 (m, 5H), 7.28 (dd, *J* = 8.5, 4.8 Hz, 6H), 7.18 (d, *J* = 8.0 Hz, 4H), 7.09 (d, *J* = 7.9 Hz, 2H), 4.77 (s, 2H), 2.45 (s, 3H), 2.34 (s, 3H); ¹³C NMR (101 MHz, CDCl₃) δ 154.63, 145.09, 142.59, 139.32, 136.88, 135.88, 135.35, 134.88, 131.44, 129.44, 129.20, 128.66, 128.26, 127.90, 127.36, 126.96, 126.81, 125.56, 124.57, 119.97, 116.35, 110.63, 77.32, 77.00, 76.68, 71.02, 48.16, 21.56; HRMS (APCI) calc. for C₃₂H₂₆IN₂O₄S⁺ [M+H]⁺: 661.0652, found 661.0653.

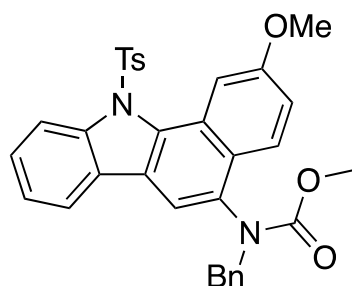
3-Benzyl-5-(2-(p-tolyl)-1-tosyl-1H-indol-3-yl)oxazol-2(3H)-one (2-40)



A mixture of **2-38a** (55 mg, 0.1 mmol), AgSbF₆ (6.9 mg, 0.02 mmol) and DCE (2 mL) was stirred at 85 °C for 12 h. The mixture was concentrated in vacuo, added to water, and extracted with EtOAc (3×10 mL). Organic layers were combined, dried over MgSO₄, filtered, concentrated, and purified by flash column chromatography to afford product **2-40** (47 mg, 88%) as a yellow oil.

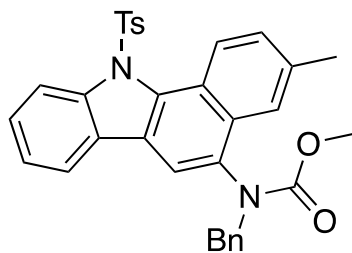
¹H NMR (400 MHz, CDCl₃) δ 8.36 (d, *J* = 8.4 Hz, 1H), 8.00 (d, *J* = 7.9 Hz, 1H), 7.39 (d, *J* = 8.4 Hz, 4H), 7.35 - 7.32 (m, 3H), 7.20 - 7.09 (m, 8H), 5.42 (s, 1H), 4.59 (s, 2H), 2.45 (s, 3H), 2.35 (s, 3H); ¹³C NMR (75 MHz, CDCl₃) δ 154.57, 145.00, 139.43, 136.45, 136.21, 135.61, 135.04, 134.29, 130.84, 129.51, 128.83, 128.80, 128.19, 127.86, 127.62, 127.07, 126.89, 125.52, 124.35, 121.28, 115.38, 111.16, 111.01, 47.58, 21.57, 21.56. HRMS (APCI) calc. for C₃₂H₂₇N₂O₄S⁺ [M+H]⁺: 535.1613, found 535.1616.

Methyl benzyl(2-methoxy-11-tosyl-11H-benzo[a]carbazol-5-yl)carbamate (2-41)



A mixture of **2-38c** (56 mg, 0.1 mmol), $\text{Ph}_3\text{PAuNTf}_2$ (7.4 mg, 0.01 mmol) and DCE (2 mL) was stirred at 50 °C for 10 h. The mixture was concentrated in vacuo, added to water, and extracted with EtOAc (3 × 10 mL). Organic layers were combined, dried over MgSO_4 , filtered, concentrated, and purified by flash column chromatography to afford product **2-41** (41 mg, 85%) as a yellow solid; Mp 150 °C; ^1H NMR (400 MHz, CDCl_3) δ 8.56 (d, J = 8.7 Hz, 1H), 8.27 (d, J = 8.3 Hz, 1H), 7.59 (s, 1H), 7.44 - 7.37 (m, 3H), 7.24 (td, J = 9.3, 8.2, 4.6 Hz, 7H), 7.06 (s, 1H), 6.99 (d, J = 7.8 Hz, 1H), 6.75 (q, J = 8.3 Hz, 5H), 5.43 (d, J = 14.8 Hz, 1H), 4.14 (d, J = 14.8 Hz, 1H), 3.97 (s, 3H), 3.60 (s, 3H), 2.16 (s, 3H); ^{13}C NMR (101 MHz, CDCl_3) δ 157.18, 155.76, 144.18, 142.32, 137.98, 136.54, 136.15, 130.95, 129.76, 129.22, 129.03, 128.22, 128.12, 127.72, 127.24, 126.97, 126.08, 125.75, 121.55, 120.36, 120.09, 119.49, 119.33, 106.28, 56.03, 55.27, 52.75, 21.40; HRMS (APCI) calc. for $\text{C}_{33}\text{H}_{29}\text{N}_2\text{O}_5\text{S}^+ [\text{M}+\text{H}]^+$: 549.1792, found 549.1791.

Methyl benzyl(3-methyl-11-tosyl-11H-benzo[a]carbazol-5-yl)carbamate (2-42)



A mixture of **2-38a** (55 mg, 0.1 mmol), $\text{RhCl}(\text{Ph}_3\text{P})_3$ (18.5 mg, 0.02 mmol), AgSbF_6 (6.9 mg, 0.02 mmol) and PhMe (2 mL) was stirred at 100 °C for 10 h. The mixture was concentrated in vacuo, added to water, and extracted with EtOAc (3 × 10 mL). Organic layers were combined, dried over MgSO_4 , filtered, concentrated, and purified by flash column chromatography to afford product **2-42** (43 mg, 78%) as a yellow solid. Mp 145 °C; ^1H NMR (400 MHz, CDCl_3) δ 8.91 (d, J = 8.7 Hz, 1H), 8.29 (d, J = 8.2 Hz, 1H), 7.57 (s, 1H), 7.52 (dd, J = 8.7, 1.7 Hz, 1H), 7.41 (t, J = 7.9 Hz, 2H), 7.29 (d, J = 7.6 Hz, 1H), 7.25 - 7.12 (m, 6H), 6.81 (d, J = 8.1 Hz, 2H), 6.74 (d, J = 8.1 Hz, 2H), 5.41 (d, J = 14.4 Hz, 1H), 4.38 (d, J = 14.4 Hz, 1H), 3.61 (s, 3H), 2.55 (s, 3H), 2.17 (s, 3H); ^{13}C NMR (101 MHz, CDCl_3) δ 157.08, 144.19, 141.79, 137.64, 136.78,

136.37, 135.96, 131.38, 130.60, 129.91, 129.19, 128.50, 128.27, 127.70, 127.50, 126.93, 126.63, 126.41, 125.63, 125.17, 121.89, 119.88, 119.20, 118.30, 54.44, 53.16, 21.97, 21.43; HRMS (APCI) calc. for C₃₃H₂₉N₂O₄S⁺ [M+H]⁺: 549.1792, found 549.1791.

6.5 Crystallographic Data

A single crystal of each compound was selected, mounted onto a cryoloop and transferred into a cold nitrogen gas stream. Intensity data were collected with a Bruker Kappa APEX-II CCD diffractometer using a micro-focused Cu-K α radiation ($\lambda = 1.54178 \text{ \AA}$). Data collections were performed at 200K, with the Bruker APEXIII suite. Unit-cell parameters determinations, integrations and data reductions were carried out with SAINT program. SADABS was used for scaling and absorption corrections. The structures were solved with SHELXT⁴⁶ and refined by full-matrix least-squares methods with SHELXL⁴⁷ using Olex2 software package⁴⁸. All non-hydrogen atoms were refined anisotropically.

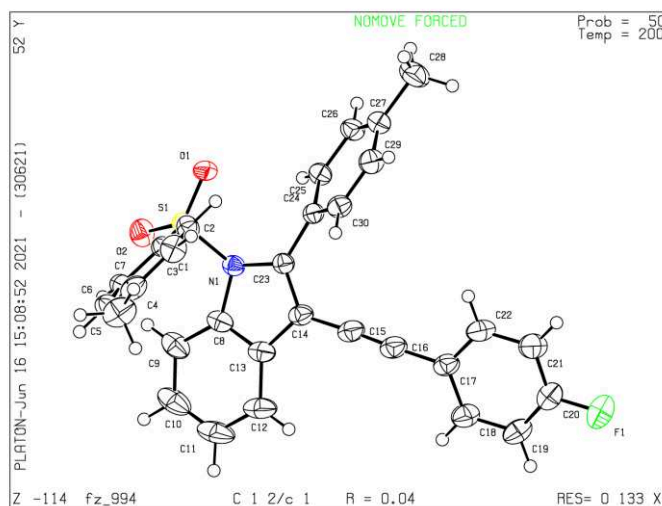
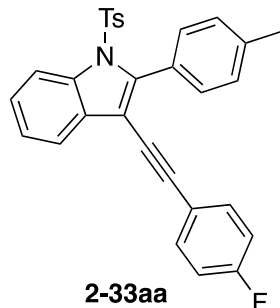
The following Table SII contains crystal data collection and structure refinement information for **2-33aa**, **2-43**, **2-40**, **2-42** and **2-38b**. These data can be obtained free of charge from The Cambridge Crystallographic Data Centre *via* www.ccdc.cam.ac.uk/data_request/cif.

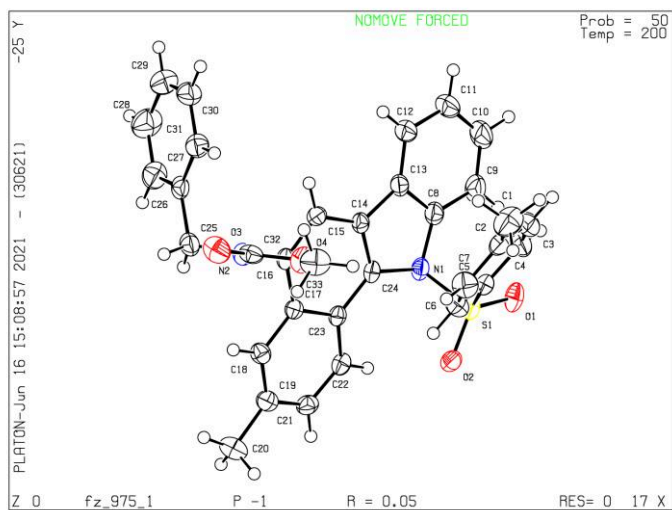
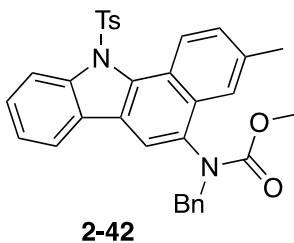
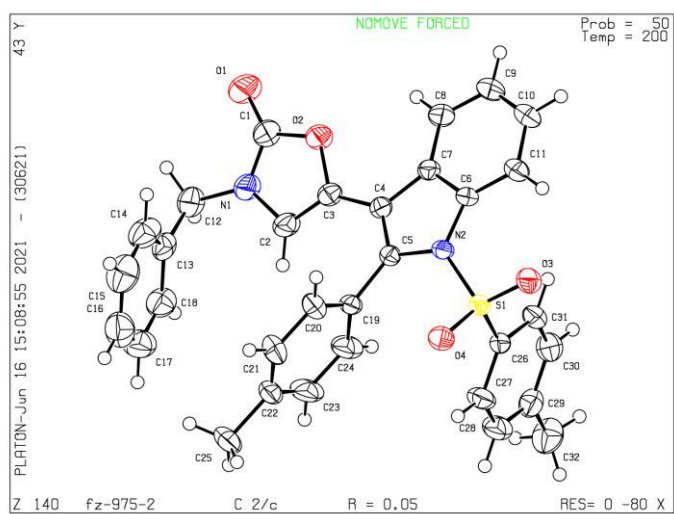
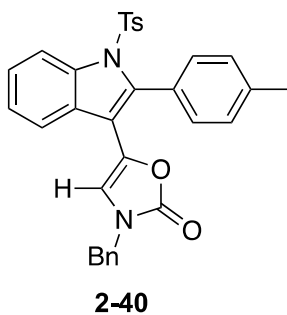
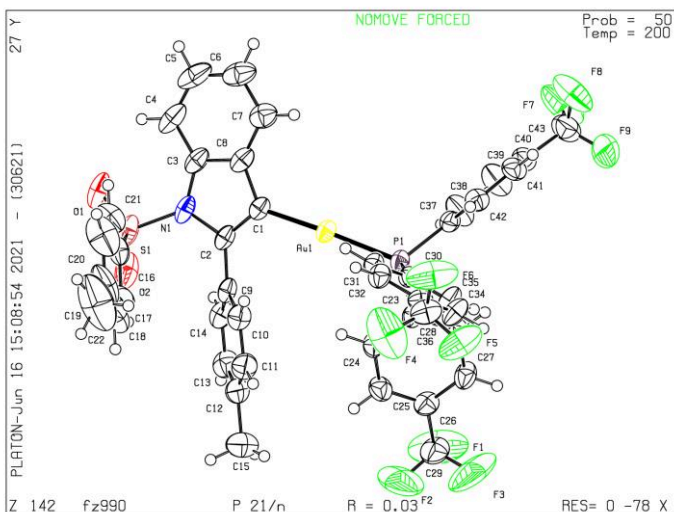
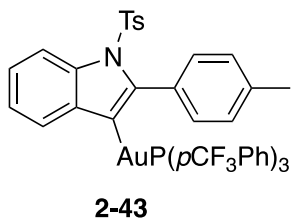
Table SII Crystallographic data for compounds **2-33aa**, **2-43**, **2-40**, **2-42**, **2-38b**

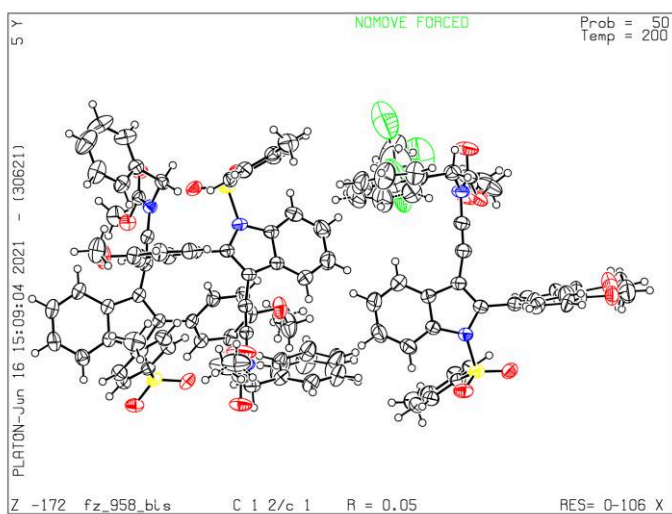
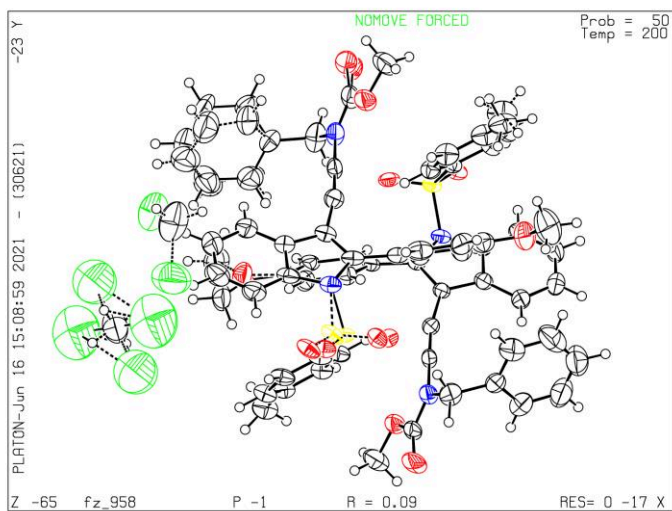
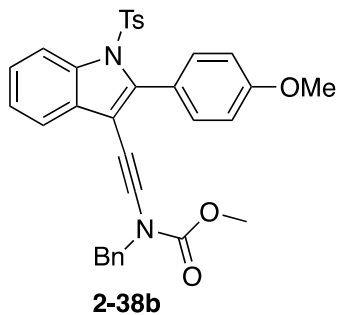
	2-33aa	2-43	2-40	2-42	2-38b	2-38b
CCDC deposit number	2090317	2090321	2090322	2090314	2090316	2090315
Empirical formula ^a	C ₃₀ H ₂₂ FNO ₂ S	C ₄₃ H ₃₀ NO ₂ F ₉ PSAu	C ₃₂ H ₂₆ N ₂ O ₄ S	C ₃₃ H ₂₈ N ₂ O ₄ S	C ₃₃ H ₂₈ N ₂ O ₅ S, 0.15(CH ₂ Cl ₂)	C ₃₃ H ₂₈ N ₂ O ₅ S, 0.2(CH ₂ Cl ₂)
<i>F</i> . <i>W</i> . [g mol ⁻¹]	479.54	1023.67	534.61	548.63	577.37	581.62
Crystal system	Monoclinic	Monoclinic	Monoclinic	Triclinic	Triclinic	Monoclinic
Space group	<i>C2/c</i>	<i>P2₁/m</i>	<i>C2/c</i>	<i>P-1</i>	<i>P-1</i>	<i>C2/c</i>
<i>a</i> [Å]	35.056(2)	11.6947(8)	21.1818(5)	11.9616(19)	12.4643(15)	75.043(3)
<i>b</i> [Å]	7.9873(5)	17.3981(10)	8.6122(2)	11.9670(19)	13.9395(17)	9.9216(3)
<i>c</i> [Å]	18.5380(11)	20.6279(14)	28.8077(7)	12.2619(19)	19.312(2)	24.6860(8)
α [°]	90	90	90	100.869(3)	75.518(3)	90
β [°]	110.312(3)	103.444(3)	91.187(2)	108.109(2)	87.281(3)	101.413(2)
γ [°]	90	90	90	116.245(3)	77.399(3)	90
<i>V</i> [Å ³]	4868.0(5)	4082.1(5)	5254.0(2)	1382.6(4)	3170.5(7)	18016.5(10)
<i>Z</i>	8	4	8	2	4	24
<i>T</i> [K]	200(1)	200(1)	200(1)	200(1)	200(1)	200(1)
λ [Å]	0.71073	0.71073	0.71073	0.71073	0.71073	1.54178
ρ_{calc} [g cm ⁻³]	1.309	1.666	1.352	1.318	1.210	1.287
μ [mm ⁻¹]	0.169 (MoK α)	3.773 (MoK α)	0.165 (MoK α)	0.159 (MoK α)	0.169 (MoK α)	1.643 (CuK α)
<i>F</i> (000)	2000.0	2008.0	2240.0	576.0	1209.0	7306.0
Measured reflections	43674	48522	42020	30735	65102	105985
Unique reflections	7551	10138	8020	6835	11385	15883
<i>R</i> _{int}	0.0328	0.0231	0.0237	0.0591	0.0632	0.0378
<i>R</i> _{sigma}	0.0230	0.0191	0.0175	0.0521	0.0521	0.0241
Reflections <i>I</i> >2 σ (<i>I</i>)	5843	8502	6701	4634	7508	13673
Parameters	318	525	354	363	901	1327
Restraints	0	0	0	0	286	441
<i>R</i> ₁ ^b [<i>I</i> >2 σ (<i>I</i>)]	0.0411	0.0293	0.0510	0.0464	0.0922	0.0478
<i>wR</i> ₂ ^c [<i>I</i> >2 σ (<i>I</i>)]	0.1089	0.0684	0.1314	0.1018	0.2517	0.1320
<i>R</i> ₁ ^b [all data]	0.0577	0.0394	0.0622	0.0834	0.1356	0.0555
<i>wR</i> ₂ ^c [all data]	0.1196	0.0732	0.1405	0.1176	0.2790	0.1382
GOF	1.031	1.022	1.094	1.015	1.116	1.038
Largest residuals [eÅ ⁻³]	-0.35 ; 0.34	-0.67 ; 1.13	-0.25 ; 0.43	-0.43 ; 0.28	-0.33 ; 0.89	-0.34 ; 0.77

^a Including solvate molecules. ^b $R_1 = \frac{\sum |F_o| - \sum |F_c|}{\sum |F_o|}$ ^c $R_2 = \frac{(\sum F_o^2 - \sum F_c^2)^2}{(\sum F_o^2)^2 + (\sum F_c^2)^2}$

X-RAY CRYSTAL STRUCTURE DETERMINATION







7. Reference

- [1] J. B. Zimmerman, P. T. Anastas, H. C. Erythropel, W. Leitner, *Science*, **2020**, 367, 397.
- [2] G. E. M. Crisenza, P. Melchiorre, *Nat. Commun.* **2020**, 11, 803.
- [3] a) C. K. Prier, D. A. Rankic, D. W. MacMillan, *Chem. Rev.* **2013**, 113, 5322; b) X. Lang, X. Chen, J. Zhao, *Chem. Soc. Rev.* **2014**, 43, 473; c) N. Corrigan, S. Shanmugam, J. Xu, C. Boyer, *Chem. Soc. Rev.* **2016**, 45, 6165; d) G. E. M. Crisenza, D. Mazzarella, P. Melchiorre, *J. Am. Chem. Soc.* **2020**, 142, 5461; e) C. G. S. Lima, T. de M. Lima, M. Duarte, I. D. Jurberg, M. W. Paixão, *ACS Catal.* **2016**, 6, 1389; f) X. Y. Yu, Q. Q. Zhao, J. Chen, W. J. Xiao, J. R. Chen, *Acc. Chem. Res.* **2020**, 53, 1066; g) X. Y. Yu, J. R. Chen, W. J. Xiao, *Chem. Rev.* **2021**, 121, 506.
- [4] E. Arceo, I. D. Jurberg, A. Álvarez-Fernández, P. Melchiorre, *Nat. Chem.* **2013**, 5, 750.
- [5] B. Liu, C. H. Lim, G. M. Miyake, *J. Am. Chem. Soc.* **2017**, 139, 13616.
- [6] S. R. Kandukuri, A. Bahamonde, I. Chatterjee, I. D. Jurberg, E. C. Escudero Adan, P. Melchiorre, *Angew. Chem. Int. Ed.* **2015**, 54, 1485.
- [7] L. Li, X. Mu, W. Liu, Y. Wang, Z. Mi, C. J. Li, *J. Am. Chem. Soc.* **2016**, 138, 5809.
- [8] P. Liu, W. Liu, C. J. Li, *J. Am. Chem. Soc.* **2017**, 139, 14315.
- [9] Q. Shi, P. H. Li, Y. Zhang, L. Wang, *Org. Chem. Front.* **2017**, 4, 1322.
- [10] H. Sahoo, A. Mandal, S. Dana, M. Baidya, *Adv. Synth. Catal.* **2018**, 360, 1099
- [11] M. Y. Wang, Y. Cao, X. Liu, N. Wang, L. N. He, S. H. Li, *Green Chem.* **2017**, 19, 1240.
- [12] Z. Xu, L. Gao, L. L. Wang, M. W. Gong, W. F. Wang, R. S. Yuan, *ACS Catal.* **2015**, 5, 45.
- [13] W. Liu, J. Li, P. Querard, C. J. Li, *J. Am. Chem. Soc.* **2019**, 141, 6755.
- [14] C. L. Wang, J. Y. Qiao, X. C. Liu, H. Song, Z. Z. Sun, W. Y. Chu, *J. Org. Chem.* **2018**, 83, 1422.
- [15] a) M. Kim, N. K. Mishra, J. Park, S. Han, Y. Shin, S. Sharma, Y. Lee, E. K. Lee, J. H. Kwak, I. S. Kim, *Chem. Commun.* **2014**, 50, 14249; b) C. Zhou, P. H. Li, X. J. Zhu, L. Wang, *Org. Lett.* **2015**, 17, 6198; c) C. L. Perrin, K. L. Chang, *J. Org. Chem.* **2016**, 81, 5631.
- [16] W. L. Lei, T. Wang, K. W. Feng, L. Z. Wu, Q. Liu, *ACS Catal.* **2017**, 7, 7941.
- [17] a) A. S. K. Hashmi, G. J. Hutchings, *Angew. Chem. Int. Ed.* **2006**, 45, 7896; b) A. Fürstner, *Chem. Soc. Rev.* **2009**, 38, 3208; c) N. Krause, C. Winter, *Chem. Rev.* 2011, 111, 1994; d) M. Bandini, *Chem. Soc. Rev.* **2011**, 40, 1358; e) R. Dorel, A. M. Echavarren, *Chem. Rev.* **2015**, 115, 9028.
- [18] L. P. Liu, G. B. Hammond, *Chem. Soc. Rev.* **2012**, 41, 3129.

- [19] a) R. Dorel, A. M. Echavarren, *Chem. Rev.* **2015**, *115*, 9028; b) C. C. Chintawar, A. K. Yadav, A. Kumar, S. P. Sancheti, N. T. Patil, *Chem. Rev.* **2021**, DOI 10.1021/acs.chemrev.0c00903.
- [20] S. G. Bratsch, *J Phys Chem Ref Data*, **1989**, *18*, 1.
- [21] a) A. S. K. Hashmi, T. D. Ramamurthi, F. Rominger, *J. Organomet. Chem.* **2009**, *694*, 592; b) W. Wang, J. Jasinski, G. B. Hammond, B. Xu, *Angew. Chem. Int. Ed.* **2010**, *122*, 7405; *Angew. Chem. Int. Ed.* **2010**, *49*, 7247; c) G. Zhang, L. Chui, Y. Wang, L. Zhang, *J. Am. Chem. Soc.* **2010**, *132*, 1474; d) J. P. Brand, Y. Li, J. Waser, *Isr. J. Chem.* **2013**, *53*, 901; e) J. P. Brand, J. Waser, *Angew. Chem. Int. Ed.* **2010**, *122*, 7462; *Angew. Chem. Int. Ed.* **2010**, *49*, 7304; f) T. de Haro, C. Nevado, *Synthesis* **2011**, 2530.
- [22] M. Joost, A. Amgoune, D. Bourissou, *Angew. Chem. Int. Ed.* **2015**, *54*, 15022.
- [23] a) B. Sahoo, M. N. Hopkinson and F. Glorius, *J. Am. Chem. Soc.* **2013**, *135*, 5505; b) M. N. Hopkinson, A. Tlahuext-Aca and F. Glorius, *Acc. Chem. Res.* **2016**, *49*, 2261.
- [24] X. Z. Shu, M. Zhang, Y. He, H. Frei and F. D. Toste, *J. Am. Chem. Soc.* **2014**, *136*, 5844.
- [25] a) L. Huang, M. Rudolph, F. Rominger and A. S. K. Hashmi, *Angew. Chem. Int. Ed.* **2016**, *55*, 4808; b) L. Huang, F. Rominger, M. Rudolph and A. S. K. Hashmi, *Chem. Commun.* **2016**, *52*, 6435; c) S. Witzel, J. Xie, M. Rudolph and A. S. K. Hashmi, *Adv. Synth. Catal.* **2017**, *359*, 1522; d) S. Witzel, K. Sekine, M. Rudolph, A. S. K. Hashmi, *Chem. Commun.* **2018**, *54*, 13802.
- [26] S. Kim, J. Rojas-Martin, F. D. Toste, *Chem. Sci.* **2016**, *7*, 85.
- [27] I. Chakrabarty, M. O. Akram, S. Biswas and N. T. Patil, *Chem. Commun.* **2018**, *54*, 7223.
- [28] a) B. Sahoo, M. N. Hopkinson, F. Glorius, *J. Am. Chem. Soc.* **2013**, *135*, 5505; b) X. Shu, M. Zhang, Y. He, H. Frei, F. D. Toste, *J. Am. Chem. Soc.* **2014**, *136*, 5844; c) M. N. Hopkinson, A. Tlahuext-Aca, F. Glorius, *Acc. Chem. Res.* **2016**, *49*, 2261; d) M. O. Akram, S. Banerjee, S. S. Saswade, V. Bedi, N. T. Patil, *Chem. Commun.* **2018**, *54*, 11069; e) B. Huang, M. Hu, F. D. Toste, *Trends in Chemistry* **2020**, *2*, 707.
- [29] a) Q. Zhou, Y. Zou, L. Lu, W. Xiao, *Angew. Chem. Int. Ed.* **2019**, *58*, 1586; b) F. Strieth-Kalthoff, M. J. James, M. Teders, L. Pitzer, F. Glorius, *Chem. Soc. Rev.* **2018**, *47*, 7190; c) F. Strieth-Kalthoff, F. Glorius, *Chem* **2020**, *6*, 1888.
- [30] Z. Xia, V. Corcé, F. Zhao, C. Przybylski, A. Espagne, L. Jullien, T. Le Saux, Y. Gimbert, H. Dossmann, V. Mouriès-Mansuy, C. Ollivier, L. Fensterbank, *Nat. Chem.* **2019**, *11*, 797.
- [31] a) G. W. Gribble, *J. Chem. Soc. Perkin Trans.* **2000**, *1*, 1045; b) J. S. S. Neto, G. Zeni, *Org. Chem. Front.* **2020**, *7*, 155 ; c) J. Dhuguru, R. Skouta, *Molecules* **2020**, *25*, 1615 ; c) M. Manickam, P. Iqbal, M. Belloni, S. Kumar, J. A. Preece, *Isr. J. Chem.* **2012**, *52*, 917; d) Z. R.

- Owczarczyk, W. A. Braunecker, A. Garcia, R. Larsen, A. M. Nardes, N. Kopidakis, D. S. Ginley, D. C. Olson, *Macromolecules*, **2013**, *46*, 1350.
- [32] Y. Liu, L. Shen, M. Prashad, J. Tibbatts, O. Repič, T. J. Blacklock, *Org. Process Res. Dev.* **2008**, *12*, 778.
- [33] Y. P. Wang, R. L. Danheiser, *Tetrahedron Lett.* **2011**, *52*, 2111.
- [34] H.-J. Knölker, K. R. Reddy, *Chem. Rev.* **2002**, *102*, 4303.
- [35] a) J. Shen, N. Li, Y. Yu, C. Ma, *Org. Lett.* **2019**, *21*, 7179; b) A. K. Ratheesh, H. A. Sparkes, K. J. R. Prasad, *Org. Biomol. Chem.* **2018**, *16*, 2527.
- [36] X. Qian, Y.-Z. Zhu, W. Y. Chang, J. Song, B. Pan, L. Lu, H. H. Gao, J. Y. Zheng, *ACS Appl. Mater. Interfaces* **2015**, *7*, 9015.
- [37] A. S. K. Hashmi, T. D. Ramamurthi, F. Rominger, *Adv. Synth. Catal.* **2010**, *352*, 971.
- [38] N. A. Takaesu, E. Ohta, L. N. Zakharov, D. W. Johnson, M. M. Haley, *Organometallics* **2017**, *36*, 2491.
- [39] Y. Zhao, J. Jin, P. W. H. Chan, *Adv. Synth. Catal.*, **2019**, *361*, 1313.
- [40] Y. Wang, R. L. Danheiser, *Tetrahedron Lett.*, **2011**, *52*, 2111.
- [41] J. Lv, B. Zhao, L. Liu, Y. Han, Y. Yuan, Z. Shi, *Adv. Synth. Catal.*, **2018**, *360*, 4054.
- [42] Y. Ye, K. P. S. Cheung, L. He, G. C. Tsui, *Org. Chem. Front.* **2018**, *5*, 1511.
- [43] N. K. Swamy, A. Yazici, S. G. Pyne, *J. Org. Chem.* **2010**, *75*, 3412.
- [44] Z. Chen, H. Jiang, Y. Li, C. Qi, *Chem. Commun.* 2010, *46*, 8049
- [45] D. Lehnher, J. M. Alzola, E. B. Lobkovsky, W. R. Dichtel, *Chem. Eur. J.* **2015**, *21*, 18122.
- [46] L. Palatinus, G. Chapuis, *J. Appl. Crystallogr.* **2007**, *40*, 786.
- [47] G. M. Sheldrick, *Acta Crystallog. Sect. C* **2015**, *71*, 3.
- [48] O.V. Dolomanov, L.J. Bourhis, R.J. Gildea, J.A.K. Howard, H. Puschmann, *J. Appl. Crystallogr.* **2009**, *42*, 339-341.

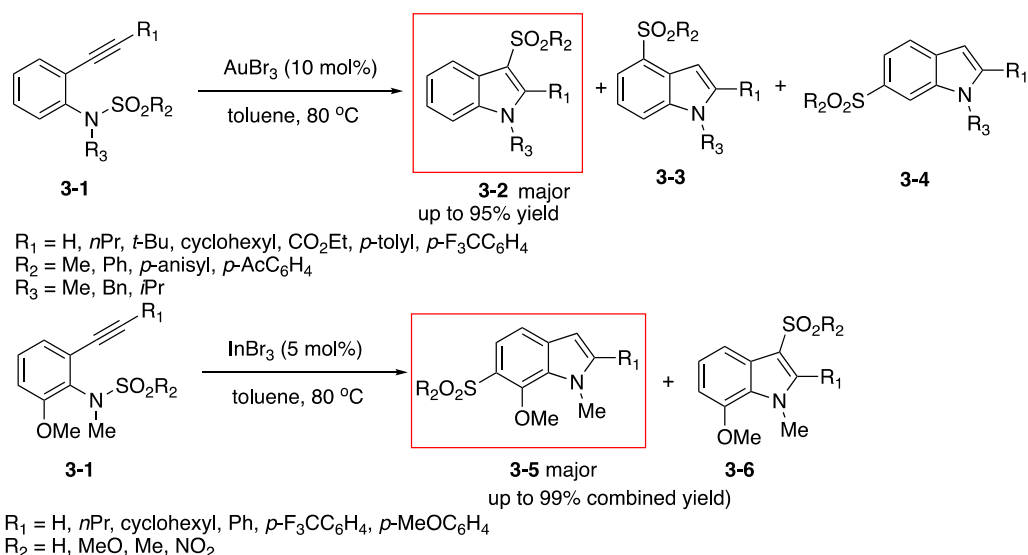
Chapter 3 Photocatalyzed Silver Catalysis

1. Background

Organic sulfones have been widely used as protecting groups or activating groups in organic synthesis, offering substantial synthetic versatility,¹ and thus playing an important role in synthetic chemistry. Most sulfonyl migrations prior to the beginning of the 21st century were originally discovered as side reactions. However, the last 20 years has seen a significant increase the number of reports about the utility of incorporating a sulfonyl molecular handle capable of migration. This short review mainly introduces gold and silver catalyzed sulfonyl migration and radical-mediated sulfonyl migration.

1.1 Gold-catalysed Sulfonyl Migration

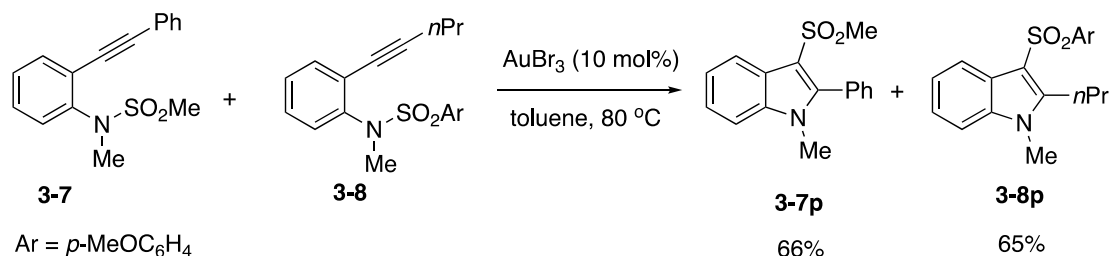
Nakamura et al. reported the gold- and indium-catalyzed synthesis of 3- and 6-sulfonylindoles from *ortho*-alkynyl-*N*-sulfonylanilines **3-1** (Scheme 3-1).² A 1,3-sulfonyl migration was observed in the presence of 10 mol% AuBr₃ in toluene at 80 °C, to afford 3-sulfonylindoles **3-2** in good to excellent yields. And minor amounts of the regioisomers **3-3** and **3-4** were also observed. Furthermore, the authors found that the reaction in the presence of InBr₃ afforded the corresponding 6-sulfonylindoles **3-5** as major product in good yields. Indicating that an unprecedented 1,7-sulfonyl migration has occurred. A methoxy group at the 6-position of the *ortho*-alkynyl-*N*-sulfonylanilines **3-1** helps the 1,7-sulfonyl migration.



Scheme 3-1 Gold- and indium-catalysed synthesis of 3- and 6-sulfonylindoles from *ortho*-alkynyl-*N*-sulfonylanilines, via 1,3- and 1,7-sulfonyl migration

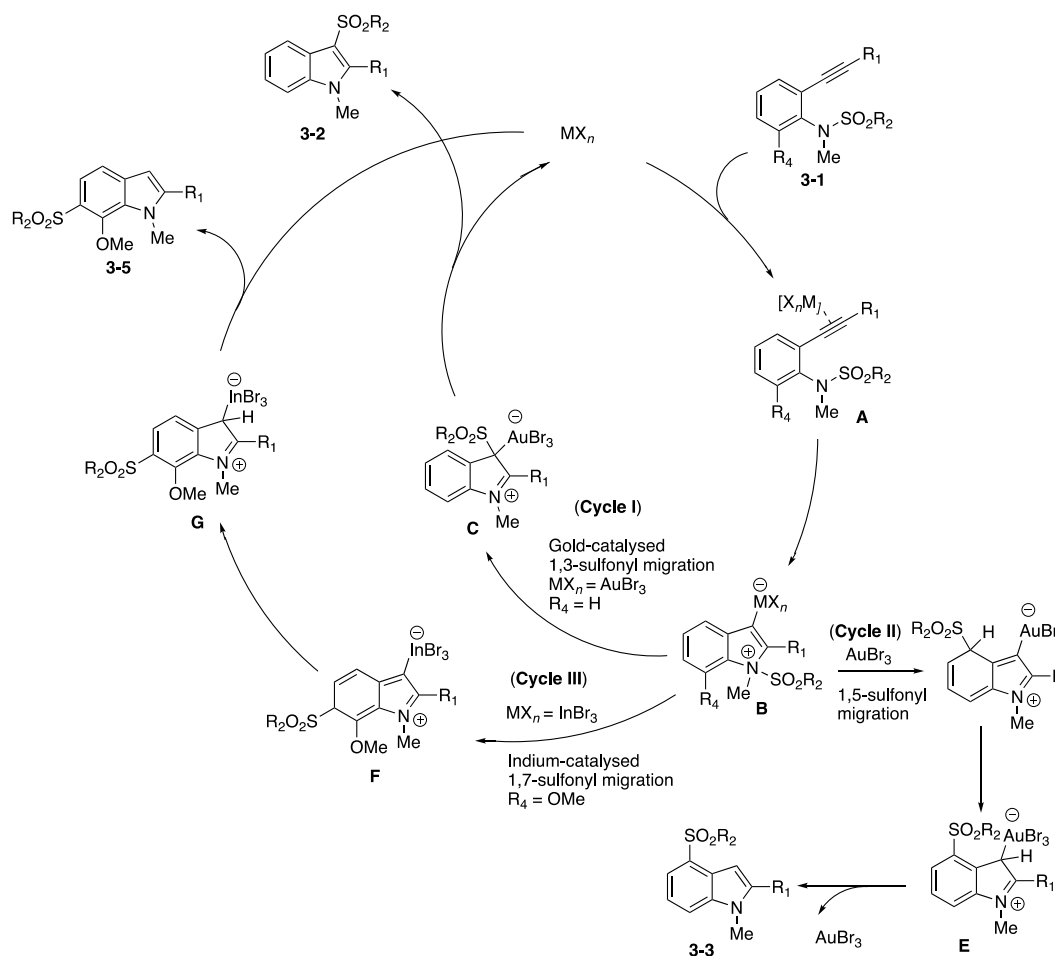
To find out if the migration of the sulfonyl group occurs in an intramolecular or intermolecular fashion, they performed crossover experiments as shown in Scheme 3-2. The reaction of a 1:1 mixture of **3-7** and **3-8** in the presence of a catalytic amount of AuBr₃ gave the

corresponding products **3-7p** and **3-8p** in 66% and 65% yields, respectively. The crossover products were not detected by GC-MS or NMR spectroscopy. Therefore, the migration of the sulfonyl group occurred in an intramolecular fashion.



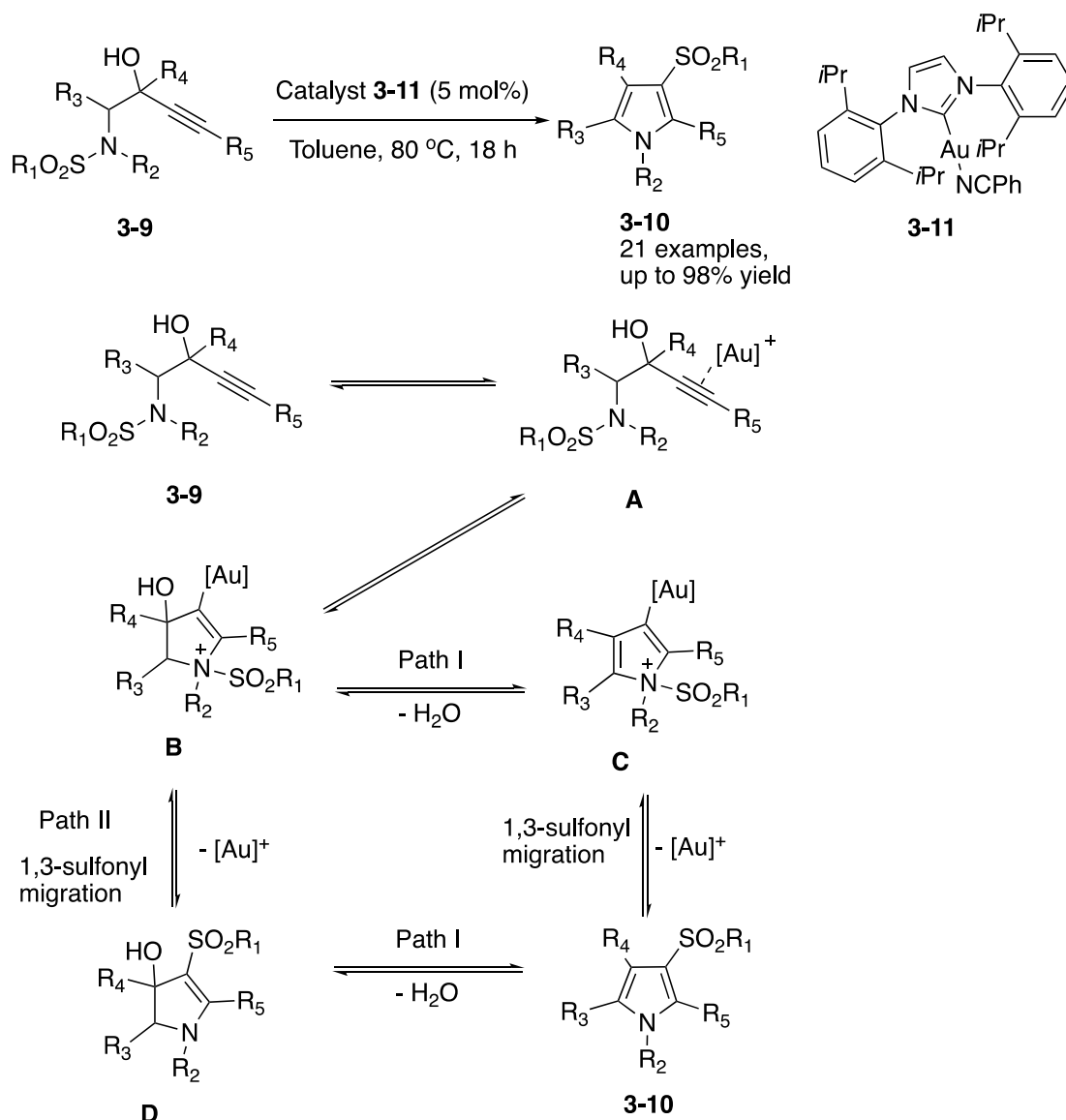
Scheme 3-2 Crossover experiments of **3-7** and **3-8**

A mechanism was proposed in Scheme 3-3 for the cyclization of **3-1**. The first step is coordination of the Lewis acidic-transition-metal complex MX_n to the alkyne moiety of **3-1** to form the intermediate π -complex **A**. The latter leads to the formation of intermediate π -complex **B**, which is formed by nucleophilic attack of the nitrogen atom on the alkynyl moiety. Then, there are two diverging pathways depending on the metal catalyst employed. For the gold-catalyzed process, the sulfonyl group migrated to the 3-position of the indole skeleton to form intermediate complex **C** (Cycle I),³ followed by elimination of AuBr_3 to afford the 3-sulfonylindole products **3-2**. 1,5-sulfonyl migration and 1,3-proton shift take place to generate intermediate **D** (Cycle II). Elimination of AuBr_3 from the resulting intermediate **E** then gives 4-sulfonylindoles **3-3**. Additionally, a consecutive 1,7-sulfonyl migration and 1,5-proton shift take place (Cycle III). Elimination of InBr_3 from the resulting intermediate **E** then gives 6-sulfonylindoles **3-5**.



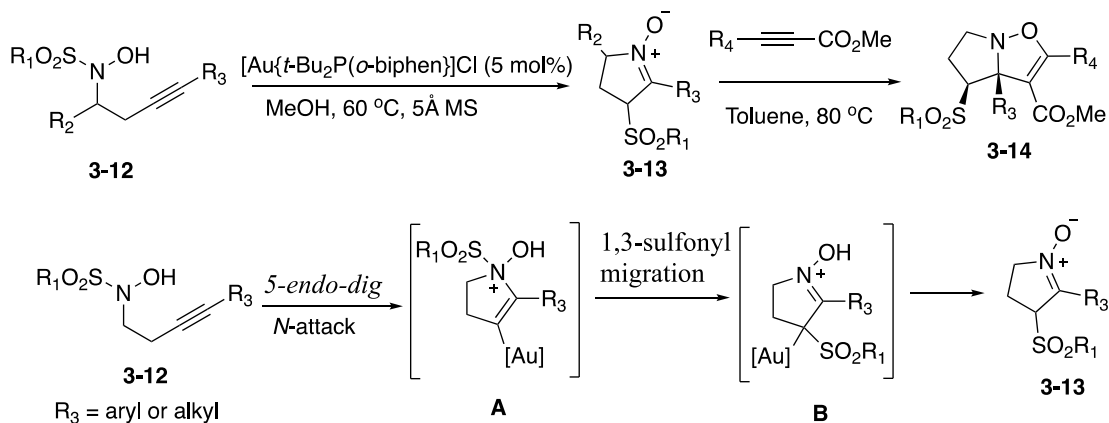
Scheme 3-3 Proposed mechanistic cycle for the gold- and indium-catalysed synthesis of 3-, 5- and 6-sulfonylindoles

Chan group reported gold(I)-catalyzed cycloisomerization of *N*-substituted, *N*-sulfonylaminobut-3-yn-2-ols **3-9**, to form the corresponding 1-substituted 3-sulfonyl-1*H*-pyrroles **3-10** with moderate to excellent yields (Scheme 3-4, catalyst **3-11**).⁴ A mechanism involving activation of the propargylic alcohol by the Au(I) catalyst was proposed. The coordination of the Au(I) catalyst with the alkyne moiety of the adduct give Au(I)-coordinated intermediate **A**. An intramolecular aminocyclisation is triggered involving anti addition of the *N,N*-disubstituted amino moiety to the triple bond affording the vinyl gold complex **B**. Then, there are two pathways. Dehydration of this species leads to the formation of the cationic pyrrole-gold adduct **C**, which subsequently undergoes an intramolecular 1,3-sulfonyl migration resulting in deauration and generation of the pyrrole product (Scheme 3-3, path I). Alternatively, vinyl gold complex **B** could undergo the deaurative 1,3-sulfonyl migration process first to give 2,3-dihydro-1*H*-pyrrol-3-ol adduct **D** that upon dehydrative aromatization would provide **3-10** (Scheme 3-4, path II).



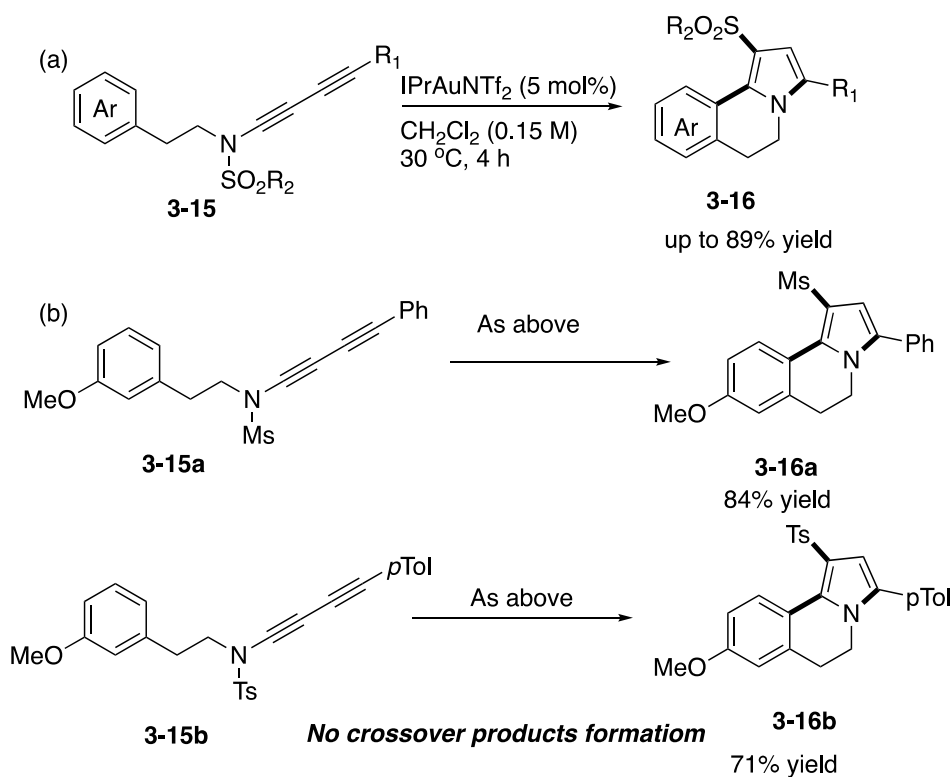
Scheme 3-4 Gold(I)-catalyzed cycloisomerization/1,3-sulfonyl migration of *N*-substituted *N*-sulfonyl-aminobut-3-yn-2-ols

The Shin group reported the gold-catalyzed synthesis of nitrones **3-13** from *N*-sulfonyl hydroxylamines **3-12** via 1,3-sulfonyl migration. In the case of internal alkynes, the nitrogen of the hydroxylamine moiety is the preferred nucleophile, which allows for a *5-endo-dig* cyclisation to occur giving **A**. Then, loss of the gold catalyst and tautomerisation of the resulting vinyl hydroxylamine leads to the nitronium **3-13**, which were confirmed by trapping with dipolarophiles via [3 + 2]-dipolar cycloaddition to form product **3-14** (Scheme 3-5).⁵



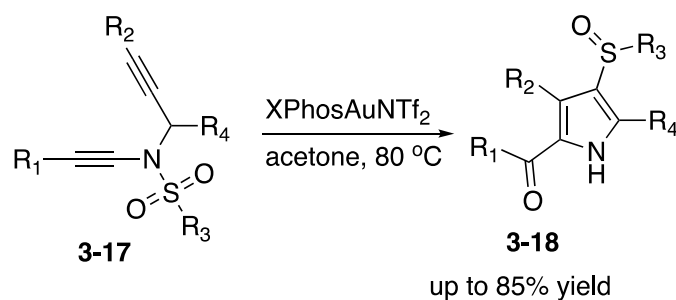
Scheme 3-5 Gold-catalysed synthesis of nitrones from *N*-sulfonyl hydroxylamines via 1,3-sulfonyl migration

Recently, Liu group developed a gold-catalyzed cascade reaction of diynamides **3-15** to generate a series of sulfone containing pyrrolo[2,1-*a*]isoquinolines **3-16** featuring the core structural motif of the lemellarin alkaloids (Scheme 3-6, a).⁶ A crossover experiment, with two different sulfonyl diynamides, did not lead to crossover products, indicating that the migration of the sulfonyl group occurs in an intramolecular fashion (Scheme 3-6, b). DFT studies suggested that the formal 1,4-sulfonyl migration is in fact two sequential 1,2-sulfonyl shifts.



Scheme 3-6 Gold-catalysed cascade reaction and crossover experiment

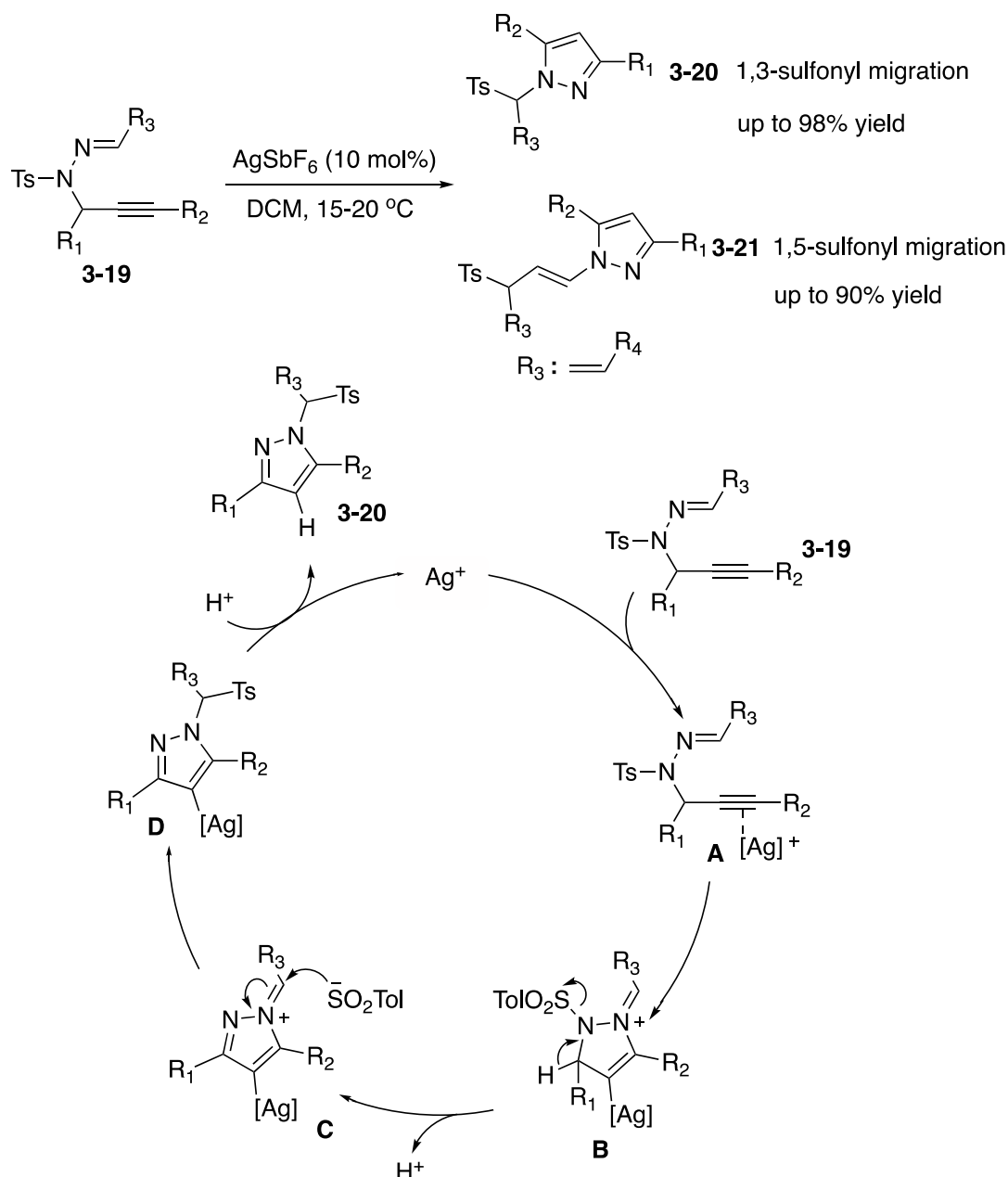
The Sahoo group recently reported a regioselective sulfonyl/sulfinyl migration cycloisomerization cascade of alkyne-tethered ynamides **1-17** in the presence of XPhos-gold catalyst to afford novel 4-sulfinylated pyrroles **1-18** in good to excellent yields (Scheme 3-7).⁷ This reaction is the first example of a general [1,3]-sulfonyl migration from the nitrogen center to the β -carbon atom of ynamides, followed by umpolung *5-endo-dig* cyclization of the ynamide α -carbon atom to the gold-activated alkyne, and final deaurative [1,5]-sulfinylation.



Scheme 3-7 Gold-catalysed regioselective sulfonyl/sulfinyl migration cycloisomerization cascade of alkyne-tethered ynamides

1.2 Silver-catalysed Sulfonyl Migration

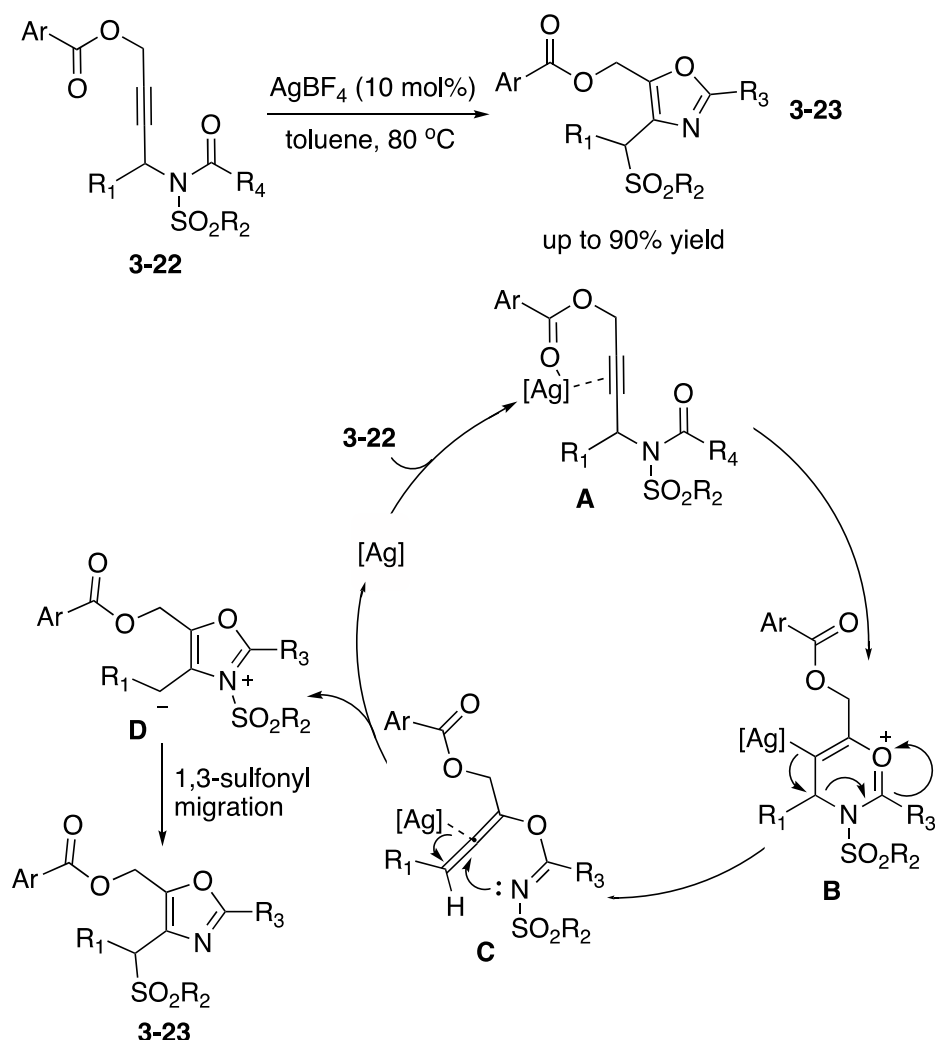
Chung group reported the silver(I)-catalyzed formation of pyrazoles **3-20/3-21** from propargyl *N*-sulfonylhydrazone **3-19**, involving a 1,3- or 1,5-sulfonyl migration (Scheme 3-8).⁸ This methodology allows for the efficient and regioselective synthesis of 1,3- and 1,5-disubstituted and 1,3,5-trisubstituted pyrazoles in moderate to excellent yields. An intermolecular sulfonyl migration was elucidated by means of crossover experiments. The author proposed the mechanism was show in Scheme 3-8. The coordination of the electrophilic silver source to the alkyne moiety of **3-19** to form the intermediate π -complex **A**. Nucleophilic cyclisation occurs yielding the silver(I) intermediate **B**. Deprotonation leads to the generation of ion pairs **C**. The sulfinate anion attacks the electrophilic iminium carbon completing the 1,3-sulfonyl migration. In instances in which the imine substituent is extended by conjugation, the sulfonate anion attacks the β -carbon leading to the preferred 1,5-sulfonyl migration. Finally, protodemetalation of **D** regenerates the catalytic silver species and gives the pyrazole products **3-20**.



Scheme 3-8 Silver(I)-catalysed synthesis of pyrazoles from propargyl *N*-sulfonylhydrazones via 1,3- or 1,5-sulfonyl migration and postulated mechanism

Wan group developed a silver(I)-catalyzed cyclization of *N*-sulfonyl propargylamides **3-22** for the synthesis of 4-(sulfonylmethyl)oxazoles **3-23** in good to excellent yields (Scheme 3-9).⁹ The introduction of the acyloxy group was found to be essential for the [3,3] rearrangement. Notably, crossover experiments indicated that the sulfonyl migration may occur in both an intra- and intermolecular manner. A plausible mechanism was proposed as depicted in Scheme 3-9. As a first step, a π -complex **A** was formed between the alkyne moiety and the Ag(I) cation. Meanwhile, the acyloxy group also coordinated with Ag(I) to facilitate subsequent transformations. Then, intermediate **B** was formed by intramolecular nucleophilic attack of the

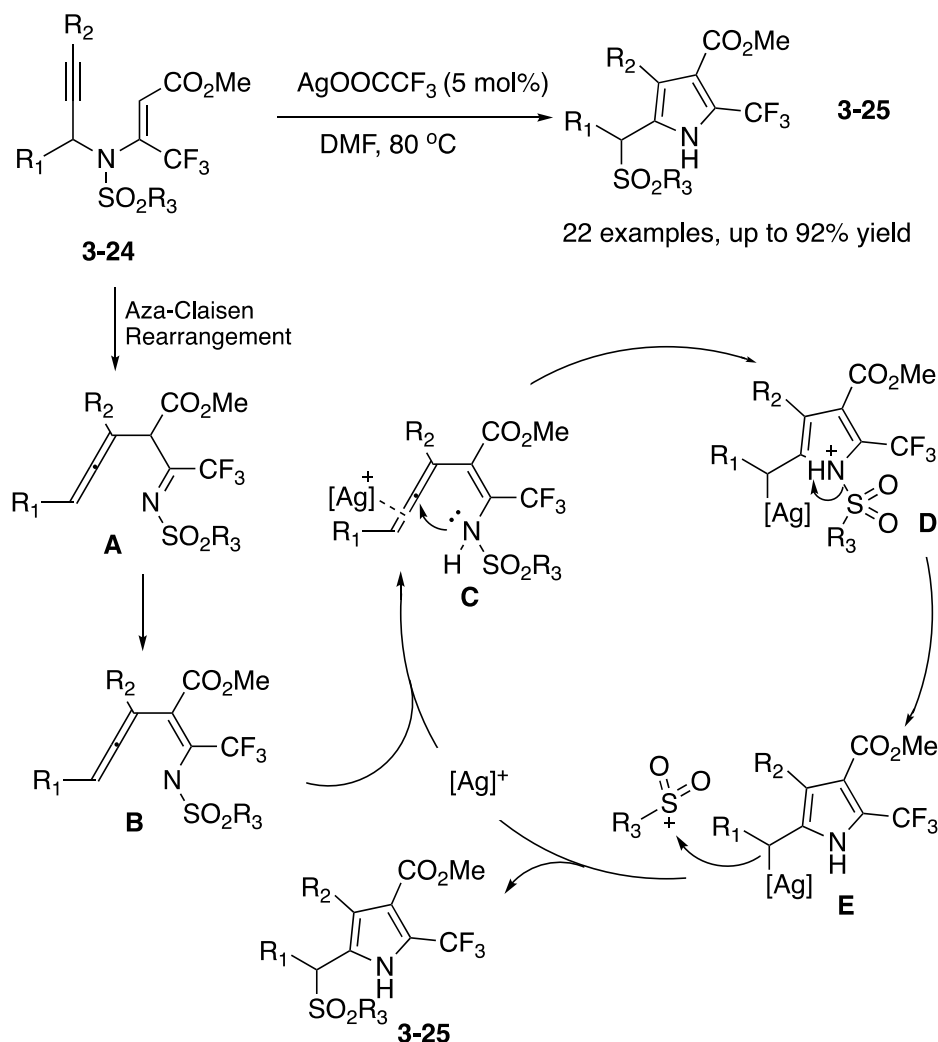
carbonyl oxygen on the amide *via* 6-*endo-dig* mode, which collapsed into the allene intermediate **C**. Nucleophilic attack of the nitrogen at the allenyl carbon followed to give a zwitterionic intermediate **D**. And then arranged to oxazole **3-23** *via* sulfonyl shift in both intra- and intermolecular manner.



Scheme 3-9 Silver-catalysed cyclisation of propargylamides in the generation of functionalised oxazoles *via* 1,3-sulfonyl migration

Wan group further developed the synthesis of 2-trifluoromethyl 5-(arylsulfonyl)methyl pyrroles **3-25** from trifluoromethyl-substituted 3-aza-1,5-enynes **3-24** *via* a cyclization/sulfonyl group migration cascade by silver catalysis (Scheme 3-10).¹⁰ Crossover experiments indicated an intermolecular process for the sulfonyl migration. Interestingly the reaction does not work with alkyl substituents at R_1 position. The author proposed the following mechanism (Scheme 3-10). 3-Aza-1,5-enyne **3-24** is transformed into intermediate **A** *via* an aza-Claisen rearrangement,¹¹ which upon isomerisation gives the allene **B**. Then, the coordination of the

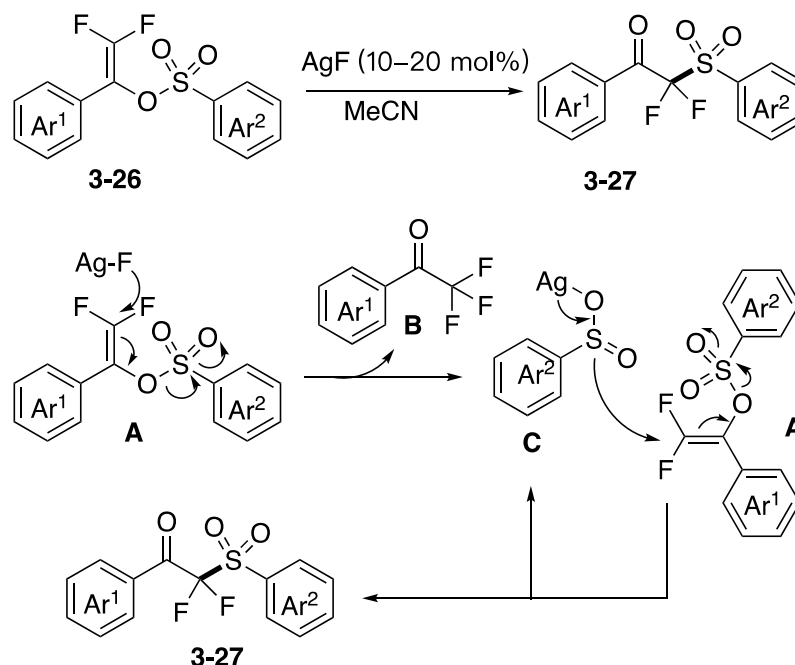
allene intermediate **B** with the silver(I) catalyst leads to cyclisation of the silver complex **C**, which cyclization provides intermediate **E**. Cleavage of the N-S bond ensues, affording the intermediate **F** and the sulfinate anion. In the last step, the organic cation displaces the Ag(I) cation to form the desired pyrroles **3-25** and releases the Ag(I) catalyst.



Scheme 3-10 Generation of 2-trifluoromethyl-5-(arylsulfonyl)methylpyrroles *via* silver-catalysed 1,3-sulfonyl migration and proposed mechanism

Very recently, Lian Group reported a silver fluoride catalyzed 1,3-sulfonyl migration of difluorovinyl sulfonates **3-26** to generate α,α -difluoro- β -ketosulfones **3-27** in excellent yields (Scheme 3-11).¹² This method features very broad functional group tolerance, high atom economy, and mild, environmentally benign reaction conditions. Furthermore, mechanistic experiments indicate that this migration proceeds in an intermolecular pathway. A plausible mechanism was presented for this 1,3-sulfonyl migration. First, silver fluoride reacts with difluorovinyl sulfonates **A** to produce the side product (trifluoromethyl)acetophenone **B** and the

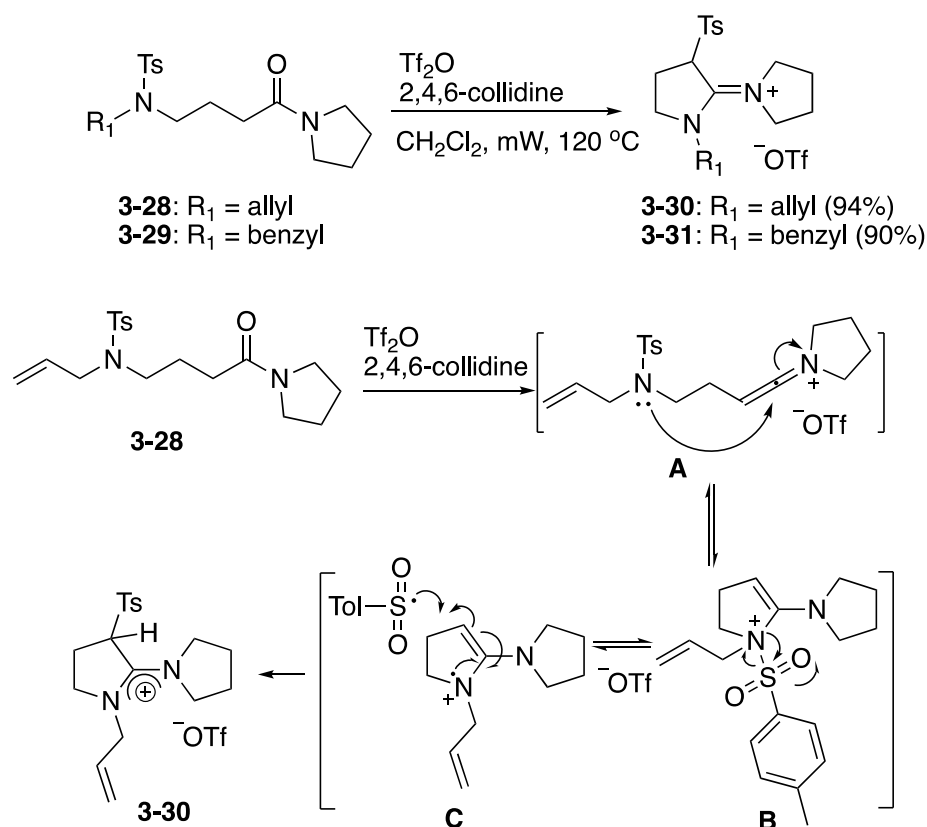
corresponding aryl sulfinate **C**. Subsequently, nucleophilic attack of the formed intermediate **C** occurs on the highly electron-deficient carbon of gem-difluorostyrenes to form the desired product α,α -difluoro- β -ketosulfones **3-27**. Meanwhile, the formed aryl sulfinate takes part in the next cycle.



Scheme 3-11 Silver catalyzed 1,3-sulfonyl migration of difluorovinyl sulfonates and plausible mechanism

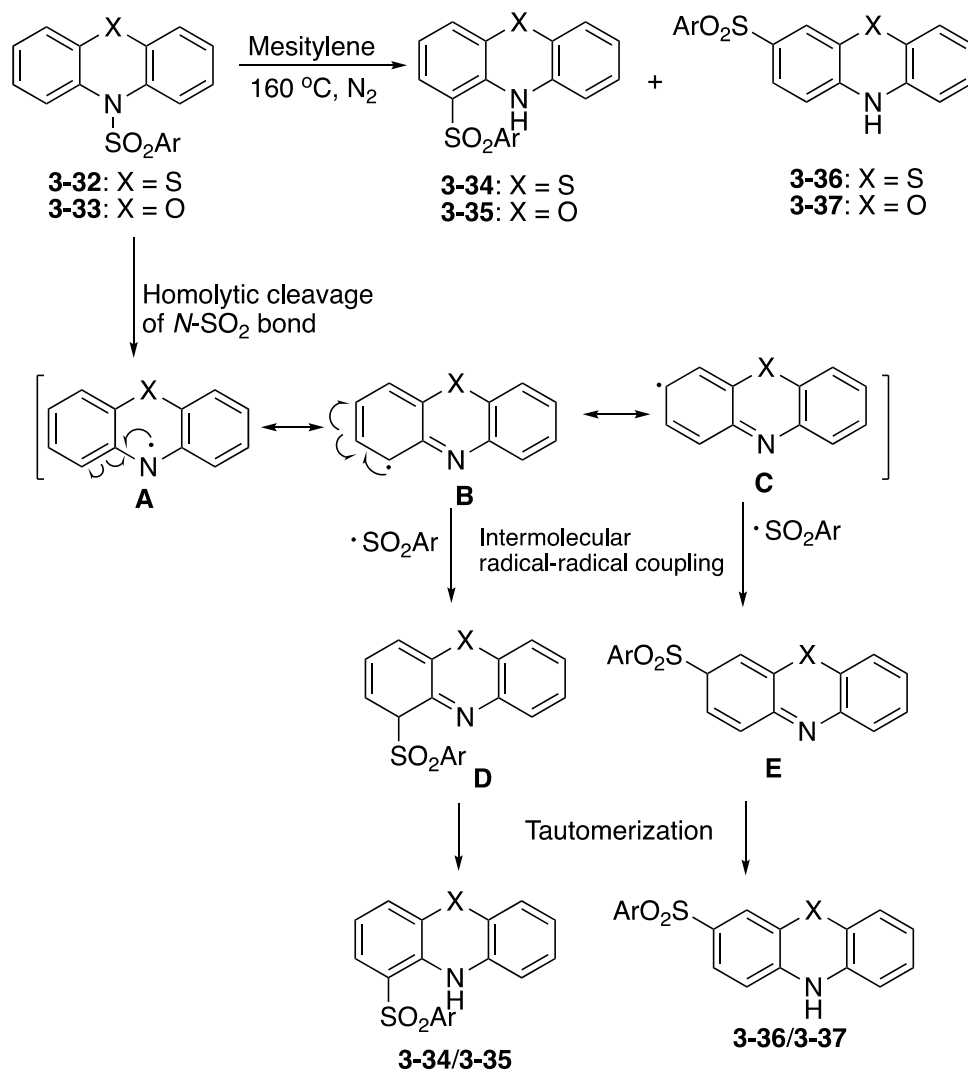
1.3 Radical-mediated Sulfonyl Migration

In 2015, Maulide group observed an unexpected nitrogen to carbon 1,3-sulfonyl migration of a tosyl group when attempting to expand the scope of electrophilic Claisen rearrangements to aza-derivatives. Aza-derivatives **3-28** - **3-29** did not afford the expected α -substituted lactams when alkyl and alkenyl oxygen-based substrates, but instead the amidinium derivatives **3-30** and **3-31**. Both the allyl and benzyl derivatives **3-28** and **3-29** underwent tosyl migration. It was postulated that the tosyl migration occurs as a result of a radical pathway, with homolytic cleavage of N-S bond in the intermediate **B**. It was suggested that recombination of the radical pair **C** to afford product **3-28** may be faster than diffusion, and that this process is more favorable energetically than migration of the allyl group (Scheme 3-12).¹³



Scheme 3-12 Generation of amidinium derivatives *via* 1,3-tosyl migration

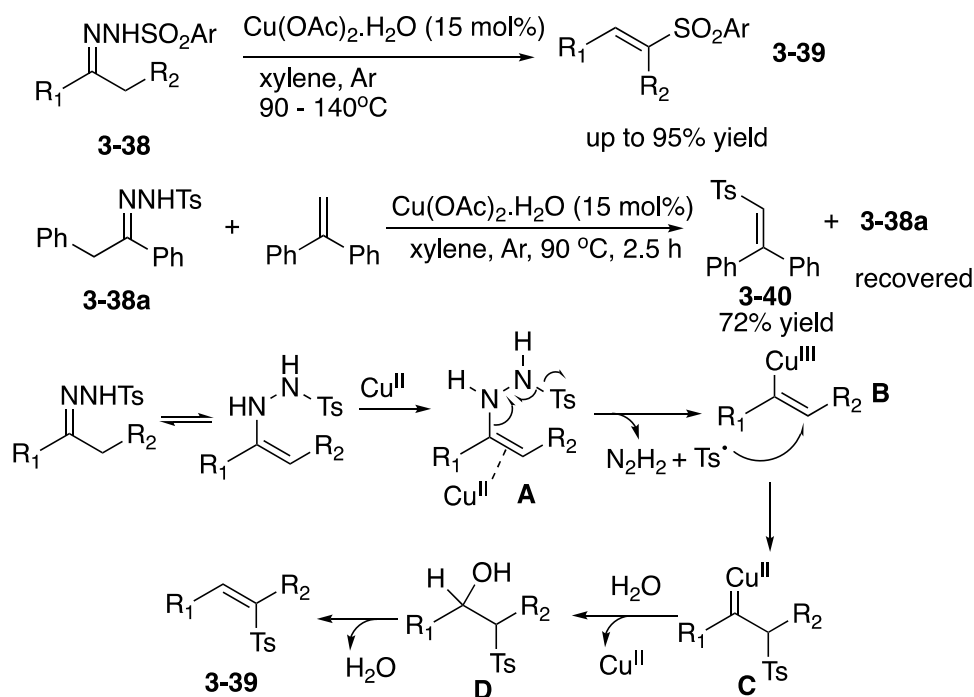
Xu group investigated thermal-induced 1,3- and 1,5-sulfonyl migration reactions of various sulphonamides.¹⁴ The results indicate that both *N*-arenesulfonylphenothiazines **3-32** and *N*-arenesulfonylphenoxazines **3-33** can undergo 1,3- and 1,5-sulfonyl migrations to afford the corresponding sulfonyl substituted phenothiazine **3-34/3-36** or phenoxazine derivatives **3-35/3-37** in modest regioselectivities and yields under thermal and neutral conditions (Scheme 3-13). And crossover experiments indicated that the sulfonyl migration was an intermolecular process. A possible mechanism involving radical-radical coupling reaction was proposed as show in Scheme 3-13. The free radical **A** and a sulfonyl radical were formed by homolytic cleavage of the N-S bond. The radical intermediates **A** can readily interconvert between the resonance structures **B** and **C** through electron delocalisation. Recombination of the sulfonyl radical with **B** or **C**, leads to formal 1,3- and 1,5-sulfonyl migrations to give intermediates **D** and **E**. Finally, isomerization of these intermediates affords the rearranged phenothiazine or phenoxazine products **3-34 - 3-37**.



Scheme 3-13 Radical-radical coupling reaction mechanism for the 1,3- and 1,5-sulfonyl migrations of *N*-arenesulfonyl-phenothiazines and phenoxazines.

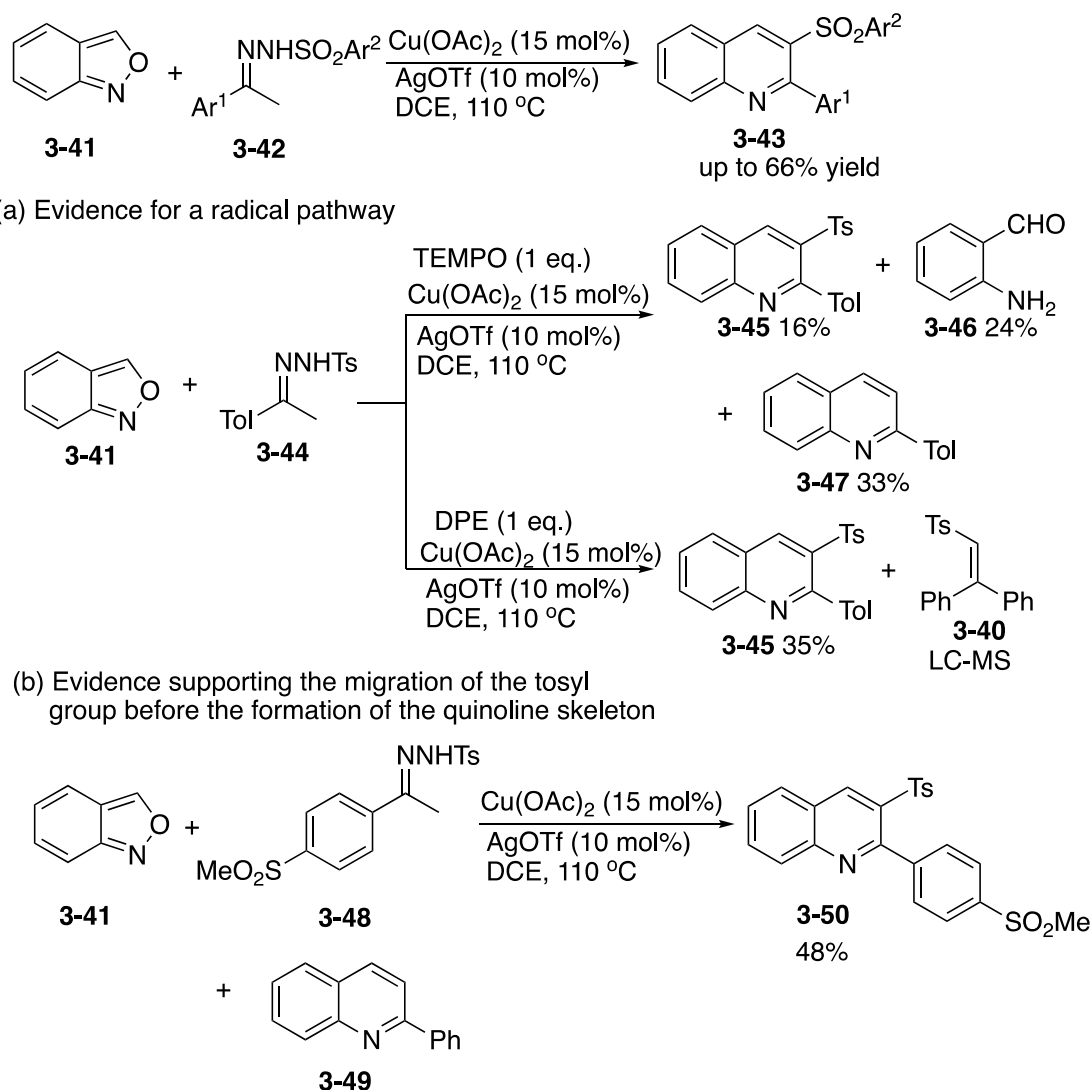
Wang group developed a copper-catalyzed radical reaction to synthesize vinyl sulfones **3-39** from *N*-sulfonylhydrazones **3-38** in good to excellent yields (Scheme 3-14).¹⁵ The radical pathway was confirmed by the addition of radical scavenger 2,2,6,6-tetramethylpiperidine-1-oxyl (TEMPO) or 1,1-diphenylethylene (DPE) to the standard reaction conditions, which completely inhibited the formation of the sulfonyl migration product. Instead **3-40** isolated as the major product in 72% yield completely replacing formation of **3-39**.

A plausible mechanism for the reaction was shown in Scheme 3-14. The *N*-tosylhydrazone isomerized. The coordination of the copper catalyst with C-C double bond and promoted the decomposition of **A** releasing N₂H₂ and tosyl free radical to provide vinyl copper complex **B**. Then, the tosyl free radical combined with **B** to give copper carbenoid **C**, which undergoes O-H insertion with water to afford to regenerate the copper catalyst and trans-elimination of H₂O to afford vinyl sulfone **3-39**.



Scheme 3-14 Copper-catalysed stereoselective synthesis of (*E*)-vinyl sulfones *via* the radical reaction of *N*-tosylhydrazones and plausible mechanism

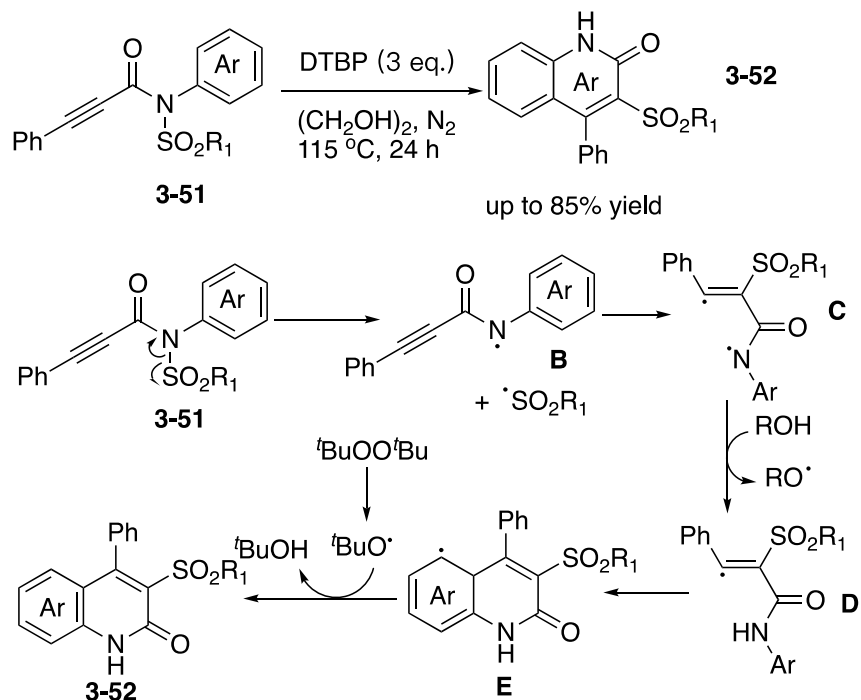
The Ji group recently developed a Cu(II)/Ag(I)-catalyzed domino reaction of *N*-sulfonylhydrazones **3-41** with anthranils **3-42** to construct 2,3-disubstituted quinoline derivatives **3-43** in one step with good yields (Scheme 3-15).¹⁶ In order to further understand the reaction mechanism, the authors carried out a series of control experiments. When 1 equiv of TEMPO was added to the reaction system of the yield of **3-45** reduced to only 16%, while also forming the decomposition product **3-46** and the quinoline **3-47**. Additionally, in the presence of the alternative radical scavenger DPE (1,1-diphenylethylene), it was found that the desired product **3-45** was obtained in 35% yield with the detection of radical trapped product **3-40** by LC-MS. These results indicated that the reaction involves a Ts radical process (Scheme 3-15, a). When **3-41** and **3-48** were reacted in the presence of the quinoline **3-50** no formation of **3-45** was observed highlighting that the sulfonyl migration occurs prior to the formation of the quinoline skeleton (Scheme 3-15, b).



Scheme 3-15 Copper(II)/silver(I)-catalysed formation of 2-aryl 3-sulfonyl disubstituted quinoline derivatives

Cheng group reported the di-tert-butyl peroxide-mediated radical rearrangement of *N*-sulfonyl-*N*-aryl propynamides **3-51** to afford 3-sulfonyl-2-(1*H*)-quinolinones **3-52** in good yields with good functional group compatibilities (Scheme 3-17).¹⁷ this procedure proceeds with sequential homolytic N-SO₂ bond cleavage and 6-*endo-dig* radical cyclization to access a variety of 2-sulfonyl-3-aryl-2(1*H*)-quinolinones **3-52** with high atom economy. Crossover experiments indicated the involvement of an intermolecular process. Additionally, a radical pathway was postulated based on the inhibition of the reaction cycle upon the addition of the radical scavengers TEMPO, BHT or galvinoxyl. A proposed mechanism was outlined in Scheme 3-17. First, the reaction is initiated by homolytic cleavage of N-SO₂ bond to afford nitrogen radical **B** and sulfonyl radical. Then the addition of sulfonyl radical to the triple bond of intermediate **B** provides radical intermediate **C**. Afterward, radical intermediate **C** abstracts

one H atom from solvent leading to radical intermediate **D**. Second, the radical cyclization takes place leading to the cyclized intermediate **E**. Meanwhile, the homolytic cleavage of DTBP produces the *t*-butoxyl radical. Finally, the *t*-butoxyl radical abstracts one hydrogen in intermediate **E** to produce the final product **3-52**.



Scheme 3-17 Di-*tert*-butyl peroxide mediated radical rearrangement of *N*-sulfonyl-*N*-aryl propynamides and proposed Mechanism

2. Project Aim and Introduction

The indole scaffold is one of a prevalent organic structure, which widely exists in many bioactive natural products and pharmaceuticals.¹⁸ Among them, 3-sulfonylindole derivatives are found in a wide variety of biologically active compounds such as a HIV-1 non-nucleoside reverse transcriptase inhibitor (I),¹⁹ norepinephrine reuptake inhibitors and 5-HT_{2A} receptor antagonists (II),²⁰ human 5-HT₆ receptor ligands (III),²¹ orexin receptor antagonists (IV) (Figure 3-1).²² Hence, there has been growing interest

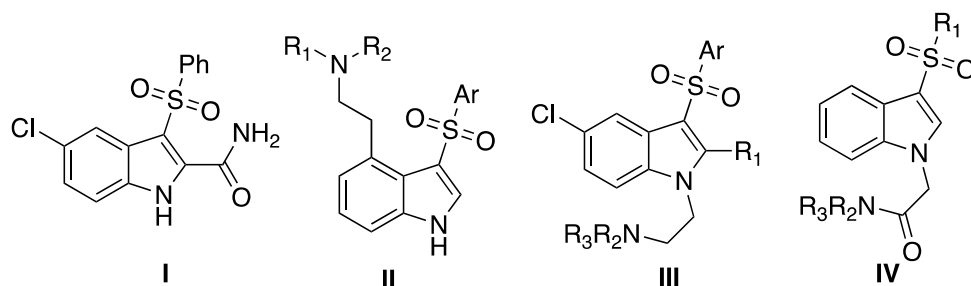


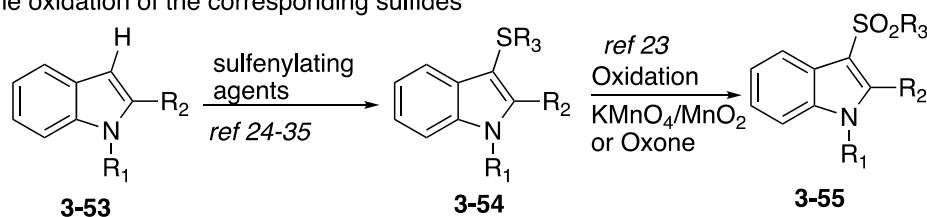
Figure 3-1 Biologically active 3-sulfonylindole derivatives

in developing a general and efficient route to access 3-sulfonylindoles. However, it is difficult to synthesize 3-sulfonylindoles directly from the corresponding non-substituted indoles by electrophilic-substitution reactions, because the electrophilicity of sulfonyl groups is much lower than that of acyl groups and halogens. In general, 3-sulfonylindoles **3-55** have been prepared by the direct C3 functionalization of indoles **3-53** with sulfenylating agents, followed by oxidation (Scheme 3-18, a).²³ To date, several sulfenylating agents such as disulfides,²⁴ thiols,²⁵ sulfinic acids,²⁶ sulfinate salts,²⁷ sulfonyl chlorides,²⁸ sulfenyl chlorides,²⁹ N-thioimides,³⁰ quinone mono-*O,S*-acetals,³¹ arylsulfonyl cyanides,³² sulfonyl hydrazides,³³ sulfoxides,³⁴ thiosulfonium salts,³⁵ and aryl boronic acids/element sulfur³⁶ have been reported to affect C3 sulfenylation.

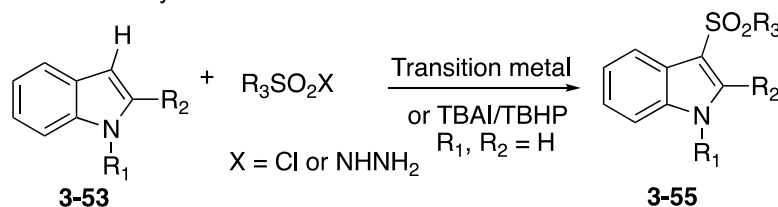
Several groups showed that 3-sulfonylindoles **3-55** can be synthesised by direct C3-sulfonylation of indoles **3-53** (Scheme 3-18, b). In 2013, Tocco et al. reported ZnO-mediated one-pot solvent-free protocol for reaction of the indoles **3-53** with sulfonyl chlorides to produce 3-sulfonylindoles **3-55**.³⁷ At the same years, Majee group reported a simple and efficient protocol for the chemoselective sulfonation of indoles using aryl sulfonyl chlorides in the presence of CuI. The reaction proceeds under mild conditions and only was applicable to indoles bearing a selection of functional groups without NH protection.³⁸ Tu group developed metal-free synthesis of bifunctionalized indole derivatives through TBHP/TBAI-mediated oxidative coupling of C2, C3-unsubstituted indoles **3-53** with arylsulfonyl hydrazide.³⁹

Undoubtedly, 3-sulfonylindoles can also be prepared the indole annulation of suitable acyclic precursors (Scheme 3-18, c). For example, Nakamura et al. reported the gold-catalysed synthesis of 3-sulfonylindoles **3-55** from *ortho*-alkynyl-*N*-sulfonylanilines **3-56**, in the presence of catalytic AuBr₃, a 1,3-sulfonyl migration was observed, to afford 3-sulfonylindoles **3-55** in good to high yields.⁴⁰ Driver group have demonstrated that rhodium(II) carboxylate complexes catalyze the migration of sulfonyl group to form 3-sulfonylindoles **3-55** from β -substituted styryl azides **3-57**.⁴¹ Back group reported the copper(II) catalyzed cyclization of sulfonyl enamines **3-58** to generate 3-sulfonylindoles **3-55** in good yields.⁴² Although these methods were available for the preparation of 3-arylsulfonylindoles by annulation of appropriate acyclic substrates, none of these methods dealt with sulfonylating reagents. During the past few years, sulfonyl hydrazides, economical and shelf-stable reagents, have received considerable attention in organic synthesis. Recently, the Kuhakarn group used sulfonyl hydrazides as the sulfur source, they reported an iodine-mediated the synthesis of 3-sulfonylindoles **3-55** from electrophilic annulation of 2-alkynyl-*N,N*-dialkylanilines **3-59** with sulfonyl hydrazides (Scheme 3-18, d).⁴³ Han and coworkers disclosed an elegant synthesis of 3-sulfonylindoles

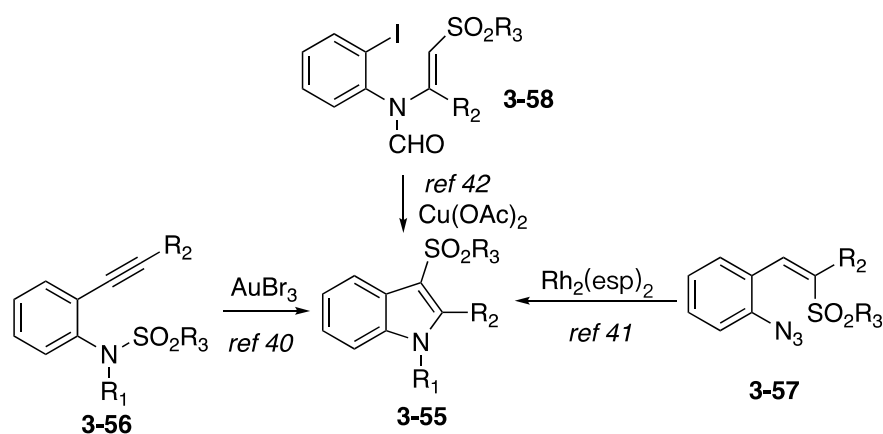
(a) The oxidation of the corresponding sulfides



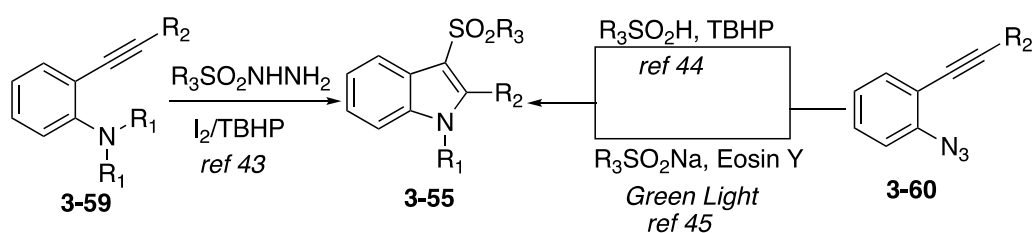
(b) Direct C3-sulfonylation of indoles³⁷⁻³⁹



(c) Indole annulation of suitable acyclic precursors



(d) The annulation of 2-alkynyl-*N,N*-dialkylanilines or 2-alkynyl-azidoarenes with sulfonyl agent

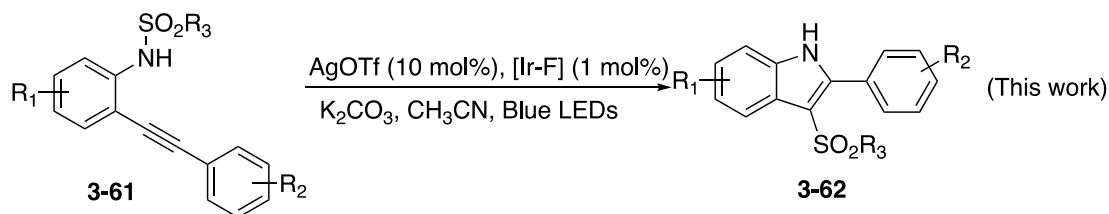


Scheme 3-18 Strategies for the synthesis of 3-sulfonylindoles

3-55 from 2-alkynylazides **3-60** employing sulfinic acids as sulfonyl agent (Scheme 3-18, d).⁴⁴ Kshirsagar group used sodium sulfonate salts instead of sulfinic acids, they disclosed a visible light induced, eosin Y photoredox catalysed a radical cascade cyclization of 2-alkynyl-azidoarenes **3-60** to produce 3-sulfonylindoles **3-55** (Scheme 3-18, d).⁴⁵ This reaction proceeds by the direct oxidation of a sulfinate anion through a reductive quenching cycle for a radical cascade cyclization of 2-alkynyl-azidoarenes.

Herein, we successfully intend to establish a facile and efficient protocol for the synthesis of bioactive 3-sulfonylindoles **3-62** by the visible-light-mediated silver catalysed tandem 1,3-

migration/cycloaddition of *ortho*-alkynyl-*N*-sulfonylanilines **3-61** (Scheme 3-19). The process occurs at room temperature upon irradiation with a sample blue LEDs. The full scope and limitation of transformation are discussed below.

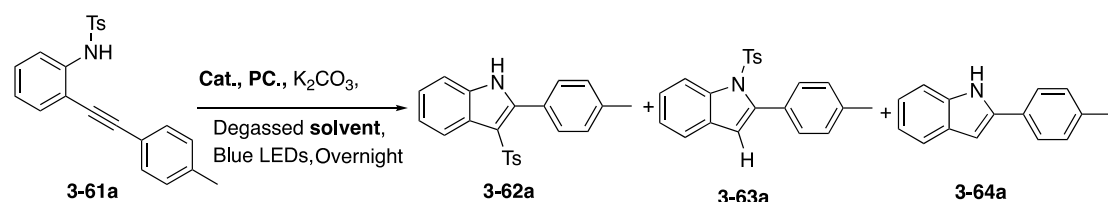


Scheme 3-19 Synthesis of 3-sulfonylindoles **3-62** from *ortho*-alkynyl-*N*-sulfonylanilines **3-61**

3. Results and Discussion

3.1 Optimization Studies

For optimization of the reactions in the present work, initially, we chose 4-methyl-*N*-(2-(*p*-tolylethynyl)phenyl)benzenesulfonamide **3-61a** as model substrate. The reaction was conducted in degassed acetonitrile at room temperature in the presence of 5 mol% [Au-CF₃] [(*p*-CF₃Ph)₃PAuCl], 1 mol% Ir[dF(CF₃)ppy]₂(dtbbpy)PF₆ (**[Ir-F]**) and 2.5 equiv of K₂CO₃, and under blue LEDs irradiated. The formation of product **3-62a** was observed in low yield (40%) (Table 3-1, entry 1). The structure of **3-62a** was confirmed by X-ray crystallography. Attempts to increase the amount of [Au-CF₃] employed (from 5 mol% to 10 mol%) did not give satisfactory results (Table 3-1, entry 3). Attempts to increase the amount of **[Ir-F]** employed (from 1 mol% to 5 mol%) gave 72% yield of **3-62a**. However, when we decreased the amount of [Au-CF₃] to 5 mol%, the yield of **3-62a** decrease to 47% (Table 3-1, entry 4). Additionally, the reaction did not give desired product when we used Ph₂CO as photocatalyst (Table 3-1, entry 5).

Table 3-1 Optimization of the Reaction Conditiona. ^a

Entry	Cat. (mol%)	Photocat. (mol%)	Solvent	Yield of 3-62a (%) ^b
1	[Au-CF ₃] (5)	[Ir-F] (1)	CH ₃ CN	40
2	[Au-CF ₃] (10)	[Ir-F] (1)	CH ₃ CN	43
3	[Au-CF ₃] (10)	[Ir-F] (5)	CH ₃ CN	72
4	[Au-CF ₃] (5)	[Ir-F] (5)	CH ₃ CN	47
5	[Au-CF ₃] (5)	Ph ₂ CO (5)	CH ₃ CN	0
6	AgOTf (10)	[Ir-F] (1)	CH₃CN	65 (3-64a, 17)
7	AgBF ₄ (10)	[Ir-F] (1)	CH ₃ CN	35 (3-64a , 14)
8	Ag ₂ CO ₃ (10)	[Ir-F] (1)	CH ₃ CN	50 (3-64a , 20)
9	AgOTf (5)	[Ir-F] (1)	CH ₃ CN	35 (3-64a , 15)
10	AgOTf (10)	[Ir-F] (5)	CH ₃ CN	47 (3-64a , 17)
11	AgOTf (10)	Ru(bpy) ₃ (PF ₆) ₂ (5)	CH ₃ CN	8 (3-63a , 58)
12	AgOTf (10)	[Ir-F] (1)	MeOH	18
13	AgOTf (10)	[Ir-F] (1)	THF	15
14	AgOTf (10)	None	CH ₃ CN	0 (3-63a , 82)
15	None	[Ir-F] (1)	CH ₃ CN	NR
16 ^c	AgOTf (10)	[Ir-F] (1)	CH ₃ CN	NR
17 ^d	AgOTf (10)	[Ir-F] (1)	CH ₃ CN	0 (3-63a , 78)

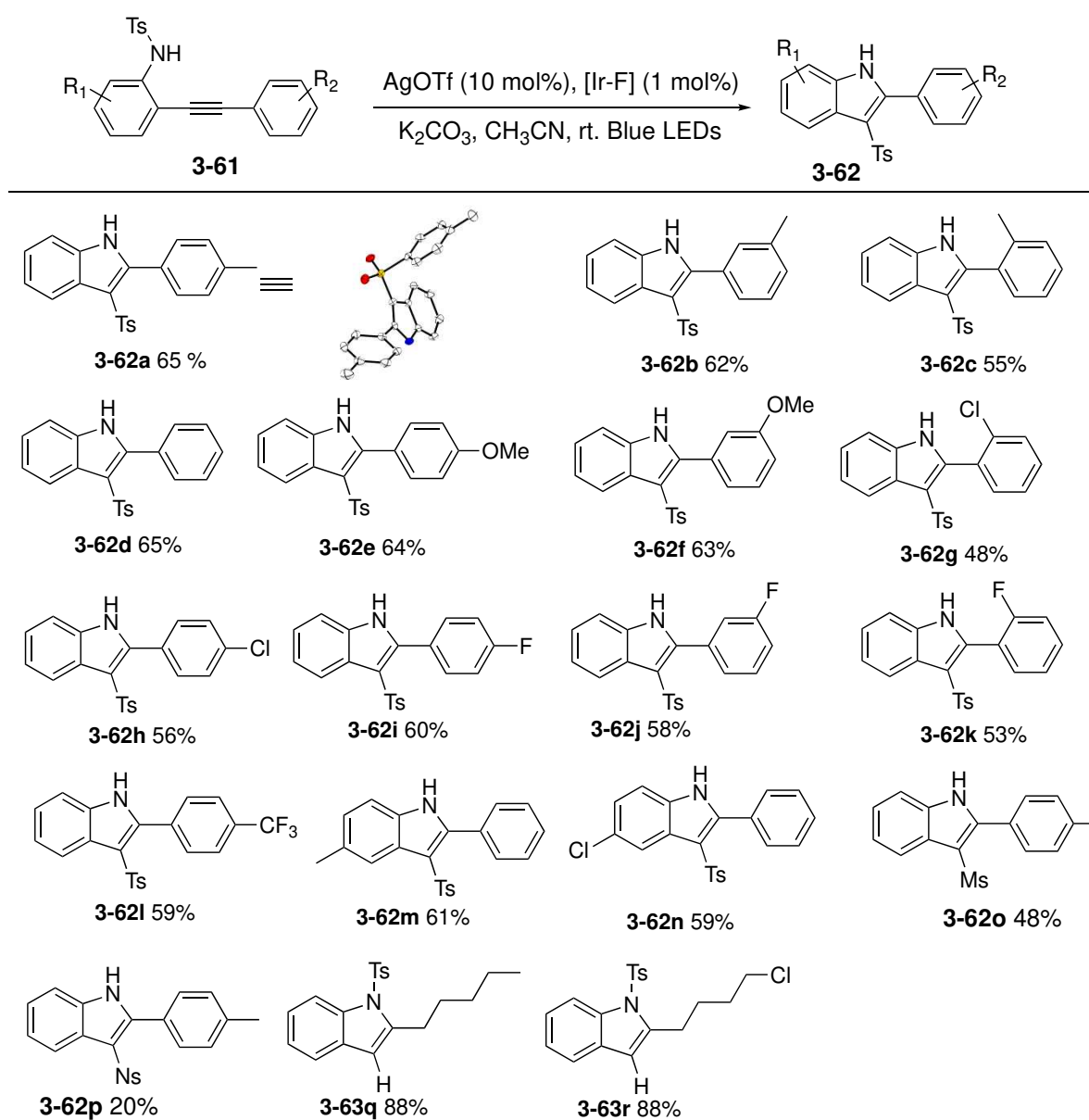
^a **3-61a** (0.2 mmol), catalyst, photocatalyst, K₂CO₃ (2.5 equiv), degassed solvent (3 mL) and stirring for overnight. [Au-CF₃] = (*p*-CF₃Ph)₃PAuCl; [Ir-F] = Ir[dF(CF₃)ppy]₂(dtbbpy)PF₆; ^b Isolated yield. ^c Without K₂CO₃; ^d No light.

Since the gold catalyst is more expensive than the silver catalyst and requires larger amount of [Ir-F], other catalysts including AgOTf, AgBF₄, and Ag₂CO₃ were examined (Table 3-1, entries 6-8). Fortunately, the desired product **3-62a** was acquired in 65% yield when AgOTf as catalyst (Table 3-1, entry 6). However, the yield of product **3-62a** decreased to 35% as the amount of catalyst decreased to 5mol% (Table 3-1, entry 9). Also, the product yield decreased when increase the amount of [Ir-F] (Table 3-1, entry 10). Additionally, only 8% desired product **3-62a** was generated when used Ru(bpy)₃(PF₆)₂ (5 mol%) instead of [Ir-F] (1 mol%) (Table 3-1, 11). The reaction was examined by changing the solvents (Table 3-1, entry

12-13) in which CH₃CN was found to be the best solvent to afford the highest yield (Table 3-1, entry 6). It has been realized that photoredox catalysts (Table 3-1, entry 14) AgOTf (Table 3-1, entry 15), K₂CO₃ (Table 3-1, entry 16), and visible light (Table 3-1, entry 17) are necessary for the reaction to occur. In front of these results, we decided to continue our study by using conditions of entry 6.

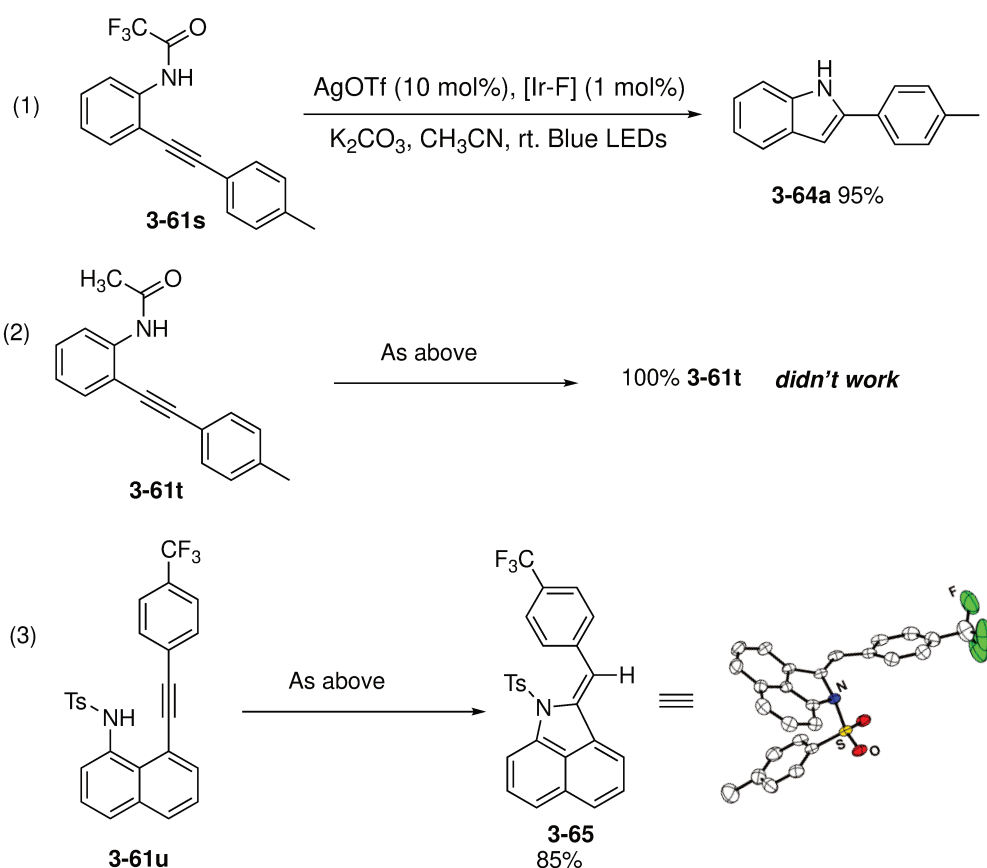
3.2 Scope and Limitation

With the optimized conditions in hand (Table 3-1, entry 6), the scope of 2-alkynylanilines **3-61** was investigated as shown in Table 3-2. First, various substituents (R₂) on the phenyl ring of the arylethynyl moiety were evaluated, which include a series of electronically different group (Me, OMe, F, Cl, CF₃). The reaction proceeded smoothly to provide the corresponding 3-sulfonylindoles **3-62a-3-62l** in moderate to good yields (from 48% to 65% yield). 2-Alkynylanilines **3-1** bearing the group Me or Cl on the phenyl ring of 2-alkynylanilines were well tolerated and yielded the corresponding 3-sulfonylindoles **3-62m-3-62n** in good yields. The influence of the steric effect was also emphasized and was found to disfavor the reactions. Thus, **3-62c**, **3-62g**, and **3-62k** were obtained in lower yields than the group in another position. In addition, *N*-(2-(*p*-tolylethynyl)phenyl)methanesulfonamide **3-61o** containing methylsulfonyl groups on the aniline nitrogen was also employed in this study. As expected, 3-(methylsulfonyl)-2-(*p*-tolyl)-1*H*-indole **3-62o** was produced in 48% yield. And when 4-nitro-*N*-(2-(*p*-tolylethynyl)phenyl)benzenesulfonamide **3-61p** was used as a starting compound, **3-62p** was isolated in 20% yield. However, when 2-alkynylanilines **3-61** bearing with alkyl group such as **3-61q** and **3-61r**, there is not tosyl migration occur. It only generated products **3-63q** and **3-63r** in 88% yield, respectively. (Notes: Starting materials from **3-61a** to **3-61p**, little amount of products **3-63** and **3-64** also were generated under optimized conditions. We did not succeed in separating them since they have similar polarity or only have a small amount.)

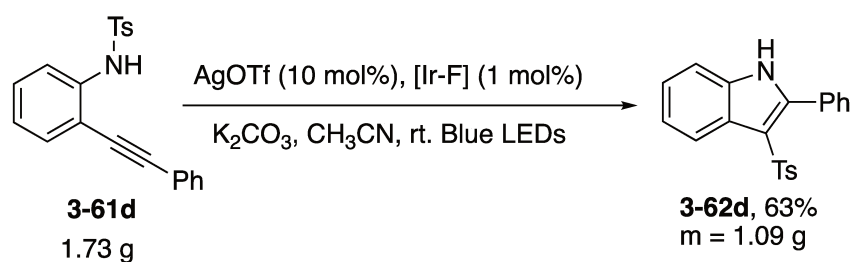
Table 3-2 Synthesis of 3-sulfonylindoles **3-62**: scope of 2-alkynylanilines **3-61**^{a,b}

^a All reactions run in degassed CH₃CN (3 mL), using **3-1** (0.2 mmol), AgOTf (10 mol%), [Ir-F] = Ir[dF(CF₃)ppy]₂(dtbbpy)PF₆ (1 mol%), and K₂CO₃ (0.5 mmol, 2.5 equiv) at room temperature under blue LEDs for overnight. ^b Isolated yields are shown.

Next, we changed the tosyl group for a trifluoroacetyl group. It only generated product **3-64a** in 95% yield (eq 1). When we used trimethylacetyl group instead of tosyl group, no desired product was obtained (eq 2). Furthermore, only polysubstituted (*Z*)-1,2-dihydrobenzo[*cd*]indoles **3-65** was formed in 85% under optimized conditions when **3-61u** was used as starting material (eq 3). And product **3-65** was unambiguously confirmed by X-ray crystallography.



To demonstrate the application of our method in organic synthesis, we tried the scale-up reaction of 4-methyl-*N*-(2-(phenylethynyl)phenyl)benzenesulfonamide **3-61d** under the standard reaction conditions. To our delight, the desired product **3-62d** could be obtained in 63% yield (Scheme 3-20).

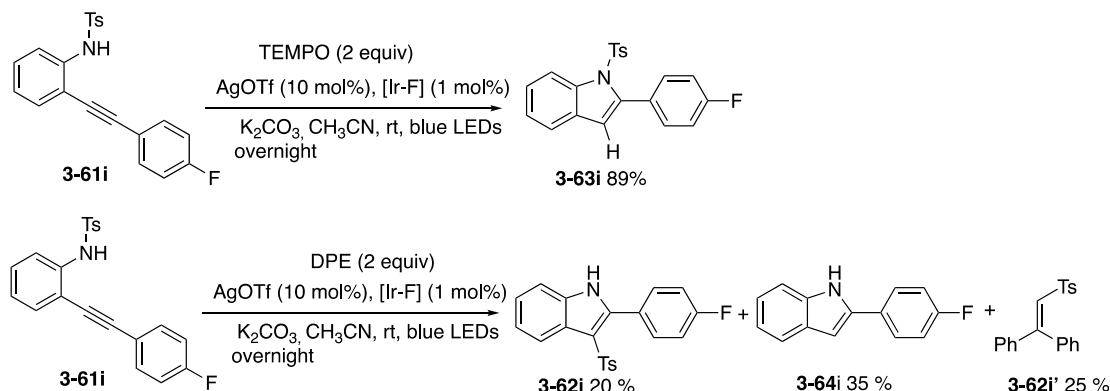


Scheme 3-20 Scale-up reaction of **3-61d**

3.3 Mechanism Investigation

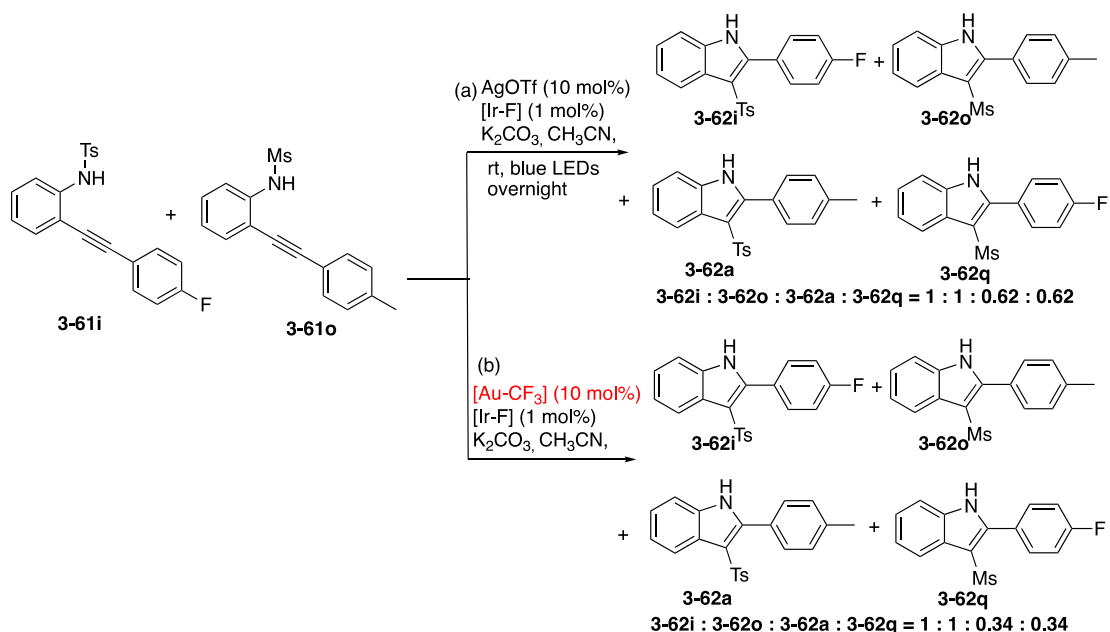
In order to further understand the reaction mechanism, we conducted some control experiments (Scheme 3-21). When 2 equivalents of TEMPO were added to the reaction system of **3-61i**, there is no desired product generated. By product **3-63i** was formed in 89%. When 2 equivalents of another radical scavenger (1,1-diphenylethylene) was added to the reaction system of **3-61i**, it was found that the desired product **3-62i** was obtained in 20% yield with the

detection of radical trapped product **3-62i'** in 25%. At the same time, the side product **4-64i** were isolated in 35% yield. These results indicated that the reaction involves a tosyl radical process.



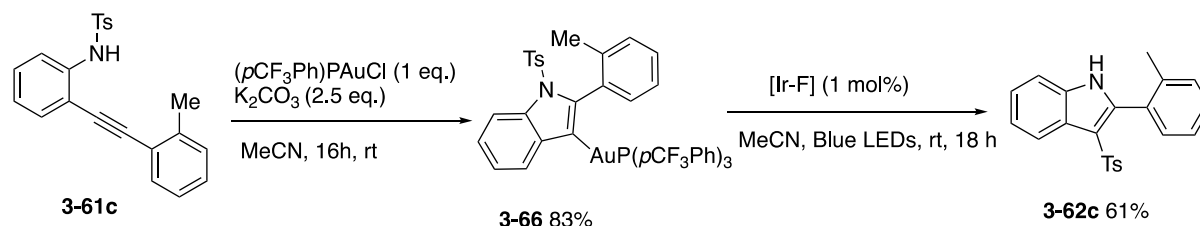
Scheme 3-21 Control experiments

To find out whether the migration of the sulfonyl group occurred in an intramolecular or intermolecular mode, a crossover experiment was performed (Scheme 3-22). The reaction of 1:1 a mixture of **3-61i** and **3-61o** in the optimized conditions to formed four 3-sulfonylindoles products in nearly 1 : 1 : 0.62 : 0.62 ratio, which was confirmed by NMR spectroscopy (Scheme 3-22, a). Interestingly, when we used $[\text{Au-CF}_3]$ instead of AgOTf, the reaction of a mixture 1:1 of **3-61i** and **3-61o** also formed four 3-sulfonylindoles products in nearly 1 : 1 : 0.34 : 0.34 ratio, which was confirmed by NMR spectroscopy (Scheme 3-22, b). These results indicated that the migration of the sulfonyl group may proceed in both intra- and intermolecular manner.



Scheme 3-22 Crossover experiment to probe the possible pathway

Based on above results, it seems that silver catalyst and [Au-CF₃] have similar value for this reaction. And it is not possible to isolate vinylsilver complexes. So, in order to gain more insights into the reaction mechanism. As shown in Scheme 3-23, we prepared vinylgold(I) **3-66** in 83% yield by an independent route.⁴⁶ Complex **3-66** was subjected under blue LEDs irradiation in the presence of 1 mol% of [Ir-F] for 18h. As expected, the migration of tosyl group was observed and the indole derivatives was isolated in 61% yield.



Scheme 3-23 The synthesis of vinylgold(I) **3-66** and further irradiation

In order to carry out NMR studies, the vinyl-gold intermediate **3-66** was engaged in photoredox conditions in NMR tube using CD₃CN under inert atmosphere. The time evolution of the intermediate formation obtained during this transformation was investigated by ³¹P NMR as shown in Figure 3-1.

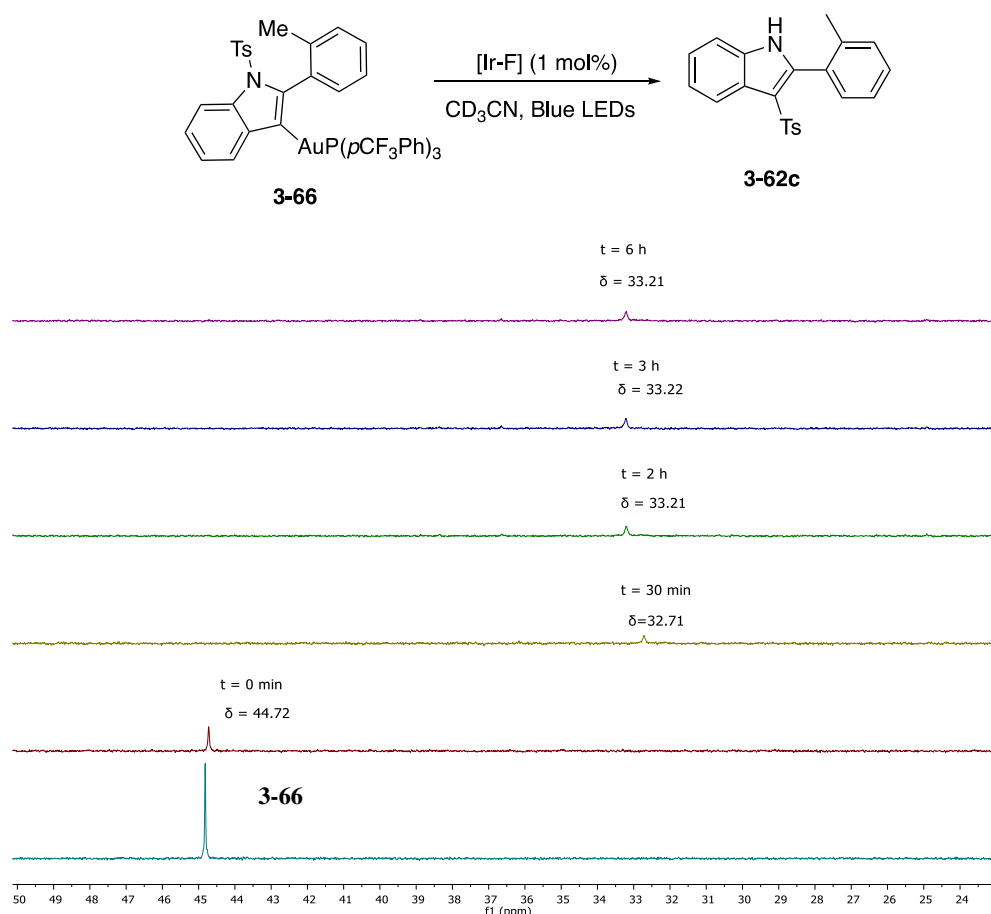
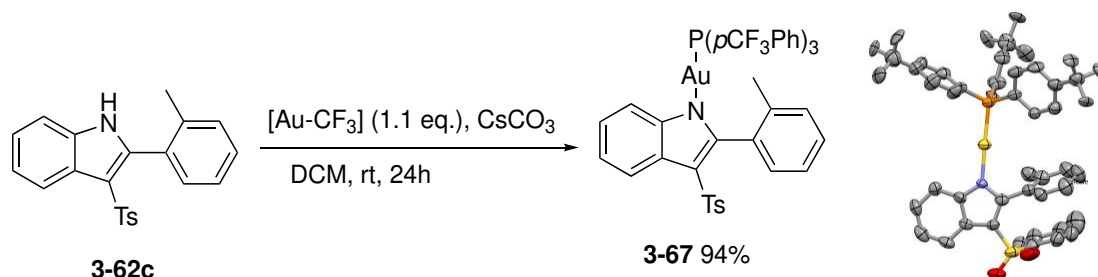


Figure 3-1 ³¹P NMR spectra of the time evolution of the intermediate formation

Interestingly, a new peak was observed and appeared at the chemical shift of 33 ppm in only 30 minutes (Figure 3-1). This result could be explained by the formation of a new gold complex intermediate imposed by the migration of tosyl group, and it is more stable during the time evolution under these conditions.

It has been reported in the literature that indole-gold complex (N-Au-P) could be obtained by reacting the indole derivative with (*p*-CF₃Ph)₃P-Au-Cl in presence of excess of CsCO₃ in DCM. Therefore, the synthesized indole **3-62c** was subjected with (*p*-CF₃Ph)₃PAuCl (1.1 equiv.) to deliver a new gold complex **3-67** in excellent yields, up to 94%. X-ray diffraction analysis of suitable crystals of **3-67** confirmed its structure. The typical chemical shift for a (*p*-CF₃Ph)₃P-Au-N environment was observed at around 33 ppm, which confirmed our observed (Scheme 3-24).



Scheme 3-24 The synthesis of gold complex **3-67**

Up to now, we still haven't got the detailed mechanism of the catalytic cycle based on above results. For that, related experiments are still going on.

3.4 Conclusion

In summary, we disclosed a visible light induced, silver-catalysed the reaction of *ortho*-alkynyl-*N*-sulfonylanilines in the presence of photocatalyst Ir[dF(CF₃)ppy]₂(dtbbpy)PF₆ ([Ir-F]) to produce 3-sulfonylindoles in moderate to good yields. This protocol not only provides a novel method for 1,3-migration/cycloaddition of *ortho*-alkynyl-*N*-sulfonylanilines but also provides a general approach for the synthesis of 3-sulfonylindole frameworks that are important in medicinal and biological chemistry. Furthermore, protodeauration products were generated when *N*-tosylalkynylamine carrying with alkyl group. Finally, mechanistic investigations indicated that the sulfonyl migration may occur in both an intra- and intermolecular manner. And related mechanism experiments are still in progress in order to understand the detailed reaction process.

4. Experimental Section

4.1 General Experimental Details

All reactions involving air sensitive reagents or intermediates were carried out in pre-heated glassware under an argon atmosphere using standard Schlenk techniques. All solvents and chemicals were used as received from suppliers (Alfa Aesar, Sigma Aldrich, TCI). Acetonitrile, tetrahydrofuran (THF), and methanol were purified by distillation over calcium hydride under dry Argon atmosphere.

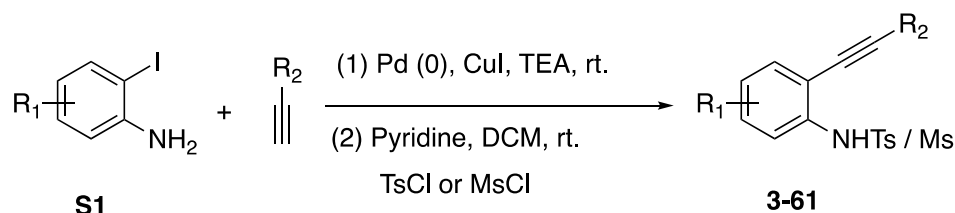
Photocatalysts $[\text{Ru}(\text{bpy})_3]_2(\text{PF}_6)_2$ and $\text{Ir}[\text{dF}(\text{CF}_3)\text{ppy}]_2(\text{dtbbpy})\text{PF}_6$ were prepared according to the procedure of Yoon⁴⁸ and Weaver⁴⁹ respectively. All gold and silver complexes were commercially available and used as received.

Chromatographic purifications of products were accomplished using force-flow chromatography (FC) on Davisil (LC60A) SI 60 Å (40 – 63 μm) silica gel according to the method of Still. Thin layer chromatography (TLC) was performed on Merck 60 F254 silica gel plates. Filtrations through Celite® were performed using Hyflo Super Cel from Fluka.

¹H NMR spectra were recorded on a Bruker 400 AVANCE or 300 AVANCE (400 and 300 MHz respectively) and are calibrated with residual CDCl₃ and DMSO protons signals at δ 7.26 ppm and δ 2.50 ppm, respectively. ¹³C NMR spectra were recorded on a Bruker 400 AVANCE or 300 AVANCE (100 and 75 MHz respectively) and are calibrated with CDCl₃ and DMSO signal at δ 77.16 ppm and δ 39.52 ppm, respectively. ¹⁹F spectra were recorded at 376.5 or 282.4 MHz and were calibrated with trifluorotoluene in CDCl₃ as external standard at δ - 63.0 ppm. Data are reported as follows: chemical shift (δ ppm), multiplicity (s = singlet, d = doublet, t = triplet, q = quartet, qt = quintuplet, m = multiplet, bs = broad signal), coupling constant (Hz) and integration. High resolution mass spectrometries were performed on a microTOF (bruker) or a LTQ-Orbitrap (Thermo Fisher Scientific) by electrospray (ESI) or Atmospheric Pressure Chemical Ionization (APCI).

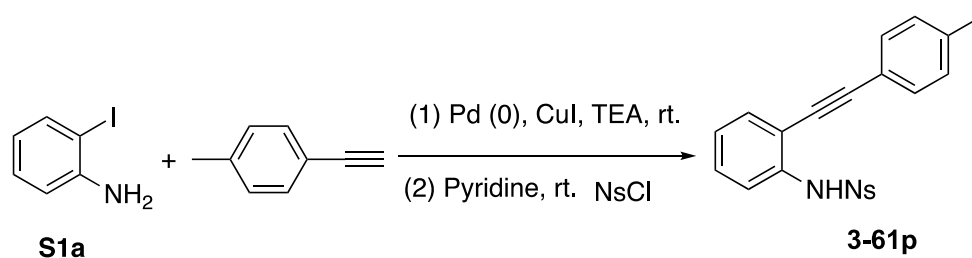
4.2 General Procedure

General Procedure 1 (GP1): Synthesis of **3-61a** - **3-61p**.⁵⁰



To a solution of corresponding 2-iodo anilines **S1** (4.0 mmol, 1.0 eq.) in dry Et₃N (5 mL), respective terminal alkynes (6.0 mmol, 1.5 eq.) and PdCl₂(PPh₃)₂ (0.04 mmol, 10 mol%) was added. After 5 min stirring at rt., CuI (0.08 mmol, 20 mol%) was added and the reaction mixture stirred at same temperature for completion (~ 4 to 12 h). After reaction completed, reaction mixture was poured into ice-cold water and extracted into EtOAc. The combined organic layer was washed with brine solution, dried and evaporated under reduced pressure. The crude residue was purified by flash chromatography on silica gel to give the products in good to excellent yields.

Then the obtained compound (1 mmol) taken in dichloromethane (20 ml) was added with pyridine (3 equiv) followed by tosyl chloride or methanesulfonyl chloride (1.3 eq) at 0 °C over a period of 15 min. After addition completes, reaction stirred at RT for ~12 hours. After reaction completed (monitored by TLC), reaction mass quenched with ice-cold water and extracted into dichloromethane. The combined organic layer was washed with 2N HCl and brine solution, and dried and evaporated to give crude residue. The obtained crude material passed through flash column chromatography to give pure product in good yield (**3-61**).

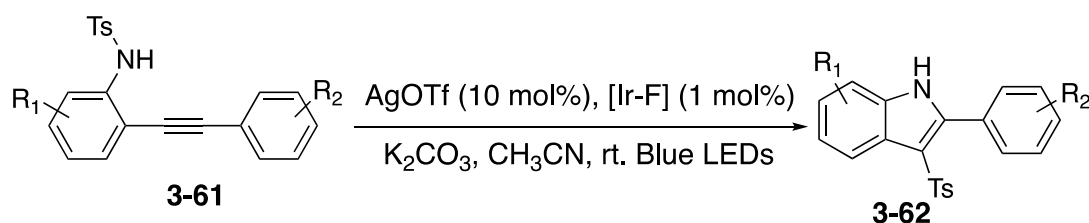


To a solution of 2-iodoaniline **S1a** (0.876 g, 4.0 mmol, 1.0 eq.) in dry Et₃N (5 mL), respective 1-ethynyl-4-methylbenzene (0.696 g, 6.0 mmol, 1.5 eq.) and PdCl₂(PPh₃)₂ (28 mg, 0.04 mmol, 10 mol%) was added. After 5 min stirring at room temperature, CuI (15 mg, 0.08 mmol, 20 mol%) was added and the reaction mixture stirred at same temperature for completion (~ 4 to 12 h). After reaction completed, reaction mixture was poured into ice-cold water and extracted into EtOAc. The combined organic layer was washed with brine solution, dried and

evaporated under reduced pressure. The crude residue was purified by flash chromatography (Pent/Et₂O: 9/1) to give the product in 92% yields as a yellow solid.

Then the obtained compound (1 mmol) taken in pyridine (10 ml) was added 4-nitrobenzenesulfonyl chloride (NsCl, 0.288 g, 1.3 eq.) at 0 °C over a period of 15 min. After addition completes, reaction stirred at RT for ~12 hours. After reaction completed (monitored by TLC), reaction mass quenched with ice-cold water and extracted into dichloromethane. The combined organic layer was washed with 2N HCl and brine solution, and dried and evaporated to give crude residue. The obtained crude material passed through flash column chromatography to give pure product (**3-61p**) in 88% yield.

General Procedure 2 (GP2): The synthesis of 3-sulfonylindoles from *ortho*-alkynyl-*N*-sulfonylanilines



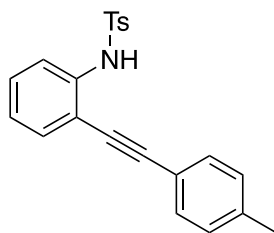
The photocatalyst Ir[dF(CF₃)ppy]₂(dtbbpy)PF₆ ([Ir-F]) (1 mol%), silver(I) complex AgOTf (10 mol %), K₂CO₃ (2.5 equiv), and *o*-alkynyl tosylanilines derivatives **3-61** (0.2 mmol, 1.0 eq.) were introduced in a *Schlenk* tube equipped with a magnetic stirring bar in which MeCN (3 mL) was added. The mixture was degassed using three freeze pump-thaw cycles and purged with Ar, then irradiated with blue LEDs light for 12h (unless mentioned). The stirring speed is equal or more than 1200 rpm. The reaction was quenched with EtOAc (5 mL) and a 2 M HCl solution (5 mL) and the solution was extracted by EtOAc (3 × 5 mL). The combined organic layer was dried over MgSO₄, filtered and concentrated under reduced pressure to give the crude product. The residue was purified by FC on silica gel to afford the desired product **3-62**.

4.3 Compound Characterizations

A. Synthesis of *ortho*-alkynyl-*N*-sulfonylanilines derivatives as substrates

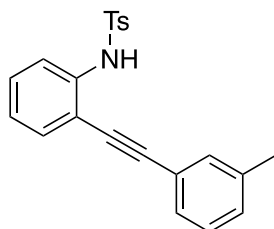
All *ortho*-alkynyl-*N*-sulfonylanilines substrates were prepared according to the procedure, as summarized before part in **General Procedure 1 (GP1)**.

4-Methyl-N-(2-(p-tolylethynyl)phenyl)benzenesulfonamide (3-61a)



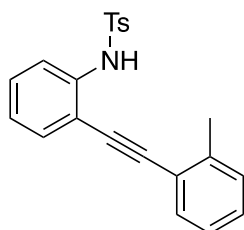
Prepared according to the general procedure GP1 on 1.0 mmol scale as a yellow solid (347 mg, 96% yield). The spectroscopic data match those previously reported in the literature.⁵⁰ ¹H NMR (400 MHz, CDCl₃) δ 7.65 (d, *J* = 8.3 Hz, 2H), 7.62 (s, 1H), 7.37 - 7.32 (m, 3H), 7.28 - 7.24 (m, 1H), 7.22 - 7.19 (m, 1H), 7.16 (dd, *J* = 12.3, 7.9 Hz, 4H), 7.03 (td, *J* = 7.6, 1.2 Hz, 1H), 2.38 (s, 3H), 2.31 (s, 3H).

4-Methyl-N-(2-(m-tolylethynyl)phenyl)benzenesulfonamide (3-61b)



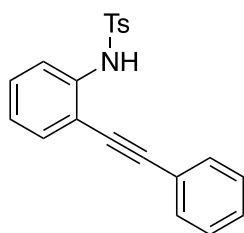
Prepared according to the general procedure GP1 on 1.0 mmol scale as a yellow solid (343 mg, 95% yield). The spectroscopic data match those previously reported in the literature.⁵⁰ ¹H NMR (300 MHz, CDCl₃) δ 7.72 (d, *J* = 8.3 Hz, 2H), 7.66 (d, *J* = 8.0 Hz, 1H), 7.39 (d, *J* = 7.7 Hz, 1H), 7.29 (d, *J* = 3.3 Hz, 5H), 7.21 (dd, *J* = 13.7, 5.9 Hz, 3H), 7.12 - 7.04 (m, 1H), 2.41 (s, 3H), 2.35 (s, 3H).

4-Methyl-N-(2-(o-tolylethynyl)phenyl)benzenesulfonamide (3-61c)



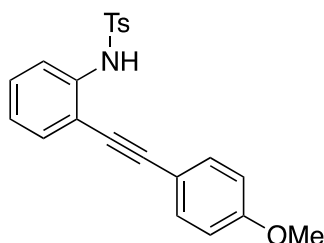
Prepared according to the general procedure GP1 on 1.0 mmol scale as a yellow solid (324 mg, 90% yield). The spectroscopic data match those previously reported in the literature.⁵⁰ ¹H NMR (400 MHz, CDCl₃): δ 7.70 (d, *J* = 8.2 Hz, 2H), 7.66 (d, *J* = 8.3 Hz, 1H), 7.46 (d, *J* = 7.5 Hz, 1H), 7.40 (td, *J* = 7.7, 1.4 Hz, 1H), 7.33 - 7.28 (m, 4H), 7.22 (td, *J* = 7.2, 1.5 Hz, 1H), 7.17 (d, *J* = 8.1 Hz, 2H), 7.07 (td, *J* = 7.6, 1.0 Hz, 1H), 2.50 (s, 3H), 2.33 (s, 3H).

4-Methyl-N-(2-(phenylethynyl)phenyl)benzenesulfonamide (3-61d)



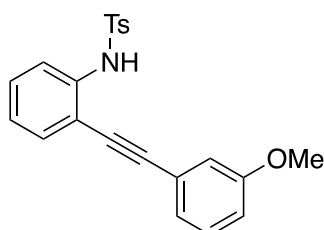
Prepared according to the general procedure GP1 on 1.0 mmol scale as a yellow solid (312 mg, 90% yield). The spectroscopic data match those previously reported in the literature.⁵⁰ ¹H NMR (300 MHz, CDCl₃) δ 7.70 (d, *J* = 8.2 Hz, 2H), 7.65 (d, *J* = 8.2 Hz, 1H), 7.50 (dd, *J* = 6.7, 3.0 Hz, 2H), 7.45 - 7.37 (m, 4H), 7.32 (s, 1H), 7.26 - 7.15 (m, 3H), 7.09 (t, *J* = 7.6 Hz, 1H), 2.37 (s, 3H).

N-(2-((4-Methoxyphenyl)ethynyl)phenyl)-4-methylbenzenesulfonamide (3-61e)



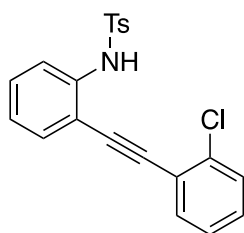
Prepared according to the general procedure GP1 on 1.0 mmol scale as a grey solid (358 mg, 95% yield). The spectroscopic data match those previously reported in the literature.⁵⁰ ¹H NMR (400 MHz, CDCl₃) δ 7.67 (d, *J* = 8.3 Hz, 2H), 7.61 (d, *J* = 8.1 Hz, 1H), 7.41 (d, *J* = 8.8 Hz, 2H), 7.35 (d, *J* = 9.0 Hz, 1H), 7.28 (d, *J* = 8.9 Hz, 1H), 7.23 - 7.15 (m, 3H), 7.05 (t, *J* = 7.6 Hz, 1H), 6.91 (d, *J* = 8.8 Hz, 2H), 3.86 (s, 3H), 2.34 (s, 3H).

N-(2-((3-Methoxyphenyl)ethynyl)phenyl)-4-methylbenzenesulfonamide (3-61f)



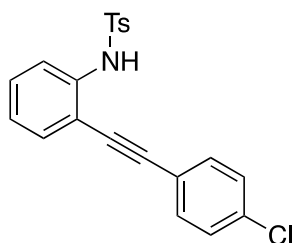
Prepared according to the general procedure GP1 on 1.0 mmol scale as a grey solid (359 mg, 96% yield). The spectroscopic data match those previously reported in the literature.⁵⁰ ¹H NMR (400 MHz, CDCl₃) δ 7.68 (d, *J* = 8.2 Hz, 2H), 7.63 (d, *J* = 8.2 Hz, 1H), 7.37 (d, *J* = 7.1 Hz, 1H), 7.28 (t, *J* = 7.9 Hz, 3H), 7.14 (s, 2H), 7.06 (dd, *J* = 10.1, 7.7 Hz, 2H), 7.00 (s, 1H), 6.94 (d, *J* = 8.3 Hz, 1H), 3.82 (s, 3H), 2.31 (s, 3H).

N-(2-((2-Chlorophenyl)ethynyl)phenyl)-4-methylbenzenesulfonamide (**3-61g**)



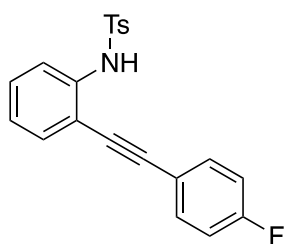
Prepared according to the general procedure GP1 on 1.0 mmol scale as a grey solid (324 mg, 85% yield). The spectroscopic data match those previously reported in the literature.⁵⁰ ¹H NMR (400 MHz, CDCl₃): δ = 7.72 (d, *J* = 8.4 Hz, 2 H), 7.69 (d, *J* = 8.5 Hz, 2 H), 7.53–7.48 (m, 2 H), 7.40 (dd, *J* = 7.7, 1.5 Hz, 1 H), 7.36–7.32 (m, 1 H), 7.32–7.27 (m, 2 H), 7.17–7.14 (m, 2 H), 7.05 (td, *J* = 7.6, 1.1 Hz, 1 H), 2.32 (s, 3H).

N-(2-((4-Chlorophenyl)ethynyl)phenyl)-4-methylbenzenesulfonamide (**3-61h**)



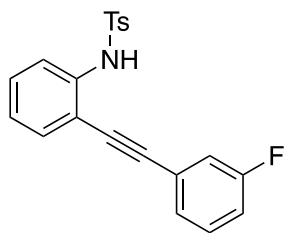
Prepared according to the general procedure GP1 on 1.0 mmol scale as a yellow solid (335 mg, 88% yield). The spectroscopic data match those previously reported in the literature.⁵⁰ ¹H NMR (300 MHz, CDCl₃) δ 7.66 (d, *J* = 8.2 Hz, 2H), 7.61 (d, *J* = 8.3 Hz, 1H), 7.37 (d, *J* = 7.6 Hz, 5H), 7.29 (d, *J* = 8.3 Hz, 1H), 7.21 - 7.13 (m, 3H), 7.07 (t, *J* = 7.6 Hz, 1H), 2.35 (s, 3H).

N-(2-((4-Fluorophenyl)ethynyl)phenyl)-4-methylbenzenesulfonamide (**3-61i**)



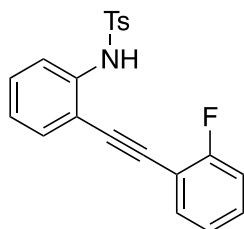
Prepared according to the general procedure GP1 on 1.0 mmol scale as a yellow solid (328 mg, 90% yield). The spectroscopic data match those previously reported in the literature.⁵⁰ ¹H NMR (300 MHz, CDCl₃) δ 7.67 (d, *J* = 8.3 Hz, 2H), 7.61 (d, *J* = 8.2 Hz, 1H), 7.50 - 7.41 (m, 2H), 7.40 - 7.27 (m, 2H), 7.18 (d, *J* = 8.0 Hz, 3H), 7.13 - 7.03 (m, 3H), 2.35 (s, 3H). ¹⁹F NMR (376 MHz, CDCl₃) δ -109.38.

N-(2-((3-Fluorophenyl)ethynyl)phenyl)-4-methylbenzenesulfonamide (**3-61j**)



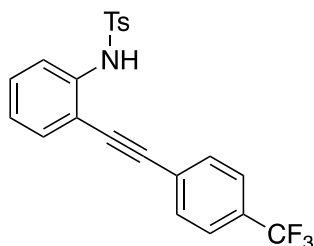
Prepared according to the general procedure GP1 on 1.0 mmol scale as a yellow solid (336 mg, 92% yield). The spectroscopic data match those previously reported in the literature.⁵⁰ ¹H NMR (400 MHz, CDCl₃) δ 7.66 (d, *J* = 8.3 Hz, 2H), 7.62 (d, *J* = 8.2 Hz, 1H), 7.39 - 7.28 (m, 4H), 7.25 (d, *J* = 8.5 Hz, 1H), 7.20 - 7.04 (m, 7H), 2.34 (s, 3H); ¹⁹F NMR (376 MHz, CDCl₃) δ -109.40.

N-(2-((2-Fluorophenyl)ethynyl)phenyl)-4-methylbenzenesulfonamide (**3-61k**)



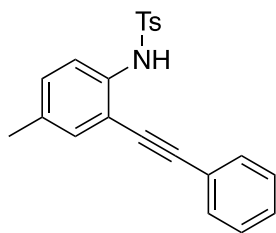
Prepared according to the general procedure GP1 on 1.0 mmol scale as a yellow solid (336 mg, 92% yield). The spectroscopic data match those previously reported in the literature.⁵⁰ ¹H NMR (400 MHz, CDCl₃) δ 7.71 (t, *J* = 9.0 Hz, 3H), 7.50 - 7.41 (m, 2H), 7.40 - 7.34 (m, 2H), 7.34 - 7.27 (m, 1H), 7.16 (dd, *J* = 11.6, 7.8 Hz, 4H), 7.05 (t, *J* = 7.6 Hz, 1H), 2.29 (s, 3H). ¹⁹F NMR (376 MHz, CDCl₃) δ -109.32.

4-Methyl-*N*-(2-((4-(trifluoromethyl)phenyl)ethynyl)phenyl)benzenesulfonamide (**3-61l**)



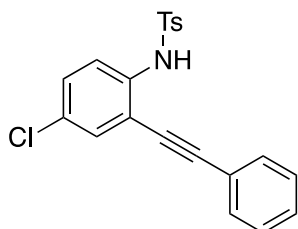
Prepared according to the general procedure GP1 on 1.0 mmol scale as a gray solid (369 mg, 89% yield). The spectroscopic data match those previously reported in the literature.⁵⁰ ¹H NMR (300 MHz, CDCl₃) δ 7.71 (d, *J* = 8.3 Hz, 2H), 7.65 (d, *J* = 7.5 Hz, 3H), 7.59 (d, *J* = 8.4 Hz, 2H), 7.45 - 7.39 (m, 1H), 7.39 - 7.31 (m, 1H), 7.29 (s, 1H), 7.19 (d, *J* = 8.2 Hz, 2H), 7.11 (t, *J* = 7.6 Hz, 1H), 2.36 (s, 3H). ¹⁹F NMR (376 MHz, CDCl₃) δ -62.89.

4-Methyl-N-(4-methyl-2-(phenylethynyl)phenyl)benzenesulfonamide (3-61m)



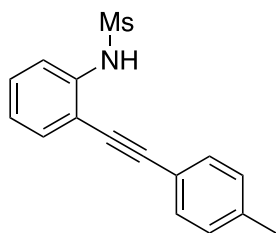
Prepared according to the general procedure GP1 on 1.0 mmol scale as a gray solid (322 mg, 89% yield). The spectroscopic data match those previously reported in the literature.⁵⁰ ¹H NMR (400 MHz, CDCl₃) δ 7.66 (d, *J* = 8.2 Hz, 2H), 7.53 (d, *J* = 8.3 Hz, 1H), 7.45 (dd, *J* = 6.6, 3.0 Hz, 2H), 7.41 - 7.34 (m, 3H), 7.20 - 7.08 (m, 5H), 2.32 (s, 3H), 2.26 (s, 3H).

N-(4-Chloro-2-(phenylethynyl)phenyl)-4-methylbenzenesulfonamide (3-61n)



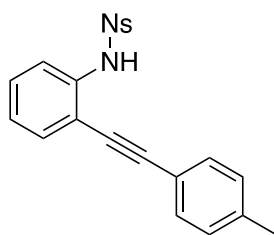
Prepared according to the general procedure GP1 on 1.0 mmol scale as a gray solid (324 mg, 85% yield). The spectroscopic data match those previously reported in the literature.⁵⁰ ¹H NMR (400 MHz, CDCl₃) δ 7.66 (s, 2H), 7.58 (s, 2H), 7.40 (t, *J* = 20.9 Hz, 6H), 7.17 (s, 3H), 2.34 (s, 3H).

*N-(2-(*p*-Tolylethynyl)phenyl)methanesulfonamide (3-61o)*



Prepared according to the general procedure GP1 on 1.0 mmol scale as a yellow solid (257 mg, 90% yield). The spectroscopic data match those previously reported in the literature.⁵⁰ ¹H NMR (400 MHz, CDCl₃) δ 7.62 (d, *J* = 8.2 Hz, 1H), 7.54 (d, *J* = 7.3 Hz, 1H), 7.43 (d, *J* = 7.9 Hz, 2H), 7.37 (t, *J* = 7.5 Hz, 1H), 7.18 (dd, *J* = 15.0, 7.7 Hz, 3H), 7.04 (s, 1H), 3.04 (s, 3H), 2.39 (s, 3H).

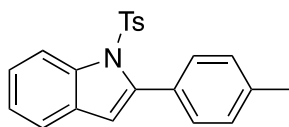
4-Nitro-N-(2-(p-tolylethynyl)phenyl)benzenesulfonamide (3-61p)



Prepared according to the general procedure GP1 on 1.0 mmol scale as a yellow solid (267 mg, 68% yield). ^1H NMR (400 MHz, CDCl_3) δ 8.16 (d, $J = 8.9$ Hz, 2H), 7.89 (d, $J = 8.8$ Hz, 2H), 7.66 (dd, $J = 8.2, 1.1$ Hz, 1H), 7.41 - 7.34 (m, 2H), 7.29 (d, $J = 8.2$ Hz, 2H), 7.23 - 7.13 (m, 4H), 2.41 (s, 3H). ^{13}C NMR (101 MHz, CDCl_3) δ 150.26, 144.58, 139.81, 136.08, 132.16, 131.34, 129.66, 129.47, 128.49, 125.98, 124.08, 122.14, 118.44, 116.24, 96.69, 82.78, 21.59. HRMS (APCI) calc. for $\text{C}_{21}\text{H}_{17}\text{N}_2\text{O}_4\text{S}^+$ $[\text{M}+\text{H}]^+$: 372.1448, found 372.1449.

B. Products of 3-sulfonylindoles

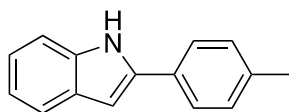
2-(p-Tolyl)-1-tosyl-1H-indole (3-63a)



The spectroscopic data match those previously reported in the literature.⁵¹

^1H NMR (400 MHz, CDCl_3): δ 8.30 (d, $J = 8.4$ Hz, 1 H), 7.43 (d, $J = 7.7$ Hz, 1 H), 7.40 (d, $J = 8.0$ Hz, 2 H), 7.36-7.32 (m, 1 H), 7.30-7.26 (m, 4 H), 7.26-7.22 (m, 3 H), 7.04 (d, $J = 8.2$ Hz, 2 H), 6.51 (s, 1 H), 2.44 (s, 3 H), 2.28 (s, 3 H).

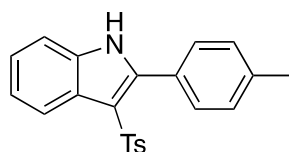
2-(p-Tolyl)-1H-indole (3-64a)



The spectroscopic data match those previously reported in the literature.⁵²

^1H NMR (400 MHz, CDCl_3): δ 8.26 (brs, 1H), 7.61 (d, $J = 7.90$ Hz, 1H), 7.56 - 7.51 (m, 2H), 7.36 (d, $J = 8.07$ Hz, 1H), 7.26 - 7.21 (m, 2H), 7.17 (t, $J = 7.57$ Hz, 1H), 7.14 - 7.08 (m, 1H), 6.77 (d, $J = 1.47$ Hz, 1H), 2.38 (s, 3H)

2-(p-Tolyl)-3-tosyl-1H-indole (3-62a)

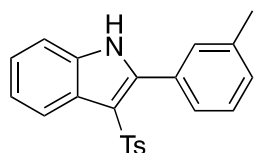


Following general procedure GP2 with 4-methyl-*N*-(2-(*p*-tolylethynyl)phenyl)benzenesulfonamide **3-1a** (72mg, 0.2 mmol). The crude product was purified by flash column chromatography (EtOAc/Petroleum ether, 1:5) to afford **3-62a** as a yellow solid (47mg, 65%).

The spectroscopic data match those previously reported in the literature.⁵¹

¹H NMR (300 MHz, CDCl₃): δ 8.63 (s, 1H), 8.27 - 8.19 (m, 1H), 7.59 (d, *J* = 8.0 Hz, 2H), 7.47 (d, *J* = 7.7 Hz, 2H), 7.39 - 7.32 (m, 1H), 7.30 - 7.22 (m, 6H), 7.10 (d, *J* = 8.0 Hz, 2H), 2.42 (s, 3H), 2.31 (s, 3H). ¹³C NMR (75 MHz, CDCl₃) δ 142.85, 142.62, 141.32, 139.95, 134.42, 130.05, 129.25, 128.88, 127.28, 127.23, 126.38, 125.94, 123.79, 122.48, 120.82, 111.10, 21.46, 21.42. HRMS calc. for [C₂₂H₂₀NO₂S]⁺ 362.1209, found 362.1207.

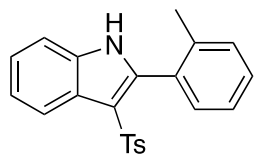
2-(*m*-Tolyl)-3-tosyl-1H-indole (**3-62b**)



Following general procedure GP2 with 4-methyl-*N*-(2-(*m*-tolylethynyl)phenyl)benzenesulfonamide **3-61b** (72mg, 0.2 mmol). The crude product was purified by flash column chromatography (EtOAc/Petroleum ether, 1:5) to afford **3-62b** as a yellow solid (45mg, 62%).

Mp 225 °C. ¹H NMR (300 MHz, CDCl₃) δ 8.63 (s, 1H), 8.29 - 8.22 (m, 1H), 7.59 (d, *J* = 8.3 Hz, 2H), 7.34 (d, *J* = 2.3 Hz, 3H), 7.29 (dd, *J* = 6.5, 2.9 Hz, 4H), 7.11 (d, *J* = 8.1 Hz, 2H), 2.38 (s, 3H), 2.31 (s, 3H); ¹³C NMR (75 MHz, CDCl₃) δ 142.92, 142.60, 141.24, 137.80, 134.44, 130.73, 130.53, 130.07, 129.21, 128.02, 127.21, 126.44, 125.93, 123.80, 122.52, 120.88, 113.26, 111.17, 21.42, 21.34. HRMS calc. for [C₂₂H₂₀NO₂S]⁺ 362.1209, found 362.1208.

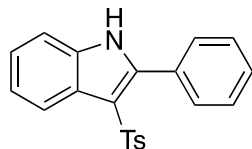
2-(*o*-Tolyl)-3-tosyl-1H-indole (**3-62c**)



Following general procedure GP2 with 4-methyl-*N*-(2-(*o*-tolylethynyl)phenyl)benzenesulfonamide **3-61c** (72mg, 0.2 mmol). The crude product was purified by flash column chromatography (EtOAc/Petroleum ether, 1:5) to afford **3-62c** as a yellow solid (40mg, 55%). Mp 220 °C. ¹H NMR (400 MHz, CDCl₃) δ 8.55 (s, 1H), 8.27 (dd, *J* = 6.5, 2.0 Hz, 1H), 7.52 (d, *J* = 8.3 Hz, 2H), 7.42 - 7.35 (m, 2H), 7.31 (ddd, *J* = 7.1, 4.9, 1.8 Hz, 2H), 7.23 (dd, *J* = 7.4, 1.2 Hz, 3H), 7.10 (d, *J* = 7.5 Hz, 2H), 2.33 (s, 3H), 1.99 (s, 3H); ¹³C

NMR (101 MHz, CDCl₃) δ 142.97, 141.79, 140.88, 138.16, 134.41, 130.88, 129.91, 129.88, 129.73, 129.18, 126.64, 125.20, 125.09, 123.72, 122.47, 120.65, 114.48, 111.20, 21.44, 19.84; HRMS calc. for [C₂₂H₂₀NO₂S]⁺ 362.1209, found 362.1206.

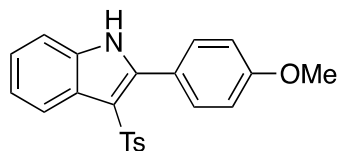
2-Phenyl-3-tosyl-1H-indole (3-62d)



Following general procedure GP2 with 4-methyl-*N*-(2-(phenylethynyl)phenyl)benzenesulfonamide **3-61d** (70mg, 0.2 mmol). The crude product was purified by flash column chromatography (EtOAc/Petroleum ether, 1:5) to afford **3-62d** as a white solid (45mg, 65%).

Mp 208 °C. ¹H NMR (300 MHz, CDCl₃) δ 8.75 (s, 1H), 8.27 - 8.21 (m, 1H), 7.58 - 7.53 (m, 4H), 7.47 - 7.35 (m, 4H), 7.31 - 7.26 (m, 2H), 7.08 (d, J = 7.9 Hz, 2H), 2.30 (s, 3H); ¹³C NMR (75 MHz, CDCl₃) δ 142.96, 142.40, 141.12, 134.53, 130.19, 130.15, 129.75, 129.25, 128.08, 126.35, 125.86, 123.87, 122.55, 120.84, 113.29, 111.27, 21.41; HRMS calc. for [C₂₁H₁₈NO₂S]⁺ 348.1053, found 348.1049.

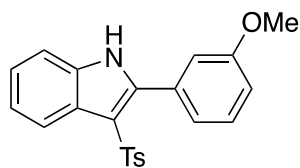
2-(4-Methoxyphenyl)-3-tosyl-1H-indole (3-62e)



Following general procedure GP2 with *N*-(2-((4-methoxyphenyl)ethynyl)phenyl)-4-methylbenzenesulfonamide **3-61e** (75mg, 0.2 mmol). The crude product was purified by flash column chromatography (EtOAc/Petroleum ether, 1:4) to afford **3-62e** as a yellow solid (48mg, 64%). Mp 211 °C.

¹H NMR (300 MHz, CDCl₃) δ 8.83 (s, 1H), 8.23 - 8.17 (m, 1H), 7.55 (d, J = 8.3 Hz, 2H), 7.51 - 7.46 (m, 2H), 7.37 - 7.31 (m, 1H), 7.29 - 7.26 (m, 1H), 7.26 - 7.23 (m, 1H), 7.08 (d, J = 8.1 Hz, 2H), 6.88 (d, J = 8.7 Hz, 2H), 3.82 (s, 3H), 2.30 (s, 3H); ¹³C NMR (75 MHz, CDCl₃) δ 160.72, 142.88, 142.61, 141.23, 134.48, 131.55, 129.24, 126.23, 125.99, 123.62, 122.39, 122.27, 120.65, 113.55, 112.43, 111.25, 55.31, 21.40. HRMS calc. for [C₂₂H₂₀NO₃S]⁺ 378.1158, found 378.1154.

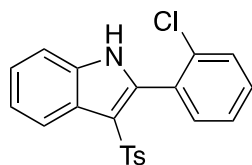
2-(3-Methoxyphenyl)-3-tosyl-1H-indole (**3-62f**)



Following general procedure GP2 with *N*-(2-((3-methoxyphenyl)ethynyl)phenyl)-4-methylbenzenesulfonamide **3-61f** (75mg, 0.2 mmol). The crude product was purified by flash column chromatography (EtOAc/Petroleum ether, 1:4) to afford **3-62f** as a yellow solid (47mg, 63%).

Mp 208 °C. ¹H NMR (300 MHz, CDCl₃) δ 8.74 (s, 1H), 8.28 - 8.21 (m, 1H), 7.58 (d, J = 8.3 Hz, 2H), 7.39 - 7.34 (m, 1H), 7.33 - 7.27 (m, 3H), 7.17 - 7.14 (m, 1H), 7.12 - 7.07 (m, 3H), 7.00 (ddd, J = 8.3, 2.5, 0.9 Hz, 1H), 3.81 (s, 3H), 2.30 (s, 3H); ¹³C NMR (75 MHz, CDCl₃) δ 159.09, 142.97, 142.11, 141.13, 134.43, 131.32, 129.24, 129.18, 126.36, 125.90, 123.90, 122.57, 122.23, 120.90, 115.94, 115.71, 113.30, 111.24, 55.39, 21.41; HRMS calc. for [C₂₂H₂₀NO₃S]⁺ 378.1158, found 378.1161.

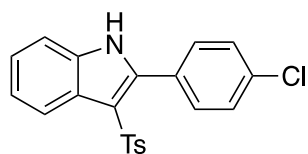
2-(2-Chlorophenyl)-3-tosyl-1H-indole (**3-62g**)



Following general procedure GP2 with *N*-(2-((2-chlorophenyl)ethynyl)phenyl)-4-methylbenzenesulfonamide **3-61g** (76mg, 0.2 mmol). The crude product was purified by flash column chromatography (EtOAc/Petroleum ether, 1:4) to afford **3-62g** as a yellow solid (37mg, 48%).

Mp 201 °C. ¹H NMR (400 MHz, CDCl₃) δ 8.71 (s, 1H), 8.20 (dd, J = 6.1, 3.2 Hz, 1H), 7.60 (d, J = 8.3 Hz, 2H), 7.56 (d, J = 7.4 Hz, 1H), 7.43 (d, J = 3.5 Hz, 2H), 7.40 - 7.34 (m, 2H), 7.31 (dd, J = 6.2, 3.2 Hz, 2H), 7.12 (d, J = 8.1 Hz, 2H), 2.32 (s, 3H); ¹³C NMR (101 MHz, CDCl₃) δ 143.11, 140.50, 138.72, 134.61, 133.98, 133.83, 131.20, 129.27, 129.25, 129.13, 126.64, 126.14, 124.87, 124.09, 122.51, 120.63, 114.83, 111.44, 21.45; HRMS calc. for [C₂₁H₁₇ClNO₂S]⁺ 382.0663, found 382.0663.

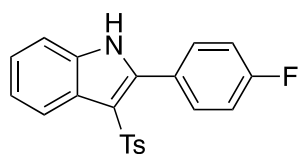
2-(4-Chlorophenyl)-3-tosyl-1H-indole (**3-62h**)



Following general procedure GP2 with *N*-(2-((4-chlorophenyl)ethynyl)phenyl)-4-methylbenzenesulfonamide **3-61h** (76mg, 0.2 mmol). The crude product was purified by flash column chromatography (EtOAc/Petroleum ether, 1:5) to afford **3-62h** as a yellow solid (43mg, 56%).

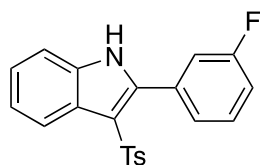
Mp 206 °C. ¹H NMR (400 MHz, DMSO-d₆) δ 12.51 (s, 1H), 8.00 (d, J = 6.7 Hz, 1H), 7.66 - 7.59 (m, 4H), 7.57 (d, J = 8.3 Hz, 2H), 7.47 (d, J = 6.9 Hz, 1H), 7.32 - 7.24 (m, 4H), 2.29 (s, 3H); ¹³C NMR (101 MHz, DMSO) δ 143.52, 141.82, 141.52, 135.52, 134.92, 132.57, 130.11, 129.47, 128.41, 126.16, 125.64, 123.96, 122.52, 120.12, 112.76, 111.80, 21.36; HRMS calc. for [C₂₁H₁₇ClNO₂S]⁺ 382.0663, found 382.0663.

2-(4-Fluorophenyl)-3-tosyl-1H-indole (3-62i)



Following general procedure GP2 with *N*-(2-((4-fluorophenyl)ethynyl)phenyl)-4-methylbenzenesulfonamide **3-61i** (73mg, 0.2 mmol). The crude product was purified by flash column chromatography (EtOAc/Petroleum ether, 1:5) to afford **3-62i** as a yellow solid (44mg, 60%). Mp 215 °C. ¹H NMR (400 MHz, CDCl₃) δ 8.55 (s, 1H), 8.28 - 8.22 (m, 1H), 7.62 - 7.54 (m, 4H), 7.41 - 7.36 (m, 1H), 7.34 - 7.29 (m, 2H), 7.16 (d, J = 8.6 Hz, 2H), 7.13 - 7.10 (m, 2H), 2.31 (s, 3H); ¹³C NMR (101 MHz, CDCl₃) δ 143.13, 141.12, 140.94, 134.40, 132.27, 132.18, 129.33, 126.33, 125.73, 124.09, 122.73, 120.92, 115.46, 115.25, 111.14, 21.44; ¹⁹F NMR (376 MHz, CDCl₃) δ -110.40; HRMS calc. for [C₂₁H₁₇FNO₂S]⁺ 366.0959, found 366.0954.

2-(3-Fluorophenyl)-3-tosyl-1H-indole (3-62j)

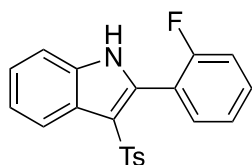


Following general procedure GP2 with *N*-(2-((3-fluorophenyl)ethynyl)phenyl)-4-methylbenzenesulfonamide **3-61j** (73mg, 0.2 mmol). The crude product was purified by flash column chromatography (EtOAc/Petroleum ether, 1:5) to afford **3-62j** as a yellow solid (42mg, 58%).

Mp 209 °C. ¹H NMR (300 MHz, CDCl₃) δ 8.55 (s, 1H), 8.28 - 8.22 (m, 1H), 7.57 (d, J = 8.4 Hz, 4H), 7.40 - 7.35 (m, 1H), 7.33 - 7.29 (m, 2H), 7.16 - 7.09 (m, 4H), 2.31 (s, 3H); ¹³C NMR (101 MHz, CDCl₃) δ 143.14, 141.12, 140.95, 134.40, 132.28, 132.19, 129.33, 126.34, 125.73,

124.11, 122.74, 120.93, 115.47, 115.25, 111.14, 21.45; ^{19}F NMR (376 MHz, CDCl_3) δ -110.37; HRMS calc. for $[\text{C}_{21}\text{H}_{17}\text{FNO}_2\text{S}]^+$ 366.0959, found 366.0956.

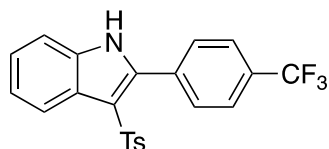
2-(2-Fluorophenyl)-3-tosyl-1H-indole (3-62k)



Following general procedure GP2 with *N*-(2-((2-fluorophenyl)ethynyl)phenyl)-4-methylbenzenesulfonamide **3-61k** (73mg, 0.2 mmol). The crude product was purified by flash column chromatography (EtOAc/Petroleum ether, 1:5) to afford **3-62k** as a yellow solid (39mg, 53%).

Mp 212 °C. ^1H NMR (400 MHz, CDCl_3) δ 8.67 (s, 1H), 8.21 – 8.16 (m, 1H), 7.65 (d, J = 8.2 Hz, 2H), 7.52 – 7.46 (m, 1H), 7.40 – 7.36 (m, 1H), 7.32 – 7.29 (m, 2H), 7.28 (d, J = 1.1 Hz, 1H), 7.26 – 7.22 (m, 1H), 7.18 – 7.11 (m, 3H), 2.33 (s, 3H); ^{13}C NMR (101 MHz, CDCl_3) δ 161.34, 158.86, 143.16, 140.71, 135.69, 134.78, 133.46, 133.44, 132.00, 131.92, 129.34, 126.53, 125.26, 124.19, 123.83, 123.79, 122.58, 120.70, 115.68, 115.46, 111.33, 21.49; ^{19}F NMR (376 MHz, CDCl_3) δ -113.08; HRMS calc. for $[\text{C}_{21}\text{H}_{17}\text{FNO}_2\text{S}]^+$ 366.0959, found 366.0955.

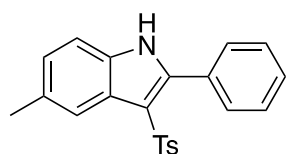
3-Tosyl-2-(4-(trifluoromethyl)phenyl)-1H-indole (3-62l)



Following general procedure GP2 with 4-methyl-*N*-(2-((4-(trifluoromethyl)phenyl)ethynyl)phenyl)benzenesulfonamide **3-61l** (83mg, 0.2 mmol). The crude product was purified by flash column chromatography (EtOAc/Petroleum ether, 1:5) to afford **3-62l** as a yellow solid (49mg, 59%).

Mp 202 °C. ^1H NMR (300 MHz, $\text{DMSO}-d_6$) δ 12.62 (s, 1H), 8.01 (dd, J = 7.9, 1.5 Hz, 1H), 7.89 (s, 2H), 7.85 (s, 2H), 7.59 (d, J = 8.3 Hz, 2H), 7.53 - 7.47 (m, 1H), 7.34 - 7.24 (m, 4H), 2.29 (s, 3H); ^{13}C NMR (101 MHz, DMSO) δ 143.15, 140.87, 140.81, 135.20, 134.32, 131.24, 129.67, 125.79, 125.04, 124.74, 124.71, 124.67, 123.70, 122.18, 119.72, 112.41, 111.85, 20.88; ^{19}F NMR (282 MHz, DMSO) δ -61.17; HRMS calc. for $[\text{C}_{22}\text{H}_{17}\text{F}_3\text{NO}_2\text{S}]^+$ 416.0854, found 416.0854.

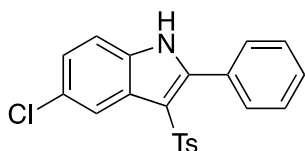
5-Methyl-2-phenyl-3-tosyl-1H-indole (3-62m)



Following general procedure GP2 with 4-methyl-*N*-(4-methyl-2-(phenylethynyl)phenyl)benzenesulfonamide **3-61m** (72mg, 0.2 mmol). The crude product was purified by flash column chromatography (EtOAc/Petroleum ether, 1:5) to afford **3-62m** as a yellow solid (44mg, 61%).

Mp 218 °C. ¹H NMR (300 MHz, CDCl₃) δ 8.76 (s, 1H), 8.03 (d, J = 1.6 Hz, 1H), 7.57 - 7.48 (m, 4H), 7.39 (dd, J = 12.8, 7.2 Hz, 3H), 7.23 (s, 1H), 7.08 (d, J = 8.2 Hz, 3H), 2.48 (s, 3H), 2.30 (s, 3H); ¹³C NMR (75 MHz, CDCl₃) δ 142.84, 142.41, 141.25, 132.87, 132.12, 130.27, 130.14, 129.59, 129.21, 127.99, 126.24, 126.12, 125.45, 120.27, 112.48, 110.98, 21.70, 21.40.

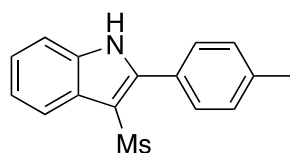
5-Chloro-2-phenyl-3-tosyl-1H-indole ((3-62n)



Following general procedure GP2 with *N*-(4-chloro-2-(phenylethynyl)phenyl)-4-methylbenzenesulfonamide **3-61n** (76mg, 0.2 mmol). The crude product was purified by flash column chromatography (EtOAc/Petroleum ether, 1:5) to afford **3-62n** as a yellow solid (45mg, 59%).

Mp 211 °C. ¹H NMR (400 MHz, CDCl₃) δ 8.71 (s, 1H), 8.27 (d, J = 1.9 Hz, 1H), 7.55 - 7.50 (m, 4H), 7.47 (d, J = 7.3 Hz, 1H), 7.43 (dd, J = 7.1, 1.3 Hz, 2H), 7.28 (d, J = 0.7 Hz, 1H), 7.25 (d, J = 2.0 Hz, 1H), 7.13 - 7.08 (m, 2H), 2.32 (s, 3H); ¹³C NMR (75 MHz, CDCl₃) δ 143.46, 143.26, 140.79, 132.82, 130.11, 130.05, 129.68, 129.36, 128.52, 128.21, 126.94, 126.37, 124.44, 120.44, 113.36, 21.44; HRMS calc. for [C₂₁H₁₇NO₂S]⁺ 382.0663, found 382.0662.

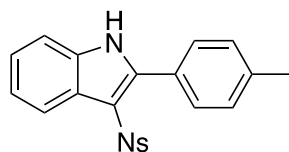
3-(Methylsulfonyl)-2-(p-tolyl)-1H-indole (3-62o)



Following general procedure GP2 with *N*-(2-(p-tolylolethynyl)phenyl)methanesulfonamide **3-61o** (57mg, 0.2 mmol). The crude product was purified by flash column chromatography (EtOAc/Petroleum ether, 1:5) to afford **3-62o** as a yellow solid (27mg, 48%).

Mp 198 °C. ^1H NMR (300 MHz, CDCl_3) δ 8.79 (s, 1H), 8.17 - 8.11 (m, 1H), 7.57 (d, $J = 8.0$ Hz, 2H), 7.46 - 7.40 (m, 1H), 7.32 (d, $J = 3.7$ Hz, 2H), 7.25 (d, $J = 6.2$ Hz, 3H), 2.98 (s, 3H), 2.40 (s, 3H); ^{13}C NMR (75 MHz, CDCl_3) δ 142.25, 140.25, 134.44, 129.91, 129.14, 126.88, 125.97, 123.95, 122.58, 120.52, 111.98, 111.30, 45.36, 21.40; HRMS calc. for $[\text{C}_{16}\text{H}_{16}\text{NO}_2\text{S}]^+$ 286.0896, found 286.0897.

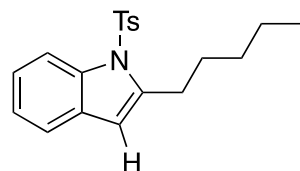
3-((4-Nitrophenyl)sulfonyl)-2-(p-tolyl)-1H-indole (3-62p)



Following general procedure GP2 with 4-nitro-*N*-(2-(p-tolylolethynyl)phenyl)benzenesulfonamide **3-61p** (78mg, 0.2 mmol). The crude product was purified by flash column chromatography (EtOAc/Petroleum ether, 1:5) to afford **3-62m** as a yellow solid (16mg, 20%).

Mp 225 °C. ^1H NMR (400 MHz, CDCl_3) δ 8.64 (s, 1H), 8.26 (dd, $J = 7.7, 1.8$ Hz, 1H), 8.12 (d, $J = 8.9$ Hz, 2H), 7.80 (d, $J = 8.9$ Hz, 2H), 7.47 (d, $J = 8.1$ Hz, 2H), 7.43 - 7.39 (m, 1H), 7.37 - 7.33 (m, 2H), 7.30 (d, $J = 7.9$ Hz, 2H), 2.47 (s, 3H); ^{13}C NMR (101 MHz, CDCl_3) δ 149.73, 149.42, 143.90, 140.73, 134.48, 130.05, 129.14, 127.49, 126.56, 125.78, 124.40, 123.94, 123.18, 120.60, 111.49, 111.41, 21.50; HRMS calc. for $[\text{C}_{21}\text{H}_{17}\text{N}_2\text{O}_4\text{S}]^+$ 393.0904, found 393.0899.

2-Pentyl-1-tosyl-1H-indole (3-63q)



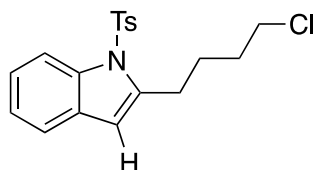
Following general procedure GP2 with *N*-(2-(hept-1-yn-1-yl)phenyl)-4-methylbenzenesulfonamide **3-61q** (68 mg, 0.2 mmol). The crude product was purified by flash column chromatography (EtOAc/Petroleum ether, 1:5) to afford **3-63q** as a yellow oil (60 mg, 88%).

The spectroscopic data match those previously reported in the literature.⁵³

^1H NMR (400 MHz, CDCl_3) δ 8.18 (dd, $J = 8.3, 1.0$ Hz, 1H), 7.68 - 7.58 (m, 2H), 7.47 - 7.37 (m, 1H), 7.29 - 7.24 (m, 1H), 7.23 (d, $J = 1.3$ Hz, 1H), 7.20 - 7.16 (m, 2H), 6.40 (q, $J = 1.1$ Hz, 1H), 2.99 (t, $J = 7.6$ Hz, 2H), 2.34 (s, 3H), 1.84 - 1.70 (m, 2H), 1.45 - 1.33 (m, 4H), 0.97 - 0.90

(m, 3H); ^{13}C NMR (101 MHz, CDCl_3) δ 144.7, 142.7, 137.4, 136.5, 130.0, 129.9, 126.4, 123.9, 123.6, 120.2, 115.0, 108.7, 31.7, 29.1, 28.7, 22.7, 21.7, 14.2.

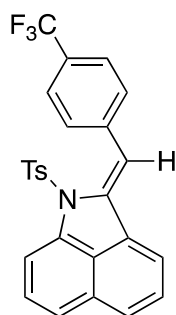
*2-(4-Chlorobutyl)-1-tosyl-1H-indole (3-63r)*⁵³



Following general procedure GP2 with *N*-(2-(6-chlorohex-1-yn-1-yl)phenyl)-4-methylbenzenesulfonamide **3-61r** (72 mg, 0.2 mmol). The crude product was purified by flash column chromatography (EtOAc/Petroleum ether, 1:5) to afford **3-63r** as a yellow oil (63 mg, 88%).

^1H NMR (400 MHz, CDCl_3) δ 8.16 (dd, $J = 8.3, 1.0$ Hz, 1H), 7.60 (d, $J = 8.4$ Hz, 2H), 7.43 - 7.39 (m, 1H), 7.25 - 7.13 (m, 4H), 6.41 (d, $J = 0.9$ Hz, 1H), 3.61 - 3.55 (m, 2H), 3.05 - 2.99 (m, 2H), 2.33 (s, 3H), 1.93 - 1.87 (m, 4H).

(Z)-1-Tosyl-2-(4-(trifluoromethyl)benzylidene)-1,2-dihydrobenzo[cd]indole (3-5)



Following general procedure GP2 with 4-methyl-*N*-(8-((4-(trifluoromethyl)phenyl)ethynyl)naphthalen-1-yl)benzenesulfonamide **3-61u** (93 mg, 0.2 mmol). The crude product was purified by flash column chromatography (EtOAc/Petroleum ether, 1:5) to afford **3-65** as a white solid (79 mg, 85%).

Mp: 177-179 °C.

^1H NMR (400 MHz, CDCl_3) δ 8.02 - 7.97 (m, 2H), 7.73 (dd, $J = 6.1, 1.8$ Hz, 1H), 7.65 (d, $J = 8.2$ Hz, 2H), 7.57 (dd, $J = 7.2, 1.4$ Hz, 1H), 7.52 - 7.49 (m, 2H), 7.48 - 7.43 (m, 2H), 7.32 - 7.27 (m, 2H), 6.98 (s, 1H), 6.86 - 6.81 (m, 2H), 2.12 (s, 3H). ^{13}C NMR (100 MHz, CDCl_3) δ 144.3, 142.1, 138.2, 137.7, 135.8, 133.3, 132.9, 131.1, 130.4, 130.2, 129.2, 129.1, 129.0, 128.8, 128.6, 128.0, 124.2, 121.9, 119.5, 115.2, 113.8, 21.9. HRMS calc. for $[\text{C}_{26}\text{H}_{19}\text{F}_3\text{NO}_2\text{S}]^+$ 465.1010, found 465.1011.

3.3 X-ray Crystal Structure Determination of Compound

A single crystal of each compound was selected, mounted onto a cryoloop and transferred into a cold nitrogen gas stream. Intensity data were collected with a Bruker Kappa APEX-II CCD diffractometer using a graphite-monochromated Mo-K α radiation ($\lambda = 0.71073 \text{ \AA}$). Data collections were performed at 200K with the Bruker APEXIII suite. Unit-cell parameters determinations, integrations and data reductions were carried out with SAINT program. SADABS was used for scaling and absorption corrections. The structures were solved with SHELXT⁵⁴ and refined by full-matrix least-squares methods with SHELXL⁵⁵ using Olex2 software package⁵⁶ or WinGX suite⁵⁷. All non-hydrogen atoms were refined anisotropically. These structures were deposited at the Cambridge Crystallographic Data Centre with numbers CCDC 2090314 to 2090317 and 2090321 to 2090323, and can be obtained free of charge *via* www.ccdc.cam.ac.uk.

Table S1 Crystal data for compound 3-62a at 200 K

Bond precision:	C-C = 0.0020 Å	Wavelength=0.71073
Cell:	a=10.5074(7) b=10.9465(7) c=15.4718(9)	
	alpha=90 beta=97.265(4) gamma=90	
Temperature:	200 K	
	Calculated	Reported
Volume	1765.27(19)	1765.27(19)
Space group	P 21/c	P 1 21/c 1
Hall group	-P 2ybc	-P 2ybc
Moiety formula	C22 H19 N O2 S	C22 H19 N O2 S
Sum formula	C22 H19 N O2 S	C22 H19 N O2 S
Mr	361.44	361.44
Dx,g cm-3	1.360	1.360
Z	4	4
Mu (mm-1)	0.200	0.200
F000	760.0	760.0
F000'	760.80	
h,k,lmax	15,15,22	15,15,22
Nref	5568	5498
Tmin,Tmax	0.940,0.970	0.697,0.746
Tmin'	0.878	
Correction method=	# Reported T Limits: Tmin=0.697 Tmax=0.746	
AbsCorr =	MULTI-SCAN	
Data completeness=	0.987	Theta(max)= 30.875
R(reflections)=	0.0415(4157)	wR2(reflections)= 0.1079(5498)
S =	1.017	Npar= 242

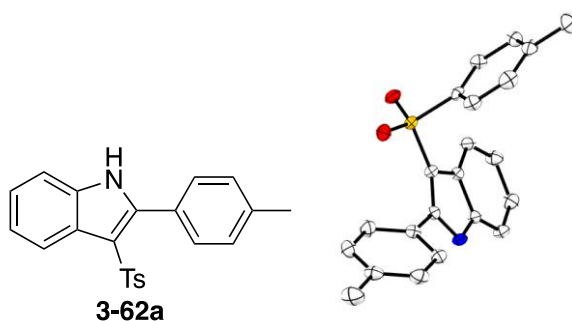


Figure S1 Crystal structure of compound **3-62a**

Table S2 Crystal data for compound 3-65 at 200 K

Bond precision:	C-C = 0.0063 Å	Wavelength=0.71073
Cell:	a=26.5846(16) b=14.1478(7) c=25.6166(16)	
	alpha=90 beta=107.864(2) gamma=90	
Temperature:	200 K	
	Calculated	Reported
Volume	9170.2(9)	9170.2(9)
Space group	P 2/c	P 2/c
Hall group	-P 2yc	-P 2yc
Moiety formula	C ₂₆ H ₁₈ F ₃ N O ₂ S	C ₂₆ H ₁₈ F ₃ N O ₂ S
Sum formula	C ₂₆ H ₁₈ F ₃ N O ₂ S	C ₂₆ H ₁₈ F ₃ N O ₂ S
Mr	465.47	465.47
D _x , g cm ⁻³	1.349	1.349
Z	16	16
Mu (mm ⁻¹)	0.189	0.189
F ₀₀₀	3840.0	3840.0
F ₀₀₀ '	3844.14	
h,k,lmax	29,15,28	29,15,28
N _{ref}	13189	13184
T _{min} ,T _{max}	0.972,0.981	0.954,1.000
T _{min} '	0.972	
Correction method= # Reported T Limits:	T _{min} =0.954 T _{max} =1.000	
AbsCorr = NUMERICAL		
Data completeness= 1.000	Theta(max)= 23.256	
R(reflections)= 0.0569(9016)	wR2(reflections)= 0.1507(13184)	
S = 1.031	Npar= 1229	

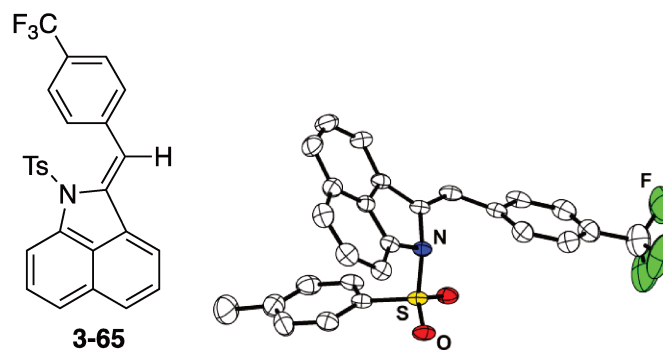


Figure S2 Crystal structure of compound **3-65**

Table S3 Crystal data for compound 3-67 at 200 K

Bond precision:	C-C = 0.0191 Å	Wavelength=1.54178
Cell:	a=12.9573(7) b=17.5613(8) c=21.5975(10)	
	alpha=90.093(2) beta=94.002(3) gamma=108.930(3)	
Temperature:	200 K	
	Calculated	Reported
Volume	4635.8(4)	4635.8(4)
Space group	P -1	P -1
Hall group	-P 1	-P 1
Moiety formula	C ₅₂ H ₅₇ Au N O ₂ P S, 0.3(C H ₂ Cl ₂)	C ₅₂ H ₅₇ Au N O ₂ P S, 0.3(C H ₂ Cl ₂), +[solvent]
Sum formula	C _{52.30} H _{57.60} Au Cl _{0.60} N O ₂ P S	C _{52.30} H _{57.60} Au Cl _{0.60} N O ₂ P S
Mr	1013.46	1013.46
D _x , g cm ⁻³	1.452	1.452
Z	4	4
Mu (mm ⁻¹)	7.335	7.336
F ₀₀₀	2058.4	2058.0
F ₀₀₀ '	2048.37	
h,k,l _{max}	15,20,25	15,20,25
N _{ref}	16463	16329
T _{min} , T _{max}	0.235, 0.598	0.162, 0.318
T _{min} '	0.089	
Correction method=	# Reported T Limits: T _{min} =0.162 T _{max} =0.318	
AbsCorr =	MULTI-SCAN	
Data completeness=	0.992	Theta(max)= 66.812
R(reflections)=	0.0827(12429)	wR2(reflections)= 0.2515(16329)
S =	1.034	N _{par} = 1157

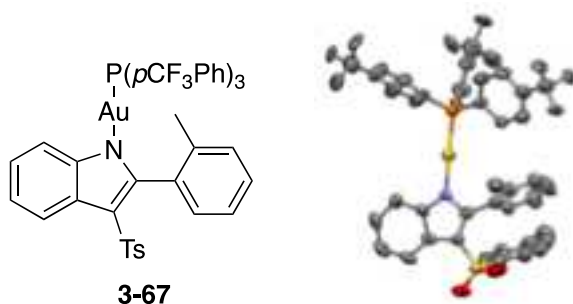


Figure S2 Crystal structure of compound **3-67**

5. Reference

- [1] Y. Fang, Z. Luo, X. Xu, *RSC Adv.* **2016**, *6*, 59661.
- [2] (a) I. Nakamura, U. Yamagishi, D. Song, S. Konta, Y. Yamamoto, *Angew. Chem. Int. Ed.* **2007**, *46*, 2284; (b) I. Nakamura, U. Yamagishi, D. Song, S. Konta, Y. Yamamoto, *Chem. Eur. J.* **2008**, *3*, 285.
- [3] Y. Horino, M. Kimura, M. Naito, S. Tanaka, Y. Tamaru, *Tetrahedron Lett.* **2000**, *41*, 3427.
- [4] W. T. Teo, W. Rao, M. J. Koh and P. W. H. Chan, *J. Org. Chem.* **2013**, *78*, 7508.
- [5] H. Yeom, E. So, S. Shin, *Chem. Eur. J.* **2011**, *17*, 1764.
- [6] J. Liu, P. Chakraborty, H. Zhang, L. Zhong, Z. X. Wang, X. Huang, *ACS Catal.* **2019**, *9*, 2610.
- [7] B. Prabagar, R. K. Mallick, R. Prasad, V. Gandon, A. K. Sahoo, *Angew. Chem., Int. Ed.* **2019**, *58*, 2365.
- [8] Y. T. Lee, Y. K. Chung, *J. Org. Chem.* **2008**, *73*, 4698.
- [9] Y. Hu, R. Yi, F. Wu and B. Wan, *J. Org. Chem.* **2013**, *78*, 7714.
- [10] Y. Zhao, H. Wang, X. Li, D. Wang, X. Xin and B. Wan, *Org. Biomol. Chem.* **2016**, *14*, 526.
- [11] (a) X. Xin, D. Wang, X. Li, B. Wan, *Angew. Chem. Int. Ed.* **2012**, *51*, 1693; (b) X. Xin, D. Wang, F. Wu, X. Li, B. Wan, *J. Org. Chem.* **2013**, *78*, 4065; (c) X. Xin, D. Wang, F. Wu, C. Wang, H. Wang, X. Li, B. Wan, *Org. Lett.* **2013**, *15*, 4512; (d) X. Xin, D. Wang, X. Li, B. Wan, *Tetrahedron*, **2013**, *69*, 10245; (e) X. Xin, H. Wang, X. Li, D. Wang, B. Wan, *Org. Lett.* **2015**, *17*, 3944.
- [12] B. Xiong, L. Chen, J. Xu, H. Sun, X. Li, Y. Li, Z. Lian, *Org. Lett.* **2020**, *22*, 9263.
- [13] M. Padmanaban, L. C. R. Carvalho, D. Petkova, J. W. Lee, A. S. Santos, M. M. B. Marques, N. Maulide, *Tetrahedron*, **2015**, *71*, 5994.
- [14] J. Wang, K.-I. Son and J. Xu, *Monatsh. Chem.* **2016**, *147*, 1637.
- [15] S. Mao, Y. Gao, X. Q. Zhu, D. D. Guo, Y. Q. Wang, *Org. Lett.* **2015**, *17*, 1692.
- [16] F. Wang, P. Xu, S. Y. Wang, S. J. Ji, *Org. Lett.* **2018**, *20*, 2204.
- [17] B. Wang, S. Jin, S. Sun, J. Cheng, *Org. Chem. Front.* **2018**, *5*, 958.
- [18] (a) M. Ishikura, T. Abe, T. Choshi, S. Hibino, *Nat. Prod. Rep.* **2013**, *30*, 694; (b) E. Stempel, T. Gaich, *Acc. Chem. Res.* **2016**, *49*, 2390; (c) A. Brancale, R. Silvestri, *Med. Res. Rev.* **2007**, *27*, 209; (d) A. J. Kochanowska-Karamyan, M. T. Hamann, *Chem. Rev.* **2010**, *110*, 4489; (e) S. Biswal, U. Sahoo, S. Sethy, H. K. S. Kumar, M. Banerjee, *Asian J. Pharm. Clin. Res.* **2012**, *5*, 1; (f) M. Z. Zhang, Q. Chen, G. F. Yang, *Eur. J. Med. Chem.* **2015**, *89*, 421.

- [19] (a) T. M. Williams, T. M. Ciccarone, S. C. MacTough, C. S. Rooney, S. K. Balani, J. H. Condra, E. A. Emini, M. E. Goldman, W. J. Greenlee, L. R. Kauffman, J. A. O'Brien, V. V. Sardana, W. A. Schleif, A. D. Theoharides, P. S. Anderson, *J. Med. Chem.* **1993**, *36*, 1291; (b) R. Silvestri, G. D. Martino, G. L. Regina, M. Artico, S. Massa, L. Vargiu, M. Mura, A. G. Loi, T. Marceddu, P. L. Colla, *J. Med. Chem.* **2003**, *46*, 2482; (c) D. Gao and T. G. Back, *Synlett*, **2013**, 389.
- [20] G. D. Heffernan, R. D. Coghlan, E. S. Manas, R. E. McDevitt, Y. Li, P. E. Mahaney, A. J. Robichaud, C. Huselton, P. Alfinito, J. A. Bray, S. A. Cosmi, G. H. Johnston, T. Kenney, E. Koury, R. C. Winneker, D. C. Deecher, E. J. Trybulski, *Bioorg. Med. Chem.* **2009**, *17*, 7802.
- [21] (a) R. Bernotas, S. Lenicek, S. Antane, G. M. Zhang, D. Smith, J. Coupet, B. Harrison, L. E. Schechter, *Bioorg. Med. Chem. Lett.* **2004**, *14*, 5499; (b) R. C. Bernotas, S. Antane, R. Shenoy, V.-D. Le, P. Chen, B. L. Harrison, A. J. Robichaud, G. M. Zhang, D. Smith, L. E. Schechter, *Bioorg. Med. Chem. Lett.* **2010**, *20*, 1657.
- [22] J. M. Bentley, T. Davenport and M. Slack, *PCT Int. Appl. WO* 2011138265A2, 2011.
- [23] (a) Y. Chen, C. Cho, F. Shi, R. C. Larock, *J. Org. Chem.* **2009**, *74*, 6802; (b) E. Vedejs, J. D. Little, *J. Org. Chem.* **2004**, *69*, 1794.
- [24] (a) J. B. Azeredo, M. Godoi, G. M. Martins, C. C. Silveira, A. L. Braga, *J. Org. Chem.* **2014**, *79*, 4125; (b) Ch. D. Prasad, S. Kumar, M. Sattar, A. Adhikary, S. Kumar, *Org. Biomol. Chem.* **2013**, *11*, 8036; (c) S. Vásquez-Céspedes, A. Ferry, L. Candish, F. Glorius, *Angew. Chem. Int. Ed.* **2015**, *54*, 5772;
- [25] (a) H. Zhang, X. Bao, Y. Song, J. Qu, B. Wang, *Tetrahedron*, **2015**, *71*, 8885; (b) S. Yi, M. Li, W. Mo, X. Hu, B. Hu, N. Sun, L. Jin, Z. Shen, *Tetrahedron Lett.* **2016**, *57*, 1912; (c) X. Liu, H. Cui, D. Yang, S. Dai, G. Zhang, W. Wei, H. Wang, *Catal. Lett.* **2016**, *146*, 1743.
- [26] (a) C.-R. Liu and L.-H. Ding, *Org. Biomol. Chem.* **2015**, *13*, 2251; (b) R. Rahaman, N. Devi, J. R. Bhagawati, P. Barman, *RSC Adv.* **2016**, *6*, 18929.
- [27] (a) F. Xiao, H. Xie, S. Liu and G.-J. Deng, *Adv. Synth. Catal.* **2014**, *356*, 364; (b) H. Rao, P. Wang, J. Wang, Z. Li, X. Sun, S. Cao, *RSC Adv.* **2014**, *4*, 49165.
- [28] (a) Z. Wu, Y. C. Li, W. Z. Ding, T. Zhu, S.-Z. Liu, X. Ren, L. H. Zou, *Asian J. Org. Chem.* **2016**, *5*, 625; (b) K. Lu, Z. Deng, M. Li, T. Li, X. Zhao, *Org. Biomol. Chem.* **2017**, *15*, 1254.
- [29] (a) H. M. Gilow, C. S. Brown, J. N. Copel, K. E. Kelly, *J. Heterocycl. Chem.* **1991**, *28*, 1025; (b) P. Hamel, *J. Org. Chem.* **2002**, *67*, 2854.
- [30] (a) E. Marcantoni, R. Cipolletti, L. Marsili, S. Menichetti, R. Properzi, C. Viglianisi, *Eur. J. Org. Chem.* **2013**, 132; (b) C. Viglianisi, E. Marcantoni, V. Carapacchi, S. Menichetti, L. Marsili, *Eur. J. Org. Chem.* **2014**, 6405; (c) P. P. Kumar, Y. D. Reddy, Ch. V. R. Reddy, B. R.

- Devi, P. K. Dubey, *J. Sulfur Chem.* **2014**, *35*, 356; (d) T. Hostier, V. Ferey, G. Ricci, D. G. Pardo, J. Cossy, *Chem. Commun.* **2015**, *51*, 13898.
- [31] M. Matsugi, K. Murata, K. Gotanda, H. Nambu, G. Anilkumar, K. Matsumoto and Y. Kita, *J. Org. Chem.* **2001**, *66*, 2434.
- [32] P. Anbarasan, H. Neumann and B. Beller, *Chem. Commun.* **2011**, *47*, 3233.
- [33] (a) F. L. Yang, S. K. Tian, *Angew. Chem. Int. Ed.* **2013**, *52*, 4929; (b) Y. Yang, S. Zhang, L. Tang, Y. Hu, Z. Zha, Z. Wang, *Green Chem.* **2016**, *18*, 2609; (c) R. Rahaman, N. Devi, K. Sarma, P. Barman, *RSC Adv.* **2016**, *6*, 10873.
- [34] J. A. Fernández-Salas, A. P. Pulis, D. J. Procter, *Chem. Commun.* **2016**, *52*, 12364.
- [35] H. Qi, T. Zhang, K. Wan, M. Luo, *J. Org. Chem.* **2016**, *81*, 4262.
- [36] J. Li, C. Li, S. Yang, Y. An, W. Wu, H. Jiang, *J. Org. Chem.* **2016**, *81*, 7771.
- [37] G. Tocco, M. Begala, F. Esposito, P. Caboni, V. Cannas, E. Tramontano, *Tetrahedron Lett.* **2013**, *54*, 6237.
- [38] M. Rahman, M. Ghosh, A. Hajra, A. Majee, *J. Sulfur Chem.* **2013**, *34*, 342.
- [39] J. K. Qiu, W. Hao, D. C. Wang, P. Wei, J. Sun, B. Jiang, S. J. Tu, *Chem. Commun.* **2014**, *50*, 14782.
- [40] I. Nakamura, U. Yamagishi, D. Song, S. Konta, Y. Yamamoto, *Angew. Chem. Int. Ed.* **2007**, *46*, 2284.
- [41] B. J. Stokes, S. Liu, T. G. Driver, *J. Am. Chem. Soc.* **2011**, *133*, 4702.
- [42] D. Gao and T. G. Back, *Chem. Eur. J.* **2012**, *18*, 14828.
- [43] J. Meesin, M. Pohmakotr, V. Reutrakul, D. Soorukram, P. Leowanawat, C. Kuhakarn, *Org. Biomol. Chem.* **2017**, *15*, 3662
- [44] F. Chen, Q. Meng, S. Han, B. Han, *Org. Lett.* **2016**, *18*, 3330.
- [45] R. S. Rohokale, S. D. Tambe, U. A. Kshirsagar, *Org. Biomol. Chem.* **2018**, *16*, 536.
- [46] A. S. K. Hashmi, T. D. Ramamurthi, F. Rominger, *Adv. Synth. Catal.* **2010**, *352*, 971.
- [47] V. Fernández-Moreira, C. Val-Campillo, I. Ospino, R. P. Herrera, I. Marzo, A. Laguna, M. C. Gimeno, *Dalton Trans.* **2019**, *48*, 3098.
- [48] M. A. Ischay, Z. Lu, T. P. Yoon, *J. Am. Chem. Soc.* **2010**, *132*, 8572.
- [49] A. Singh, K. Teegardin, M. Kelly, K. S. Prasad, S. Krishnan, J. D. Weaver, *J. Organomet. Chem.* **2015**, *776*, 51.
- [50] (a) J. Lv, B. Zhao, L. Liu, Y. Han, Y. Yuan, Z. Shi, *Adv. Synth. Catal.* **2018**, *360*, 4054; (b) Y. Li, J. Li, S. N. Yu, J. Wang, Y. M. Yu, J. Deng, *Tetrahedron* **2015**, *71*, 8271; (c) Y. Ye, K. P. S. Cheung, L. He, G. C. Tsui, *Org. Chem. Front.* **2018**, *5*, 1511.
- [51] J. McNulty, K. Keskar, *Eur. J. Org. Chem.* **2014**, 1622.

- [52] I. T. Alt, B. Plietker, *Angew. Chem. Int. Ed.* **2016**, *55*, 1519.
- [53] A. Bruneau, K. P. J. Gustafson, N. Yuan, C. W. Tai, I. Persson, X. Zou, J. E. Bäckvall, *Chem. Eur. J.* **2017**, *23*, 12886.
- [54] L. Palatinus, G. Chapuis, *Journal of Applied Crystallography* **2007**, *40*, 786.
- [55] G. M. Sheldrick, *Acta Crystallographica Section C* **2015**, *71*, 3.
- [56] O.V. Dolomanov, L.J. Bourhis, R.J. Gildea, J.A.K. Howard, H. Puschmann, *Journal of Applied Crystallography* **2009**, *42*, 339.
- [57] L. J. Farrugia, *Journal of Applied Crystallography* **1999**, *32*, 837.

Chapter 4 Bisphosphine Allene based Ligands: from Coordination to Catalysis

1. Background

1.1 Organophosphorus Compounds

Organophosphorus (OP) compounds are organic compounds containing carbon-phosphorus (C-P) bonds or phosphoric acid derivatives carrying organic groups.¹ Organophosphorus compounds are characterized by an unusually large variety of structures and a wide range of uses. The reason is that phosphorus is able to form stable compounds with a coordination number of 1 to 6, and an oxidation state of - III to + V. Moreover, phosphines are an important class of organophosphorus compounds. They are derived from phosphine [7803-51-2], PH_3 . Successive formal substitution of 1, 2, or 3 hydrogen atoms of PH_3 by alkyl or aryl groups gives primary, secondary, and tertiary phosphines. Common examples for organophosphorus include phosphines, phosphinites, phosphonites, phosphites, phosphinous amides, phosphinous diamides, phosphinous triamides, phosphonium salts, phosphine oxides, phosphinates, phosphonates, phosphates, phosphinothioates, phosphonothioates, and phosphorothioates (Figure 4-1).

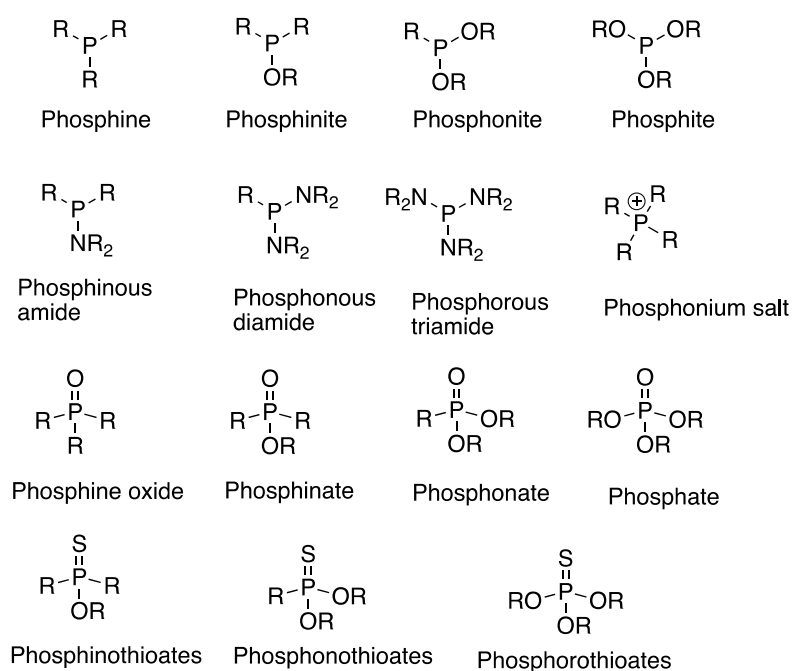


Figure 4-1 Examples of organophosphorus compounds

OP compounds are incredibly diverse with respect to chemical structure and attendant physical-chemical properties; accordingly, the uses of these compounds cover a wide range. Thus, depending on their molecular structures, OP compounds have been found mainly in agriculture as insecticides, herbicides, and plant growth regulators.² They have also been used

as nerve agents in chemical warfare (e.g., Sarin gas), and as therapeutic agents, such as ecothiopate used in the treatment of glaucoma.³ In academic researches organophosphorus compounds find important applications in organic synthesis (Wittig, Mitsunobu, Staudinger, organocatalysis etc.).⁴ The use of organophosphorus compounds as achiral or chiral ligands for transition metal-catalyzed transformations is also rapidly growing in both laboratory synthesis and industrial production.⁵ Furthermore, organophosphorus compounds can be used as flame retardants for fabrics and plastics, plasticising and stabilising agents in the plastics industry, selective extractants for metal salts from ores, additives for petroleum products, and corrosion inhibitors.¹

1.2 Phosphine Ligand and Analogues

The most common phosphine ligands are of the type PR_3 . They are three-fold symmetric with equivalent substituents. Most phosphines are colourless, often pyrophoric, distillable oils with unpleasant alliaceous odours. Furthermore, phosphorus, as with the other heavier pnictogens, differs from nitrogen in that the P(V) oxidation state is readily accessible. For this reason, phosphines are often prone to oxidation in air and must be manipulated under an inert atmosphere. Phosphine ligands are good σ -donors by virtue of the lone pair of electrons in the sp_3 hybridized orbital (Figure 4-2, a). The nature of the substituents has a dramatic effect on the σ -basicity of phosphines, where electron withdrawing substituents decrease the availability of the lone pair with a concomitant decrease in donor ability. Thus, an approximate basicity scale can be constructed such that $PR^{\text{alkyl}}_3 > PR^{\text{aryl}}_3 > P(OR)_3 > PX_3$; Furthermore, PR_3 ligands can act as π -acceptor ligands by interaction of the metals d-orbitals with an appropriate orbital of the ligand (Figure 4-2, b). This gives solubilization and stabilization to organometallic complexes by forming complexes with various transition metal species including latter-period transition metals and others. Thus, phosphines are often used as ligands in metal complex catalysis and they have become a popular reagent for organocatalysis.⁶

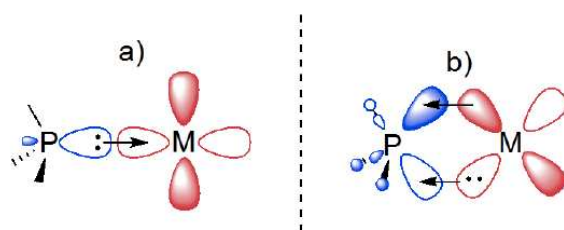
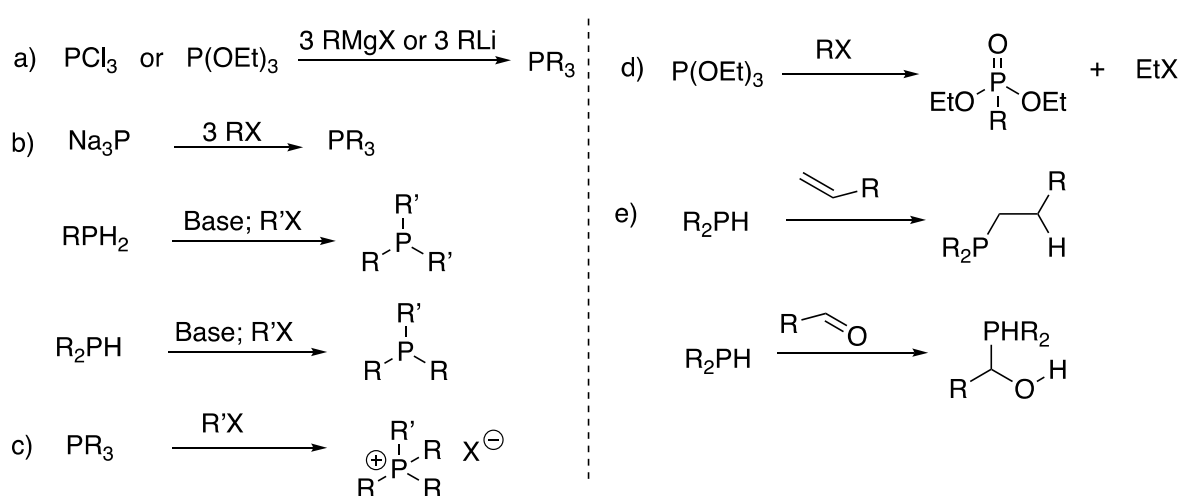


Figure 4-2 Orbital interactions and bonding of PR_3 donors with d-block metals. a) σ bonding; b) π backbonding

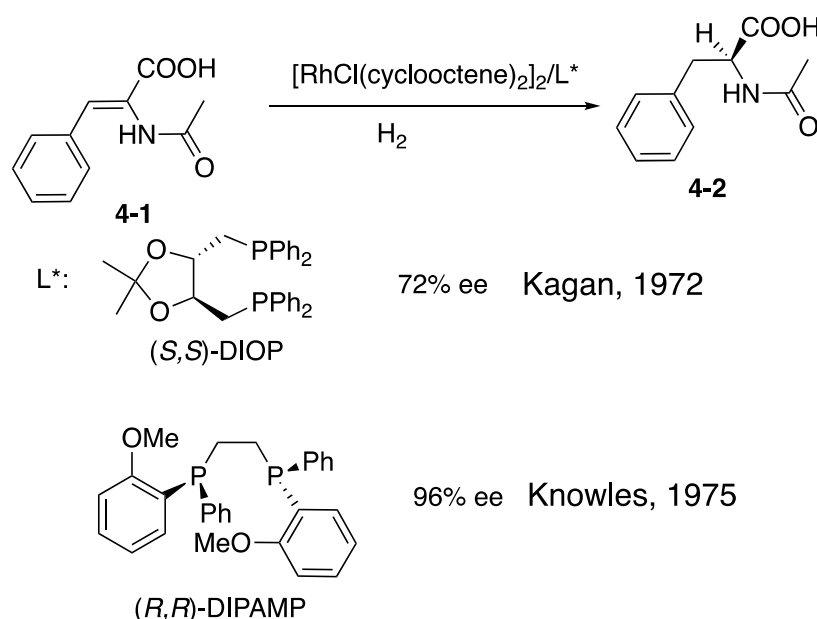
Numerous methods have been developed for the synthesis of phosphines and other phosphorus containing species. The most common of these falls into one of two categories. The first category utilizes an electrophilic phosphorus center such as PCl_3 or $\text{P}(\text{OEt})_3$ in combination with a nucleophile such as Grignard reagents, alkyl/aryl lithium species, alcohols or amines (Scheme 4-1, a). The second and perhaps most straightforward procedure for the formation of P-C bonds however, is *via* the formal deprotonation of a primary or secondary phosphine to give an anionic phosphido species. Phosphides, in addition to displaying a rich coordination chemistry in their own right,⁷ are strong nucleophiles and are thus useful reagents for organic synthesis (Scheme 4-1, b).⁸ This methodology is particularly useful in synthesizing asymmetrically substituted phosphines.⁹ Neutral P(III) species are also often effective nucleophiles and can take part in nucleophilic substitution reactions.¹⁰ However, the initial product of these reactions is either a 4 coordinate phosphonium species (Scheme 4-1, c) or an oxidized P(V) species (e.g. Michaelis-Arbusov reaction.¹¹ Scheme 4-1, d) which must undergo further synthetic preparation in order to be used as a ligand. The P-H bonds of primary and secondary phosphines have been shown to add across multiple bonds in numerous unsaturated compounds, especially alkenes, alkynes and carbonyls (Scheme 4-1, e).¹² These reactions may occur spontaneously but are often promoted *via* the action of base, free radicals, UV light or metal catalysts. Such hydrophosphination reactions are often problematic as they have the potential to produce numerous regio- and stereo-isomers. Many primary and secondary phosphines are commercially available but are easily synthesized *via* the reduction of halo phosphines or P(OR) groups with LiAlH_4 , NaBH_4 or hydrosilanes. Similarly, trivalent species can be accessed *via* reduction of the P(V) intermediates in the presence of strong reducing agents.



Scheme 4-1 Some common P-C bond forming reactions

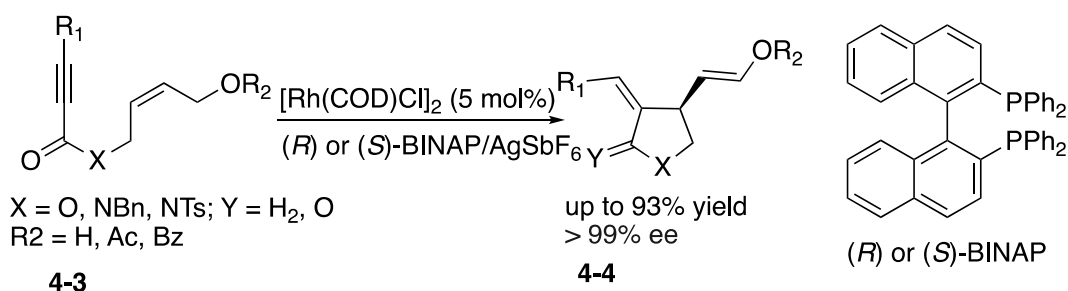
1.3 Phosphine Ligand in Asymmetric Catalysis

Optically active phosphine ligands have played a significant role in transition-metal-catalyzed asymmetric reactions. Knowles and Horner reported the first asymmetric reaction by homogeneous transition-metal catalysts, methylphenylpropylphosphine was used as a chiral monodentate phosphine ligand with a rhodium catalyst which gave 4-15% *ee* in asymmetric hydrogenation of prochiral olefins.¹³ In 1972, Kagan found that a bisphosphine ligand, DIOP, derived from tartaric acid, is much more effective for the rhodium-catalyzed asymmetric hydrogenation, producing amino acids **4-2**.¹⁴ Later, Knowles disclosed (*R,R*)-DIPAMP as a P-sterogenic ligand for asymmetric hydrogenation of *a*-acetamidoacrylic acids **4-1** to form product **4-2** with excellent enantioselectivity of 96% (Scheme 4-2).¹⁵



Scheme 4-2 Rh-catalyzed asymmetric hydrogenation of **4-1**

Since these findings, the development of chiral phosphine ligands has been concentrated into the design and preparation of bisphosphine compounds.¹⁶ In 1980, Noyori reported an axially chiral ligand, BINAP, which expanded the scope of transition-metal catalyzed asymmetric hydrogenations.¹⁷ Since then optically pure BINAPs have been used as bidentate ligands for transition metals such as rhodium, palladium, silver and gold. For examples, Zhang group developed Rh-catalyzed cycloisomerization of 1,6-enyne **4-3** using an air-stable $[\text{Rh}(\text{COD})\text{Cl}]_2$ precursor with commercially available BINAP. In this reaction, a variety of 1,6-enyne substrates with a functional group (OH, OAc, OBz, alkyl) in the allylic position can be cycloisomerized in excellent yields, regio-, and enantioselectivity to form the corresponding products **4-4** (Scheme 4-3).¹⁸



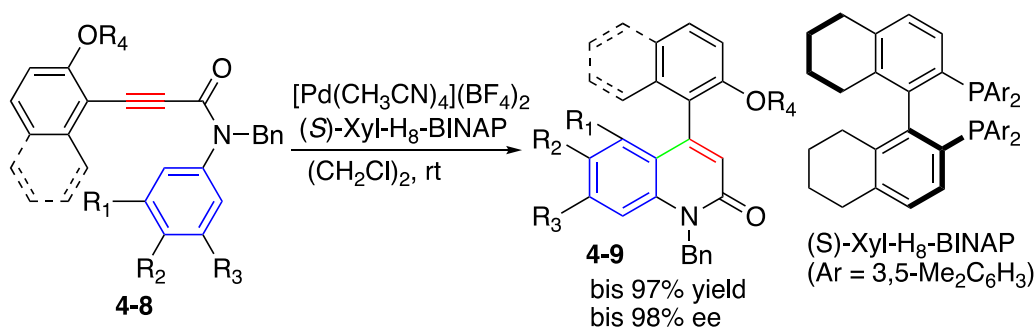
Scheme 4-3 Rh-catalyzed cycloisomerization of 1,6-enyne

Tanaka group developed the cationic Rhodium(I)/H₈-BINAP complex catalyzed asymmetric [2+2+2] cyclization of 1,6-enynes **4-5** and electron-deficient ketones **4-6** to give fused dihydropyrans **4-7** containing two quaternary carbon centers with excellent regio-, diastereo-, and enantioselectivity (Scheme 4-4).¹⁹



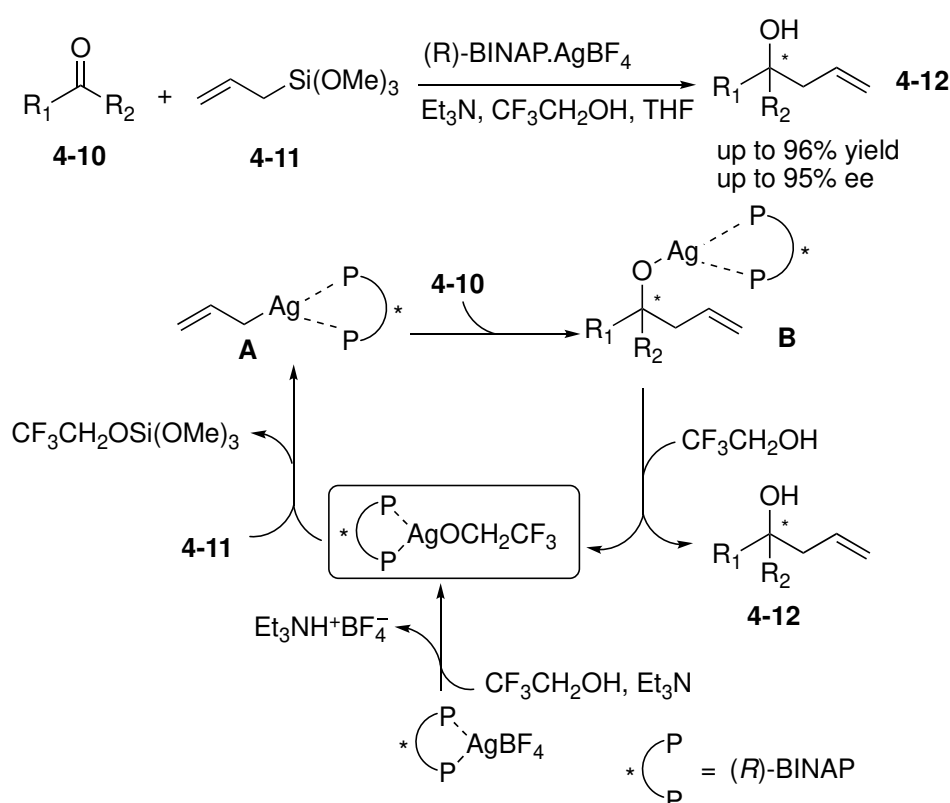
Scheme 4-4 Rhodium-catalyzed asymmetric [2+2+2] cyclization of 1,6-enyne and electron-deficient

Few years later, the same group developed the palladium (II)/(*S*)-xyl-H₈-BINAP complex-catalyzed enantioselective intramolecular hydroarylation of alkynes **4-8** to form axially chiral 4-aryl 2-quinolinones **4-9** at room temperature (Scheme 4-5).²⁰ Axially chiral 4-aryl 2-quinolinones are valuable compounds, which have been found as core structures of pharmaceutically active compounds and chiral ligands.²¹



Scheme 4-5 Palladium (II)/(*S*)-xyl-H₈-BINAP complex-catalyzed enantioselective intramolecular hydroarylation of alkynes

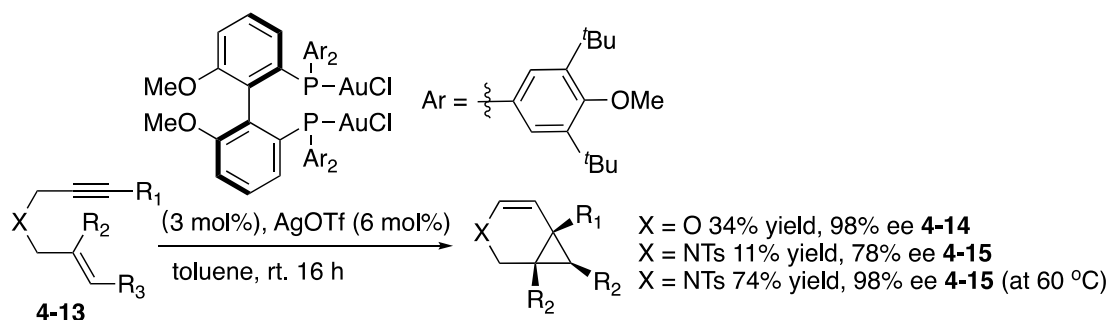
Bamba group developed asymmetric allylation reaction of aldehydes or ketones **4-10** with allyltrimethoxysilane **4-11** by using a BINAP·AgBF₄ complex as the chiral precatalyst and triethylamine as the base in the presence of 2,2,2-trifluoroethanol. Optically active homoallylic alcohols **4-12** with up to 95 % *ee* were obtained in moderate to high yields through the in situ generated of chiral allyl silver catalyst (Scheme 4-6).²² Additionally, the author developed a plausible catalytic cycle was shown in Scheme 4-6. Initially, (R)-BINAP·AgBF₄ reacts with trifluoroethanol in the presence of triethylamine to afford the corresponding (R)-BINAP·AgOCH₂CF₃ complex, which was the true catalyst in the present asymmetric allylation reaction. Subsequently, the thus-generated chiral silver alkoxide attacks allyltrimethoxysilane **4-11** to yield chiral allyl silver species **A**. The following addition reaction of chiral allyl silver **A** with carbonyl compound **4-10** provides **B** as the chiral silver alkoxide of the homoallylic alcohol. Finally, protonation of **B** with CF₃CH₂OH results in the formation of optically active homoallylic alcohol **4-12** with regeneration of the chiral silver alkoxide. Rapid alcoholysis of silver alkoxide **B** promotes the catalytic cycle efficiently.



Scheme 4-6 Silver/(R)-BINAP complex-catalyzed aldehydes or ketones with allyltrimethoxysilane and the proposed mechanism

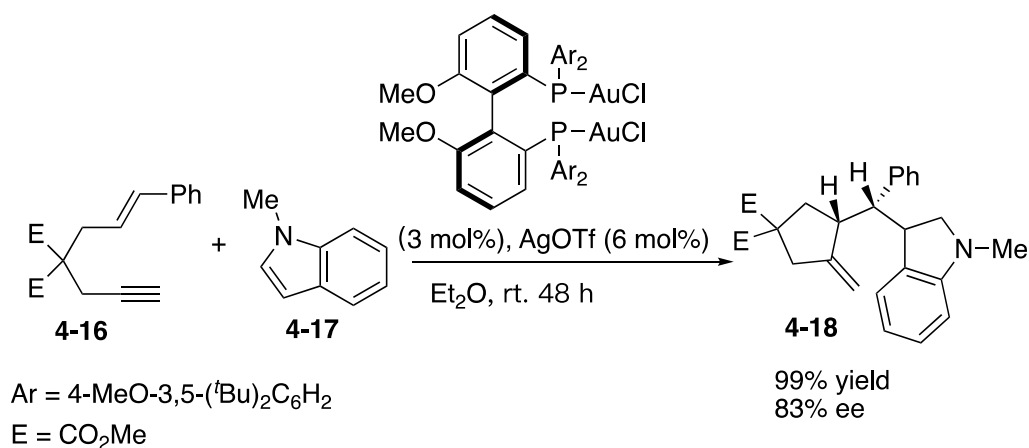
Michelet group developed an asymmetric gold-catalyzed cycloisomerization reaction that provides bicyclo-[4.1.0]heptene derivatives **4-14**, **4-15**. The combination of atropisomeric

chiral ligand 4-MeO-3,5-(*t*-Bu)₂-MeOBIPHEP associated to Au(I) and silver salts promotes the enantioselective rearrangement of oxygen and nitrogen-tethered 1,6-enynes **4-13** under mild conditions. Although, the reactions to afford the products **4-14** and **4-15** in moderated yields, this chiral ligand can induce excellent enantioselectivities of the reactions with 98% and 78% *ee* respectively. Moreover, in the case of *N*-Tosyl group tether (substrate), the yield of product **4-15** increased to 74% with 98% *ee* when the reaction temperature increased to 60 °C (Scheme 4-7).²³



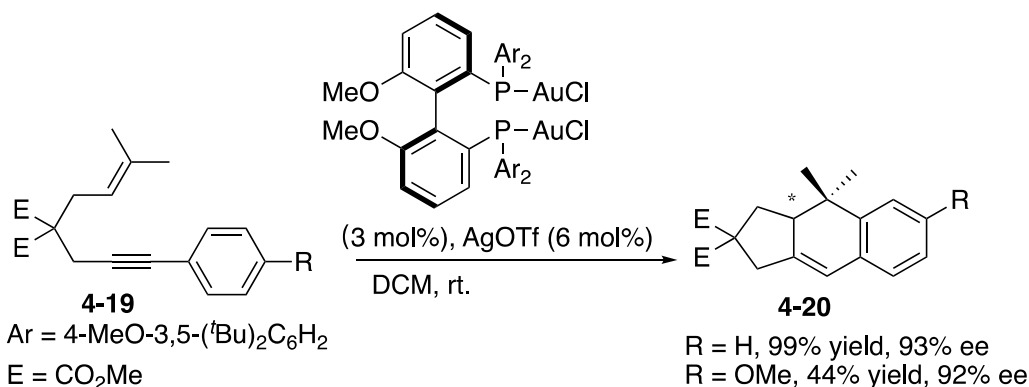
Scheme 4-7 Gold-catalyzed cycloisomerization of heteroatom tethered 1,6-enynes

Additionally, the same group reported the reaction of enyne **4-16** with methylindole **4-17** provided cyclic product **4-18** in high yields (up to 99%) and *ee* (up to 83%) by using the same gold complex bearing a chiral bisphosphine ligand (Scheme 4-8).²⁴



Scheme 4-8 Asymmetric gold(I)-catalyzed cyclization of 1,6-enyne **4-16**

Using a similar gold catalyst as before, intramolecular cycloisomerization of 1,6-enynes bearing aryl or alkenyl substituents produce formal [4+2] adducts. The enantioselective cyclization of malonate enyne **4-19** afforded the tricyclic products **4-20** in excellent yield and enantioselectivity (Scheme 4-9).²⁴ It is remarkable to note that no reaction occurred in the presence of chiral platinum complexes.²⁵



Scheme 4-9 Cycloisomerization of **4-19** with the cationic gold complexes from (*R*)-4-MeO-3,5-(^tBu)₂-MeOBIPHEP(AuCl)₂

To date, many chiral P,P-ligands have been prepared and have played a successful role in transition-metal-catalyzed asymmetric reactions. BPPM (Achiwa),²⁶ CHIRAPHOS, (*S*)-PROPHOS (Bosnich),²⁷ DUPHOS (Burk),²⁸ BICP (Zhang),²⁹ PHANEPHOS (Rossen),³⁰ PENNPHOS (Zhang),³¹ BIPHEMP (Schönholzer),³² P-PHOS (Chan),³³ SEGPHOS (Mikami),³⁴ TANGPHOS (Zhang)³⁵ and ZHAOPHOS (Zhao)³⁶ are some of the successful examples in this field (Figure 4-3).

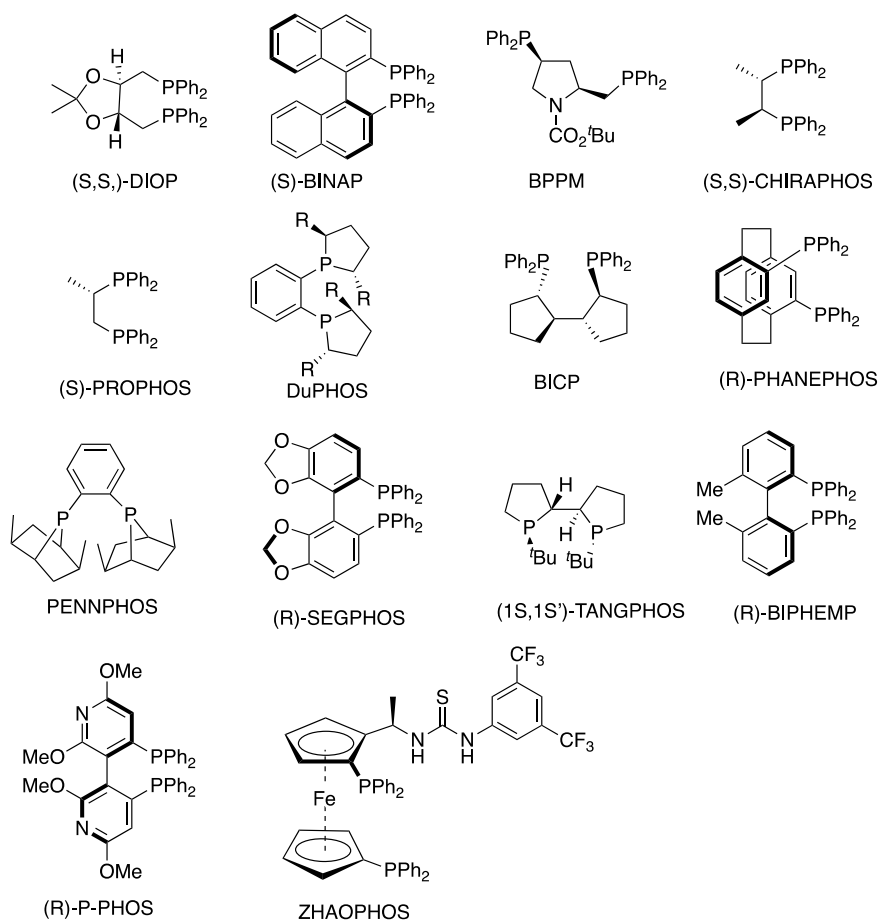
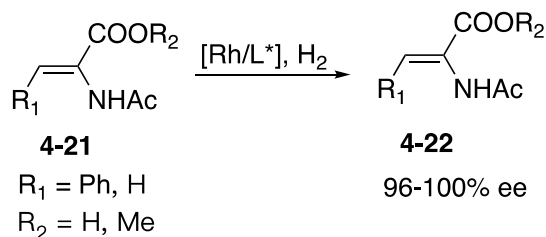


Figure 4-3 Chiral diphosphine ligands

These ligands were extensively employed in Rh-catalyzed asymmetric hydrogenation of enamides **4-21** giving rise to the corresponding amino acid derivatives **4-22** with high enantioselectivities (Scheme 4-10).³⁷



Scheme 4-10 Asymmetric hydrogenation of enamides using chiral diphosphine ligands

Up to now, chiral organophosphorus ligands are continuing to be modified for specific selective reactions to reach enantioselective products with high *ees*. Our research aimed to design new axially chiral phosphine ligands in order to broaden the family of available ligands and investigate on their reactivity and selectivity in asymmetric reactions.

1.4 Allene Syntheses

Allenes contain two cumulated π -bonds, with the double bonds located in mutually perpendicular planes. The C1 and C3 carbons of an allene are sp^2 -hybridized, whereas the central C2 carbon is sp -hybridized (Figure 4-4). Allenes, served as key structural motifs, have been found in over 150 biologically active natural products, such as Panacene, Grasshopper ketone, Icariside B₁ and (+)-Scorodonin, as well as marketed drugs such as Enprostil and Fenpropalene (Figure 4-5).³⁸ In particular, allenenes represent one of the most valuable and versatile building blocks for the synthesis of complex molecules.³⁹ An allene with two different substituents on each of the two carbon atoms will be chiral because there will no longer be any mirror planes. The chirality of these types of allenenes was first predicted in 1875 by Jacobus Henricus van 't Hoff, but not proven experimentally until 1935.⁴⁰ Two years later, Burton and Pechmann accidentally synthesized the first allene, which was penta-2,3-dienedioic acid.⁴¹ Allene synthesis has intrigued and inspired chemists during the last several decades. One of the earliest methods for the synthesis of allenenes is the isomerization of alkynes (Scheme 4-11). Isomerization is a chemical process in which an atom or group rearranges within a molecule, resulting in a structural reorganization without a change in the molecular formula.

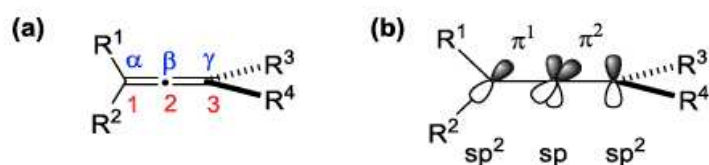


Figure 4-4 Cumulated π -bond system of allenes

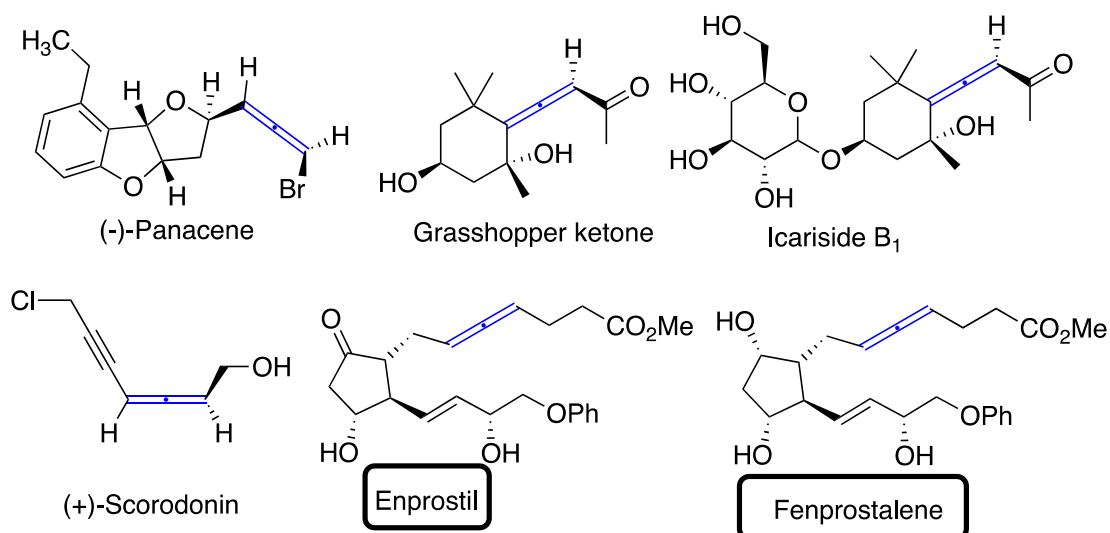
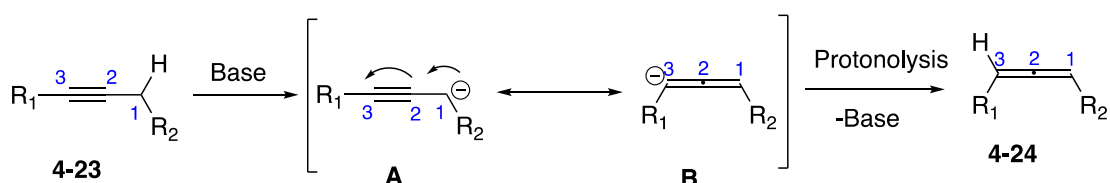


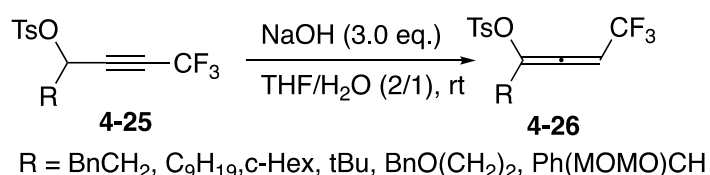
Figure 4-5 Representative bioactive molecules based on an allenyl skeleton and marketed drugs

Under basic conditions, the isomerization step of alkyne **4-23** takes place by deprotonation at C₁ and the generation of the propargyl carbanion intermediate **A**, which is also delocalized as C₃ carbanion corresponding to allenyl anion **B**. Protonation at C₃ affords allene **4-24**.⁴²



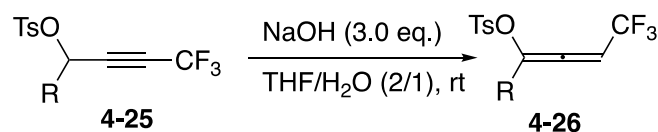
Scheme 4-11 Isomerization of alkynes in basic conditions

In 2010, the Yamazaki group developed propargylic tosylates **4-25** with the CF₃ group at the terminal *sp* carbon atom. Those isomerize to allenyl tosylates **4-26** smoothly at room temperature in the presence of sodium hydroxides in a water-organic biphasic solvent system (Scheme 4-12).⁴³



Scheme 4-12 Isomerization of **4-25** to form allenyl tosylates **4-26**

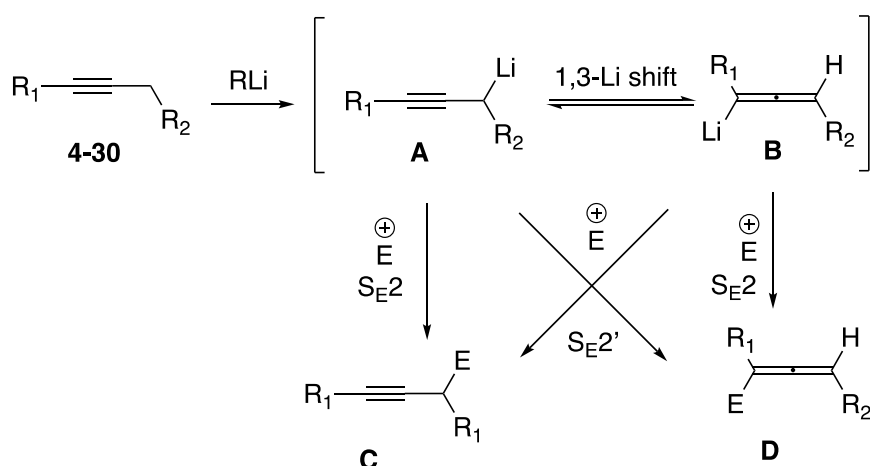
Quite excitingly, an enantioselective isomerization of 3-alkynonates **4-27** to optically active 2,3-dienonates **4-29** with chiral bicyclic guanidine **4-28** as base was also developed (Scheme 4-13).⁴⁴



R = BnCH₂, C₉H₁₉, *o*-Hex, *t*Bu, BnO(CH₂)₂, Ph(MOMO)CH

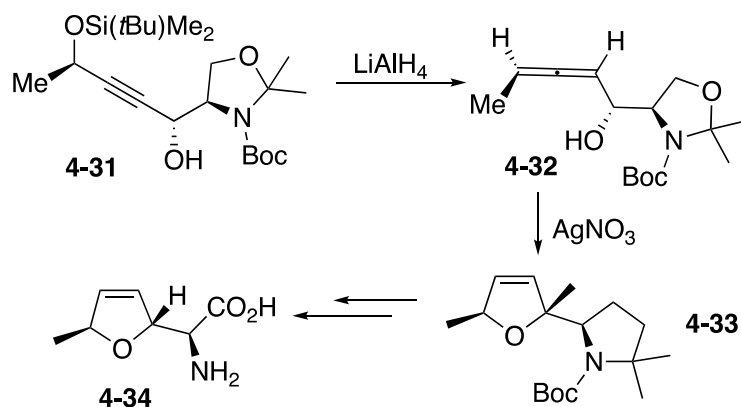
Scheme 4-13 Enantioselective isomerization of 3-alkynonates

In the case of using organolithium reagents such as LDA and butyllithium, as shown in Scheme 4-14, the deprotonation of alkyne **4-30** forms intermediate alkynyllithium **A**, leading to form allenyl and/or propargyllithium **B** in an equilibrium mixture. The process can provide electrophilic-substituted products **C** and **D** by either S_E2 or S_E2' pathways, depending on an electrophile and the reaction conditions.^{38g}

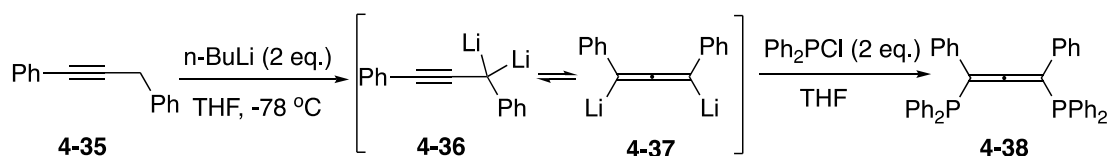


Scheme 4-14 Metallotropic rearrangement of alkyne and electrophilic substitution reaction of **A** and **B**

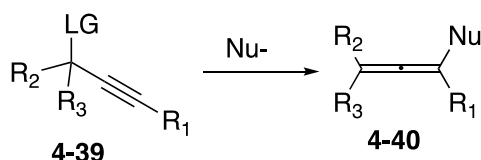
A corresponding example was given by Standaert group in the total synthesis of (+)-furanomycin **4-34**. In this synthetic strategy, treatment of the propargylic silyl ether **4-31** with LiAlH₄ led to the *syn*-stereoselective formation of the hydroxyallene **4-32**, albeit with an unsatisfactory chemical yield (25-50%). The latter allene was then transformed into the antibiotic amino acid, furanomycin (**4-34**), by silver-mediated cycloisomerization to the dihydrofuran **4-33** and elaboration of the side chain (Scheme 4-15).⁴⁵



Another interesting example about the synthesis of allenes bearing phosphine moieties was developed by Schmidbaur group in 1989.⁴⁶ So far, this is the only study dealing with the isomerization of the alkyne and electrophilic trapping to synthesize allene bisphosphines **4-38**. First, treatment of 1,3-diphenyl-1-propyne **4-35** with two equivalents of *n*-butyllithium to deprotonate the two acidic protons at the propargylic position. In the same line, two possible intermediates were also generated in equilibrium mixture, which are alkynyl-di-lithium **4-36** and allenyl-di-lithium **4-37**. The allenyl-di-lithium **4-37** would react with two equivalents of chlorodiphenyl phosphine. The allenyl bisphosphine **4-38** was obtained in 49% yield (Scheme 4-16).

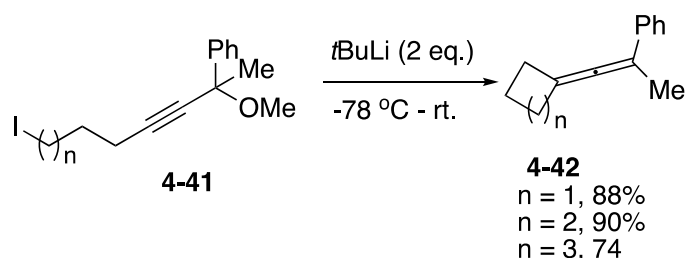


Substitution reaction of propargylic compounds **4-39** with a leaving group is the most commonly employed and convenient method for the synthesis of allenes **4-40**. A variety of labile groups, including propargylic acetates, mesylates, carbonates, and halides, etc. have been used as leaving groups (Scheme 4-17).⁴⁷



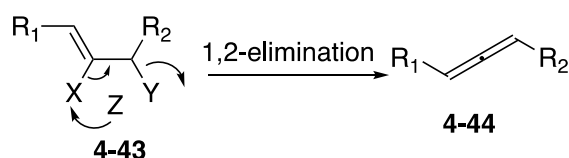
One of the very few examples of intramolecular substitution reaction of propargylic substrates with organolithium reagents was reported by Bailey and Aspris (Scheme 4-18).⁴⁸ Iodine-lithium exchange of propargyl ethers **4-41** at low temperature led to the corresponding

alkyllithium compounds which cyclized to furnish exocyclic allenes of the type **4-42** upon warming to room temperature. Four-, five- and six-membered rings were efficiently formed in good to excellent yield by *exo-dig* ring closure.

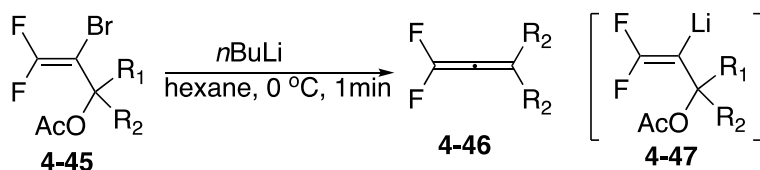


Scheme 4-18 The synthesis of alkenyldenecycloalkanes **4-42**

1,2-Elimination of two groups from a vinyl precursor **4-43** represents a common class of reactions used to access allenes **4-44** (Scheme 4-19). For example, allenes can be obtained by dehydrohalogenation of 2-halopropene derivatives using strong bases,⁴⁹ or by *syn*-selenoxide elimination of vinyl selenides.⁵⁰ This elimination protocol has been recently applied to the synthesis of 1,1-difluoroallenes (Scheme 4-20).⁵¹ Upon treatment with *n*-butyl lithium, 2-bromo-3,3-difluoroallylic acetates **4-45** underwent lithium-bromide exchange, followed by 1,2-elimination of lithium acetate to afford mono- and disubstituted 1,1-difluoroallenes **4-46** in high yields. Similarly, Yamazaki *et al.* used zinc-mediated 1,2-elimination of 2-iodo-3-trifluoromethylallylic acetates to prepare the potentially important CF₃-substituted allenes.⁵²

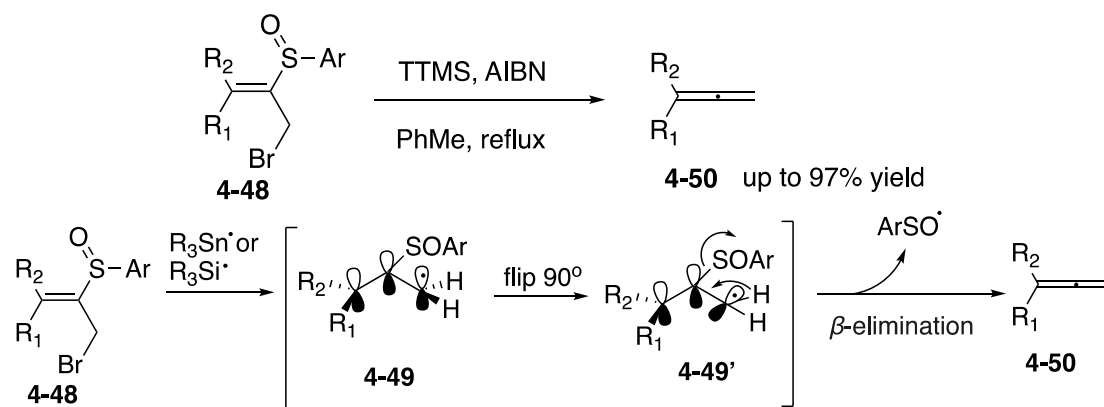


Scheme 4-19 Synthesis of allenes involving 1,2-elimination



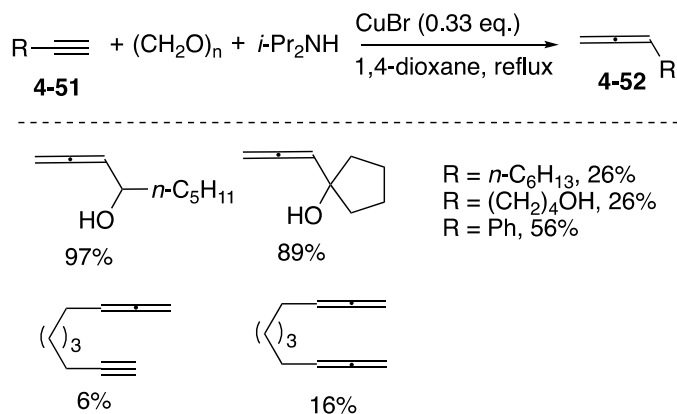
Scheme 4-20 Synthesis of 1,1-difluoroallenes **4-46**

Furthermore, our group has developed a new route to prepare functionalized allenes **4-49** *via* radical β -elimination of vinyl sulfoxides **4-48** in the presence of tris(trimethylsilyl)silane (TTMS) and 2,2'-azobis(2-methylpropanitrile) (AIBN). This reaction does not proceed at low temperature, nor with sulfur groups other than sulfoxide and sulfimide.⁵³ A noteworthy feature of this system is that a conjugated radical **4-49** needs to flip by 90° to provide **4-49'**, which can then undergo β -elimination to form desired products **4-50**.



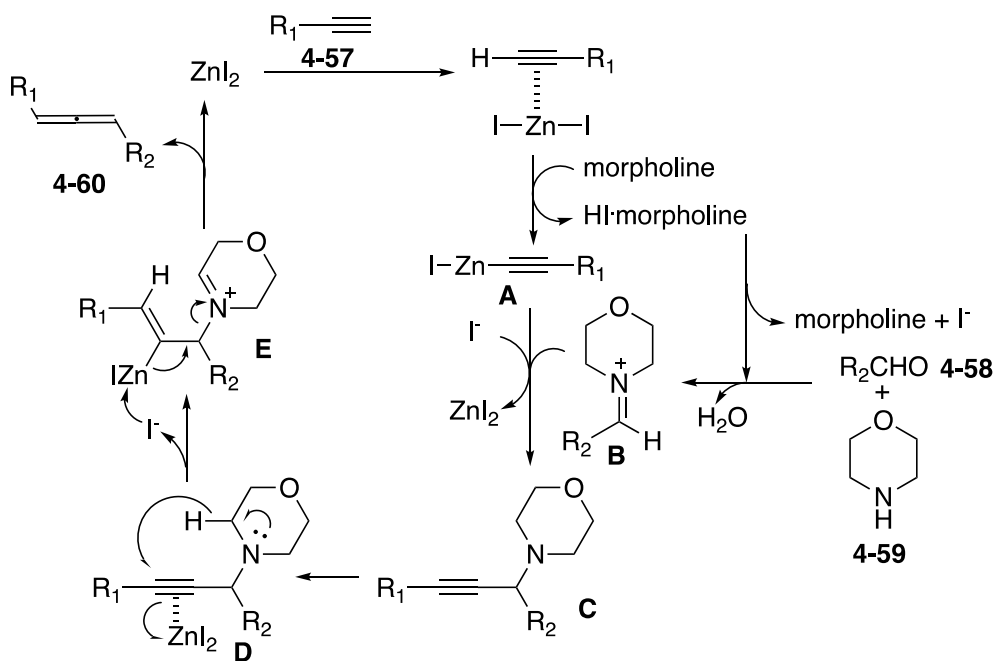
Scheme 4-21 The synthesis of monosubstituted allene **4-50**

Monosubstituted allenes could also be synthesized *via* the Crabbé homologation reaction of terminal alkynes. In 1979, Crabbé et al. reported the first CuBr-mediated allenation of terminal alkynes (ATA) **4-51** with paraformaldehyde to prepare monosubstituted allenes **4-52** in the presence of diisopropylamine (Scheme 4-22). This reaction involves copper-catalyzed addition of terminal alkyne to the *in situ* formed Schiff base and hydride migration to the carbon-carbon triple bond in an S_N2' substitution manner. It should be noted that the α -hydroxy substitution significantly increased the reactivity of the alkynes, while phenyl substitution and long carbon-chain alkyl substitutions led to lower yields. Moreover, the reaction of nona-1,8-diyne only afforded monosubstituted allene product in 6% yield and bisallene product in 16% yield.⁵⁴



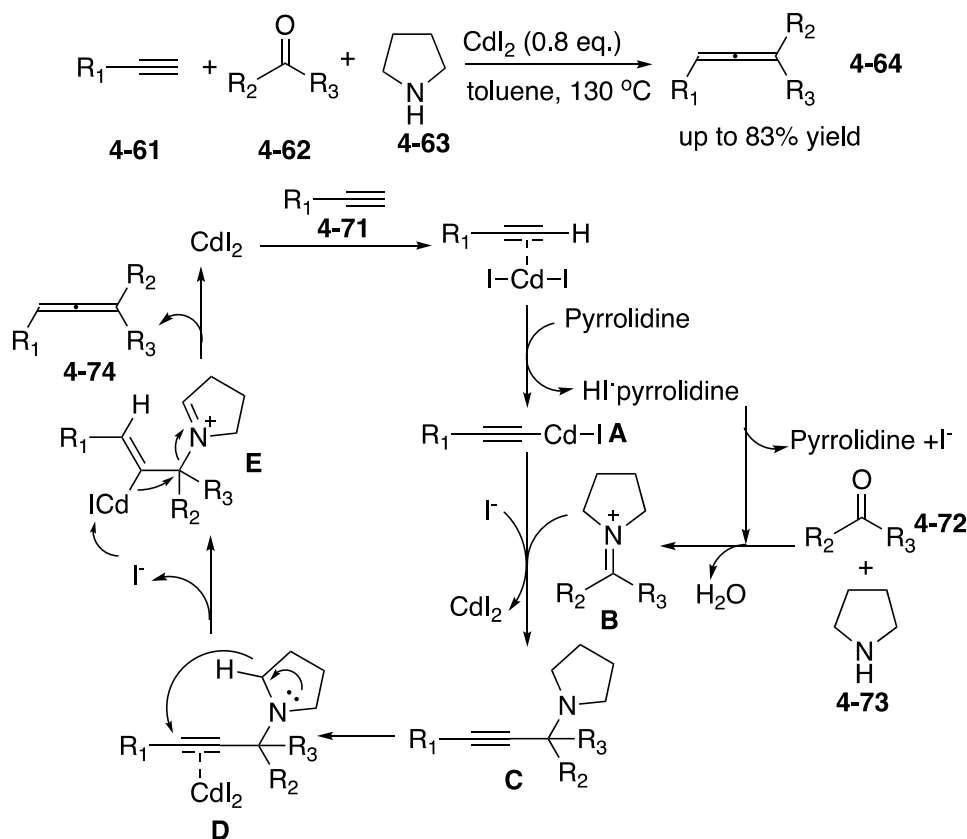
Scheme 4-22 Original allenation of terminal alkynes (ATA) reaction by Crabbé

The usefulness of this reaction has inspired several modifications to improve efficiency or expand the reaction scope. It was found that microwave irradiation could accelerate reaction rate, reducing reaction time from usually 6-24 h to 1-20 min (Scheme 4-23).⁵⁵



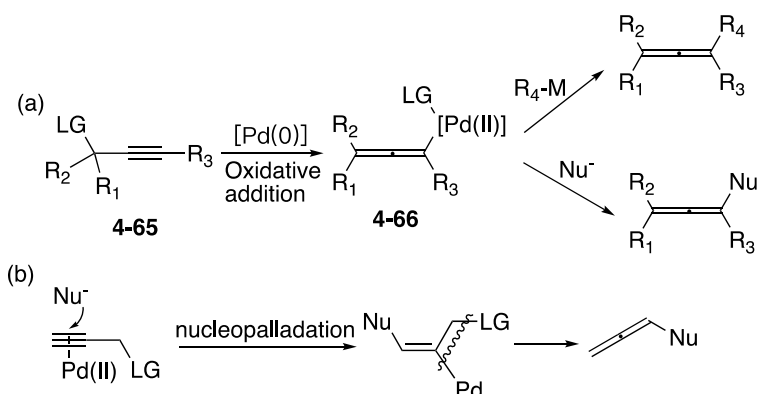
Scheme 4-26 A possible mechanism

Ma group has also developed the ATA reaction with ketones **4-62** under the promotion of CdI_2 (0.8 equiv.) with pyrrolidine **4-63** as the matched amine. With this protocol, a series of different trisubstituted allenes **4-61** have been successfully prepared in high yield (Scheme 4-27). This protocol was operationally simple and all the starting materials are basic chemicals readily available, showing the potential synthetic utility of this method. Additionally, the author proposed a plausible mechanism as shown in Scheme 4-27. Alkynyl cadmium species **A**, generated from terminal alkyne in the presence of pyrrolidine, would react with the ketoniminium **B** formed *in situ* from ketone and pyrrolidine, to give the corresponding propargylic amine **C**. The carbon-carbon triple bond in propargylic amine **C** coordinates to CdI_2 forming complex **D**, which would be followed by 1,5-hydride transfer and β -elimination to afford the corresponding trisubstituted allene **4-64**.⁵⁸



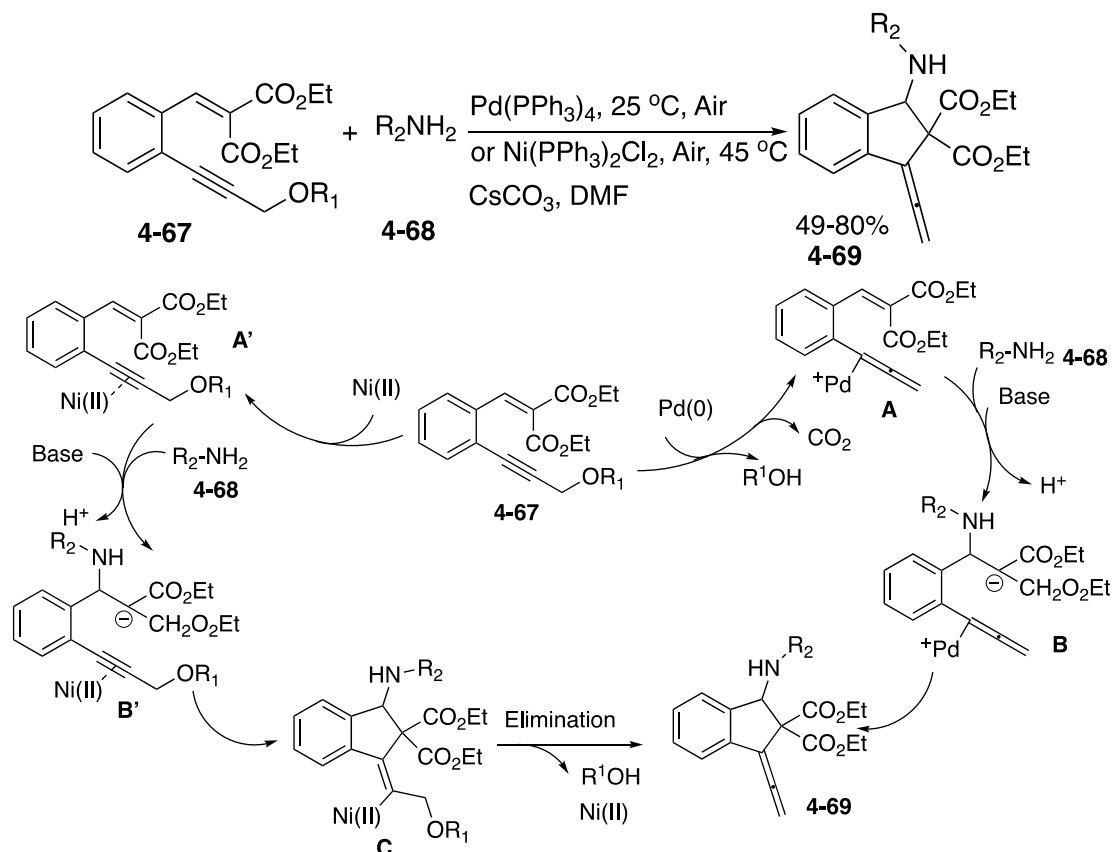
Scheme 4-27 Synthesis of trisubstituted allenes *via* CdI₂ promoted ATA reactions from terminal alkynes, ketones, and pyrrolidine and a plausible mechanism

Palladium-catalyzed cross-coupling reactions of propargyl substrates with organometallic reagents or nucleophiles constitute an important method to allenic compounds. For Pd(0)-mediated coupling, the reaction may be initiated by oxidative addition of Pd(0) to the corresponding propargylic compounds **4-65** with a good leaving group forming allenylpalladium intermediate **4-66**,⁵⁹ followed by treatment with organometallic reagents or nucleophiles to generate the corresponding allenes (Scheme 4-28, a). For Pd(II)-mediated reactions, the initial step usually involved nucleopalladation (Scheme 4-28, b).⁶⁰



Scheme 4-28 The synthesis of allenic compounds *via* Palladium-catalyzed cross-coupling reactions

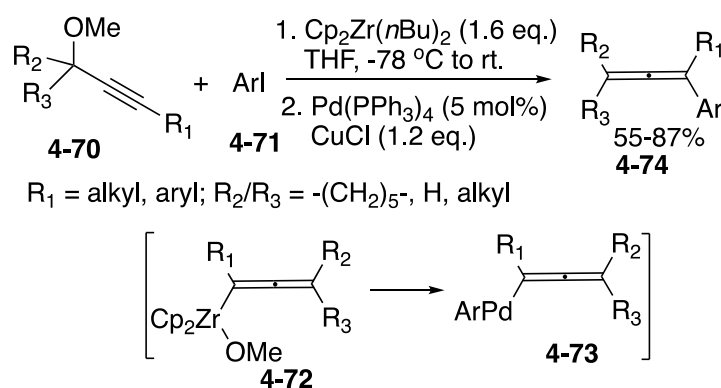
The allenylpalladium intermediate formed by oxidative addition of Pd(0) to propargylic carboxylate could be trapped by nucleophiles, which gave a variety of functionalized allenes.⁶¹ Liang group intercepted the allenylpalladium complex by carbon nucleophiles generated *in situ* by Michael addition of arylamines **4-68** to diethyl 2-{2-[3-(ethoxycarbonyloxy)prop-1-ynyl]benzylidene} malonate **4-67** (Scheme 4-29). The reaction offered an efficient route to highly substituted indenenes with an allene moiety **4-69**. Ni(II) also worked well for this reaction, which coordinated to the triple carbon-carbon bond to facilitate the attack of nucleophiles.⁶²



Scheme 4-29 The synthesis of allenylidene derivatives *via* palladium- or nickel-catalyzed tandem Michael addition-cyclization reaction and possible mechanism

The plausible reaction mechanism was proposed for this novel cascade transformation as shown in Scheme 4-29. As the first step: decarboxylation of propargylic compound **4-67** catalyzed by Pd(0) generates an allenylpalladium complex **A** or the Ni(II) species coordinates to the alkyne triple bond of **4-67** to afford **A'**. Then, the base mediates a Michael addition which affords intermediate **B** or **B'**, respectively. Finally, **B** undergoes regioselective intramolecular stabilized carbon nucleophilic attack to afford product indene **4-69**; on the other hand, **B'** could also undergo the same attack with the activated triple bond to afford vinyl intermediate **C** and then β -heteroatom elimination to form indene **4-69**.

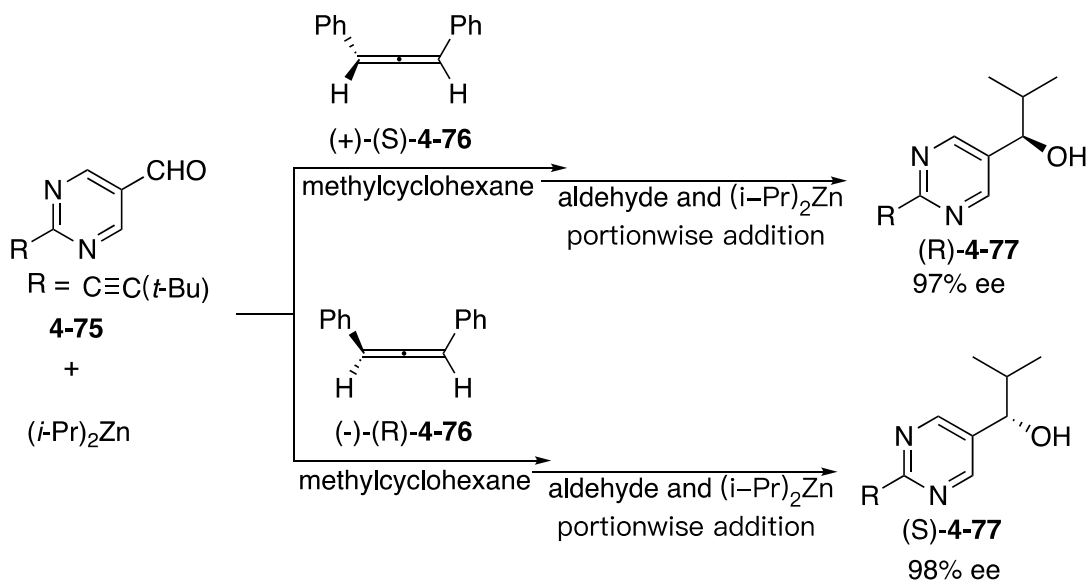
Treatment of propargylic ether **4-70** with $\text{Cp}_2\text{Zr}(n\text{-Bu})_2$ led to allenic/propargylic zirconium reagents. Their ratio depended on the substitution pattern of starting propargylic ethers. Aryl- or alkyl-substituted propargylic ethers favored the allenic zirconium, whereas TMS-substituted propargylic ethers preferred to produce alkyne zirconium. These reagents, upon coupling with aryl iodides **4-71** in the presence of $\text{Pd}(\text{PPh}_3)_4/\text{CuCl}$, gave multisubstituted allenes **4-74** in moderate to good yields (Scheme 4-30).⁶³



Scheme 4-30 The synthesis of multi substituted allenes **4-74** in the presence of $\text{Pd}(\text{PPh}_3)_4/\text{CuCl}$

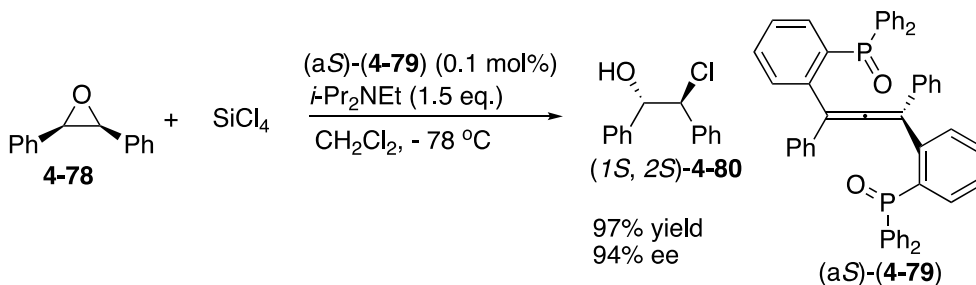
1.5 Allenes in Catalysis

Nowadays, there is a growing interest regarding the development of methods to synthesize structurally complex and biological active products incorporating allenes. Allenes can also be used as organocatalysts or as ligands in organometallic catalysis when it substituted by coordinating groups. There are indeed some examples about the use of allenes as organocatalyst in asymmetric reactions. In 2002, Soai group found that optically pure allenes could be applied as efficient organocatalysts in asymmetric reactions. They reported that 1,3-disubstituted chiral allenes **4-76** induce asymmetry in the enantioselective addition of $(i\text{-Pr})_2\text{Zn}$ to 2-(alkynyl)pyrimidine-5-carbaldehyde **4-75**. Highly enantiomerically enriched pyrimidin-5-yl alkanol **4-77** was obtained by combination asymmetric autocatalysis (Scheme 4-31). In addition, chiral allenes **4-76** are hydrocarbon compounds without any heteroatom. The ee value of (*S*)-**4-76** / (*R*)-**4-76** was 99.5%, which was determined by HPLC analysis with a chiral stationary phase. These results were very significant in that chiral hydrocarbon compounds without any stereogenic center can act as chiral inducers in asymmetric synthesis.⁶⁴



Scheme 4-31 Enantioselective addition of $(i\text{-Pr})_2\text{Zn}$ to aldehyde *via* chiral allenyl phosphine oxides as asymmetric autocatalysts

Few years later, Ready group successfully prepared optically pure allenyl phosphine oxides **4-79**.⁶⁵ They investigated the catalysis of the asymmetric addition of SiCl_4 to *meso*-epoxides with these organocatalysts. Similar reaction has been studied by Denmark group. They demonstrated that optically active phosphorus triamides could catalyze this transformation;⁶⁶ subsequent reports revealed the utility of pyridine *N*-oxide and phosphine oxides.⁶⁷ Mechanistically, these reactions are thought to involve the coordination of one or more Lewis bases to SiCl_4 to generate a more Lewis acidic species $(\text{LB})_n\text{SiCl}_3^+$ (LB = Lewis base) capable of activating the epoxide toward ring opening.^{66b} Here, Ready group developed allenyl phosphine oxides **4-79** can catalyze the addition of SiCl_4 to *cis*-stilbene oxide **4-78** with high enantioselectivity, which generated a diastereoselective chlorohydrin (*1S, 2S*)-**4-80** in 97% yield and 94% *ee* (Scheme 4-32).



Scheme 4-32 Asymmetric addition of SiCl_4 to *cis*-stilbene oxide in the presence of chiral allenyl phosphine oxides

The allene functional group was known to act as a ligand in transition metal complexes through its double bonds. To date, allenes have been observed in the coordination sphere of

transition metals in a variety of contexts. Complexes of Au,⁶⁸ Os,⁶⁹ Mn,⁷⁰ W,⁷¹ Co⁷² and Pt⁷³ that involve direct binding of the allene to a transition metal were known. Furthermore, allene-containing phosphines have been characterized as ligands for Fe⁷⁴ by Doherty group in 1996 and Os⁷⁵ by Xia group in 2010. Both of them are η^2 -allene complexes (Figure 4-6).

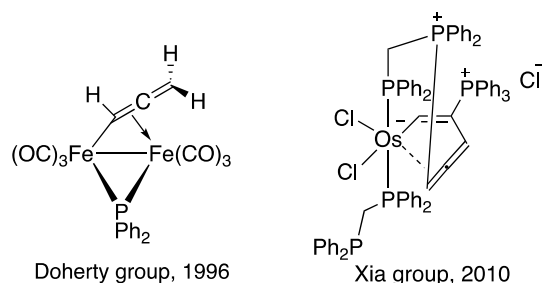
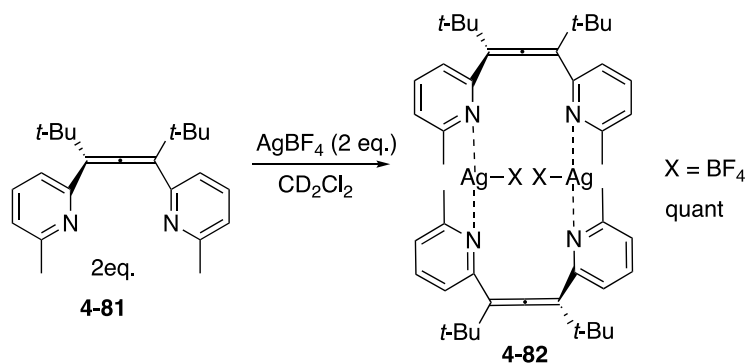


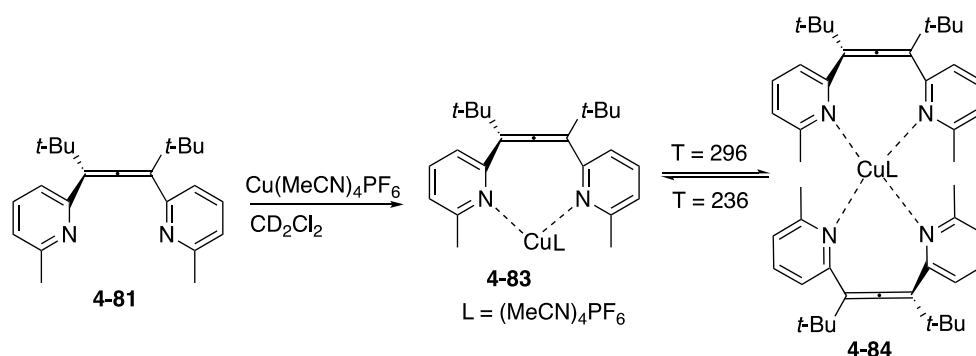
Figure 4-6 η^2 -allene complexes

Substituted pyridines group on allenes could also coordinate to transition metals since pyridines constitute one of the most established and well performing classes of ligands for transition metal complexes. In 2008, Krause group synthesized allenic bipyridine ligands **4-81** from propargylic acetate with PhZnCl, which was used as a nucleophile for the transmetalation step in palladium catalytic process. Their complexation to silver and copper salts was studied to form the corresponding complexes through nitrogen coordination of the pyridine groups, characterized by mass spectrometry (ESI), NMR spectroscopy, and X-ray crystallography. Bis(pyridyl)allene-silver complex **4-82** was formed by the complexation of allenes **4-81** with silver salts *via* the coordination of two silver atoms to both nitrogen atoms of each ligand (Scheme 4-33). On the other hand, the complexation with copper salts forms 1:1 complex (Ligand/Cu) **4-83** at 236 K. The copper complexation led to the 2:1 complex **4-84** when the temperature was increased to 296 K (Scheme 4-34).⁷⁶

For all of these complexes, very few catalytic reactions have been reported with some of these allene-metal complexes, and progress in this field is slow, probably due to the ability of metals to activate the allene towards nucleophilic attack, which disrupts the allene backbone.⁷⁷

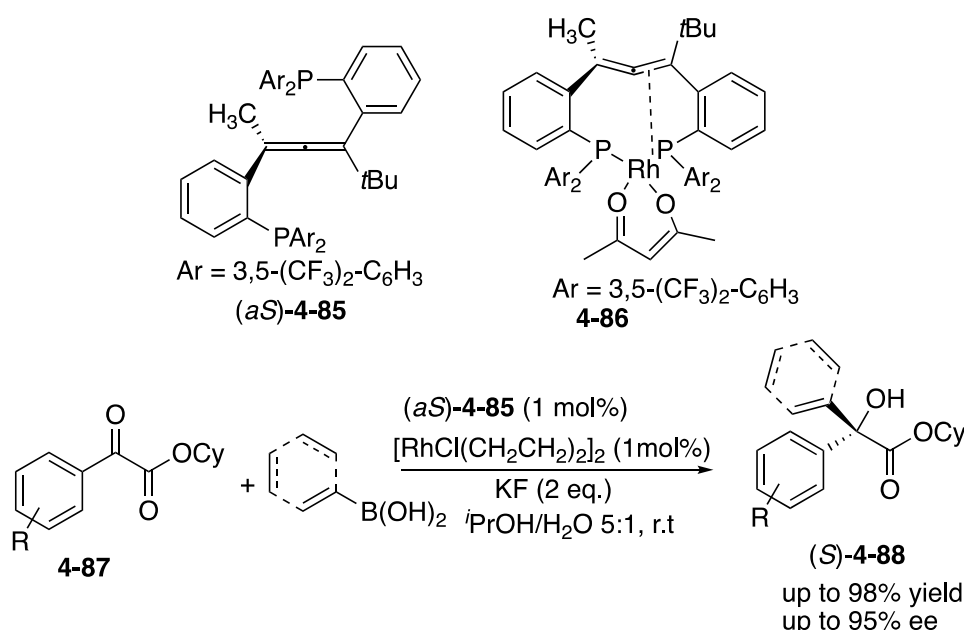


Scheme 4-33 Allene complexation mode (**4-82**) of silver salt 2:2 (Ligand/Ag)



Scheme 4-34 Allene complexation modes (**4-83** and **4-84**) of copper salt 2:1 and 1:1 (Ligand/Cu).

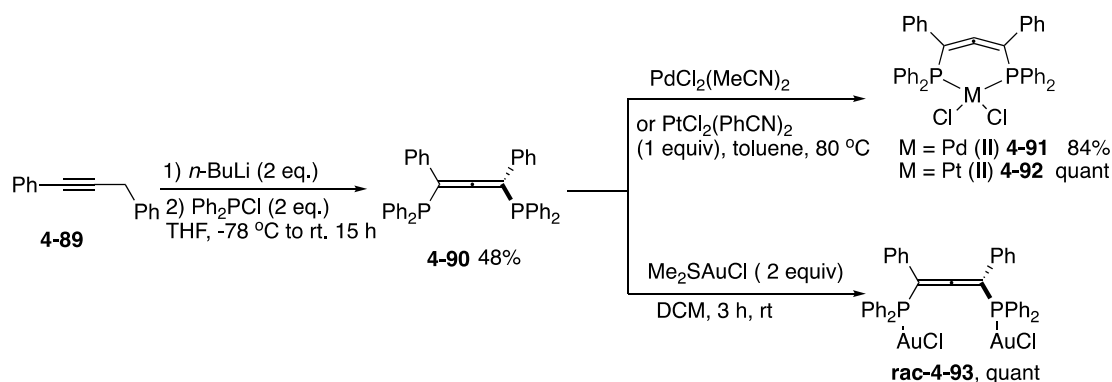
In 2011, The Ready group then further adapted the parent structure **4-79** to append phosphine groups bearing CF_3 electron withdrawing group in place of the phosphine oxide ones. The resulting ligand **4-85** could coordinate to Rh(I), featuring also coordination from the allene moiety, and provide η^2 -allene complex **4-86**. Interestingly, the coordination complex could be isolated and characterized by X-ray analysis. It evidenced the coordination of the rhodium center by two phosphine groups and one allene bond. This complex proved to be a highly efficient catalyst for the enantioselective rhodium(I)-catalyzed addition of arylboronic acids to α -keto ester **4-87**. This transformation provides synthetically valuable tertiary alcohols **4-88** in good to excellent yields in high ees (Scheme 4-35).⁷⁸



Scheme 4-35 Enantioselective Rh(I)-allene complexes catalyzed addition of boronic acids to α -ketoesters

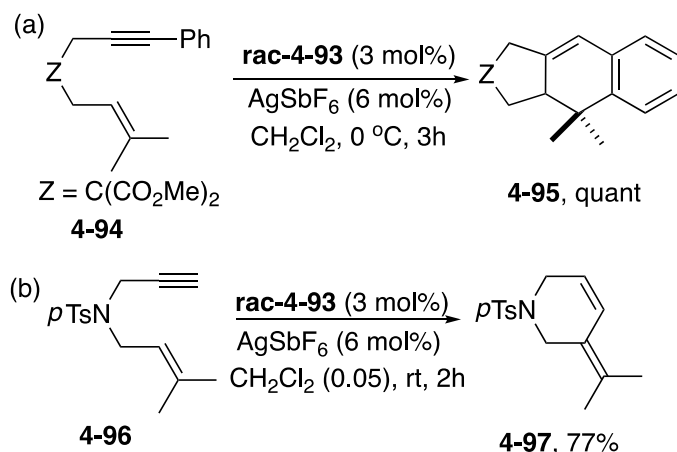
Recently, our group reported that bisphosphine allene ligands form complexes with Pd(II) and Pt(II) in a 1:1 ligand to metal ratio to give Pd and Pt mononuclear complexes **4-91**, **4-92**,

respectively with good yields. In the same vein, bisphosphine allene ligands with Au(I) in a 1:2 ratio yielded quantitatively to dinuclear gold(I) complexes **rac-4-93**.⁷⁹ The synthesis of bisphosphine allene ligand **4-90** has been previously described by Schmidbaur group.⁴⁶ 1,3-Diphenyl-1-propyne **4-89** was prepared *via* a palladium coupling reaction of 2-propynylbenzene and iodobenzene and then used as a precursor for allenyl bisphosphine **4-90**.⁸⁰ The precursor **4-89** was deprotonated with two equivalents of *n*-butyllithium to generate an alkynyllithium intermediate, by undergoing the isomerization to form an allenyllithium intermediate in equilibrium. After adding two equivalents of chlorodiphenylphosphine at -78 °C, the mixture was slowly warmed to rt for 15 h and concentrated under reduced pressure. The residue was precipitated in the mixture of ethanol and water (1:1) to provide a brown solid in 48% yield (Scheme 4-36).



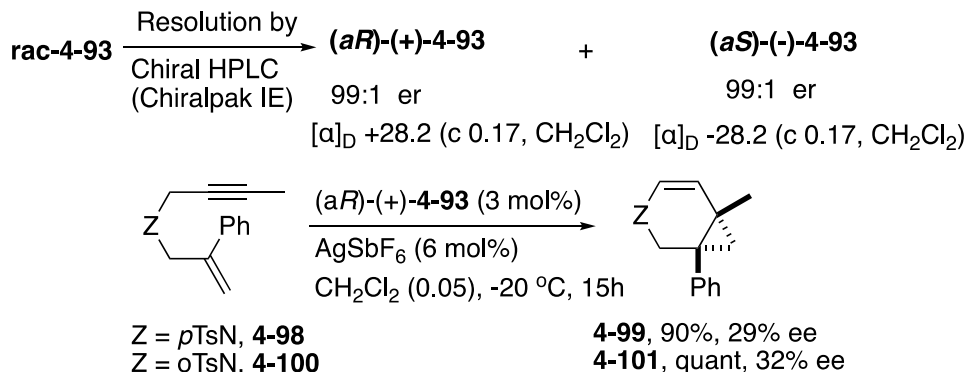
Scheme 4-36 The synthesis of mononuclear Pd and Pt bisphosphine allene complexes and dinuclear gold(I) bisphosphine allene complexes

The precatalyst **rac-4-93** in the presence of a silver salt proved to be very active and robust in a series of prototypical gold-catalyzed reactions. For examples, the reaction of enyne **4-94** was carried out in CH_2Cl_2 with a catalytic 1:1 mixture of **rac-4-93** (3 mol%) and AgSbF_6 (6 mol%) to afford tricyclic product **4-95** in quantitative yield (Scheme 4-37, reaction a). The reaction of prototypical *N*-tethered 1,6-enyne **4-96** was run in similar catalytic reaction, which afforded diene product **4-97** in 74% yield (Scheme 4-37, reaction b).⁷⁹



Scheme 4-37 Preliminary catalytic testing of **rac-4-93**

Additionally, the enantiomers of complex **rac-4-93** were nicely separated by preparative chiral chromatography on a Chiralpak IE column by Dr. Nicolas Vanthuynne (iSm2, Aix-Marseille Université). Each enantiomer was obtained a high *ee* of 98%. Then the catalytic activity of (*aR*)-(+)-**4-93** was evaluated for the asymmetric cycloisomerisation of 1,6-enynes **4-98** and **4-100**. The expected azabicyclo[4.1.0]heptenes **4-99** and **4-101** were obtained in good yields and with promising *ee* values of 29 and 32%, respectively (Scheme 4-38).⁷⁹ Those results gave promising hits for asymmetric catalysis.



Scheme 4-38 Resolution of **rac-4-93** and further asymmetric catalysis

In previous works, bisphosphine allene ligand **4-90** was difficult to isolate since phosphine functional groups on allene were easily oxidized, such as mono- and bisphosphine oxide-containing allenes were formed. In average, this procedure gave **4-90** in low yield (38%). Although this work in the coordination of bisphosphine allene **4-90** with palladium, platinum and gold salts has allowed the formation of original coordination complexes, it is limited to obtain chiral digold complex **4-93**. So it appeared necessary to develop new methods to form bisphosphine allene ligand **4-90** in good yields and further synthesize a variety of chiral metal bisphosphine allene complexes.

Owing to the great examples of allene applications in organometallic chemistry, we want enlarge the scope of the preliminary findings. We will notably focus on the asymmetric catalysis since the initial set of findings proved to be quite encouraging. To do that, a new family of stable allene phosphine ligands will be prepared. We will therefore vary the substitution of the allene backbone. The substituents with different steric and electronic properties will be introduced. We aimed to apply them as chiral organocatalysts and as ligands for various metals.

1.6 Luminescence Properties

Fluorescence, phosphorescence and chemiluminescence are three main forms of luminescence. Phosphorescence and fluorescence are two forms of photoluminescence. In photoluminescence, a substance's glow is triggered by light, in contrast to chemiluminescence, where the glow is caused by a chemical reaction. Both fluorescence and phosphorescence are based on the ability of a substance to absorb light and emit light of a longer wavelength and therefore lower energy. The main difference is the time in which it takes to do so.

In fluorescence, the emission is basically immediate and therefore generally only visible, if the light source is continuously on (such as UV lights); while phosphorescent material can store the absorbed light energy for some time and release light later, resulting in an after glow that persists after the light has been switched off. Depending on the material, this afterglow can last anywhere from a few seconds to hours.

One radiative mechanism by which excited electrons may relax is a light-emitting transition from the lowest excited state (S_1) to ground state (S_0) in a fast (10^{-9} to 10^{-6} sec) process called fluorescence. The energy difference is dissipated by emitting a photon. Due to the electron having shed some of the original excitation energy by vibrational relaxation, the emitted photon will be of lower energy and thus of longer wavelength. However, this is different for phosphorescence. Fast (10^{-12} to 10^{-9} sec) intersystem crossing from singlet excited state (S_1) to an energetically favorable triplet excited state (T_1) leads to inversion of the electron spin. Triplet excited states are characterized by parallel spin of both electrons and are metastable. Relaxation occurs *via* phosphorescence, which results in another flip of the electron spin and the emittance of a photon. The return to relaxed singlet ground state (S_0) might occur after considerable delay (10^{-3} to >100 sec). Additionally, more energy is dissipated by non-radiative processes during phosphorescent relaxation than in fluorescence, therefore the energy difference between the absorbed and emitted photon is bigger and the wavelength shift more pronounced. Thus, phosphorescence is characterized by a bigger Stokes shift than fluorescence (Figure 4-7).⁸¹

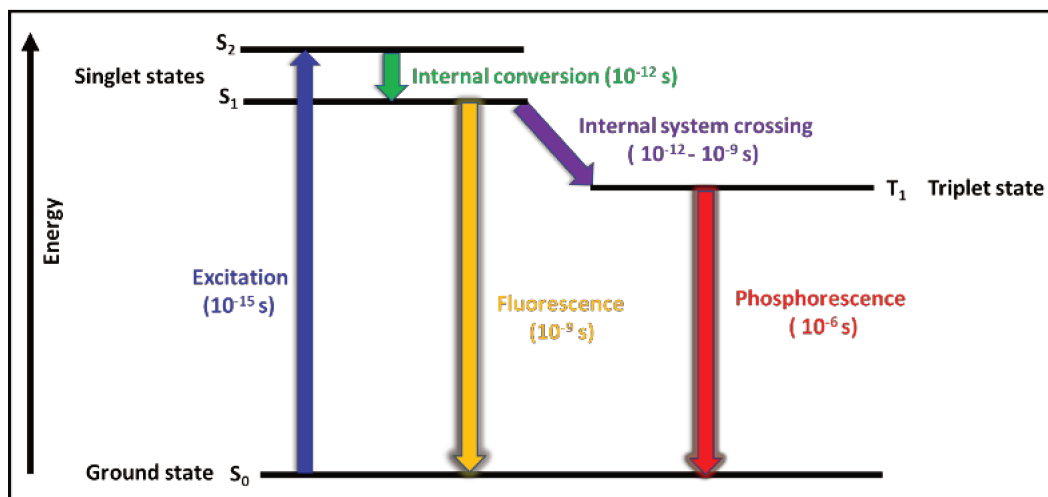


Figure 4-7 Fluorescence and phosphorescence mechanism in a substance

Au(I) alkynyl complexes⁸² have generated much interest associated with their use in the synthesis of organometallic rigid oligomers, polymers, molecular triangles, macrocycles, and catenanes.⁸³ Another interesting feature of these complexes is their luminescence, which can be employed for the design of sensors or optical devices and is strongly influenced by the presence of aurophilic interactions.⁸⁴ Several examples of luminescent chemosensors containing Au(I)-alkynyl units have been described.⁸⁵ In these systems, the alkynyl ligands contain a crown ether, a calixarene, or a calix crown host, which interacts with metal ions, giving rise to a detectable perturbation of the luminescence of the Au-alkynyl unit.

The luminescence of gold(I) acetylides was first reported by Che in 1993⁸⁶ and has been extensively studied by his group and also by Yam's group.⁸⁷ These properties have found interest in the use of the systems in a wide range of different applications.

The gold(I) alkynyl system supported by an auxiliary phosphine ligand represents the major class of luminescent gold(I) complexes. The first group is represented with the general formula $R_3P-Au-C\equiv C-R_1$ where R corresponds to a wide range of aromatic or aliphatic phosphines and R_1 to the huge number of organic groups linked to the acetylene moiety. M. Laguna, P. Dyson and co-workers synthesized and characterized the first examples of phosphine-gold-alkynyl-aliphatic **4-102** type of complexes, which containing the stable and water-soluble PTA and DAPTA ligands (Figure 4-8).⁸⁸ All of them were synthesized by the reaction of $AuCIPR_3$ with the alkynyl ligand under basic conditions to deprotonate the terminal alkynyl proton and promote coordination to gold(I) atom.⁸⁸ The compounds display solid state broad emission bands when they were excited at *ca.* 370-380 nm with maxima centered in the range 485-505 nm. The origin of the emission was attributed to a $\pi \rightarrow \pi^*(C\equiv C)$ or $\sigma(Au-P) \rightarrow \pi^*(C\equiv C)$ transitions, as reported for similar Au(I) alkynyl phosphine derivatives.

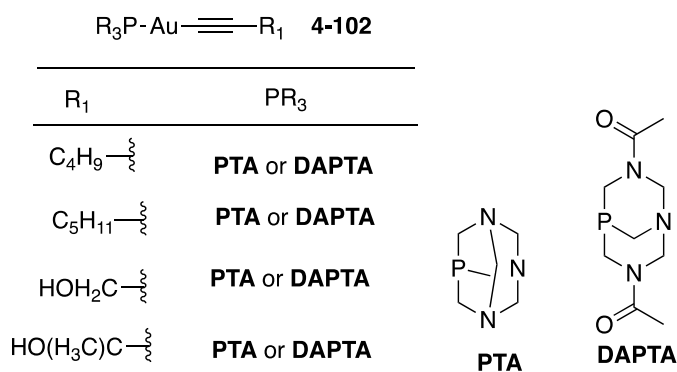


Figure 4-8 Chemical structure of the aliphatic gold(I) phosphine complexes **4-102**

Another phosphine-gold alkynyl-aromatic chromophore type of complexes has also been reported in literature. For example, urea-based gold(I) acetylide complexes **4-103a-g**, **4-104a-b** and **4-105a-b** were synthesized and characterized by Chao's group (Figure 4-9).⁸⁹ X-ray crystal structures of some of the compounds could be solved and demonstrate the presence of aurophilic contacts in some of the compounds. Complexes **4-103a-g**, **4-104b**, and **4-105a-b** show intense luminescence both in the solid state and in degassed THF solution at 298 K. Anion binding properties of all complexes have been studied by UV-vis and ¹H NMR titration experiments. In general, the log K values of **4-103a-g** with the same anion in THF depend on the substituent R on the acetylide ligand of **4-103a-g**: R = NO₂ > CF₃ ≥ Cl > H > CH₃ ≈ ^tBu ≥ OCH₃.

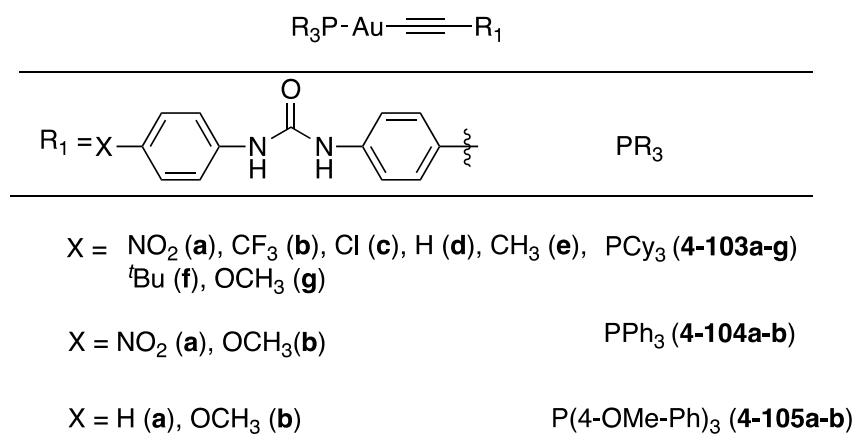
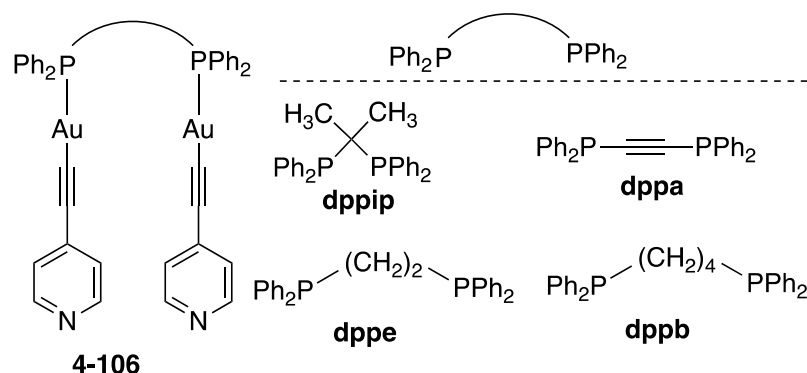


Figure 4-9 Chemical structure of the C-aromatic gold(I) phosphine complexes

The second group of alkynyl-gold(I)-phosphane derivatives are those systems containing polyphosphines. The series of dinuclear gold(I) (4-pyridyl)ethynyl complexes **4-106** were characterized by Lima group (Scheme 4-39).⁹⁰ The absorption spectra of the compounds obtained in dichloromethane solution are comparable, as expected by the fact that the chromophoric units ((4-pyridyl)ethynyl and diphenylphosphine) are constant within the series. All the compounds show a vibronically resolved band around 280 nm as shown in Figure 4-10,

while in the case of dppip, significant broadening of the bands was observed. The presence of aurophilic interactions in dppip leads to band broadening due to π - π stacking of the ethynylpyridine moieties and the appearance of a new band at ~ 310 nm corresponding to a $\sigma_{\text{Au-Au}}^* \rightarrow \pi^*$ transition. Additionally, they provided theoretical calculations and emission features of a series of alkynyl gold(I) complexes with the same chromophoric unit ((4-pyridyl)ethynyl). There is not a straightforward correlation between the presence of a $\sigma_{\text{Au-Au}}^* \leftarrow \pi^*$ transition and the presence or absence of an emission band. The analysis of the decaytimes, quantum yields and thus, the corresponding calculated rate constants demonstrated the existence of a correlation between Au(I)···Au(I) distance and the radiative rate constant for the deactivation of the emissive triplet states.



Scheme 4-39 Polynuclear gold(I) alkyne complexes with diphosphane bridging ligands

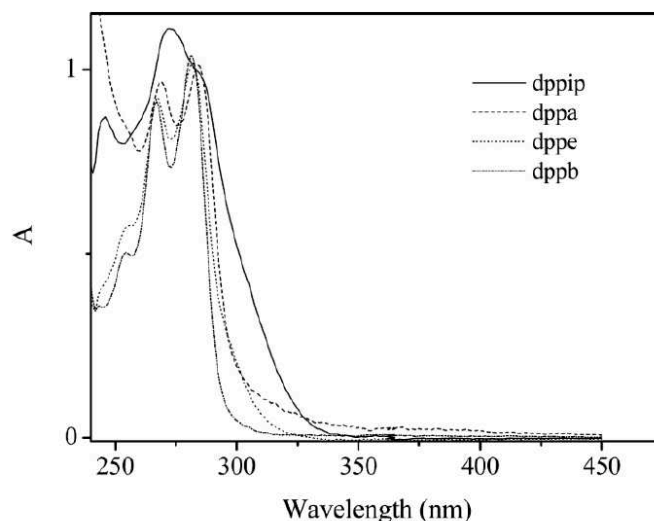


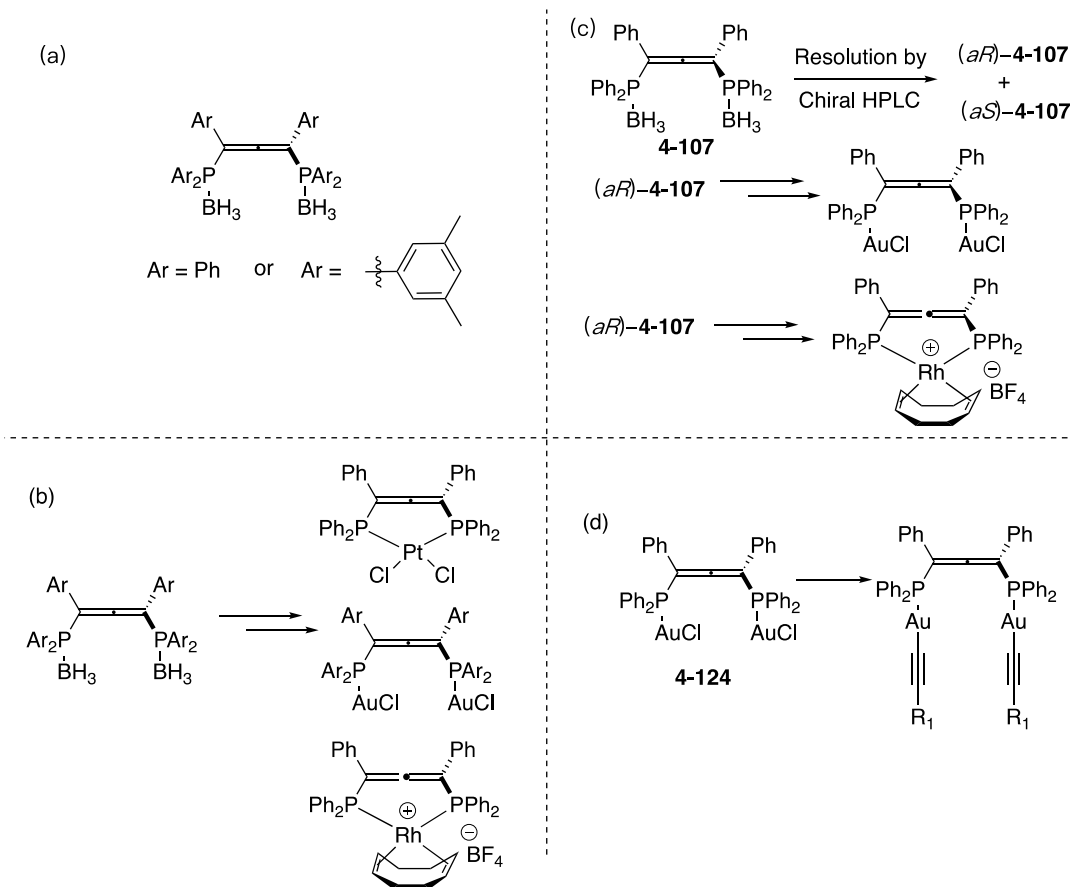
Figure 4-10 Absorption spectra of the gold(I) (4-pyridyl)ethynyl derivatives (in DCM at rt)

2. Objective of the Project

Based on previous works, we aimed herein at synthesizing a novel class of allenes bearing phosphine borane groups. Compared with bisphosphine allene **4-90**, allenyl bisphosphine diborane offers the following advantages: (a) it is very stable in the air since the borane group

protects both phosphine groups on the allene; (b) it is easy to isolate with high yields by chromatography; (c) the borane group can be deprotected easily; (d) The enantiomers of allenyl bisphosphine boranes can be separated by preparative chromatography which opens an access to other chiral metal-allenyl bisphosphine complexes besides chiral digold complex **4-93**.

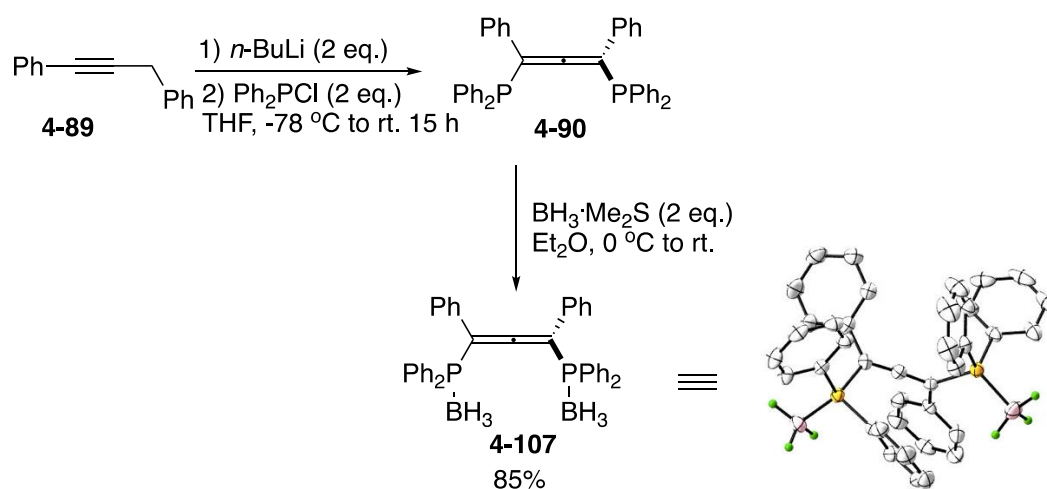
Therefore, the first objective was to synthesize allenyl bisphosphine boranes carrying different group (Scheme 4-40, a). The second objective is to prepare metal-allenyl bisphosphine complexes (Pt, Au, and Rh) starting from allenyl bisphosphine boranes (Scheme 4-40, b). The third objective is the separation of the enantiomers of allenyl bisphosphine boranes **4-107** by preparative chiral chromatography on a Chiralpak column. Then, starting from chiral allenyl bisphosphine boranes **4-107**, we planned to synthesize chiral digold complexes **4-124**, which will be analysed by specific rotation to check whether racemization occurs during the reaction. Furthermore, synthesis of chiral rhodium (I) allenyl bisphosphine complexes **4-127** starting from chiral allenyl bisphosphine boranes **4-112** will be attempted. Then, evaluation of the rhodium (I) allenyl bisphosphine complexes **4-127** in catalysis and asymmetric catalysis (Scheme 4-40, c) will be pursued. The fourth objective is to synthesize dinuclear alkynyl gold(I) complexes bearing allenyl biphosphine ligands and further study the luminescence properties of these complexes (Scheme 4-40, d).



Scheme 4-40 Objectives of allene compounds

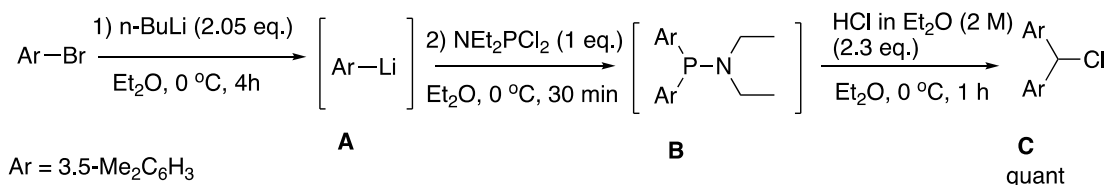
3. Synthesis of Allenyl Bisphosphine Boranes

Based on previous works, allenyl bisphosphine **4-90** can be formed following Schmidbauer's procedure.⁴⁶ It is very sensitive to air which gives a challenge for its purification and limits its application. Protecting the bisphosphine group by using $\text{BH}_3 \cdot \text{Me}_2\text{S}$ provided allenyl bisphosphine-borane adduct **4-107** in 85% yield. ^{31}P NMR analysis showed a singlet peak at 22.1 ppm. Allenyl bisphosphineborane **4-107** was characterized by X-ray crystallography. To our delight, we can synthesize the desired product **4-107** on a gram scale in good yield by following this procedure.

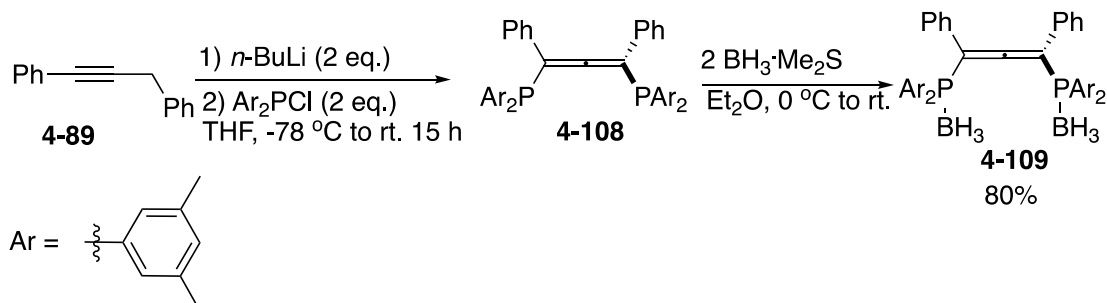


Scheme 4-41 Synthesis of allenyl bisphosphine borane ligand **4-107** by one-pot

To extend the scope of allenyl bisphosphine boranes, the synthesis of allene **4-114** was aimed. To do that, chlorodiarylphosphine reagents were prepared following the procedure from the Alexakis' group.⁹¹ The reaction starts from the Li-Br exchange to generate aryllithium intermediate **A**. Dichloro-diethylphosphinamine (NEt_2PCl_2) was added as an electrophile to be trapped by two equivalents of aryl anion from intermediate **A**. This led to form diaryl diethylphosphinamine **B**. The amine group was removed by the solution of hydrochloric acid 2 M in Et_2O to furnish chlorodiarylphosphines **C** in quantitative yield (Scheme 4-43). With chlorodiarylphosphines **C** in hand, we prepared organolithium intermediate from **4-89** with *n*-butyllithium under the same conditions as for allenyl bisphosphine **4-107**. Then, we used chlorobis(3,5-dimethylphenyl)phosphane **C** as an electrophile to provide allenyl bisphosphine **4-108**, which further treatment with two equivalents of borane dimethyl sulfide complex to generated allenyl bisphosphine borane **4-109** in 80% yield (Scheme 4-42).

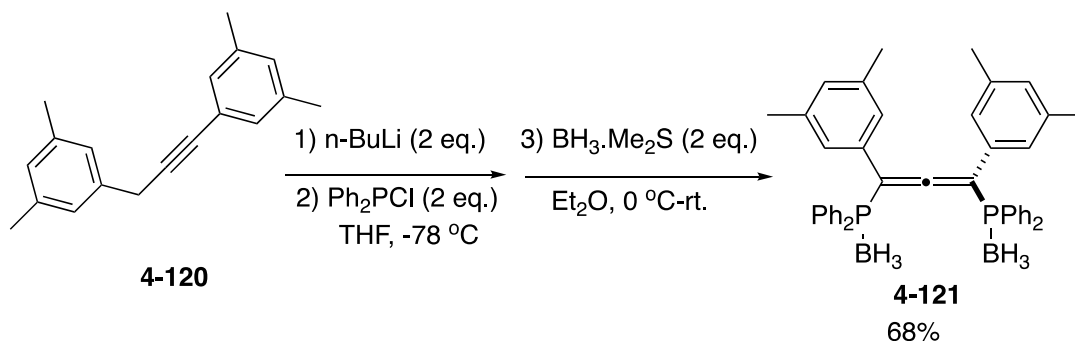


Scheme 4-42 Synthesis of chlorodiarylposphine reagents **C**



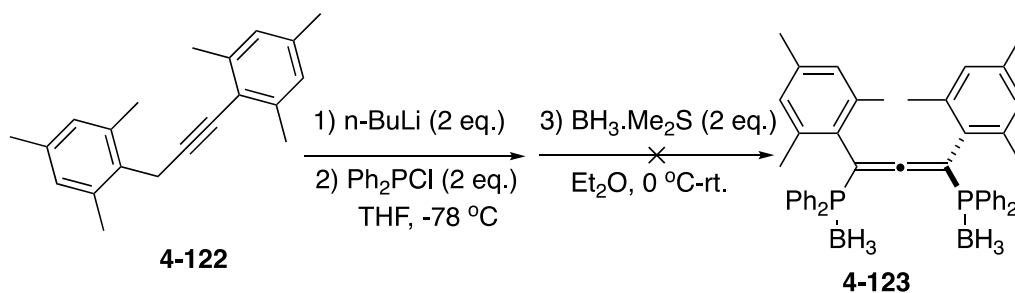
Scheme 4-43 Changing electrophilic reagents to synthesize **4-109**

Following above procedure, **4-121** can be synthesized in good yield starting from the 5,5'-(prop-1-yne-1,3-diyl)bis(1,3-dimethylbenzene) precursor **4-120**, which could be formed *via* a palladium coupling reaction of 1-ethynyl-3,5-dimethylbenzene and 1-(bromomethyl)-3,5-dimethylbenzene (Scheme 4-44).



Scheme 4-44 Changing precursor as **4-120** to prepare allene **4-121**

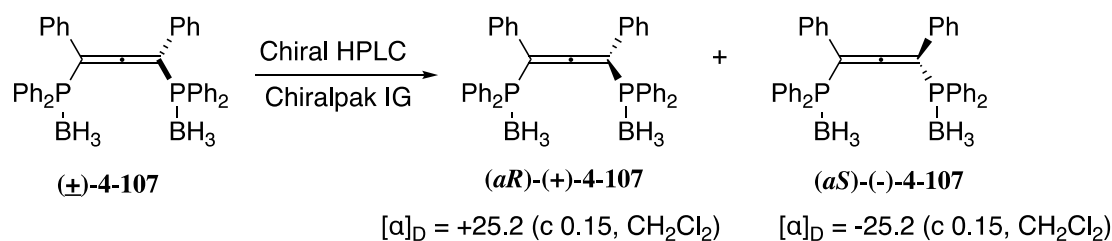
On the other hand, we also tested 2,2'-(prop-1-yne-1,3-diyl)bis(1,3,5-trimethylbenzene) **4-122** as a precursor, which was prepared *via* a palladium coupling reaction of 2-(chloromethyl)-1,3,5-trimethylbenzene and 2-ethynyl-1,3,5-trimethylbenzene. The precursor **4-122** was treated with *n*-butyllithium and chlorodiphenylphosphine for overnight. Then, treatment with borane-dimethyl sulfide complex following the same procedure as above. ³¹P NMR of this reaction was recorded and showed several peaks occurring in the range of -23 to -81ppm. We were unable to isolate **4-123** (Scheme 4-45).



Scheme 4-45 Changing precursor as **4-122** to prepare allene **4-123**

4. Resolution of Racemic Allene Bisphosphine Borane

Based on previous work in our group, we know it is impossible to separate allene **4-90** by using preparative chiral HPLC since oxidation to give mono- and bisphosphine oxide-containing allene occurred. Therefore, we are interested in the separation of the two enantiomers of racemic allene **4-107** in large scale by using preparative chiral HPLC. This analysis was performed in collaboration with Dr. Nicolas Vanthuyne (iSm2, Aix-Marseille Université). Fortunately, racemic allene **4-107** was successfully separated in large scale. The separation was conducted by Chiralpak IG column and detecting by UV-detection at 254 nm (Figure 4-11, a) and circular dichroism (Figure 4-11, b). Two enantiomers of (*aR*)-(+)-**4-107** with $[\alpha]_{\text{D}} = +25.2$ (c 0.15, CH₂Cl₂) and (*aS*)-(-)-**4-107** with $[\alpha]_{\text{D}} = -25.2$ (c 0.15, CH₂Cl₂) were obtained in excellent enantiomeric excess (*ee* > 99%) (Scheme 46).



Scheme 4-46 Resolution of racemic allene bisphosphine borane ligands by chiral HPLC

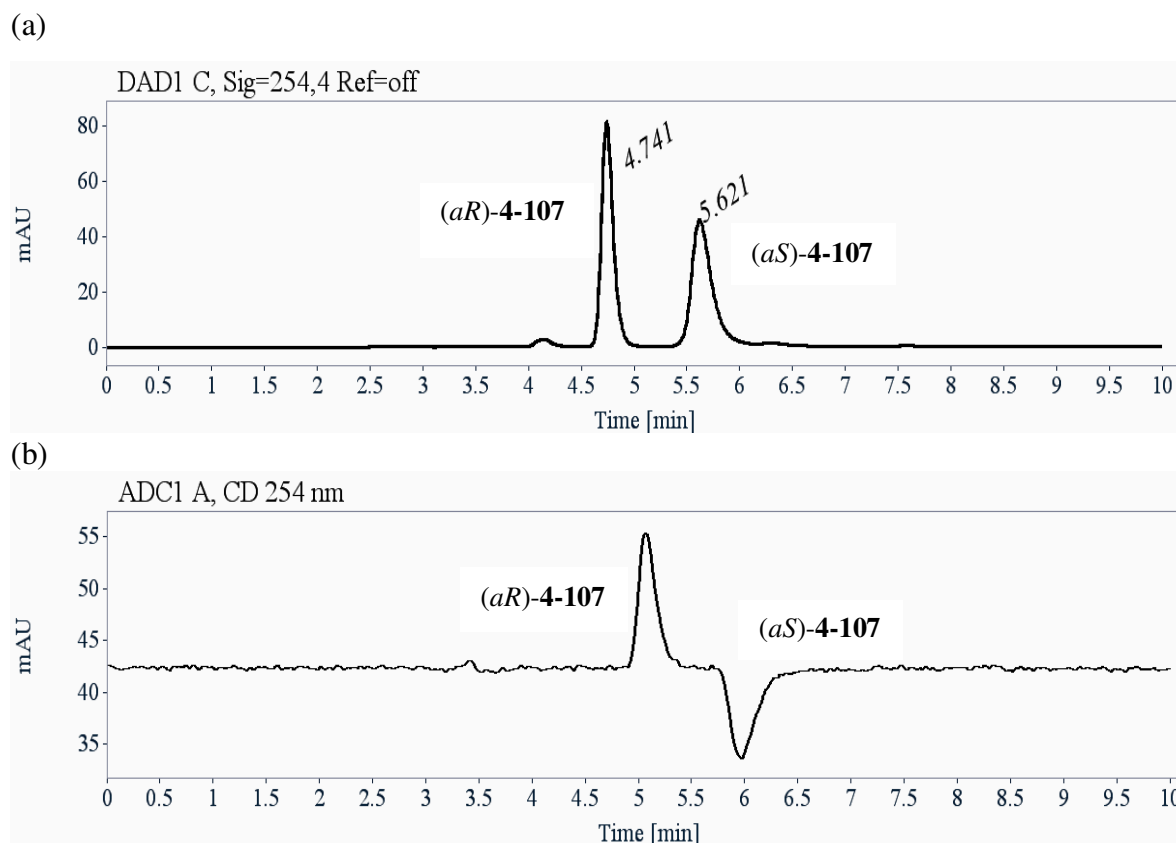
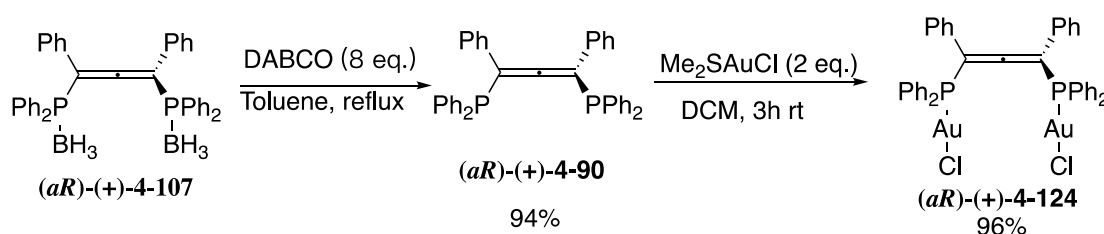


Figure 4-11 Preparative chiral HPLC of (\pm) -**4-107**. The chromatographic conditions: Chiralpak IG (250x10 mm), hexanes/ dichloromethane (60/40) as mobile phase, flow-rate = 5 mL/min, (a) UV detection at 254 nm and (b) circular dichroism detection

In order to expand its application, we synthesized digold allene complex (aR) - $(+)$ -**4-124** starting from chiral allene (aR) - $(+)$ -**4-107**, which was deprotected by using DABCO to provide allene (aR) - $(+)$ -**4-90**. Based on previous works, the gold(I) coordinated to the phosphorus atoms of **4-90** selectively to afford the dinuclear gold bisphosphine complex (aR) - $(+)$ -**4-124** in 96% yield with $[\alpha]_D = +28.2$ (c 0.17, CH_2Cl_2) (the same specific rotation values as previous), which means there is no oxidation and racemization following this procedure. And the spectroscopic data match those previously reported by our group (Scheme 4-46).⁷⁹

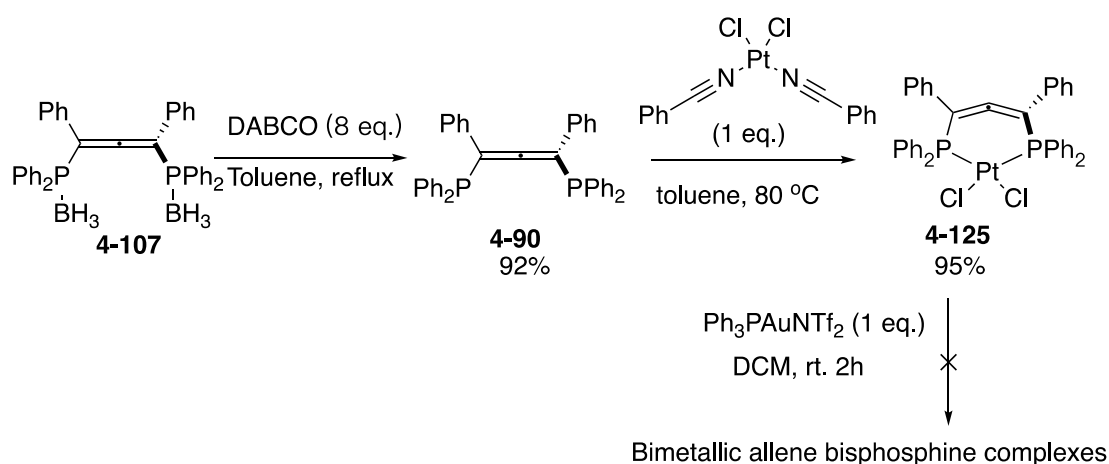


Scheme 4-46 The synthesis of (aR) - $(+)$ -**4-124** from chiral allene (aR) - $(+)$ -**4-107**

5. Metal-allenyl Bisphospine Complexes

5.1 Platinum-allenyl Bisphospine Complex

Platinum complexes bearing phosphine moieties have also been reported in the literature.⁹² Based on previous study, we envisaged the preparation of a platinum complex starting from allene **4-107**, the BH₃ group being removed by treatment with eight equivalents of DABCO in toluene to form allene **4-90** in 92% yield. Then, treatment with one equivalent of *cis*-bis(benzonitrile)dichloroplatinum(II) afforded the mononuclear platinum-allene bisphosphine complex **4-125** in quantitative yield (Scheme 4-44). The method is simple to operate and adequate to synthesize pure allene **4-90**. The spectroscopic data match those previously reported by our group.⁷⁹ Additionally, we further add gold complexes Ph₃PAuNTf₂ in order to check whether cationic gold could coordinate to the allene moiety and new bimetallic allene bisphosphine complexes could be formed. Unfortunately, we did not obtain the desired product regardless of the conditions used (Scheme 4-47).



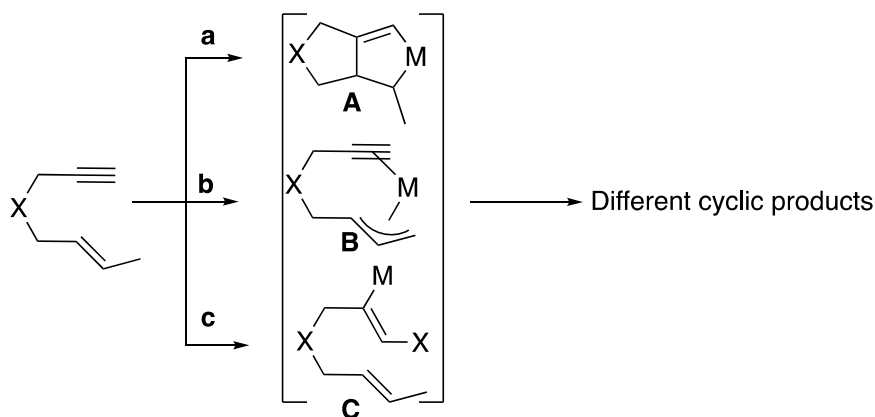
Scheme 4-47 Synthesis of platinum-allene bisphosphine complex **4-125** starting from allene **4-107** and further testing

5.2 Gold-allenyl Bisphosphine Complex

Dinuclear gold phosphine complexes bearing axial chiral ligands (*C*₂-Symmetry) have been successfully prepared by gold(I) salts and applied in asymmetric catalytic reactions.⁹³ In previous works, we have synthesized dinuclear gold-bisphosphine complex **4-124** from allene **4-107**. Based on this result, we also prepared dinuclear gold bisphosphine complex **4-126** starting from allenes bisphosphine borane **4-109** following the same procedure as Scheme 4-46, the yield is up to 92% (Scheme 4-49).

6. Rhodium (I)-catalyzed Cyclization Reactions of 1,6-Enynes

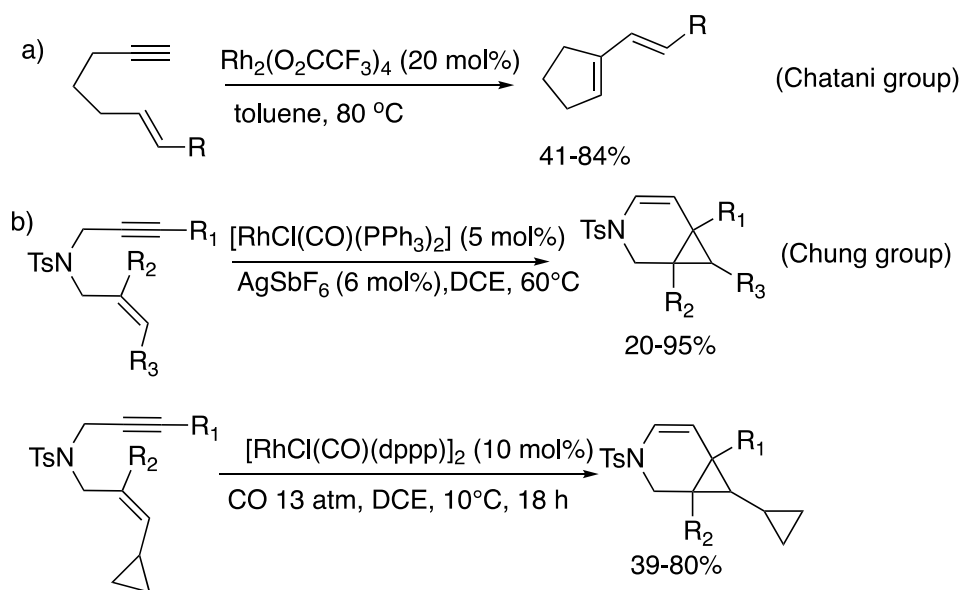
The transition metal-catalyzed cycloisomerization of enynes is a powerful method for accessing cyclic structures of higher molecular complexity from acyclic precursors. Considering the mechanistic rationales of the transition-metal-catalyzed cycloisomerization of enynes, different pathways can be considered depending on the reaction conditions and on the choice of the precatalyst. Generally, the complexation of the metal to an alkene or alkyne allows the activation of either both moieties or only one of them. Depending on the unsaturation which will react first. Generally, the complexation of the metal to an alkene or alkyne allows the activation of either both moieties or only one of them. Depending on the unsaturation which will react first, three main mechanisms are described in the literature to describe these reactions (Scheme 4-52). The simultaneous complexation of both unsaturations leads preferentially to the metallacycle intermediate **A**, which is usually followed by β -H elimination and reductive elimination to complete the catalytic cycle (Scheme 4-52, a). Almost all the transition-metal complexes could react to generate such intermediates. However, their reactivity can be quite different. The presence of a functional group in the allylic position allows the formation of a π -allyl complex **B** which could further react with the triple bond (Scheme 4-52, b). And finally, the activation of the alkyne to form the corresponding vinylmetal complex **C**, which is followed by a cyclization of the *5-exo-dig* or *6-endo-dig* type (depending on the vinylmetal complex formed) and β -H elimination to complete the cycle (Scheme 4-52, c).⁹⁴



Scheme 4-52 Three mechanistic pathways of 1,6-enynes cycloisomerization

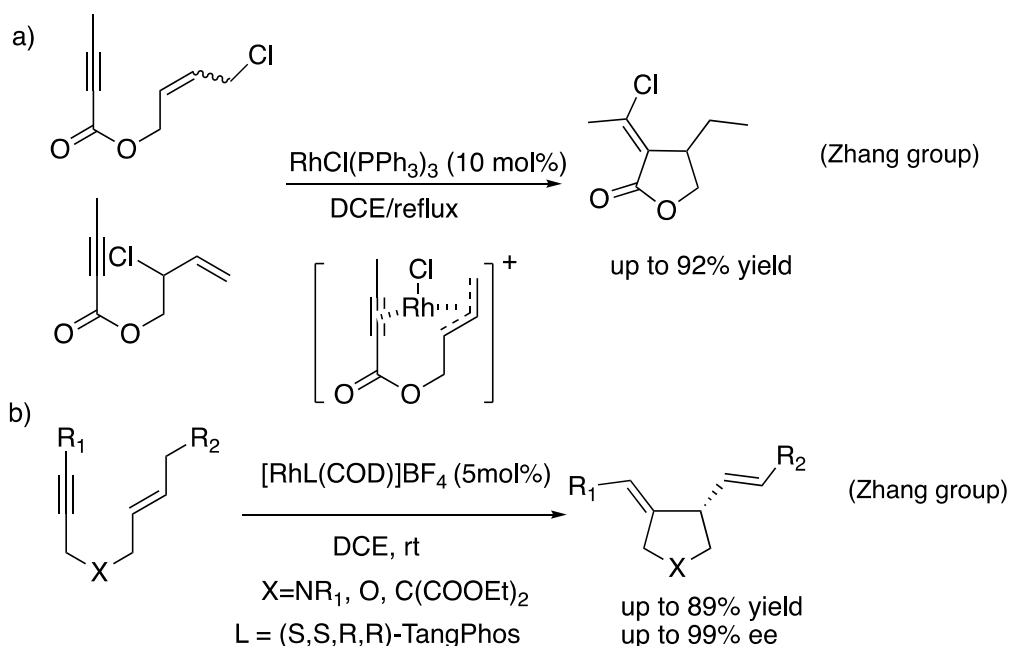
Until now, several Rhodium(I)-catalyzed cycloisomerization reactions of 1,6-enynes have been disclosed. Chatani group reported the $\text{Rh}_2(\text{O}_2\text{CCF}_3)_4$ -catalyzed skeletal reorganization of 1,6-enynes leading to 1-vinylcycloalkenes (Scheme 4-53, a). Chung group reported rhodium(I)-catalyzed cyclopropanation reactions of nitrogen-tethered 1,6-enynes to azabicyclo[4.1.0]heptenes. Moreover, Rhodium(I)-catalyzed tandem cycloisomerization and

carbonylative [3+3+1] cycloaddition reactions of a cyclopropenyne have been observed (Scheme 4-53, b).⁹⁵



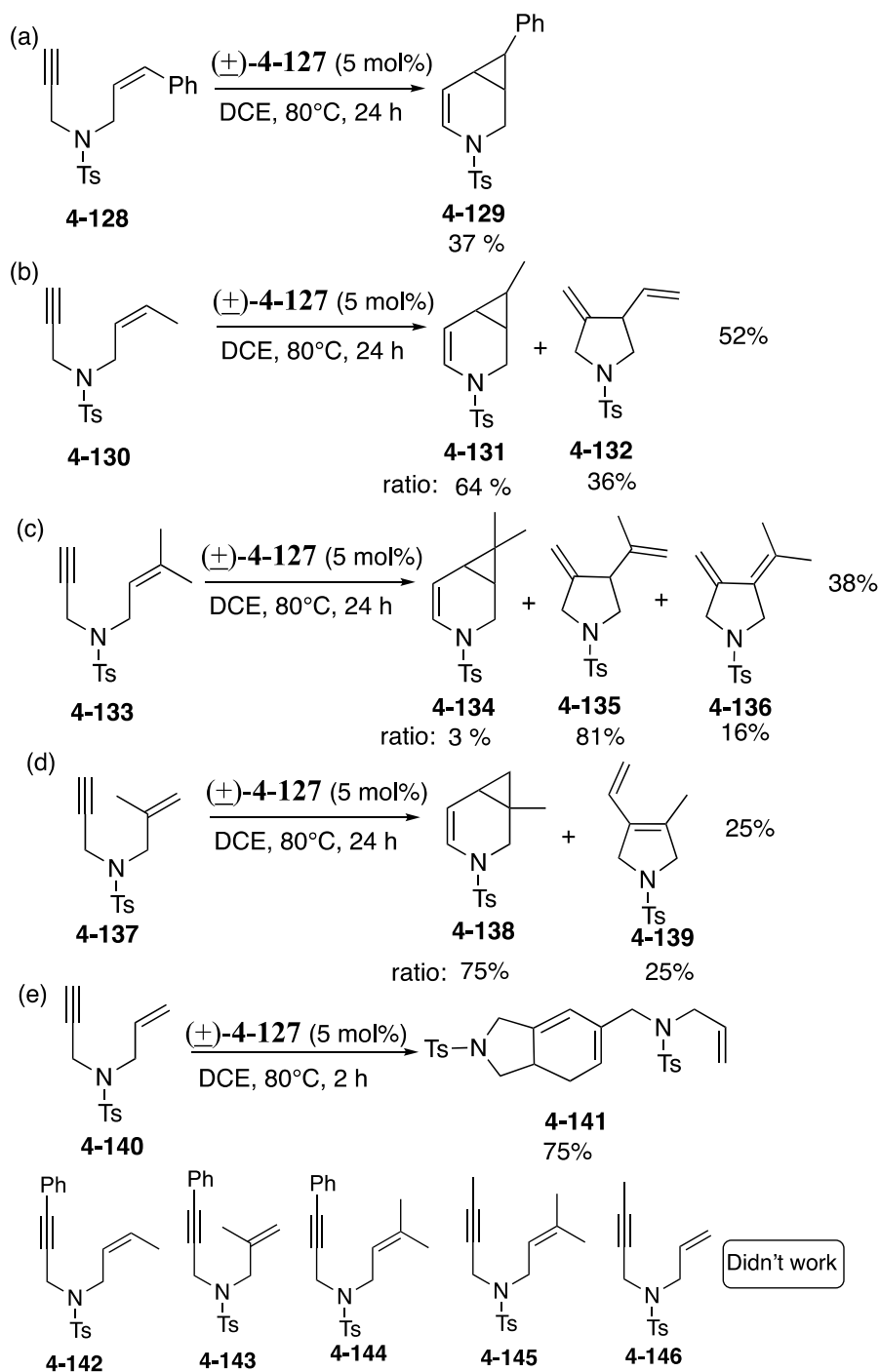
Scheme 4-53 Rhodium-catalyzed cycloisomerization of 1,6-enynes

Zhang group developed Rh(I)-catalyzed enyne cycloisomerization reaction with an intramolecular halogen shift proceeding through a π -allyl rhodium intermediate, then followed by a 5-*exo-dig* cyclization. Coordinatively unsaturated rhodium species ($[\text{Rh}(\text{COD})\text{Cl}]_2 + \text{dppb} + \text{AgSbF}_6$) only catalyzes the reaction with enyne substrates bearing a *Z*-form double bond (Scheme 4-54, a). Recently, Zhang group also developed rhodium(I)-catalyzed asymmetric cycloisomerization of (*E*)-1,6-enynes that afford highly functionalized five-membered cycles. This novel process enables (*E*)-1,6-enynes with a wide range of functionalities, including nitrogen-, oxygen-, and carbon tethered (*E*)-1,6-enynes to undergo cycloisomerization with excellent enantioselectivity, in a high-yielding and operationally simple manner (Scheme 4-54, b).⁹⁶



Scheme 4-54 Rhodium(I)-catalyzed cycloisomerization of 1,6-enynes a 5-*exo-dig* process

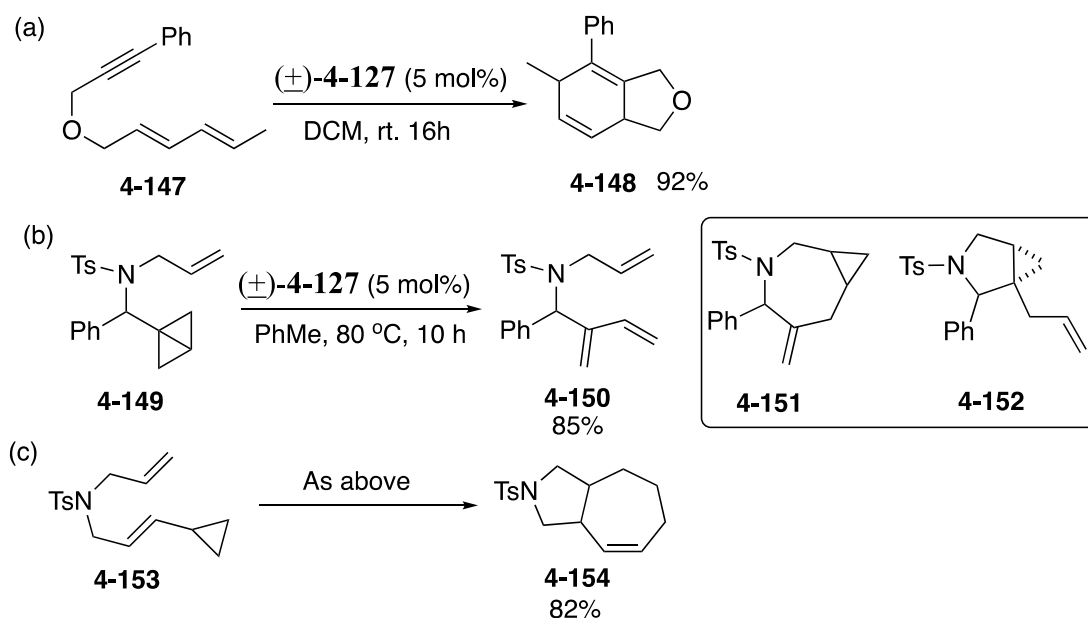
Based on the above results, we decided to test the racemic rhodium complex (\pm)-**4-118** as a precatalyst in cycloisomerization reactions of 1,6-enyne substrates to examine the reactivity and selectivity (Scheme 4-55). This work was performed in collaboration with Grédy Kiala, master student (Master 2, 2017) under the supervisions of Dr. Virginie Mouriés-Mansuy. Firstly, the reaction was run using enyne **4-128** and 5 mol% of rhodium complex (\pm)-**4-127**. This cyclization reaction gave six-membered cyclic product **4-129** in 37% yield (Scheme 4-55, a). When we experimented with enyne **4-130** under the same conditions, the products were generated in 52% yield. The ratio of six-membered cyclic product **4-131** five-membered cyclic product **4-132** was 64%:36% (Scheme 4-55, b). The reaction of the enyne **4-133** gave products in 38% yield, here, the ratio of product **4-135** and **4-136** and **4-134** was 81%:16%:3% (Scheme 4-55, c). The reaction of enyne **4-137** was also examined under the same conditions. Major six-membered cyclic product **4-138** and minor product **4-139** were obtained in ratio 75%:25% with 25% yield (Scheme 4-55, d). The reaction of the enyne **4-140** could not afford similar cycloisomerization pattern as product **4-138**. The reaction gave a cyclic product **4-141** in good yield (Scheme 4-55, e). Instead, the reaction of the enynes bearing a prenyl functional group (**4-142** - **4-144**) or methyls group (**4-145** - **4-146**) under the same conditions, did not give any products.



Scheme 4-55 Rhodium-catalyzed cycloisomerization of 1,6-enynes

We next attempted to evaluate the reactivity and selectivity of our rhodium complex $(\pm)\text{-4-127}$ with different type of substrates, such as diene-yne **4-147** and bicyclo[1.1.0]butane **4-149**, in skeletal rearrangement reactions under the condition reaction in Scheme 4-56. Cycloadduct **4-148** could be obtained in the presence of 5 mol% rhodium complexes $(\pm)\text{-4-127}$ in DCM at room temperature (Scheme 4-56, a). However, the reaction of bicyclo[1.1.0]butane **4-149** with 5 mol% rhodium complexes $(\pm)\text{-4-127}$ in PhMe at 80 °C did not give cycloadduct **4-151** and/or **4-152**. Both of them have been reported by Wipf in a rhodium(I)-catalyzed cycloisomerizations

of bicyclobutanes.⁹⁷ Instead product **4-150** was obtained in 85% (Scheme 4-56, b) when we used the compound **4-153** bearing a vinylcyclopropanes instead of bicyclo[1.1.0]butane as in **4-149**, [5 + 2] cycloaddition product **4-154** was obtained in 82% yield under the same conditions (Scheme 4-56, c).



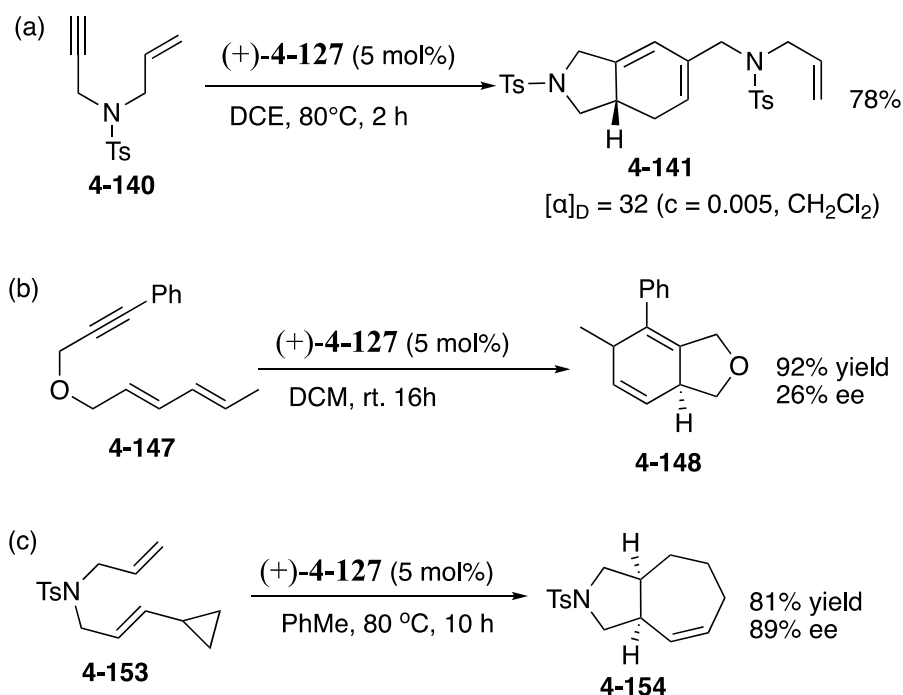
Scheme 4-56 Further catalytic tests with rhodium complexes (\pm)-**4-127**

7. Asymmetric Catalysis with Chiral Rh Complexes **4-127**

Racemic allene bisphosphine borane ligand **4-107** was separated by preparative chiral HPLC. Then, the rhodium complexes (*aS*)- and (*aR*)-**4-107** were synthesized start from (*aS*)- and (*aR*)-**4-107**, respectively and then used in asymmetric catalytic reactions. We selected some interesting rhodium(I)-catalyzed asymmetric reactions.

According to the successful cycloisomerization of 1,6-enynes by using racemic rhodium complex (\pm)-**4-127**, we then evaluated the catalytic activity of (+)-**4-127** for the asymmetric cycloisomerisation of 1,6-enynes **4-140** and **4-147**. The corresponding products **4-141** and **4-148** were obtained in 78% and 92%, respectively. We have tried to get *ee* value by HPLC. No *ee* could be precisely determined but final products exhibited optical rotation ($[\alpha]_D$ value). Products **4-141** and **4-148** were shown optical rotation value, which was $[\alpha]_D = +32$ ($c = 0.005$, CH_2Cl_2) and $[\alpha]_D = +25$ ($c = 0.005$, CH_2Cl_2), respectively (Scheme 4-57, a and b). We deduced the *ee* values of the **4-148** was 26% based on optical rotation of the literature ($[\alpha]_D = +85.3$, $c = 2.71$ in CHCl_3 , 88% *ee*).⁹⁸ The reaction of **4-153** also was examined with 5 mol% (+)-**4-127** in toluene at 80 °C for 10 h. Cyclic product **4-154** was obtained in 81% yield with $[\alpha]_D = +28$

(c 0.01, CH₂Cl₂) (Scheme 4-57, c). We also deduced the *ee* values of the **4-154** was 89% based on optical rotation of the literature ($[\alpha]_D = +30.1$, $c = 0.47\%$, CDCl₃, 96% *ee*).⁹⁹

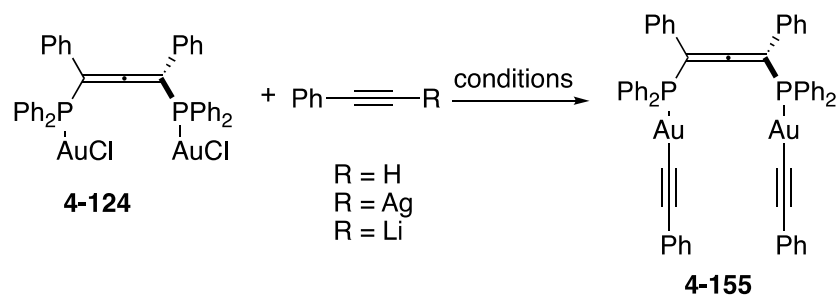


Scheme 4-57 Asymmetric catalysis of optically pure rhodium complexes (+)-**4-127**.

So these preliminary testings of the optically pure rhodium complexes (+)-**4-127** gave promising hits for asymmetric catalysis.

8. Gold-allenyl Bisphosphine Complex

Dinuclear gold alkynyl complexes bearing phosphine moieties have been reported in the literature.¹⁰⁰ We envisaged the preparation of a new gold complex with dinuclear gold bisphosphine complex **4-124**, which is the substitution of chlorine of **4-124** by an alkynyl group (Scheme 4-58). Several reaction conditions were carried out for the chlorine substitution reaction by phenylacetylene.



Scheme 4-58 Substitution of chloride by phenylacetylide

First, we tried the reaction of complexes **4-124** with phenylacetylene (R = H) under basic conditions. Unfortunately, we did not obtain the desired product regardless which conditions

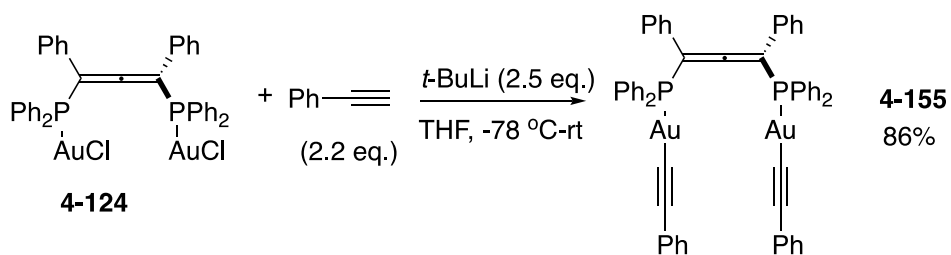
were used (Table 4-1, entries 1-3). Then, we used silver phenylacetylene (R = Ag) instead of phenylacetylene (R = H), which was prepared by trimethyl(phenylethynyl)silane treatment with AgNO₃ (1 eq.) in MeOH at room temperature. When acetone or the mixture solvent of DCM/DMF (v/v = 1/1) were used as solvent at room temperature, no target product was generated (Table 4-1, entries 4-5). To our delight, dinuclear gold alkynyl phosphine complex **4-155** was formed in DMSO or DCM solvent at 60 °C in 51% and 35% yield, respectively (Table 4-1, entries 6-7). Gratifyingly, when phenylethynyl lithium (R = Li) was used as a reagent instead of phenylacetylene, the yield of complex **4-155** increased to 85% (Table 4-1, entry 8). Phenylethynyl lithium was formed from phenylacetylene treatment with *n*-Buli (1eq.) in THF at -78°C.

Based on these results, we did the reaction of complex **4-124** with phenylacetylene in the presence of *t*-BuLi in THF under argon from -78 °C to room temperature. Dinuclear gold alkynyl phosphine complex **4-155** could be generated in 86% yield (Scheme 4-59). The absorption spectra of complex **4-155** obtained in DCM solution with different concentration as shown in Figure 4-11. The maximum absorption is around 270 nm and 283 nm. The absorption peak signal increases with the increase of complex **4-155** concentration from 5 μM to 25 μM. No absorption when the concentration is 1 μM and 2 μM.

Table 4-1 Screening the optimized reaction conditions^a

Entry	R	Base (3 eq.)	Solvent	T (°C)	4-155 (Yield %)
1	H	KOH	MeOH	rt	0
2	H	NaOH	DCM/MeOH (1/1)	rt	0
3	H	Na	EtOH/THF (1/1)	rt	0
4	Ag		Acetone	rt	0
5	Ag		DCM/DMF (1/1)	rt	0
6	Ag		DMSO	60	51
7	Ag		DCM	60	35
8	Li		THF	-78 - rt	85

^a Reaction conditions: **4-124** (0.05 mmol), base (3 eq.), phenylacetylene (2.2 eq.), solvent (2 mL), rt or 60 °C, or from -78 °C to rt.



Scheme 4-59 The synthesis of dinuclear gold alkynyl phosphine complex **4-155**

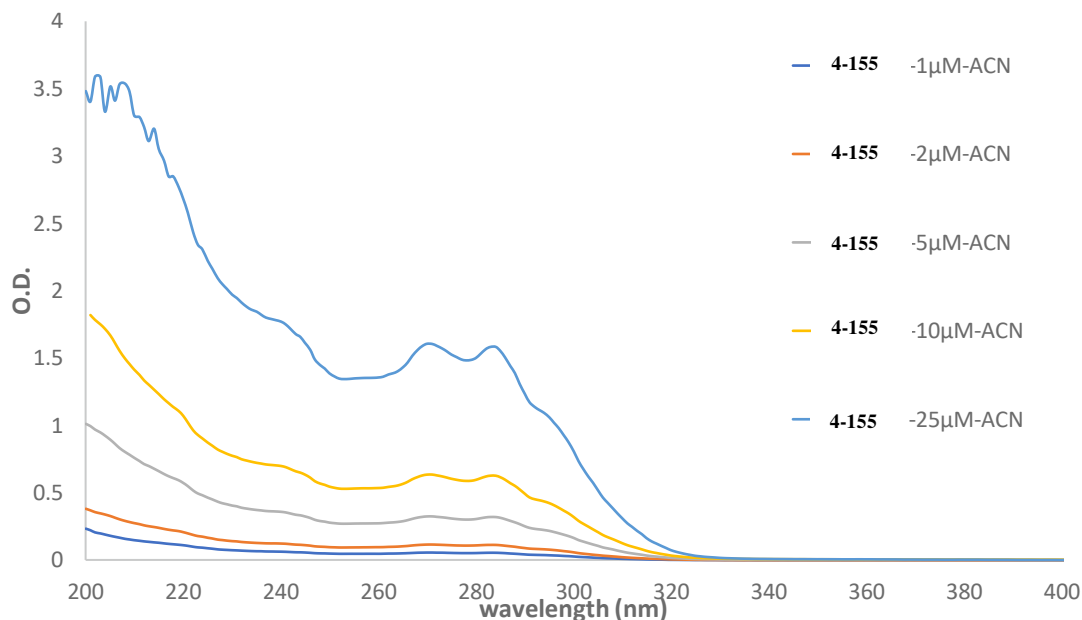
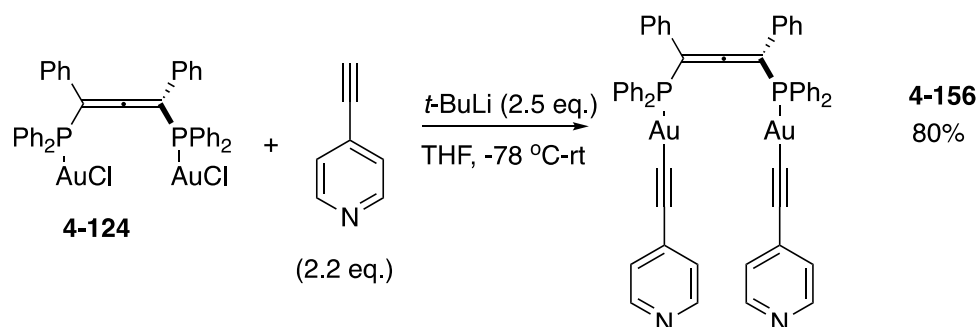


Figure 4-12 Absorption spectra of complex **4-155** (DCM solution, rt)

Similar reaction conditions can be used for the reaction of complex **4-124** with 4-ethynylpyridine to synthesize new complex **4-156** in 80% yield (Scheme 4-60). The absorption of complex **4-156** is shown on Figure 4-13, which was similar as the absorption of complex **4-155**. The maximum absorption is around 285 nm. No absorption when the concentration of complex **4-156** is 1 μM . It shows absorption starting from 2 μM concentration.



Scheme 4-60 The synthesis of dinuclear gold alkynyl phosphine complex **4-156**

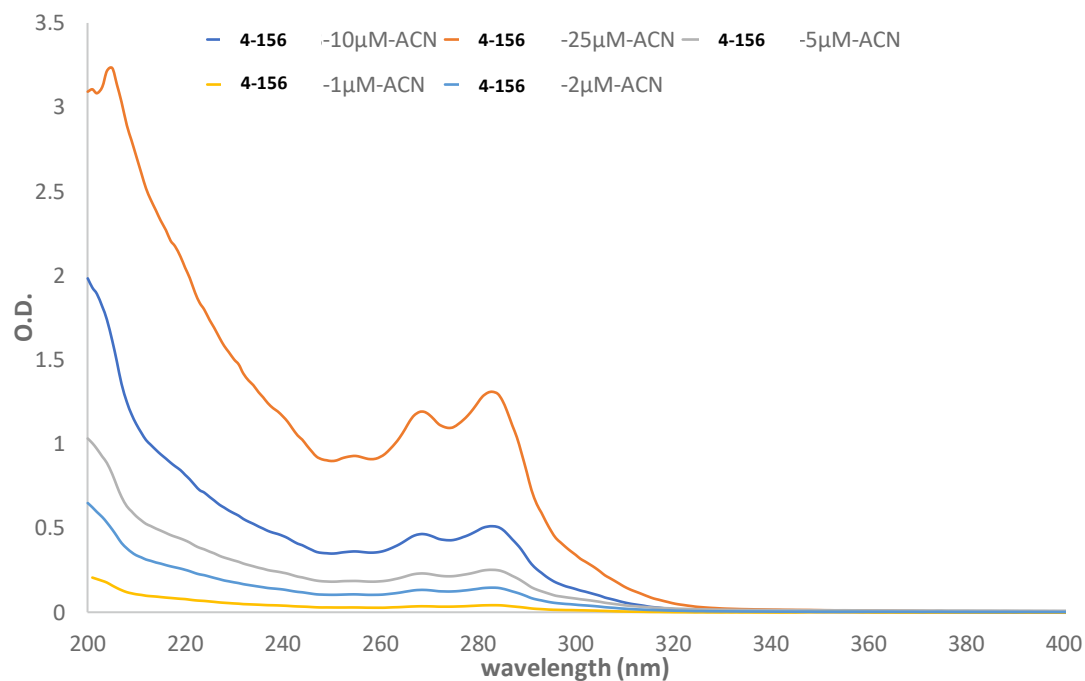


Figure 4-13 Absorption spectra of complex **4-156** (DCM solution, rt)

As expected, the absorption spectra of all gold(I) complexes **4-155** and **4-156** obtained are essentially similar to each other because of the similarity of the chromophoric centers mainly localized on the allene gold alkynyl ligand (Figure 4-12, Figure 4-13).

9. Conclusion and Perspectives

Allenes bisphosphine borane **4-107**, **4-109** and **4-121** were successfully prepared and the chiral complexes (*aR*)- and (*aS*)- **4-107** were obtained by preparative chiral HPLC. Allenyl bisphosphine borane **4-107** can be deprotected in the presence of DABCO to form allenyl bisphosphine ligand **4-90**, which easily coordinates to various metals such as platinum, gold and rhodium furnishing metal complexes. The rhodium(I) complex (\pm)-**127** bearing allenyl bisphosphine complex could be used as a precatalyst in some rhodium catalysis. It was initially used as a catalyst in cycloisomerization reactions with 1,6-enynes. The reaction successfully furnished the desired products in fair to good yields except the enyne bearing a prenyl functional group (**4-142** - **4-144**) or methyl group (**4-145** - **4-146**). Additionally, chiral rhodium complexes (+)- and (-)-**127** were generated starting from chiral allenyl bisphosphine borane derivatives (+)- and (-)-**127**, respectively. These enantiomers were investigated in asymmetric reactions in order to prepare enantiomerically pure products. The reactions of enynes **4-140**, **4-147**, and **4-153** could generate products with excellent yields. The reactions of enynes **4-140**, **4-147**, and **4-153** could generate products with excellent yields. No *ee* could be precisely determined but final products exhibited optical rotation ($[\alpha]_D$ value). We deduced the *ee* values of the **4-148** was 26% and the **4-154** was 89% based on optical rotation of the literature. These suggest enantiomeric enrichment.

Dinuclear gold alkynyl phosphine complexes **4-155** and **4-156** could be synthesized starting from gold(I) allenyl bisphosphine complex (\pm)-**124** *via* substitution of chlorides by phenylacetylene and 4-ethynylpyridine group in the presence of *t*-BuLi, respectively.

As perspectives, we are continuing to investigate the ability of allenyl bisphosphine borane substrate **4-107** for its catalytic activity and preparing new allenyl bisphosphine complexes. We will also continue to investigate the ability of optically pure rhodium complex **4-127** to produce various chiral products. Moreover, we will investigate luminescence properties of dinuclear gold alkynyl phosphine complexes **4-155** and **4-156**.

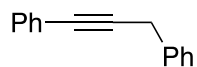
10. Experimental Section

10.1 General Information

All reactions were performed under argon atmosphere, in flame dried glassware with magnetic stirring using standard Schlenk techniques, unless otherwise mentioned. All solvents were freshly distilled prior to use: Et₂O and THF over sodium and benzophenone; CH₂Cl₂ and toluene over CaH₂. DMF and DMSO was dried and degassed before using. Technical grade solvents for extraction and chromatography were used without distillation. *t*-Butyllithium was purchased as a 2.5 M solution in hexanes and titrated before using. NaH was purchased as a 60% suspension in mineral oil and washed with pentane under argon atmosphere before using. All other reagents were purchased from commercial sources (Sigma-Aldrich, Alfa Aesar, Fluorochem, Strem Chemicals) and were used without purification, unless otherwise noted. Column chromatography was performed on Merck Geduran SI 60 A silica gel (35-70 mm). Analytical Thin-layer chromatography (TLC) was performed on Merck 60 F254 silica gel and visualized either with a UV lamp (254 nm), or using solutions of para-anisaldehyde-sulfuric acid-acetic acid in EtOH or KMnO₄-K₂CO₃ in water followed by heating. UV-Vis-NIR was recorded using JASCO V670 spectrophotometer or a Cary 5000 spectrophotometer (kinetic follow of the aziridination of trans-chalcone). Wavelengths (λ) are given in nanometer (nm) and molar extinction coefficients (ϵ) are given in M⁻¹.cm⁻¹. ¹H NMR and ¹³C NMR spectra were recorded at room temperature unless otherwise required on a Bruker Avance 300 MHz or a Bruker Avance 400 MHz spectrometer. Trimethoxybenzene was used as an internal standard to determine ¹H NMR yield. ³¹P NMR spectra were recorded at 122 MHz or 162 MHz and data are reported as follows: chemical shift in ppm with an internal probe of H₃PO₄ (85% in H₂O, δ 0.0). Shifts (δ) are given in parts per million (ppm) and coupling constants (J) are given in Hertz (Hz). High resolution mass spectra (HRMS) were obtained using a mass spectrometer MicroTOF from Bruker with an electron spray ion source (ESI) and a TOF detector at Institut Parisien de Chimie Moléculaire. Melting points (m.p.) were recorded with a SMP₃ Stuart Scientific melting point apparatus. Optical rotations were determined using a JASCO P2000. Chiral HPLC analyses were achieved on an Agilent 1260 infinity unit with pump, autosampler, oven, DAD and Jasco CD-2095 circular dichroism detector, controlled by a SRA Instrument software (Marcy l'Etoile, France) at Institut des Sciences Moléculaires de Marseille (iSm2).

10.2 General Experimental Details and Compound Characterizations

*Prop-1-yne-1,3-diyl*dibenzene (**4-89**)

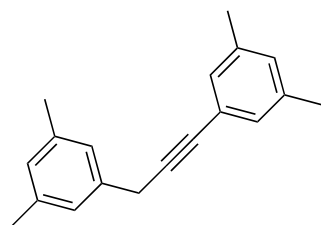


To a solution of PdCl₂(PPh₃) (240 mg, 0.34 mmol, 0.02 equiv) in Et₃N (50 mL) was added 3-phenyl-1-propyne (2.0 g, 17.2 mmol, 1.0 equiv) and PhI (2.88 mL, 25.8 mmol, 1.5 equiv) and stirred at rt. CuI (40 mg, 0.18 mmol, 0.01 equiv) was then added portion-wise into the mixture. After stirring for 2 h, the mixture was filtered over a short pad of Celite® to remove the black solid. The solution was added a saturated NH₄Cl solution (20 mL) and diluted with EtOAc (20 mL). The aqueous solution was extracted with EtOAc (2x 20 mL). The combined organic layers were washed with brine (10 mL), dried over anhydrous MgSO₄, filtered and concentrated under reduced pressure. The product was purified by flash chromatography (100% pentane) to afford **4-89** (1.30 g, 79% yield) as yellow oil.

The characterization data were identical to those previously reported.⁸⁰

¹H NMR (400 MHz, CDCl₃) δ 7.71 (d, *J* = 8.0 Hz, 1H), 7.47-7.42 (m, 3H), 7.37-7.26 (m, 5H), 7.11 (t, *J* = 7.8 Hz, 1H), 3.85 (s, 2H); ¹³C NMR (75 MHz, CDCl₃) δ 136.9, 131.8, 128.7, 128.4, 128.1, 127.9, 126.8, 123.8, 87.7, 82.8, 25.9.

*5,5'-(Prop-1-yne-1,3-diyl)*bis(*1,3*-dimethylbenzene) (**4-120**)

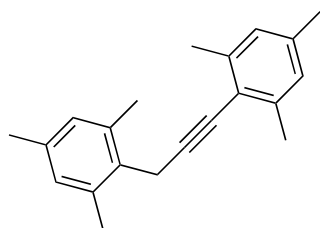


To a solution of Pd(OAc)₂ (340 mg, 1.52 mmol, 0.1 equiv), X-phos (1.08 g, 2.28 mmol, 0.15 eq.) and Cs₂CO₃ (8 g, 22.7 mmol 1.5 eq.) in dry THF (100 mL) was added 1-(bromomethyl)-3,5-dimethylbenzene (3 mg, 15.2 mmol, 1.0 equiv) and 1-ethynyl-3,5-dimethylbenzene (2.95 g, 22.7 mmol, 1.5 equiv) and stirred at 80 °C. After stirring for 6 h, the mixture was filtered over a short pad of Celite® to remove the black solid. The solution was diluted with EtOAc (20 mL). The aqueous solution was extracted with EtOAc (2x 20 mL). The combined organic layers were washed with brine (10 mL), dried over anhydrous MgSO₄, filtered and concentrated under reduced pressure. The product was purified by flash chromatography (100% pentane) to afford **4-120** (2.6 g, 69% yield) as yellow oil.

¹H NMR (400 MHz, CDCl₃) δ 7.12 (s, 2H), 7.05 (s, 2H), 6.95 (d, *J* = 1.9 Hz, 1H), 6.91 (s, 1H), 3.77 (s, 2H), 2.35 (s, 6H), 2.31 (s, 6H); ¹³C NMR (101 MHz, CDCl₃) δ 138.07, 137.75, 136.75,

129.66, 129.37, 128.22, 125.82, 123.44, 87.08, 82.63, 25.58, 21.30, 21.11; HRMS (APCI) calc. for $C_{19}H_{20}^+$ $[M+H]^+$: 249.1565, found 249.1565.

2,2'-(Prop-1-yne-1,3-diyl)bis(1,3,5-trimethylbenzene) (**4-122**)

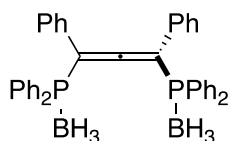


To a solution of $Pd(OAc)_2$ (331 mg, 1.48 mmol, 0.1 equiv), X-phos (1.05 g, 2.22 mmol, 0.15 eq.) and Cs_2CO_3 (7.2 g, 22.2 mmol, 1.5 eq.) in dry THF (50 mL) was 2-(chloromethyl)-1,3,5-trimethylbenzene (2.5 g, 14.8 mmol, 1 eq.) and 2-ethynyl-1,3,5-trimethylbenzene (2.56g, 17.76 mmol, 1.2 eq.) and stirred at 80 °C. After stirring for 6 h, the mixture was filtered over a short pad of Celite® to remove the black solid. The solution was diluted with EtOAc (20 mL). The aqueous solution was extracted with EtOAc (2x 20mL). The combined organic layers were washed with brine (10 mL), dried over anhydrous $MgSO_4$, filtered and concentrated under reduced pressure. The product was purified by flash chromatography (100% pentane) to afford **4-122** (2.4g, 60%) as yellow solid

M.p. = 121-124°C;

1H NMR (400 MHz, $CDCl_3$) δ 6.87 (s, 2H), 6.80 (s, 2H), 3.74 (s, 2H), 2.43 (s, 6H), 2.31 (s, 6H), 2.27 (s, 3H), 2.24 (s, 3H); ^{13}C NMR (101 MHz, $CDCl_3$) δ 139.90, 136.73, 136.05, 135.88, 131.70, 128.88, 127.34, 120.64, 94.96, 77.92, 21.21, 20.93, 20.86, 19.97, 19.86. HRMS (APCI) calc. for $C_{21}H_{25}$ $[M+H]^+$: 276.1878, found 276.1878.

1,3-Bis(diphenylphosphino borane)-1,3-diphenylpropa-1,2-diene (**4-107**)



To a solution of **4-89** (1.50 g, 7.81 mmol, 1 equiv) in THF (80 mL) was added *n*-BuLi (6.50 mL of a 2.5 M in hexanes, 16.17 mmol, 2.1 equiv) at -78 °C. After 1 h, the solution of chlorodiphenyl phosphine (3.0 mL, 16.17 mmol, 2.1 equiv) in THF (10 mL) was added into the mixture at the same temperature. The mixture was slowly warmed to rt for 15 h and concentrated under reduced pressure to form crude product **4-90**. Which is stable under argon atmosphere. A solution of **4-90** in 50 mL Et_2O , then slowly added $BH_3 \cdot Me_2S$ (2 eq.) at 0 °C. The mixture was slowly warmed to rt for 1h. The solution was added H_2O (20 mL) and CH_2Cl_2 (20 mL). The aqueous solution was extracted with CH_2Cl_2 (2x 20 mL). The combined organic

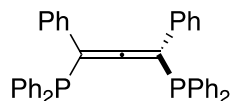
layers were washed with brine (10 mL), dried over anhydrous MgSO₄, filtered and concentrated under reduced pressure. Purification by chromatography on silica gel using DCM/pentane (1/2) as eluent to afford **4-107** (3.9 g, 85% yield) as a yellow solid.

M.p. = 210-212°C;

¹H NMR (400 MHz, CDCl₃) δ 7.64 - 7.14 (m, 30H), 1.29 (s, 6H); ¹³C NMR (101 MHz, CDCl₃) δ 213.30, 133.69, 133.56, 133.16, 133.03, 131.72, 131.69, 131.40, 131.37, 130.91, 130.85, 130.79, 130.74, 128.85, 128.85, 128.72, 128.71, 128.58, 128.58, 128.54, 128.53, 128.47, 128.47, 128.42, 128.42, 128.40, 127.65, 127.65, 127.29, 126.54, 102.59, 102.47, 101.93, 101.81; ³¹P NMR (162 MHz, CDCl₃) δ 22.12; ¹¹B NMR (96 MHz, CDCl₃) δ -36.28; HRMS (ESI) calcd. for C₃₉H₃₆B₂P₂ ([M + H]⁺) 589.2478 found 589.2479.

Chiral HPLC separation Chromatographic conditions: Chiralpak IG (250x10 mm), hexanes/dichloromethane (60/40) as mobile phase, flow-rate = 5 mL/min, (a) UV detection at 254 nm (first column) and circular dichroism detection (second column). Retention time for first enantiomer = 4.74 min [(-, CD 254 nm)-**4-107**] with ee > 99%, [α]_D = 25.2 (c 0.15, CH₂Cl₂), (*R*)-form; for second enantiomer = 5.62 min[(+, CD 254 nm)] with ee > 99%, [α]_D = - 25.2 (c 0.15, CH₂Cl₂), (*S*)-form.

1,3-Bis(diphenylphosphino)-1,3-diphenylpropa-1,2-diene (4-90)

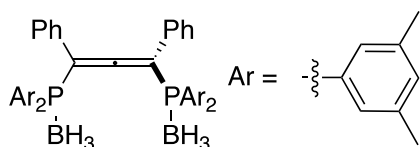


To a solution of **4-107** (117 mg, 0.2 mmol, 1 equiv) in fresh degassed toluene (5 mL) was added DABCO (179 mg, 1.6 mmol, 8 equiv), then reflux for 1 h. The mixture was slowly warmed to rt and concentrated under reduced pressure. Then filtered over a small column of neutral aluminum oxide and washed with 30 mL mixture solvent of DCM/pentane (1/2). The solvent was removed on the rotary evaporator to form **4-90** (103 mg, 92%) as white solid (Note: The product was stable in the solid under argon atmosphere.)

The characterization data were identical to those previously reported.⁴⁶

¹H NMR (400 MHz, CDCl₃) δ 7.47 (d, J = 8.4 Hz, 5H), 7.35-7.12 (m, 22H), 7.01 (t, J = 7.7 Hz, 3H); ¹³C NMR (100 MHz, CDCl₃) δ 209.9 (d, ²J_{CP} = 3.5 Hz, C), 136.0, 135.9, 135.8, 135.6, 135.2, 135.0, 134.9, 134.8, 133.8, 133.6, 132.0, 131.7, 131.6, 129.6, 129.2, 128.8, 128.7, 128.6, 128.5, 128.4, 128.3, 128.2, 128.1, 128.0, 127.7, 127.4, 127.2, 127.1, 127.0, 105.0 (d, ¹J_{CP} = 3.6 Hz, C), 104.8 (d, ¹J_{CP} = 3.0 Hz, C); ³¹P NMR (162 MHz, CDCl₃) δ -8.8.

1,3-Bis(bis(3,5-dimethylphenyl)phosphino borane)-1,3-diphenylpropa-1,2-diene (4-109)

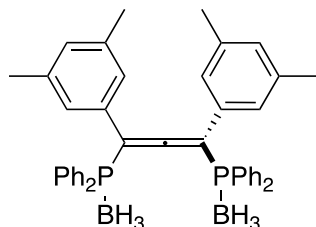


To a solution of **4-89** (1.0 g, 5.19 mmol, 1 equiv) in THF (67 mL) was added *n*-BuLi (4.30 mL of a 2.5 M in hexanes, 10.7 mmol, 2.07 equiv) at -78 °C. The solution of chlorobis(3,5-dimethylphenyl) phosphine (3.0 g, 10.9 mmol, 2.1 equiv) in THF (7 mL) was added into the mixture at the same temperature. The mixture was slowly warmed to rt for 15 h and concentrated under reduced pressure to obtain **115** (3.5 g, quant) as brown oil. Which is stable under argon atmosphere. A solution of **4-108** in 50 mL Et₂O, then slowly added BH₃.Me₂S (2 equiv) at 0 °C. The mixture was slowly warmed to rt for 1h. The solution was added H₂O (20 mL) and CH₂Cl₂ (20 mL). The aqueous solution was extracted with CH₂Cl₂ (2x 20 mL). The combined organic layers were washed with brine (10 mL), dried over anhydrous MgSO₄, filtered and concentrated under reduced pressure. Purification by chromatography on silica gel using DCM/pentane (1/2) as eluent to afford **4-109** (2.9 g, 80% yield) as a yellow solid.

M.p. = 220-222°C;

¹H NMR (400 MHz, CDCl₃) δ 7.35 - 7.23 (m, 10H), 7.22 - 7.11 (m, 10H), 7.05 (s, 2H), 2.25 (s, 12H), 2.20 (s, 12H), 1.30 (d, J = 3.0 Hz, 6H). ³¹P NMR (162 MHz, CDCl₃) δ 21.50; ¹¹B NMR (128 MHz, CDCl₃) δ -36.35.

1,3-Bis(diphenylphosphino borane)-1,3-bis(3,5-dimethylphenylpropa)-1,2-diene (4-121)



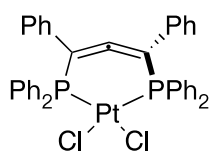
To a solution of **4-120** (1.0 g, 5.19 mmol, 1 equiv) in THF (67 mL) was added *n*-BuLi (4.30 mL of a 2.5 M in hexanes, 10.7 mmol, 2.07 equiv) at -78 °C. The solution of chlorobis(3,5-dimethylphenyl) phosphine (3.0 g, 10.9 mmol, 2.1 equiv) in THF (7 mL) was added into the mixture at the same temperature. The mixture was slowly warmed to rt for 15 h and concentrated under reduced pressure to obtain **115** (3.5 g, quant) as brown oil. Which is stable under argon atmosphere. Then slowly added BH₃.Me₂S (2 equiv) at 0 °C. The mixture was slowly warmed to rt for 1h. The solution was added H₂O (20 mL) and CH₂Cl₂ (20 mL). The aqueous solution was extracted with CH₂Cl₂ (2x 20 mL). The combined organic layers were washed with brine (10 mL), dried over anhydrous MgSO₄, filtered and concentrated under

reduced pressure. Purification by chromatography on silica gel using DCM/pentane (1/2) as eluent to afford **4-121** (2.9 g, 80% yield) as a yellow solid.

M.p. = 216-219°C;

^1H NMR (400 MHz, CDCl_3) δ 7.57 - 7.34 (m, 20H), 6.92 (d, J = 13.3 Hz, 6H), 2.24 (s, 12H), 1.47 - 0.92 (m, 6H); ^{13}C NMR (101 MHz, CDCl_3) δ 213.60, 137.91, 133.78, 133.69, 133.40, 133.31, 131.65, 131.63, 131.42, 131.40, 130.81, 130.76, 130.72, 130.68, 130.09, 128.80, 128.70, 128.67, 128.61, 128.57, 128.03, 127.63, 127.06, 126.50, 126.48, 126.45, 102.09, 101.50, 21.34; ^{31}P NMR (162 MHz, CDCl_3) δ 21.57; ^{11}B NMR (128 MHz, CDCl_3) δ -36.02; HRMS (ESI) calcd. for $\text{C}_{43}\text{H}_{45}\text{B}_2\text{P}_2$ ($[\text{M} + \text{H}]^+$) 645.3104 found 645.3108.

Dichloroplatinum(II)-(1,3-Diphenylpropa-1,2-diene-1,3-diyl)-bis(diphenylphosphine) (**4-125**)

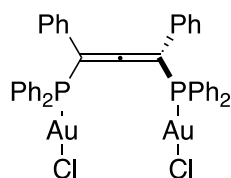


To a solution of **4-90** (117 mg, 0.2 mmol, 1 equiv) in fresh degassed toluene (10 mL) was added DABCO (179 mg, 1.6 mmol, 8 equiv), then reflux for 1 h. The mixture was slowly warmed to rt and concentrated under reduced pressure. Then filtered over a small column of neutral aluminum oxide and washed with 30 mL mixture solvent of DCM/pentane (1/2) under nitrogen flow. The solvent was removed on the rotary evaporator to form **4-125** (103 mg, 92%) as white solid (Note: The product was stable in the solid under argon atmosphere.) A solution of **4-125** (103 mg, 0.185 mmol, 1 equiv) and *cis*-bis(benzonitrile)dichloroplatinum(II) (82 g, 0.185 mmol, 1 equiv) in toluene (6 mL) was stirred at 80 °C for 20 h. The mixture was filtered over a short pad of Celite[®] and concentrated under reduced pressure. The product was recrystallized by diffusion of toluene into the solution of crude product in CHCl_3 to give **4-117** (145 mg, 0.95) as a brown solid. (Note: the product is not stable in the air and moisture).

The characterization data were identical to those previously reported.⁷⁹

^1H NMR (300 MHz, CDCl_3) δ 10.54-10.47 (m, 3H), 9.73-9.66 (m, 6H), 9.28-9.13 (m, 11H), 8.98 (t, J = 7.5 Hz, 3H), 8.79 (t, J = 7.7 Hz, 4H), 8.07 (d, J = 7.6 Hz, 3H); ^{13}C NMR (100 MHz, CD_2Cl_2) δ 198.9 (t, $^2J_{\text{CP}} = 5.1$ Hz, C), 136.6, 136.5, 134.2, 134.1, 133.2, 131.8, 131.7, 131.1, 130.0, 129.9, 129.8, 129.7, 129.2, 128.9, 128.7, 128.5, 128.4, 128.3, 128.2, 128.0, 104.5; ^{31}P NMR (162 MHz, CDCl_3) δ 98.7 (P-Pt, $^1J_{\text{P-Pt}} = 4371$ Hz).

Dichlorogold(I)-(1,3-diphenylpropa-1,2-diene-1,3-diyl)-bis(diphenylphosphine) (**4-124**)

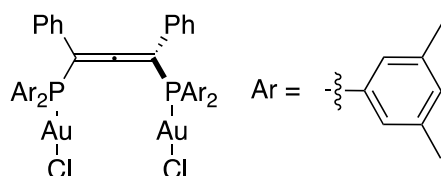


To a solution of **4-107** (117 mg, 0.2 mmol, 1 equiv) in fresh degassed toluene (10 mL) was added DABCO (179 mg, 1.6 mmol, 8 equiv), then reflux for 1 h. The mixture was slowly warmed to rt and concentrated under reduced pressure. Then filtered over a small column of neutral aluminum oxide and washed with 30 mL mixture solvent of DCM/pentane (1/2) under nitrogen flow. The solvent was removed on the rotary evaporator to form **4-90** (105 mg, 94%) as white solid (Note: The product was stable in the solid under argon atmosphere.) A solution of **4-90** (105 mg, 0.185 mmol, 1 equiv) and AuCl(Me₂S) (106 mg, 0.37, 2 equiv) in CH₂Cl₂ (5 mL) was stirred at rt for 3 h. The mixture was concentrated under reduced pressure. The residue was purified by a precipitation with pentane and CH₂Cl₂ to obtain **4-124** (182 mg, 96%) as a white solid.

The characterization data were identical to those previously reported.⁷⁹

¹H NMR (400 MHz, CDCl₃) δ 7.60-7.31 (m, 30H); ¹³C NMR (100 MHz, CDCl₃) δ 213.1, 135.2, 135.1, 135.0, 134.1, 134.0, 133.5, 132.9, 132.7, 132.4, 131.8, 131.5, 130.3, 130.2, 130.1, 129.8, 129.7, 129.6, 129.5, 129.4, 129.3, 129.2, 129.1, 129.0, 128.9, 127.8, 127.7, 127.5, 127.2, 126.8, 126.6, 104.4, 103.9; ³¹P NMR (162 MHz, CDCl₃) δ 30.2.

(1,3-Diphenylpropa-1,2-diene-1,3-diyl)-bis(chlorogold(I) bis(3,5-dimethylphenylphosphine))
(4-126)

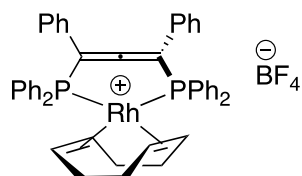


To a solution of **4-109** (69 mg, 0.1 mmol, 1 equiv) in fresh degassed toluene (10 mL) was added DABCO (89 mg, 0.8 mmol, 8 equiv), then reflux for 1 h. The mixture was slowly warmed to rt and concentrated under reduced pressure. Then filtered over a small column of neutral aluminum oxide and washed with 20 mL mixture solvent of DCM/pentane (1/2) under nitrogen flow. The solvent was removed on the rotary evaporator to form **4-108** (60 mg, 90%) as yellow solid (Note: The product was stable in the solid under argon atmosphere.) A solution of **4-108** (60 mg, 0.089 mmol, 1 equiv) and AuCl(Me₂S) (52 mg, 0.178, 2 equiv) in CH₂Cl₂ (5 mL) was stirred at rt for 3 h. The mixture was concentrated under reduced pressure. The residue was purified by a precipitation with pentane and CH₂Cl₂ to obtain **4-126** (93 mg, 92%) as a white solid.

The characterization data were identical to those previously reported.⁷⁹ (Note: the product is stable in the air and moisture).

¹H NMR (300 MHz, CDCl₃) δ 7.66-7.63 (m, 4H), 7.37-7.34 (m, 6H), 7.24-7.20 (m, 6H), 7.09 (s, 2H), 6.93 (d, J = 15 Hz, 4H), 2.25 (s, 12H), 2.15 (s, 12H); ¹³C NMR (75 MHz, CDCl₃) δ 212.3, 139.1, 138.7, 136.4, 134.3, 133.1, 131.4, 130.53, 129.2, 127.8, 127.3, 126.6, 126.5, 125.7, 104.5, 103.8, 21.4; ³¹P NMR (162 MHz, CDCl₃) δ 29.3.

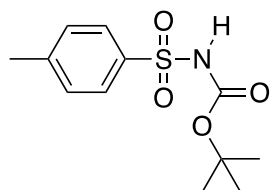
Rhodium-allene bisphosphine complex (4-127)



To a solution of **4-107** (117 mg, 0.2 mmol, 1 equiv) in fresh degassed toluene (10 mL) was added DABCO (179 mg, 1.6 mmol, 8 equiv), then reflux for 1 h. The mixture was slowly warmed to rt and concentrated under reduced pressure. Then filtered over a small column of neutral aluminum oxide and washed with 30 mL mixture solvent of DCM/pentane (1/2) under nitrogen flow. The solvent was removed on the rotary evaporator to form **4-90** (103 mg, 92%) as white solid (Note: The product was stable in the solid under argon atmosphere.) A solution of **4-90** (103 mg, 0.185 mmol, 1 equiv) and bis(1,5-cyclooctadiene) rhodium(I) tetra fluoroborate (75 mg, 0.185 mmol, 1 equiv) in 10 mL DCM, the mixture was stirred at room temperature for 3h. Then half of the solvent was evaporated on vacuum, the residue was precipitated with the mixture solvent of pentane/Et₂O (7/3) to afford the complex **4-127** after filtration, which is brown solid (135 mg, 85%).

M.p. = 204-212°C; ¹H NMR (400 MHz, CD₂Cl₂) δ 8.48-8.29 (m, 4H), 7.84-7.74 (m, 6H), 7.54-7.41 (m, 2H), 7.35-7.31 (m, 4H), 7.12 (t, 3J = 7.5 Hz, 2H), 7-6.96 (m, 4H), 6.90 (t, 3J = 7.7 Hz, 4H), 5.87 (d 3J = 7.7 Hz, 4H), 5.03-4.92 (m, 2H), 4.31 (q 3J = 8 Hz, 2H), 2.69-2.63 (m, 4H), 2.16-2.10 (m, 4H); ¹³C NMR (100 MHz, CD₂Cl₂) δ 192.93, 136.62, 136.47, 133.37, 133.27, 132.97, 132.89, 132.55, 131.65, 130.22, 130.11, 129.74, 129.70, 128.67, 128.91, 128.84, 128.68, 128.59, 128.35, 128.21, 104.19, 103.7, 102.98, 94.24, 32.96, 27.81; ³¹P NMR (162 MHz, CD₂Cl₂) δ 102.31 (d, ¹J_{P-Rh} = 171.1 Hz); ¹⁹F NMR (376 MHz, CD₂Cl₂) δ -153.84 (d, ¹J_{B-F} = 19.2 Hz). HRMS (ESI) Calcd for C₄₇H₄₂P₂Rh(CH₃OH) (M+CH₃OH) 803.21, found 803.1947.

N-Boc-*p*-toluenesulfonamide (**S1**)

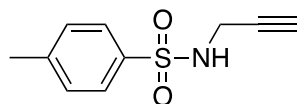


To a solution of *p*-toluenesulfonamide (7.0 g, 40.9 mmol, 1 equiv) in CH₂Cl₂ (40 mL) were added Et₃N (6.25 mL, 45.0 mmol, 1.1 equiv) and DMAP (0.5 g, 4.09 mmol, 0.1 equiv) at rt. The reaction was cooled to 0 °C and the solution of Boc₂O (10.3 g, 47.0 mmol, 1.15 equiv) in CH₂Cl₂ (80 mL) was added to the solution and then warmed to rt. After stirring for 15 h, the mixture was concentrated under reduced pressure and then dissolved in Et₂O (50 mL). A solution of 1 M HCl (20 mL) was added. The aqueous phase was extracted with Et₂O (3 x 50 mL). The combined organic layers were washed with brine (20 mL), dried over anhydrous Mg₂SO₄, filtered and concentrated under reduced pressure. Purification by recrystallization in refluxing hexanes/Et₂O (9/1) for overnight afforded **S1** (11.3 g, quant) as a white solid.

The characterization data were identical to those previously reported.¹⁰²

¹H NMR (300 MHz, CDCl₃) δ 7.90 (d, *J* = 8.4 Hz, 2H), 7.34 (d, *J* = 8.5 Hz, 2H), 2.45 (s, 3H), 1.38 (s, *J* = 0.7 Hz, 9H).

4-Methyl-*N*-(*prop*-2-yn-1-yl)benzenesulfonamide (**S2**)



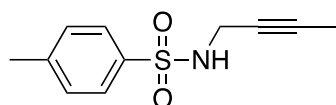
To a solution of **S1** (2.0 g, 7.4 mmol, 1 equiv) in DMF (8 mL) was added K₂CO₃ (1.5 g, 11.1 mmol, 1.5 equiv). After stirring at rt for 1 h, 3-bromoprop-1-yne (0.66 mL, 7.4 mmol, 1 equiv) was added and the resulting yellow solution was stirred for 18 h. The reaction mixture was diluted with Et₂O (20 mL) and quenched with a saturated aqueous NH₄Cl solution (30 mL). The aqueous phase was extracted with Et₂O (2x30 mL). The combined organic layers were washed with brine (20 mL), dried over anhydrous MgSO₄, filtered and concentrated under reduced pressure. The resulting crude product was dissolved in CH₂Cl₂ (6 mL) and trifluoroacetic acid (2.2 mL, 24.5 mmol, 3.3 equiv) was added. The resulting mixture was stirred for 20 h. A solution of NaHCO₃ (20 mL) was slowly added, then the mixture was diluted with CH₂Cl₂ (20 mL). The aqueous phase was extracted with CH₂Cl₂ (3x 20 mL). The combined organic layers were washed with brine (20 mL), dried over anhydrous MgSO₄, filtered and concentrated under reduced pressure. Purification by column chromatography on

silica gel using EtOAc/pentane (1/9) as eluent afforded **S2** (1.25 g, 80% yield) as a pale brown solid pure product **S2**.

The characterization data were identical to those previously reported.¹⁰²

¹H NMR (400 MHz, CDCl₃) δ 7.77 (d, *J* = 8.3 Hz, 2H), 7.32 (d, *J* = 8.0 Hz, 2H), 3.83 (d, *J* = 2.5 Hz, 2H), 2.43 (s, 3H), 2.11 (t, *J* = 2.5 Hz, 1H).

N-(But-2-ynyl)-4-methyl(benzenesulfonamide (**S3**))

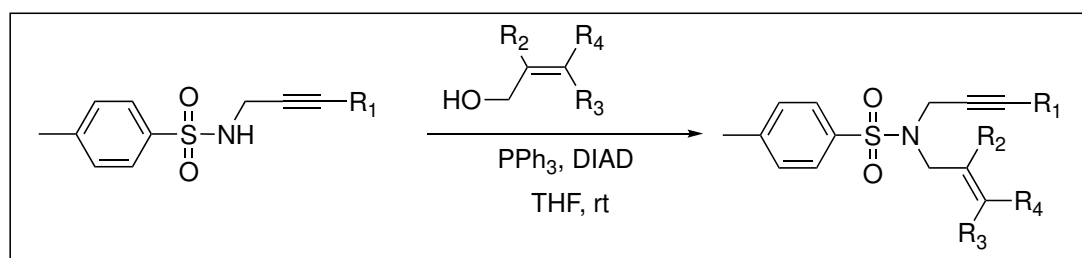


To a solution of **S1** (2.0 g, 7.4 mmol, 1 equiv) in DMF (8 mL) was added K₂CO₃ (1.5 g, 11.1 mmol, 1.5 equiv). After stirring at rt for 1 h, 1-bromobut-2-yne (0.66 mL, 7.4 mmol, 1 equiv) was added and the resulting yellow solution was stirred for 18 h. The reaction mixture was diluted with Et₂O (20 mL) and quenched with a saturated aqueous NH₄Cl solution (30 mL). The aqueous phase was extracted with Et₂O (2x30 mL). The combined organic layers were washed with brine (20 mL), dried over anhydrous MgSO₄, filtered and concentrated under reduced pressure. The resulting crude product was dissolved in CH₂Cl₂ (6 mL) and trifluoroacetic acid (2.2 mL, 24.5 mmol, 3.3 equiv) was added. The resulting mixture was stirred for 20 h. A solution of NaHCO₃ (20 mL) was slowly added, then the mixture was diluted with CH₂Cl₂ (20 mL). The aqueous phase was extracted with CH₂Cl₂ (3x 20 mL). The combined organic layers were washed with brine (20 mL), dried over anhydrous MgSO₄, filtered and concentrated under reduced pressure. Purification by column chromatography on silica gel using EtOAc/pentane (1/9) as eluent afforded **S3** (1.10 g, 67% yield) as a pale brown solid.

The characterization data were identical to those previously reported.¹⁰²

¹H NMR (400 MHz, CDCl₃) δ 7.77 (d, *J* = 8.3 Hz, 2H), 7.31 (d, *J* = 8.0 Hz, 2H), 4.40 (bs, 1H), 3.77 (dq, *J* = 4.9, 2.4 Hz, 2H), 2.43 (s, 3H), 1.61 (t, *J* = 2.4 Hz, 3H).

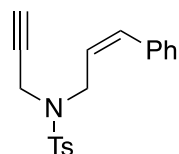
GP1: General produce for the synthesis of nitrogen-tethered 1,6-enyne derivatives



To a solution of **S2** (1.0 equiv) or **S3** in freshly distilled THF at rt were added triphenyl phosphine (1.5 equiv) and the desired allylic alcohol (1.5 equiv). Diisopropylazodicarboxylate

(1.5 equiv) was added dropwise to the mixture. The resulting yellow-orange mixture was stirred at rt for 15-18 h. The mixture was diluted with EtOAc (50 mL) and quenched with a saturated aqueous NH₄Cl solution (50 mL). The aqueous phase was extracted with EtOAc (2x30 mL). The combined organic layers were washed with brine (20 mL), dried over anhydrous MgSO₄, filtered and concentrated under reduced pressure. Purification by column chromatography on silica gel afforded the desired products.

4-Methyl-N-(3-phenylallyl)-N-(prop-2-yn-1-yl)benzenesulfonamide (4-128)

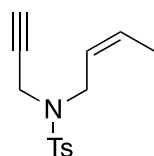


The compound was prepared according to the general procedure **GP1**, using **S2** (0.47 g, 2.24 mmol, 1 equiv), 3-phenylprop-2-en-1-ol (0.45 g, 3.36 mmol, 1.5 equiv), PPh₃ (0.90 g, 3.36 mmol, 1.5 equiv) and diisopropylazodicarboxylate (0.70 mL, 3.36 mmol, 1.5 equiv). Purification by chromatography on silica gel using EtOAc/pentane (1/10) as eluent to afford **4-128** (0.626 g, 86% yield) as a white solid.

The characterization data were identical to those previously reported.¹⁰²

¹H NMR (300 MHz, CDCl₃) δ 7.79 (d, *J* = 8.1 Hz, 2H), 7.37 - 7.27 (m, 7H), 6.60 (d, *J* = 15.8 Hz, 1H), 6.10 (dt, *J* = 15.8, 6.8 Hz, 1H), 4.15 (d, *J* = 2.4 Hz, 2H), 4.02 (d, *J* = 6.8 Hz, 2H), 2.45 (s, 3H), 2.07 (s, 1H).

N-(But-2-en-1-yl)-4-methyl-N-(prop-2-yn-1-yl)benzenesulfonamide (4-130)

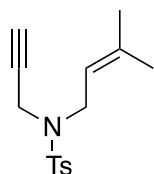


The compound was prepared according to the general procedure **GP1**, using **S2** (0.47 g, 2.24 mmol, 1 equiv), but-2-en-1-ol (0.24 g, 3.36 mmol, 1.5 equiv), PPh₃ (0.90 g, 3.36 mmol, 1.5 equiv) and diisopropylazodicarboxylate (0.70 mL, 3.36 mmol, 1.5 equiv). Purification by chromatography on silica gel using EtOAc/pentane (1/10) as eluent to afford **4-130** (0.47 g, 80% yield) as a white solid.

The characterization data were identical to those previously reported.¹⁰²

¹H NMR (300 MHz, CDCl₃) δ 7.73 (d, *J* = 8.0 Hz, 2H), 7.29 (d, *J* = 8.1 Hz, 2H), 5.77 - 5.66 (m, 1H), 5.42 - 5.32 (m, 1H), 4.09 (s, 2H), 3.77 (d, *J* = 6.6 Hz, 2H), 2.43 (s, 3H), 2.01 (s, 1H), 1.70 (d, *J* = 6.2 Hz, 3H).

4-Methyl-N-(3-methylbut-2-en-1-yl)-N-(prop-2-yn-1-yl)benzenesulfonamide (4-133)

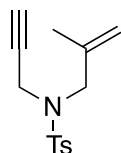


The compound was prepared according to the general procedure **GP1**, using **S2** (0.47 g, 2.24 mmol, 1 equiv), 3-methylbut-2-en-1-ol (0.29 g, 3.36 mmol, 1.5 equiv), PPh₃ (0.6 g, 3.36 mmol, 1.5 equiv) and diisopropylazodicarboxylate (0.7 mL, 3.36 mmol, 1.5 equiv). Purification by chromatography on silica gel using EtOAc/pentane (1/10) as eluent afforded **4-133** (0.56 g, 90%) as pale yellow liquid.

The characterization data were identical to those previously reported.¹⁰³

¹H NMR (400 MHz, CDCl₃) δ 7.73 - 7.75 (m, 2H), 7.28 - 7.30 (m, 2H), 5.08 - 5.12 (m, 1H), 4.07 (d, *J* = 2.4 Hz, 2H), 3.81 (d, *J* = 7.3 Hz, 2H), 2.43 (s, 3H), 1.98 (t, *J* = 2.5 Hz, 1H), 1.72 (s, 3H), 1.70 (s, 3H).

4-Methyl-N-(2-methylallyl)-N-(prop-2-yn-1-yl)benzenesulfonamide (4-137)

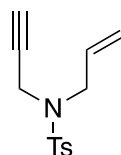


The compound was prepared according to the general procedure **GP2**, using **S2** (0.47 g, 2.24 mmol, 1 equiv), 2-methylprop-2-en-1-ol (0.24 g, 3.36 mmol, 1.5 equiv), PPh₃ (0.6 g, 3.36 mmol, 1.5 equiv) and diisopropylazodicarboxylate (0.7 mL, 3.36 mmol, 1.5 equiv). Purification by chromatography on silica gel using EtOAc/pentane (1/10) as eluent afforded **4-128** (0.53 g, 89%) as a colorless solid.

The characterization data were identical to those previously reported.¹⁰⁴

¹H-NMR (300 MHz, CDCl₃): δ 7.67 (d, *J* = 8.12 Hz, 2H), 7.22 (d, *J* = 7.93 Hz, 2H), 4.91-4.90 (m, 2H), 3.92 (d, *J* = 2.45 Hz, 2H), 3.66(s, 2H), 2.35 (s, 3H), 1.89 (t, *J* = 2.54 Hz, 1H), 1.69 (s, 3H).

N-Allyl-4-methyl-N-(prop-2-yn-1-yl)benzenesulfonamide (4-140)



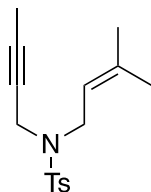
The compound was prepared according to the general procedure **GP2**, using **S2** (0.47 g, 2.24 mmol, 1 equiv), prop-2-en-1-ol (0.23 mL, 3.36 mmol, 1.5 equiv), PPh₃ (0.6 g, 3.36 mmol, 1.5 equiv) and diisopropylazodicarboxylate (0.7 mL, 3.36 mmol, 1.5 equiv). Purification by

chromatography on silica gel using EtOAc/pentane (1/10) as eluent afforded **4-128** (0.47 g, 85%) as white solid.

The characterization data were identical to those previously reported.¹⁰⁵

¹H NMR (300 MHz, CDCl₃) δ 7.78-7.70 (m, 2H), 7.30 (d, *J* = 8.0 Hz, 2H), 5.84-5.63 (m, 1H), 5.37-5.18 (m, 2H), 4.15-4.06 (m, 2H), 3.83 (dd, *J* = 7.2, 5.6, 2H), 2.43 (s, 3H), 2.02 (t, *J* = 2.5 Hz, 1H)

N-(But-2-yn-1-yl)-4-methyl-*N*-(3-methylbut-2-en-1-yl)benzenesulfonamide (**4-145**)

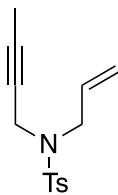


The compound was prepared according to the general procedure **GP1**, using **S3** (0.50 g, 2.24 mmol, 1 equiv), 3-methylbut-2-en-1-ol (0.34 mL, 3.36 mmol, 1.5 equiv), PPh₃ (0.6 g, 3.36 mmol, 1.5 equiv) and diisopropylazodicarboxylate (0.7 mL, 3.36 mmol, 1.5 equiv). Purification by chromatography on silica gel using EtOAc/pentane (1/10) as eluent afforded **4-145** (0.64 g, 98%) as yellow oil.

The characterization data were identical to those previously reported.¹⁰⁵

¹H NMR (400 MHz, CDCl₃) δ 7.74 (d, *J* = 8.2 Hz, 2H), 7.29 (d, *J* = 7.9 Hz, 2H), 5.12-5.08 (m, 1H), 3.99 (q, *J* = 2.4 Hz, 2H), 3.78 (d, *J* = 6.9 Hz, 2H), 2.42 (s, 3H), 1.72 (s, 3H), 1.67 (s, 3H), 1.54 (t, *J* = 2.4 Hz, 3H).

N-Allyl-*N*-(but-2-yn-1-yl)-4-methylbenzenesulfonamide (**4-146**)

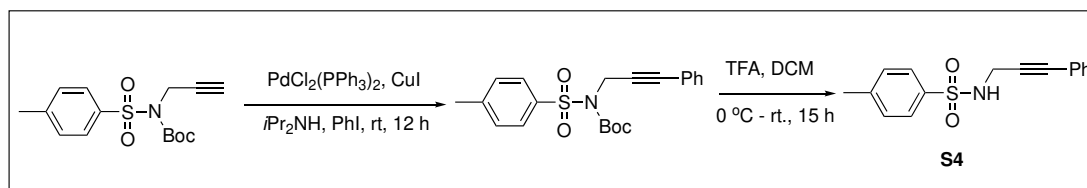


The compound was prepared according to the general procedure **GP1**, using **S3** (0.50 g, 2.24 mmol, 1 equiv), prop-2-en-1-ol (0.23 mL, 3.36 mmol, 1.5 equiv), PPh₃ (0.90 g, 3.36 mmol, 1.5 equiv) and diisopropylazodicarboxylate (0.70 mL, 3.36 mmol, 1.5 equiv). Purification by chromatography on silica gel using EtOAc/pentane (1/10) as eluent to afford **4-146** (0.51 g, 86% yield) as a white solid.

The characterization data were identical to those previously reported.¹⁰⁶

¹H NMR (300 MHz, CDCl₃) δ 7.65 (d, *J* = 8.0 Hz, 2H), 7.22 (d, *J* = 7.9 Hz, 2H), 5.70-5.55 (m, 1H), 5.22 (s, 1H), 5.13 (d, *J* = 10.3 Hz), 3.93 (s, 2H), 3.72 (d, *J* = 5.8 Hz, 2H), 2.33 (s, 3H), 1.45 (s, 3H).

GP2: General Procedure for the Sonogashira Coupling

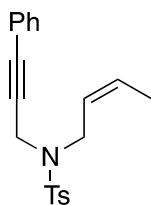


CuI (0.12 g, 0.65 mmol, 0.1 equiv) and $\text{PdCl}_2(\text{PPh}_3)_2$ (0.23 g, 0.32 mmol, 0.05 equiv) were suspended in $i\text{-Pr}_2\text{NH}$ (10 mL), and the resulting mixture was stirred for 10 minutes. Then, *N*-**Boc-S2** (2.0 g, 6.47 mmol, 1 equiv) and iodobenzene (0.94 mL, 8.41 mmol, 1.3 equiv) was added. The reaction was stirred at rt until TLC showed total conversion. The crude mixture was diluted with Et_2O , filtered over a short pad of Celite®. Purification by chromatography on silica gel using EtOAc /pentane (1/9) as eluent afforded yellow solid (2.13 g, 92% yield). The product was dissolved in CH_2Cl_2 (9 mL) and trifluoroacetic acid (3.0 mL, 38.95 mmol, 6 equiv) was added. The resulting mixture was stirred for 20 h. The mixture was slowly added NaHCO_3 (20 mL) and CH_2Cl_2 (20 mL). The aqueous phase was extracted with CH_2Cl_2 (3x 20 mL). The combined organic layers were washed with brine (20 mL), dried over anhydrous MgSO_4 , filtered and concentrated under reduced pressure to give **S4** (1.50 g, 81% yield) as a pale yellow solid without purification.

The characterization data were identical to those previously reported.¹⁰⁴

^1H NMR (400 MHz, CDCl_3) δ 7.82 (d, $J = 8.4$ Hz, 2H), 7.29-7.26 (m, 3H), 7.25-7.24 (m, 1H), 7.23-7.22 (m, 1H), 7.14 (d, $J = 1.6$ Hz, 1H), 7.12(d, $J = 2.0$ Hz, 1H), 4.72 (t, $J = 6.2$ Hz, 1H), 4.08 (d, $J = 6.4$ Hz, 2H), 2.35 (s, 3H).

N-(*But-2-en-1-yl*)-*N*-(3-phenylprop-2-yn-1-yl)benzenesulfonamide (**4-142**)

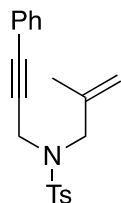


The compound was prepared according to the general procedure **GP1** using **S4** (0.50 g, 1.75 mmol, 1 equiv), but-2-en-1-ol (0.23 mL, 2.76 mmol, 1.5 equiv), PPh_3 (0.70 g, 2.76 mmol, 1.5 equiv) and diisopropylazodicarboxylate (0.6 mL, 2.76 mmol, 1.5 equiv). Purification by chromatography on silica gel using EtOAc /pentane (1/10) as eluent afforded **4-142** (0.49 g, 82% yield) as a white solid.

The characterization data were identical to those previously reported.¹⁰⁷

^1H NMR (400 MHz, CDCl_3) δ 7.77 (d, J = 8.3 Hz, 2H), 7.28-7.21 (m, 5H), 7.08 (d, J = 1.4 Hz, 1H), 7.06 (d, J = 1.7 Hz, 1H) 5.77-5.72 (m, 1H), 5.47-5.40 (m, 1H), 4.29 (s, 2H), 3.82 (d, J = 6.8 Hz, 2H), 2.33 (s, 3H), 1.71 (dd, J = 6.5, 1.6 Hz, 3H).

4-Methyl-N-(2-methylallyl)-N-(3-phenylprop-2-yn-1-yl)benzenesulfonamide (4-143)

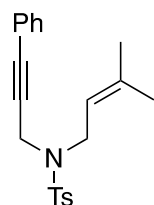


The compound was prepared according to the general procedure **GP1** using **S4** (0.50 g, 1.75 mmol, 1 equiv), 2-methylprop-2-en-1-ol (0.2 g, 2.76 mmol, 1.5 equiv), PPh_3 (0.70 g, 2.76 mmol, 1.5 equiv) and diisopropylazodicarboxylate (0.6 mL, 2.76 mmol, 1.5 equiv). Purification by chromatography on silica gel using EtOAc/pentane (1/10) as eluent afforded **4-143** (0.52 g, 88% yield) as a white solid.

The characterization data were identical to those previously reported.¹⁰⁸

^1H NMR (300 MHz, CDCl_3) δ 7.80 (d, J = 8.1 Hz, 2H), 7.32 - 7.22 (m, 5H), 7.06 (d, J = 7.5 Hz, 2H), 5.03 (s, 2H), 4.28 (s, 2H), 3.82 (s, 2H), 2.35 (s, 3H), 1.83 (s, 3H).

4-Methyl-N-(3-methylbut-2-en-1-yl)-N-(3-phenylprop-2-yn-1-yl)benzenesulfonamide (4-144)

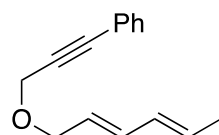


The compound was prepared according to the general procedure **GP1** using **S4** (1.0 g, 3.49 mmol, 1 equiv), 3-methylbut-2-en-1-ol (0.35 mL, 3.49 mmol, 1 equiv), PPh_3 (0.9 g, 3.49 mmol, 1 equiv) and diisopropylazodicarboxylate (0.7 mL, 3.49 mmol, 1 equiv). Purification by chromatography on silica gel using EtOAc/pentane (1/10) as eluent to afford **4-144** (0.71 g, 58% yield) as a white solid.

The characterization data were identical to those previously reported.¹⁰⁴

^1H NMR (300 MHz, CDCl_3) δ 7.78 (d, J = 8.2, 2H), 7.27-7.21 (m, 5H, Har), 7.06 (d, J = 6.4, 2H), 5.25- 5.10 (t, J = 7.2, 1H), 4.28 (s, 2H), 3.88 (d, J = 7.4 Hz, 2H), 2.33 (s, 3H), 1.75 (s, 3H), 1.70 (s, 3H).

(3-Hexa-2,4-dienyloxy-prop-1-ynyl)-benzene (4-147)

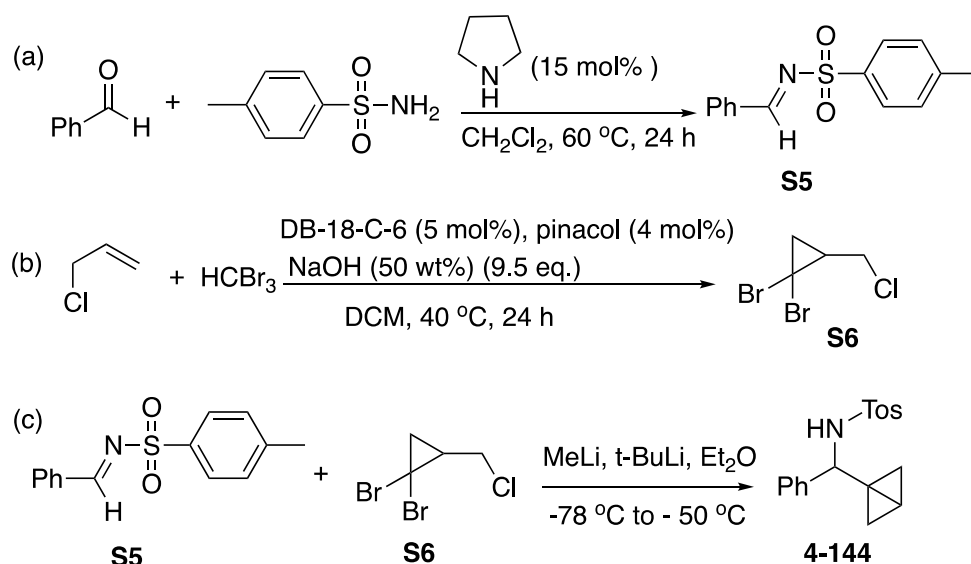


To a suspension of $\text{PdCl}_2(\text{PPh}_3)_2$ (70.2 mg, 0.10 mmol) and CuI (9.5 mg, 0.05 mmol) was added iodobenzene (1.12 ml, 10.0 mmol), diethylamine (15 ml), and 1-prop-2-ynoxy-hexa-2,4-diene (0.68 g, 5.0 mmol) under argon atmosphere, and the mixture was refluxed for 3 h (monitored by TLC). After cooled to room temperature, the resultant mixture was added to ether, and then filtered by celite. After evaporation under reduced pressure, the resultant residue was purified by silica-gel chromatography to give the titled compound **4-147** (0.95 g, 90% yield) as colorless oil.

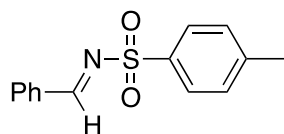
The characterization data were identical to those previously reported.⁹⁸

^1H NMR (300 MHz, CDCl_3) δ 1.79 (dd, $J = 6.9, 0.6$ Hz, 3H), 4.17 (d, $J = 6.3$ Hz, 2H), 4.38 (s, 2H), 5.63-5.82 (m, 2H), 6.06-6.15 (m, 1H), 6.29 (dd, $J = 15.0, 10.5$ Hz, 1H), 7.31-7.36 (m, 3H), 7.46-7.49 (m, 2H).

The synthesis of 4-149



(*E*)-*N*-Benzylidene-4-methylbenzenesulfonamide (**S5**)

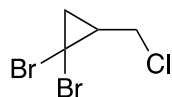


A solution of 4-methylbenzenesulfonamide (5 g, 29.2 mmol) in 100 ml dry DCM, benzaldehyde (3.7 g, 34.87 mmol) and pyrrolidine (0.31 g, 4.38 mmol) was added dropwise to the mixture. The resulting yellow solution was stirred for 24 h. The reaction mixture was filtered and the solvent was removed under reduced pressure to get yellow solid. Then added 10 mL EtOAc to the remaining solid, the result mixture was filtered and the solvent was removed by evaporation, and washed by the mixture solvents of Et₂O and pentane (15/25) to afford **S5** (6.2 g, 82% yield) as white solid

The characterization data were identical to those previously reported.¹⁰⁹

¹H NMR (300 MHz, CDCl₃) δ 8.95 (s, 1H), 7.86 - 7.80 (m, 4H), 7.43 - 7.38 (m, 2H), 7.28 - 7.25 (m, 2H), 2.36 (s, 3H);

1,1-Dibromo-2-(chloromethyl)cyclopropane (S6)



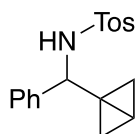
250 mL flask was charged dibenzo-18-crown-6 (DB18C6) (2.14 g, 5.93 mmol, 5 mol%), pinacol (608 mg, 5.14 mmol, 4 mol%) under a N₂ atmosphere. DCM (75 mL) was added to the solids followed by allyl chloride (15.75 mL, 193 mmol, 1.5 equiv) and bromoform (11.25 mL, 129 mmol, 1 equiv). To the resulting solution, a solution of sodium hydroxide (48.9 g, 1.22 mol, 9.5 equiv) in water (49 mL) was added all at once. The flask was equipped with a reflux condenser and a N₂ balloon and the reaction was stirred for 20 h at 40 °C (full consumption of bromoform is recommended, as the presence of this compound in the reaction mixture complicates the purification procedure).

The reaction mixture was allowed to cool down to r.t. and poured into a 500 mL beaker containing 250 mL of pentane. The mixture was gently stirred with a glass stick and sonicated for five minutes. The mixture was let to sediment for 20 minutes and the supernatant pentane was passed through a celite/silica plug, collecting the solution. Extra attention should be paid to avoid pouring the black precipitate or the water phase over the filter. The black precipitate was washed two times with 250 mL of pentane repeating the stirring-sonication-plug procedure. The solvent was then evaporated, and the resulting residue was redissolved in 300 mL of pentane. The mixture was filtered through a thin layer of silica and the silica filter was washed with further 200 mL of pentane. Evaporation of solvent led to a turbid liquid, which was passed through a Pasteur containing a small amount of oven-dried MgSO₄ to afford the pure intermediate trihalide **S6** (16.0 g, 51% yield) as a colorless liquid.

The characterization data were identical to those previously reported.¹¹⁰

¹H NMR (CDCl₃, 400 MHz) δ 3.65 (d, *J* = 7.4 Hz, 2H), 2.08 – 2.00 (m, 1H), 1.93 (dd, *J* = 10.3, 7.6 Hz, 1H), 1.48 (appt, *J* = 7.5 Hz, 1H);

N-(Bicyclo[1.1.0]butan-1-yl)(phenyl)methyl)-4-methylbenzenesulfonamide (4-149)



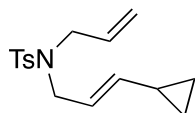
A solution of 1,1-dibromo-2-(chloromethyl)cyclopropane **S6** (5.0 g, 20 mmol) in dry Et₂O (30 mL) was cooled to -78 °C and treated dropwise with a solution of MeLi (15 mL, 20 mmol, c =

1.4 M in Et₂O). The reaction mixture was allowed to warm up to -50 °C over 1 h, cooled to -78 °C and treated with a solution of t-BuLi (12 mL, 20 mmol, c = 1.7 M in pentane). After 20 min, a solution of *N*-benzylidene-4-methylbenzenesulfonamide **S5** (2.6 g, 10 mmol) in THF (20 mL) was added. The reaction mixture was allowed to warm up to rt, quenched with sat. NH₄Cl and extracted (3x) with Et₂O. The combined organic layers were washed with water and brine, dried (Na₂SO₄), and evaporated. The oil was purified by chromatography on SiO₂ (hexanes/EtOAc, 4:1) to afford **4-149** (1.9 g, 61%) as colorless oil.

The characterization data were identical to those previously reported.⁹⁷

¹H NMR (300 MHz, CDCl₃) δ 7.65-7.62 (m, 2 H), 7.21-7.18 (m, 5 H), 7.12-7.08 (m, 2 H), 4.96 (d, *J* = 6.6 Hz, 1 H), 4.76 (d, *J* = 6.8 Hz, 1 H), 2.40 (s, 3 H), 1.51 (t, *J* = 4.6 Hz, 1 H), 1.27 (d, *J* = 4.9 Hz, 2 H), 0.64 (d, *J* = 0.8 Hz, 1 H), 0.55 (br s, 1 H).

(E)-*N*-Allyl-*N*-(3-cyclopropylallyl)-4-methylbenzenesulfonamide (**4-153**)



Vinylcyclopropane alcohol (91.0 mg, 929 μmol)¹¹³, *N*-allyl-*p*-toluenesulfonamide (196 mg, 929 μmol)¹¹⁴ and triphenylphosphine (290 mg, 1.11 mmol) were weighed out in an oven-dried 50 mL round-bottom flask with stir bar. This material was taken up in THF (20 mL), and diisopropylazodicarboxylate (DIAD, 224 mg, 217 μL, 1.11 mmol) was added over 2 min. The yellow solution was stirred 14 h before it was concentrated by rotary evaporation and purified by flash column chromatography, eluting with 10% Et₂O/ pentane. Product-containing fractions were identified and concentrated by rotary evaporation to get product **4-153** (0.168 g, 62% yield) as a colorless oil.

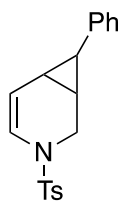
The characterization data were identical to those previously reported.⁹⁸

¹H NMR (400 MHz, CDCl₃) δ 7.79 (d, *J* = 8.2 Hz, 2H), 7.29 (d, *J* = 8.2 Hz, 2H), 5.65-5.56 (m, 1H), 5.28-5.21 (m, 1H), 5.15-5.14 (m, 2H), 5.11-5.01 (m, 1H), 3.79 (d, *J* = 6.4 Hz, 2H), 3.32 (d, *J* = 6.7 Hz, 2H), 2.42 (s, 3H), 1.32-1.27 (m, 1H), 0.69-0.65 (m, 2H), 0.31-0.27 (m, 2H).

GP2: Rhodium catalyzed cycloisomerization of enynes

To a solution of [Rh] (5 mol%) in dry and degassed solvent was added 1,6-enyne (1 equiv). The mixture was stirred at 80 °C for 24 h and monitored by TLC. When the reaction was complete, the mixture was filtered over a short pad of Celite® and washed with CH₂Cl₂. The solution was concentrated under reduced pressure. Subsequent purification by flash chromatography on silica gel afforded the desired products.

7-Phenyl-*3*-tosyl-*3*-azabicyclo [4.1.0] hept-4-ene (**4-129**)

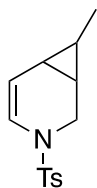


The compound was prepared according to the general procedure **GP2** from enyne **4-128**. Using enyne substrate **4-128** (100 mg, 0.38 mmol, 1 equiv), (\pm)-**4-127** (16.2 mg, 0.019 mmol, 0.05 equiv). Purification by chromatography on silica gel using EtOAc/pentane (1/15) as eluent afforded **4-129** (0.037 g, 37% yield) as a colorless oil.

The characterization data were identical to those previously reported.¹¹¹

¹H RMN (400 MHz, CDCl₃) δ 7.71-7.68 (m, 2H), 7.37-7.35 (m, 2H), 7.24-7.19 (m, 2H), 7.15-7.11 (m, 1H), 6.81-6.78 (m, 2H), 6.42 (d, J = 8.0 Hz, 1H), 5.51 (dd, J = 8.0, 5.4 Hz, 1H), 4.03 (dt, J = 12.1, 1.3 Hz, 1H), 3.16 (dd, J = 12.0, 2.9 Hz, 1H), 2.24 (s, 3H), 1.92-1.88 (m, 1H), 1.62 (dd, J = 5.1, 3.8 Hz, 1H), 1.51-1.42 (m, 1H); ¹³C NMR (75 MHz, CDCl₃) δ 143.94, 140.64, 134.93, 130.04, 128.52, 127.24, 126.04, 125.42, 121.58, 111.34, 40.32, 31.29, 29.08, 21.70, 19.53.

7-Methyl-3-tosyl-3-azabicyclo[4.1.0]hept-4-ene (**4-131**)

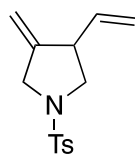


The compound was prepared according to the general procedure **GP2** from enyne **4-130**. Using enyne **4-130** (100 mg, 0.38 mmol, 1 equiv), (\pm)-**4-127** (16.2 mg, 0.019 mmol, 0.05 equiv). Purification by chromatography on silica gel using EtOAc/pentane (1/15) as eluent afforded **4-131** as a colorless oil.

The characterization data were identical to those previously reported.¹¹¹

¹H RMN (400 MHz, CDCl₃) δ 7.65-7.61 (m, 2H), 7.31-7.29 (m, 2H), 6.28 (d, J = 8.1 Hz, 1H), 5.40 (dd, J = 8.1, 5.4 Hz, 1H), 3.88 (dt, J = 11.5, 1.3 Hz, 1H), 2.94 (dd, J = 11.5, 3.1 Hz, 1H), 2.41 (s, 3H), 1.27-1.18 (m, 1H), 0.96 (d, J = 6.0 Hz, 3H), 0.83 (ddd, J = 8.8, 5.4, 3.8 Hz, 1H), 0.75-0.63 (m, 1H); ¹³C NMR (101 MHz, CDCl₃) δ 143.72, 134.97, 129.82, 127.20, 120.85, 111.98, 40.84, 26.51, 21.82, 21.67, 17.56, 15.56.

3-Methylene-1-tosyl-4-vinylpyrrolidine (4-132)

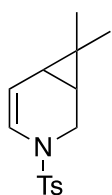


The compound was prepared according to the general procedure **GP2** from enyne **4-130**. Using enyne **4-125** (100 mg, 0.38 mmol, 1 equiv), (\pm)-**4-118** (16.2 mg, 0.019 mmol, 0.05 equiv). Purification by chromatography on silica gel using EtOAc/pentane (1/15) as eluent afforded **4-127** as a colorless oil.

The characterization data were identical to those previously reported.¹¹²

¹H NMR (400 MHz, CDCl₃) δ 7.72-7.70 (m, 2H), 7.34-7.32 (m, 2H), 5.54-5.47(m, 1H), 5.12-5.08 (m, 2H), 4.97 (dd, J = 2.0, 4.0 Hz, 1H), 4.86 (dd, J = 2.0, 5.0 Hz, 1H), 3.99 (qd, J = 2.5, 14 Hz, 1H), 3.72 (qd, J = 2.5, 14 Hz, 1H), 3.63 (dd, J = 8.0, 9.5 Hz, 1H), 3.26-3.21 (m, 1H), 2.87 (dd, J = 9.0, 9.0 Hz, 1H), 2.43 (s, 3H); ¹³C NMR (75 MHz, CDCl₃) δ 146.7, 143.7, 135.6, 133.0, 129.7, 127.8, 118.0, 108.2, 53.2, 51.9, 47.7, 21.5.

7,7-Dimethyl-3-tosyl-3-azabicyclo[4.1.0]hept-4-ene (4-134)

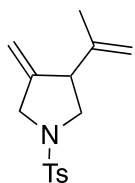


The compound was prepared according to the general procedure **GP2** from enyne **4-133**. Using enyne **4-133** (100 mg, 0.36 mmol, 1 equiv), (\pm)-**4-127** (15.48 mg, 0.018 mmol, 0.05 equiv). Purification by chromatography on silica gel using EtOAc/pentane (1/15) as eluent afforded **4-134** as a colorless oil.

The characterization data were identical to those previously reported.¹¹²

¹H NMR (400 MHz, CDCl₃) δ 7.66-7.65 (m, 2H), 7.03-7.28 (m, 2H), 6.59 (d, J = 8.5 Hz, 1H), 5.06 (dd, J = 4.5, 8.5 Hz, 1H), 3.48 (dd, J = 2.0, 12 Hz, 1H), 3.36 (dd, J = 6.0, 12 Hz, 1H), 2.42 (s, 3H), 1.05-1.02 (m, 4H), 0.97 (dd, J = 5.0, 5.5 Hz, 1H), 0.73 (s, 3H); ¹³C NMR (75 MHz, CDCl₃) δ 143.6, 134.8, 129.6, 127.2, 122.3, 104.3, 38.6, 27.3, 25.3, 21.8, 21.5, 18.7, 14.0.

3-Methylene-4-(prop-1-en-2-yl)-1-tosylpyrrolidine (4-135)

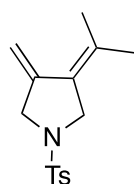


The compound was prepared according to the general procedure **GP2** from enyne **4-133**. Using enyne **4-133** (100 mg, 0.36 mmol, 1 equiv), (\pm)-**4-127** (15.48 mg, 0.018 mmol, 0.05 equiv). Purification by chromatography on silica gel using EtOAc/pentane (1/15) as eluent afforded **4-135** as a colorless oil.

The characterization data were identical to those previously reported.¹¹²

¹H NMR (400 MHz, CDCl₃) δ 7.72-7.70 (m, 2H), 7.34-7.32 (m, 2H), 5.00 (m, 1H), 4.86-4.80 (m, 3H), 3.91-3.87 (m, 1H), 3.82-3.77 (m, 1H), 3.47 (dd, $J = 8.0, 9.5$ Hz, 1H), 3.32-3.29 (m, 1H), 3.12 (dd, $J = 7.0, 9.5$ Hz, 1H), 2.43 (s, 3H), 1.58 (s, 3H); ¹³C NMR (75 MHz, CDCl₃) δ 145.8, 143.7, 142.7, 129.7, 129.6, 127.8, 114.2, 108.3, 52.2, 51.9, 50.8, 21.5, 18.6.

3-Methylene-4-(propan-2-ylidene)-1-tosylpyrrolidine (4-136)

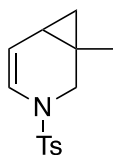


The compound was prepared according to the general procedure **GP2** from enyne **4-136**. Using enyne **4-133** (100 mg, 0.36 mmol, 1 equiv), (\pm)-**4-127** (15.48 mg, 0.018 mmol, 0.05 equiv). Purification by chromatography on silica gel using EtOAc/pentane (1/15) as eluent afforded **4-136** as a colorless oil.

The characterization data were identical to those previously reported.¹¹²

¹H NMR (400 MHz, CDCl₃) δ 7.74 (d, $J = 8.3$ Hz, 2H), 7.29 (d, $J = 8.1$ Hz, 2H), 5.18-4.97 (m, 1H), 4.91-4.75 (m, 1H), 4.07 (d, $J = 2.5$ Hz, 2H), 3.81 (d, $J = 7.1$ Hz, 2H), 2.42 (s, 3H), 1.72 (s, 3H), 1.67 (s, 3H).

1-Methyl-3-tosyl-3-azabicyclo[4.1.0]hept-4-ene (4-138)



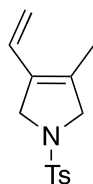
The compound was prepared according to the general procedure **GP2** from enyne **4-137**. Using enyne **4-137** (100 mg, 0.38 mmol, 1 equiv), (\pm)-**4-127** (16.2 mg, 0.019 mmol, 0.05 equiv). Purification by chromatography on silica gel using EtOAc/pentane (1/15) as eluent afforded **4-138** as a colorless oil.

The characterization data were identical to those previously reported.¹¹³

¹H NMR (400 MHz, CDCl₃) δ 7.65 (d, $J = 8.2$ Hz, 2H), 7.31 (d, $J = 8.3$ Hz, 2H), 6.28 (d, $J = 7.9$ Hz, 1H), 5.39 (dd, $J = 7.9, 5.7$ Hz, 1H), 3.84 (d, $J = 11.3$ Hz, 1H), 2.72 (d, $J = 11.3$ Hz, 1H), 2.42 (s, 3H), 1.11 (s, 3H), 0.92 (dt, $J = 9.4, 5.0$ Hz, 1H), 0.62 (dd, $J = 8.1, 4.4$ Hz, 1H), 0.56 (t,

$J = 4.3$ Hz, 1H) ppm; ^{13}C NMR (101 MHz, CDCl_3) δ 143.7, 135.2, 129.9, 127.2, 120.5, 112.8, 46.1, 25.9, 22.1, 21.7, 20.4, 16.1.

3-Methyl-1-tosyl-4-vinyl-2,5-dihydro-1H-pyrrole (4-139)

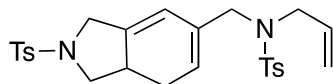


The compound was prepared according to the general procedure **GP2** from enyne **4-137**. Using enyne **4-137** (100 mg, 0.38 mmol, 1 equiv), (\pm)-**4-127** (16.2 mg, 0.019 mmol, 0.05 equiv). Purification by chromatography on silica gel using EtOAc/pentane (1/15) as eluent afforded **4-139** as a colorless oil.

The characterization data were identical to those previously reported.¹¹⁴

^1H NMR (400 MHz, CDCl_3) δ 7.73 (d, $J = 8.0$ Hz, 2H), 7.32 (d, $J = 8.0$ Hz, 2H), 6.43 (dd, $J = 10.8, 17.6$ Hz, 1H), 5.12 (d, $J = 10.8$ Hz, 1H), 4.96 (d, $J = 17.6$ Hz, 1H), 4.20 (s, 2H), 4.07 (s, 1H), 2.43 (s, 3H), 1.70 (s, 3H); ^{13}C NMR (75 MHz, CDCl_3) δ 143.4, 134.1, 131.6, 129.8, 129.4, 127.6, 127.5, 115.2, 59.2, 54.7, 21.5, 11.4.

N-Allyl-4-methyl-N-((2-tosyl-2,3,7,7a-tetrahydro-1H-isoindol-5-yl)methyl)benzenesulfonamide (4-141)

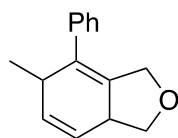


The compound was prepared according to the general procedure **GP2** from enyne **4-140**. Using enyne **4-140** (100 mg, 0.4 mmol, 1 equiv), (\pm)-**4-127** (17.2 mg, 0.02 mmol, 0.05 equiv). Purification by chromatography on silica gel using EtOAc/pentane (1/15) as eluent afforded **4-141** (0.149 g, 75% yield) as a colorless oil.

^1H NMR (400 MHz, CDCl_3) δ 7.77-7.58 (m, 4H), 7.31 (m, 4H), 5.74 (d, $J = 2.8$ Hz, 1H), 5.50-5.35 (m, 2H), 5.08-4.95 (m, 2H), 4.16-3.99 (m, 1H), 3.88-3.83 (m, 1H), 3.80-3.59 (m, 5H), 2.94-2.71 (m, 1H), 2.66 (m, 1H), 2.43 (s, 3H), 2.41 (s, 3H), 2.32-2.12 (m, 1H), 1.76 (m, 1H); ^{13}C NMR (100 MHz, CDCl_3) δ 143.72, 143.31, 139.56, 137.35, 132.91, 132.31, 131.88, 129.76, 129.68, 127.77, 127.12, 122.32, 118.99, 116.53, 54.46, 50.46, 49.28, 37.39, 26.57, 21.56, 21.51; MS (ESI) Calcd for $\text{C}_{26}\text{H}_{30}\text{O}_4\text{S}_2(\text{Na})$ $[\text{M}+\text{Na}]$ 521.1523, found 521.1539.

Specific rotation analysis: Prepared **4-141** by using **4-140** (1 equiv), (*aR*)-(+)-**4-127** (5 mol%) in DCE at 80 °C for 2 h. $[\alpha]_{\text{D}} = 32$ ($c = 0.005$, CH_2Cl_2).

6-Methyl-7-phenyl-1,3,3a,6-tetrahydroisobenzofuran (4-148)



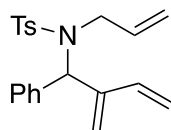
The compound was prepared according to the general procedure **GP2** from enyne **4-147**. Using enyne **4-147** (100 mg, 0.47 mmol, 1 equiv), (\pm)-**4-127** (19 mg, 0.02 mmol, 0.05 equiv). Purification by chromatography on silica gel using EtOAc/pentane (1/15) as eluent afforded **4-148** (0.091 g, 92% yield) as a colorless oil.

The characterization data were identical to those previously reported.¹¹⁴

¹H NMR (400 MHz, CDCl₃) δ 7.33 (t, $J = 7.6$ Hz, 2H), 7.24 (tt, $J = 7.3$ Hz and $J = 1.4$ Hz, 1H), 7.11 (d, $J = 7.9$ Hz, 2H), 5.81 (d, $J = 11.3$ Hz, 1H), 5.79 (d, $J = 11.6$ Hz, 1H), 4.29 (dt, $J = 13.1$ Hz and $J = 1.8$ Hz, 1H), 4.24 (t, $J = 7.5$ Hz, 1H), 4.13 (ddd, $J = 13.1$ Hz and $J = 3.3$ and 1.5 Hz, 1H), 3.39 (dd, $J = 10.9$ Hz and $J = 7.3$ Hz, 1H), 3.28-3.21 (m, 1H), 3.20-3.12 (m, 1H), 0.94 (d, $J = 7.3$ Hz, 3H); ¹³C NMR (101 MHz, CDCl₃) δ 140.4, 135.0, 134.8, 132.2, 128.4, 128.2, 126.7, 121.9, 72.3, 68.4, 41.2, 34.7, 20.3.

Specific rotation analysis: Prepared **4-148** by using **4-147** (1 equiv), (*aR*)-(+)-**4-127** (5 mol%) in DCM at rt for 16 h. $[\alpha]_D = 25$ (c 0.005, CH₂Cl₂).

N-Allyl-4-methyl-*N*-(2-methylene-1-phenylbut-3-en-1-yl)benzenesulfonamide (**4-150**)

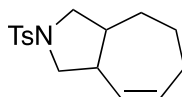


A solution of **4-149** (100 mg, 0.28 mmol) and (\pm)-**4-127** (12.6 mg, 5 mol%) in toluene. The reaction mixture was degassed and placed in an oil bath (80 °C). After 10 h, the mixture was cooled to rt, concentrated in vacuo, and the dark-brown oil was purified by chromatography on SiO₂ (Hex:EtOAc, 4:1) to afford **4-150** (0.084 g, 85 %) as a clear, colorless oil.

The characterization data were identical to those previously reported.⁹⁷

¹H NMR (300 MHz, CDCl₃) δ 7.50 (d, $J = 8.3$ Hz, 2 H), 7.20-7.09 (m, 9 H), 7.04-7.01 (m, 2 H), 6.95 (dd, $J = 7.2, 2.2$ Hz, 2 H), 6.21 (dd, $J = 17.8, 11.2$ Hz, 1 H), 5.99 (s, 1H), 5.32 (s, 1 H), 5.06 (d, $J = 7.7$ Hz, 1 H), 5.05 (s, 1 H), 4.98 (d, $J = 11.3$ Hz, 1 H), 4.49, 4.41 (AB, $J = 15.9$ Hz, 2 H), 2.40 (s, 3 H); ¹³C NMR (75 MHz, CDCl₃) δ 143.6, 143.0, 137.9, 137.5, 137.2, 136.9, 129.5, 129.2, 128.6, 128.4, 127.8 (2), 127.5, 127.0, 119.7, 115.6, 63.1, 49.9, 21.5.

Cycloadduct **4-154:**



A solution of **4-153** (100 mg, 0.34 mmol) and (\pm)-**4-127** (15 mg, 5 mol%) in toluene.

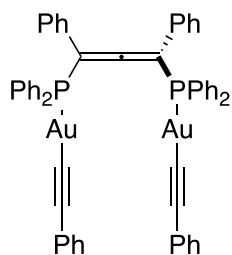
The reaction mixture was degassed and placed in an oil bath (80 °C). After 10 h, The crude product mixture was concentrated by rotary evaporation, and the residue was purified by flash column chromatography eluting with 5% Et₂O/pentane to afford **4-154** (0.081 g, 82 %) as a colorless oil.

The characterization data were identical to those previously reported.¹¹⁵

¹H NMR (400 MHz, CDCl₃) δ 7.70 (d, *J* = 8.1 Hz, 2H), 7.31 (d, *J* = 7.9 Hz, 2H), 5.62-5.56 (m, 1H), 5.22-5.17 (m, 1H), 3.49-3.41 (m, 2H), 2.97-2.87 (m, 3H), 2.43 (s, 3H), 2.23-2.15 (m, 2H), 1.99-1.93 (m, 1H), 2.62-1.53 (m, 2H), 1.44-1.28 (m, 2H); ¹³C NMR (100 MHz, CDCl₃) δ: 143.3, 133.6, 130.8, 129.5 (2C), 127.6 (2C), 127.5, 54.6, 53.1, 41.5, 40.8, 29.2, 28.7, 23.8, 21.5.

Specific rotation analysis: Prepared **4-154** by using **4-153** (1 equiv), (*aR*)-(+)-**4-127** (5 mol%) in toluene at 80 °C for 10 h. [α]_D = 38 (c 0.005, CH₂Cl₂).

*Diphenylacetylenegold(I)-(1,3-diphenylpropa-1,2-diene-1,3-diyl)-bis (diphenylphosp hine) (**4-155**)*

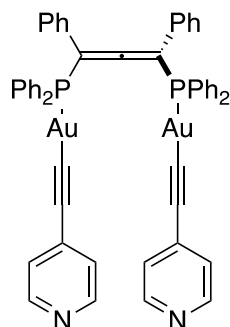


A solution of *t*-BuLi (0.25 mmol, 2.5 equiv, 1.7 M in pentane) was added *via* syringe to a solution of phenylacetylene (23 mg, 0.22 mmol, 2.2 equiv) in 5 mL of THF at -78 °C under argon. A solution of dichlorogold(I)-(1,3-diphenylpropa-1,2-diene-1,3-diyl)-bis(diphenylphosp hine) (**4-124**) (103 mg, 0.1 mmol, 1 equiv) in 2 mL THF was immediately added all at once at -78 °C. The cold bath was removed, reaction mixture was allowed to warm to 25 °C on its own and stirred for 5 h in the absence of light, followed by solvent removal *via* rotary evaporation at ambient temperature. The product was recrystallized by diffusion of cyclohexane into the solution of crude product in CH₂Cl₂ to give white crystals **4-155** (99 mg, 86%).

M.p. = 222-224°C;

¹H NMR (400 MHz, CDCl₃) δ 7.54 (dd, *J* = 19.9, 7.6 Hz, 15H), 7.47 - 7.04 (m, 25H); ¹³C NMR (101 MHz, CDCl₃) δ 213.28, 135.25, 135.11, 134.23, 134.09, 132.72, 132.33, 130.76, 130.69, 129.45, 129.33, 129.22, 129.08, 128.50, 128.17, 128.01, 127.92, 127.76, 127.72, 127.68, 126.88, 124.85, 104.72, 104.21; ³¹P NMR (162 MHz, CDCl₃) δ 39.20; HRMS (ESI) calcd. for C₅₅H₄₁Au₂P₂ ([M + H]⁺): 1156.1936, found 1156.1938.

Di(4-ethynylpyridine)gold(I)-(1,3-diphenylpropa-1,2-diene-1,3-diyl)-bis (diphenylphosphine)
(4-156)



A solution of *t*-BuLi (0.25 mmol, 2.5 equiv, 1.7 M in pentane) was added *via* syringe to a solution of 4-ethynylpyridine (23 mg, 0.22 mmol, 2.2 equiv) in 5 mL of THF at -78 °C under argon. A solution of dichlorogold(I)-(1,3-diphenylpropa-1,2-diene-1,3-diyl)-bis(diphenylphosphine) (**4-124**) (103 mg, 0.1 mmol, 1 equiv) in 2 mL THF was immediately added all at once at -78 °C. The cold bath was removed, reaction mixture was allowed to warm to 25 °C on its own and stirred for 5 h in the absence of light, followed by solvent removal *via* rotary evaporation at ambient temperature. The product was recrystallized by diffusion of cyclohexane into the solution of crude product in CH₂Cl₂ to give yellow crystals **4-156** (93 mg, 80%).

M.p. = 228-230°C;

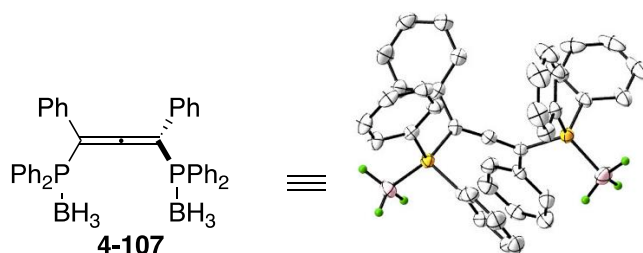
¹H NMR (400 MHz, CDCl₃) δ 8.53 - 8.50 (m, 2H), 7.61 - 7.45 (m, 15H), 7.44 - 7.31 (m, 21H);

³¹P NMR (122 MHz, CDCl₃) δ 38.94; HRMS (ESI) calcd. for C₅₃H₃₉Au₂N₂P₂ ([M + H]⁺): 1158.1841, found 1158.1840.

10.3 Crystallographic Data

A single crystal of each compound was selected, mounted onto a cryoloop, and transferred in a cold nitrogen gas stream. Intensity data were collected with a BRUKER Kappa-APEXII diffractometer with graphite-monochromated Mo-K α radiation. Data collections were performed with APEX2 suite (BRUKER). Unit-cell parameters refinement, integration and data reduction were carried out with SAINT program (BRUKER). SADABS (BRUKER) was used for scaling and multi-scan absorption corrections. In the WinGX suite of programs,¹¹⁶ the structure was solved with different programs (cf cif files) and refined by full-matrix least-squares methods using SHELXL-14.¹¹⁷

The following table contains crystal data collection and structure refinement information for allene **4-107**. Crystallographic data for this structure was deposited at the Cambridge Crystallographic Data Centre. Data can be obtained free of charge via www.ccdc.cam.ac.uk.



Bond precision:	C-C = 0.0035 Å	Wavelength=1.54178
Cell:	a=9.5122 (3) b=17.4616 (5) c=19.7590 (5)	
	alpha=90 beta=90.522(1) gamma=90	
Temperature: 200 K		
	Calculated	Reported
Volume	3281.80 (16)	3281.80 (16)
Space group	C c	C 1 c 1
Hall group	C -2yc	C -2yc
Moiety formula	C39 H36 B2 P2	C39 H36 B2 P2
Sum formula	C39 H36 B2 P2	C39 H36 B2 P2
Mr	588.24	588.24
Dx, g cm ⁻³	1.191	1.191
Z	4	4
Mu (mm ⁻¹)	1.386	1.386
F000	1240.0	1240.0
F000'	1245.12	
h,k,lmax	11,20,23	11,20,23
Nref	5802[2906]	5685
Tmin,Tmax	0.716,0.779	0.668,0.753
Tmin'	0.578	
Correction method=	# Reported T Limits: Tmin=0.668 Tmax=0.753	
AbsCorr =	MULTI-SCAN	
Data completeness=	1.96/0.98	Theta(max)= 66.617
R(reflections)=	0.0223(5646)	wR2(reflections)= 0.0580(5685)
S =	1.054	Npar= 413

11. Reference

- [1] a) L. D. Quin, *A Guide to Organophosphorus Chemistry*; Wiley: New York, **2000**; b) Y. A. Vereshchagina, E. A. Ishmaeva, V. V. Zverev, *Russ. Chem. Rev.* **2005**, *74*, 297.
- [2] a) H. Morales-Rojas, R. A. Moss, *Chem. Rev.* **2002**, *102*, 2497; b) J. Wu, H. R. Hudson, *Chem. Rev.* **2002**, *102*, 7, 2497.
- [3] a) P. F. Burd, C. B. Ferry, J. W. Smith, *British J. Pharm.* **1989**, *98*, 243; b) K., Peter, *Curr. Med. Chem.* **2003**, *10*, 2705; c) Z. Wang, X. Han, L. Wang, Z. Zhai, *Chin. Sci. Bull.* **2004**, *49*, 1437.
- [4] a) M. K. Dipl. Chem., R. Breinbauer, *Angew. Chem. Int. Ed.* **2004**, *43*, 3106; b) Y. Du, X. Lu, C. Zhang, *Angew. Chem. Int. Ed.* **2003**, *42*, 1035; (c) C. Lu, X. Lu, *Org. Lett.* **2002**, *4*, 4677; d) X. Lu, C. Zhang, Z. Xu, *Acc. Chem. Res.* **2001**, *34*, 535; (e) H. Guo, Y. C. Fan, Z. Sun, Y. Wu, O. Kwon, *Chem. Rev.* **2018**, *118*, 10049.
- [5] W. Tang, X. Zhang, *Chem. Rev.* **2003**, *103*, 3029.
- [6] A. G. Orpen, N. G. Connelly, *Organometallics* **1990**, *9*, 1206.
- [7] a) U. Seegerer, R. Felsberg, S. Blaurock, G. A. Hadi, E. Hey-Hawkins, *Phosphorus. Sulfur. Silicon Relat. Elem.* **1999**, *144*, 477; b) T. Li, S. Kaerche, P. W. Roesky, *Chem. Soc. Rev.* **2014**, *43*, 42.
- [8] R. Waterman, *Dalt. Trans.* **2009**, *104*, 18.
- [9] A. Grabulosa, J. Granell, G. Muller, *Coord. Chem. Rev.* **2007**, *251*, 25.
- [10] W. A. Henderson, S. A. Buckler, *J. Am. Chem. Soc.* **1960**, *82*, 5794.
- [11] a) A. E. Arbuzov, *J. Russ. Phys. Chem. Soc.* **1906**, 687; b) A. E. Arbuzov, *Chem. Zentralblatt* **1906**, 1639; c) A. Michaelis and R. Kaehne, *Berichte der Dtsch. Chem. Gesellschaft*, **1898**, *31*, 1048.
- [12] V. Koshti, S. Gaikwad, S. H. Chikkali, *Coord. Chem. Rev.* **2014**, *265*, 52.
- [13] a) W. S. Knowles, M. J. Sabacky, *Chem. Commun.* **1968**, 1445; b) L. Horner, H. Siegel, H. Buthe, *Angew. Chem. Int. Ed.* **1968**, *80*, 1034.
- [14] H. B. Kagan, T. P. Dang, *J. Am. Chem. Soc.* **1972**, *94*, 6429.
- [15] W. S. Knowles, M. J. Sabacky, B. D. Vineyard, D. J. Weinkauff, *J. Am. Chem. Soc.* **1975**, *97*, 2567.
- [16] a) A. Miyashita, A. Yasuda, H. Takaya, K. Toriumi, T. Ito, T. Souchi, R. Noyori, *J. Am. Chem. Soc.* **1980**, *102*, 7932; b) R. Noyori, H. Takaya, *Acc. Chem. Res.* **1990**, *23*, 345; c) T. Ohta, H. Takaya, M. Kitamura, K. Nagai, R. Noyori, *J. Org. Chem.* **1987**, *52*, 3174; d) R. Noyori, T. Ohkuma, M.

- Kitamura, H. Takaya, N. Sayo, H. Kumobayashi, S. Akutagawa, *J. Am. Chem. Soc.* **1987**, *109*, 5856; e) R. Noyori, T. Ohkuma, *Angew. Chem. Int. Ed.* **2001**, *40*, 40.
- [17] a) M. Wadamoto, N. Ozasa, A. Yanagisawa, H. Yamamoto, *J. Org. Chem.* **2003**, *68*, 5593; b) M. Lin, G. Y. Kang, Y. A. Guo, Z. X. Yu, *J. Am. Chem. Soc.* **2012**, *134*, 398; c) A. Yanagisawa, H. Nakashima, Y. Nakatsuka, A. Ishiba, H. Yamamoto, *Bull. Chem. Soc. Jpn.* **2001**, *74*, 1129; d) A. Najib, K. Hirano, M. Miura, *Chem. Eur. J.* **2018**, *24*, 6.
- [18] (a) P. Cao, B. Wang, X. Zhang, *J. Am. Chem. Soc.* **2000**, *122*, 6490; (b) P. Cao, X. Zhang, *Angew. Chem. Int. Ed.* **2000**, *39*, 410; (c) A. Lei, M. He, X. Zhang, *J. Am. Chem. Soc.* **2002**, *124*, 8198; (d) A. Lei, M. He, S. Wu, X. Zhang, *Angew. Chem. Int. Ed.* **2002**, *41*, 3457; (e) A. Lei, J. P. Waldkirch, M. He, X. Zhang, *Angew. Chem. Int. Ed.* **2002**, *41*, 4526.
- [19] K. Tanaka, Y. Otake, H. Sagae, K. Noguchi, M. Hirano, *Angew. Chem. Int. Ed.* **2008**, *120*, 1332.
- [20] T. Shibuya, Y. Shibata, K. Noguchi, K. Tanaka, *Angew. Chem. Int. Ed.* **2011**, *123*, 4049.
- [21] (a) T. N. Glasnov, W. Stadlbauer, C. O. Kappe, *J. Org. Chem.* **2005**, *70*, 3864; (b) N. Arshad, J. Hashim, C. O. Kappe, *J. Org. Chem.* **2008**, *73*, 4755.
- [22] A. Yanagisawa, N. Yang, K. Bamba, *Eur. J. Org. Chem.* **2017**, 6614.
- [23] C. M. Chao, D. Beltrami, P. Y. Toullec, V. Michelet, *Chem. Commun.* **2009**, 6988.
- [24] C. M. Chao, M. R. Vitale, P. Y. Toullec, J. P. Genêt, V. Michelet, *Chem. Eur. J.* **2009**, *15*, 1319.
- [25] P. Y. Toullec, C. M. Chao, Q. Chen, S. Gladiali, J. P. Genet, V. Michelet, *Adv. Synth. Catal.* **2008**, *350*, 2401
- [26] K. J. Achiwa, *J. Am. Chem. Soc.* **1976**, *98*, 8256.
- [27] a) M. D. Fryzuk, B. J. Bosnich, *J. Am. Chem. Soc.* **1977**, *99*, 6262; b) M. D. Fryzuk and B. Bosnich, *J. Am. Chem. Soc.* **1978**, *100*, 17, 5491.
- [28] M. J. Burk, *J. Am. Chem. Soc.* **1991**, *113*, 8518.
- [29] G. Zhu, P. Cao, Q. Jiang, Q. Zhang, *J. Am. Chem. Soc.* **1997**, *119*, 1799.
- [30] P. J. Pye, K. Rossen, R. A. Reaner, N. N. Tsou, R. P. Volante, P. J. Reider, *J. Am. Chem. Soc.* **1997**, *119*, 6207.
- [31] Q. Jiang, Y. Jiang, D. Xiao, P. Cao, X. Zhang, *Angew. Chem. Int. Ed.* **1998**, *37*, 1100.
- [32] R. Schmid, M. Cereghetti, B. Heiser, P. Schönholzer, *Helv. Chim. Acta* **1998**, *71*, 897.
- [33] C. Pai, C. Lin, C. Chen, A. S. C. Chan, *J. Am. Chem. Soc.* **2000**, *122*, 11513.
- [34] M. Hatano, M. Terada, K. Mikami, *Angew. Chem. Int. Ed.* **2001**, *40*, 249.
- [35] W. Tang, X. Zhang, *Angew. Chem. Int. Ed.* **2002**, *41*, 1612.

- [36] Q. Zhao, S. Li, K. Huang, R. Wang, X. Zhang, *Org. Lett.* **2013**, *15*, 15, 4014.
- [37] I. Ojima, *Catalytic Asymmetric Synthesis*, 2nd ed.; Wiley-VCH: Weinheim, **2000**.
- [38] a) J. Meinwald, K. Erickson, M. Hartshorn, Y. C. Meinwald, T. Eisner, *Tetrahedron Lett.* **1968**, 2959; b) T. E. DeVile, M. B. Hursthouse, S. W. Russell, B. C. L. Weedon, *J. Chem. Soc. Chem. Commun.* **1969**, 754; c) F. Abe, T. Yamauchi, *Phytochem.* **1993**, *33*, 1499; d) R. Kinnel, A. J. Duggan, T. Eisner, J. Meinwald, *Tetrahedron Lett.* **1977**, 3913; e) A. Hoffmann-Roder, N. Krause, *Angew. Chem. Int. Ed.* **2004**, *43*, 1196; f) H. F. Schuster, G. M. Coppola, *Alkenes in Organic Synthesis*; Wiley-VCH: New York, **1984**; g) N. Krause, A. S. K. Hashmi, *Modern Allene Chemistry*; Wiley-VCH: Weinheim, **2004**.
- [39] a) D. J. Pasto, *Tetrahedron*, **1984**, *40*, 2805; b) S. Ma, *Chem Rev.* **2005**, *105*, 2829; c) K. M. Brummond, J. E. Deforrest, *Synthesis*, **2007**, 795.
- [40] a) J. H. Van't Hoff, *La Chimie dans l'Espace*, Bazendijk: Rotterdam, **1875**; b) P. Maitland, W. H. Mills, *Nature* *135*, **1935**, 994.
- [41] B. S. Burton, von Pechmann, *H. Ber. Dtsch. Chem. Ges.* **1887**, *20*, 145.
- [42] M. D. Carr, L. H. Gan, I. Reid, *J. Chem. Soc. Perkin Trans.* **1973**, *2*, 668.
- [43] Y. Watanabe and T. Yamazaki, *J. Fluorine Chem.* **2010**, *131*, 646.
- [44] H. Liu, D. Leow, K. W. Huang, C. H. Tan, *J. Am. Chem. Soc.* **2009**, *131*, 7212.
- [45] M. P. VanBrunt, R. F. Standaert, *Org. Lett.* **2000**, *2*, 705.
- [46] H. Schmidbaur, C. M. Frazão, G. Reber, G. Müller, *Chem. Ber.* **1989**, *122*, 259.
- [47] a) P. Rona, P. Crabbe, *J. Am. Chem. Soc.* **1969**, *91*, 3289; b) A. Claesson, L. I. Olsson, *J. Chem. Soc. Chem. Commun.* **1979**, 524; c) G. B. Hammond, *J. Fluorine Chem.* **2006**, *127*, 476; d) S. Ma, E. I. Negishi, *J. Am. Chem. Soc.* **1995**, *117*, 6345; e) N. Krause, A. Hoffmann-Roder, *Tetrahedron*, **2004**, *60*, 11671.
- [48] W. F. Bailey, P. H. Aspris, *J. Org. Chem.* **1995**, *60*, 754.
- [49] a) S. Ma, S. Yu, S. Yin, *J. Org. Chem.* **2003**, *68*, 8996; b) G. Buono, *Tetrahedron Lett.* **1972**, *13*, 3257; (d) G. Buono, *Synthesis*, **1981**, 872.
- [50] a) T. Miura, M. Kobayashi, *J. Chem. Soc. Chem. Commun.* **1982**, 438; b) T. G. Back, S. Collins, R. G. Kerr, *J. Org. Chem.* **1983**, *48*, 3077; c) T. G. Back, S. Collins, U. Gokhale, K. W. Law, *J. Org. Chem.* **1983**, *48*, 4776.
- [51] M. Yokota, K. Fuchibe, M. Ueda, Y. Mayumi, J. Ichikawa, *Org. Lett.* **2009**, *11*, 3994.
- [52] T. Yamazaki, T. Yamamoto and R. Ichihara, *J. Org. Chem.* **2006**, *71*, 6251.
- [53] V. Mouries, B. Delouvrie, E. Lacote, L. Fensterbank, M. Malacria, *Eur. J. Org. Chem.* **2002**, 1776.
- [54] P. Crabbe, H. Fillion, D. Andre, J. L. Luche, *J. Chem. Soc. Chem. Commun.* **1979**, 859.

- [55] a) H. Nakamura, T. Sugiishi, Y. Tanaka, *Tetrahedron Lett.* **2008**, *49*, 7230; b) S. Ma, S. Wu, *J. Org. Chem.* **1999**, *64*, 9314; c) A. Basak, S. Das, D. Mallick, E. D. Jemmis, *J. Am. Chem. Soc.* **2009**, *131*, 15695.
- [56] B. Chen, N. Wang, W. Fan, S. Ma, *Org. Biomol. Chem.* **2012**, *10*, 8465.
- [57] J. Kuang, S. Ma, *J. Am. Chem. Soc.* **2010**, *132*, 1786.
- [58] X. Tang, C. Zhu, T. Cao, J. Kuang, W. Lin, S. Ni, J. Zhang, S. Ma, *Nat. Commun.* **2013**, *4*, 2450.
- [59] a) C. Bruneau, C. Darcel, P. H. Dixneuf, *Curr. Org. Chem.* **1997**, *1*, 197; (b) M. Yoshida, M. Hayashi, K. Shishido, *Org. Lett.* **2007**, *9*, 1643; (c) M. Yoshida, H. Ueda, M. Ihara, *Tetrahedron Lett.* **2005**, *46*, 6705; (d) D. Girard, S. Broussous, O. Provot, J. D. Brion, M. Alami, *Tetrahedron Lett.* **2007**, *48*, 6022; (e) R. Riveiros, J. P. Sestelo, L. A. Sarandeses, *Synthesis*, **2007**, 3595; (f) M. Yoshida, T. Okada, K. Shishido, *Tetrahedron*, **2007**, *63*, 6996.
- [60] a) S. Ma, *Chem. Rev.* **2005**, *105*, 2829; b) S. Ma, *Top. Organomet. Chem.* **2005**, *14*, 183.
- [61] a) H. P. Bi, X. Y. Liu, F. R. Gou, L. N. Guo, X. H. Duan, X. Z. Shu, Y. M. Liang, *Angew. Chem. Int. Ed.* **2007**, *46*, 7068; b) H. P. Bi, L. N. Guo, F. R. Gou, X. H. Duan, X. Y. Liu, Y. M. Liang, *J. Org. Chem.* **2008**, *73*, 4713; c) H. P. Bi, X. Y. Liu, F. R. Gou, L. N. Guo, X. H. Duan, Y. M. Liang, *Org. Lett.* **2007**, *9*, 3527.
- [62] Y. Shi, J. Huang, Y. F. Yang, L. Y. Wu, Y. N. Niu, P. F. Huo, X. Y. Liu, Y. M. Liang, *Adv. Synth. Catal.* **2009**, *351*, 141.
- [63] F. Sasaki, T. Endo, M. Noguchi, K. Kawai, T. Nakano, *Appl. Organomet. Chem.* **2008**, *22*, 128.
- [64] I. Sato, Y. Matsueda, K. Kadowaki, S. Yonekubo, T. Shibata, K. Soai, *Helv. Chim. Acta* **2002**, *85*, 3383.
- [65] X. Pu, X. Qi, J. M. Ready, *J. Am. Chem. Soc.* **2009**, *131*, 10364.
- [66] a) S. E. Denmark, P. A. Barsanti, K.T. Wong, R. A. Stavenger, *J. Org. Chem.* **1998**, *63*, 2428; b) S. E. Denmark, P. A. Barsanti, G. L. Beutner, T. W. Wilson, *Adv. Synth. Catal.* **2007**, *348*, 567.
- [67] a) B. Tao, M. M. C. Lo, G. C. Fu, *J. Am. Chem. Soc.* **2001**, *123*, 353; b) M. Nakajima, M. Saito, M. Uemura, S. Hashimoto, *Tetrahedron Lett.* **2002**, *43*, 8827; c) E. Tokuoka, S. Kotani, H. Matsunaga, T. Ishizuka, S. Hashimoto, M. Nakajima, *Tetrahedron: Asymmetry* **2005**, *16*, 2391.
- [68] T. J. Brown, A. Sugie, M. G. Dickens, R. A. Widenhoefer, *Organometallics* **2010**, *29*, 4207.

- [69] R. Castro-Rodrigo, M. A. Esteruelas, A. M. Lopez, S. Mozo, E. Onate, *Organometallics* **2010**, *29*, 4071.
- [70] S. Sentets, R. Serres, Y. Ortin, N. Lugan, G. Lavigne, *Organometallics* **2008**, *27*, 2078.
- [71] L. Lee, I.Y. Wu, Y.-C. Lin, G. H. Lee, Y. Wang, *Organometallics* **1994**, *13*, 2521.
- [72] J. M. O'Connor, M. C. Chen, B. S. Fong, A. Wenzel, P. Gantzel, A. L. Rheingold, I. A. Guzei, *J. Am. Chem. Soc.* **1998**, *120*, 1100.
- [73] M. A. Bennett, L. Kwan; A. D. Rae; E. Wenger; A. C. Willis, *Dalton Trans.* **2002**, 226.
- [74] S. Doherty, M. R. J. Elsegood, W. Clegg, D. Mampe, N. H. Rees, *Organometallics* **1996**, *15*, 5302.
- [75] H. Zhang, R. Lin, G. Hong, T. Wang, T. B. Wen, H. Xia, *Chem. Eur. J.* **2010**, *16*, 6999.
- [76] S. Löhr, J. Averbeck, M. Schürmann, N. Krause, *Eur. J. Inorg. Chem.* **2008**, 552.
- [77] a) J. M. Alonso, M. T. Quirós, M. P. Muñoz, *Org. Chem. Front.* **2016**, *3*, 1186; b) M. P. Muñoz, *Chem. Soc. Rev.* **2014**, *43*, 3164; c) M. P. Muñoz, *Org. Biomol. Chem.* **2012**, *10*, 3584; d) N. Krause, C. Winter, *Chem. Rev.* **2011**, *111*, 1994; e) A. S. K. Hashmi, L. Schwarz, J. H. Choi, T. M. Frost, *Angew. Chem. Int. Ed.* **2000**, *39*, 2285.
- [78] F. Cai, X. Pu, X. Qi, V. Lynch, A. Radha, J. M. Ready, *J. Am. Chem. Soc.* **2011**, *133*, 18066.
- [79] A. Vanitcha, C. Damelinourt, G. Gontard, N. Vanthuyne, V. Mouries-Mansuy, L. Fensterbank, *Chem. Commun.* **2016**, *52*, 6785.
- [80] X. Zhang, S. Sarkar, R. C. Larock, *J. Org. Chem.* **2006**, *71*, 236.
- [81] M. Omary, H. Patterson, *Encyclopedia of Spectroscopy and Spectrometry*, 3rd ed; Elsevier Ltd, **2016**; p 636-656.
- [82] a) J. Vicente, M. T. Chicote, M. D. Abrisqueta, *J. Chem. Soc. Dalton Trans.* **1995**, 497; b) J. Vicente, M. T. Chicote, M. M. Álvarez-Falcón, P. G. Jones, *Organometallics* **2005**, *24*, 2764; c) J. Vicente, M. T. Chicote, M. M. Álvarez-Falcón, P. G. Jones, *Organometallics* **2005**, *24*, 4666.
- [83] a) J. Vicente, M. T. Chicote, M. M. Álvarez-Falcón, M. A. Fox, D. Bautista, *Organometallics* **2003**, *22*, 4792; b) J. Vicente, M. T. Chicote, M. M. Álvarez-Falcon, P. G. Jones, *Chem. Commun.* **2004**, 2658; c) C. P. McArdle, S. Van, M. C. Jennings, R. J. Puddephatt, *J. Am. Chem. Soc.* **2002**, *124*, 3959; (d) N. C. Habermehl, M. C. Jennings, C. P. McArdle, F. Mohr, R. J. Puddephatt, *Organometallics* **2005**, *24*, 5004.
- [84] a) P. Pyykkö, *Angew. Chem. Int. Ed.* **2004**, *43*, 4412; b) J. Vicente, P. González-Herrero, Y. García-Sánchez, P. G. Jones, M. Bardají, *Inorg. Chem.* **2004**, *43*, 7516.

- [85] a) X. X. Lu, C. K. Li, E. C. C. Cheng, N. Y. Zhu, V. W. W. Yam, *Inorg. Chem.* **2004**, *43*, 2225; b) S. K. Yip, E. C. C. Cheng, L. H. Yuan, N. Y. Zhu, V. W. W. Yam, *Angew. Chem. Int. Ed.* **2004**, *43*, 4954; c) V. W. W. Yam, K. L. Cheung, L. H. Yuan, K. M. C. Wong, K. K. Cheung, *Chem. Commun.* **2000**, 1513.
- [86] D. Li, X. Hong, C. M. Che, W. C. Lo and S. M. Peng, *J. Chem. Soc. Dalton Trans.* **1993**, 2929.
- [87] a) V. W. W. Yam, S. W. K. Choi, *J. Chem. Soc. Dalton Trans.* **1996**, 4227; b) W. Lu, H. F. Xiang, N. Zhu, C. M. Che, *Organometallics* **2002**, *21*, 2343; c) H. Y. Chao, W. Lu, Y. Li, M. C. W. Chan, C. M. Che, K. K. Cheung, N. Zhu, *J. Am. Chem. Soc.* **2002**, *124*, 14696.
- [88] E. Vergara, E. Cerrada, A. Casini, O. Zava, M. Laguna, P.J. Dyson, *Organometallics* **2010**, *29*, 2596.
- [89] Y.P. Zhou, M. Zhang, Y.H. Li, Q.R. Guan, F. Wang, Z.J. Lin, C.K. Lam, X.L. Feng, H.Y. Chao, *Inorg. Chem.* **2012**, *51*, 5099.
- [90] L. Rodríguez, M. Ferrer, R. Crehuet, J. Anglada, J. C. Lima, *Inorg. Chem.* **2012**, *51*, 7636.
- [91] D. Müller, L. Guénée, A. Alexakis, *Eur. J. Org. Chem.* **2013**, *2013*, 6335.
- [92] a) V. Michelet, L. Charruault, S. Gladiali, J. P. Genêt, *Pure Appl. Chem.* **2006**, *78*, 397; b) X. Han, R. A. Widenhoefer, *Org. Lett.* **2006**, *8*, 3801; (c) D. Brissy, M. Skander, H. Jullien, P. Retailleau, A. Marinetti, *Org. Lett.* **2009**, *11*, 2137; (d) K. Ishida, H. Kusama, N. Iwasawa, *J. Am. Chem. Soc.* **2010**, *132*, 8842.
- [93] a) C. M. Chao, D. Beltrami, P. Y. Toullec, V. Michelet, *Chem. Commun.* **2009**, 6988. b) C. M. Chao, M. R. Vitale, P. Y. Toullec, J. P. Genêt, V. Michelet, *Chem. Eur. J.* **2009**, *15*, 1319; c) A. Pradal, C. M. Chao, M. R. Vitale, P. Y. Toullec, V. Michelet, *Tetrahedron* **2011**, *67*, 4371; d) M. A. Abadie, X. Trivelli, F. Medina, F. Capet, P. Roussel, F. Agbossou-Niedercorn, C. Michon, *ChemCatChem* **2014**, *6*, 2235; e) Y. M. Wang, A. D. Lackner, F. D. Toste, *Acc. Chem. Res.* **2014**, *47*, 889.
- [94] C. Aubert, O. Buisine, M. Malacria, *Chem. Rev.* **2002**, *102*, 813.
- [95] a) K. Ota, S. I. Lee, J. M. Tang, M. Takachi, H. Nakai, T. Morimoto, H. Sakurai, K. Kataoka, N. Chatani, *J. Am. Chem. Soc.* **2009**, *131*, 15203; b) S. Y. Kim, Y. K. Chung, *J. Org. Chem.* **2010**, *75*, 1281.
- [96] a) X. Tong, D. Li, Z. Zhang, X. Zhang, *J. Am. Chem. Soc.* **2004**, *126*, 7601; b) X. Deng, S. F. Ni, Z. Y. Han, Y. Q. Guan, H. L. Dang, X. M. Zhang, *Angew. Chem. Int. Ed.* **2016**, *55*, 6295.
- [97] M. A. A. Walczak, P. Wipf, *J. Am. Chem. Soc.* **2008**, *130*, 6924.
- [98] K. Aikawa, S. Akutagawa, K. Mikami, *J. Am. Chem. Soc.* **2006**, *128*, 12648.

- [99] P. A. Wender, L. O. Haustedt, J. Lim, J. A. Love, T. J. Williams, J. Y. Yoon, *J. Am. Chem. Soc.* **2006**, *128*, 19, 6302
- [100] a) L. Rodríguez, M. Ferrer, R. Crehuet, J. Anglada, J. C. Lima, *Inorganic Chem.* **2012**, *51*, 7636; b) I. Strel'nik, V. Sizov, V. Gurzhiy, E. Grachova, *Inorganic Chem.* **2020**, *59*, 244.
- [101] M. Barbazanges, M. Augé, J. Moussa, H. Amouri, C. Aubert, C. Desmarets, L. Fensterbank, V. Gandon, M. Malacria, C. Ollivier, *Chem. Eur. J.* **2011**, *17*, 13789.
- [102] R. Liu, D. Yang, F. Chang, L. Giordano, G. Liu, A. Tenaglia, *Asian J. Org. Chem.* **2019**, *8*, 2011.
- [103] J. Teske, B. Plietker, *ACS Catal.* **2016**, *6*, 7148.
- [104] A. Gansäuer, M. Otte, L. Shi, *J. Am. Chem. Soc.* **2011**, *133*, 416.
- [105] F. Kramm, J. Teske, F. Ullwer, W. Frey, B. Plietker, *Angew. Chem. Int. Ed.* **2018**, *57*, 13335.
- [106] F. Schröder, C. Tugny, E. Salanouve, H. Clavier, L. Giordano, D. Moraleda, Y. Gimbert, V. Mouriès-Mansuy, J.-P. Goddard, L. Fensterbank, *Organometallics* **2014**, *33*, 4051.
- [107] S. Lee, S. Kim, S. Kim, Y. Chung, *Synlett* **2006**, *2006*, 2256.
- [108] S. Y. Kim, Y. K. Chung, *J. Org. Chem.* **2010**, *75*, 1281.
- [109] M. Barbarotto, J. Geist, S. Choppin, F. Colobert, *Tetrahedron: Asymmetry* **2009**, *20*, 2780.
- [110] A. Fawcett, T. Biberger, V. K. Aggarwal, *Nat. Chem.* **2019**, *11*, 117.
- [111] J. A. Johnson, B. M. Petersen, A. Kormos, E. Echeverría, Y. S. Chen, J. Zhang, *J. Am. Chem. Soc.* **2016**, *138*, 10293
- [112] T. Ozawa, T. Kurahashi, S. Matsubara, *Org. Lett.* **2012**, *14*, 3008.
- [113] M. Dieckmann, Y. Jang, N. Cramer, *Angew. Chem. Int. Ed.* **2015**, *54*, 12149.
- [114] T. Kitamura, Y. Sato, M. Mori, *Adv. Synth. Catal.* **2002**, *344*, 678.
- [115] P. A. Wender, L. O. Haustedt, J. Lim, J. A. Love, T. J. Williams, J. Y. Yoon, *J. Am. Chem. Soc.* **2006**, *128*, 19, 6302.
- [116] L. J. Farrugia, *J. Appl. Crystallogr.* **1999**, *32*, 837.
- [117] G. M. Sheldrick, *Acta Crystallogr. Sect. C Struct. Chem.* **2015**, *71*, 3.

General Conclusion

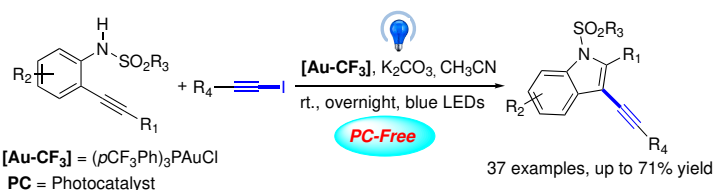
This Ph.D work has been aimed at studying gold(I) and silver-catalyzed reactions under visible light. And, we also aimed at synthesizing a novel class of allenes bearing phosphine borane groups and further study their applications. All the works were summarized in Figure GC.

Based on our previous works on gold catalysis and photocatalysis, firstly, we present a novel photosensitizer- and external oxidant-free photoredox gold-catalyzed Csp^2 - Csp cross coupling of *o*-alkynyl NTs amide and aryl iodoalkynes. This reaction occurs smoothly at room temperature in the presence of a gold (I) complex and K_2CO_3 , which offers various 2,3-disubstituted indole derivatives. The scope of the transformation is wide, and the limitations are discussed. We found that the reaction was well tolerated with iodoalkynes bearing an alkyl chain. Donor alkyl groups on the alkyne of *o*-alkynyl NTs amide were also competent providing 2-alkyl indoles. The process can give corresponding 2,3-disubstituted indole derivatives in quite good yields when Ts group was instead by Ms, Ns, and SES. Of note, iodo-ynamides that have very rarely been used in any organometallic cross coupling reaction could be used as electrophiles. The resulting alkynylated indoles lend themselves to various post-functionalization providing valuable scaffolds. In the end, NMR monitoring experiments on the vinylgold(I) intermediate showed that photocatalyst, especially [Ir-F], is not conducive to generate desired product. Further investigations of the reaction mechanism are ongoing (Figure GC I).

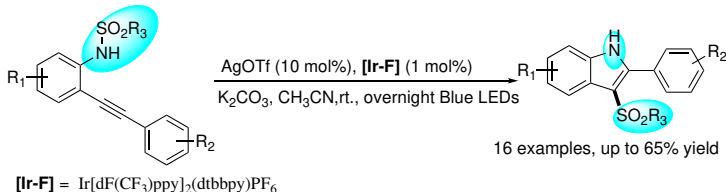
Later, we developed a new method for the synthesis of 3-sulfonylindole derivatives devised from *ortho*-alkynyl-*N*-sulfonylanilines in the presence of a catalytic mixture of Ag (I) and Ir(III) under blue LEDs irradiation. This protocol provided a general approach for the synthesis of 3-sulfonylindole frameworks that are important in medicinal and biological chemistry. Of note, when *N*-tosylalkynylamine bearing with alkyl group, provided protodeauration products in high yields instead of 3-sulfonylindole. Mechanistic investigations indicated that the sulfonyl migration may occur in both an intra- and intermolecular manner. And related mechanism experiments are still in progress in order to understand the detailed reaction process (Figure GC II).

Based on our previous works on biphosphine allenes **A**, which can be prepared in good yield following Schmidbaur's procedure. But shown sensitivity to air which is a challenge for its purification and limits its application, here, we developed a novel method for protecting the

(I) Gold(I) Catalysis Under Visible Light



(II) Silver (I) Catalysis Under Visible Light



(III) Allenes Bisphosphine Borane and Their Applications

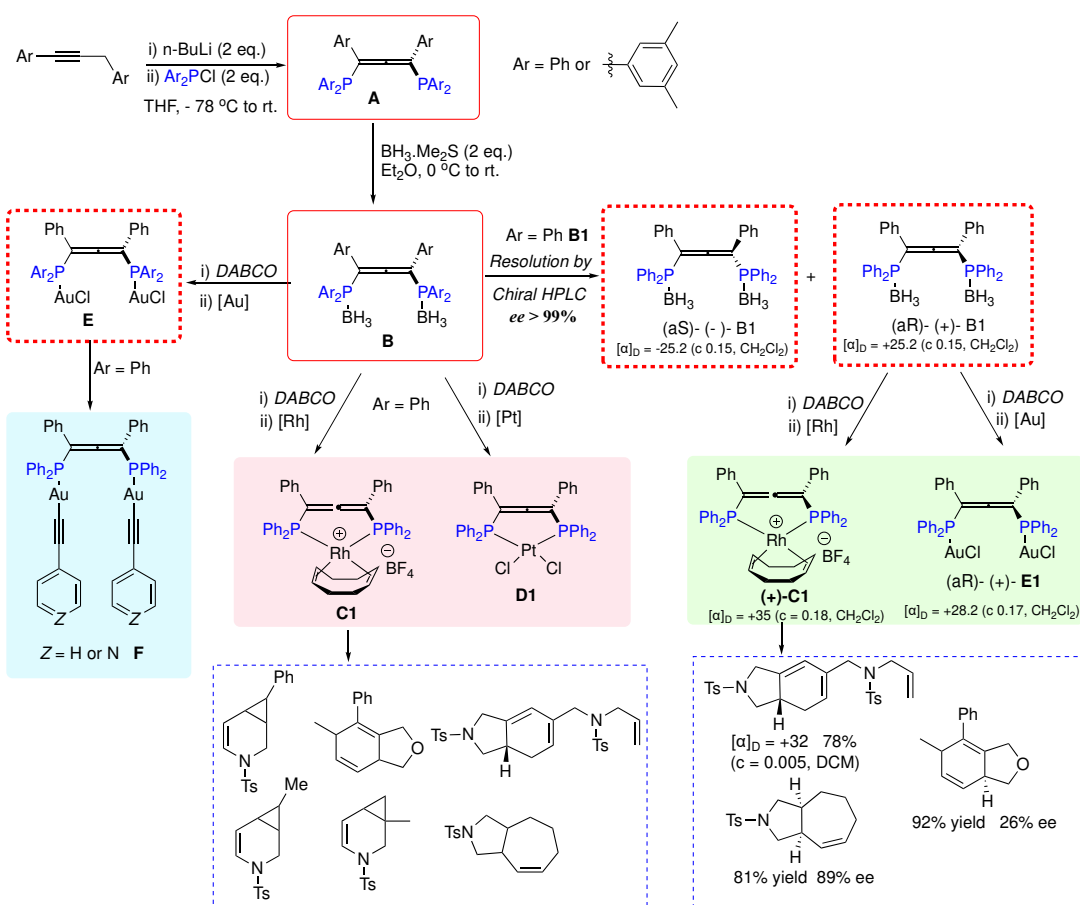


Figure GC Summary of gold(I) and silver(I) catalysis under visible light and allenes bisphosphine borane and their applications

bisphosphine group by using $\text{BH}_3 \cdot \text{Me}_2\text{S}$ (2 eq.). It provided several allenyl bisphosphine borane compounds **B** bearing different substituents in moderate to excellent yields under the mild conditions. This structure was characterized by NMR analysis and X-ray crystallography. Interestingly, protecting group BH_3 can be removed by using DABCO to form bisphosphine allenes **A**, which then directly coordinates with an equivalent of $\text{Rh}(\text{COD})_2\text{BF}_4$ or *cis*-

bis(benzonitrile)dichloroplatinum(II) to provide corresponding mononuclear rhodium-allene bisphosphine complex **C1** and platinum-allene bisphosphine complex **D1** in excellent yields. Several dinuclear gold bisphosphine complex **E** can be smoothly synthesized by starting from allenes bisphosphine borane **B** following the same procedure as above. Mononuclear rhodium-allene bisphosphine complex **C1** can be used as a catalyst in cycloisomerization reactions of 1,6-enynes to afford the cyclic products in good to excellent yields.

Additionally, we are able to separate the two enantiomers of racemic allenyl bisphosphine borane **B1** in large scale by using preparative chiral HPLC. This analysis was performed in collaboration with Dr. Nicolas Vanthuyne. The separation was conducted by Chiralpak IG column and detection by UV-detection at 254 nm and circular dichroism. Two enantiomers of (*aR*)-(+)-**B1** with $[\alpha]_D = +25.2$ (c 0.15, CH₂Cl₂) and (*aS*)-(-)-**B1** with $[\alpha]_D = -25.2$ (c 0.15, CH₂Cl₂) were obtained in excellent enantiomeric excess (*ee* > 99%). In order to expand its application, we synthesized digold complex (*aR*)-(+)-**E1** starting from chiral allene (*aR*)-**B1**, which was deprotected by using DABCO to provide allene (*aR*)-**A1**. Based on previous works, the gold(I) coordinated to the phosphorus atoms of **A1** selectively to afford the dinuclear gold bisphosphine complex (*aR*)-(+)-**E1** in 96% yield with $[\alpha]_D = +28.2$ (c 0.17, CH₂Cl₂) (the same specific rotation values as previous), which means there is no oxidation and racemization following this procedure. Based on this result, we also prepared enantio-enriched rhodium-allenyl bisphosphine complex (+)-**C1** from enantiopure allenes bisphosphine boranes (*aR*)-(+)-**B1** follow the same procedure in excellent yield with $[\alpha]_D = +35$ (c = 0.18, CH₂Cl₂). Dinuclear gold alkynyl phosphine complex **F** can be generated from the reaction of complex **C1** with phenylacetylene or 4-ethynylpyridine in the presence of *t*-BuLi in THF under argon from -78 °C to room temperature. We will investigate luminescence properties of dinuclear gold alkynyl phosphine complexes **F** in the future (Figure GC III).

The chiral rhodium complex (+)-**C1** was tested in similar catalytic reactions. Unfortunately, no *ee* could be precisely determined but final products exhibited optical rotation ($[\alpha]_D$ value). We deduced the *ee* values based on optical rotation of the literature. So these preliminary tests of the optically pure rhodium complexes (+)-**C1** gave promising hits for asymmetric catalysis (Figure GC III).

Gold(I) and Silver(I)-Catalyzed Reactions under Visible Light Bisphosphine Allene based Ligands: from Coordination to Catalysis

Abstract: This thesis has focused on the study of gold(I) and silver(I) catalyzed reactions under visible light, and the synthesis of a novel class of allenyl bisphosphine borane compounds and their applications. Firstly, we present a novel gold-catalyzed Csp^2 - Csp cross coupling of *o*-alkynyl NTs amide and iodoalkynes. Various 2,3-disubstituted indole derivatives were synthesized from moderate to good yields in the absence of photosensitizer and external oxidant. The scope of the transformation is wide, and the limitations are discussed. Later, we reported the first facile and efficient protocol for the synthesis of bioactive 3-sulfonylindoles in good yields *via* the visible-light-mediated silver-catalyzed tandem 1,3-migration/cycloaddition of *ortho*-alkynyl-*N*-sulfonylanilines. This reaction occurs smoothly in the presence of a catalytic mixture of Ag (I) and Ir(III) under blue LEDs irradiation. In the end, we developed a novel facile method to prepare allenyl bisphosphine borane compounds in good to excellent yields. Borane protecting group can be easily removed by using DABCO to liberate the bisphosphine allenes, which then directly coordinate with metals such as Rh, Pt and Au to form the corresponding metal-allenyl phosphine complexes. Additionally, the allenyl bisphosphine borane can be separated in large scale by using preparative chiral HPLC. Chiral gold(I) and rhodium-allenyl bisphosphine complexes can be synthesized without oxidation and racemization occurring in the process. This chiral rhodium complex was tested in asymmetric catalysis for generating various chiral cyclic products, which gave promising hits for asymmetric catalysis. Furthermore, dinuclear gold alkynyl phosphine complexes can be synthesized starting from dinuclear gold-allenyl phosphine complexes.

Keywords: gold catalysis, silver catalysis, visible light, *o*-alkynyl-*N*-sulfonylanilines, iodoalkynes, 3-sulfonylindoles, 1,3-migration, allenyl bisphosphine borane, bisphosphine allene

Réactions catalysées par l'or (I) et l'argent (I) sous la lumière visible Ligands à base d'allène bisphosphine : de la coordination à la catalyse

Résumé: Ce travail de thèse traite de réactions catalysées par des complexes d'or(I) et d'Ag(I) sous lumière visible, mais aussi sur la synthèse d'une nouvelle famille d'allènes bisphosphine borane et de leurs applications. Dans un premier temps nous exposerons les résultats obtenus lors de réactions de couplage croisé Csp^2 - Csp catalysées par des complexes d'or(I) sous LED bleues entre des dérivés NTs-benzylamine *o*-alcyne et des iodoalcynes. Ainsi différentes indoles 2,3-disubstitués ont été obtenues avec des rendements modérés à bons. Cette réaction a lieu en absence de photosensibilisateur et d'oxydant externe. Le champ d'application de cette transformation est large et les limites seront discutées. Nous présenterons aussi une synthèse efficace et de mise en œuvre facile, de 3-sulfonylindoles, composés ayant des propriétés bioactives intéressantes. Les composés sont obtenus avec de bons rendement Cette réaction se fait *via* une séquence cycloaddition/migration 1,3 de groupement sulfonyl d'*ortho*-alkynyl-*N*-sulfonylanilines catalysée par des complexes d'or(I) ou Ag(I) et de complexe d'Ir(III), sous irradiation par des LED bleues. Pour terminer, nous avons développé une nouvelle méthode, facile, de synthèse de bisphosphine allénique boranes chirales avec des rendements bons à excellent sans modifier le motif allénique. La phosphine a pu être facilement libérée en présence de DABCO. La diposphine correspondante a permis la formation de complexes de Rh(I), Pt(I) et Au(I) de façon efficace. Une bisphosphine allène borane chirale a pu être préparée en grande échelle et séparée par HPLC préparative permettant l'accès à chaque énantiomère. Les complexes d'or(I) et de rhodium(I)-allenyl bisphosphines énantiopures ont pu être préparés sans qu'aucune racémisation ne se produise. Les complexes énantiopures de Rh(I) ont été testé en catalyse asymétrique dans des réactions de cycloaddition. Une énantioselectivité a été observée et la détermination des ratios énantiomériques est en cours. Par ailleurs, des complexes dinucléaires d'or(I)-alcynyl-bisphosphine peuvent être synthétisés à partir de complexes dinucléaires d'or-allenyl-phosphine.

Mots clés: catalyse à l'or, catalyse à l'argent, lumière visible, *o*-alkynyl-*N*-sulfonylanilines, iodoalcynes, 3-sulfonylindoles, migration-1,3, allenyl bisphosphine borane, bisphosphine allène